The Detection of Potential Drug Resistance Markers Using Proteomic Technologies

A thesis submitted for the degree of Ph.D.

By

Lisa Murphy M. Sc.

The experimental work described in this thesis was carried out under the supervision of

Professor Martin Clynes Ph. D.

and

Dr. Joanne Keenan

National Institute for Cellular Biotechnology
School of Biological Sciences,
Dublin City University, Dublin 9, Ireland.

I hereby certify that this material, which I now submit for assessment on the programme of study leading to the award of Ph D is entirely my own work and has not been taken from the work of others save and to the extent that such work has been cited and acknowledged within the text of my work

Signed Lisa Murphy **ID No** 52170004

Date 18/12/2006

This thesis is dedicated to my father and the memory of my mother

Acknowledgements

It is a pleasure to thank the many people who made this thesis possible

I would like to thank Prof Martin Clynes for giving me the opportunity to do this PhD and for his constant support, advice and patience

I cannot express enough my gratitude to Dr Joanne Keenan for her fantastic support, guidance, constant enthusiasm and inspiration Over the past four years, she provided encouragement, sound advice, great company, good teaching and lots of great ideas I would have been lost without her

On a different note, I would like to thank Maxwell House for keeping me thinking and to all my coffee and lunch buddies - Paula, Vanesa, Laura, Naomi, Sandra and Erica for their great friendship You kept me all sane and stress free especially when the end was in sight

To everybody in the tox lab – Vanesa, Paula, Laura, Naomi, Sharon, Dermot, Aoife, Joanne, Rob, Norma, Brendan, Denis and Brigid for helping to keep my days in the lab eventful and lively

I am particularly grateful to everybody in the proteomics lab for all the help over the years, especially Will, Mick, Andrew and Paul

Also thanks to Rob for all his help with various problems (computers and otherwise) over the years To Joe and Ultan for all the "behind the scenes" work and to Carol and Yvonne in the office A huge thanks to everybody else I have failed to mention, you have not been forgotten

I cannot end without thanking my family for their constant support and encouragement in everything I do

The Detection of Potential Drug Resistance Markers Using Proteomic Technologies

Abstract

This thesis sets out to increase our knowledge of mechanisms by which lung cancer cells develop resistance to chemotherapeutic agents To further investigate drug resistance in lung cancer, a panel of four cell lines were chosen for pulse-selection with chemotherapeutic agents The cell lines include two squamous (SKMES-1 and DLRP) and two small cell lung carcinoma (DMS-53 and NCI-H69) cell lines The chemotherapy naive cell lines were pulse-selected rather than continuously selected with clinically relevant concentrations of taxotere, taxol, carboplatin and/or VP-16 The resulting twelve novel cell lines were tested for resistance to a cross-section of chemotherapeutic agents, for changes in invasiveness, motility, adhesiveness and for expression of the multidrug resistance (MDR) efflux pump proteins, P-gp and MRP-1 The SKMES-taxane selected variants were chosen for further analysis because the resistance profile was unstable and the concentration of drug used for selection was at a clinically achievable level Proteomic analysis was used to identify proteins associated with the development of taxol and taxotere resistance in these cell lines Proteomic analysis also revealed the differences between resistance to taxol and taxotere Loss of resistance was observed in both taxane resistant variants of SKMES-1 By monitoring the differential protein expression over time, proteins involved in the loss of resistance were identified

Adriamycin and mitoxantrone resistance was also studied in the squamous lung cell line DLKP While the main mechanism of resistance in these cell lines is associated with a drug pump, little information on cytoplasmic changes is available Proteomic analysis investigated these changes and elucidated the mechanisms involved in adriamycin and mitoxantrone resistance to identify putative markers with possible prognostic/diagnostic value A comparison of the proteins altered in adriamycin and mitoxantrone-resistant variants was carried out as these drugs are intercalating agents with mitoxantrone being an analogue of adriamycin and inducing less cardiotoxicity Multidrug resistance is a major problem in lung cancer, there is a need to understand the common mechanisms involved The proteins involved in the development of taxane resistance in SKMES-1 showed some cross over with other chemotherapeutic drugs namely adriamycin or mitoxantrone in DLKP

Abbreviations

2D-DIGE	-	Two dimensional-difference gel electrophoresis
2-DE	-	2-Dimensional Electrophoresis
5-FU	-	5-Fluorouracil
5dUMP	-	5-fluoro deoxyuridine monophosphate
5dUTP	-	5-fluoro-2-deosyuridine triphosphate
5FTUP	-	5-fluorouridine triphosphate
ABC	-	ATP Binding Cassette
ALL	-	Acute lymphocytic leukaemia
AML	-	Acute myeloid leukemia
ATCC	-	American Tissue Culture Collection
ATP	-	Adenosine-triphosphate
BCRP	-	Breast cancer resistance protein
BSA	-	Bovine Serum Albumin
BVA	-	Biological variation analysis
CA	-	Carrier ampholyte
CA125	-	Cancer antigen 125
cDNA	-	Complementary DNA
Da	-	Daltons
DIA	-	Differential In-Gel Analysis
DMEM	-	Dulbecco's Minimum Essential Medium
DNA	-	Deoxyribonucleic Acid
DNase	-	Deoxyribonuclease
DEPBG	-	Demethylepipodophyllin benzylidene glucoside
DEPC	-	Diethyl Pyrocarbonate
DMF	-	Dimethylformamide
DMSO	-	Dimethyl sulfoxide
DTE	-	Dithioerythritol
DTT	-	Dithiothreitol
ECACC	-	European Collection of cell cultures
ECL	-	Enhanced chemiluminescence
ECM	-	Extracellular matrix
EDTA	-	Ethylene diamine tetracetic acid
ESI	-	Electrospray ionisation

FCS	-	Fetal Calf Serum
FGF	-	Fibroblast growth factor
GSH	-	Glutathione
GTP	-	Guanosine Triphosphate
HEPES	-	N-[2-Hydroxyethyl]piperazine-N'-[2-ethanesulphonic acid]
HCC	-	Hepatocellular carcinoma
HCL	-	Hydrochloric acid
HPLC	-	High performance liquid chromatography
HSP	-	Heat shock protein
IC_{50}	-	Inhibitory Concentration 50%
IEF	-	Isoelectric Focusing
IHC	-	Immunohistochemistry
IMS	-	Industrial Methylated Spirits
IPG	-	Immobilised pH gradients
JNK	-	c-jun N-terminal kinase
kDa	-	Kilo Daltons
LF	-	Laminar Flow
LRP	-	Lung Resistance Protein
M	-	Molar
MALDI	-	matrix assisted laser desorption ionisation
MDR	-	Multiple Drug Resistance
MEM	-	Minimum Essential Medium
min	-	Minute(s)
MITOX	-	Mitoxantrone
mA	-	Milliamps
mM	-	Millimolar
MMPs	-	Matrix metalloproteinases
mRNA	-	Messenger RNA
MW	-	Molecular Weight Marker
MRP	-	Multidrug Resistance-associated Protein
MVP	-	Major Vault Protein
MS	-	Mass Spectrometer
N/A	-	Not applicable
NSAIDS	-	Non-Steroidal Anti-Inflammatory Drugs

NSCLC	-	Non Small Cell Lung Cancer
OD	-	Optical Density
PBS	-	Phosphate Buffered Saline
P-gp	-	P-glycoprotein
PGP9 5	-	Protein gene product 9 5
pI	-	Isoelectric point
PMF	-	Peptide mass fingerprinting
PMT	-	Photo multiplier tube
Q-TOF	-	Quadrupole time-of-flight
RNA	-	Ribonucleic Acid
RNase	-	Ribonuclease
rpm	-	Revolution(s) Per Minute
SCLC	-	Small Cell Lung Carcinoma
SELDI	-	Surface Enhanced Laser Desorption/Ionisation
SiRNA	-	Small interfering RNA
SDS-PAGE	-	Sodium Doedecyl Sulphate Polyacrylamide electrophoresis
TBP	-	Tributylphosphine
TEMED	-	N, N, N', N'-Tetramethyl-Ethylenediamine
TOF	-	Time-of-flight
Tris	-	Tris(hydroxymethyl)aminomethane
TS	-	Thymidylate Synthase
Txl	-	Taxol
TXT	-	Taxotere
UHP	-	Ultra high pure water
UK	-	Unknown
V	-	Volts
VCR	-	Vincristine
v/v	-	Volume per volume
w/v	-	Weight per volume

Table of Contents

4.0 Discussion

Section 1.0: Introduction

1 Introduction

Cancer is a major health issue accounting for 1 in 4 deaths in the United States in 2002, second only to heart disease (American Cancer Society statistics, 2005) Of the different types, lung cancer is the most lethal with 1 2 million cases diagnosed world wide each year and 1 2 million deaths (Seve and Dumontet, 2005) At approximately 20%, lung cancer is the leading cause of cancer deaths in Ireland Statistics show the incidences to be below the European average for men but over double for women (O' Connell, 2004) Less than 1% of cases occur before the age of 40, with a rapid increase thereafter particularly in the 65-70 age group Over 90% of lung cancers are due to smoking tobacco and are therefore preventable However, despite numerous programmes aimed at stopping smokers, 29% of adults and over 30% of teenagers still smoke Currently greater than 75% present with advanced stage disease Despite recent advances in research, there has only been a modest increase in survival and this scenario presents an important area for the detection of early stage cancers and identification of more effective treatments

Surgery provides the only curative treatment for lung cancer but resection is only possible in 30% of patients at diagnosis (Sandler *et al*, 2004) due to the late stage of presentation (Danesi *et al*, 2003) The poor survival rates are due to the cancer's propensity for early spread, the lack of effective screening for early diagnosis, the inability of systemic therapy to cure metastatic disease and the poor understanding of the biology of the tumours (Bunn, 2002, Niklinski and Hirsch, 2002)

Histologically lung cancers are classified into four groups, namely small cell lung cancer, adenocarcinoma, squamous cell carcinoma and large cell carcinoma However, for clinical and therapeutic purposes, lung cancers are divided into two groups, small cell carcinoma (SCLC) and non-small cell carcinomas (NSCLC)

While non small cell lung carcinomas (which constitute 80% of lung cancers) often show intrinsic multidrug resistance, small cell lung carcinomas, which causes 20% of all lung cancers, usually respond well to various anticancer agents initially However, SCLC acquires drug resistance with a two-year survival rate less than 10% (Wilhelm and Kolesar, 2005) This type of lung cancer differs both biologically and clinically

from the other histological types of lung cancer in that it has unique neuroendocrine and metastatic phenotypes SCLC cells can secrete up to 30 regulatory peptides and hormones and express receptors for over half of these factors Many of these peptides function as autocrine growth factors, which activate G protein-coupled receptors This establishes a positive feed-back loop which stimulates cell proliferation (Strassheim *et al*, 2000) This factor and the metastatic phenotype contribute to the greater mortality rate of SCLC patients

Non-small cell lung carcinomas have more phenotypic heterogeneity than SCLC (Gazdar, 1985) and are less sensitive to cytotoxic drugs The overall 5 year survival rate of patients with NSCLC has remained at less than 15% for the past 20 years (Rosel *et al*, 2004) Nearly all patients with NSCLC eventually develop metastatic disease (Boonstra *et al*, 2004) with an average survival period of 8 to 10 months The standard chemotherapy regime consists of a range of combinations of carboplatin, cisplatin, taxol, taxotere, gemcitabine, vinorelbine, ifosfamide and VP-16 However, results from randomised trials have illustrated that the following combinations - cisplatin and gemcitabine, cisplatin and vinorelbine and cisplatin or carboplatin with taxol or taxotere, failed to show differences in response rates and thus failed to improve survival rates The response rates in question failed to exceed 40% regardless of the combination used (Scagliatti *et al*, 1999)

The treatment of patients with chemotherapeutic drugs is seriously hampered by the development of resistance (both single agent and or multiple) (Boonstra *et al*, 2004) There are multiple mechanisms of drug resistance in lung cancer, acquired in SCLC and often inherent in NSCLC (Scagliatti *et al*, 1999) Acquired resistance is particularly problematic as tumours not only develop resistance to the original treatment but can also become cross-resistant to other drugs thereby developing multiple drug resistance (Longely and Johnston, 2005)

1.1 Multidrug resistance (MDR)

One of the major factors leading to drug resistance is decreased drug accumulation. Drug resistance mechanisms develop at many levels including drug inactivation, alterations in the target, increased drug efflux, processing of drug-induced damage and evasion of apoptosis (Longely and Johnston, 2005). Multidrug resistance occurs when cells are exposed to only one drug, yet display cross-resistance to an array of structurally unrelated compounds. Huge advances have been made in understanding the biology of lung cancer and the mechanisms of drug resistance. MDR has been classified based on the specific cellular targets involved: they are – classical multidrug resistance (MDR/P-gp), non P-gp MDR (MRP), atypical MDR (mediated through altered expression of topoisomerases II) and lung cancer resistance-related protein (LRP) (Scagliotti, *et al.*, 1999). However, other mechanisms of resistance include, an increase in detoxification due to enhanced activity of glutathione s-transferase, failure to engage the proper response, which leads to apoptosis of damaged cells and an increase in the metabolism of the drug to less toxic molecules (Longely and Johnston, 2005).

To help identify these molecular mechanisms, cell lines resistant to chemotherapeutic drugs have been developed. From analysis of lung cancer, it is apparent that a range of resistance mechanisms exist. The two most commonly found mechanisms are the overexpression of P-glycoprotein and the MDR related protein MRP – both of which are involved in the first stage of the development of multidrug resistance. It has been recognised that the development of MDR is a multifactorial process involving several cellular pathways. The first line of defence is to prevent accumulation of chemotherapeutics within the cell and this is achieved by means of the following membrane pumps.

1.1.1 P-glycoprotein (P-gp)

P-gp is one of the most widely studied and best characterised markers of MDR. Identified by Juliano and Ling in 1976, it is a 170 kDa member of the superfamily of ATP-binding cassette (ABC) membrane transporters (Tellingen, 2001). It is composed of 12 transmembrane domains and 2 ATP-binding domains (Figure 1.1). The protein is naturally expressed in the epithelial cells of the liver and kidney and also in the capillaries of the testes, ovaries and adrenal gland. In these cells, P-gp functions to pump toxins and xenobiotics (including anticancer agents) out of cells (Scagliotti *et al.*, 1999; Filipits, 2004).

Encoded by the *mdr-1* gene, P-gp is one of the key proteins that confer MDR in cancer. It is an ATP-dependant drug efflux pump which mediates drug resistance by actively extruding drugs from the cells (Lavie and Liscovitch, 2000).

The drugs most often involved in P-gp-mediated MDR are of fungal or plant origin, including anthracyclines, taxanes, epipodphyllotoxins and vinca alkaloids. Cancers that are intrinsically resistant to cytotoxic drugs such as renal, pancreatic and hepatocellular carcinomas often (over-) express P-gp. Interestingly, cancers with no or low basal levels of P-gp such as small cell lung carcinomas show higher expression levels after chemotherapy treatment (Filipits, 2004). It appears that P-gp alone is not sufficient in conferring a complete MDR phenotype in all cancer cells. Acquisition of MDR involves other mechanisms that often act concurrently to prevent or circumvent the lethal effects of chemotherapy drugs (Lavie and Liscovitch, 2001).

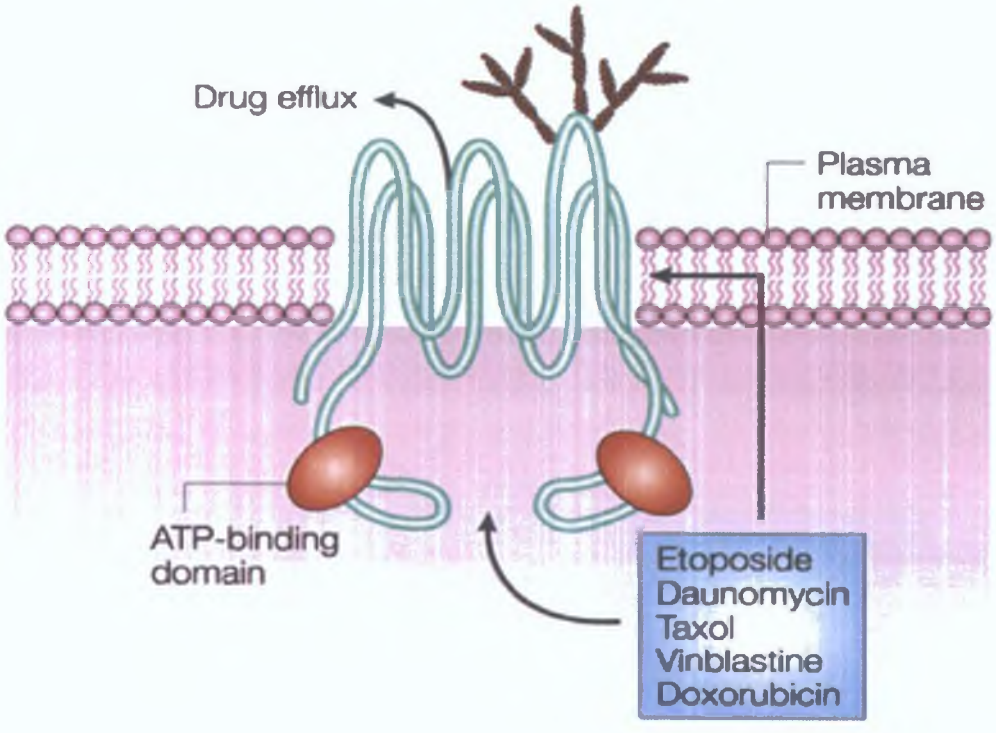

Figure 1.1 P-glycoprotein as a transmembrane drug efflux pump (Sorrentino, 2002).

The expression and/or activity of P-gp has been associated with unfavourable outcome in for example, paediatric acute lymphoblastic leukaemia, ovarian and diffuse large B-cell lymphoma patients (Swerts *et al*, 2006, Yakirevich *et al*, 2006, Ohsawa *et al*, 2005)

A possible strategy against MDR is to co-administer efflux pump inhibitors, although these agents may actually increase the side effects of chemotherapy by blocking physiological anticancer drug efflux from normal cells Even though efforts to overcome MDR using first and second generation reversal agents (e g verapamil, cyclosporine A, quinidine) or analogues of the first-generation drugs (e g dexverapamil, valspodar, cinchonine), have begun, few significant advances have resulted Clinical trials with third generation modulators (e g biricodar, zosuquidar, and laniquidar) specifically developed for MDR reversal are ongoing Results are not encouraging, as the perfect reversing agent may not exist

Antisense strategies targeting the MDR1 messenger RNA have been developed Guo *et al* (2005) used the antisense peptide nucleic acid delivery system via liposomes to inhibit the expression of P-gp in the human neuroblastoma cell line, SK-N-SH The result was an efficient and specific decrease in P-gp expression of SK-N-SH cells

1 1 2 Multidrug resistance protein 1 (MRP1)

The subfamily C of the ABC transporter family comprises six members of the multidrug resistance protein (MRP) family (Figure 1 2) They function in the transport of organic anions (MRP1-3) and nucleotides (MRP5) (Schrenk *et al*, 2001) First discovered by Cole and Deeley in 1992, MRP1 is a 190 kDa protein, mainly localised in the plasma membrane (Borst *et al*, 1999)

The genes encoding MRP1 and P-gp are evolutionarily very distant, with the primary structure of the two proteins being dissimilar, sharing only 15 percent ammo acid identity (Cole *et al*, 1992) The resistance profile of MRP1 is somewhat different to that of P-gp-mediated resistance although many cancer drugs are affected by both mechanisms Overexpression of MRP1 increases resistance to several anticancer drugs, such as anthracyclines, vincristine, vinblastine, and VP-16 The specific exceptions are the taxanes and mitoxantrone (Filipits, 2004)

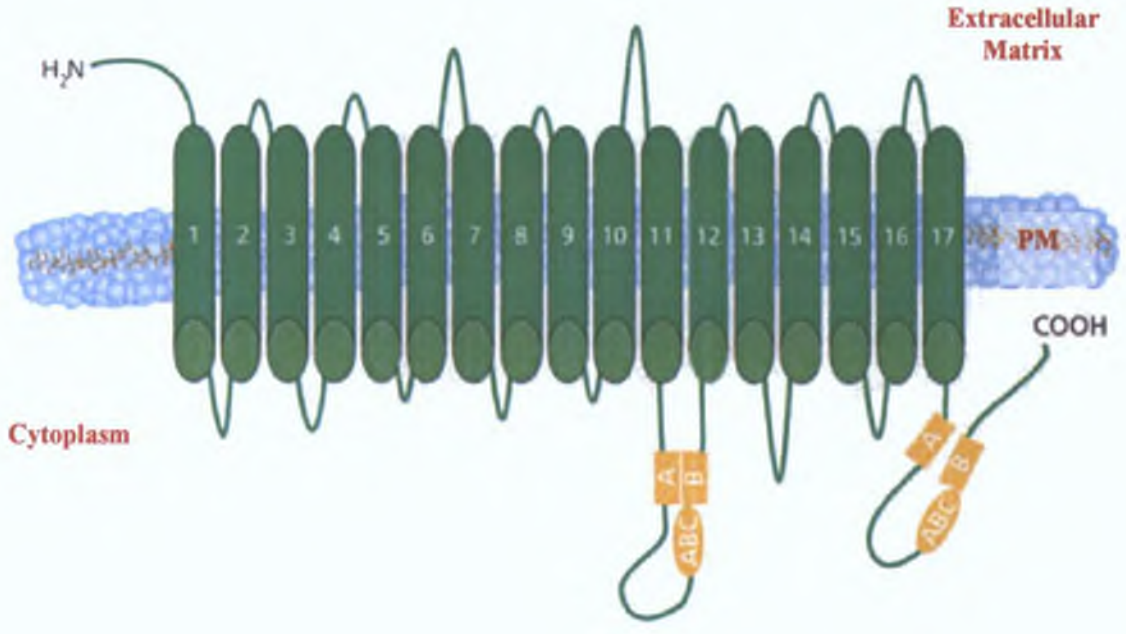

Figure 1.2 Schematic representation of MRP1 (adapted from this website: www.sigma-aldrich.com). PM=Plasma membrane; 1-17=Transmembrane domains 1-17; COOH=Carboxy terminus; NH_2=Amino terminus

MRP1 has been detected in almost all solid and haematological cancers. The clinical significance of high levels of MRP1 has been associated with poor patient outcomes in lung, endometrial, breast, gastric carcinomas, neuroblastomas and acute myeloid leukaemia (Chauncey, 2000; Young *et al.*, 2001).

1.1.3 MRP2 (cMOAT)

Canalicular multi-specific organic anion transporter (cMOAT or MRP2), an isoform of MRP1, is mainly expressed in the canalicular membrane of hepatocytes and the proximal tubules of the kidney. It shows 49% identity with human MRP1 at the protein level and is associated with hepatobiliary secretion of bilirubin-glucuronide (Young *et al.*, 2001; Filipits, 2004). The substrate specificity is similar to MRP1, but in contrast to MRP1 it can confer resistance to cisplatin.

In recombinant systems, MRP2 expression enhanced resistance to VP-16, vincristine, cisplatin, doxorubicin, and epirubicin. Using antisense cDNA, sensitivity to cisplatin, vincristine and doxorubicin was restored in cell lines expressing MRP2 (Lockhart *et al.*,

2003) MRP2 has been demonstrated to transport vinblastine in association with glutathione (GSH) The GSH co-transport mechanism provides a plausible explanation of how MRP2 and MRP1 confer resistance to some of the anti-cancer agents that form conjugates *in vivo* (Leslie *et al*, 2001) To date, there has been no demonstrated correlation between MRP2 expression and clinical outcome (Lockhart *et al*, 2003)

1 1 4 Lung resistance protein

The lung resistance protein, also known as the major vault protein (MVP), is not an ABC transporter but is often expressed in high levels in non P-gp drug-resistant cell lines and tumours The LRP gene codes for a protein that has a molecular mass of 110 kDa (Scaglioti *et al*, 1999) The LRP/MVP is the most abundant protein of the vault complex Vaults are large, abundant ribonucleoprotein particles localised in the cytoplasm The function of vault proteins is still unclear However, it has been suggested that vaults may regulate nucleocytoplasmic as well as vesicular transport of different substrates, including cytostatic drugs

Analysis of advanced ovarian tumour samples has illustrated that the expression of LRP/MVP at diagnosis was an independent poor prognostic factor for response to chemotherapy Lung resistance protein is also an indicator of poor response to platin or alkylating agents (Filipits, 2004)

1 2 Chemotherapy drugs

Currently, chemotherapy can offer improvement in medium term survival of lung cancer but overall survival is poor Chemotherapy is the use of pharmaceutical agents for the treatment of a disease and overall has been very successful in the treatment of certain types of cancer Chemotherapeutic drugs have been discovered through many different approaches ranging from empirical screening to rational design with a strong contribution from serendipity along the way

The aim of chemotherapy is to kill the tumour cells with the least possible effect on normal cells (Debatin, 2000) Chemotherapy is often used in combination with surgery or other therapies such as radiotherapy, known as adjuvant chemotherapy It is especially important for increased survival in cancer patients where these other treatments have failed (Akehurst *et al*, 2002)

1 2 1 The taxanes (Taxol and Taxotere)

The taxanes are a group of drugs, which include taxol and taxotere Taxol, purified by Bristol-Meyers Squibb, was originally isolated from the bark of the slow-growing Pacific yew, *Taxus brevifolia* by Wall and Wani in 1979 Taxol is a complex diterpene with a taxane ring structure fused with a 4-membered oxetan ring, an ester side chain at position C-13 and a benzoyl side chain at position C-2 (see Figure 1 3)

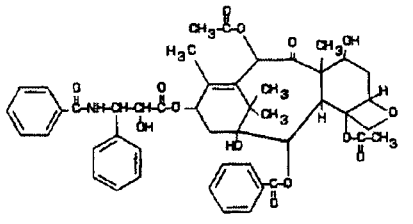

Figure 1 3 Structure of taxol

Taxol was approved by the Federal Drug Agency (FDA) for treatment of breast, ovarian and NSCLC (He *et al*, 2001) Schiff *et al* (1979), were the first group to report that taxol promoted the assembly of microtubules *in vitro* in the absence of guanosine triphosphate (GTP), which is usually required The resulting microtubules were also discovered to be stable against conditions favouring depolymerisation

Taxotere is synthesised from a precursor, isolated from the needles of the European yew, *Taxus baccata* Taxotere is not identical in structure to taxol, having two modifications, a tert-butoxycarbonyl group at C-3' and a hydroxyl group on the C-10 position (see Figure 1 4) The two drugs have similar mechanisms of action even though taxotere is approximately twice as potent an inhibitor of microtubule depolymerisation relative to taxol (Gelman, 1994)

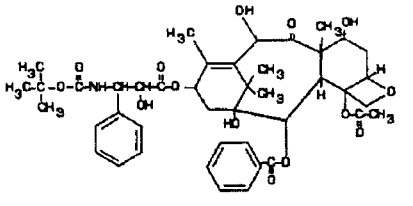

Figure 1 4 Structure of taxotere

Microtubules which primarily consist of alpha (α) and beta (β) tubulin heterodimers, are intrinsically dynamic polymers They play a crucial role in mitotic spindle assembly, the mitotic checkpoint and chromosomal development (Yvon *et al*, 1999) The taxane drugs cause interruption of mitotically-specific microtubule processing at the G2-M phase of cell division They promote the assembly of microtubules and block their disassembly thereby preventing cancer cells from dividing The result is cancer cell death and the promotion of dysfunctional microtubules (Calderoni and Cerny, 2001) Interestingly, both taxanes bind to the β-subunit of tubulin but the microtubules produced by taxotere are larger than those produced by taxol This may explain why taxotere appears to be approximately twice as potent as taxol (Vaishampayan *et al*, 1999)

There are at least two important mechanisms of resistance to the taxanes The MDR phenotype is acquired resistance conferred by both taxanes and many other chemotherapeutic drugs The energy-dependent P-gp efflux pump transports chemotherapeutic drugs through the cell membrane reducing the accumulation of intracellular taxol/taxotere (Chiou *et al*, 2003) The other major mechanism involves a mutation of the gene encoding for one of the tubulin subunits (Schibler and Cabral, 1986) or alterations in the expression of the subunits The result is the production of structurally altered tubulin subunits with have diminished capacity of depolymerisation (Calderoni and Cerny, 2001) Studies have shown that taxane treatment has improved clinical outcome and survival For example, taxotere as a neoadjuvant single agent is effective in treating patients with large locally advanced breast cancer, giving durable clinical and pathological responses, and good survival outcome in patients with clinical responses (Tham *et al*, 2005)

Recent advances in the design and preclinical evaluations are leading to the generation of new synthetic taxane anticancer agents These agents have been designed to have fewer side effects, superior pharmacological properties and improved activity against drug-resistant human cancers Structure-activity relationship studies discovered a series of highly active second-generation taxanes such as Ortataxel, DJ-927 and BAY 59-8862 (Geney *et al*, 2005, Shionoya *et al*, 2003, Ferlini *et al*, 2003)

Ortataxel (SB-T-101131, IDN5109, BAY59-8862), currently in phase II trials, exhibits excellent activity against a variety of drug-sensitive and drug-resistant cancer cell lines, as well as human tumour xenografts in mice. Photoaffinity labelling of the microtubules and P-gp revealed the drug-binding domain in tubulin as well as in P-gp (Geney *et al.*, 2005). The drug is characterized by its high tolerance, antitumour efficacy, ability to overcome multidrug resistance and oral bioavailabilty. After treatment of head and neck squamous cell carcinoma with ortataxel *in vitro,* Bcl-2 and Bcl-XL were down-regulated, Bax was up-regulated, and caspase-3 was activated. Supernatant concentration of vascular endothelial growth factor and interleukin-8 were decreased. Immunohistochemistry analysis showed that ortataxel inhibited tumour angiogenesis and induced apoptosis, producing a decreased blood vessel density and increased apoptosis index (Sano *et al.*, 2006).

Taxol and taxotere are substrates for P-gp. In contrast, ortataxel is effective against P-gp-expressing cells by virtue of modulation of P-gp-mediated transport. Modulation of the drugs mitoxantrone, daunorubicin and adriamycin retention and cytotoxicity by ortataxel was studied in cell lines overexpressing P-gp, MRP-1 and breast cancer resistance protein. Ortataxel effectively modulated drug retention and cytotoxicity in all cell lines (Minderman *et al.*, 2004).

1.2.3 The platinum drugs (Cisplatin and Carboplatin)

In 1965, Rosenberg and co-workers first reported the inhibition of cell division in *Eschericia coli* by the electrolysis products from a platinum electrode. As a result cisplatin was the first platinum complex discovered to have a broad range of antitumour activity (Figure 1.5). Further research resulted in the synthesis of more platinum analogues, carboplatin being the most widely studied.

Cisplatin is an established antitumour agent for the treatment of advanced NSCLC and in cisplatin-based adjuvant chemotherapy. Cisplatin is a square planar coordination complex with a central platinum atom surrounded by two labile chlorine atoms and two relatively inert ammonia moieties in the *cis* configuration (Wang and Lippard, 2005). The ability of cisplatin or carboplatin to form covalent intra-strand and inter-strand cross-links with the genomic DNA is thought to cause its cytotoxic effects. Besides their effect on lung cancer, the platinum drugs are extremely effective when used on most testicular cancers, head and neck and on a subset of ovarian and bladder tumours.

However, almost half the women with ovarian cancers present with tumours that are intrinsically resistant to the platinum compounds Moreover, a significant number of the tumours that respond well initially eventually acquire resistance As a result, the cells' ability to limit these DNA lesions or its ability to repair or tolerate these lesions once formed, should influence its survival Therefore resistance to platinum based therapy poses a major problem (Wernyj and Morin, 2004) Cisplatin treatment is severely limited by neurotoxicity side effects which can cause peripheral neuropathy, tinnitus and hearing loss Carboplatin (Figure 1 6) is less potent than cisplatin and its side effects are different in that it has less renal and gastrointestinal toxicity but it has more hematological toxicity (Wang and Lippard, 2005)

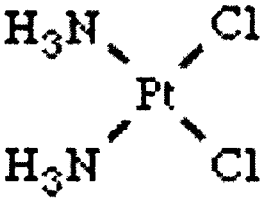

Cisplatin

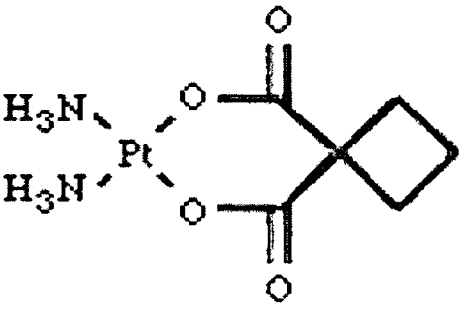

Carboplatin

Figure 1 5 Structure of cisplatin

Figure 1 6 Structure of carboplatin

Mechanisms of cellular platinum resistance identified to date include, decreased cisplatin accumulation *via* increased drug inactivation by protein and non-protein thiols, enhanced DNA adduct repair, alteration in the sorts of platinum-DNA adducts formed and increased tolerance to platinum-DNA damage However, the underlying molecular bases for these chemoresistance mechanisms are still poorly understood (Johnson *et al*, 1996) Chemoresistance to cisplatin remains one of the major obstacles to the successful treatment of NSCLC

1 2 4 5-fluorouracil (5-FU)

The drug 5-fluorouracil (an antimetabolite) and its derivatives are among the most useful drugs in the treatment of solid tumours but not traditionally used in lung cancer First designed and synthesised by Heidelberger and co-workers in 1957, its chemistry and mechanism of action has been studied extensively (Longley *et al*, 2003) It is

widely used to treat colorectal, breast, head and neck, non-small-cell lung cancer, pancreatic cancer and leukaemias (Maring *et al*, 2005) However, as it is unusual to observe complete remission when 5-FU is used alone, it is therefore more used as a combinational drug For example the combination of 5-FU with oxahplatm and irinotecan which act on targets distinct from 5-FU have improved the response rates of advanced colorectal cancer to 40-50% (Longley *et al*, 2003)

Targeting rapidly dividing cells, the main side effects of 5-FU are on the bone marrow and intestinal and oral mucosa The result is a decrease in platelet and leukocyte production Other side effects include diarrhoea and neurological problems such as somnolence and ataxia

Resistance is still a significant limitation to its clinical use Understanding the mechanisms involved is vital to overcoming resistance

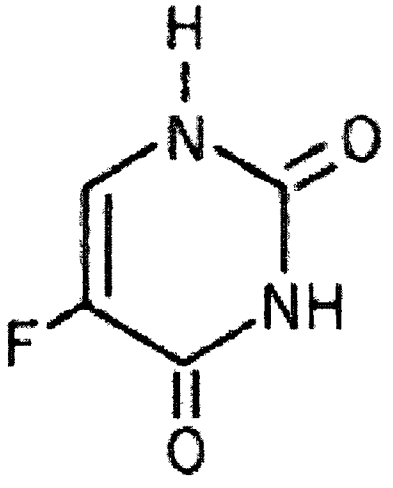

Figure 1 7 Structure of 5-FU

An analogue of uracil, 5-FU has a fluorine atom at its C-5 position instead of hydrogen (Figure 1 7) On entering the cell, it is converted to several active antimetabolites 5 fluoro-2-deoxyuridine monophosphate (5dUMP), 5 fluoro-2-deoxyuridine triphosphate (5dUTP) and 5-fluorouridine triphosphate (5FUTP) 5FUTP is incorporated into the RNA causing errors in transcription and translation and alters mRNA stability 5dFUMP inhibits the action of the enzyme essential in DNA synthesis, *thymidylate synthase (TS)* (Pinedo and Peters, 1988, Grem, 2000)

These mechanisms may vary in importance and differ between cell lines Intrinsic or acquired resistance to 5-FU is usually caused by aberration in its metabolism

amplification or alteration of TS, deficiency anabolism or transport or increased catabolism Any of the above can result in resistance (Pinedo and Peters, 1988)

TS expression effectively predicts resistance to 5-FU There is an approximate 50% failure rate among patients with low TS mRNA Aschele *et al* (2002) reported that the correlation between intratumoral TS levels and clinical response to 5-FU depended strongly on the schedule of administration/biochemical modulators that is used in different 5-FU regimens This data strengthens the notion that different 5-FU schedules have different mechanisms of cytotoxicity Cascinu *et al* (1999) confirmed the ability of TS protein expression to predict for response to 5-FU The study provided further evidence for the existence of different patterns of TS expression among different metastatic sites, which may have a significant impact on the choice of drugs and the design of new treatments in advanced colon cancer

1 2 5 Adriamycin

Adriamycin is an anthracycline antibiotic, isolated from *Streptomyces peucetus* It was recognised to have antineoplastic activity over four decades ago but it was not until 1984 that the anthracyclines were discovered to be inhibitors of topoisomerases II It is this ability that appears to be the primary mechanism of action for tumour cytotoxicity (Tewey *et al*, 1984)

The drug has a broad spectrum of antitumour activity and is used to treat solid tumours including breast, bladder, endometrium, lung, ovarian, stomach and thyroid carcinomas It is also effective against soft tissue sarcomas and many cancers of the blood (Hortobagyi, 1997) However, adriamycin treatment often causes nausea vomiting, anorexia, diarrhoea and in some cases cardiotoxicity (Nielsen *et al*, 1996, Monneret, 2001) Adriamycin is composed of four rings linked *via* a glycosidic bond to daunosamine - an amino sugar (Figure 1 8)

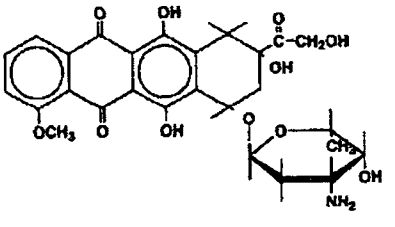

Figure 1 8 Structure of adriamycin

The planar moiety of the drug permits intercalation between the bases of the double helix resulting in the DNA extending and unwinding It also modifies the ability of the nuclear hehcases to dissociate the duplex DNA into single DNA strands therefore hindering the process of DNA strand separation Moreover, all active anthracyclines are anthraquinones Quinones can undergo one and two electron reductions producing reactive compounds that damage macromolecules and lipid membranes (Myers *et al*, 1977) It is this free radical formation that causes damage to heart tissues

The main mechanisms of resistance to adriamycin are –

(1) The classic MDR phenotype i e increased drug efflux, due to overexpression of P-glycoprotein, MRP family members and LRP (Clynes *et al*, 1998, Borst *et al*, 1999)

(2) Increased glutathione transferases content and detoxification mechanisms

(3) Alteration in topoisomerase II activity due to decreased cellular expression of the enzyme or changes in activity such as decreased drug-induced DNA cleavage, differential expression of topoisomerase isoforms, altered subcellular distribution of topoisomerase II and changes in extrinsic factors modulating topoisomerase II activity (Skovsgaard *et al*, 1994)

1.2.6 Etoposide (VP-16)

Etoposide, also commonly known as VP-16 (Figure 1 9) is a semi-synthetic derivative of podophyllotoxin and is used in the treatment of certain neoplastic diseases Podophylhn-containing materials have been used as medications by various cultures for over 1000 years In the 19th century, podophyllin was found to be topically effective in the treatment of skin cancer and in 1946 its antimitotic properties were discovered In the 1950s, researchers at Sandoz Pharmaceuticals developed several derivatives, which were found to have antitumour activity against L1210 leukaemia The most effective of these derivatives was 4'-demethylepipodophyllin benzylidene glucoside (DEPBG) Further development of DEPBG resulted in two analogues being synthesised (Hande, 1998) They were named VP-16 and teniposide

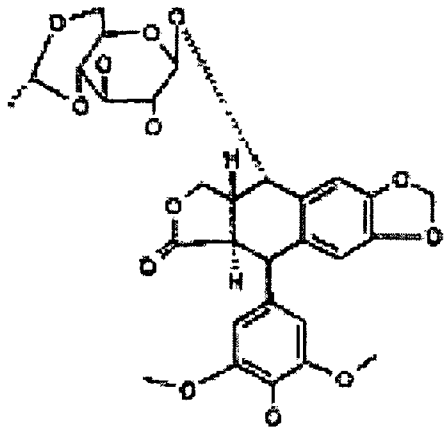

Figure 1 9 Structure of etoposide

VP-16 has shown activity against testicular cancers, acute myeloid leukaemia, Hodgkin's disease, non-Hodgkin's lymphoma, lung, gastric, breast and ovarian cancers as well as Kaposi's sarcoma The major toxicities attributable to VP-16 are bone marrow depression, nausea, diarrhoea, mucositis and hypotension (Hande, 1998)

VP-16's mechanism of action involves the poisoning of topoisomerase II enzymes whose function is to temporarily break DNA strands and reseal the breaks This results in the DNA being sufficiently untangled to allow transcription and replication to occur VP-16 poisons topoisomerase II by increasing the steady state concentration of their covalent DNA cleavage complexes This converts the topoisomerases into toxins that introduce high levels of transient protein-associated breaks in the genome of the treated cells

The replication machinery (helicases), which attempts to traverse the covalently bound topoisomerase roadblock, does not function properly This results in disruption of the cleavage complex and conversion of the transient DNA breakage into permanent double-stranded helices, which are no longer held together by the proteinaceous bridges It is these breaks that become targets for recombination, sister chromatid exchange, the generation of large deletions or insertions and the production of chromosomal aberrations ultimately leading to apoptosis and cell death (Hande, 1998)

Development of resistance to VP-16 can be due to reduced levels of topoisomerase II within the target cells Moreover, mutations or alterations in drug binding sites on topoisomerase II are associated with resistance to VP-16 Increased expression of MDR-1 also confers resistance to VP-16

1 2 7 Vinca alkaloids - vincristine

Vincristine and vinblastine are naturally occurring alkaloids found in minute quantities in the leaves of the Madagascar periwinkle plant *Catharanthus roseus* The plant was initially used by a variety of cultures for the treatment of diabetes However, while it was under investigation as a source of oral hypoglycaemic agents, it was noted that extracts could reduce white blood cell counts Subsequently it was found to be active against lymphocytic leukaemia in mice, which led to the isolation of vincristine (Pratt *et al*, 1994, Cragg and Newman, 2005) Both drugs are members of a general class of drugs that function as mitotic inhibitors which interfere with the function of microtubules, a class of long, tube-like cellular organelles approximately 250nm in diameter (Pratt *et al*, 1994) Microtubules and microfilaments play an important role in the movement of cells relative to each other and in the movement of organelles within the cytoplasm of a single cell

Vincristine is an asymmetrical and dimeric molecule composed of a dihyrdoindole nucleus, vindoline, linked by a carbon-carbon bond to an indole nucleus, catharanthine (Figure 1 10)

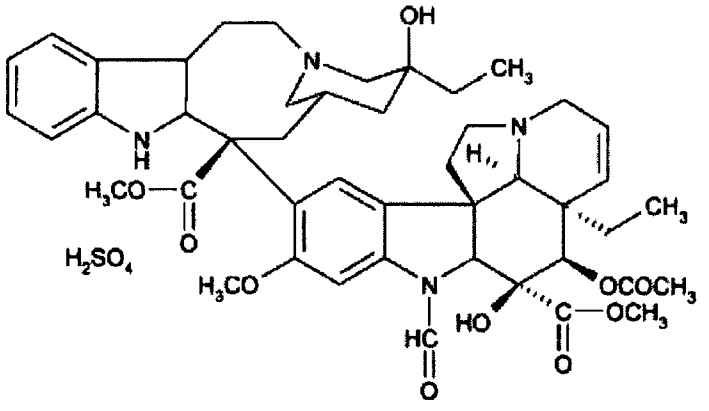

Figure 1 10 Structure of vincristine

Vincristine arrests the cell cycle in G2/M phase by blocking mitotic spindle formation High concentrations of vincristine result in a depolymerisation of the microtubules This prevents the binding of tubulin to microtubule proteins - this mechanism contrasts to that of the taxanes which stabilise the tubules In turn this induces apoptosis *in vitro* or tumour necrosis *in vivo*, triggers Raf-1 activation, phosphorylation of Bcl-2 family proteins and induction of p53 expression Low concentrations of vincristine stabilise the spindle apparatus resulting in the failure of chromosomes to segregate, leading to

metaphase arrest and inhibition of mitosis (Bruchovsky *et al*, 1965, Gidding *et al*, 1999)

Vincristine is most frequently used in paediatric oncology and is also used to treat acute lymhoblastic leukaemia Wilms' tumour, Hodgkin's disease and non-Hodgkin's lymphoma Vincristine is also very commonly used in combination with other chemotherapeutics (Lofgren *et al*, 2004)

Mechanisms of vincristine resistance include the amplification of P-gp, MRP1 and LRP Decreased binding affinity of tubulin for vincristine also plays a role in vincristine resistance This may be due to changes in the tubulin isoforms expressed or different tubulin levels Altered stability of microtubules may also result in changes in the equilibrium between free and polymerised tubulin in cells (Gidding *et al*, 1999)

1 2 8 Mitoxantrone

Mitoxantrone, an aminoalkylamino-disubstituted anthraquinone with anti-cancer activity was developed in the 1980s as a doxorubicin analogue in a program to find a cytotoxic agent with decreased cardiotoxicity compared with doxorubicin (Figure 1 11) (Fox *et al*, 2004, Gutierrez *et al*, 2000) The drug was developed from a rational design of screening of anthranquinone-based intercalating agents (Alderden *et al*, 2006)
It has a broad spectrum of antitumour activity and is used to treat acute leukaemia, malignant lymphoma, non-small cell lung cancer, melanoma, lymphoma symptomatic hormone-refractory prostate cancer, breast and colon cancers (Parker *et al*, 2004, Fox, 2004, Towatari *et al*, 1998)

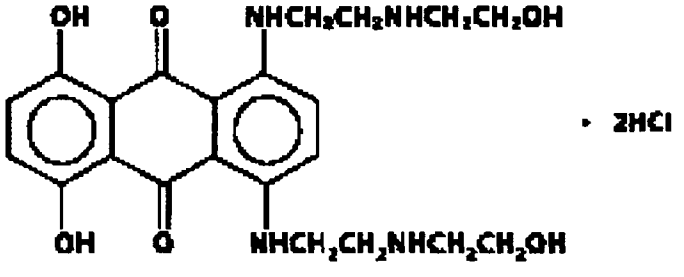

Figure 1.11 Structure of mitoxantrone

The drug binds with high affinity to DNA in a sequence specific manner and unwinds the closed circular complex It inhibits nucleic acid synthesis and causes strands of DNA to break *in vivo* (Twentyman *et al* , 2004) The intercalation with the DNA leads to cytotoxicity via inhibition of topoisomerase II The interaction with DNA is thought to be stabilised by two cationic alkylamino side chains, which form electrostatic interactions and hydrogen bonds with the strand of DNA Investigations have identified that the cationic alkylamino group in mitoxantrone derivatives are important in the nuclear localisation, DNA binding and the inhibition of DNA synthesis (Alderden *et al* , 2006) Mitoxantrone is a substrate for P-gp mediated efflux however, when used as a selecting agent it frequently selects for non-P-glycoprotein-mediated multidrug resistance in *in vitro* models (Futscher *et al* , 1994)

1.3 Cancer and proteomics

Cancer is a multi-faceted disease that presents many challenges to clinicians and cancer-researchers alike who search for more effective ways to combat this devastating disease. Tumour development is a complex process, requiring the co-ordinated interactions of many proteins, signal pathways and cell types (Negm *et al.*, 2002) and as such is an ideal candidate for proteomic analysis.

Proteomics analysis attempts to identify the protein complement expressed by the genome (Wilkins and Williams, 1993) and is the systematic separation, identification and characterisation of proteins present in a biological sample (Kennedy, 2000). Proteomics includes not only the identification of proteins but also the determination of their locations, modifications, interactions, activities and ultimately their functions. Proteomics is regarded as the sister technology to genomics (Kennedy, 2000) complementing the knowledge derived from genomic analysis. The ultimate goals of proteomics go beyond a catalogue of proteins expressed by healthy and diseased cells. The eventual objective is to elucidate the organisation and dynamics of the metabolic, signalling and regulatory networks through which the life of the cell is transacted. Cancer proteomics seeks to understand how networks become dysfunctional, predict how their function can be manipulated through interventions by drugs or genetic manipulations (Anderson *et al.*, 2000) and enables the identification of disease-specific proteins, drug targets and markers of drug efficacy and toxicity. Furthermore, cancer proteomics seeks to identify markers to improve diagnosis, classification of tumours and also to define targets for more effective therapeutic measures (Simpson and Dorow, 2001). Given the late stage at which cancers often present, the identification of early detection biomarkers by proteomic analysis will offer better prognosis and aid in individualizing treatments for certain cancers.

Analysis of the proteome has added layers of complexity compared to the genome. A simple gene can encode multiple different proteins by alternative splicing of the mRNA transcript, by varying translation start or stop sites, by frameshifting during which a different set of triplet codons in the mRNA is translated or by posttranslational modifications (Anderson and Seilhamer, 1997). A single protein may be multifunctional and conversely similar functions may be performed by different proteins (Fields, 2001). The result is a proteome estimated to be an order of magnitude more complex than the genome.

For the past 26 years, high-resolution two-dimensional gel electrophoresis (2-DE) using isoelectric focusing/sodium dodecyl sulfate-polyacrylamide gel electrophoresis (IEF/SDS-PAGE) has been the technology of choice for analysing the protein content of tissues and fluids followed by mass spectrometry It has also been used to study changes in global patterns of gene expression elicited by a wide range of gene effectors (Celis and Gromov, 1999) Originally introduced in 1975, Farrell and Klose demonstrated the ability to separate proteins based on their isoelectric points and molecular weights by 2-DE on polyacrylamide gels In the first dimension, proteins were separated according to their isoelectric point (pI) along a pH gradient using carrier ampholyte (CA) containing polyacrylamide gels cast in narrow tubes In the second dimension proteins were separated according to their molecular weights in SDS-PAGE

1 4 The development of immobilised pH gradient-based 2-DE

For many years 2-DE technology relied on the use of carrier ampholite to establish a pH gradient This technique proved to be difficult, labour intensive and a major contributor to the variability of 2-DE patterns (Celis and Gromov, 1999) The problems associated with CA-based separations included gaps and drift in the gel patterns resulting from discontinuities in the pH gradient (Hanash *et al* , 1991) These difficulties prompted the development of immobilised pH gradients (IPG) for first dimension separation IPGs are formed by the co-polymerization of buffering groups of acrylamide derivatives into a polyacrylamide gel matrix They contain chemically immobilised buffering and titrant groups that cannot migrate in the electric field This allows steady state focussing and eliminates the problem of cathodic drift (Molloy, 2000) Their development meant that 2-DE became more reproducible, allowing inter-laboratory comparison of results (Bjellquist *et al* , 1982) Narrow-range strips, suitable for focussing proteins over wide pH units (3-10) or single pH range (11-12) (Cordwell *et al* , 2000) became available (Gorg *et al* , 1999) Loading capacity increased (up to 5 milligrams) on wide pH ranges (Hanash *et al* , 1991) enhancing the detection of less abundant proteins and subsequently providing enough amounts for protein sequencing Rabilloud *et al* (1994) improved the resolution by applying the sample during the rehydration step thus eliminating its precipitation More acidic and basic proteins could be separated with increased resolution (Gorg *et al* , 1988) It also enabled exact control of protein amounts and sample volumes loaded Sanchez *et al* (1997) developed a simple and inexpensive

methacrylate rehydration chamber, which could accommodate 10 immobilised IPG strips

Two-dimensional electrophoresis continues to deliver high quality protein resolution and dynamic range for the proteomics researcher However, in order to remain the preferred method for protein separation and characterization, several key steps needed to be implemented to ensure high quality sample preparation and speed of analysis The following describes the progress made towards establishing 2-DE as an optimal separation tool for proteomics research

1 5 Sample preparation

A suitable sample preparation is critical for high quality accurate and reliable 2-DE results The method involves preparation/purification of cells, cell lysis and solubilisation However, there is no unique way to prepare samples, therefore each protocol differs depending on the type of sample used Similarly, sample selection and handling are of utmost importance, for example, the use of fresh tumour tissue for 2-DE analysis was reported to be superior to a frozen sample (Alaiya *et al*, 2002) An effective sample preparation will solubilise all proteins, prevent protein aggregation during focusing, prevent chemical modification of the protein, may remove abundant proteins or non-relevant classes, remove contaminating nucleic acids and other interfering molecules and yield proteins of interest at detectable levels Solubilisation is achieved by the use of chaotropes, detergents and reducing agents

1 5 1 Chaotropes

Chaotropes disrupt hydrogen bonding thereby leading to protein unfolding and denaturing Urea is a popular uncharged chaotrope used in 2-DE It is typically used at the highest possible concentration (usually 5-9 8 M) with an accompanying surfactant Rabilloud *et al* (1997) utilised the high loading capacity of IPGs to resolve hydrophobic proteins In the process they improved their solubility by using a combination of detergents and chaotropes They showed for example, that addition of thiourea, CHAPS and sulphobetain surfactants (SB3-8, SB3-10 and ASB14) to the lysis solution which contained urea resulted in much improved solubilisation as well as transfer to the SDS gel

The use of thiourea is recommended for use with IPGs, which are prone to absorptive losses of hydrophobic and isoelectrically neutral proteins Thiourea (at 2M) when used

in conjunction with high concentrations of urea, adds to the power of the solubilisation solution This was dramatically illustrated with high recoveries seen on 2-DE gels from separations of nuclear proteins and integral membrane proteins when compared to classical solubilisation solutions (Rabilloud *et al* , 1997)

1 5 2 Surfactants

Surfactants must be included in the solubilisation solution as they act synergistically with chaotropes They prevent hydrophobic interactions, which might occur via chaotrope-generated exposure of hydrophobic domains These hydrophobic stretches must be protected or protein loss can occur through aggregation and adsorption This is therefore essential for proteins that have one or more such domains One of the most commonly used surfactant, SDS, needs dilution to 0 3% or less so as not to interfere with the first dimension The preferred option is to avoid SDS and include a nonionic or zwitterionic surfactant in the sample solubilisation solution A zwitterionic surfactant such as CHAPS shows superior efficiency over non-ionic detergents such as Nonidet P-40 (NP-40) and TritonX-100 (Molloy, 2000) However, 0 5 % of TritonX-100 is often used in conjunction with a zwitterionic surfactant to aid in the solubilisation of membrane proteins Moreover, typically less than 1 % of carrier ampholytes are added to help reduce the problem of protein-matrix interactions and to overcome the detrimental effects caused by salt boundaries The salt concentration must be below 10 mM by dilution as it interferes with the IEF, otherwise the samples must be desalted by dialysis

1 5 3 Reducing agents

Thiol reducing agents break intra- and inter-molecular disulphide bonds and are critical for protein solubilisation The most common agents are cyclic reducing agents such as dithiothreitol (DTT) and dithioerythritol (DTE) These reagents work through an equilibration reaction However, loss of the agent through migration in the pH gradient (DTT and DTE are mildly acidic) can contribute to horizontal streaking therefore IEF should not be carried out for excessively long focussing times Iodoacetamide is subsequently used to remove excess DTT, which is responsible for causing "point streaking" in silver stained gels (Gorg *et al* , 2000) Phosphines are an alternative to thiol reducing agents Tributylphosphine (TBP) is uncharged and maintains reducing conditions throughout the IEF process This minimises the problem of aggregation

(Molloy, 2000) TBP has been successfully applied to hydrophobic proteins (Gorg *et al*, 2000)

1 5 4 Tissue heterogeneity

Tissue heterogeneity is another key problem It is important that a cell population be "pure and relevant" (i e free from stroma, blood, serum etc) In this context, the impact of cancer cell lines derived from tissue samples cannot be overstated Many different methods have been developed to minimise or eliminate "non relevant" cell types in tissue samples Using Dynabeads, Reymond *et al* (1997) isolated human colorectal tissue from normal tissue to look at the contribution of the normal cells surrounding the cancer to the cancer growth and development Proteolytic enzymes are a prime example of this as they are often expressed by tumour surrounding fibroblasts but not by tumour cells (Okada *et al*, 1995) Banks *et al* (1999) used laser capture microdissection on cervix tissue to cleanly remove the epithelium from underlying stroma

1 5 5 Subcellular fractionation

The problem of limited dynamic range exists as low copy number proteins are rarely visualised and successfully identified from 2-DE gels In mRNA-based approaches the dynamic range spans five orders of magnitude This is a severe limiting factor as the dynamic range of some proteins may be as great as seven to eight orders of magnitude coupled with limited dynamic ranges of staining techniques such as silver versus coomassie It is therefore more practical to think of the dynamic range of 2-DE/MS in terms of what can be observed on a gel – typically three orders of magnitude for silver staining However, the dynamic range of a method is only limited to the number of enrichment or prefractionating steps performed (Ho *et al*, 2006)

Subcellular fractionation of cellular organelles can enrich cells for analysis and reduce the complexity of the protein mixture Prefractionation of proteins can be achieved either by

(1) Isolating the cell compartments and/or organelles (ribosomes, mitochondria or plasma membrane) by high-speed centrifugation
(2) Sequential extraction procedures with increasingly stronger solubilising buffers (e g aqueous buffers, ethanol or chloroform/methanol and detergent based extraction solutions)

(3) Precipitation e g TCA/acetone precipitation is a very successful method for (a) inactivating proteases, (b) enriching alkaline proteins such as ribosomes in a total cell lysate and (c) removing interfering compounds
(4) Chromatography, free flow electrophoresis and/or affinity purification
(5) Commercially available kits such as PlusOne 2-DE clean up kit (Amersham Biosciences, UK) which can be bought to remove substance that may interfere with the IEF such as salts, nucleic acids lipids or polysaccharides (Shaw and Riederer, 2003)

This subsequently enhances resolution and a higher number of spots can therefore be separated The technique also increases the success rate of protein identification thereby decreasing the ambiguity of the protein mixtures Subcellular fractionation requires large quantities of biopsy material which can therefore only be applicable to some tumour groups (Alaiya, 2002b)

1 6 Limitations associated with 2-DE

While IPG strips revolutionised IEF, some limitations still remain All limitations are linked to the enormous chemical diversity of proteins and to their divergent expression in cells and tissues In order to achieve the goal of visualising a near-to-total proteome using 2-DE, it has become essential to improve existing techniques in each of the areas defined as causing limitations including resolution and protein binding capability, low abundance proteins, hydrophobic and membrane proteins, staining sensitivity, streaking, gel matching and automation

1 6 1 Resolution and protein loading capacity

Resolution (i e the distance between spots on a 2-DE gel) and protein loading capacity (i e the amount of protein per spot) can limit proteome analysis by 2-DE as it restricts detection to only a minute fraction of the proteins present This can be overcome by using 18 cm narrow-range IPG strips (1 pH unit) Moreover this can avoid the presence of multiple proteins per spot and/or cross contamination of spots These new strips have a higher protein loading capacity and higher resolving power compared to the medium- to wide-pH range IPG strips As the resolution increases, image analysis becomes easier and complex protein patterns can be compared in a more efficient and reproducible way (Langen and Roder, 2000)

1 6 2 Low abundance proteins

Low abundance proteins are rarely visualised on traditional 2-DE gels due to overwhelming quantities of abundant soluble proteins obscuring their detection or due to low solubility (Herbert *et al*, 2001) Although 2-DE is the highest resolution technique currently available for resolving protein mixtures, low abundance proteins can be problematic to detect in a whole cell lysate or in treated body fluids Currently, proteins present at a copy number of 1000-3000 per cell are visible with silver staining whereas only the significantly more abundant proteins can be seen with standard coomassie-type stains Complete recovery and enrichment of selective fractions permit global and targeted proteomics Low abundance proteins and biomarkers are often masked and therefore require unique tools to observe and compare genuinely representative data sets

1 6 3 Hydrophobic membrane proteins

The under-representation of membrane proteins on 2-DE gels is caused by their being poorly soluble in the aqueous media used in standard IEF (Santoni *et al*, 2000) There has been a gradual improvement in detecting highly hydrophobic membrane proteins using 2-DE Heat is applied to the protein sample along with SDS (an anionic detergent) in denaturing zone electrophoresis to disrupt noncovalent interactions However, an intrinsic surface charge on the protein is required when separating via pI Continued improvements are seen with novel reagents for solubilisation and separation of hydrophobic proteins including chaotropes, surfactants and reducing agents (Molloy, 2000)

1.6 4 Streaking

Streaks are a major problem for both beginners and experts alike They are also the most time-consuming trouble-shooting problem There are a variety of reasons for this problem and the following are some of the causes and remedies

1.6.4 1 Protein solubility

Protein solubility is a major bottleneck in proteomics It leads to streaky 2-DE gel patterns and/or protein smears To ensure optimum results, special attention must be

paid to the following cell lysis conditions, inactivation of proteases, choice and concentration of detergents, chaotropes and reducing agents New approaches have considerably improved the solubilisation, but much progress remains to be made Such improvement will also allow for higher protein loading onto narrow gradients, which should, in turn, allow the visualization of the less abundant proteins of the proteome and further increase the scope of proteomics

1.6.4.2 Horizontal and vertical streaks

Another problem in proteomics is that of horizontal streaking, which can be localised to different areas of the gel They can be caused by protein overloading, protein interactions with contaminants (DNA, RNA, lipids etc) and poor solubility near the pI Streaking localised to the basic region is caused by over focussing or depletion of DTT during IEF However, increasing the concentration of DTT used causes distorted patterns To diminish these streaks IPG strips in the range of 6-12 should be used instead of 6-10 (Gorg *et al* , 2000) In contrast, vertical streaks are caused by salt fronts, protein aggregates and/or insufficient focussing in the first dimension (Gorg *et al* , 2000) However, dialysis of the sample can eliminate salt fronts (Rabilloud, 1996) Slow sample entry can also avoid salt fronts and use of iodoacetamide avoids the problems associated with DTT migration

1 6 4.3 Detergent/chaotrope smear

The traditional detergents such as TritonX-100 and NP-40 cause background smears when silver stain is used CHAPS eliminates this problem (Gorg *et al* , 2000)

1.6 5 Automation and high-throughput analysis

Despite improvements in the field of proteomics such as the ability to run 10 or even 20 second dimension SDS gels in parallel, 2-DE is a time consuming, labour intensive, poorly reproducible and poorly automated technology Recent improvements include, the production of ready-made gels (IPG DryStrips and Excel Gel SDS, GE Healthcare) on stable plastic supports, the introduction of IPGphor, the automation of silver staining devices and the development of fluorescent labelling which is less labour intensive Currently, IPGphor, in conjunction with the ready-made IPG strips, has enabled sample in-gel rehydration IEF which can be performed unattended overnight This is an important step in the automation of the 2-DE process

Whilst automating the transfer from the first to the second dimension gels in itself would be convenient, in reality it is not the running of the 2-DE gels but their subsequent analysis that is the bottleneck in most proteomic projects. Automation of many of the individual steps in the process could increase throughput. For example, matching 2-DE gels, picking the polypeptide spots, digestion and processing for mass spectrometry (MS) and database searches could all be automated using robotic and software technology currently available or being developed (Lopez, 1999).

1.7 Fluorescence 2D difference gel electrophoresis

Traditional 2-DE is a well-established high-resolution technique for the simultaneous separation and display up to thousands of proteins. However it is both time-consuming and labour intensive as many gels must be run, analysed and compared in order to generate statistically significant differences between two or more proteomes. Moreover, reproducibility between gels (technical variations in sample preparation and gel running conditions) hinders efficient matching. This matching is critical to establish proteins with altered expression levels (Tannu and Hemby, 2006).

Two dimensional difference gel electrophoresis (2D-DIGE) introduced by Unlu *et al.* (1997), has made it possible to detect and quantify differences between experimental pairs of samples resolved on one gel system. The technique involves prelabelling the protein samples with different spectrally-resolvable fluorescent dyes so they can be mixed together, co-separated and visualised on a single 2-DE gel. Such dye triplets include the three mass- and charge-matched N-hydroxyl succinimidyl ester derivatives of the fluorescent cyanine dyes (Cy2, Cy3 and Cy5 - GE Healthcare) which are covalently bound or the three stains LUCY-506, LUCY-565 and LUCY-569 from Sigma which possess distinct excitation and emission spectra. The Cy dyes are used to differentially label the lysine residues of the protein samples.

During labelling, the dyes undergo a nucleophilic substitution reaction with the ε-amino group of lysine residues on protein resulting in the formation of an amide bond. The dye: protein ratio is optimised so that only 5% of the protein sample is labelled (where the protein is abundant). This method ensures that only proteins with a single dye molecule are visualised and those containing multiple dye molecules are minimised. Where the protein concentration is low, saturation labelling can be used. The result of this labelling system is co-migration of proteins originating from separate samples. For example, healthy and tumour cells can be labelled with different fluorochromes,

combined and run on the same gel. The advantage of this method over conventional 2-DE is that the samples are exposed to the same chemical environments and electrophoretic conditions. Gel-to-gel variation is reduced as co-migration is guaranteed for identical proteins from separate samples. The result is higher throughput of experiment and data analysis (Tonge *et al.*, 2001). The remaining Cy2 is used as an internal control for a number of gels, to allow more accurate statistical analysis of protein expression differences across many gels can be made (Gharbi *et al.*, 2002).

Gharbi *et al.* (2002) evaluated the 2D-DIGE technique using a model breast cancer cell system. They investigated an ErbB-2-mediated transformation in a cell line system, which comprised an immortalised luminal epithelial cell line and a derivative that stably overexpressed ErbB-2 at a similar level to that seen in breast carcinomas. They determined that 2D-DIGE is a sensitive and reproducible technique for differential expression analysis when compared with data from subsequent matrix assisted laser desorption ionisation mass spectrometry-compatible silver staining. Results revealed that Cy dye labelling is in fact more sensitive than silver staining (less than one nanogram of protein could be detected versus five nanograms with silver staining). It was also discovered that the fluorescent protein stain (SyproRuby) is much more sensitive than silver staining and produces more uniform staining from gel-to-gel. Staining with SyproRuby (or SyproOrange or SyproRed) involves a noncovalent reaction whereby the fluorescent compounds bind to the SDS surrounding the proteins. The staining shows little to no protein variability and is usually completed after 2-3 hours (although staining overnight produces better results) with little or no destaining required.

Gharbi *et al.* (2002) were able to detect 35 distinct protein spots, which showed consistent differences in expression levels between the two cell lines. The spots were present in all gel images and were detectable by SyproRuby. The numerous proteins detected by 2D-DIGE are now implicated in ErbB-2-mediated transformation and may represent future targets for breast cancer therapies.

In summary, this proteomic approach is sensitive, MS compatible, reproducible and can be used for the rapid identification of differences in the protein content of two separate cell lysate samples. It provides the basis for detecting proteins associated with a diseased state via their altered levels of expression when compared to a control. The ability to detect low levels of protein is important for proteomics research and 2D-DIGE technology supports this by detecting proteins, which are less abundant. This technique

can detect changes in protein abundance as low as 10% with a 95% confidence ($p<0.05$) for proteins

1.8 Fluorescent staining versus silver staining

Silver staining or fluorescent compounds can detect, with high sensitivity, proteins separated by 2-DE An advantage of both is that they are compatible with MS (used for subsequent protein analysis) Silver staining methods are ideal for (i) the detection of trace components within a protein sample and (ii) the analysis of protein samples that are present in only limited amounts The detection limit is as low as 0 1 ng protein per spot However, despite the many advantages, silver staimng has several limitations such as (i) the poor reproducibility of several stains, (ii) limited dynamic range, (iii) the fact that some specific spots stain poorly, negatively or not at all and (iv) the labour intensive nature of the staining process (Gorg *et al* , 2000)

In contrast, fluorescent staining is more reproducible, easier to perform and can be more sensitive than silver staining which is routinely used to study differential expression This approach is expected to be more amenable to automation However, this technique also has limitations i e (i) photography or electronic image acquisition is required to document results and (ii) there are still only a limited number of fluorescent cyanin dyes available including (Cy3, Cy5, and Cy2), the post-electrophoretic fluorescent dyes, ruthenium and SyproRuby The latter is more sensitive than both SyproRed and SyproOrange (Gorg *et al* , 2000)

1 9 Evolution of mass spectrometry

As proteomics research evolves, so too does the technology used in this field In the last decade, explosive progress m the areas of protein science, bioinformatics and in cell and molecular biology has resulted in an increased demand for the development of instrument technology Mass spectrometry permits the identification of proteins to be automatically carried out at high speeds and with high sensitivity Currently it is not possible to use nucleotide sequence data to gain insights into how different basic biological processes (such as cell differentiation, receptor activation, signal transduction and malignant transformation) work in biological systems Consequently, studies of protein expression, interaction, post-translational modifications and the resulting repercussions in living organisms have to be made at the protein level (Ekstrom *et al* , 2000) Since gel electrophoresis is the most common method for separation of proteins

it has became desirable to combine gel electrophoresis with a sensitive detection method (Neubauer and Mann, 1999)

For protein identification, the traditional, slow system of Edman sequencing has mostly given way to mass spectrometry MS now drives the progress of proteomics and has become a powerful, rapid and sensitive tool for the analysis of proteins Proteomics is now utterly dependent on new generations of mass spectrometers produced by companies such as Finnigan, Micromass and others

Traditional protein techniques rely on digestion of gel-separated proteins into peptides by a sequence specific protease such as trypsin Peptides are analysed and not the proteins because gel-separated proteins are difficult to elute and analyse via MS In contrast, peptides are easily eluted and even small sets of peptides are sufficient to identify a particular protein, a procedure referred to as peptide mass fingerprinting (PMF) Mass spectrometric study of gel-separated proteins is leading to a renaissance in biochemical approaches to protein function Mass spectrometers have also been connected to liquid chromatography systems to identify proteins and study proteomics Protein characterisation will continue to improve in throughput, sensitivity and completeness with continual developments in MS and 2-DE technology

1 9 1 Mass spectrometers

A mass spectrometer measures the mass-to-charge ratio of ions This is achieved by ionizing the sample and separating ions of differing masses and recording their relative time of flight by measuring intensities of ion flux A typical mass spectrometer comprises three parts an ion source, a mass analyzer, and a detector system (Figure 1 12)

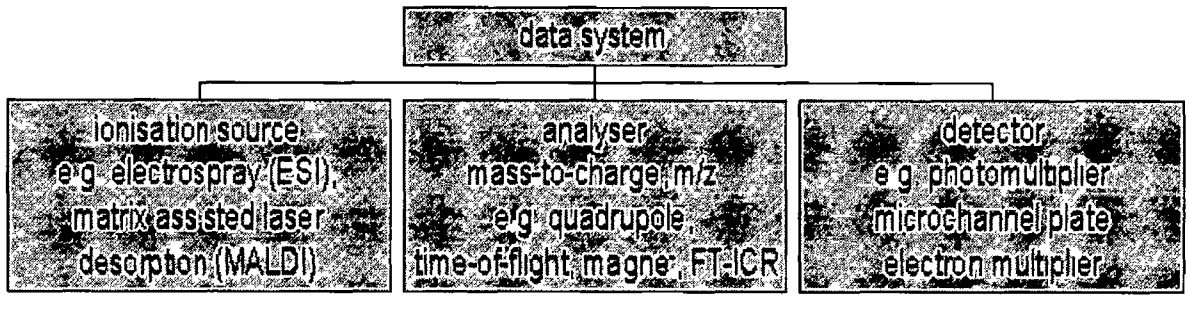

Figure 1 12 Schematic of a mass spectrometer

The first step is an ionisation source such as matrix-assisted laser desorption ionisation (MALDI) or electrospray ionisation (ESI) In MALDI, peptides are embedded in a matrix and excited by a laser to allow them to fly In ESI, charged droplets enter a gas phase and are ionised The flexibility to combine ionisation sources with mass analysers has brought forward numerous types of MS instruments with varying mass accuracy, sensitivity and most importantly, applications The sample is introduced into the ionisation source then ionised, as ions are easier to manipulate than neutral molecules The ions are then extracted into the analyser region of the mass spectrometer where they are separated according to their mass (m)-to-charge-(z) ratios (*m/z*) (Wasinger and Corthals, 2002) Examples of mass analysers include quadrupole, ion trap or time-of-flight (TOF) tubes A quadrupole consists of four parallel metal rods that have fixed DC and alternating RF potentials applied to them Generated ions pass along the middle of the quadrupole Their motion depends on the electric fields so only ions of a ceretain *m/z* will be in resonance and pass through to the detector The RF is altered to bring ions of differing m/z into focus on the detector and generate a mass spectrum

The separated ions are detected (examples include an electron multiplier, photomultiplier or conversion dynode) and this signal is sent to a data system where the *m/z* ratios are stored together with their relative abundance for presentation in the format of a *m/z* spectrum (Yates, 2000) The analyser, detector and often the ionisation source, are maintained under high vacuum to give the ions a reasonable chance of travelling from one end of the instrument to the other without any hindrance from air molecules

For proteomics, gel spots on a 2D gel are usually attributable to one protein To identify the protein, the gel spot is excised and digested proteolytically The peptide masses resulting from the digestion can be determined by mass spectrometry using peptide mass fingerprinting (PMF) This uses the masses of the proteolytic peptides as input to a search of a database of predicted masses that would arise from digestion of a list of known proteins If a protein sequence in the reference list gives rise to a significant number of predicted masses that match the experimental values, the protein is identified as present in the original sample PMF servers on the internet include, Mascot, Aldente (Phenyx), MassSearch, Mowse, MS-Fit (Protein Prospector), PepMAPPER, PeptideSearch, Profound (Prowl) and XProteo

The performance of existing mass spectrometers for proteomics research has gradually improved with technology developments The instruments can be grouped into two

categories single stage mass spectrometers for peptide analysis (for example MALDI and MALDI-TOF) and tandem MS-based systems for sequencing (for example triple quadropole ion-trap and hybrid quadropole-TOF) (Gygi and Aebersold, 2000)

1.9 2 MALDI mass spectrometry

To identify a protein/peptides by mass spectrometry, the sample must first be ionised MALDI involves the bombardment of sample molecules with a laser light to bring about sample ionisation Typical MALDI mass spectrometers have a pulsed nitrogen laser of wavelength 337 nm or an Er-YAG laser operating in the infrared wavelength range of 2 94 μm The sample is dissolved in a volatile solvent, usually with traces of trifluoroacetic acid An aliquot of this removed and mixed with an equal volume of a solution containing a vast excess of the matrix The matrix is a highly absorbing compound, examples of which include sinapinic acid, which is typically used for protein analysis and alpha-cyano-4-hydroxycinnamic acid (CHCA), often used for peptide analysis The choice of matrix is important for the control of fragmentation The final solution is applied to the sample target, dried and inserted into the high vacuum of the mass spectrometer The laser is fired, the energy arriving at the sample/matrix surface is optimised and data accumulated until a *m/z* spectrum of reasonable intensity has been amassed The time-of-flight analyser separates ions according to their *m/z* ratios by measuring the time it takes for ions to travel through a field free region known as the flight or drift tube (Figure 1 13) The heavier ions are slower than the lighter ones The *m/z* scale is calibrated with known samples that can either be analysed independently (external calibration) and/or pre-mixed with the sample and matrix (internal calibration)

MALDI MS has numerous advantages over other ionisation methods for peptide mapping Sample preparation is simple and when combined with a TOF analyser, it is a sensitive and fast method for peptide mass mapping (Jensen *et al* , 1997) However, the main drawback of MALDI is that it is difficult to analyse low molecular weight compounds (<1,000 m/z) because the matrix that allows MALDI to work interferes in this mass range (Peterson, 2006) Moreover, a visible coomassie stained spot (100 femtomoles) of material is required for peptide fingerprinting analysis

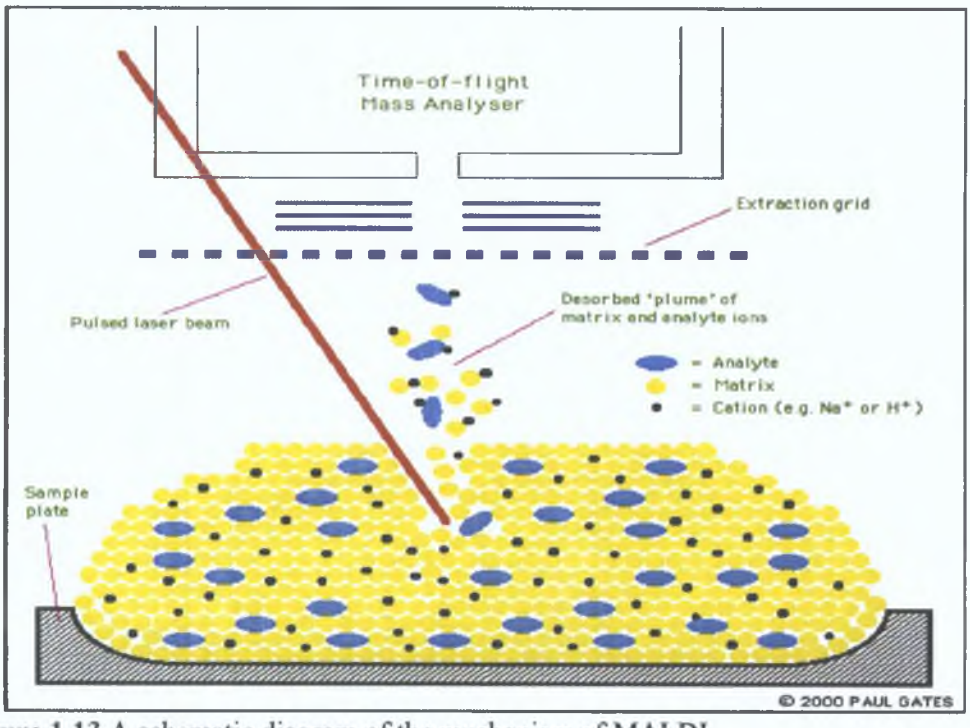

Figure 1.13 A schematic diagram of the mechanism of MALDI

An initial problem with this technology occurred when the energy spread among the ions and led to broad peaks. This was therefore limiting in both resolution and mass assignment accuracy. In order to counteract this, TOF instruments now use delayed extraction i.e. they allow equilibration of the energy distribution until it reaches a narrow range before ion acceleration. These TOF analysers have the advantage of being relatively inexpensive and simple to operate (Costello, 1999).

1.9.3 Electrospray ionisation

ESI utilises the potential difference between a capillary and the inlet of the mass spectrometers to cause charged droplets to be released from the tip of a capillary. As the droplets evaporate, gas phase charged ionisation is desorbed from the droplets. ESI permits a constant ionisation and monitoring. However, it is more sensitive to contaminating buffers and detergents than MALDI (McDonald and Yates, 2000).

The technique involves generating a very fine liquid aerosol through electrostatic charging, rather than the more familiar gas (pneumatic) methods. Electrospray uses electricity instead of gas to form the droplets. In electrospray, a liquid is passed through a nozzle. A plume of droplets is generated by electrically charging the liquid to a very high voltage. The charged liquid in the nozzle becomes unstable as it is forced to hold more and more charge. Soon the liquid reaches a critical point, at which it can hold no more electrical charge and at the tip of the nozzle it blows apart into a cloud of tiny,

highly charged droplets. These droplets are repelled from the needle towards the source-sampling cone on the counter electrode (shown in blue in Figure 1.14).

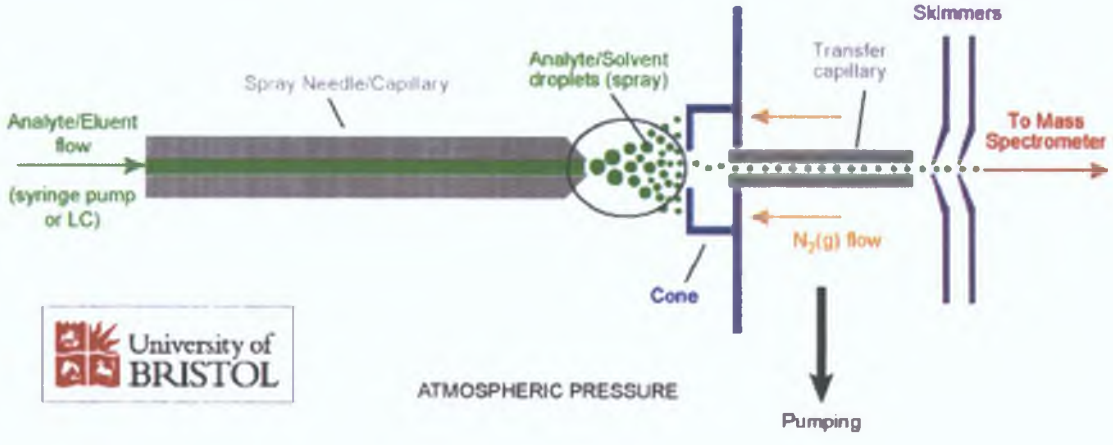

Figure 1.14 A diagram of an ESI source (http://www.chm.bris.ac.uk/ms/theory/esi-ionisation.html)

The solvent evaporates as the droplets travel the distance between the needle tip and the cone (circled in black Figure 1.14). This evaporation causes the droplet to shrink until it reaches the point where the surface tension cannot sustain the charge any longer (the Rayleigh limit, Figure 1.15). At this point a "Coulombic explosion" occurs and the droplet is ripped apart. Smaller droplets are formed, which can repeat the process as well as naked charged analyte molecules, which can be single or multiple charged. This method of ionisation is very soft i.e. little residual energy is retained by the analyte upon ionisation. ESI-MS is therefore an important technique in biological studies where the analyst often requires that non-covalent molecule-protein or protein-protein interactions are representatively transferred into the gas-phase. The major disadvantage is that very little (typically zero) fragmentation is produced. For structural elucidation studies, this leads to the requirement for tandem mass spectrometry where the analyte molecules can be fragmented.

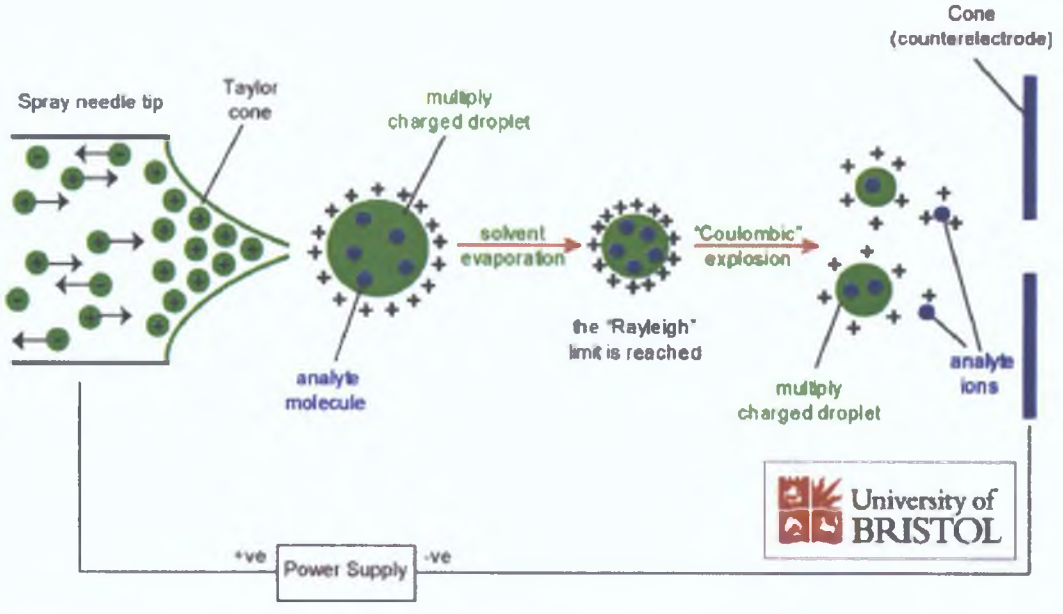

Figure 1.15 A schematic of the mechanism of ion formation in ESI.

1.9.4 Other mass spectrometers

Tandem mass spectrometers are built out of two mass spectrometers. The first one selects the peptides by mass one by one and the second mass spectrometer reads out the intensities of the fragment ions of each peptide. Many different combinations of mass spectrometers have been tried. A popular configuration today is a quadrupole linked to a time-of-flight (called a Q-TOF) or one time-of-flight linked to another time-of-flight (called a TOF-TOF).

Liquid chromatography/MS is a hyphenated technique, which combines the separation power of high performance liquid chromatography (HPLC) with the detection power of mass spectrometry. Even with a very sophisticated MS instrument, HPLC is still useful to remove the interferences from the sample that would impact the ionisation. An interface eliminates the solvent and generates gas phase ions, which are then transferred to the optics of the mass spectrometer. Most instruments use an atmospheric pressure ionisation technique, which combine the solvent elimination and ionisation steps. This is achieved through a particle beam, which separates the sample from the solvent allowing the introduction of the sample in the form of dry particles into the high vacuum region.

1 10 Surface enhanced laser desorption/ionisation (SELDI)

Recent advances in proteomics, especially technologies that allow rapid "fingerprint" profiling of multiple biomarkers (e g SELDI technology) have improved the discovery, identification and characterisation of potential cancer-associated biomarkers The proteomic approach is likely to discover many biomarkers and it is predicted that in future, high-throughput proteomics will be integrated into a clinical setting to identify those patients who are at risk (Negm *et al* , 2002)

Any experiment that involves a limited number of proteins, for example, those used in a purified protein complex are not amenable to 2D-gel separation, which is tedious and difficult Methods such as high performance liquid chromatography, gel filtration or one-dimensional chromatography are alternatives These techniques separate and concentrate proteins sufficiently well to be identified by MS However, they do not allow quantification Various strategies have been developed to overcome problems of limited sample volume

The advent of MS-based protein biochip technology enabled complex biological systems to be routinely analysed under non-denaturing conditions and their protein contents purified The technology also enabled studies for the purpose of biomarker discovery, toxicological investigation and also basic research to be performed (Merchant and Weinberger, 2000, Weinberger *et al* , 2000) MS-protein biochip technology was based upon the principles of surface enhanced laser desorption/ionisation This is commercially embodied in the ProteinChip systems offered by Ciphergen Biosystems (Fremont, CA, USA) In 1993, Hutchens and Yip introduced the idea of SELDI This novel strategy for MS analysis of macromolecules simplified sample extraction and facilitated on-probe investigation of biopolymers when compared to conventional approaches like MALDI

SELDI is an affinity-based mass spectrometric method in which proteins of interest are selectively adsorbed onto a chemically modified surface on the biochip Impurities are then removed by washing with a suitable buffer The technology allows sensitive and high throughput profiling of complex biological specimens

Crude biological samples, for example serum or cell lysates, can be applied directly to the ProteinChip Arrays. After a short incubation period, the unbound proteins are washed off the surface retaining only proteins interacting with the chemistry of the array surface. After washing, energy-absorbing molecules are applied to the array as a final step. They are then analyzed in the ProteinChip Reader, a TOF mass spectrometer. The mass values and signal intensities for the detected proteins and peptides are viewed and then transferred to software in-depth analysis (Figure 1.16).

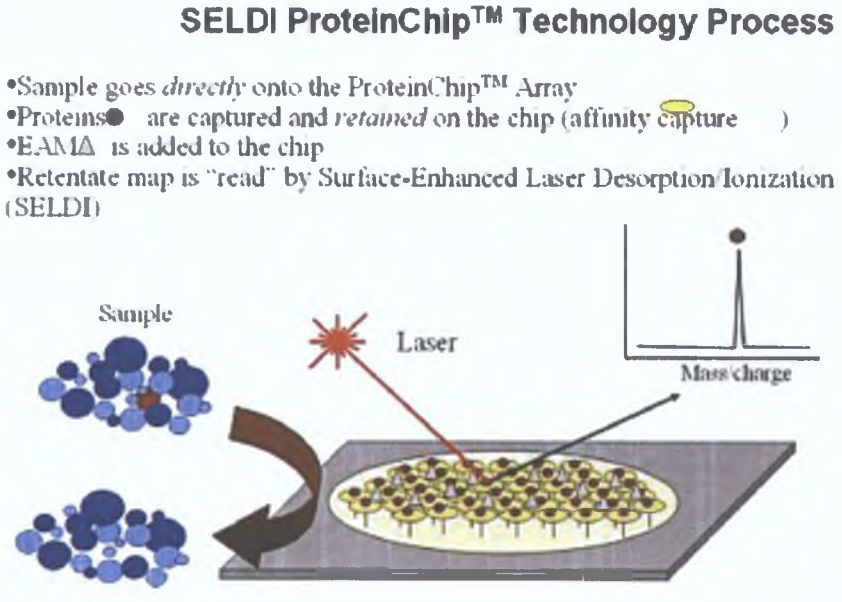

Figure 1.16 A schematic of the mechanism of SELDI.

1.10.1 Advantages of SELDI technology

ProteinChip technology has several advantages over the conventional proteomic technologies (2-DE and MS). These advantages include speed of detection (hours versus days), coverage of a broader region of the proteome, small sample requirement and combination of discovery of biomarkers and diagnostic assays in one system compared to MS, which is limited to the discovery of biomarkers only. Another advantage of the system is that it is automated for high throughput compatibility (Zhang *et al.*, 2004). The development of SELDI and subsequent ProteinChip technology enabled the exploitation of protein separation and detection strategies that were not previously possible with existing techniques.

The potential of biomarker discovery in proteomics research is enormous It is therefore becoming increasingly important that high throughput automated systems are developed Ciphergen's novel technology satisfies this growing need for powerful, mechanised bench-top systems for clinical proteomic applications Recent developments have boosted system throughput by automated sample preparation and loading This eliminates the need for tedious sample preparation allows for greater precision and most importantly speeds up the entire process

Reproducibility is a major problem of the SELDI/MS method especially if the identities of the peaks are unknown Irreproducibility between laboratories is exemplified in ovarian cancer studies, one of which was published by Petricom's group All three papers report different key discriminatory peaks, which still have not been identified Moreover, re-analysis of the raw data identified bioinformatic artifacts, which could invalidate the original conclusions More recently, careful evaluation of methods of sample collection and processing for proteomic analysis by SELDI-TOF revealed that preanalytic variables such as sample handling could markedly influence results The original data published by Petricoin *et al* (2002) have never been reproduced A recent study further attempted to validate three previously identified breast cancer biomarkers by SELDI-TOF using patients from another institution (Li *et al*, 2005) Among the three previously identified candidate biomarkers, one was not reproduced

1 11 The application of proteomics to cancer research

As cancer is a multifaceted disease with alterations in protein expression across a diverse range of cellular pathways, proteomics offers an unrivalled opportunity to investigate and view the global changes that mark cancer In view of the current state of the technology in genetic cancer research, clinicians are still faced with difficulty in the early detection and diagnosis of pre-clinical lesions In addition, it is difficult to predict disease-specific biological behaviour, i e whether or not a tumour will metastasise or resist cytostatic or radiation therapies The ultimate goals of cancer proteomics are to enhance and improve molecular classification of tumours and to develop more sensitive biomarkers for disease prognosis and treatment sensitivity There is an increasing interest in both academia and the biopharmaceutical industry in the proteomic approach to the discovery of drug development (Alaiya *et al*, 2002)

The following sections with tables 1 1 and 1 2 are overviews of the potential approaches of proteomics to study different human cancers

1.11 1 Molecular markers

Markers constitute major targets for the early detection of cancer and identification of cancer risk (Negm *et al*, 2002) Important properties of a marker are sensitivity, selectivity and specificity irrespective of the source of measurement (e g tissue or body fluids) The specificity of many currently used markers is questionable and only detecting late stage malignancies Traditionally, prostatic carcinoma is diagnosed *via* biopsy after discovery of elevated blood levels of prostatic specific antigen (PSA) In normal males, PSA is present at 1 ng/ml However, for both prostatic carcinoma and benign prostatic hyperplasia PSA levels can be elevated to 4-10 ng/ml (Merchant and Weinberger, 2000) Moreover, PSA shows wide variations in both specificity and sensitivity when used to analyse prostate cancer The serum marker α-fetoprotein is used to diagnose hepatocellular carcinoma However, high levels of this marker are also detected in patients suffering from ovarian or testicular cancers and also in patients with liver cirrhosis Cancer antigen 125 (CA125) is used in screening ovarian cancer While increased levels of CA125 are detected in 50% of patients with stage I and in >90% of women with more advanced stages the marker is also elevated in benign cases (e g uterine fibroids, endometriosis, tubo-ovarian abscess etc) and ectopic pregnancy (Ahmed *et al*, 2005) resulting in predictive value of less than 10% as a single marker (Cohen *et al*, 2001) When combined with transvaginal ultrasound, sensitivity and specificity are increased

Diagnostic markers are used to aid histopathological classification of tumours Lung cancer for example, can be classified into squamous, small and large cell carcinomas as well as adenocarcinomas In addition, lung malignancies are divided into primary carcinomas and metastases originating from extrapulmonary malignancies Markers must be developed to classify all these tumours Recently TA02 was discovered to be expressed in primary lung adenocarcinomas but not in metastases from colo-rectal malignancies allowing for diagnosis and treatment (Alaiya *et al*, 2002) In general, where a fairly large number of markers have been described, there are only a few which can predict the treatment outcome in each individual patient The general consensus is that a panel of markers should be used, thereby identifying targets with greater sensitivity, specificity and selectivity Cancer proteomics can be used to enhance and

improve molecular classification of tumours and develop more sensitive biomarkers for disease prognosis and treatment sensitivity.

1.11.2 Lung cancer

The lung is a very common site for metastasis from tumours growing at other sites in the body. Lung cancer has a propensity for early spread and usually presents at a very late stage (Danesi *et al.*, 2003). Phenotypic and genotypic heterogeneity of lung cancer likely precludes the identification of a single predictive marker and suggests the importance of identifying and measuring multiple markers. To date no satisfactory biomarkers are available to screen for lung cancer. Numerous proteomic analyses of lung cancer tissues have been carried out and results are summarized in Table 1.1. Analysing these reports together, we can assume that the common identified proteins such as α-enolase and triosephosphate isomerase appear to be increased in lung cancer tissues.

Seike *et al.* (2005) performed proteomic analysis on 30 lung cancer cells lines with three different histological backgrounds (squamous cell carcinoma, small cell lung carcinoma and adenocarcinoma) to elucidate the mechanisms that determine histological phenotypes. Hierarchical clustering and principal component analysis divided the cell lines according to their histology. Spot ranking analysis identified 32 protein spots essential for the classification. Following this, lung cancer cells, isolated from tumour specimens by laser capture microdissection were successfully classified on the basis of the expression pattern of the protein spots

Liu *et al.* (2004) reported that the expressions of TEF1d, vimentin, cytokeratin 8, YB-1, PCNA, Nm23, hnRNP A2/B1, pyruvate kinase M2 and HSP90b increased, while those of 14-3-3d and pyruvate kinase M1 decreased in four NSCLC cell lines (H1299, H23, H226, SW-1573) compared with those in normal human bronchial epithelial cells (HBE4-E6/E7 and NHBE-8917).

Tyan *et al.* (2005) analyzed pleural effusion from lung adenocarcinoma patients for early detection of lung adenocarcinoma. They identified 44 of 472 proteins which included, retinoblastoma binding protein 7, synaptic vesicle membrane protein, corticosteroid binding globulin precursor, PR-domain containing protein 11, envelope

glycoprotein, MSIP043 protein and titin Many of these have not been previously reported in plasma and may represent proteins specifically present in pleural effusion Retinoblastoma binding protein 7 is of interest as it may play a role in the regulation of cell proliferation and differentiation

At present, α-enolase and triosephosphate isomerase have been identified as the two proteins that commonly increase in lung cancer tissues and are expected to be used as biomarkers However, further proteomic studies using sputum and pleural effusion from lung cancer patients are necessary

There is a need therefore for markers, which can distinguish primary lung adenocarcinomas from distant metastases (Alaiya *et al*, 2000a) such as surfactant proteins Surfactants TAO1 and TAO2 (35 kDa markers) were found by 2-DE to be significantly overexpressed m approximately 90% of all primary lung adenocarcinomas but were absent in secondary adenocarcinomas metastasised from colo-rectum and mammary glands (Hirano *et al*, 1997) Chuman *et al* (1999) determined that TAO2 was identical to Napsin A, a member of the aspartic protease family It is thought to be involved in the cleavage of pro-surfactant proteins that are produced by the type II pneumocystis

The SELDI-TOF-MS ProteinChip system is currently used try to identify biomarkers for cancers Yang *et al* (2005) used SELDI profiling to distinguish between NSCLC and normal subjects with relatively high sensitivity and specificity Both NSCLC and SCLC patients were chosen for the study to develop a broad biomarker panel for screening a diverse, high-risk population

A total of 208 serum samples, including 158 lung cancer patients and 50 healthy individuals, were randomly divided into a training set and a blinded test set Five protein peaks at 11493, 6429, 8245, 5335 and 2538 Da were automatically chosen as a biomarker pattern in the training set This SELDI pattern yielded a sensitivity of 86 9%, a specificity of 80 0% and a positive predictive value of 92 4% They identified Cyfra21-1 and NSE in the 208 serum samples Based on the results of the test set, they found that the SELDI marker pattern showed a sensitivity of 91 4% in the detection of NSCLC The pattern also had a sensitivity of 79 1% in the detection of lung cancers in stages I/II NSCLC

Zhukov *et al* (2003) identified specific protein peak patterns in malignant lung tumours and pre-malignant airway epithelium showing neoplastic transformation using lung tumour specimens The study could detect "malignant" protein signatures, which could lend themselves to identification of populations at high-risk of lung cancer and for monitoring response to lung cancer chemo-preventative agents The samples were laser capture microdissected to obtain pure cell populations from frozen sections of normal lung, atypical adenomatous hyperplasia and malignant tumours SELDI mass spectrometry generated protein profiles in each epithelial cell type Three peaks at 17-23 kDa mass range from tumour cells were markedly increased compared with normal cells The peak at 17250 Da was not detected in any of the normal cells This peak appeared to be present at low levels in the atypical cell samples

Brichory *et al* (2001) identified circulating tumour antigens or their related autoantibodies Their study provides a means for early cancer diagnosis as well as leads for therapy The aim of the study was to identify proteins that commonly induce a humoral response in lung cancer using a proteomic approach and to investigate biological processes associated with the development of autoantibodies Solubilized proteins from the lung adenocarcinoma cell line, A549 and from lung tumours were subjected to two-dimensional PAGE Western blot analyses of 54 sera from newly diagnosed patients with lung cancer, 60 patients with other cancers and from 61 non-cancer controls were tested for primary antibodies Sera from 60% of patients with lung adenocarcinoma and 33% of patients with squamous cell lung carcinoma but none of the controls exhibited IgG-based reactivity against proteins identified as glycosylated annexins I and/or II Immunohistochemistry revealed that annexin I was expressed diffusely in neoplastic cells in lung tumour tissues, whereas annexin II was predominant at the cell surface IL-6 levels were significantly higher in the sera of antibody-positive patients compared to antibody-negative patients and controls An immune response due to annexin I and II autoantibodies is commonly found in lung cancer It is associated with high circulating levels of an inflammatory cytokine

Brichory *et al* (2001b) using 2-DE identified proteins that commonly induce an antibody response in lung cancer Sera from 64 newly diagnosed patients with lung cancer, 99 patients with other types of cancer, and 71 non-cancer controls were analysed for antibody-based reactivity against lung adenocarcinoma proteins Autoantibodies

against a protein identified by MS as protein gene product 9 5 (PGP 9 5) were detected in sera from 9 of 64 patients with lung cancer and not in the controls Circulating PGP 9 5 antigen was found in sera from two additional patients with lung cancer, without detectable PGP 9 5 autoantibodies It is a neurospecific polypeptide previously proposed as a marker for non-small cell lung cancer, based on its expression in tumour tissue The PGP 9 5 was present at the cell surface and secreted by of the A549 cell line PGP 9 5 may therefore have utility in lung cancer screening and diagnosis

Zhong *et al* (2005) used a fluorescent protein microarray to identify and measure multiple non-small cell lung cancer-associated antibodies They show how simultaneous measurements can be combined into a single diagnostic assay T7 phage cDNA libraries of NSCLC were first biopanned with plasma samples from normal patients and patients with NSCLC to enrich the component of tumor-associated proteins They were then applied to microarray slides Two hundred and twelve immunogenic phage-expressed proteins were identified from roughly 4,000 clones, using high-throughput screening with patient plasmas and assayed with 40 cancer and 41 normal plasma samples Twenty patient and 21 normal plasma samples were randomly chosen and used for statistical determination of the predictive value of each putative marker Measurements of the 5 most predictive phage proteins were combined in a logistic regression model that achieved 90% sensitivity and 95% specificity in prediction of patient samples

1.11 3 Ovarian cancer

Ovarian cancer is an example of a disease with numerous diagnostic difficulties (Alaiya *et al*, 2000b) It is often very difficult to distinguish between benign, borderline and malignant ovarian cancer The application of new emerging genomic and proteomic technologies to the early detection of ovarian cancer provides a direct approach to understanding the role of proteins in the biology of the disease, monitoring its progression and also evaluating the therapeutic and side effects of drugs (Lafky and Maihle, 2002) However, analysis of a panel of markers is a possible approach to the diagnostic problems Alaiya *et al* (1999) showed (via 2-DE) that the expression of a number of proteins, namely the proliferating cell nuclear antigen, oncoprotein 18, phosphorylated heat shock protein 60 (pHSP 60), HSP 90 and elongation factor 2 were high in ovarian carcinomas In contrast, expression of tropomyosin 1 and 2 was

decreased in the same carcinomas compared to the benign tumours They were able to use a set of 9 proteins to discriminate between benign and malignant ovarian tumours

Petricoin *et al* (2002) combined SELDI-TOF mass spectrometry and bioinformatics to analyse proteomic sera patterns The result was a "fingerprint" that is capable of distinguishing the serum profiles of ovarian cancer patients from those of a control group Proteomic spectra were generated from serum samples (50 samples from a control group and 50 from patients with ovarian cancer) A "training set" of spectra, derived from the samples were subsequently analysed by an iterative searching algorithm This identified a proteomic pattern that distinguished cancer from non-cancer This fingerprint consisted of 5 distinguishing mass/charge spectra values The pattern was used to classify an independent set of 116 masked serum samples They were able to identify 50 out of 50 malignant ovarian cancer tumours, 18 of which had stage I ovarian cancer (100% sensitivity) and 63 out of 66 unaffected individuals (95% specificity) Generation of the mass spectra only required a small serum sample and the results were obtained in under 30 minutes Cost-effective and high-throughput screening is therefore possible It could be argued that complex serum patterns may neglect the underlying pathological state of an organ like the ovary The technology could also reveal new insights into the biology of the ovarian cancer

1 11 4 Breast cancer

Early attempts to resolve proteins from breast material by 2-DE were impeded due to the lack of reproducibility, low sensitivity and use of biopsy material which contained a mixed cell population However, several technological advances now enable systematic proteomic analysis of normal, luminal and myoepithelial breast cells (Page *et al* , 1999) Differential analysis identified 170 proteins that were elevated between two breast cell types Muscle-specific enzyme isoforms and contractile intermediate filaments including tropomyosin and smooth muscle α-protein were detected in the myoepithelial cells Furthermore, a large number of cytokeratin subclasses and isoforms characteristic of luminal cells were detected in this cell type (Page *et al* , 1999)

Molecular events leading to breast epithelial cell carcinogenesis involve modification in the structure and expression of both oncogenic (*ras*) and suppressive genes (*p53*) This leads to unbalanced growth characterised by high rates of proliferation and eventually

migration There is also a tendency to survive environmental stress better, which would under normal circumstances lead to apoptosis

Growth factors, such as the fibroblast growth factor (FGF), are involved in control of cell proliferation, differentiation and survival Adriaenssens *et al* (2002) used proteomic methods to study both rapid (occurring in the first minutes) changes in protein tyrosine phosphorlyation and the modifications in protein synthesis that are induced by FGF-2 They discovered several proteins as being the FGF receptor substrates, namely the oncogenic protein Src, the MAP kinases (p42/p44) and the FGF receptor substrate Further work enabled them to identify 14-3-3 and oncogenic mRNA *H19* gene, which regulates cancer cell growth via 2-DE

Li *et al* (2002) have utilised SELDI MS technology in conjunction with bioinformatics tools to facilitate the discovery of new and better tumour biomarkers to detect breast cancer They screened for potential biomarkers in 169 serum samples This included samples from 103 breast cancer patients at three different clinical stages of the disease The samples were diluted and applied to immobilised metal affinity capture Ciphergen ProteinChip Arrays which had previously been activated with Ni^{2+} The proteins that bound to the chelated metal were then analysed on a ProteinChip Reader Model PBS III and the complex protein profiles were compared and analysed Zhang and his colleagues selected three biomarkers based on their collective contribution to the optimal separation between stages 0-III breast cancer patients and controls There was a 93% sensitivity for all cancer patients and a specificity of 91% for all controls

1 11 5 Prostate cancer

Qu *et al* (2002) evaluated and developed a proteomic approach to enable the simultaneous detection and analysis of proteins for the differentiation of prostate cancer from non-cancer patients Serum samples from 197 prostate cancer patients, 92 samples from men with benign prostatic hyperplasia and 96 from healthy individuals (396 in total) were randomly divided into test (n=60) and training sets (n=326) They were then analysed by SELDI mass spectrometry Computer analysis detected 124 peaks in the training set The peaks were subsequently analysed by an algorithm in order to develop a profile for separating prostate cancer from non-cancer groups The classifier was challenged with the test set, following which two classifiers were developed The AdaBoost classifier, which achieved a 100% sensitivity and specificity, thus separated

the cancer from the non-cancer patients The second classifier, namely Boosted Decision Feature Selection Classifier, achieved a specificity of 97 9 and sensitivity of 98 5% for the test set

Levner (2005) reran the boosted feature extraction algorithm on the same prostate samples but used an updated cross-validation scheme on the same data set They compared their results to those of Qu *et al* (2002) Their algorithm attained 100% specificity and 96 25% sensitivity

Table 1 1 summarises a range of proteomically analysed reported proteins from human cancers

Cancer	Up-regulated	Down-regulated	Reference
Oral Tongue	Myosin heavy chain 1, Galectin 1, haemoglobin HSP 60 and 27, calgranulin B nuclear fragile X mental retardartion protein	myosin light chains tropomyosin ATP-synthase β chain crystalline αB	He *et al* (2004)
Neuroblastoma	peptidyl-propyl cis-trans isomerase A, nucleophosmin stathmin	Adrenodoxin, carbonic anhydrase III, aldose reductase related protein 1	Campostrini *et al* (2004)
Esophageal	PCNA, eIF-1A, RNA binding motif protein 8A, Keratin 1 Transmembrane protein 4 Ubiquitin C-terminal esterase Fascin, Thioredoxin peroxidase, AKR family 1, GST M2, gp96, Reticulocalbin, Proteasome subunit b type 4, Prosomal protein p30-33k	Galectin-7, Fatty acid-binding protein, S100 A9, TGase 3, Annexm I, Transgelin, Tropomyosin, SCCA1 Proteinase, inhibitor,Clade B, HSP27, Desmin, Proteasome subunit b type 9, Keratin 8 and 13	Zhou *et al* (2005)
Colorectal	Adenosyl homocysteinase, Leukocyte elastase inhibitor Macrophage capping protein Biliverdin reductase A, pridoxal kinase, Annexin 1 fragment, alpha tubulin, elongation factor 1-d, tropomyosin alpha & alpha chain, Actin fragment, annexin 3, 4, 5, microtuble-associated protein RP/EB, GST-P, cathepsin fragment, 14-3-3 proteins, proteasome subunit a type 6, Triosephosphate isomerase, P13693 translationally controlled tumor protein, nucleoside diphosphate kinase A, Calgranulin B,S100 A9	Puromycin-sensitive aminopeptidase NADH-ubiquinone oxidoreductase Succinate dehydrogenase subunit A Aldehyde dehydrogenase Myosin regulatory light chain 2 Selenium-binding protein Creatin kinase B chain Placental thrombin inhibitor Vimentin, Desmin Carbonic anhydrase I Tubulin b 5 chain	Friedman *et al* (2004)
HCC	PCNA, eIF-5a, E-FABP, Lactoylglutathione lyase APC-binding protein EB1	Galectin-1	Fujii *et al* (2005)

Table 1 1 Summary of proteomically analysed reported proteins (in a range) of human cancers

HCC - Hepatocellular carcinoma.

1.12 Proteomics and the study of chemoresistance

Resistance to chemotherapy is multifactorial and may be affected by the cell cycle stage and proliferation status, biochemical mechanisms such as detoxification, cellular drug transport or DNA replication and repair mechanisms

Chemotherapy of cancer can fail for a variety of reasons, as many factors can conspire to limit its effectiveness, including problems of delivery and penetration Some cancers, such as prostate tumours and melanomas are intrinsically resistant to most anti-tumour drugs (section 1 1) However, ovarian cancer or small cell lung cancer respond to chemotherapy and appear to disappear altogether, only to return later as drug resistant tumours It is thought that 30% of all cancer patients undergoing chemotherapy encounter acquired drug resistance (Kerbel, 1997)

Proteomic technology has been applied to the problem of chemoresistance to successfully determine alterations in protein expressions after exposure of the cells to a cytotoxic agent However the technology has been unable to accurately detect the classic proteins involved in multi-drug resistance, for example P-gp and MRP These proteins are extremely basic and hydrophobic and are therefore problematic to detect by traditional proteomic gel based methods

It appears that exposure of cells to chemotherapy drugs results in the activation of different mechanisms of resistance that a specific drug-resistant phenotype consists of several molecular mechanisms that are simultaneously active and that hypothesis that many metabolic pathways are affected during the resistance process Even though the differential expression levels of such proteins is not clear proof of their role in drug resistance *per se*, some are very likely to be involved in the resistance phenotype, and therefore may be potential targets for new drugs

1 12 1 Ovarian cancer

Cisplatin is the most common therapeutic agent used for chemotherapy in ovarian carcinoma Despite a good response to surgery and initial chemotherapy essentially based on cisplatin compounds, late tumour detection and frequent recurrences with chemoresistance acquisition are responsible for poor prognosis Several mechanisms have been implicated in cisplatin resistance but they are not sufficient to explain this resistance emergence Few mechanistic proteomic studies have been applied to describe chemoresistance emergence in ovarian cancers

Le Moguen *et al.* (2006) applied proteomics coupled with MS to identify proteins associated the development of chemoresistance using carboplatin sensitive and resistant ovarian cell lines IGROV1 and IGROV1-R10 respectively. Of the 40 identified proteins, cytokeratins 8 and 18 and aldehyde dehydrogenase 1 were overexpressed in IGROV1-R10, whereas annexin IV was down-regulated. Other differentially regulated proteins included: HSP 27, 60 and 70, actin, stathmin, GST, peroxiredoxin, aldolase, alpha enolase, GAPDH, Triosephosphate isomerase 1, inorganic pyrophosphatase, chloride intracellular channel I, hnRPC, Translation elongation factor 1, Proliferation-associated protein 2G4, 14-3-3 Sigma (stratifin), Nucleoside-diphosphate kinase 1 isoform b and ATPase synthase.

1.12.2 Breast cancer

The estrogen receptor has proven to be an extraordinarily successful target for breast cancer treatment and prevention. Tumours positive for the receptor are commonly treated with antagonists of estrogen, as their growth depends on the presence of this hormone. The non-steroidal drug tamoxifen is the first line treatment even though only 60% of the patients are estrogen-receptor positive and one-third of them initially fails to respond or develops resistance during treatment. Besada *et al.* (2006) established a pair of xenograft breast tumours, sensitive and resistant to tamoxifen, 3366 and 3366/TAM respectively. They compared the protein expression profiles using 2-DE. Twelve proteins were found up-regulated in the tamoxifen-resistant line, while nine were down-regulated. Biological functions of these proteins are related to cell–cell adhesion and interaction, signal transduction, DNA and protein synthesis machinery, mitochondrial respiratory chain, oxidative stress processes and apoptosis. Three of the identified proteins (ALG-2 interacting protein and two GDP-dissociation inhibitors) could be directly involved in the resistance phenomenon. The proteins identified were Endothelial actin-binding protein filamin A, vinculin, protein disulfide isomerase A3,actin, cytoplasmic 1, beta actin, 40S ribosomal protein SA (precursor), 34-kDa laminin receptor, VDAC protein 1, Peroxiredoxin 4, ubiquinol-cytochrome c reductase, lysophospholipase I, acyl-protein, thioesterase 1, peroxiredoxin 1 11 SPFH domain family member 40S ribosomal protein SA, 67-kDa laminin receptor GMP synthase, 60S acidic ribosomal protein, Heat-shock 27 kDa protein, DJ-1 protein Parkinson disease, cyclophilin A, peptidylproly, isomerase A, Inorganic pyrophosphatase, translationally-

controlled tumor Rho GDP dissociation inhibitor (GDI) alpha protein 1, glyoxalase I, lactoylglutathione lyase

Gregory *et al* (2004) used SELDI to study the proteomic changes in response to taxol, 5-FU, adriamycin and cyclophosphamide chemotherapy in the plasma of sixty-nine patients with stage I- III breast carcinoma They also profiled 15 healthy plasma samples and plasma from patients with cancer to identify breast carcinoma-associated protein markers Plasma was sampled on day 0 before chemotherapy and on day 3 post-treatment in the 69 patients or 3 days apart in the 15 healthy women Twenty-nine patients received preoperative and 40 received postoperative treatment

A single protein peak, induced by taxol (and to a lesser extent by FAC) was identified at 2790 m/z in 80% of patients treated preoperatively It was also detected with lesser intensity in approximately 40% of patients treated postoperatively However no direct correlation between the induction of m/z 2790 during a single dose of treatment and the final response of the tumour to preoperative treatment was found The group found five other peaks that distinguished between normal and breast cancer patients The peaks were also found in patients that had tumours removed surgically These peaks represent candidate markers of micrometastatic disease after surgery

1 12 3 Prostate cancer

Temporarily effective agents against prostate cancer include chemotherapy and androgen therapy Studies are ongoing to test agents that target proteins responsible for autocrine and paracrine stimulated growth However, there are limitations on current laboratory models to test the effect of these agents on cell growth and protein targets Dvorzhinskily *et al* (2004) developed a coculture model that can distinguish paracrine stimulated growth and effects on proteins

They observed that LNCaP prostate cancer cells and an immortalized rat prostate cell line transfected to overexpress the antiapoptotic resistance protein Bcl-2 were stimulated to grow via autocrine effects from extra cells in an upper chamber of their system Two-dimensional differential in gel electrophoresis found four proteins (Triosephosphate isomerase 1, Phosphoglycerate Kinase, enolase and aldolase), which increased after autocrine-induced growth stimulation

1 12.4 Cervical cancer

Lee *et al* (2005) exposed the HPV-16 positive CaSKi, HPV-18 positive HeLa and the HPV-negative C33A cervical carcinoma cell lines to taxol to determine the cytotoxic effects Two-dimensional electrophoresis and MALDI-ToF-MS identified several cellular proteins that are responsive to taxol treatment in HeLa cells Exposure to taxol elevated mainly apoptosis-related, immune response-related and cell cycle checkpoint proteins Growth factors, oncogene-related proteins and transcription regulated-related proteins were mainly down-regulated Taxol showed anti-profilerative activity via the membrane death receptor-mediated apoptotic pathway with the activation of caspase-8 in a TRAIL-dependant fashion as well as the mitochondrial apoptotic pathway with down-regulation of bcl-2 by cytosolic cytochrome c release Two-dimensional electrophoresis identified 47 proteins, which exhibited significant changes in taxol-treated cells compared to control cells with 24 of these proteins being down-regulated and 23 up-regulated

Castagna *et al* (2004) applied proteomics to study the effects of cisplatin on the cervix squamous cell carcinoma cell line A431 that was resistant to the drug (A431Pt) A four way comparison was applied as follows 1) A431 *versus* A431/Pt cells, 2) A431 *versus* A431 cisplatin exposed cells, 3) A431/Pt *versus* *A*431/Pt cisplatin exposed cells and 4) A431 cisplatin exposed cells *versus* A431/Pt cisplatin exposed cells Proteins found to be differentially regulated included the chaperones (heat-shock proteins HSP60, HSP90, HSC71, heat-shock cognate 71 kDa protein), the calcium-binding proteins (calmodulin, calumenin), proteins involved in drug detoxification (peroxiredoxins PRX 2 and PRX 6 and glutathione-*S* -transferase, GST), anti-apoptotic proteins (Bcl-3 and 14-3-3) and finally ion channels (such as VDAC-1, voltage-dependent anion-selective channel) switched on as a result of cisplatin exposure

For example, there was up-regulation of HSC71, HSP60, 14-3-3 and GST in A431/Pt cells compared to the parent The results are consistent with the expression of defence factors to protect the cells from drug-induced damage

Cancer (Drug)	Up-regulated	Down-regulated	Reference
Gastric (D)/(M)	Annexin I		Sinha *et al* (1998)
Gastric (M)	Thioredoxin		
Gastric (C)		Pyruvate Kinase M2	Yoo *et al* (2004)
Pancreatic (D)	Cofilin		Sinha *et al* (1999)
Pancreatic (M)	Cofihn Epidermal Fatty Acid bp Stratifin		
Fibrosarcoma (M)	Rho-GDP Dissociation inhibitor		Sinha *et al* (1999)
Colon (M)	Adenine Phosphoribosyl Transferase		Sinha *et al* (1999)
	Breast Cancer Specific Gene 1		
Colon (5-FU)	Metabotropic Glutamate Receptor 4		Yoo *et al* (2004)
Colon (5-FU)		F1 F0 -ATP Synthase	Shin *et al* (2005)
Melanoma (V)	Translationally Controlled Tumor Protein		Sinha *et al* (2000)
Melanoma (C)	Human Elongation Factor 1-δ		
Melanoma (F)	Tetratricopeptide Repeat Protein		
Melanoma (VP)	14-3-3-γ		
Neuroblastoma (VP)	Peroxiredoxin I β-Galactoside Soluble Lectin Binding Protein Vimentin Heat Shock Protein 27 HnRPK	dUTP Pyrophosphatase	Urbani *et al* (2005)
Breast (MEL)	Retinoic Acid Binding Protein II Macrophage Migration Inhibition Factor	Calreticulin Cyclophin A Heat Shock Protein 27	Hathout *et al* (2002)
Breast (A)	Annexin I Neuronal Ubiquitin Carboxyl Hydrolase Isoenzyme L1 Glutathione-S-Transferase pi Nicotinamide N-Methyltransferase Interleukin-18 Precursor	Catechol-O - Methyltransferase	Gehrmann *et al* (2004)

Table 1 2 Summary of studies using 2-DE and MS for analysis of chemotherapy resistance in cell lines Drugs D – daunorubicin, M – mitoxantrone, C – cisplatin, F – fotemustine, V – vindesine, VP – etoposide, MEL, melphalan and A – adriamycin

1 13 Conclusion

Proteomic technologies including high resolution 2-DE, protein arrays and advances in mass spectrometry are providing the tools needed to discover and identify disease-associated biomarkers Recent advances in MS, especially platforms that permit rapid "fingerprint" profiling, will most assuredly enhance the discovery, identification and characterisation of potential cancer associated biomarkers Furthermore, improvements in preparation of cancer samples particularly laser capture microdissection has provided a reproducible approach to procure pure populations of cells This technology coupled with 2-DE and MS has significantly aided the elucidation of the differential expression profiles between malignant, benign and normal cell populations Moreover, the development and application of learning algorithms and bioinformatics to the data generated by these proteomic technologies will be essential in determining the clinical potential of protein biomarkers

The ability to discover and subsequently routinely monitor multiple changes in protein composition simultaneously from only a small sample (e g of blood) will enable the realisation of three important goals in medicine Firstly, it will enable the earliest possible detection of disease onset Secondly, it will provide the ability to accurately assess disease type and level of disease progression Finally, it will also provide the ability to routinely monitor how a patient is responding to a chosen therapy

Two-dimensional electrophoresis remains a major component of proteomics and its high-resolution power makes it a challenge to other existing separation techniques However, it is still labour intensive and requires skill to generate highly reproducible results Despite the interesting results derived from 2-DE technology, especially in the area of cancer research, the many drawbacks of this technology preclude its wide acceptance in routine clinical use There is an obvious need to further develop and generate equally sensitive separation methods that unify both high sample throughput and reproducibility ProteinChips will ultimately permit researchers to scan thousands of proteins in a variety of proteomic experiments including differential expression, response to drugs and importantly in the identification of disease specific markers

1.14 Aims of Thesis

The central aim of this work was to investigate the mechanisms of drug resistance in lung cancer using proteomic technologies through the following approaches

Establishment of clinically relevant drug-resistant variants

- Many cell lines used as models for studying drug resistance are established with clinically unachievable concentrations or do not reflect the patients treatment regime To establish drug resistant variants of two squamous (SKMES and DLRP) and two small cell lung carcinoma (DMS-53 and NCI-H69) cell lines, chemotherapy-naive cell lines were chosen and pulse-selected (rather than continuously) with clinically-relevant concentrations The aim of carrying out this procedure was three-fold Firstly, it was designed to establish variants to reflect the clinical scenario Secondly, it facilitated analysis of the role of MDR proteins P-gp and MRP1 in cells with clinically relevant resistance Finally, these studies would contribute to an understanding of the relationship between drug resistance and invasive phenotypes

Increased understanding of adriamycin resistance

- The second aim was to gain further understanding of drug resistance in adriamycin-resistant variants of DLKP by studying differential protein expression using proteomic technologies The use of variants with high resistance profiles will help to select those changes involved in resistance specifically DLKP, a poorly differentiated squamous lung cell line, was previously exposed continuously to increasing concentrations of adriamycin resulting in the cell line, DLKP-A This cell line was further selected by continuous exposure to adriamycin creating DLKP-A10 Two clonal sub-populations were also isolated from DLKP-A by clonal dilution, DLKP-A5F and DLKP-A2B Each of the above four cell lines has differing levels of resistance to adriamycin and also exhibits cross-resistance profiles to a number of chemotherapeutic drugs While the main mechanism of resistance in these cell lines is associated with P-gp (no detectable levels of MRP), little information on cytoplasmic changes is available This work set out to investigate such changes The objective is to increase our understanding of the mechanisms involved in adriamycin

resistance and to identify putative markers with possible prognostic/diagnostic value.

Increased understanding of mitoxantrone resistance

- Mitoxantrone, an analogue of adriamycin with lower levels of toxicity provides a useful means of studying resistance further. A proteomic investigation was carried out to study the differential protein expression caused by mitoxantrone resistance in the already established DLKP-Mitox cell line. While the main mechanism of resistance in this cell line may be associated with BCRP (increased expression of BCRP at the mRNA levels, no detectable levels of P-gp and MRP1), little information on cytoplasmic changes is available. This work set out to investigate such changes to increase our understanding of the mechanisms involved in mitoxantrone resistance to identify putative markers with possible prognostic/diagnostic value. It was also of interest to compare proteins altered in DLKP versus DLKP-A with DLKP versus DLKP-Mitox as both adriamycin and mitoxantrone are alkylating agents and mitoxantrone is an analogue of adriamycin with less cardiotoxicity.

Investigation of clinically relevant taxane resistance

- The fourth aim is to determine the cellular components that are involved in taxol and taxotere resistance in the squamous lung cancer cell lines, SKMES-Txl and SKMES-Txt respectively. The parental cell line, not previously documented to be exposed to drug was selected with clinically relevant concentrations of the taxanes (taxol and separately taxotere), drugs traditionally used in the treatment of lung cancer. Proteomic analysis of these cell lines was used to generate a list of differentially expressed proteins that should provide insights into common mechanisms of taxane resistance as well as differences between the taxol and the more potent taxotere. Taxol and taxotere have similar mechanisms of action even though taxotere is approximately twice as potent an inhibitor of microtubule depolymerisation relative to taxol (Gelman, 1994). Moreover, there is a geographical bias with taxol predominately used in America and taxotere in Europe. Currently, while there is much known about the mechanism of action of the taxanes, little is known about the differences induced by taxol and taxotere. It is

hypothesised that proteomic investigation of taxol- and taxotere-selected variants will yield differential protein expression profiles that may contribute to understanding the differences in action of taxol and taxotere

Investigation into unstable resistance

- An unforeseen but fortunate result of taxane selection with SKMES was the observed loss of resistance in both taxane-resistant variants of SKMES By monitoring the differential protein expression over time, the proteins specifically involved in the loss of resistance may be identified

Investigation into common markers for resistance

- Do proteins involved in taxane resistance show cross-over with other chemotherapeutic drugs (namely adriamycin or mitoxantrone)? Multi-drug resistance is classified as resistance not only to the selecting drug but also to a range of structurally distinct chemotherapeutics As multidrug resistance is a major problem in lung cancer, there is a need to understand the common mechanisms involved A further aim of this work was to identify common pathways or intermediaries from the proteomic analysis that may provide targets that may act to reduce resistance and cross-resistance

Section 2.0: Materials and Methods

2.1 Preparation of cell culture media

Ultrapure water (UHP) was purified to a standard of 12-18 MΩ/cm resistance by a reverse osmosis system (Millipore MilliI-RO 10 Plus, Elgastat UHP) Glassware required for cell culture related applications were soaked in a 2% RBS-25 (AGB Scientific) for 1 hour, washed in an industrial dishwasher, using Neodisher detergent and rinsed twice with UHP All thermostable solutions, water and glassware were sterilised by autoclaving at 121°C for 20 minutes at 15 bar (Thermolabile solutions were filtered through 0 22 μm sterile filters (Millipore, Millex-GV SLGV025BS))

All 1X basal media were prepared in-house as follows 10X media was added to sterile UHP water, buffered with HEPES (N-(2-Hydroxyethyl) piperazine-N-(2-ethanesulfonic acid) and $NaHCO_3$ as required and adjusted to pH 7 5 using sterile 1 5 N NaOH or 1 5 N HCl The media was then filtered through sterile 0 22μm bell filters (Gelman, 12158) and stored in sterile 500ml bottles at 4°C Sterility checks on all media bottles for bacterial, yeast and fungal contamination were made using Colombia blood agar (Oxoid, CM217), Sabauraud dextrose (Oxoid, CM217) and Thioglycolate broths (Oxoid, CM 173) respectively All sterility checks were then incubated at both 25°C and 37°C

Basal media were stored at 4°C for up to three months in the dark Complete media was then prepared as follows supplements of 2mM L-glutamine (Gibco, 11140-0350) for all basal media and 1ml 100X non-essential amino acids (Gibco, 11140-035) and 100mM sodium pyruvate (Gibco, 11360-035) were added to MEM Other components were added as described in Table 2 1 Complete media was stored at 4°C for a maximum of one month in the dark

Cell Line	Basal Media	FCS (%)	Additions
DLKP	ATCC	5	-
DLRP	ATCC	5	-
DMS-53	RPMI 1640	10	Sodium pyruvate
NCI-H69	RPMI 1640	10	Sodium pyruvate
SKMES	MEM	10	Sodium pyruvate, non-essential amino acids

Table 2 1 Additional components in media

2.2 Cells and cell culture

All cell culture work was carried out in a class II laminar air-flow cabinet (Holten) All experiments involving cytotoxic compounds were conducted in a cytotoxic laminar air-flow (LF) cabinet (Gelman Sciences, CG series or Holten Maxisafe) Before and after use the LF cabinet was cleaned with 70% industrial methylated spirits (IMS) Any items brought into the cabinet were also swabbed down with IMS At any time, only one cell line was used in the LF cabinet and upon completion of work with any given cell line, a 15 minutes clearance was given to eliminate any possibilities of cross-contamination between the various cell lines The cabinet was cleaned weekly with Virkon (Antech International, P0550) and IMS Details pertaining to the cell lines used for the experiments are provided in Tables 2 2 and 2 3 All cells were incubated at 37°C and where required, in an atmosphere of 5% CO_2 Cells were fed with fresh media or subcultured (see section 2 5 1) every 2-3 days or as required in order to maintain active cell growth

Cell line	Cell type	Source	Developer
DLKP	Poorly differentiated squamous cell lung carcinoma	NCTCC*	Law *et al* (1992)
DLKP-A	Adriamycin resistant variant of DLKP	NCTCC	Redmond *et al* (1992)
DLKP-A10	Adriamycin resistant variant of DLKP-A	NCTCC	Cleary *et al* (1997)
DLKP-A5F	Clonal subpopulation of DLKP-A	NCTCC	Heenan *et al* (1997)
DLKP-A2B	Clonal subpopulation of DLKP-A	NCTCC	Heenan *et al* (1997)

Table 2 2 Description of DLKP and variants described in this thesis * NCTCC, National cell and tissue culture centre

Cell line	Cell type	Source
DLRP	Poorly differentiated squamous cell lung carcinoma	NCTCC
DLRP-Cpt	Carboplatm resistant variant of DLRP	NCTCC*
DLRP-Txt	Taxotere resistant variant of DLRP	NCTCC*
DMS-53	Small cell lung cancer	ECACC**
DMS-Cpt	Carboplatin resistant variant of DMS-53	NCTCC*
DMS-Txt	Taxotere resistant variant of DMS-53	NCTCC*
DMS-Txl	Taxol resistant variant of DMS-53	NCTCC*
NCI-H69****	Small cell lung cancer	ATCC***
H69-Cpt5 & H69 Cpt-10	Carboplatm resistant variants of NCI-H69	NCTCC*
H69-VP480	VP-16 resistant variants of NCI-H69	NCTCC*
SKMES	Squamous cell lung carcinoma	ATCC
SKMES-Cpt30 SKMES-Cpt100	Carboplatin resistant variant of SKMES	NCTCC*
SKMES-Txl	Taxol resistant variant of SKMES	NCTCC*
SKMES-Txt	Taxotere resistant variant of SKMES	NCTCC*

Table 2 3 Description of other cell lines described in this thesis

* - developed during the course of these studies

** ECACC - European collection of cell cultures

*** ATCC - American Tissue Culture Collection

**** Morphology resembles floating aggregates, characteristic of SCC

2 2 1 Subculturing of adherent cell lines

Waste cell culture medium was removed from the tissue culture flask and discarded into a sterile bottle The flask was then rinsed out with 1ml of trypsin/EDTA solution (0 25% trypsin (Gibco, 043-05090), 0.01% EDTA (Sigma, E9884) solution in PBS (Oxoid, BRI4a)) to ensure the removal of any residual media Depending on the size of the flask,

2-5ml of trypsin was then added to the flask, which was then incubated at 37°C, for approximately 5 minutes, until all of the cells detached from the inside surface of the flask monitored by microscopic observation Adding an equal volume of complete media to the flask deactivated the trypsin The cell suspension was removed from the flask and placed in a sterile universal container (Sterilin, 128a) and centrifuged at 1000rpm for 5 minutes The supernatant was then discarded from the universal and the pellet was suspended gently in complete medium A cell count was performed and an aliquot of cells was used to seed a flask at the required density All cell waste and media exposed to cells were autoclaved before disposal

2 2.2 Subculturing of floating aggregate cell lines

The cell suspension was removed from the flask and placed in a sterile universal container and centrifuged at 1000g for 5 minutes The supernatant was then discarded from the universal and the pellet was suspended in complete medium The aggregates were broken up by gently pipetting the suspension up and down using a 10 ml pipette A cell aliquot was used to seed a flask

2.3 Assessment of cell number and viability

Prior to cell counts, cells were prepared for subculturing as detailed in 2 2 1 or 2 2 2 depending on adherent or floating aggregates An aliquot of the cell suspension was then added to trypan blue (Gibco, 525) at a ratio of 5 1 The mixture was incubated for 3 minutes at room temperature An aliquot (10µl) was then applied to the chamber of a glass coverslip-enclosed haemocytometer For each of the four grids, cells in the 16 squares were counted The average of the four grids were multiplied by a factor of 10^4 volume of the grid) and the relevant dilution factor to determine the average cell number per ml in the original cell suspension Non-viable cells stained blue, while viable cells excluded the trypan blue dye as their membrane remained intact and remained unstained On this basis, percentage viability could be calculated

2 4 Cryopreservation of cells

Cells for cryopreservation were harvested in the log phase of growth and counted as described in Section 2 2 1 or 2 2 2 Cell pellets were resuspended in a suitable volume of serum An equal volume of a 10 - 20 % DMSO/serum solution was added dropwise with mixing, to the cell suspension The suspension was then aliqoted in 1 ml volumes to cryovials (Greiner, 122278) and immediately placed in the vapour phase of a liquid nitrogen container After four hours, vials were transferred to the liquid phase for long term storage (- 196°C)

2 4.1 Thawing of cryopreserved cells

A volume of 5ml of fresh growth medium was added to a sterile universal The cryopreserved cells were removed from the liquid nitrogen and thawed at 37°C quickly The cells were removed from the vials and transferred to the aliquoted media The resulting cell suspension was centrifuged at 1,000 rpm for 5 minutes The supernatant was removed and the pellet resuspended in fresh culture medium An assessment of cell viability on thawing was then carried out (Section 2 3) Thawed cells were then added to an appropriately sized tissue culture flask with a suitable volume of growth medium and allowed to attach overnight The following day, flasks were refed with fresh media to remove any non-viable cells

2 5 Monitoring of sterility of cell culture solutions

Sterility testing was performed in the case of all cell culture media and cell culture related solutions Samples of prepared basal media were incubated at 37°C for a period of seven days This ensured that no bacterial or fungal contamination was present in the media or the solutions

2 6 Serum batch testing

To prevent batch to batch variation (a common problem in foetal calf serum (FCS) in cell culture), a range of FCS batches were screened and the most suitable was chosen for a block of work (Sigma, F7524) Screening involved growing cells in 96-well plates and growth was recorded as a percentage of growth of a serum with known acceptable growth rate as described in section 2 8 4

2.7 *Mycoplasma* analysis of cell lines

Mycoplasma testing was carried out in house by Ms Aine Adams and Mr Michael Henry at the NCTCC Both direct and indirect methods were used In the indirect method, *Mycoplasma* negative NRK (Normal rat kidney fibroblast) cells were exposed to conditioned media of the test sample Hoechst staining specific for DNA shows positive for *Mycoplasma* when viewed in the extracellular spaces In the direct method, conditioned media were incubated on cells specifically to encourage *Mycoplasma* growth

2.8 Miniaturised *in vitro* toxicity assays

2.8.1 *In vitro* toxicity assay for anchorage dependant cell lines

Cells in the exponential phase of growth were harvested by trypsinisation (section 2 2 1) Cell suspensions containing $1x10^4$ cells/ml in the appropriate culture medium, were aliquotted at 100µl/well in 96-well plates (Costar, 3599) using a multichannel pipette Plates were agitated gently in order to ensure even dispersion of cells over a given surface Cells were then incubated overnight at 37°C and 5% CO_2 Cytotoxic drug dilutions were prepared at 2X their final concentration in cell culture medium Volumes of the drug dilutions (100µl) were then added to each well using a multichannel pipette Plates were then mixed gently as above Cells were incubated for a further 6-7 days at 37°C and 5% CO_2 until the control wells had reached approximately 80-90% confluency Assessment of cell survival in the presence of drug was determined by the acid phosphatase assay (section 2 8 4) The concentration of drug which caused 50% cell kill (IC_{50} of the drug) was determined from a plot of the % survival (relative to the control cells) versus cytotoxic drug concentration

2.8 2 *In vitro* toxicity assay for floating aggregate cell lines

Cells in the exponential growth phase were harvested as in section 2 2 2 However, the cell pellet was suspended in 500 µl of Cell Dissociation solution (Sigma, C5914) The suspension was then incubated at 37^0C for approximately 10 minutes after which a p200 gilson was used to aid in the disruption of the clumps The assay was set up as described in 2 8 1 except $3.5x10^5$ cells/ml was prepared in RPMI medium and aliquotted at 100µl/well Cells were incubated for a further 9-10 days

2.8.3 Combination toxicity assays

As described in section 2 2 1 or 2 2 2, plates were seeded at $1x10^4$ cells/ml and incubated overnight Cytotoxic drug dilutions and non-steroidal anti-inflammatory drug (NSAID) dilutions were prepared at 4X their final concentration in media Volumes of 50µl of the drug dilution and 50µl of the NSAID dilution were then added to each relevant well and the final volume in all wells was brought up to 200µl with media where necessary All potential toxicity-enhancing agents were dissolved in DMSO, ethanol or media Stock solutions were prepared at approximately 15mg/10ml media, filter sterilised with a 0 22µm low protein binding filter (Millex-GV, SLGV025BS) and then used to prepare all subsequent dilutions Cells were incubated for a further 6-7 days at 37°C in an atmosphere containing 5% CO_2 At this point the control wells would have reached approximately 80-90% confluency Cell number was assessed using the acid phosphatase assay (section 2 8 4)

2.8.4 Assessment of cell number - acid phosphatase assay for anchorage dependant cell lines

Following the incubation period of 6-7 days, the media with the chemotherapy drug was removed from the plates and disposed (Table 2 5) Each well on the plate was washed twice with 100µl PBS and to each well, 100µl of freshly prepared phosphatase substrate (10mM *p*-nitrophenol phosphate (Sigma 104-0) in 0 1M sodium acetate (Sigma, S8625), 0 1% triton X-100 (BDH, 30632), pH 5 5) was added The plates were then incubated in the dark at 37°C for about 2 hours, monitoring colour development The enzymatic reaction was stopped by the addition of 50µl of 1N NaOH The plate was read in a dual beam plate reader at 405nm with a reference wavelength of 620nm

2 8 5 Assessment of cell number - modified acid phosphatase assay for floating aggregate cell lines

For the anchorage-independent cell lines (NCI-H69 and variants), the same procedure was followed as described above with the following exceptions Washing involved centrifuging the plates and aspirating off the supernatant The plates were incubated for a period of approximately 5 hours before the assay was stopped

2.9 Safe handling of cytotoxic drugs

Cytotoxic drugs were handled with extreme caution at all times in the laboratory, due to the potential risks in handling these drugs Disposable nitrile gloves were worn at all times and all work was carried out in cytotoxic cabinets All drugs were stored in a safety cabinet at room temperature or in designated areas at 4°C or -20°C The storage and means of disposal of the cytotoxic drugs used in this work are outlined in Table 2 5

Cytotoxic Agent	Storage	Disposal*
Adriamycin	4°C in dark	Incineration
Taxol	Room temperature in dark	Incineration
Carboplatin	Room temperature in dark	Incineration
Vincristine	4°C in dark	Incineration
Taxotere	Room temperature in dark	Incineration
VP-16	Room temperature in dark	Incineration
5-fluorouracil	Room temperature in dark	Incineration
Cisplatin	Room temperature in dark	Incineration

Table 2 5 Storage and disposal details for chemotherapeutic agents

*Platinum and non-platinum waste were stored separately prior to incineration

2.10 Pulse selection of parent cell lines

Taxanes and carboplatin are the drugs of choice for treatment of NSCLC while VP- 16 and carboplatin are the drugs of choice for SCLC SKMES-1, DLRP (squamous) and DMS-53 (SCLC) were all selected with carboplatin, taxotere SKMES-1 and DMS-53 were treated with taxol NCI-H69 (SCLC) was pulsed with VP-16 or carboplatin

2 10 1 Assay to determine drug concentration for pulse selection

Cells were seeded into 25cm^2 flasks at 3 × 10^5 cells per flask and as per miniaturized assay After overnight incubation (37°C), media was removed and a range of drug concentrations added for 4 hours Cells were washed and allowed to grow for 5-7 days until the control was 80% confluent The end point was determined by cell counting (2 2 1) Concentrations chosen for pulse selection of DMS-53, NCI-H69 and SKMES-1 gave an 80-90% kill, i e IC_{80} - IC_{90}. DLRP was pulsed with taxotere and carboplatin at

a concentration that gave a much lower kill, since these cells were found to recover poorly when pulsed at higher doses. (Table 2.6).

Cell Line	Taxol (ng/ml)	Taxotere (ng/ml)	VP-16 (ng/ml)	Carboplatin (μg/ml)
DLRP	Not Treated	5	Not Treated	15
DMS-53	60	40	Not Treated	5
SKMES-1	120	60	Not Treated	100 and 30
NCI-H69	Not Treated	Not Treated	480	10 and 5

Table 2.6 Concentrations used for pulse-selection

2.10.2 Pulse selection

Cells at 70-80% confluency in 75cm^2 flasks were exposed to the chosen concentration of taxol, taxotere, VP-16 or carboplatin for 4 hours. After this period, the drug was removed and the flasks were rinsed and fed with fresh complete media. The cells were then grown in drug-free media for 6 days, refeeding every 2-3 days. This was repeated once a week for ten weeks. Where cells did not recover sufficiently from the previous pulse, more time was required to complete the pulses. Invasive potential (see section 2.11) and sensitivity to the selecting drug and a variety of cytotoxic drugs was the determined using miniaturised toxicity assays (see section 2.8.1 and 2.8.2).

2.11 Invasion techniques

2.11.1 *In vitro* invasion assays

Invasion assays were performed using the method of Albini (1998). Matrigel (Sigma E-1270) (11mg/ml) was diluted to 1mg/ml in serum-free culture media. Matrigel was kept ice-cold at all times. Into each insert (Falcon 3097) (8.0μm pore size, 24-well format), which stands on 24-well plate (Costar) 100μl of 1mg/ml Matrigel was placed. The insert and the plate were incubated for one hour at 37°C to allow the gel to polymerise. Cells were harvested and resuspended in culture media containing 5% FCS at the concentration of 1×10^6 cells/ml. Excess media was removed from the inserts, and they were rinsed in culture media. To each insert, 100μl of the suspension cells were added. A further 100μl of culture media was added to each insert and 500μl of culture media

containing 5% FCS was added to the well underneath the insert (no serum gradient was used) Cells were incubated at 37°C for 24 hours After this time period, the inner side of the insert was wiped with a cotton swab dampened with PBS, while the outer side of the insert was stained with 0 25% crystal violet for 10 minutes and then rinsed in UHP and allowed to dry The inserts were then viewed and photographed under the microscope at 10X The invasion assays were quantified by counting cells within a graticule at 40X magnification, use of positive and negative control confirmed the assay procedure

2.11.2 Motility assays

The procedure for carrying out motility assays was identical to the procedure used for invasion assays (section 2 11 1) with the exception that the inserts were not coated with ECM The procedure for quantitative analysis was identical to that of the invasion assays

2.11.3 Adhesion assays

The ECM protein matrigel was diluted to 1mg/ml with PBS A volume of 250µl was placed into wells of a 24-well plate The plates were gently tapped to ensure that the base of each well was completely covered with the solution The plates were then left overnight at 4°C The ECM solutions were then removed from the wells and the wells rinsed twice with sterile PBS To each well, 0 5ml of a sterile 0 1% BSA/PBS solution was dispensed to reduce non-specific binding The plates were incubated at 37°C for 20 minutes and rinsed twice with PBS

Cells were set up in 75cm^2 flasks, grown to about 80% confluency, harvested and resuspended in serum-free medium A 1ml volume of cells was then plated at a concentration of 2 5 × 10^4 cells per well in triplicate and incubated at 37°C for 60 minutes Control wells were those which had firstly been coated but contained no cells and secondly not been coated After 60 minutes, the medium was removed from the wells and rinsed gently with PBS This was then removed and 200µl of freshly prepared phosphatase substrate (10mM *p*-nitrophenol phosphate (Sigma 104-0) in 0 1M sodium acetate (Sigma, S8625), 0 1% triton X-100 (BDH, 30632), pH 5 5) was added to each well The plates were then incubated in the dark at 37°C for 2 hours The enzymatic

reaction was stopped by the addition of 100µl of 1M NaOH The plate as read in a dual beam plate reader at 405nm with a reference wavelength of 620nm

2 11.4 Zymography

Zymography was used to assess the level of proteolytic activity of different proteinases in cell culture supernatants The choice of substrate incorporated into the resolving gel depends on substrate specificity of the species of enzyme to be detected (Johansson *et al*, 1986) Gelatin as a substrate for matrix metalloproteinases (MMPs), serine and cysteine protemases, was used in these experiments

The 10% acrylamide gels were prepared by incorporating gelatin within the polymerized acrylamide matrix The quantities for one gel are given in Table 2 7

Components	**Resolving gel**	**Stacking gel**
Acrylamide	3 3 mls	0 5 mls
3mg/ml Gelatin (Sigma, G-8150)	2 5 ml	-
1 875M-Tris/HCl, pH 8 8	2 5 ml	-
1 25M-Tris/HCl, pH 6 8	-	0 8 ml
Ultrapure water	1 7 ml	2 ml
10% Ammonium persulphate (Sigma, A-1433)	33 µl	33 µl
TEMED (Sigma, T-8133)	5 µl	5 µl

Table 2 7 Preparation of resolving and stacking gel for zymography

Cells were grown in T75 flasks Once cells were about 80% confluent, they were rinsed twice with sterile PBS, followed by 2-hour incubation with serum-free medium The cells were then grown in fresh serum-free medium for another 24-72 hours (dependmg on their growth rate) After the relevant time period, supernatants were collected and concentrated in centrifugal concentrators (Vivascience, VS2012) Protein was quantified using a Bio-Rad protein assay kit (Bio-Rad, 500-0006) Samples were mixed 3 1 with 4X sample buffer (20% glycerol, 0 25M Tris-HCl, pH 6 8, 0 1% (w/v) bromophenol blue) and were loaded onto the gel A 5µl aliquot of boiled broad size range protein marker (New England Biolabs, 7708S) was also loaded onto the gel The gels were run

at 30 mA per gel in 1X running buffer (14 4g Glycine, 3 03g Tris and 1g SDS in 1L UHP) until the dye front reached the bottom of the gel Following electophoresis, the gels were soaked in 2 5% Triton-X-100 with gentle shaking for 30 minutes at room temperature The gels were then rinsed in substrate buffer (50mM Tris-HCl, pH8 0, 5mM $CaCl_2$) and incubated for 24 hours in substrate buffer at 37°C The gels were then stained with Coomassie blue (2 5mg/ml) for 2 hours by shaking and destained in 25% acetic acid until clear bands were visible The gels were then scanned To identify the different classes of proteinases that were being secreted, inhibitors of protemases were added to 2 5% Triton-X-100 m substrate buffer The inhibitors used in this study are listed in Table 2 8

Inhibitor	Enzyme inhibited	Concentration used
EDTA	MMPs	30 mM
PMSF	Serine protemases	1 mM

Enhancer	Enzyme enhanced	Concentration used
Cysteine	Cysteine proteinases	10 mM

Table 2 8 Inhibitors and enhancers of different classes of proteinases used in gelatin zymography

2.11.5 3D-*in vitro* invasion assays

The hanging drop method was performed using an adapted method from Robinson *et al*, (2004) Cells were harvested and resuspended at a concentration of $1x10^6$ cells/ml in complete media Volumes of 20µL aliquots were deposited onto the underside lid of 10mm tissue culture dish The lid was then inverted over 10ml sterile UHP or complete media to create hanging drops on the upper lid Drops were incubated under tissue culture conditions for 24 hours Aggregates were added to a tissue culture dish precoated with Agar (5%) and overlaid with 10ml complete media to prevent attachment and allow dense spheroid profile formation for 24hrs After this time, the spheroids were transferred to a 24-well plate coated with matrigel or collagen type I for the 3-D *in vitro* invasion assay

A volume of 250µL of matrigel (1mg/ml) was added 24 well plates and allowed to settle overnight at 4°C The excess media was removed and washed twice with PBS The

spheroid was carefully placed into matrigel ensuring only one spheroid was implanted. The spheroid was then incubated for 2hrs at 37°C in 5% CO_2. After this time, the well was overlaid with 500µL of media. The implanted spheroid was monitored at 24hrs, 48hrs, 72hrs and up to 7 days. The rate of invasion was measured by the distance (µm) of invasion of the cells from the original spheroid with a graticule in the microscope at 4x magnification.

2.12 Western blotting

2.12.1 Whole cell extract preparation

Cells were grown to 80-90% confluency in 75cm^2 flasks. Cells were trypsinised (section 2.2.1) and washed twice with ice-cold PBS. All procedures from this point forward were performed on ice. Cells were resuspended in 100-200µl of NP-40 complete lysis buffer (50mM Tris-HCl (pH 7.5), 150 mM NaCl, 0.5%, NP-40 and UHP) and incubated on ice for 30 minutes. Immediately before use, 10µl of the 100X stocks listed in Table 2.7 were added to 1ml of lysis buffer.

100X stock	**Preparation instructions**
100mM DTT	154 mg in 10ml UHP
100mM PMSF	174 mg in 10ml 100% ethanol (Lennox, 608)
100X Protease inhibitors	2.5 mg/ml leupeptin, 2.5 mg/ml aprotinin, 15 mg/ml benzamidine and 1mg/ml trypsin inhibitor in UHP water

Table 2.7 NP-40 lysis buffer 100X stocks

After incubation on ice, lysates were centrifuged on a bench centrifuge at 14,000rpm for 15 minutes at 4°C. Supernatant containing extracted protein was transferred to a fresh chilled eppendorf tube. Protein concentration was quantified using the Biorad assay as detailed in section 2.12.2. Samples were then stored in aliquots at -80°C.

2.12.2 Protein quantification

Protein levels were determined using the Bio-Rad protein assay kit (Bio-Rad, 500-0006) as follows. A 2mg/ml bovine serum albumin (BSA) solution (Sigma, A9543) was prepared freshly in lysis buffer. A protein standard curve (0, 0.2, 0.4, 0.6, 0.8 and 1.0mg/ml) was prepared from the BSA stock with dilutions made in lysis buffer. The

Bio-Rad reagent was diluted 1 5 in UHP water A 20µl volume of protein standard dilution or sample (diluted 1 10) was added to 980µl of diluted dye reagent and the mixture vortexed All samples were assayed in triplicate After 5 minutes incubation, absorbance was assessed at 570nm The concentration of the protein samples was determined from the plot of the absorbance at 570nm versus the concentration of the protein standard

2 12.3 Gel electrophoresis

Proteins for analysis by Western blotting were resolved using SDS-polyacrylamide gel electrophoresis (SDS-PAGE) Using the Atto dual mini slab kit (AE 6450) the stacking and resolving gels were prepared as illustrated in Table 2 8 The gels were set in clean 9cm x 8cm gel cassettes, which consisted of 2 glass plates separated by a rubber gasket to a width of 1mm The resolving gel was added to the gel cassette and allowed to set Once the resolving gel had set, stacking gel was poured on top A comb was placed into the stacking gel after pouring, in order to create wells for sample loading (maximum sample loading volume of 15-20µl)

Components	10% Resolving Gel	5% Stacking Gel
Acrylamide stock	4 6 ml	670µl
UHP water	5 6ml	2 7ml
1 875 M Tris-HCl pH 8 8	3 5ml	-
1 25 M Tris-HCl pH 6 8	-	500µl
10% SDS	140µL	40µL
10% NH_4- persulfate*	140µL	40µL
TEMED*	5 6µL	4µL

Table 2 8 Preparation protocol for SDS-PAGE gels (2 x 0 75mm gels)

* Added immediately before pouring

The acrylamide stock in Table 2 8 consists of a 30% (29 1) ratio of acrylamide bis-acrylamide (Sigma, A2792) In advance of samples being loaded in to the relevant sample wells, 20µg of protein was diluted in 10X loading buffer Molecular weight markers (Sigma, C4105) were loaded alongside samples The gels were run at 250V and

45mA until the bromophenol blue dye front was found to have reached the end of the gel, at which time sufficient resolution of the molecular weight markers was achieved

2.12.4 Western blotting

Western Blotting was performed by the method of Towbin *et al* (1979) Once electrophoresis had been completed, the SDS-PAGE gel was equilibrated in transfer buffer (25mM Tris (Sigma, T8404), 192mM glycine (Sigma, G7126), pH 8 3-8 5) for approximately 30 minutes Five sheets of Whatman 3mm filter paper were soaked in freshly prepared transfer buffer These were then placed on the cathode plate of a semi-dry blotting apparatus (Bio-rad) Air pockets were then removed from between the filter paper PVDF membrane (Boehringer Mannheim 1722026) or nitrocellulose membrane (Amersham Pharmacia Biotech, RPN 303D), which had been equilibrated in the same transfer buffer, was placed over the filter paper on the cathode plate Air pockets were once again removed The gels were then aligned onto the membrane Five additional sheets of transfer buffer-soaked filter paper were placed on top of the gel; all air pockets removed and excess transfer buffer removed from the cathode plate The proteins were transferred from the gel to the membrane at a current of 34mA at 15V for 30-40 minutes, until all colour markers had transferred

Following protein transfer, membranes were stained using Ponceau (Sigma, P7170) to ensure efficient protein transfer The membranes were then blocked overnight using 5% milk powder (Cadburys, Marvel skimmed milk) in PBS at 4°C The membranes were washed with PBS prior to addition of the primary antibody

Membranes were treated with primary antibody for 2-3 hours at room temperature (or overnight at 4°C) and a negative control where the membrane was exposed to antibody diluent was also performed Antibodies were prepared in 1% Marvel in PBS Primary antibody was removed after this period and the membranes rinsed 3 times with PBS containing 0 5% Tween 20 (Sigma P1379) for a total of 15-30 minutes The primary antibody dilutions are illustrated in Table 2 9

Secondary antibody (1 in 1,000 dilution of anti-mouse IgG peroxidase conjugate (Sigma, A4914) in PBS, was added for 1 5 hour at room temperature The membranes were washed three times thoroughly in PBS containing 0 5% Tween for 15 minutes each time

Primary Antibody	Dilution
β-actin (Sigma, A5441)	1:10,000
P-gp (Santa Cruz, SC-13131)	1:200

Table 2.9 List of primary antibodies and dilutions

2.12.5 Enhanced chemiluminescence (ECL) detection

Immunoblots were developed using an Enhanced Chemiluminescence kit (Amersham, RPN2109), which facilitated the detection of bound peroxidase-conjugated secondary antibody. Following the final washing, membranes were subjected to ECL. A layer of parafilm was flattened over a glass plate and the membrane placed gently upon the plate. A volume of 3ml of a freshly prepared 50:50 mixture of ECL reagents was used to cover the membrane. The ECL reagent mixture was completely removed after a period of one minute and the membrane wrapped in clingfilm. All excess air bubbles were removed. The membrane was then exposed to autoradiographic film (Kodak, X-OMATS) for various times (from 10 seconds to 30 minutes depending on the intensity of the signal). The exposed autoradiographic film was developed for 3 minutes in developer (Kodak, LX-24). The film was then washed in water for 15 seconds and transferred to a fixative (Kodak, FX-40) for 5 minutes. The film was washed with water for 5-10 minutes and left to dry at room temperature.

2.13 Proteomic protocols: sample preparation - total protein extraction

In order to obtain between 5-10 mg of protein, at least $3x10^7$ cells were required. Cells were therefore grown to 70-80% confluency in 175cm^2 flasks, trypsinised and counted (section 2.2.1), washed three times with 50 ml ice cold PBS or sucrose solution and the resulting pellet was left on ice for up to 30 minutes. After 30 minutes, 1ml of either of the following complete lysis buffers: (8M urea (Sigma, U6504), 30mM, Tris Base (Sigma, T1378) (1M not pH'd), 4 % (w/v) CHAPS (Sigma, C5070), pH to 8.5 with dilute HCl) or ((5 M urea (Sigma, U6504), 2M thiourea (Sigma 88810) 30mM, Tris Base (Sigma, T1378) (1M not pH'd), 4 % (w/v) CHAPS (Sigma, C5070), pH to 8.5 with dilute HCl) was added to the pellet. Immediately before use, 10µl of the 100X stocks of DNase and RNase were added to 1ml of lysis buffer.

The lysate was then put through a 1 ml syringe with a 21 gauge needle 5 times. The cell lysate was placed on an orbital shaker and shaken for 1 hour at room temperature. The protein lysate was then transferred to an eppendorf and centrifuged at 13,000 rpm for 15

minutes The resulting supernatant was transferred to a fresh microcentrifuge tube and its pH was checked to ensure it was between pH 8 0-9 0 by spotting 3 µl onto a pH indicator strip The sample was then divided into smaller aliquots and stored at –80°C The protein concentration was quantified using the Biorad method outlined in section 2 12 2 At least 6 biological replicates of each cell line were prepared

Different protein loadings for isoelectric focussing were used for 2-DE These volumes were dependent on whether or not the samples were to be used for screening, DIGE analysis or for the identification of proteins of interest by mass spectrometry (see section 2 17 2)

2.14 Labeling of cell lysates for DIGE

2.14.1 Preparation of CyDye DIGE fluor minimal dyes for protein Labelling

2.14 1.1 Preparation of dye stock solution (1 nmol/µl)

The three CyDye DIGE Fluor Minimal dyes (Cy3, Cy5 and Cy2 (Amersham, 25-8010-65) were thawed from –20 °C to room temperature for 5 minutes To each microfuge tube dimethylformamide (DMF) (Aldrich, 22,705-6) was added to a concentration of 1 nmol/ µl Each microfuge tube was vortexed vigorously for 30 seconds to dissolve the dye The tubes were then centrifuged for 30 seconds at 14,000rpm in a microcentrifuge The reconstituted dyes were stored at –20 °C for up to two months

2.14.2 Preparation of 10 µl working dye solution (200 pmol/µl)

On thawing, the dye stock solutions were centrifuged in a microcentrifuge for 30 seconds To make 10 µl of the three working dye solutions, 8 µl of DMF was added to three fresh eppendorfs labelled Cy2, Cy3 and Cy5 A 0 2 nmol/µl volume of each of the reconstituted dye stock solutions was added to their respective tubes The dyes were stored at -20 °C in tinfoil in the dark for 3 months

2.14.3 Protein sample labelling

A volume of the 6 control samples and 6 treated protein samples equivalent to 50 µg was placed into twelve eppendorf tubes (6 for Cy3 and the other 6 for Cy5) They were labelled with the minimal dyes as follows, Control 1-3 and Treated 1-3 were labelled with 1 µl each of Cy3 and Control 4-6 and Treated 4-6 were labelled with 1 µl each with

Cy5 Each tube was mixed by vortexing, centrifuged and then left on ice for 30 minutes in the dark To stop the reaction, 1 µl of 10 mM lysine was added, the tubes were vortexed, centrifuged briefly and left on ice for 10 minutes in the dark The labelled samples were stored at –80 °C The Cy2 pool for each gel (50 µg) contained a 4·17 µg aliquot of each of the 12 protein samples (6 control and 6 treated) To this tube 1 µl of working dye solution was added

2.14 4 Preparing the labelled samples for the first dimension

The protein samples labelled with Cy2 (pooled internal standard), Cy3 and Cy5 were thawed on ice (in the dark), combined by placing into a single eppendorf tube and mixed An equal volume of 2X sample buffer (2 5 ml rehydration buffer stock solution (8M urea, 4 % CHAPS), pharmalyte broad range pH4-7 (2%) (Amersham, 17-6000-86), DTT (2%) (Sigma, D9163)) was added to the labelled protein samples The mixture was left on ice for at least 10 minutes then applied to Immobiline DryStrips for isoelectric focussing

2.15 First dimension separation - isoelectric focussing methodologies

Isoelectric focussing of all samples were carried out using immobiline pH gradient (IPG) strips

2.15.1 Strip rehydration using Immobiline DryStrip reswelling tray

The protective lid was removed from the Immobilme Dry Strip Reswellmg tray The tray was levelled using the spirit level A 350µl volume of rehydration buffer solution (with 2 % pharmalyte broad range pH4-7 and 2 % DTT) was slowly pipetted into the centre of each slot, all air bubbles generated were removed The cover film from the IPG strip (Amersham, 17-1233-01) was removed and positioned with the gel side down and lowered To ensure the entire strip was evenly coated the strip was gently lifted and lowered onto the entire surface of the solution avoiding trapping air bubbles

Each strip was overlaid with about 3 ml IPG Cover Fluid (Amersham, 17-1335-01) starting on both ends of the strip, moving to the centre The protective lid was then replaced and the strips were left at room temperature to rehydrate overnight (or at least 12 hours)

2 15 2 Isoelectric focussing using the IPGphor manifold

Following the rehydration procedure, the Manifold (Amersham) was placed onto the IPGphor unit by inserting the "T" shape into the hollow provided A 9 ml volume of Cover Fluid was placed into each of the twelve lanes in the tray m order to cover the surface Two wicks (Amersham, 80-6499-14) per strip were placed on tinfoil and 150 µl of UHP was pipetted onto each one to rehydrate them The rehydrated strips were placed in the correct orientation (+ to anode) and aligned just below the indented mark, to allow for the wicks to overlap the strip The rehydrated wicks were then placed over both the cathodic and anodic ends of all the strips The wicks were checked to ensure they were positioned over the gel portion of the strip and avoiding the indent in the lane so as to guarantee a good contact with the electrodes The sample cups (Amersham,-80-6498-95) were then positioned approximately 1 cm from the cathodic end of the strip and an insertion tool was used to securely "click" the cups into place The electrodes were then fitted with their "Cams" open and in direct contact with the wicks

The amount of protein loaded per strip was 75ug for screening, 150ug for DIGE or 400ug for spot picking The protein samples were prepared by centrifuging to remove any insoluble material and the appropriate volume was loaded with a pipette tip placed just beneath the surface of the cover fluid The cover of the IPGphor unit was closed and the desired programme selected The temperature was set for 20°C with 50µA/strip The IEF parameters are as follows step 1 300 volts for 3 hours (step-and-hold), step 2 600 volts for 3 hours (gradient), step 3 1000 volts for 3 hours (gradient), step 4 8000 volts for 3 hours (gradient) The IEF was left at 8000 volts (step-and –hold) until ready for SDS-PAGE step On completion of the IEF run, the strips were drained of the cover fluid and stored in glass tubes at –80°C or used directly in the second dimension

2.16 Second Dimension – SDS polyacrylamide gel electrophoresis

2.16.1 Casting gels in the ETTAN Dalt-12 gel caster

The 12 5 % acrylamide gel solution was prepared in a glass beaker (acrylamide/bis 40 %, 1 5 M Tris pH 8 8, 10 % SDS) Prior to pouring, 10 % ammonium persulfate and neat TEMED were added

Two types of plates were used, low fluorescent for DIGE experiments and hinged for preparative and screening silver stained gels All plates (both normal hinged and low

fluorescent) and casting equipment were inspected to ensure they were clean The gel caster frame was placed on a level bench leaning on its "legs" so that the back of the caster was open and facing the operator The plates were assembled so that the front and back plates were evenly aligned and all seals and hinges in place A thin spacer was placed in the gel caster unit followed by an assembled plate followed by a thin spacer then another plate The plates were positioned in the caster unit so that the lower, front plate was the furthest away from the operator and the spacers packed with their curved edges to the top This layering was repeated until all 14 plates and spacers were in place All plates and spacers were checked to ensure they were packed tightly together so as to minimise any gaps and air pockets If all 14 gels were not required, up to 4 dummy plates could be substituted instead of the glass plates When the desired amount of plates had been added, the thicker spacers were placed next to bring the level marginally over the edge of the back of the caster The backing plate was then added to the caster frame and screwed into place with the 6 screws provided The silicone tubing was added to the outlet of the glass beaker and the glass tube was inserted to the other end of the silicone tubing The glass tube was inserted into the inlet of the reservoir and the glass beaker containing the gel solution was then clamped to a retort stand The gel solution was held in place using arterial clamps on the top tube and the tube running down from the reservoir to the caster chamber The top tube was unclamped and the gel solution was allowed to fill the tubing and the reservoir dram Air bubbles that had been generated were dislodged by flicking the tube When all air bubbles had been removed the bottom clamp was released allowing the gel solution into the gel caster When the gel solution reached the indicator line across the top of the caster, the bottom and top tubes were reclamped The displacement solution (0 375M Tris-Cl 1 5M pH8 8, 30% glycerol, UHP and bromophenol blue) was added to the reservoir and the glass tubing was slowly removed from the reservoir inlet The clamp was removed from the bottom tube allowing the displacement solution into the tube and forcing the remaining gel solution into the gel caster The gels were overlaid with 1 ml saturated butanol or sprayed with 0 1 % SDS solution The gels were left to set for at least three hours at room temperature Following this, the caster was gently unlocked and the gels removed and rinsed with distilled water If the gels were not used immediately they were stored for up to four days in 1X running buffer at 4 °C

If gels were to be used for "spot picking" the plates were silanised to stick the acrylamide mixture to the plates A volume of 2ml of (8ml ethanol, 200µl glacial acetic

acid, 10µl bind-silane and 1 8ml UHP) was pipetted over the glass plate and wiped over with a lint free cloth This was left to air dry for 15 minutes, after which 2ml ethanol and 2 ml UHP were each pipetted over the plate and wiped off respectively The plate was left to air dry for approximately 1 hour 30 minutes

2 16.2 Preparing the ETTAN DALT 12 electrophoresis unit

The electrophoresis chamber was prepared by adding 6 48 litres of UHP and 720 ml of 10X SDS running buffer The pump was then turned on to cool the system to 10 °C

2 16.3 Equilibration of focussed Immobiline DryStrips

The SDS equilibration buffer (30% glycerol, 6M urea, 50nm 1 5M Tris-Cl pH 8 8, 2% SDS, bromophenol blue and UHP) which had been prepared, aliquotted into 30 ml volumes and frozen at –20°C was allowed to thaw to room temperature Two SDS equilibration buffer solutions with DTT (65 mM) or iodoacetamide (240 mM) (Sigma, I1149) were then prepared Using a forceps, the IPG strips* were removed from the IPGphor unit, the cover fluid was drained off by holding the strips at an angle and they were placed into individual glass tubes with the support film toward the wall Equilibration buffer (10 mls containing DTT) was added to each tube and incubated for 15 minutes with gentle agitation using an orbital shaker During this equilibration step, the gel cassettes were rinsed with UHP and then the tops rinsed with 1X running buffer After the first equilibration, DTT containing equilibration solution was removed and 5 mls of the iodoacetamide containing equilibration buffer added The strips were incubated for 10 minutes with gentle agitation During this equilibration step, the agarose overlay solution (0 5% agarose in running buffer) was prepared and 50 ml of 1X running buffer was placed in a glass tube

*If the strips had been frozen at this stage they were left at room temperature to thaw before the DTT-containing equilibration solution was added

2.16.4 Loading the focussed Immobiline DryStrips

Using a forceps and holding the anode end, the IPG strips were rinsed in 1X SDS electrophoresis running buffer and placed between the two glass plates of the gel The strip was pushed down gently using a thin plastic spacer until it came in contact with the surface of the gel Any air bubbles trapped between the gel surface and the strip were gently removed Approximately 1 ml of the 0 5 % agarose overlay solution was applied over the IPG strip to seal it in place

2.16.5 Inserting the gels into the Ettan DALT 12 electrophoresis buffer tank

When the running buffer reached the desired temperature (10°C) the loaded gel cassettes were wetted with UHP and inserted into the tank through the slots provided in the same orientation When all 12 slots were filled the upper chamber was filled, 2X running buffer was added to the upper chamber until the mark on the side of the chamber was reached The cover of the unit was replaced and the required running conditions selected The unit was run for 18–24 hours at 1 5 Watts per gel at 10°C or until the bromophenol blue dye front reached the bottom of the gel When the run was completed, the gel cassettes were removed from the tank one at a time using the DALT cassette removal tool and rinsed with UHP to remove the running buffer

2.17 Method for scanning DIGE labelled samples

The Typhoon Variable Mode Imager (GE Healthcare) was turned on and left to warm up for 30 minutes prior to scanning The scanning control software was opened and the fluorescence mode was selected The appropriate emission filters and lasers were then selected for the separate dyes (Cy2 520 BP40 Blue (488), Cy3 580 BP30 Green (532) and Cy5 670 BP 30 Red (633)) The first gel was placed in the scanner and pre-scanned at a 1000 pixel resolution in order to obtain the correct photo multiplier tube (PMT) value (to prevent saturation of the signal from high abundant spots) Once the correct PMT value was found, the gel was scanned at 100 pixel resolution, resulting in the generation of three images, one each for Cy2, Cy3 and Cy5 Once the scanning was completed, the gel images were imported into the ImageQuant software All gels were cropped identically to facilitate spot matching in the Decyder BVA module

2.18 Analysis of gel images

2.18.1 Differential in-gel analysis (DIA)

The DIA module processes a triplet of images from a single gel The internal standard is loaded as the primary image followed by the secondary and tertiary image, derived from, for example, a control and treated sample Spot detection and calculation of spots properties were performed for each image from the same gel The software determined the margins of the spots, quantified the spot intensities and calculated the relative spot intensity as the ratio between the total intensity of the gel and the intensity of each individual spot The protein spots were then normalised using the m-gel linked internal standard The data from the first gel was XML formatted and exported into the Biological Variation Analysis (BVA) software for further analysis This procedure was repeated for each gel in the experiment

2.18.2 Biological variation analysis (BVA)

Once all gels from the experiment were loaded into the BVA module, the experiment design was set up and the images were assigned into three groups (standard, control and treated) The spots on the gels were then matched across all gels in the experiment

This module detects the consistency of the differences between samples across all the gels The software standardises the relative spot intensity of the Cy5 image to that of the Cy3 image in the same gel The standardised spot intensity was then averaged across the triplicate gels The BVA module detected the consistency of the differences between samples across all the gels and applied statistics to associate a level of confidence for each of the differences The protein spots with statistically significant protein expression changes were designated "proteins of interest" and placed in a pick list

Preparative gels for spot picking with 400 ug of protein/gel were focussed and run out on SDS-PAGE gels The gels were then stained with colloidal coomassie (section 2 21 2) Spots that showed differential protein expression were picked with the ETTAN Spot Picker (section 2 22)

2 20 Stainıng methods

2 20.1 Sılver stainıng 2-D electrophoresıs gels (used to screen samples)

Thıs method ıs used to screen protein samples prıor to labellıng wıth the Cy Dyes After 2-DE, the gels were removed from the plates by very carefully placıng a ruler between the two plates at the top rıght hand corner and the top plate removed gradually Usıng the ruler, the sıde borders of the gel were cut away ın lıne wıth the ends of the IPG strıp at the top of the gel The strıp and agarose were then removed and the gel was lıfted gently and placed ın a gel box contaınıng fixıng solutıon (50ml ethanol, 12 5 ml acetıc acıd (Lennox, 351) and 62 5 ml UHP) The gel boxes were placed on an orbıtal shaker and fixed for at least 30 mınutes (usually overnıght) After fixıng, solutıon was drained from the gels The gels were then washed three tımes wıth 150 ml of UHP for 5 mınutes each tıme and draıned The gels were next sensıtısed (60ml ethanol, 13 6g sodıum acetate, 0 4g sodıum thıosulfate and UHP ın 200ml) for 30 mınutes on the orbıtal shaker

Usıng the method outlıned above the gels were washed three tımes (for 10 mınutes) Followıng the washes, 200 ml of sılver staınıng solutıon was added and the boxes returned to the orbıtal shaker After 20 mmutes the sılver solutıon (0 5g sılver nıtrate, 80ul formaldehyde and 200ml UHP) was draıned and the gels were washed twıce for 5 mınutes each wıth UHP After the last wash, 200 ml of developer (5g sodıum carbonate, 40ul formaldehyde and 200ml UHP) was added to each of the boxes The gels were placed on the orbıtal shaker and allowed to develop When the desıred amount of spots appeared the developer was draıned ınto the sılver contaınıng 5 L drum (thıs precıpıtated out the sılver) and 200 ml of stoppıng solutıon (2 92g EDTA and 200ml UHP) was added The gels were left on the belly dancer for at least 10 mınutes The gels were then scanned at > 300 resolutıon

2.20.2 Brılliant blue G Colloıdal coomassıe staınıng of preparatıve gels for spot pıckıng

After electrophoresıs, the smaller lower plates wıth the gels attached were placed ın the gel boxes contaınıng fixıng solutıon (7% glacıal acetıc acıd ın 40% (v/v) methanol (Aldrıch, 200-659-6)) for at least one hour Durıng thıs step a 1X workıng solutıon of Brılliant Blue G colloıdal coomassıe (Sıgma, B2025) was prepared by addıng 800ml UHP to the stock bottle When the fixıng step had nearly elapsed a solutıon contaınıng 4 parts of 1X workıng colloıdal coomassıe solutıon and 1 part methanol was made, mıxed

by vortexing for 30 seconds and then placed on top of the gels The gels were left to stain for 2 hours To destain, a solution containing 10% acetic acid in 25% methanol was poured over the shaking gels for 60 seconds The gels were then rinsed with 25% methanol for 30 seconds and then destained with 25% methanol for 24 hours The glass surface was dried and two reference markers (Amersham) attached to the underside of the glass plate before scanning The resulting image was imported into the ImageMaster software (Amersham) and the spots were detected, normalised and the reference markers selected While keeping the shift key depressed, all spots of interest were manually selected The resulting image was saved and exported into the Ettan Spot Picker software

2.21 Spot picking

The stained gel was placed in the tray of the Ettan Spot Picker (Amersham, 18-1145-28) with reference markers (Amersham, 18-1143-34) aligned appropriately and covered with UHP The imported pick list was opened, the syringe primed and the system was set up for picking the spots from the pick list The spots were robotically picked and placed in 96-well plates, which were stored at 4°C until spot digestion

2.22 Spot digestion and identification with MALDI-TOF

The 96-well plate was placed in the Ettan Digester (Amersham, 18-1142-68) to digest the protein as follows Step 1 – the gel plugs were washed three times for 20 minutes each with 50µl 50mM ammonium bicarbonate (Sigma, A6141) in 50% methanol Step 2 – the gel plugs were washed twice for 15 minutes with 50µl 70% acetonitrile (Sigma, 34967) The gel plugs were left to dry for at least 60 minutes After drying, the individual gel pieces were rehydrated in 10µl digestion buffer (12 5ng trypsin (Promega, V5111) per µl of 10% acetonitrile, 40mM ammonium bicarbonate) Exhaustive digestion was carried out overnight at 37°C After digestion, the samples were transferred as follows Step 1 – A volume of 40µl of 0 1% trifluoroacetic acid (Sigma, 302031) in 50% acetonitrile was added to the wells, mixed and left for 20 minutes A volume of 60µl of this solution was transferred to a fresh 96-well plate Step 2 - A volume of 30µl of 0 1% trifluoroacetic acid in 50% acetonitrile was added to the wells, mixed and left for 20 minutes A volume of 50µl of this solution was transferred to the fresh 96-well plate The liquid in the plate was vacuum-dried in a maxi dry plus After drying, the 96-well plate was placed in the Ettan Spotter (Amersham, 18-1142-67)

for spotting onto the target plates A volume of 3µl of 0 5% trifluoroacetic acid in 50% acetomtrile was added to the desiccated peptides and mixed 5 times A volume of 0 3µl of this mixture was spotted onto the target plate after which a volume of 0 3µl matrix solution [7 5mg/ml a-cyano-4-hydroxycinnamic acid (LaserBio labs, 28166-41-8) in 0 1% trifluoroacetic acid in 50% acetonitrile]

The target plate was placed in the MADLI-ToF (Amersham, 11-0010-87) instrument The system was set up as follows the target plate was disengaged from the machine A new empty run list was opened In the acquisition mode of the "favorites" icon, the "spectrum processes", specifically PepMix 4 (LaserBio labs, C104) was picked, and "protein digest optimised" were successively selected and dragged to positions 1 and 2-24 respectively on the target slide Within the identification section of favorites, "protein digest Homo sapiens IAA" was selected and dragged to positions 2-24 on the target slide The run list for slide 1 was saved and associated to position 1 on the previously disengaged tray Selecting process and play then started the MALDI

Mass spectra were recorded operating in the positive reflector mode at the following parameters accelerating voltage 20 kV, and pulsed extraction on (focus mass 2500) Internal and external calibration was performed using trypsin autolysis peaks at 842 509 m/z, 2211 104 m/z and PepMix 4 respectively Calibration usmg Pep4 was performed as follows Once two spectra were generated for the PepMix 4 mix (position 1 on the slide), the acquisition of spectra was stopped The first spectrum of sample one was selected and the calibrant peaks readjusted for accuracy The five individual peaks cover the 500-3500 Da mass range and include bradykinin fragment 1-5 (573 315), angiotensin II human (1046 5424), neurotensin (1672 9176) and insulin B chain oxidised (3494 6514) Once calibration was completed it was saved as the new "system calibration" The MALDI was then restarted The mass spectra generated for each of the proteins were analyzed usmg MALDI evaluation software (Amersham Biosciences) Protein identification was achieved with the PMF Pro-Found search engine for peptide mass fingerprints

An example of a mass spectra generated for annexin A1 is seen in Figure 2 1, whereby the sequence coverage is 26 4% with seven of the 15 peptides used 907 419, 1261 623, 1549 833, 1677 909, 1701 891, 1738 722 and 1904 004 The sequence coverage with peptide information and p value for each of identified proteins in the thesis is presented in the appendices

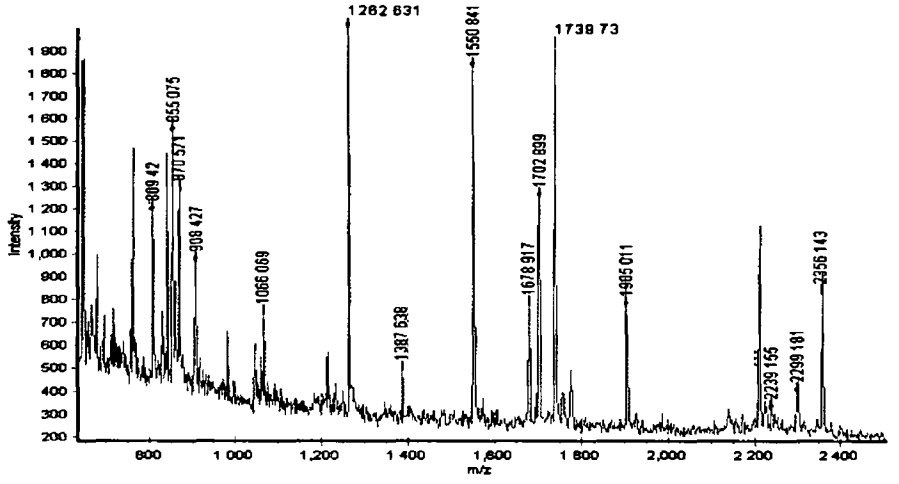

Figure 2.1 Mass spectra for the annexin 1 protein with sequence coverage of 26.4%

2.23 PathwayAssist of identified proteins

PathwayAssist is a product aimed at the visualisation and analysis of biological pathways, gene regulation networks and protein interaction maps The PathwayAssist automated software is comprised of two tools, namely MedScan and ResNet The Medscan algorithm is a text-mining tool that extracts biological interaction information by reading digital text documents (e g biomedical journal articles and abstracts) It efficiently scans sentences searching for co-occurrences of biological terms to locate connecting verbs such as *binds, inhibits, modulates or phosphorylates* - between the co-occurring terms The ResNet database is a repository of over 500,000 biological interactions for more than 50,000 proteins including human, mouse, rat, yeast, drosophila, and *C eligans*, which are extracted from the current literature PathwayAssist permits the identification of biological interactions among genes and proteins of interest from the published literature, and provides links to the supporting sentences in the matching journal article citations (for articles available online in PubMed) The software can also connect two genes/proteins with the shortest possible path, import a list of genes/protems, which can then be arranged into a pathway and finally find common upstream and downstream regulators of a gene/protein

Section 3.0: Results

3 1 Development of multidrug resistant variants by pulse selection

Two squamous and two small cell lung carcinoma cell lines were chosen for drug treatment on the basis of no previous exposure to chemotherapeutic drugs Each parental cell line was pulsed with two clinically relevant drugs namely a taxane (taxotere and/or taxol) and a platinum drug (carboplatin), which are commonly used to treat lung cancer (Table 3 1 1) The two squamous cell carcinomas cell lines (SKMES-1 and DLRP) and one small cell carcinoma cell line, DMS-53 were pulsed with a taxane and carboplatin, whereas the NCI-H69 cell line was pulsed with carboplatin and VP-16 Pulse selection of the cell lines with taxol, taxotere, VP-16 and carboplatin resulted in the establishment of twelve novel drug resistant variants These were denoted "-Txl", "-Txt", "-VP" and "-Cpt" for the taxol, taxotere, VP-16 and carboplatin-selected cells respectively

Cell Line	Taxol (ng/ml)	Taxotere (ng/ml)	VP-16 (ng/ml)	Carboplatin (μg/ml)
DLRP	Not Treated	5	Not Treated	15
DMS-53	60	40	Not Treated	5
SKMES-1	120	60	Not Treated	100 and 30
NCI-H69	Not Treated	Not Treated	480	10 and 5

Table 3 1 1 Lung cancer cell lines and drug concentrations used for pulse selections

3.1 1 Determination of sensitivity of parental cell lines to chemotherapeutic agents

The parent cell lines were analysed using an *in vitro* toxicity assay to determine the IC_{50} value (drug concentration that kills half of the cell population) of the drugs chosen for drug selection and the following panel of drugs adriamycin, cisplatin, 5-fluorouracil and vincristine (section 2 8 1)

The parent cell lines examined showed quite marked differences in sensitivity to the range of drugs tested (Table 3 1 2) The cell line SKMES-1 is 3-fold more resistant to cisplatin compared to DLRP By contrast, DLRP is 14-fold, 5 6-fold, 7 5-fold and 7 3-fold more resistant to 5-FU, adriamycin, taxol and VP-16 respectively compared with SKMES-1 Interestingly, both squamous cell carcinoma cell lines show similar resistance patterns to taxotere and vincristine Within the small cell carcinoma group, NCI-H69 is more sensitive to all drugs except adriamycin and taxol in comparison to DMS-53 DMS-53 in turn is more resistant to the taxanes and vincristine when compared with both squamous cell lines

Drug	SKMES-1 (ng/ml)	DLRP (ng/ml)	DMS-53 (ng/ml)	NCI-H69 (ng/ml)
Taxotere	0 7 ± 0 06	0 7 ± 0 1	8 2 ± 0 3	0 23 ± 0 03
Taxol	1 2 ± 0 1	9 ± 0 9	12 9 ± 1 3	13 3 ± 2 3
Adriamycin	7 3 ± 0 4	40 7 ± 3 1	15 ± 1 7	42 3 ± 6 4
Carboplatin	4600 ± 200	3500 ± 360 6	1200 ± 100	740 ± 112 7
Cisplatin	671 7 ± 77 5	223 ± 21 4	151 7 ± 12 6	110 ± 20
5-FU	89 3 ± 6 6	1250 ± 132 3	733 3 ± 57 7	90 ± 10
Vincristine	3 8 ± 0 3	3 3 ± 0 2	8 5 ± 0 9	3 9 ± 0 3
VP-16	60 3 ± 1 9	438 3 ± 40 7	295 ± 22 9	72 ± 2

Table 3 1 2 IC_{50} values for a range of chemotherapeutic drug acting on the cell lines SKMES-1, DLRP, DMS-53 and NCI-H69 The values are given as the average IC_{50} value ± the standard deviation on a minimum of three repeats

3.1.2 Establishment of taxotere-selected variant of SKMES-1

The SKMES-1 cell line was exposed to an IC_{90} value (determined from a pulse exposure in a 25 cm^2 flask) of 60ng/ml taxotere for four hours, once a week for ten consecutive weeks. The cell line resulting from this exposure was designated SKMES-Txt.

Toxicity assays were carried out at the following time points:

1: after the final pulse - before cells were frozen in liquid nitrogen,

2: after one month in liquid nitrogen

3: after fifteen months storage in liquid nitrogen (Table 3.1.3)

Cell Line	Liquid Nitrogen Storage Time
SKMES-Txt	Pre-Storage
SKMES-Txt	One Month
SKMES-Txt	Fifteen Months

Table 3.1.3 Summary of SKMES-Txt selections

3.1.2.1 Morphology of the taxotere variant of SKMES-1

The morphology of SKMES-Txt was found to have changed during the selection procedure with taxotere (Figures 3.1.1 and 3.1.2). The cell line (similar to the parent) required cell-to-cell contact for growth. Images were taken at 10X magnification.

Figure 3.1.1 SKMES-1

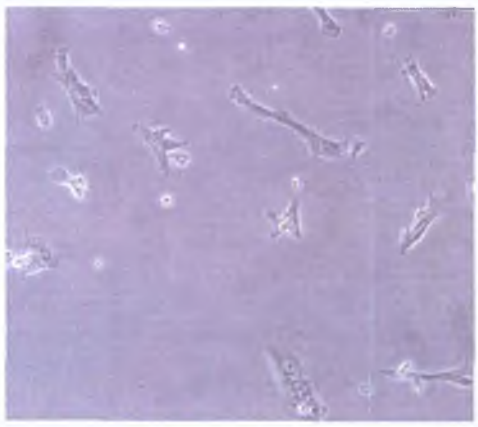

Figure 3.1.2 SKMES-Txt

3 1.2 2 Resistance and cross-resistance profiles of SKMES-Txt immediately after pulse selection

After the final pulse with taxotere, SKMES-Txt was left to recover for one week before toxicity assays were carried each week for one month for eight drugs as described in section 2 8

SKMES-Txt was 16-fold resistant to taxotere when tested one week after pulsing The resistance increased and stabilised in weeks 2, 3 and 4 (26 7-fold, 26 7-fold and 25 3-fold respectively) (Table 3 1 4, Figure 3 1 3)

Stable cross-resistance developed to Adriamycin and VP-16 (2 1-fold and 3 7 fold respectively) Moreover, as a result of the selection process, the cell line developed unusual cross-resistance to 5-FU (13-fold) SKMES-Txt developed no cross-resistance to the platinum drugs (Table 3 1 5, Figure 3 1 4)

Drug	SKMES-1	Week 1	Week 2	Week 3	Week 4
Taxotere (ng/ml)	0 71 ± 0 06	11 4 ± 1 7	19 ± 1 8	19 ± 2 9	19 4 ± 1 6

Table 3 1 4 IC_{50} values for taxotere acting on the cell line SKMES-Txt before freezing Toxicity assays were only carried out once at each week and are given as the average

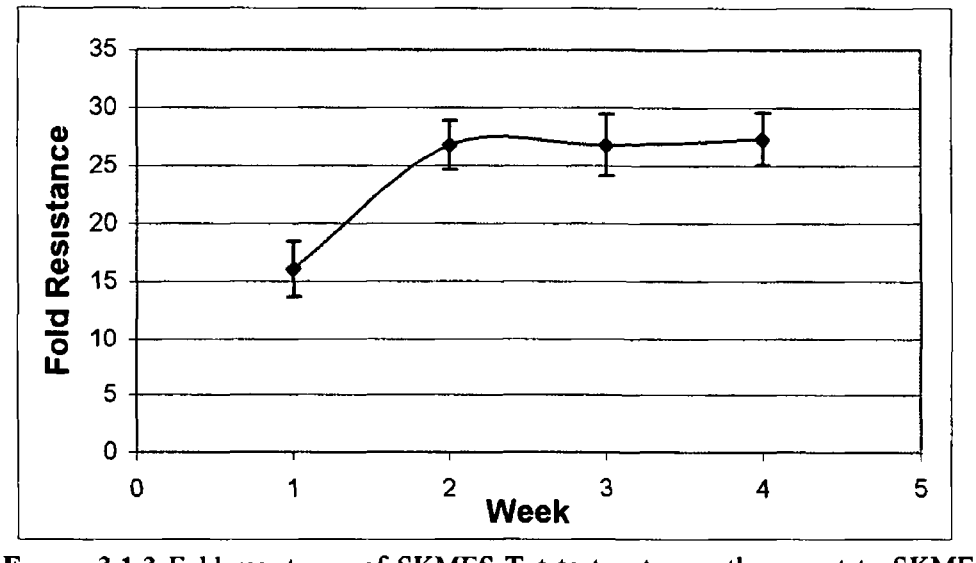

Figure 3 1 3 Fold resistance of SKMES-Txt to taxotere with respect to SKMES-1 over four weeks, as determined by comparing IC_{50} values IC_{50} value ± standard deviation of the eight rows of a 96 well plate

Drug	IC_{50} SKMES-1 (ng/ml)	IC_{50} SKMES-Txt (ng/ml)	Fold Resistance
Carboplatin	3350 ± 200	3120 ± 216	0.93
Cisplatin	671.7 ± 72.2	682 ± 53.7	1
5-FU	85 ± 8.75	1115 ± 164	13
VP-16	66.8 ± 6.98	250 ± 56	3.7
Adriamycin	7 ± 0.74	14.5 ± 2.7	2.1

Table 3.1.5: IC_{50} values for a range of chemotherapeutic drugs acting on the cell line SKMES-Txt before freezing. Toxicity assays were carried out once at each week. Values are given as the average of four IC_{50} values ± standard deviation over the month.

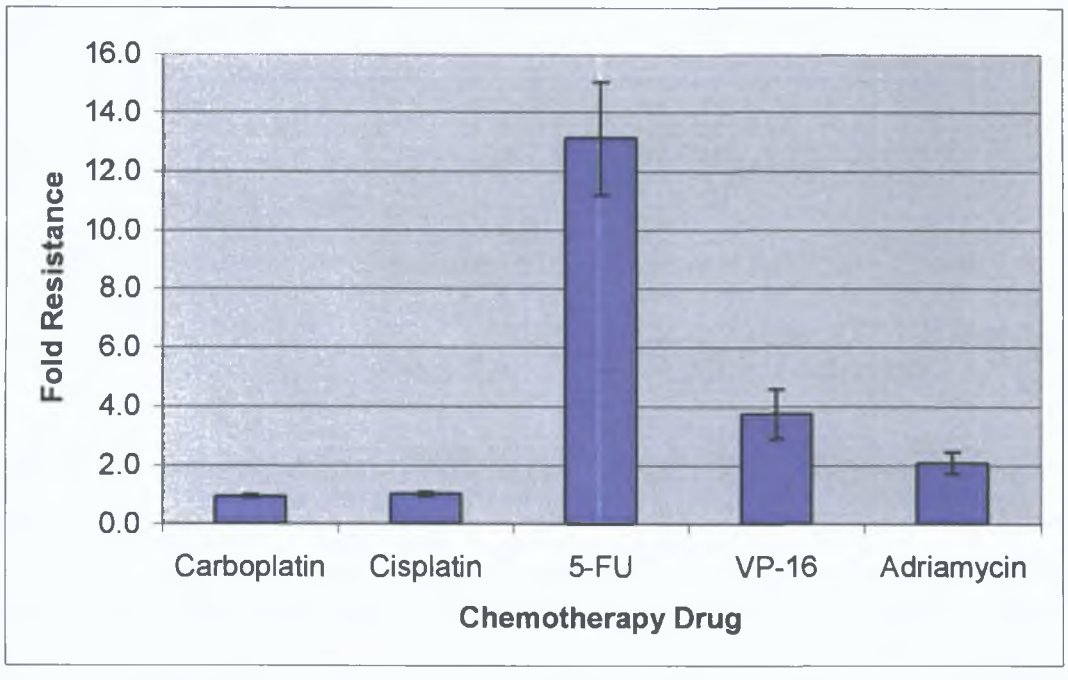

Figure 3.1.4 The fold increases in resistance in SKMES-Txt with respect to SKMES-1 over four weeks, as determined by comparing IC_{50} values.

3 1 2 3 Resistance and cross-resistance profiles of SKMES-Txt after one-month storage in liquid nitrogen

After a period of one-month storage in liquid nitrogen, SKMES-Txt were thawed and the resistance and cross-resistance measured for eight drugs as described in section 2 8 The toxicity assays were carried out on each of the eight drugs every week for at least one month after thawing (Figure 3 1 5)

The resistance to taxol and taxotere was found to have altered with one-month storage in liquid nitrogen

SKMES-Txt was 5 6-fold resistant when tested one week after thawing The resistance increased and stabilised in weeks 2 and 3 (29-fold and 30 9-fold respectively) however, resistance fell sharply to 16 6-fold by week 4 Unstable cross-resistance to taxol also developed in this cell line The cell line was 63-fold resistant when tested one week after thawing (Table 3 1 6) Interestingly, taxol resistance fell at each of the subsequent weeks tested (Figure 3 1 5)

Similar to results to cells tested immediately after pulse selection, stable cross-resistance developed to adriamycin, vincristine and VP-16 (7 3-fold, 19 6-fold and 3 8 fold respectively) Moreover, as a result of the selection process, the cell line developed unusual cross-resistance to 5-FU (13 2-fold) SKMES-Txt developed no cross-resistance to the platinum drugs (Table 3 1 7, Figure 3 1 6)

IC_{50} values of SKMES-Txt (ng/ml)					
Drug	**SKMES-1**	**Week 1**	**Week 2**	**Week 3**	**Week 4**
Taxotere	0 71 ± 0 06	4 ± 0 4	21 ± 2 8	22 ± 2 8	11 8 ± 0 3
Taxol	1 2 ± 0 1	63 ± 11	49 9± 5 1	36 2 ± 4 8	30± 2 1

Table 3 1 6 IC_{50} values for a range of chemotherapeutic drugs acting on the cell line SKMES-Txt after one month frozen The values are given as the average IC_{50} value ± the standard deviation on two repeats for taxotere and once for taxol

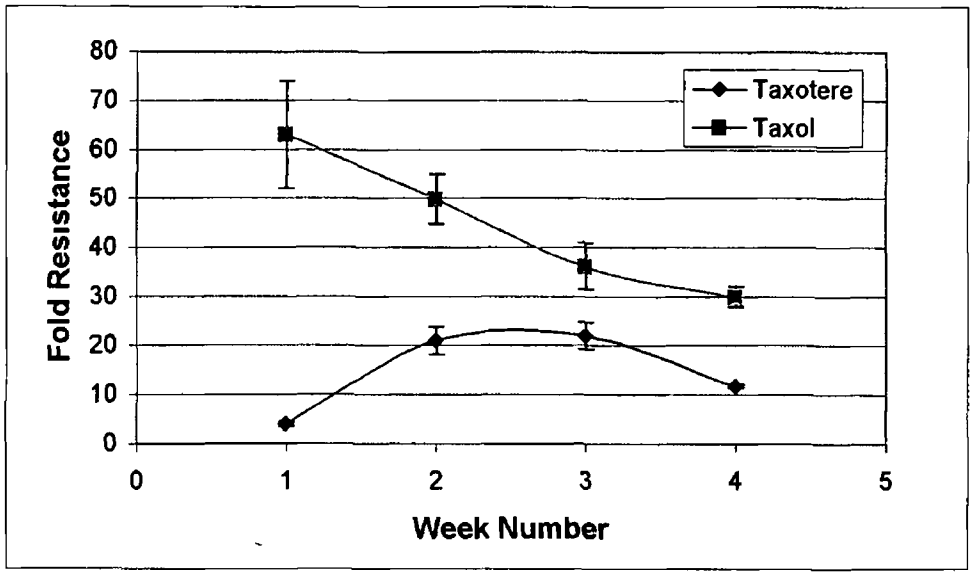

Figure 3 1 5 The fold increases in resistance to the taxanes in SKMES-Txt with respect to SKMES-1 over four weeks, as determined by comparing IC_{50} values

Drug	IC_{50} SKMES-1 (ng/ml)	IC_{50} SKMES-Txt (ng/ml)	Fold Resistance
Carboplatin	3350 ± 200	3350 ± 290	1
Cisplatin	671 7 ± 72 2	687 ± 33	1 02
5-FU	85 ± 8 75	1123 ± 170	13 2
VP-16	66 8 ± 6 98	259 ± 20 7	3 8
Vincristine	1 15 ± 0 07	22 5 ± 3 2	19 6
Adriamycin	7 ± 0 74	51 16 ± 4 3	7 3

Table 3 1 7 IC_{50} values for a range of chemotherapeutic drugs acting on the cell line SKMES-Txt after one-month storage in liquid nitrogen The values are given as the average IC_{50} value ± the standard deviation on a minimum of three repeats The fold increases in resistance to chemotherapeutic drugs in SKMES-Txt with respect to SKMES-1, as determined by comparing IC_{50} values

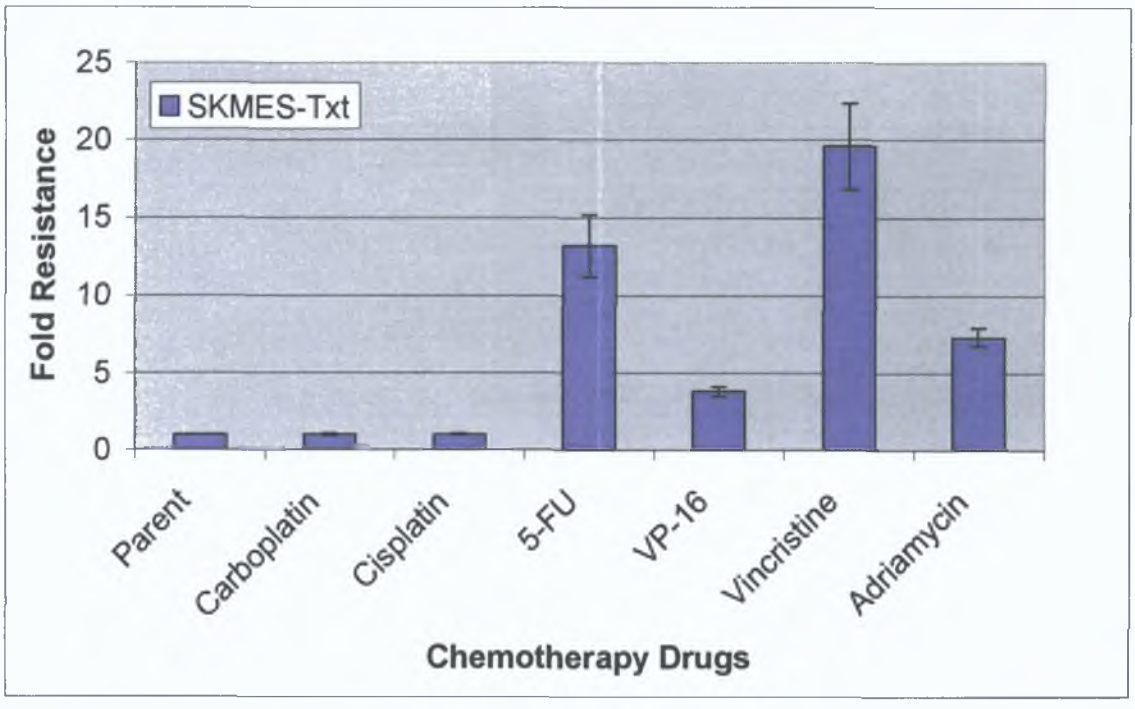

Figure 3.1.6 The fold increases in resistance to chemotherapeutic drugs in SKMES-Txt with respect to SKMES-1, as determined by comparing IC_{50} values

3.1.2.4 Resistance profiles of SKMES-Txt after fifteen-months storage in liquid nitrogen

After a period of fifteen-months storage in liquid nitrogen, SKMES-Txt were thawed and the resistance and cross-resistance measured for eight drugs as described in section 2.8.The toxicity assays were carried out on each of the eight drugs every week for at least six weeks after thawing.

Table 3.1.8 and Figures 3.1.7 and 3.1.8 demonstrate that SKMES-Txt has lost further resistance to all drugs tested when compared to pre-freezing and after one-month storage in liquid nitrogen (Tables 3.1.4 3.1.6). Taxotere and taxol resistance has fallen sharply with long-term storage in this cell line. The cell line after fifteen-months storage in liquid nitrogen is 5.9-fold and 4.4-fold resistant to taxotere at weeks 2 and 4 compared to 29-fold and 16.6-fold at the same weeks after one-month storage in liquid nitrogen. There is a significant loss of resistance to taxol, the cell line is now 10.6-fold resistant at week 2 (was 41.5-fold). This Figure drops to 5.3-fold at week 4 (was 25-fold). Resistance to both taxanes continued to fall at each subsequent week tested.

Stable but lower cross-resistance to 5-FU and vincristine developed (8 ± 0.6 and 3.4 ± 0.5 fold respectively, values averaged over 6 weeks ± standard deviation). SKMES-Txt

retained the same cross-resistance to VP-16 and adriamycin but resistance to both drugs decreases over the six weeks tested

	Fold Resistance of SKMES-Txt				
Drug	**Week 2**	**Week 3**	**Week 4**	**Week 5**	**Week 6**
Taxotere	5 9 ± 0 2	4 6 ± 0 2	4 4 ± 0 1	2 7 ± 0 1	3 7 ± 0 2
Taxol	10 6 ± 0 6	9 4 ± 1	7 8 ± 0 1	5 3 ± 0 7	6 6 ± 0 7
5-FU	9 6 ± 0 4	7 7 ± 0 01	Not done	7 6 ± 0 06	8 7 ± 0 7
Adriamycin	4 3 ± 0 4	2 8 ± 0 1	4 6 ± 0 4	2 5 ± 0 06	2 9 ± 0 4
VCR	4 5 ± 0 6	3 1 ± 0 2	4 0 ± 0 7	3 0 ± 0 09	3 6 ± 0 1
VP-16	11 8 ± 0 97	4 5 ± 0 1	5 6 ± 0 2	3 9 ± 0 08	6 3 ± 0 1

Table 3 1 8 The fold increase in resistance to chemotherapeutic drugs in SKMES-Txt with respect to SKMES-1 after fifteen months storage in liquid nitrogen, as determined by comparing IC_{50} values The values are given as the average IC_{50} value ± the standard deviation on a minimum of three repeats

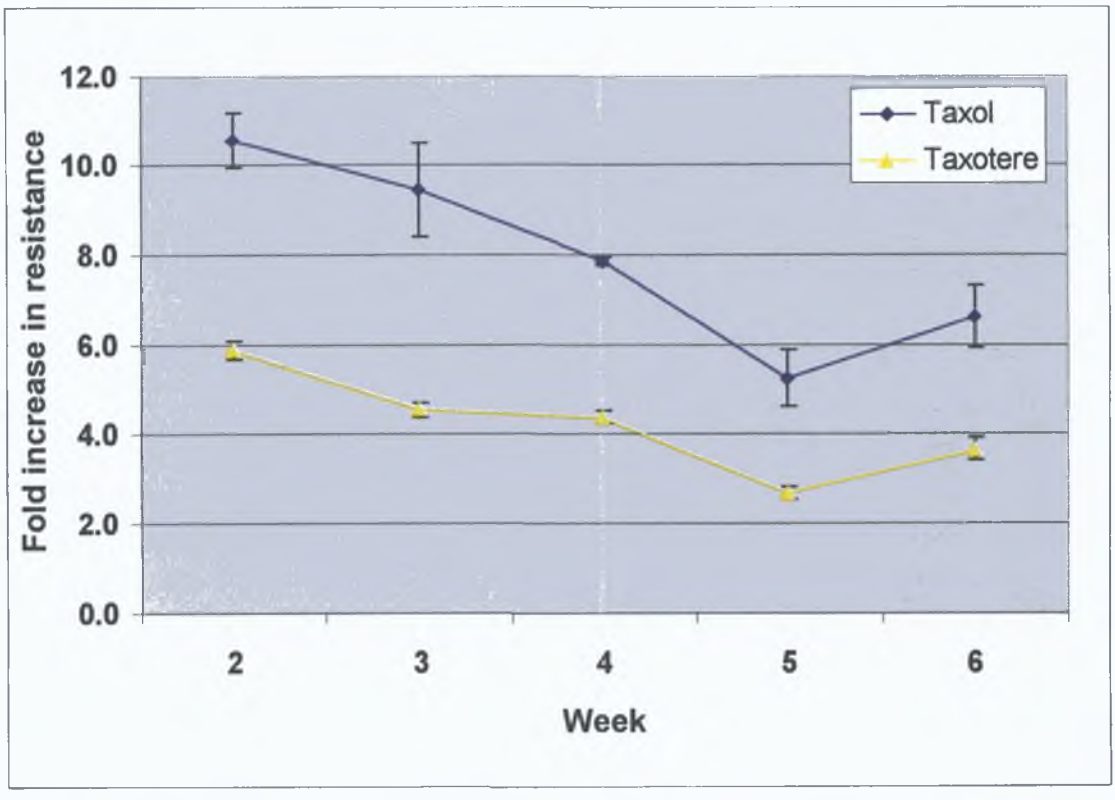

Figure 3.1.7 Fold Resistance of SKMES-Txt to Taxol and Taxotere over 6 weeks after 15 months in liquid nitrogen with respect to SKMES-1 as determined by comparing IC_{50} values.

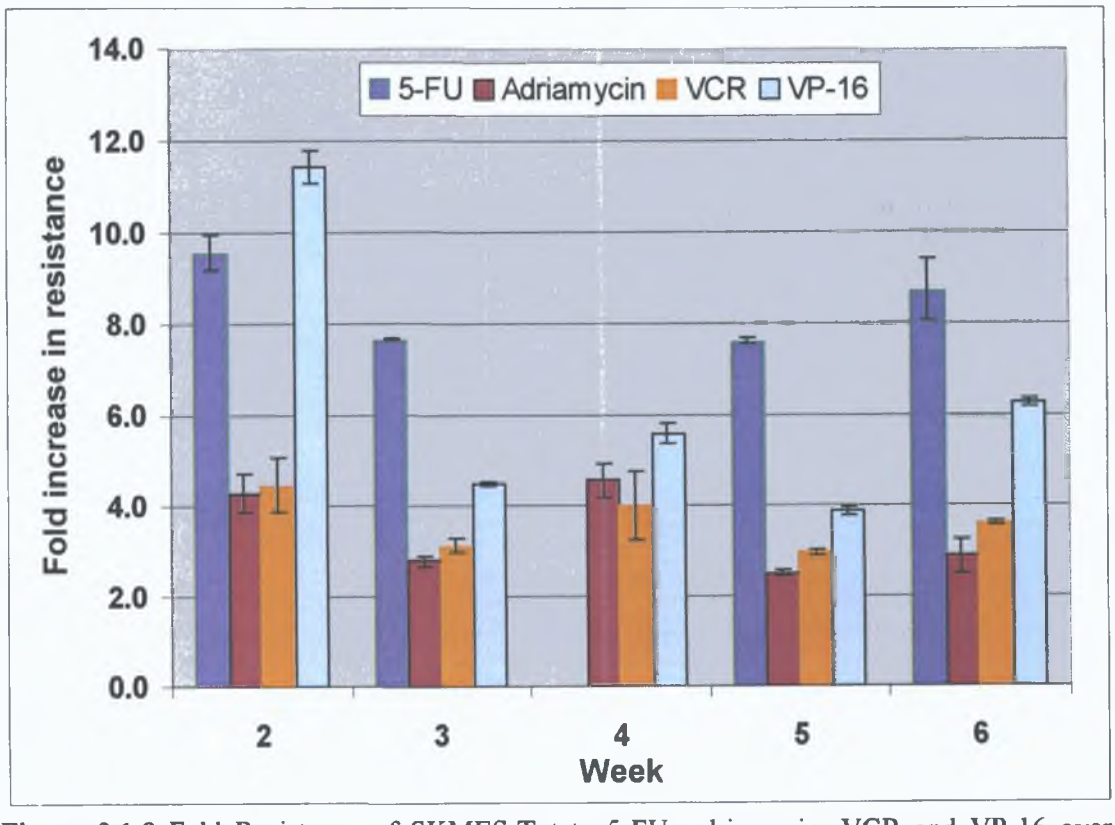

Figure 3.1.8 Fold Resistance of SKMES-Txt to 5-FU, adriamycin, VCR and VP-16 over 6 weeks after 15 months in liquid nitrogen with respect to SKMES-1, as determined by comparing IC_{50} values.

3.1.2.5 Establishment of SKMES-Txt(11)

It was decided to attempt to further increase the resistance of SKMES-Txt to taxotere. The cell line was cultured for seven weeks then exposed to 60ng/ml taxotere for four hours. The cell line was left to recover for one week. The cell line resulting from this exposure to taxotere was designated SKMES-Txt(11).

Table 3.1.9 and Figure 3.1.9 demonstrates the effect of an additional pulse of taxotere on SKMES-Txt after seven weeks in culture. The pulse resulted in a cell line that is now 169-fold resistant to taxotere and 41-fold cross-resistant to taxol.

Drug	**Week 4**	**Week 5**	**Week 6**	**Week 7**	**Week 7 pulse11**
Taxol	7.8 ± 0.1	5.3 ± 0.7	6.6 ± 0.7	7.3 ± 0.8	41.1 ± 1
Taxotere	4.4 ± 0.1	2.7 ± 0.1	3.7 ± 0.2	3 ± 0.2	169 ± 0.0

Table 3.1.9: The fold increase in resistance to the taxanes after a pulse with taxotere at week 7 in SKMES-Txt with respect to SKMES-1 after fifteen months storage in liquid nitrogen, as determined by comparing IC_{50} values. The values are given as the average IC_{50} value ± the standard deviation on a minimum of three repeats.

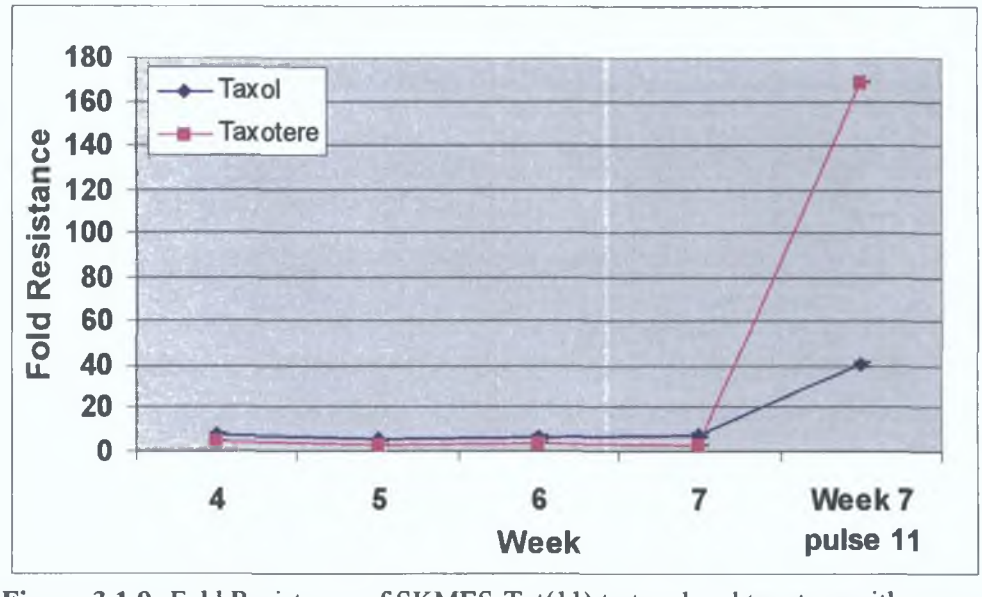

Figure 3.1.9: Fold Resistance of SKMES-Txt(11) to taxol and taxotere with respect to SKMES-1, as determined by comparing IC_{50} values.

3 1 3 Development of the taxol resistant variant of SKMES-1

SKMES-1 was also exposed to an IC_{90} (determined from a pulse selection in a 25 cm^2 flask) value of 120ng/ml of taxol for four hours, once a week for ten consecutive weeks (section 2 10) The cell line resulting from this exposure was designated SKMES-Txl Toxicity assays were performed after the cell line was frozen in liquid nitrogen for one-month and eight months (Table 3 1 10)

Toxicity assays were carried out at the following time points

1 after one month in liquid nitrogen

3 after eight months storage in liquid nitrogen (Table 3 1 3)

Cell Line	Liquid Nitrogen Storage Time
SKMES-Txl	One Month
SKMES-Txl	Eight Months

Table 3 1 10 Summary of SKMES-Txl selections

3.1 3 1 Morphology of the Taxol Variant of SKMES-1

The morphology of SKMES-Txl was found to have changed during the selection procedure with taxol (Figures 3 1 10 and 3 1 11) The cell line (like the parent and SKMES-Txt) required cell-to-cell contact for growth Images were taken at 10X magnification

Figure 3 1 10 SKMES-1

Figure 3 1 11 SKMES-Txl

3.1 3.2 Resistance profiles of SKMES-Txl after one-month storage in liquid nitrogen

The resistance and cross-resistance profiles of SKMES-Txl were determined for eight drugs using the long-term toxicity assay (section 2 8 1) The toxicity assays were carried out on each of the eight drugs two, three and four weeks after the final 12ng/ml pulse with taxol Table 3 1 12 shows the fold resistance patterns of SKMES-Txl to each of the drugs after one-month storage in liquid nitrogen

SKMES-Txl developed high but unstable resistance to taxol with 72 9-fold resistance on week 2, which dropped to 12 9-fold 4 weeks after thawing (Table 3 1 12, Figure 3 1 11) The results also demonstrate that SKMES-Txl developed unstable cross-resistance to all other chemotherapy drugs tested Unusual cross-resistance to 5-FU (15 1-fold at week 2) developed while little cross-resistance to the platinum drugs is seen (Figure 3 1 13)

	IC_{50} values of SKMES-Txl (ng/ml)			
Drug	**SKMES-1**	**Week 2**	**Week 3**	**Week 4**
Taxotere	0 7 ± 0 06	21 8 ± 3 1	13 8 ± 1 8	6 9 ± 0 14
Taxol	1 2 ± 0 1	87 5 ± 10 6	72 5 ± 3 5	15 5 ± 0 56
Adriamycin	7 3 ± 0 4	29 2 ± 1 1	26 5 ± 2 6	8 95 ± 0 63
Carboplatin	4600 ± 200	6050 ± 353	6500 ± 141	1500 ± 141
Cisplatin	671 7 ± 77 5	680 ± 99	1125 ± 247	170 ± 14
5-FU	89 3 ± 6 6	1350 ± 212	730 ± 28 2	700 ± 14
Vincristine	3 8 ± 0 3	56 ± 8 4	52 5 ± 6 3	3 3 ± 0 3
VP-16	60 3 ± 1 9	720 ± 28 2	600 ± 127	410 ± 28 2

Table 3 1 11 IC_{50} values for a range of chemotherapeutic drugs acting on the cell line SKMES-Txl after one-month storage in liquid nitrogen The values are given as the IC_{50} value from a 96 well plate at each week Toxicity assays were carried out once for each drug at each week

Drug	SKMES-1	Week 2	Week 3	Week 4
Taxotere	1	31.1	19.7	9.8
Taxol	1	72.9	60.4	12.9
Adriamycin	1	4	3.6	1.2
Carboplatin	1	1.3	1.41	0.3
Cisplatin	1	1	1.67	0.25
5-FU	1	15.1	8.2	7.8
Vincristine	1	17.7	13.8	0.86
VP-16	1	11.9	9.9	6.8

Table 3.1.12: The fold increase in resistance to chemotherapeutic drugs in SKMES-Txl with respect to SKMES-1 after one-month storage in liquid nitrogen, as determined by comparing IC_{50} values

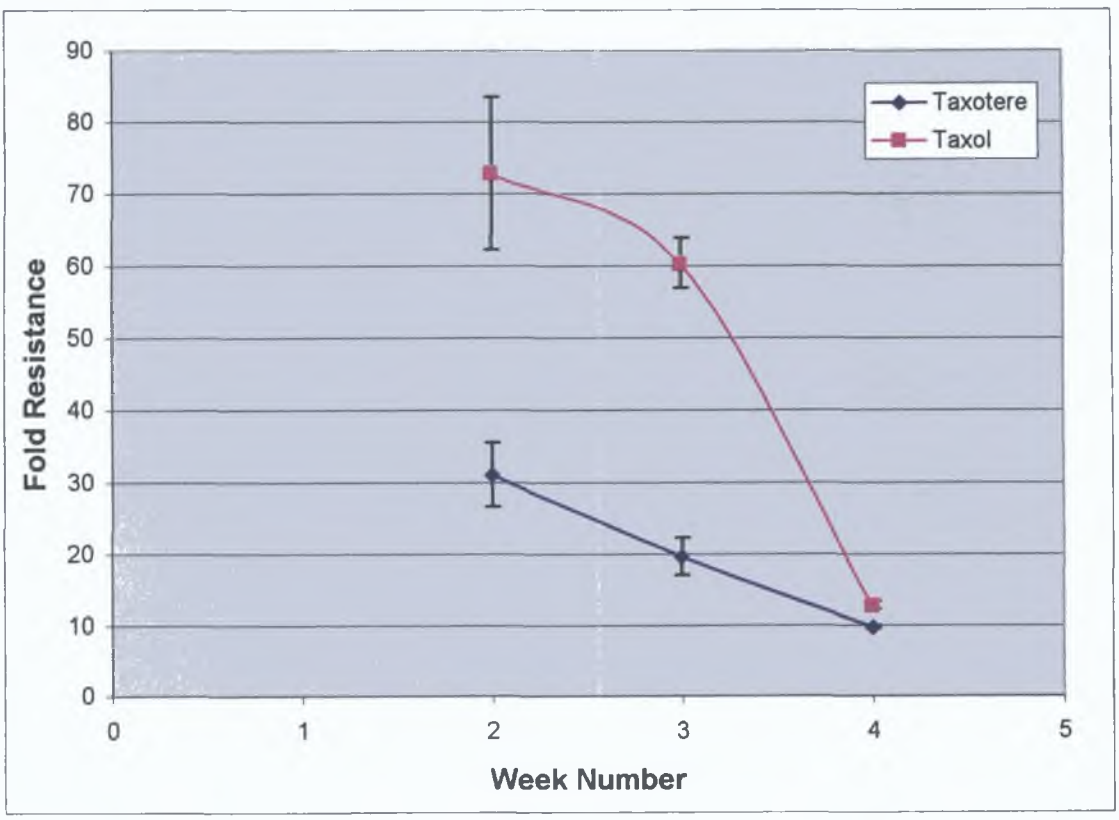

Figure 3.1.12 Fold Resistance of SKMES-Txt to taxol and taxotere with respect to SKMES-1, as determined by comparing IC_{50} values

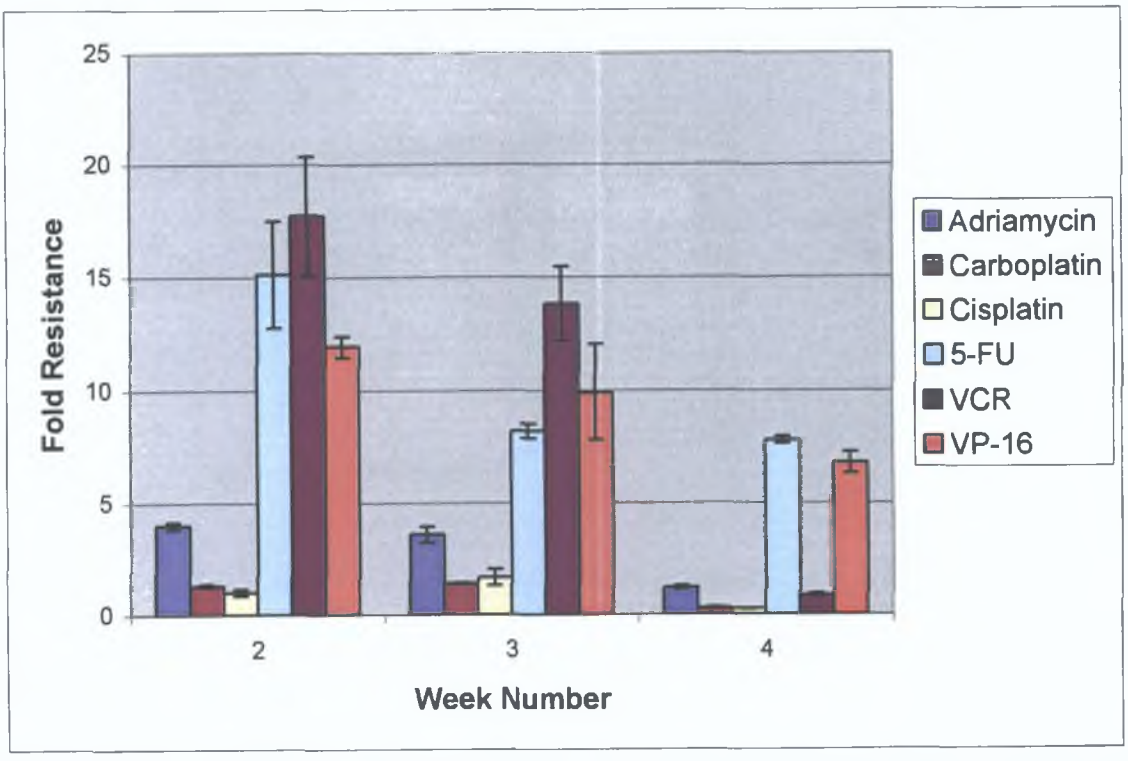

Figure 3.1.13 Fold Resistance of SKMES-Txt to adriamycin, carboplatin, cisplatin, 5-FU, VCR and VP-16 s with respect to SKMES-1, as determined by comparing IC_{50} values

3 1 3 3 Resistance profiles of SKMES-Txl after eight months storage in liquid nitrogen

After eight-months storage in liquid nitrogen the cells were again tested for resistance and cross-resistance to a range of chemotherapeutic drugs

Table 3 1 13 and Figures 3 1 14 and 3 1 15 demonstrate that SKMES-Txl has lost resistance to all drugs tested when compared to Tables 3 1 12 Taxotere and taxol resistance has fallen sharply with storage in this cell line The cell line is now 4 4-fold resistant to taxotere at week 2 (was 28 6-fold) and 3-fold at week 4 (was 9 7-fold) There is a significant loss of resistance to taxol, the cell line is now 8-fold resistant at week 2 (was 76 7-fold) and 5 1-fold at week 4 (was 15 2) Resistance to both taxanes stabilises at from week 4 onwards

Stable but lower cross-resistance to 5-FU, adriamycin and VP-16 developed (7 8 ± 0 3, 2 7 ± 0 4 and 4 5 ± 0 6-fold respectively, values averaged over 6 weeks ± standard deviation)

	Fold Resistance of SKMES-Txl				
Drug	**Week 2**	**Week 3**	**Week 4**	**Week 5**	**Week 6**
Taxol	8 ± 0 3	12 5 ± 0 1	5 1 ± 0 4	5 2 ± 0 3	5 8 ± 0 3
Taxotere	4 4 ± 0 2	6 7 ± 0 2	3 ± 0 1	2 3 ± 0 2	2 95 ± 0 14
Adriamycin	2 8 ± 0 1	2 3 ± 0 1	3 3 ± 0 1	2 4 ± 0 05	2 54 ± 0 04
5-FU	8 2 ± 0 1	7 5 ± 0 4	Not determined	7 5 ± 0 1	7 8 ± 0 1
VCR	3 2 ± 0 1	5 6 ± 0 2	3 ± 0 2	2 8 ± 0 1	3 1 ± 0 1
VP-16	5 1 ± 0 3	4 ± 0 1	4 6 ± 0 2	3 8 ± 0 05	4 9 ± 0 5

Table 3 1 13 The fold increase in resistance to chemotherapeutic drugs in SKMES-Txl with respect to SKMES-1 after eight-months storage in liquid nitrogen, as determined by comparing IC_{50} values, n=3

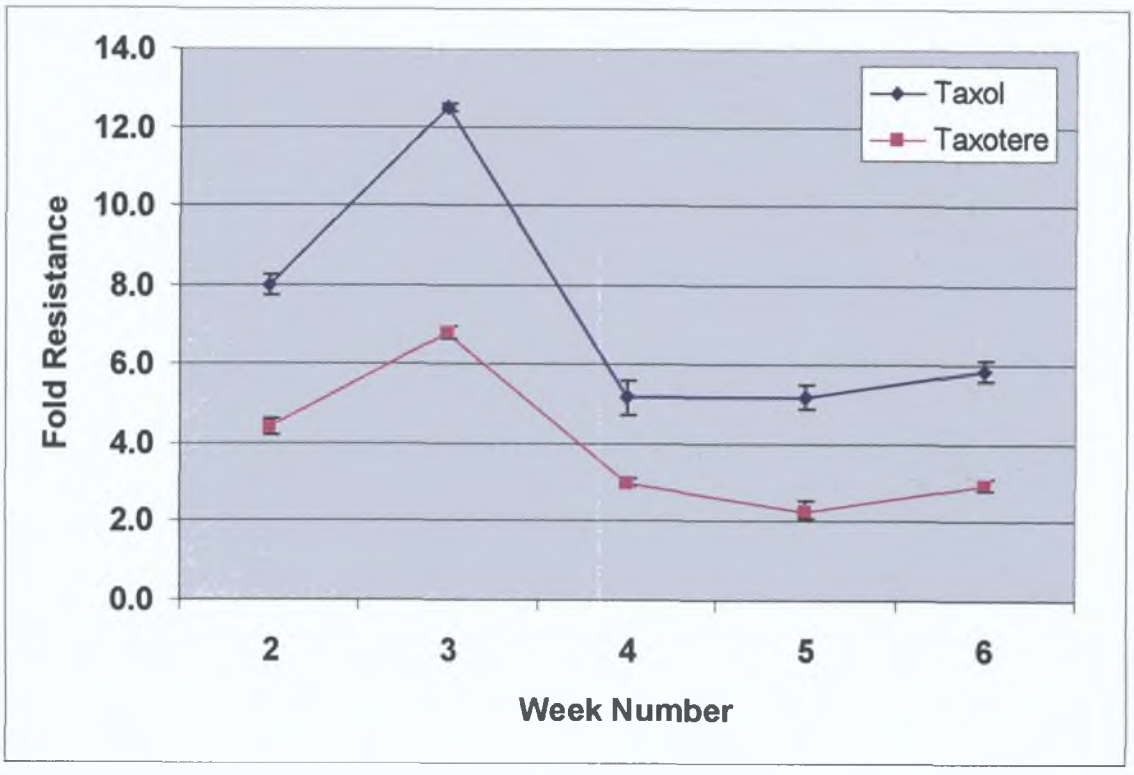

Figure 3.1.14 Fold Resistance of SKMES-Txl to Taxol and Taxotere over 6 weeks with respect to SKMES-1, as determined by comparing IC_{50} values

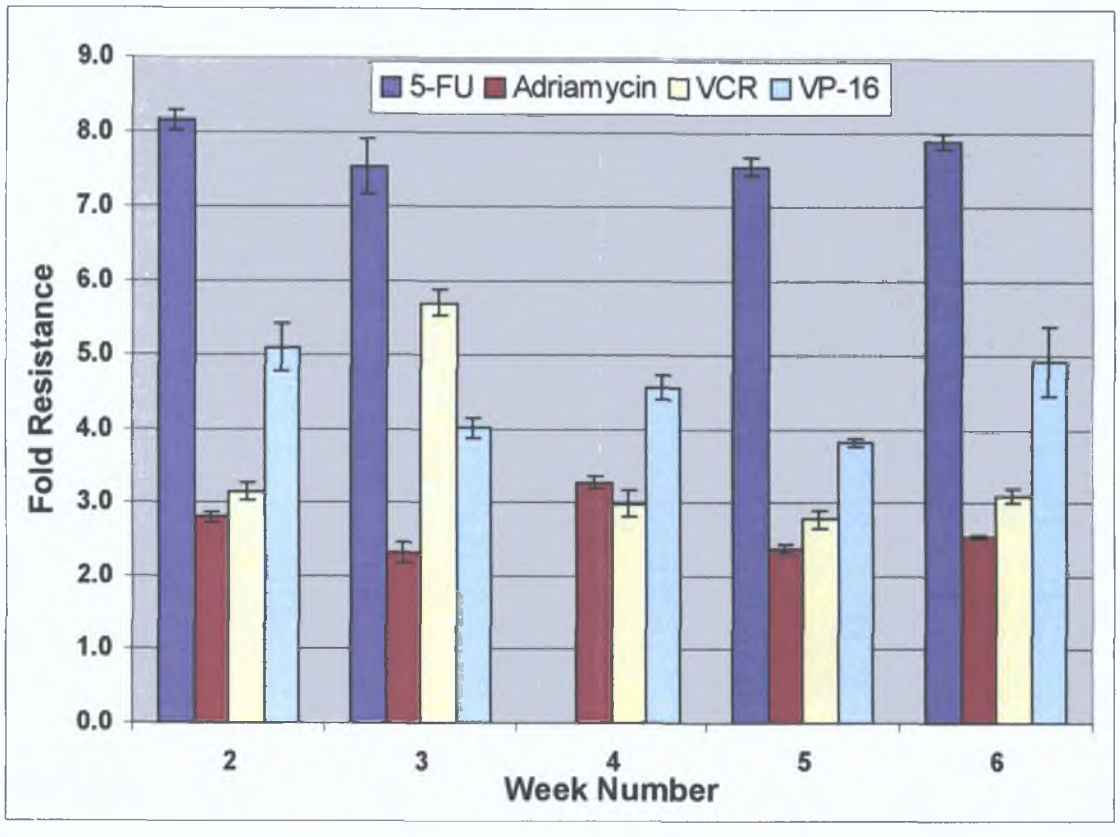

Figure 3.1.15 Fold Resistance of SKMES-Txl to 5-FU, adriamycin, VCR and VP-16 over 6 weeks with respect to SKMES-1, as determined by comparing IC_{50} values.

3.1 3 4 Establishment of SKMES-Txl(11)

In an attempt to further increase the resistance of SKMES-Txl to taxol, the cell line was cultured for seven weeks then exposed to 120ng/ml taxotere for four hours The cell line was left to recover for one week The cell line resulting from this exposure to taxol was designated SKMES-Txl(11)

Table 3 1 14 demonstrates the effect of an additional pulse of taxol on SKMES-Txl after seven weeks in culture The pulse resulted in a cell line that is now 14 4-fold resistant and 4-fold cross-resistant to taxol and taxotere respectively at week 11 where it was 5-fold and 2 5-fold previously

	Fold Resistance of SKMES-Txl				
Drug	**Week 4**	**Week 5**	**Week 6**	**Week 7**	**Week 7 pulse11**
Taxol	5 1 ± 0 4	5 2 ± 0 3	5 8 ± 0 3	5 ± 0 38	14 4 ± 1 6
Taxotere	3 ± 0 1	2 3 ± 0 2	2 95 ± 0 14	2 5 ± 0 1	4 ± 0 1

Table 3 1 14 The fold increase in resistance to the taxanes after a pulse with taxol at week 7 in SKMES-Txl with respect to SKMES-1 after eight months storage in liquid nitrogen, as determined by comparing IC_{50} values, n=3

3 1 4 Establishment of carboplatin selected variants of SKMES-1

The sensitivity of SKMES-1 to carboplatin necessitated two approaches to obtain pulse-selected variants In the first approach, as with other cell lines in this project, the SKMES-1 cell line was exposed to an IC_{90} value of 100 μg/ml carboplatin for four hours, once a week for four consecutive weeks (section 2 10) However, the fourth pulse resulted in almost total cell death The cells were left to recover to almost full confluency before being pulsed again Each of the next four pulses resulted in almost total cell death so the cells were again left to recover after each pulse The final two pulses were consecutive (i e no longer than a week between pulses), as resistance to carboplatin had developed The cell line resulting from this exposure was designated SKMES-Cpt100

In the second approach, pulse selection was performed at an IC_{50} concentration (30μg/ml) The cell line could then be pulsed for four hours once a week for ten consecutive weeks similar to the regime used for other cell lines in this project The cell line resulting from this exposure was designated SKMES-Cpt30

3 1 4 1 Morphology of the carboplatin resistant variants of SKMES-1

The morphology of SKMES-Cpt100 was found to have changed during the selection procedure with carboplatin, these cells are bigger than the parent In contrast, selection with a lower concentration of carboplatin resulted in a cell line with smaller cells It was observed that this cell line (like the parent and the taxane-selected variants) also required cell-to-cell contact for growth as a high growth rate was seen with high cell density (Figures 3 1 16-18)

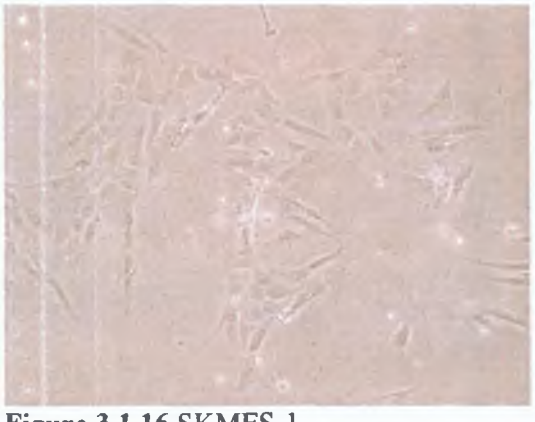

Figure 3.1.16 SKMES-1

Figure 3.1.17 SKMES-Cpt30

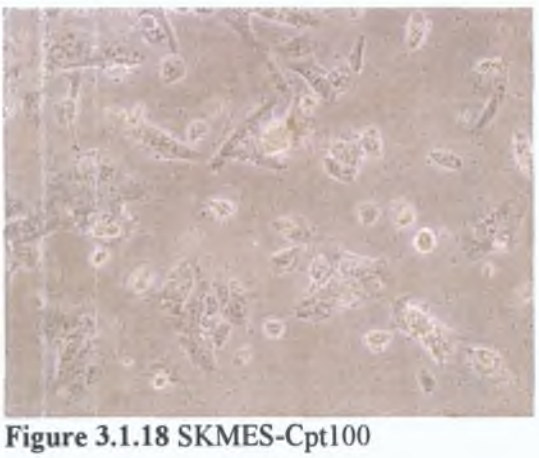

Figure 3.1.18 SKMES-Cpt100

3.1.4.2 Resistance profiles of platinum variants

The resistance and cross-resistance profiles were determined for eight drugs (Table 3.1.15). The toxicity assays were carried out on the SKMES-Cpt100 and SKMES-Cpt30 variants to eight drugs each week for one month after the final 100ug/ml and 30ug/ml pulses with carboplatin. Table 3.1.16, Figure 3.1.19 show the fold resistance patterns of both variants to each of the drugs.

The toxicity profiles demonstrate that the carboplatin resistance of both carboplatin variants was not significantly increased in comparison to the parental cell line, despite the fact that high cell kill was observed during selection with both concentrations of carboplatin.

SKMES-Cpt100 exhibited no cross-resistance to taxotere whereas SKMES-Cpt30 was 2.5-fold resistant. SKMES-Cpt30 became sensitised to 5-FU (0.8-fold), vincristine (0.6-fold) and adriamycin (0.3-fold). SKMES-Cpt100 developed 5.2-fold resistance to 5-FU. Both cell lines showed similarly low levels of cross-resistance to cisplatin and VP-16.

Drug	SKMES-1 (ng/ml)	SKMES-Cpt100 (ng/ml)	SKMES-Cpt30 (ng/ml)
Taxotere	0 7 ± 0 06	0 6 ± 0 1	1 8 ± 0 2
Taxol	2 ± 0 2	4 ± 0 2	4 4 ± 0 2
Adriamycin	7 3 ± 0 4	6 5 ± 0 9	2 1 ± 0 3
Carboplatin	4596 7 ± 150	9233 3 ± 896 3	5333 3 ± 642 9
Cisplatin	671 9 ± 77 5	1165 ± 74 7	1036 ± 31 6
5-FU	89 3 ± 6 6	466 7 ± 75 7	73 3 ± 11 5
Vincristine	3 8 ± 0 3	1 8 ± 0 2	2 4 ± 0 1
VP-16	60 3 ± 1 9	128 3 ±17 6	141 ± 7 9

Table 3 1 15 IC_{50} values for a range of chemotherapeutic drugs acting on the squamous lung carcinoma cell lines SKMES-1, SKMES-C100 and SKMES-C30 The values are given as the average IC_{50} value ± the standard deviation on a minimum of three repeats

Drug	SKMES-Cpt100	P value	SKMES-Cpt30	P value
Taxotere	0 8	0 001	2 5	0 004
Taxol	3 2	0 06	3 6	0 001
Adriamycin	0 9	0 008	0 3	0 000
Carboplatin	2	0 005	1 2	0 18
Cisplatin	1 7	0 079	1 5	0 007
5-FU	5 2	0 011	0 8	0 124
Vincristine	0 5	0 036	0 6	0 005
VP-16	2 1	0 343	2 3	0 002

Table 3 1 16 The fold increase in resistance to chemotherapeutic drugs of SKMES-Cpt100 and SKMES-Cpt30 with respect to SKMES-1, as determined by comparing IC_{50} values

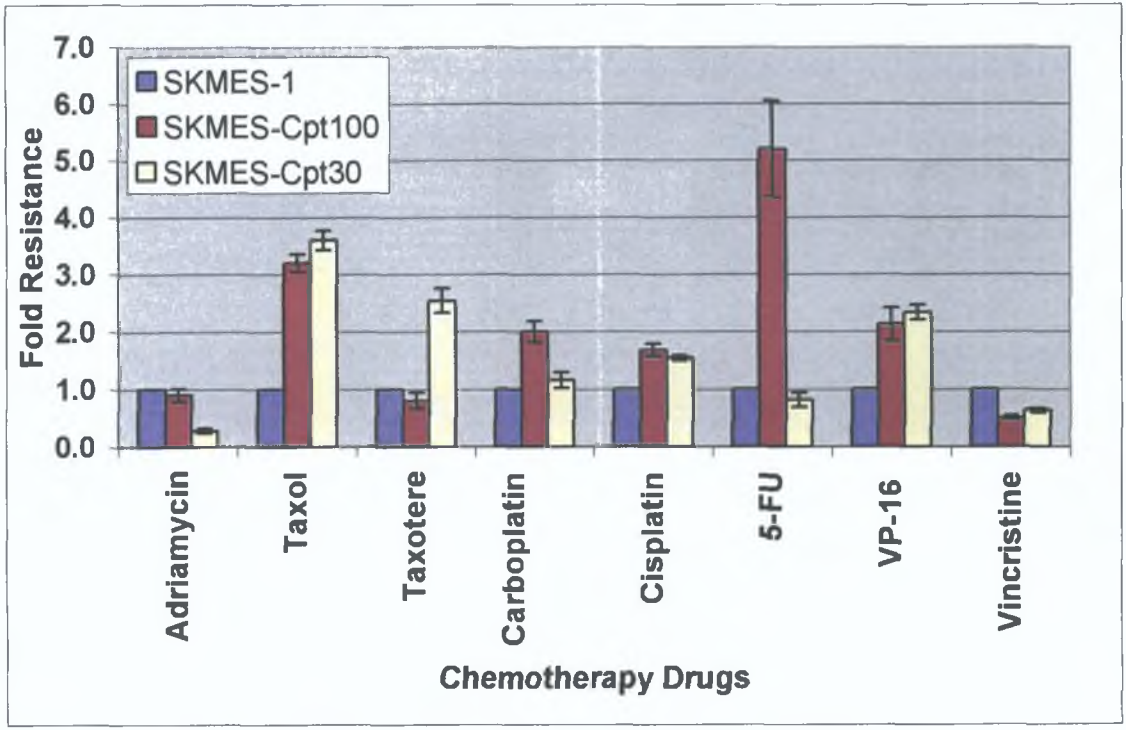

Figure 3.1.19 Resistance Profiles of SKMES-Cpt100 and SKMES-Cpt30

3 1.5 Development of the DLRP-Cpt and DLRP-Txt selected variants

The DLRP squamous cell line (developed in this laboratory) proved to be highly sensitive to carboplatin drug treatment Pulse selection at an IC_{90} value of 100ug/ml carboplatin for four hours, once a week for 4 consecutive weeks resulted in total cell death (section 2 10) It was therefore decided to reduce the carboplatin pulse concentration to an IC_{50} level (50 μg/ml) The result was total cell death at pulse 4 Subsequently, the cell line was pulsed with 15 μg/ml (IC_{10}) of carboplatin All pulses at this concentration resulted in high cell kill so the cells were allowed to recover after each pulse The cell line resulting from this exposure was designated DLRP-Cpt

Similarly to the DLRP carboplatin selections, DLRP proved to be highly sensitive to taxotere drug treatment Pulse selection at an IC_{90} value of 60ng/ml of taxotere for four hours, once a week for 4 consecutive weeks resulted in total cell death The taxotere concentration had to be reduced to 5 ng/ml All pulses at this concentration resulted in high cell kill so the cells were allowed to recover after each pulse The cell line resulting from this exposure to taxotere was designated DLRP-Txt

3 1 5 1 Morphology of the taxotere and carboplatin selected variants of DLRP

The morphology of DLRP-Txt and DLRP-Cpt cell lines were found to have changed during the selection procedure with both drugs The cells have rounded up and almost lost their dendritic-like appearance in both cases The two cell lines required increased cell-to-cell contact for growth in comparison to the parent (which also required it) but to a lesser degree As a result of drug treatment both cell lines developed sensitivity to trypsin and also required their own conditioned media for growth (Figures 3 1 20-22)

Figure 3 1 20 DLRP

Figure 3 1 21 DLRP-Cpt

Figure 3 1 22 DLRP-Txt

3 1 5 2 Resistance profiles of DLRP selections

The resistance and cross-resistance profiles were determined in triplicate for eight drugs using the long-term toxicity assay

The results demonstrate that no resistance to carboplatin developed in DLRP-Cpt despite the fact that high cell kill was observed during selection process (Table 3 1 17-18, Figure 3 1 23) Cross-resistance to VP-16 and taxotere was observed (1 2-fold and 4 6-fold respectively) Interestingly, the cell line became sensitised to adriamycin (0 5-fold) and to cisplatin (0 8-fold) and 5-FU (0 9-fold) to a lesser degree

DLRP-Txt developed low but statistically significant resistance to taxotere (4 4-fold) This cell line also developed cross-resistance to adriamycin (2 7-fold) and to a lesser degree carboplatin, 5-FU, vincristine and VP-16 (1 2-fold, 1 3-fold, 1 5-fold, 1 4-fold and 1 2-fold respectively)

Drug	DLRP (ng/ml)	DLRP-Cpt (ng/ml)	DLRP-Txt (ng/ml)
Taxotere	0 7 ± 0 1	3 2 ± 0 2	3 1 ± 0 4
Taxol	9 ± 0 9	8 7 ± 0 9	11 1 ± 1
Adriamycin	40 7 ± 3 1	21 8 ± 1 8	108 3 ± 7 6
Carboplatin	3500 ± 360 6	3500 ± 300	4633 3 ± 152 8
Cisplatin	223 ± 21 4	174 7 ± 25	198 3 ± 2 9
5-FU	1250 ± 132 3	1150 ± 50	1933 3 ± 230 9
Vincristine	3 3 ± 0 2	3 9 ± 0 5	4 7 ± 0 7
VP-16	438 3 ± 40 7	526 7 ± 25 2	533 3 ± 70 2

Table 3 1 17 IC_{50} values for a range of chemotherapeutic drugs acting on the squamous lung carcinoma cell lines DLRP, DLRP-Cpt and DLRP-Txt The values are given as the average IC_{50} value ± the standard deviation on a minimum of three repeats

Drug	DLRP-Cpt	P value	DLRP-Txt	P value
Taxotere	4 6	0 001	4 4	0 008
Taxol	1 0	0 698	1 2	0 051
Adriamycin	0 5	0 002	2 7	0 001
Carboplatin	1 0	1 00	1 3	0 02
Cisplatin	0 8	0 065	0 9	0 182
5-FU	0 9	0 321	1 5	0 019
Vincristine	1 2	0 147	1 4	0 052
VP-16	1 2	0 043	1 2	0 132

Table 3 1 18 The fold increase in resistance to chemotherapeutic drugs of DLRP-Cpt and DLRP-Txt with respect to DLRP, as determined by comparing IC_{50} values

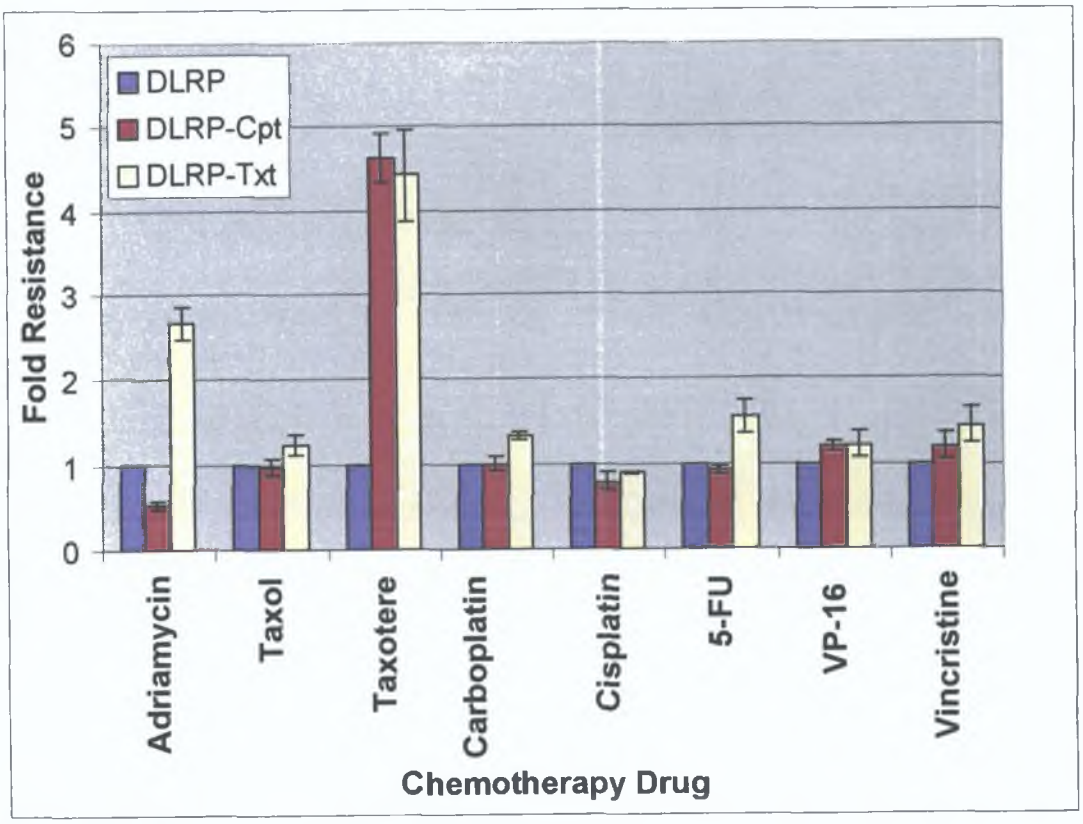

Figure 3.1.23 Resistance Profiles of DLRP Selections

3 1 6 Establishment of taxane and carboplatin selected variants of the small cell lung carcinoma cell line DMS-53

The DMS-53 cell line was exposed to an IC_{90} value of 40 ng/ml of taxotere and an IC_{90} value of 60 ng/ml of taxol respectively The cell line was pulsed for four hours, once a week for 10 consecutive weeks with both drugs individually (section 2 10) The cell lines resulting from the taxane exposures were designated DMS-Txt and DMS-Txl respectively

The DMS-53 cell line was also exposed to an IC_{90} value of 5ug/ml of Carboplatin The cell line was pulsed for four hours, once a week for 10 consecutive weeks The cell lines resulting from the carboplatin exposure was designated DMS-Cpt

3 1 6 1 Morphology of the taxane and carboplatin resistant variants of DMS-53

The morphologies of the three MDR variants of DMS-53 appeared to change during the selection procedure with carboplatin, taxotere and taxol When trypsinised, DMS-53 forms spheroids if agitated too severely The three drug selected variants retain this ability If these spheroids are broken into single cells and placed in a fresh flask, they will attach and grow as a monolayer (Figures 3 1 24-27)

The two taxane-selected variants have gained the ability to overcome contact inhibition, i e they grow on top of each other Cells maintained viability in suspension (if reseeded in a new flask, they would re-attach and grow)

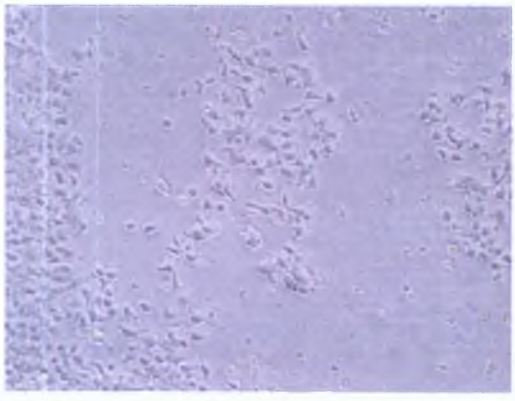

Figure 3.1.24 DMS-53

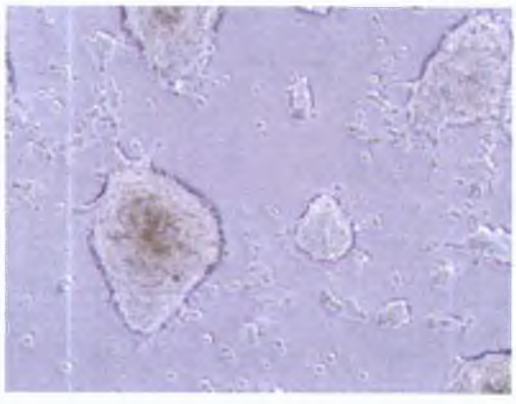

Figure 3.1.25 DMS-Txt

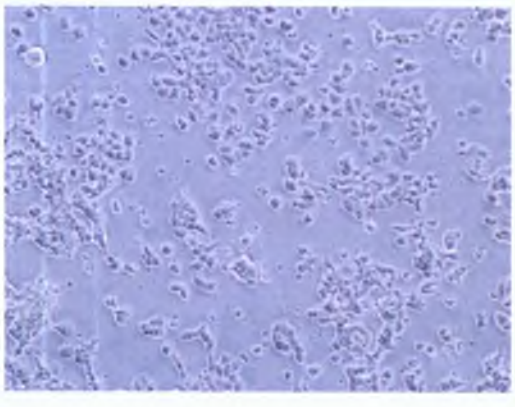

Figure 3.1.26 DMS-Cpt

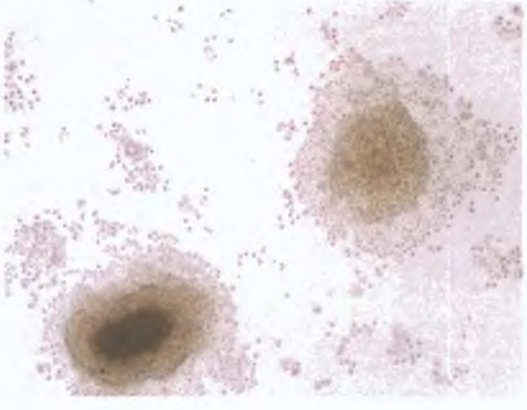

Figure 3.1.27 DMS-Txl

3.1.6.2 Resistance profiles of drug selected variants

The resistance and cross-resistance profiles were determined for eight drugs using the long-term toxicity assay (Table 3.1.19). The toxicity assays were carried out on each of the eight drugs each week for at least one month after the final pulses with carboplatin, taxotere and taxol. Table 3.1.20 shows the fold resistance patterns of both variants to each of the drugs.

Table 3.1.20 and Figure 3.1.28 represents the fold increase in resistance of DMS-Cpt, DMS-Txt and DMS-Txl with respect to DMS-53. The results demonstrate that DMS-Cpt only developed 1.6-fold resistance to carboplatin despite the fact that high cell kill was observed during the selection process. The cell line also developed 2.1-fold, 1.4-fold and 1.4-fold cross-resistance to cisplatin, adriamycin and taxol respectively. However, DMS-Cpt became sensitised to taxotere (0.5-fold) and vincristine (0.8-fold). Moreover, cross-resistance to VP-16 and 5-FU was not significantly increased in comparison to the parental cell line.

DMS-Txt developed low but statistically significant stable resistance to taxotere, taxol, adriamycin, vincristine and cisplatin (1 8-fold, 5 9-fold, 1 3-fold, 1 6-fold and 1 4-fold respectively) No change in resistance to carboplatin, 5-FU or VP-16 was observed

DMS-Txl developed low but statistically significant resistance to taxol, adriamycin, vincristine and carboplatin (6 3-fold, 1 6-fold, 3 3-fold and 1 2-fold respectively) No change in resistance was observed to 5-FU, cisplatin, taxotere or VP-16

Drug	DMS-53 (ng/ml)	DMS-Cpt (ng/ml)	DMS-Txt (ng/ml)	DMS-Txl (ng/ml)
Taxotere	8 2 ± 0 3	3 8 ± 0 4	14 6 ± 2 2	8 8 ± 1 5
Taxol	12 9 ± 1 3	18 7 ± 2 5	75 7 ± 4	81 ± 2 5
Adriamycin	15 ± 1 7	20 3 ± 3 1	19 5 ± 0 9	24 ± 2 5
Carboplatin	1200 ± 100	1840 ± 52 9	1210 ± 17 3	1406 7 ± 100 7
Cisplatin	151 7 ± 12 6	324 ± 46 8	210 ± 26 5	148 3 ± 12 6
5-FU	733 3 ± 57 7	863 ± 118 5	723 3 ± 75 1	760 ± 121 7
Vincristine	8 5 ± 0 9	6 6 ± 0 8	13 7 ± 1 3	28 3 ± 1 5
VP-16	295 ± 22 9	321 7 ± 40 7	334 3 ± 34 3	271 1 ± 12 6

Table 3 1 19 IC_{50} values for a range of chemotherapeutic drugs acting on the small cell lung carcinoma cell lines DMS-53, DMS-Cpt, DMS-Txt and DMS-Txl The values are given as the average IC_{50} value ± the standard deviation on a minimum of three repeats

Drug	DMS-Cpt	P value	DMS-Txt	P value	DMS-Txl	P value
Taxotere	0.5	0.000	1.8	0.034	1.1	0.528
Taxol	1.4	0.04	5.9	0.001	6.3	0.002
Adriamycin	1.4	0.079	1.3	0.029	1.6	0.003
Carboplatin	1.6	0.000	1.0	0.323	1.2	0.034
Cisplatin	2.1	0.018	1.4	0.034	1.0	0.762
5-FU	1.2	0.189	1.0	0.864	1.0	0.755
Vincristine	0.8	0.49	1.6	0.005	3.3	0.000
VP-16	1.1	0.393	1.1	0.184	0.9	0.217

Table 3.1.20: The fold increase in resistance to chemotherapeutic drugs of DMS-Cpt, DMS-Txt and DMS-Txl with respect to DMS-53, as determined by comparing IC_{50} values.

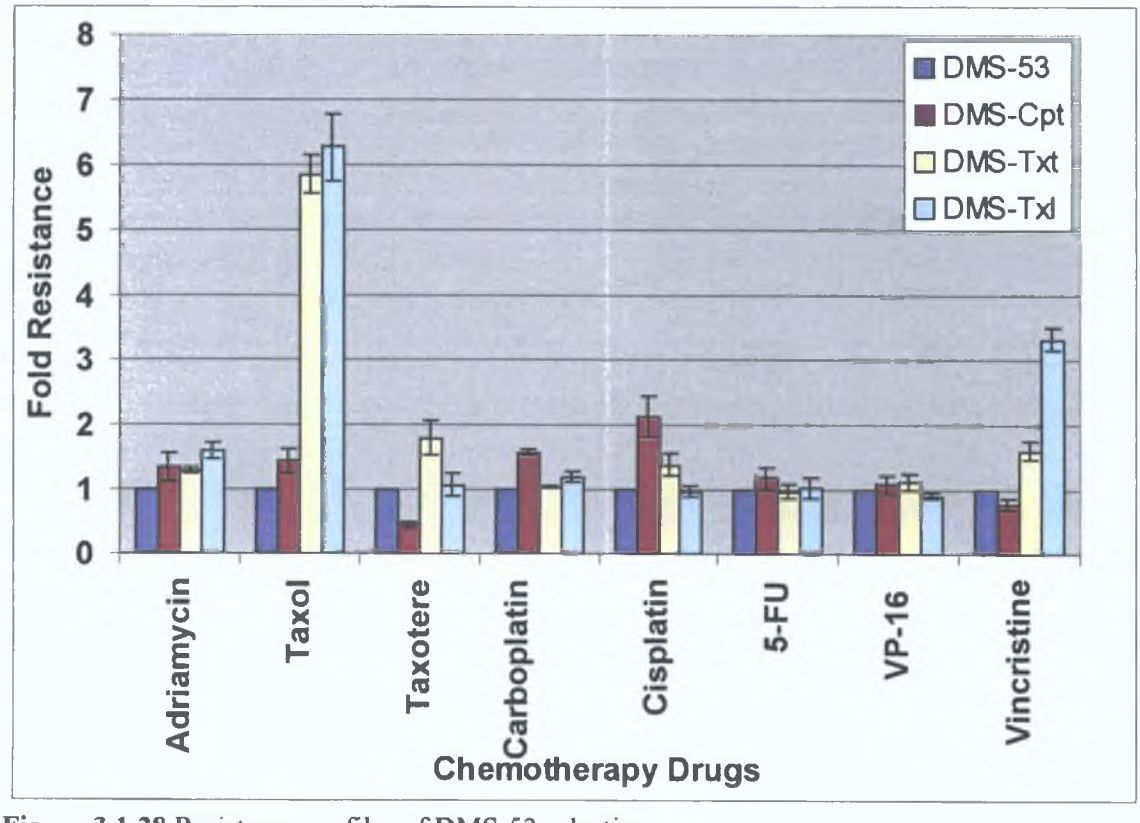

Figure 3.1.28 Resistance profiles of DMS-53 selections

3.1.7 Development of the NCI-H69 VP-16 and carboplatin selected variants

The NCI-H69 cell line was exposed to IC_{90} concentration of 480 ng/ml of VP-16. The cell line was also exposed to IC_{90} and IC_{50} values of 10 ug/ml and 5 ug/ml of carboplatin respectively. The cell line was pulsed for four hours, once a week for 10 consecutive weeks with all concentrations of both drugs individually (section 2.10). The cell line resulting from the VP-16 exposures was designated H69-VP480. The cell lines resulting from the carboplatin exposures were designated H69-Cpt10 and H69-Cpt5.

3.1.7.1 Morphology of the VP-16 and carboplatin resistant variants of NCI-H69

The morphology of NCI-H69 variants was not found to have changed during the selection procedure with carboplatin and VP-16 (Figure 3.1.29).

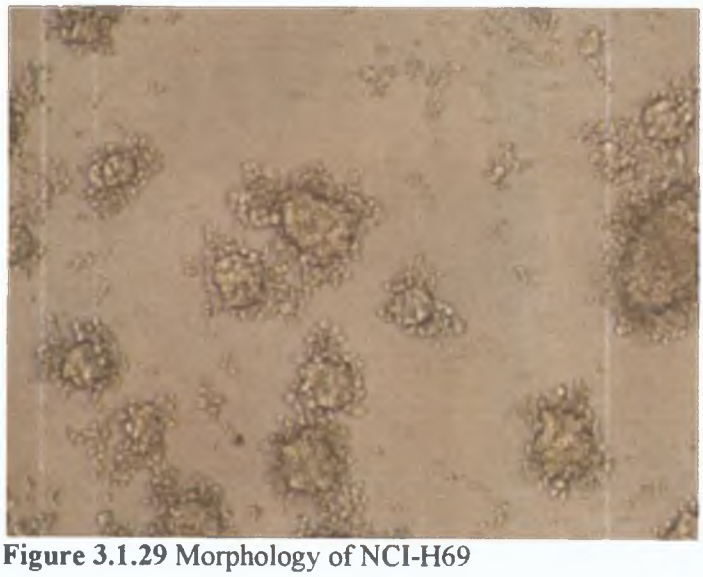

Figure 3.1.29 Morphology of NCI-H69

3 1 7 2 Resistance profiles of drug selected variants

The resistance and cross-resistance profiles were determined for eight drugs using the long-term toxicity assay (Table 3 1 21 and 3 1 22) The toxicity assays were carried out on each of the eight drugs each week for one month after the final pulses with carboplatin and VP-16 (section 2 8 2)

Table 3 1 23 and Figure 3 1 31 represent the fold resistance values of each of the chemotherapeutic agents for the parental NCI-H69 cell line and its VP-16 and carboplatin selected variants H69-VP480, H69-Cpt10 and H69-Cpt5 The results demonstrate that the VP-16 resistant variant developed 2 9-fold resistance to VP-16 and exhibited cross resistance to carboplatin (1 6-fold), cisplatin (1 2-fold), taxotere (2 4-fold) and 5-FU (3 9-fold) The cell line became sensitised to taxol (0 3-fold resistant), adriamycin (0 4-fold resistant) and vincristine (0 8-fold resistant)

The results also reveal that although pulsed with half the concentration of carboplatin, the H69-Cpt5 variant developed higher resistance and cross-resistance to carboplatin (2 2-fold), 5-FU (8 6-fold) and VP-16 (2 fold) In contrast, H69-Cpt10 developed higher cross-resistance to taxotere (5 4-fold) and cisplatin (3-fold) Interestingly both platinum-resistant variants became sensitised to the same drugs namely, taxol, adriamycin and vincristine

Drug	NCI-H69 (ng/ml)	H69-VP480 (ng/ml)
Taxotere	0 23 ± 0 03	0 6 ± 0 1
Taxol	13 3 ± 2 3	4 3 ± 0 7
Adriamycin	42 3 ± 6 4	17 ± 1 8
Carboplatin	740 ± 112 7	1206 7 ± 11 5
Cisplatin	110 ± 20	138 7 ± 5 5
5-FU	90 ± 10	353 3 ± 20 8
Vincristine	3 9 ± 0 3	3 3 ± 0 4
VP-16	72 ± 2	306 7 ± 38 8

Table 3 1 21 IC_{50} values for a range of chemotherapeutic acting on the small cell lung carcinoma cell line NCI-H69 and the VP-16 resistant variant The values are given as the average IC_{50} value ± the standard deviation on a minimum of three repeats

Drug	NCI-H69 (ng/ml)	H69-Cpt10 (ng/ml)	H69-Cpt5 (ng/ml)
Taxotere	0 23 ± 0 03	1 3 ± 0 2	0 6 ± 0 1
Taxol	13 3 ± 2 3	4 2 ± 0 5	5 9 ± 1 7
Adriamycin	42 3 ± 6 4	19 1 ± 0 8	20 7 ± 2 4
Carboplatin	740 ± 112 7	1166 7 ± 57 7	1600 ± 173 2
Cisplatin	110 ± 20	355 ± 47 7	259 7 ± 31
5-FU	90 ± 10	760 ± 36 1	773 3 ± 97 1
Vincristine	3 9 ± 0 3	0 7 ± 0 1	3 6 ± 0 2
VP-16	72 ± 2	75 7 ± 7 5	144 ± 12 3

Table 3 1 22 IC_{50} values for a range of chemotherapeutic acting on the small cell lung carcinoma cell line NCI-H69 and the carboplatin resistant variants The values are given as the average IC_{50} value ± the standard deviation on a minimum of three repeats

Drug	H69-VP480	P value	H69-Cpt10	P value	H69-Cpt5	P value
Taxotere	2 4	0 022	5 4	0 006	2 4	0 004
Taxol	0 3	0 014	0 3	0 016	0 4	0 012
Adriamycin	0 4	0 016	0 5	0 023	0 5	0 018
Carboplatin	1 6	0 18	1 6	0 01	2 2	0 003
Cisplatin	1 2	0 243	3 0	0 006	2 2	0 005
5-FU	3 9	0 000	8 4	0 000	8 6	0 006
Vincristine	0 8	0 114	0 2	0 001	0 9	0 189
VP-16	2 9	0 026	1 1	0 49	2 0	0 008

Table 3 1 23 The fold increase in resistance to chemotherapeutic drugs in H69-VP480, H69-Cpt10 and H60-Cpt5 with respect to NCI-H69, as determined by comparing IC_{50} values

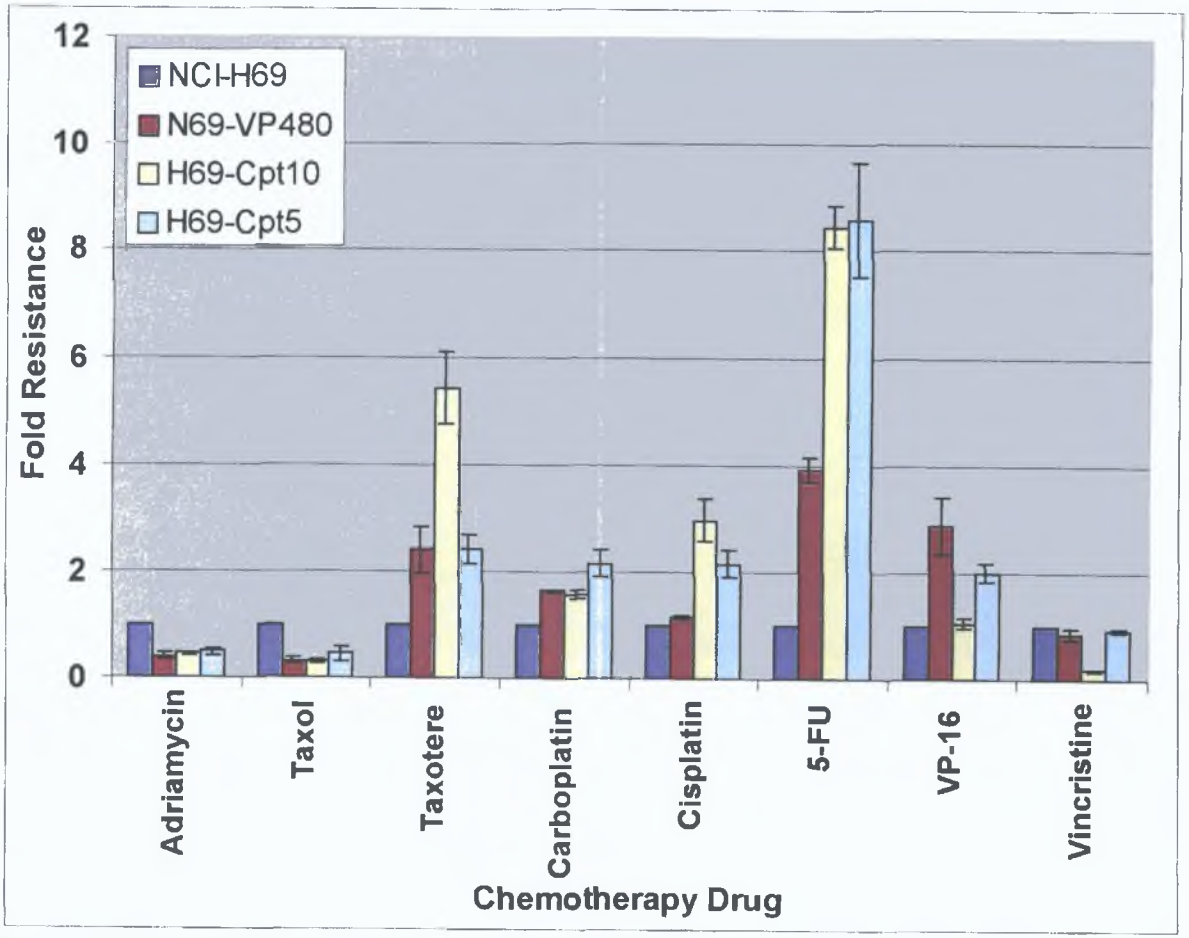

Figure 3.1.30: Fold resistance profiles of NCI-H69 Selections

3 2 Analysis of multidrug resistant variants using *in vitro* invasion assays

Invasion assays were performed, as described in Section 2 11, to assess the ability of each of the following four cell lines SKMES-1, DLRP, NCI-H69 and DMS-53 and their drug selected variants to invade through matrigel Cell culture inserts were coated with matrigel and placed in medium containing 24-well plates prior to cell addition Cells were considered invasive if they migrated through the matrigel and the 8 μM porous membrane and attached to the underside of the membrane within 24 hours The nasal carcinoma cell lines RPMI-2650 and its melphalan-selected variant RPMI-Melphalan were used as negative and positive controls respectively The images presented are representative of at least three separate experiments, are at a magnification of 10X and are stained with crystal violet

3 2 1 Invasion potential of SKMES-1 and MDR variants

The ability of SKMES-1, both the taxane and the carboplatin-selected variants to invade through matrigel was assessed in a 24-hour invasion assay The SKMES-1 parental cell line is highly invasive (Figure 3 2 1) Increased invasion was observed in the taxane-selected variants, SKMES-Txt (Figure 3 2 2) and SKMES-Txl (Figure 3 2 3) compared with the parent SKMES-Cpt100 is more invasive than the parent (Figure 3 2 5) By contrast, SKMES-Cpt30 is less invasive i e fewer cells attached to the underside of the membrane, compared with the parental cell line (Figure 3 2 4) A change in morphology as a result of the selection process is seen in SKMES-Txt and SKMES-Cpt100 compared to the parent (Figures 3 2 2 and 3 2 5)

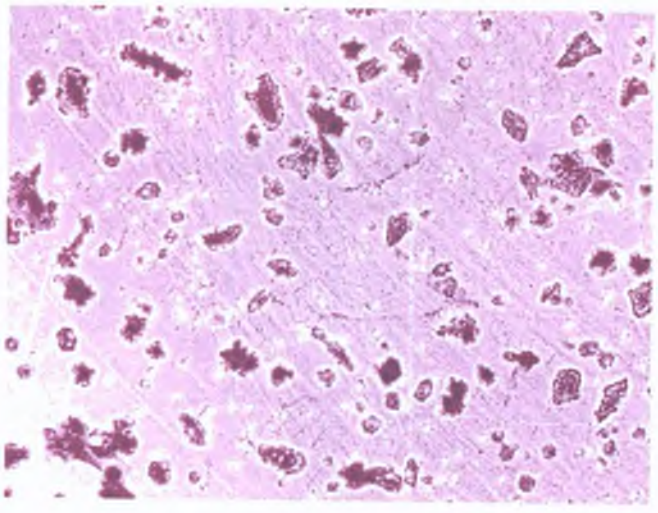

Figure 3.2.1 Invasion of SKMES-1

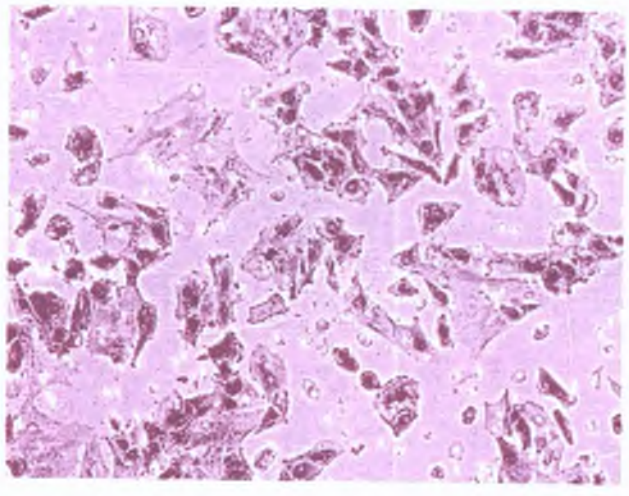

Figure 3.2.2 Invasion of SKMES-Txt

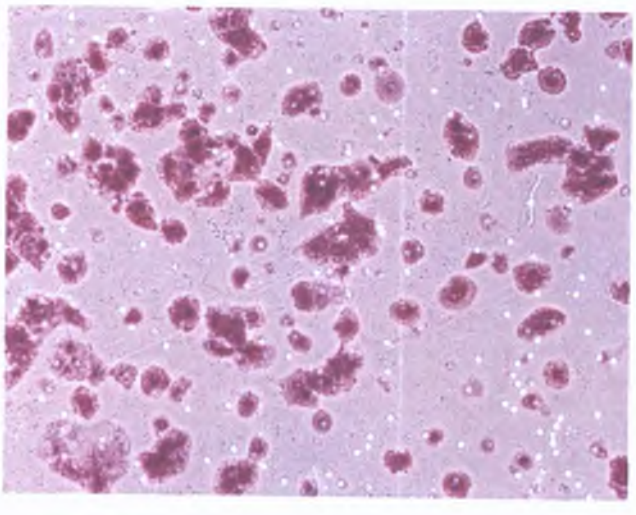

Figure 3.2.3 Invasion of SKMES-Txl

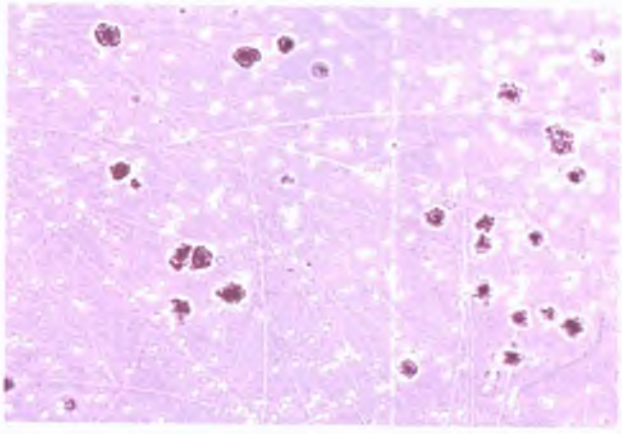

Figure 3.2.4 Invasion of SKMES-Cpt30

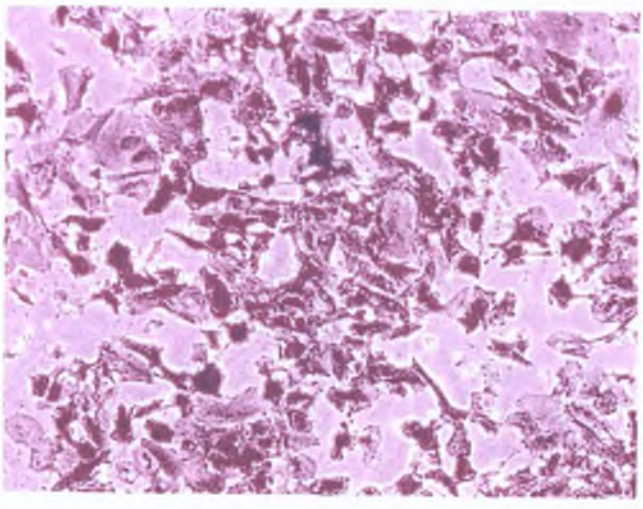

Figure 3.2.5 Invasion of SKMES-Cpt100

3.2.2 Quantification of invasion

The invasion assays were quantified by counting cells with a graticule at 40X magnification (Table 3.2.1, Figure 3.2.6). The data shows that selection of SKMES-1 with lower levels of carboplatin results in a less invasive cell line. By contrast, the taxane drugs and the higher carboplatin pulse produces more invasive cell lines. Table 3.2.2 and Figure 3.2.7 demonstrates that both taxane variants become more invasive with time.

Cell Line	Average cell count/area/view	P value
SKMES-1	8.2 ± 1.03	-
SKMES-C30	2.5 ± 0.25	0.008
SKMES-C100	11.5 ± 1.5	0.04
SKMES-Txt	17.8 ± 0.58	0.0005
SKMES-Txl	11 ± 0.64	0.015

Table 3.2.1 Quantification of SKMES-1 and pulse-selected variants

The values are given as the average cell counts/area/view ± the standard deviation on a minimum of three repeats.

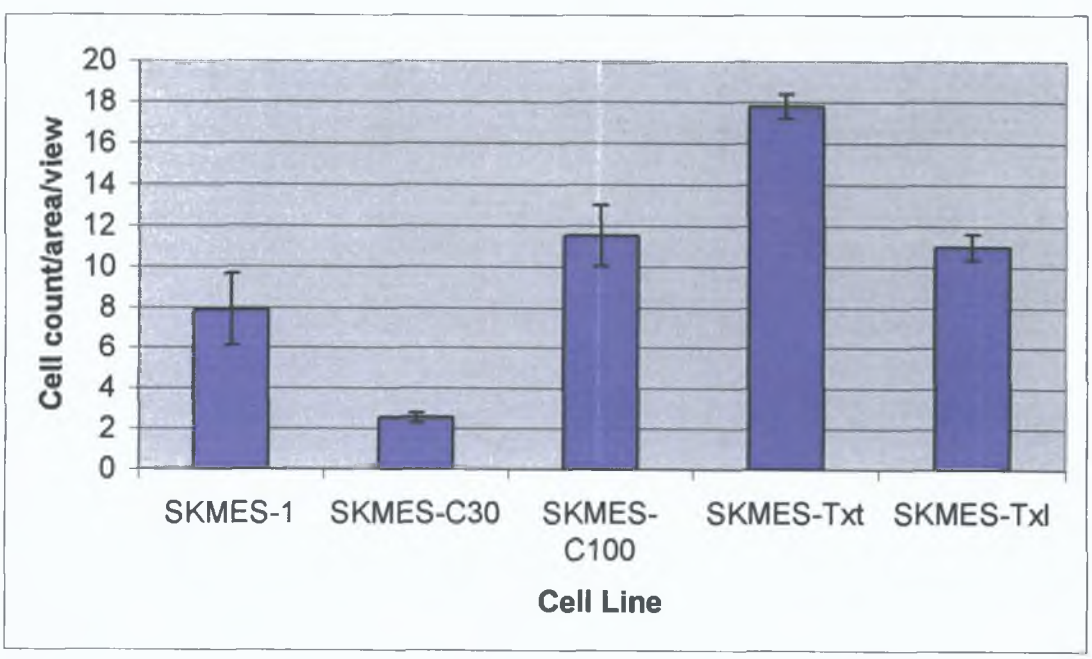

Figure 3.2.6 Quantification of SKMES-1 and pulse selected variants

Due to the unstable nature of both SKMES-Txt and SKMES-Txl variants, their invasiveness was assessed at both weeks 2 and 7 where decreasing drug resistance was observed.

Drug selection with taxotere and taxol appears to induce invasion compared to the control (2.17-fold and 1.34-fold respectively). However, at week 7 when drug resistance has fallen by 2.2-fold in both cell lines (to their selecting drug), the taxol-selected variant was 5-fold more invasive than the control whereas the invasive potential of the selected variant has only increased by 3.3-fold (Table 3.2.2 and Figure 3.2.7).

	Average cell count/area/view		**P value**
Cell Line	**Week 2**	**Week 7**	**Week 7**
SKMES-1	$8.2 \pm 1.03^{\#}$		-
SKMES-Txt	17.8 ± 0.58	27 ± 1.4	$1 * 10^{-4}$
SKMES-Txl	11 ± 0.64	41.3 ± 2.17	0.0002

Table 3.2.2 Quantification of SKMES-1 and taxane-selected variants

The values are given as the average cell counts/area/view ± the standard deviation on a minimum of three repeats. # The invasiveness of the SKMES-1 cell line was assessed over one-month; the value given is the average cell counts/area/view ± the standard deviation over this time on a minimum of four repeats.

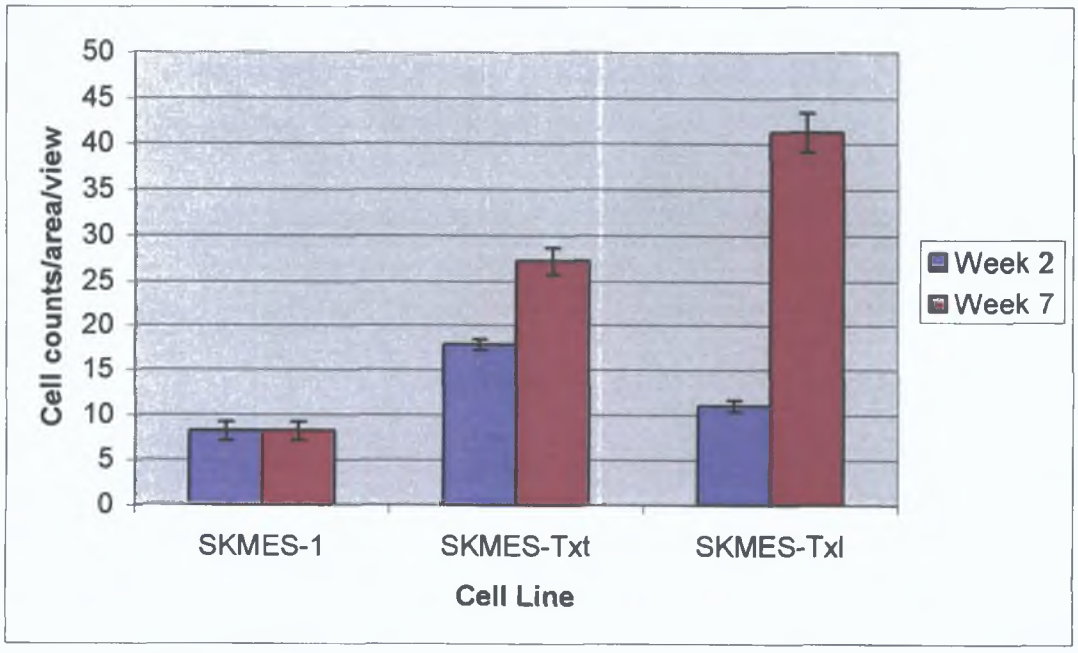

Figure 3.2.7 Quantification of invasion in SKMES-1 and taxane-selected variants

3.2.3 Invasion potential of SKMES-1 and SKMES-Taxol in collagen Type I

Invasion assays were also carried out whereby cells were induced to grow as spheroids using the hanging droplet technique with subsequent growing in a petri dish of media for a total four days (section 2.11.1). The spheroids were then transferred to a well of a 24-well plate coated in collagen type I. The invasion through the collagen was measured using a graticule at 20X magnification. Images were taken at 4X magnification.

The results reveal that both SKMES-1 and the taxane variants are invasive after 24 hours in collagen type I (Figures 3.2.8-13). However, the taxol and taxotere variants are less invasive than the parent over seven days (Table 3.2.3 and Figure 3.2.14).

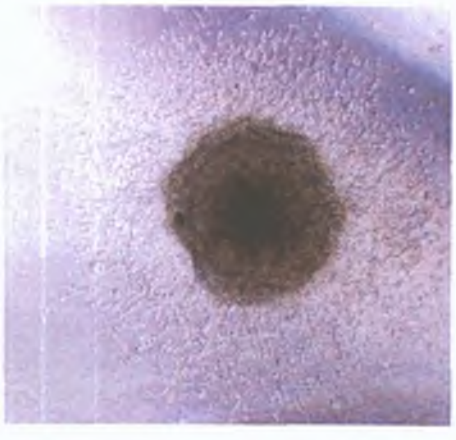

Figure 3.2.8 SKMES-1 day 1

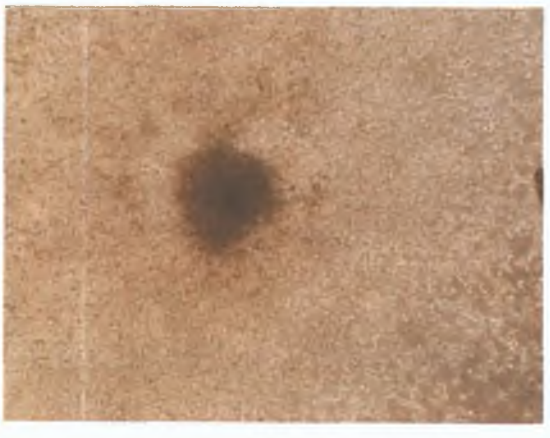

Figure 3.2.9 SKMES-1 day 3

Figure 3.2.10 SKMES-Txl day 1

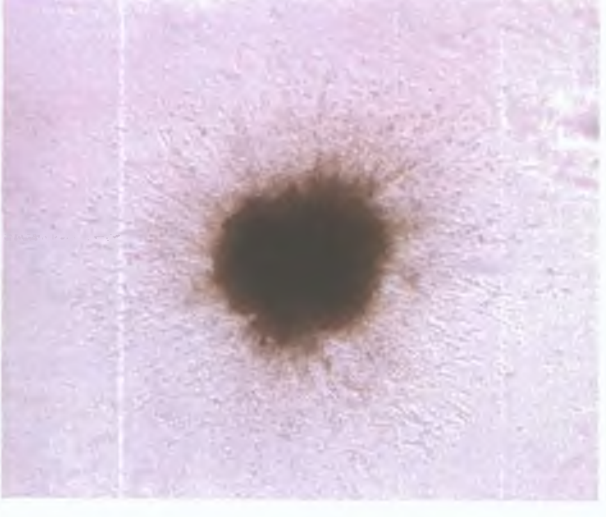

Figure 3.2.11 SKMES-Txl day 3

Figure 3.2.12 SKMES-Txt day 1

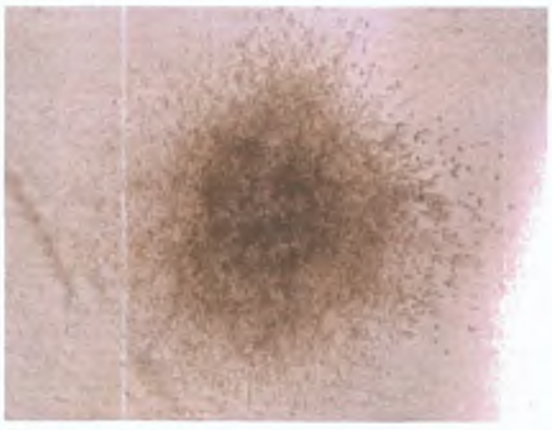

Figure 3.2.13 SKMES-Txt day 3

Invasion Through Collagen Type I (μMeters)			
Day	**SKMES-1**	**SKMES-Txt**	**SKMES-Txl**
2	113 ± 8	64 ± 4	45 ± 6
3	139 ± 15	75 ± 11	60 ± 8
4	159 ± 11	79 ± 10	68 ± 3
5	186 ± 8	105 ± 8	83 ± 4
7	246 ± 16	126 ± 3	109 ± 8

Table 3.2.3 Quantification of invasion of SKMES-1 and taxane variants in collagen type I. Values are given as the average invasion (at 20X magnification) in micrometers ± the standard deviation on four repeats.

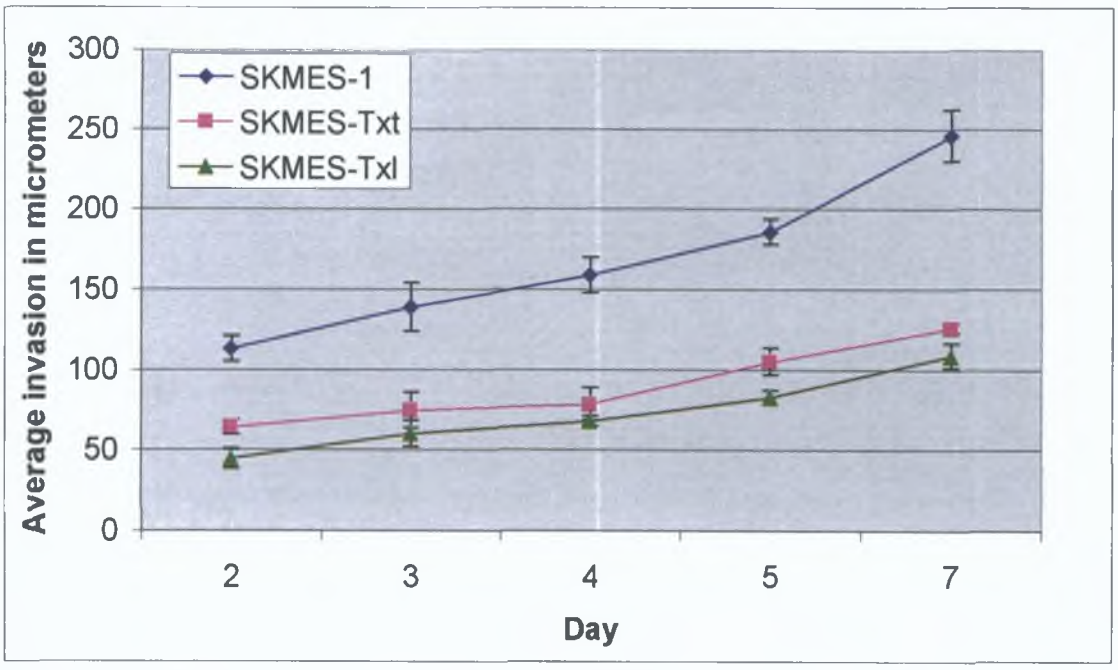

Figure 3.2.14 Quantification of invasion of SKMES-1 and taxane variants in collagen type I

3.2.4 Invasion potential of DLRP and MDR variants

The ability of DLRP and its taxotere and carboplatin selected variants to invade through matrigel was assessed in a 24-hour assay. DLRP, DLRP-Cpt and DLRP-Txt display varying levels of invasion at 10X magnification (Figure 3.2.15, 3.2.16 and 3.2.17). Both drug-selected variants (DLRP-Cpt and DLRP-Txt) are highly invasive. The invasion assays were quantified by counting at 40X magnification. The data shows that selection with carboplatin had no effect on invasion. However, selection with taxotere resulted in a slightly more invasive cell line (1.3-fold compared to the control) (Figure 3.2.18 and Table 3.2.4).

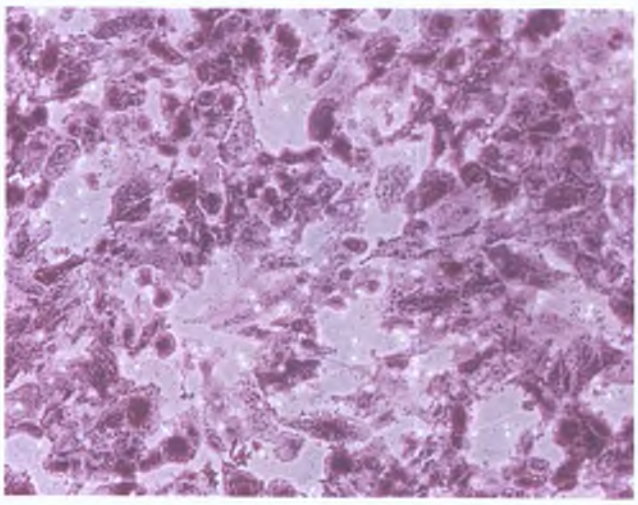

Figure 3.2.15 Invasion of DLRP

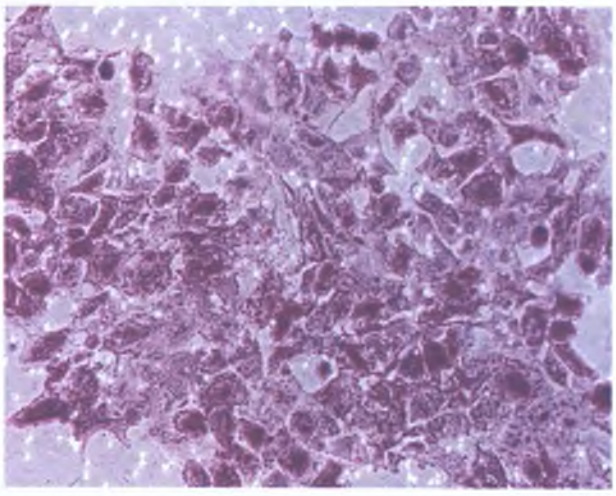

Figure 3.2.16 Invasion of DLRP-Cpt

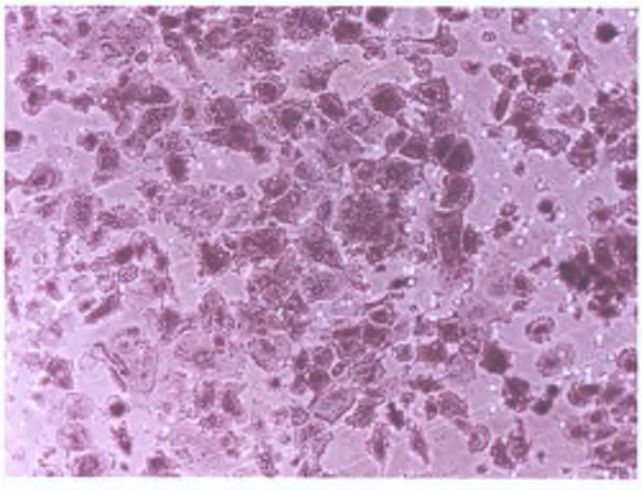

Figure 3.2.17 Invasion of DLRP-Txt

Cell Line	Average cell count/area/view	P value
DLRP	11.7 ± 1.2	-
DLRP-Cpt	11.4 ± 1.2	0.47
DLRP-Txt	15.4 ± 0.2	0.007

Table 3.2.4 Quantification of invasion of DLRP and pulse selected variants

The values are given as the average cell counts/area/view ± the standard deviation on a minimum of three repeats.

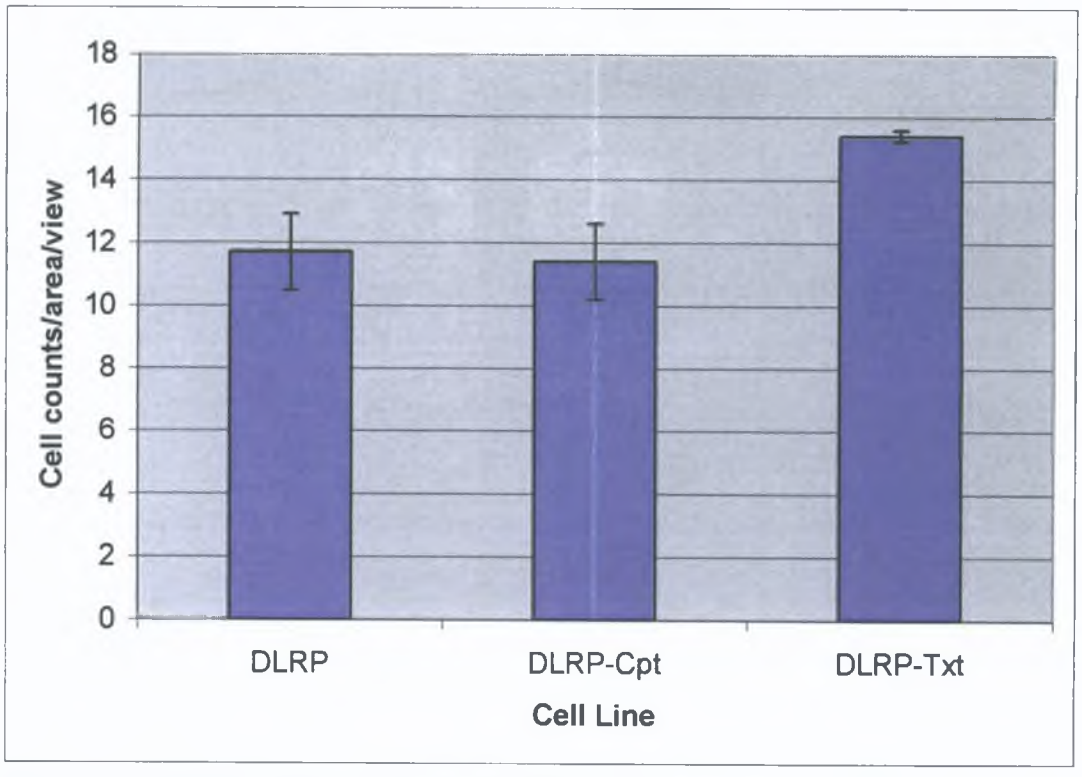

Figure 3.2.18 Quantification of invasion of DLRP and pulse selected variants

3.2.6 Invasion potential of DMS-53 and MDR variants

The DMS-53 small cell lung cell line is non-invasive after 24 hours (Figure 3.2.19). Pulse selection of DMS-53 with taxotere, taxol and carboplatin, showed no change in invasion potential at 24 hours. DMS-53 and variants were also non-invasive after 48 and 72 hours. Invasion assays were carried out in triplicate at each time point.

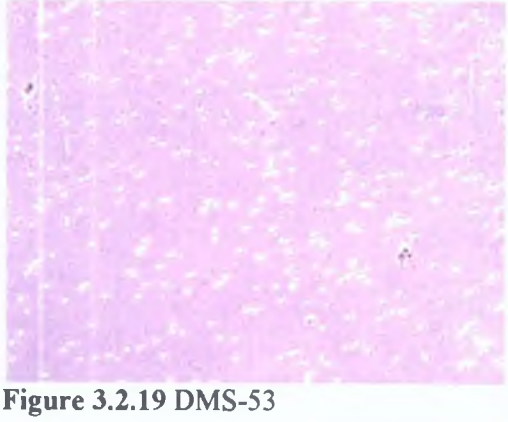

Figure 3.2.19 DMS-53

3.2.7 Invasion potential of DMS-53 and drug selected variants in collagen Type I

To assess this lack of invasion further, additional invasion assays were carried out as described in section 2.11.1 whereby cells were induced to grow as spheroids and placed in collagen type I. In all cases no invasion was observed after 10 days in collagen type I (Figures 3.2.20 – 3.2.23). Invasion assays were carried out in triplicate.

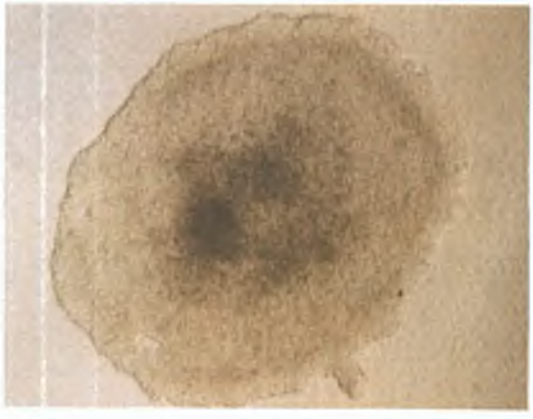

Figure 3.2.20 DMS-53

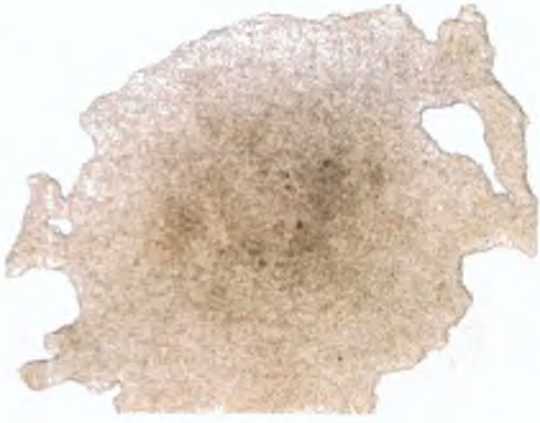

Figure 3.2.21 DMS-Txl

Figure 3.2.22 DMS-Txt

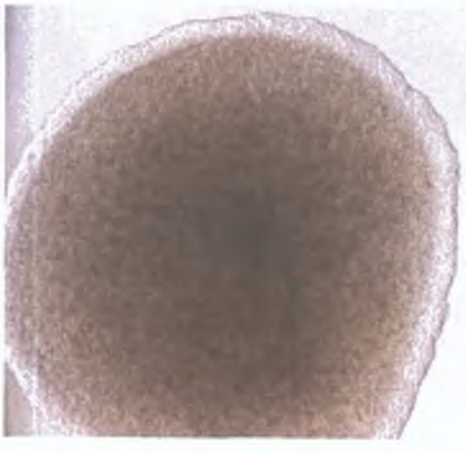

Figure 3.2.23 DMS-Cpt

3.2.8 Invasion potential of DMS-53 and drug selected variants in matrigel

To assess this further, additional invasion assays were carried out as described in section 2.11.1 whereby cells were induced to grow as spheroids and placed in matrigel. In all cases no invasion was observed after 10 days in matrigel (Figures 3.2.24 – 3.2.27). Invasion assays were carried out in triplicate.

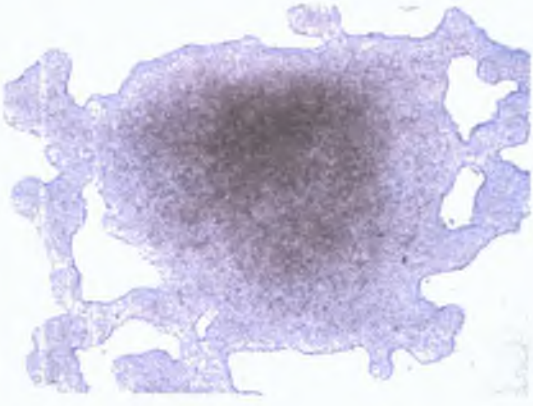

Figure 3.2.24 DMS-53

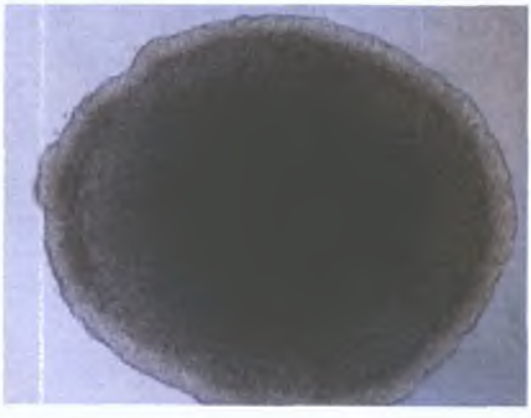

Figure 3.2.25 DMS-Txl

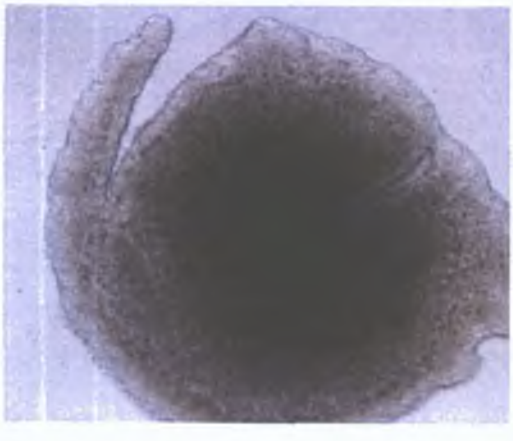

Figure 3.2.26 DMS-Txt

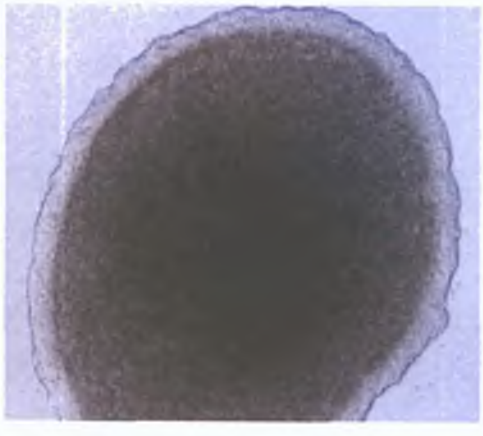

Figure 3.2.27 DMS-Cpt

3.2.9 Invasion potential of NCI-H69 and MDR variants

NCI-H69 small cell lung cell line is non-invasive after 24 hours in matrigel (Figure 3.2.28). Pulse selection of H69 with VP-16 and carboplatin, showed no change in invasion potential after 24 hours and 48 hours. Invasion assays were carried out in triplicate at each time point.

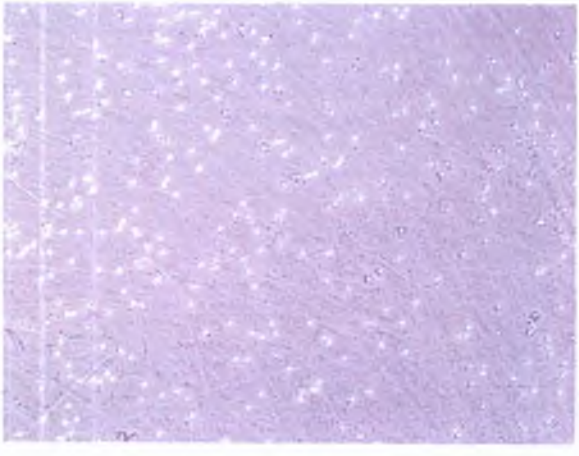

Figure 3.2.28 NCI-H69

3.2.10 Invasion potential of NCI-H69 and drug selected variants in collagen Type I

Invasion assays were also carried out whereby cells were induced to grow as spheroids using the hanging droplet technique with subsequent growing in a petri dish of media for a total four days (section 2.11.1). The spheroids were then transferred to a 24-well plate coated in collagen type I. Results revealed that the NCI-H69 cell line and all the pulse selected variants are non-invasive after 10 days in collagen type I (Figures 3.2.29-3.2.32). Invasion assays were carried out in triplicate.

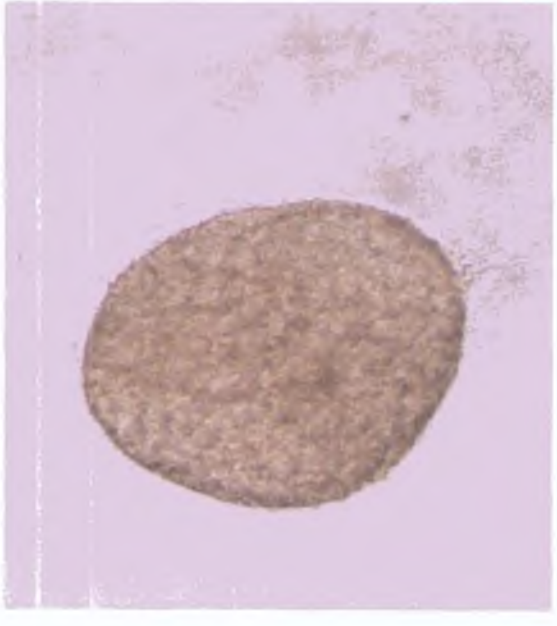

Figure 3.2.29 NCI-H69

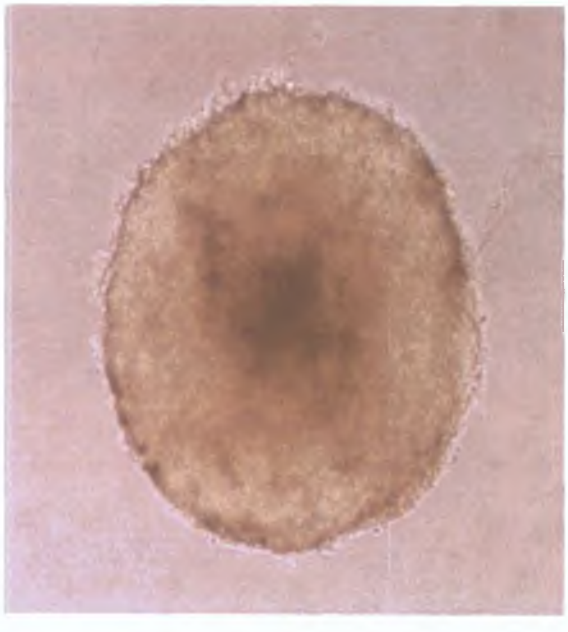

Figure 3.2.30 H69-Cpt100

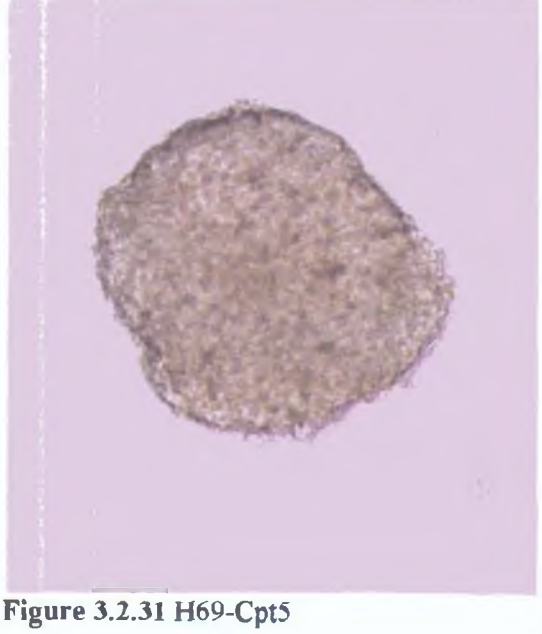

Figure 3.2.31 H69-Cpt5

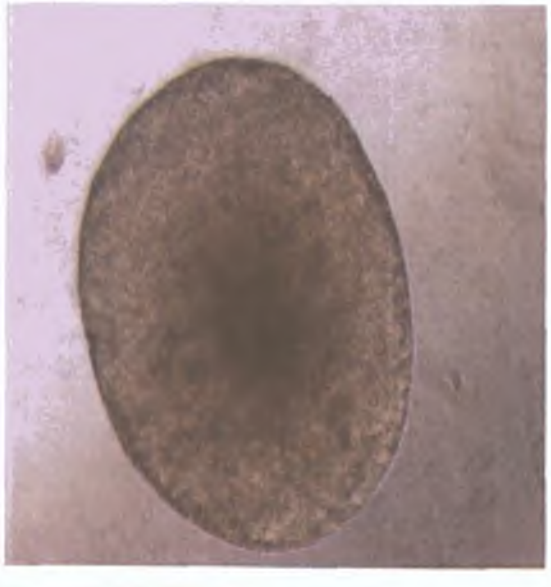

Figure 3.2.32 H69-VP480

3.2.11 Invasion potential of NCI-H69 and drug selected variants in matrigel

Spheroids were also transferred to a 24-well plate coated in matrigel. Results revealed that the NCI-H69 cell line and all the MDR variants are also non-invasive after 10 days in matrigel (Figures 3.2.33-3.2.36). Invasion assays were carried out in triplicate.

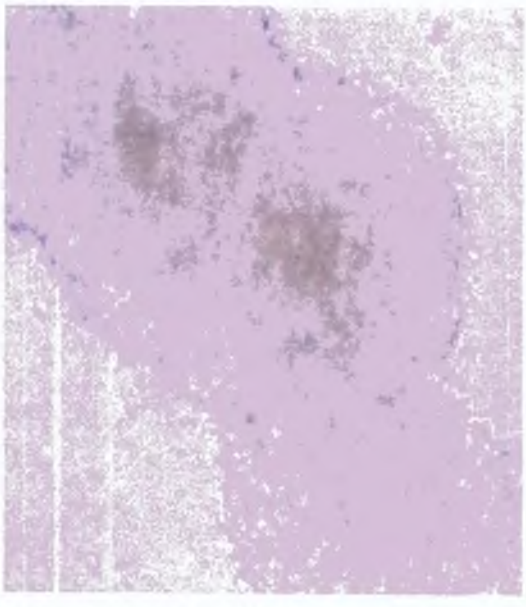

Figure 3.2.33 NCI-H69

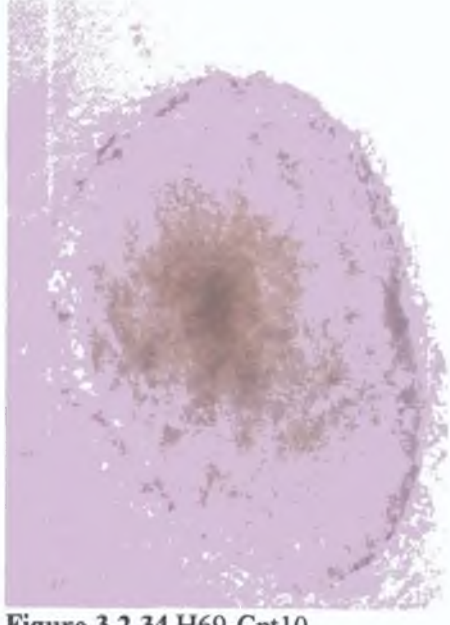

Figure 3.2.34 H69-Cpt10

Figure 3.2.35 H69-Cpt5

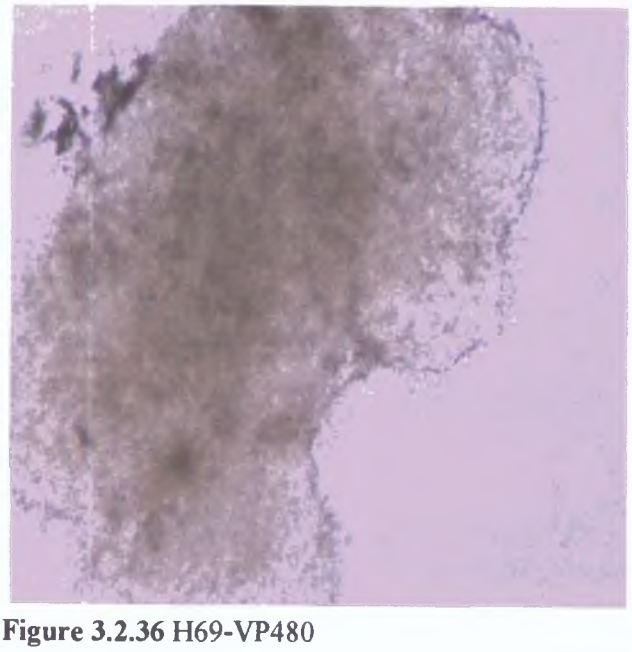

Figure 3.2.36 H69-VP480

3.2.12 Analysis of drug resistant variants using *in vitro* motility assays

Motility assays were carried out as described in section 2.12 to compare the locomotive ability of the four parental cell lines (SKMES-1, DLRP, NCI-H69 and DMS-53) and their drug selected variants. The procedure used to demonstrate cell motility was similar to that used for the invasion assays except that the inserts were not coated with ECM prior to the addition of the cells. Cells were considered motile if they migrated through the 8 μM porous membrane and attached to the underside within 24 hours. The images presented are representative of at least three separate experiments, are at a magnification at 10X and stained with crystal violet.

3.2.13 Motility of SKMES-1 and MDR variants

The motility of SKMES-1 and SKMES-Cpt100 was assessed in a 24-hour motility assay. The results obtained demonstrate that the highly invasive cell line SKMES-Cpt100 is more motile that SKMES-1 (Figures 3.2.37 and 3.2.38).

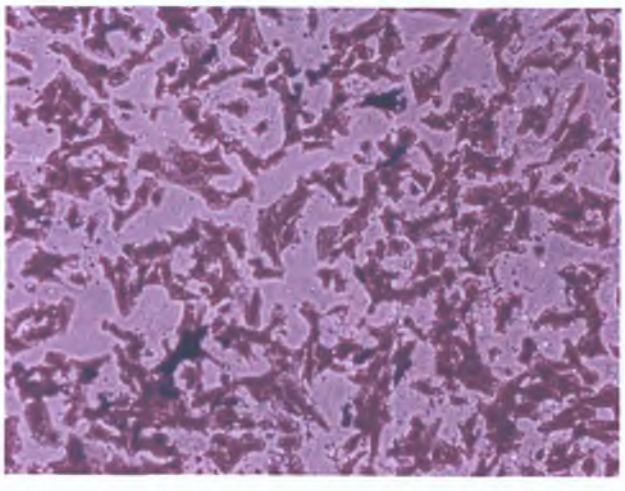

Figure 3.2.37 Motility of SKMES-1

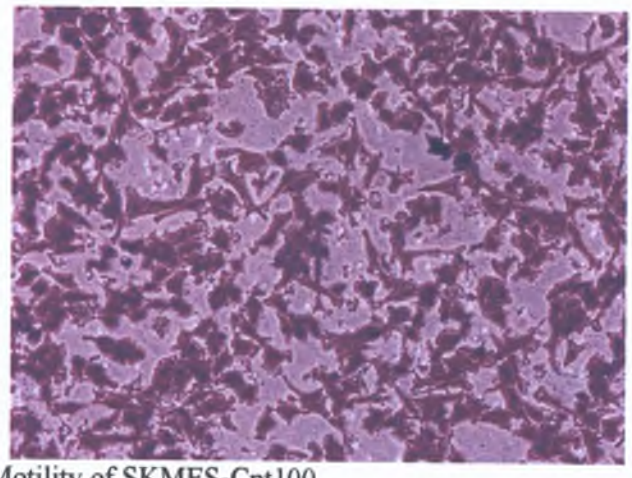

Figure 3.2.38 Motility of SKMES-Cpt100

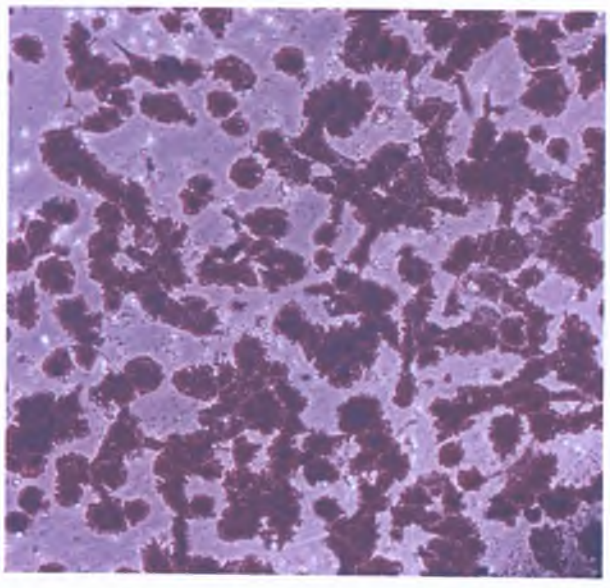

Figure 3.2.39 Motility of SKMES-Cpt30

3.2.14 Quantification of motility assays

The motility assays were quantified by counting cells using a graticule at 40X magnification (Table 3.2.5, Figure 3.2.40). The data shows that selection of SKMES-1 with higher levels of carboplatin has no significant effect on motility whereas pulse selection with lower levels of carboplatin results in a less motile cell line.

Cell Line	Average cell count/area/view	P Value
SKMES-1	26.2 ± 1.1	-
SKMES-C30	17.33 ± 1.73	0.0006
SKMES-C100	28.2 ± 1.1	0.09

Table 3.2.5 Quantification of motility of SKMES-1 and pulse selected variants

The values are given as the average cell counts/area/view ± the standard deviation on a minimum of three repeats.

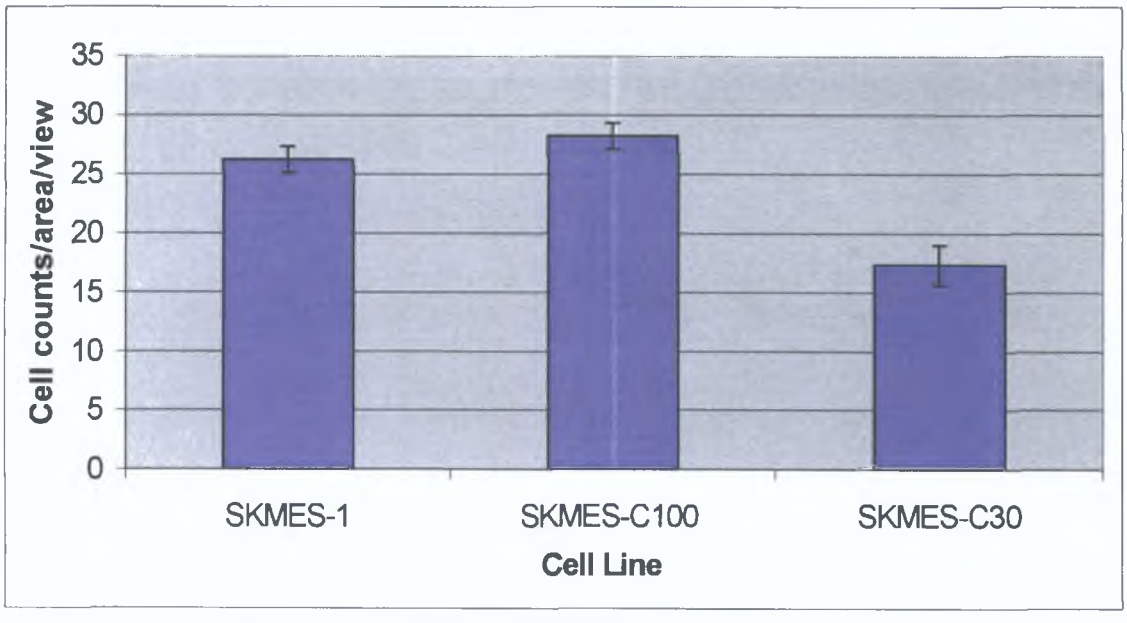

Figure 3.2.40 Quantification of motility of SKMES-1 and pulse selected variants

3.2.15 Motility of DLRP and MDR variants

The motility of DLRP and both drug selected variants DLRP-Cpt and DLRP-Txt were assessed in a 24-hour motility assay. The results obtained demonstrate that there is little change in the motility of the three cell lines (Figures 3.2.41 - 3.2.43).

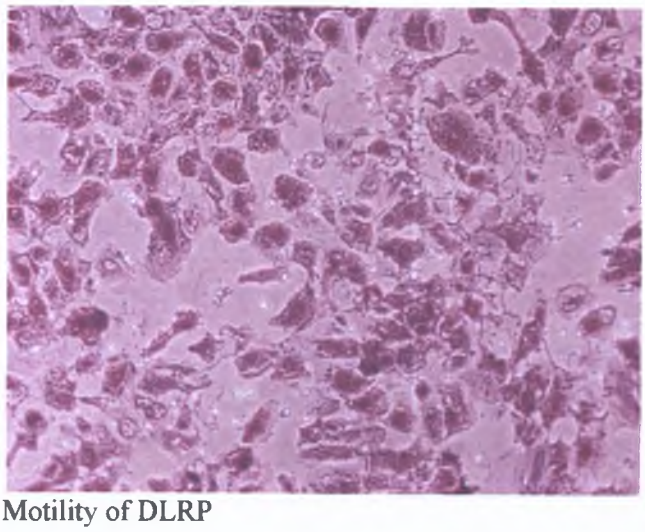

Figure 3.2.41 Motility of DLRP

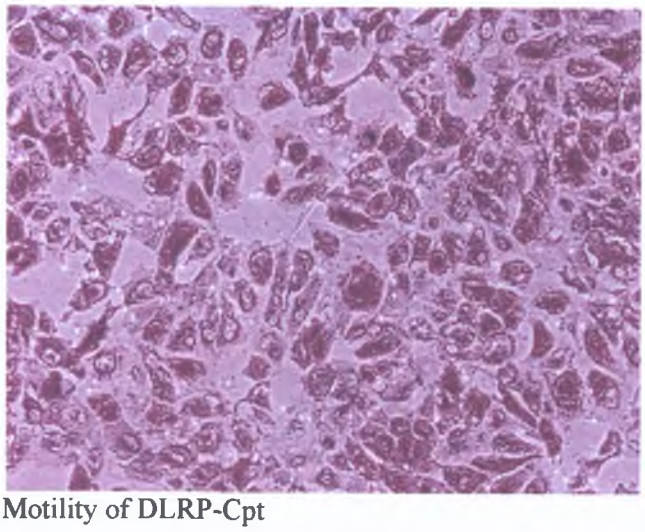

Figure 3.2.42 Motility of DLRP-Cpt

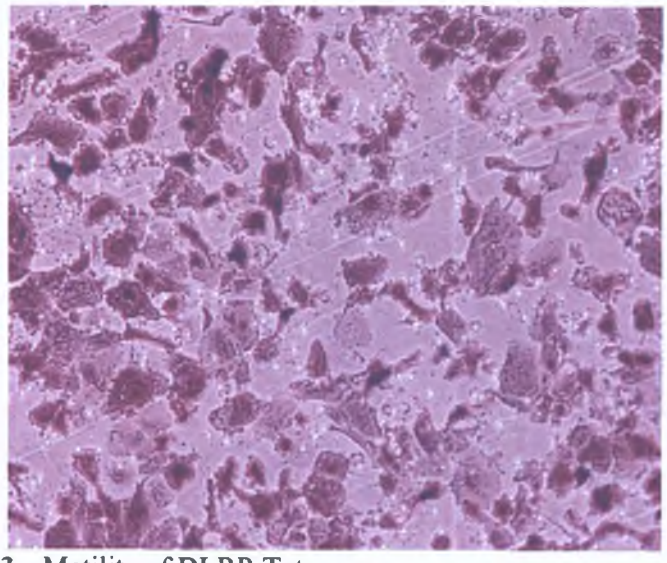

Figure 3.2.43 Motility of DLRP-Txt

3.2.16 Quantification of motility assays

The motility assays were quantified by counting cells using a graticule at 40X magnification (Table 3.2.6, Figure 3.2.44). The data shows that selection of DLRP with taxotere and carboplatin had no significant effect on motility.

Cell Line	Average cell count/area/view	P value
DLRP	18.1 ± 1.3	-
DLRP-Cpt	19.1 ± 1.0	0.005
DLRP-Txt	17 ± 0.5	0.31

Table 3.2.6 Quantification of motility of DLRP and pulse selected variants

The values are given as the average cell counts/area/view ± the standard deviation on a minimum of three repeats.

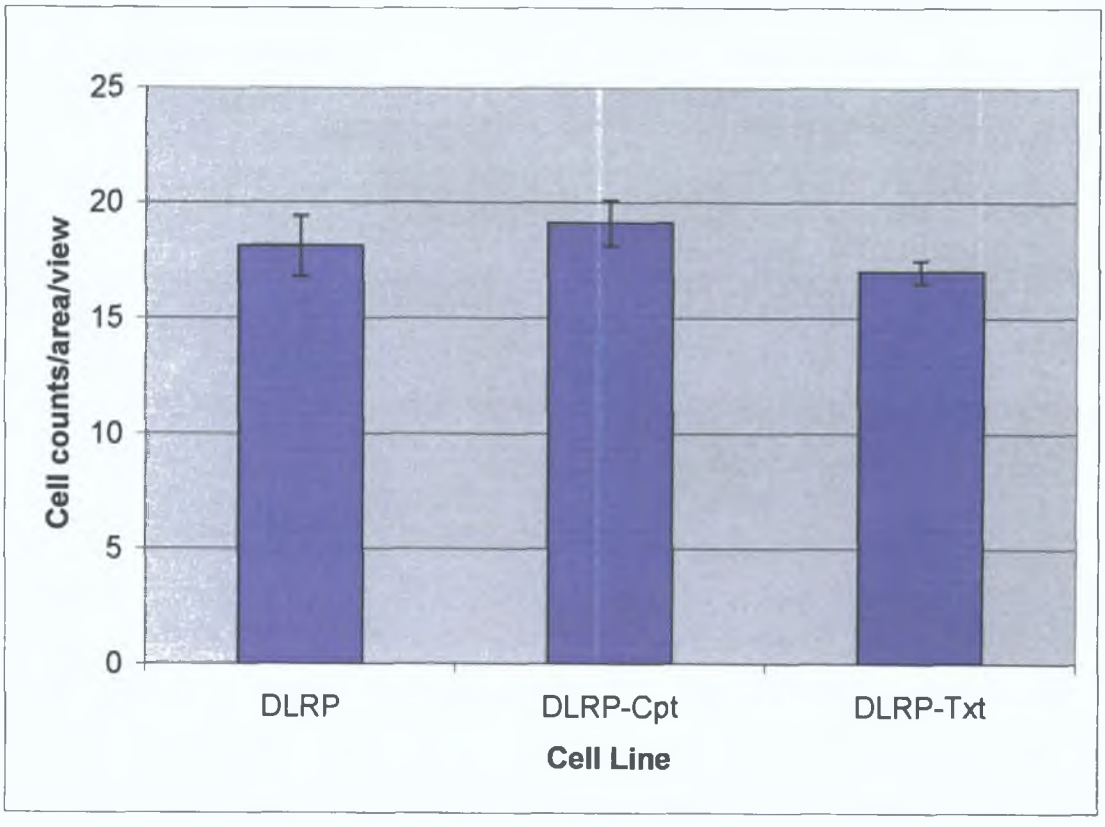

Figure 3.2.44 Quantification of motility of DLRP and pulse selected variants

3 2 17 Analysis of drug resistant variants using *in vitro* adhesion assays

To analyse the adhesiveness of the four parental cell lines to matrigel (SKMES-1, DLRP, NCI-H69 and DMS-53) and their drug selected variants to matrigel adhesion assays were carried out as described in section 2 11 3 The adhesion assays presented are representative of three separate experiments

3.2 18 Adhesion of SKMES-1 and MDR variants

Table 3 2 7, Figures 3 2 45 and 3 2 46 show the levels of adhesion of SKMES-1 and the taxane- and carboplatin-selected variants (after two and seven weeks culture) to matrigel after 1 hour SKMES-Txt is more adhesive to matrigel than either the parent or taxol-selected variant The taxol-selected variant is less adhesive than the parent Loss of adhesion is seen in both taxane cell lines with respect to time SKMES-Txt is 2 45-fold less adhesive at week 7 compared to week 2 SKMES-Txl is also less adhesive at week 7 compared to week 2, revealing that loss of adhesion to matrigel is greater in the taxotere-selected variant than in taxol-selected variant

	Fold Adhesion			
Cell Line	**Week 2**	**P value**	**Week 7**	**P value**
SKMES-1	1 ± 0 09			
SKMES-Txt	3 85 ± 0 29	0 001	1 4 ± 0 13	0 01
SKMES-Txl	0 83 ± 0 08	0 1	0 44 ± 0 05	0 002
SKMES-Cpt100	2 51 ± 0 14	0 0002	-	-
SKMES-Cpt30	1 21 ± 0 35	0 4	-	-

Table 3 2 7 Quantification of adhesion of SKMES-1 and drug selected variants

The values are given as the fold adhesion compared to the parental cell line ± the standard deviation on a minimum of three repeats

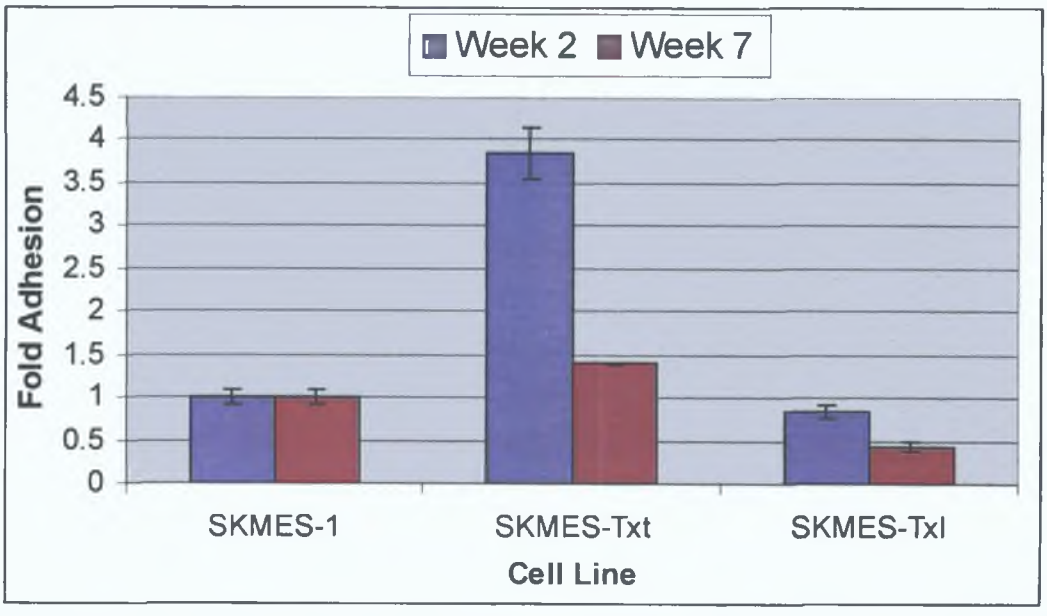

Figure 3.2.45 Quantification of adhesiveness of SKMES-1 and taxane selected variants to matrigel

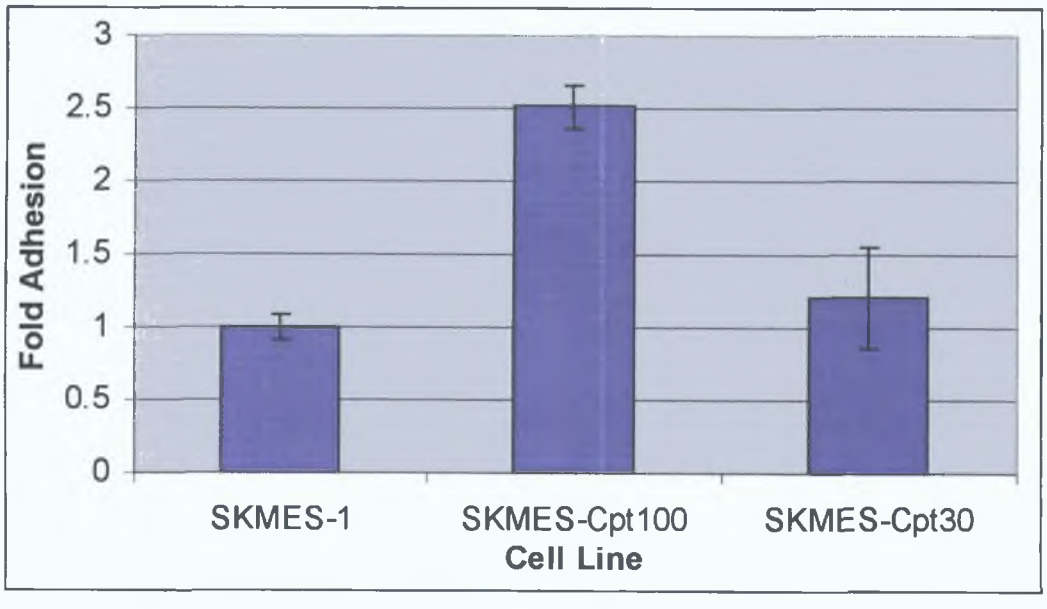

Figure 3.2.46 Quantification of adhesiveness of SKMES-1 and carboplatin selected variants to matrigel

3.2.19 Adhesion of DLRP and MDR variants

Table 3.2.8 and Figure 3.2.47 show the adhesiveness of DLRP and pulse-selected variants to matrigel after 1 hour. Both DLRP-Cpt and DLRP-Txt are less adhesive to matrigel in comparison to the parent with DLRP-Cpt being statistically the least adhesive of the three.

Cell Line	Fold Adhesion	P value
DLRP	1 ± 0.023	-
DLRP-Txt	0.91 ± 0.125	0.006
DLRP-Cpt	0.62 ± 0.05	0.02

Table 3.2.8 Quantification of adhesion of DLRP and selected variants to matrigel

The values are given as the fold adhesion to matrigel relative to the parental cell line ± the standard deviation on a minimum of three repeats.

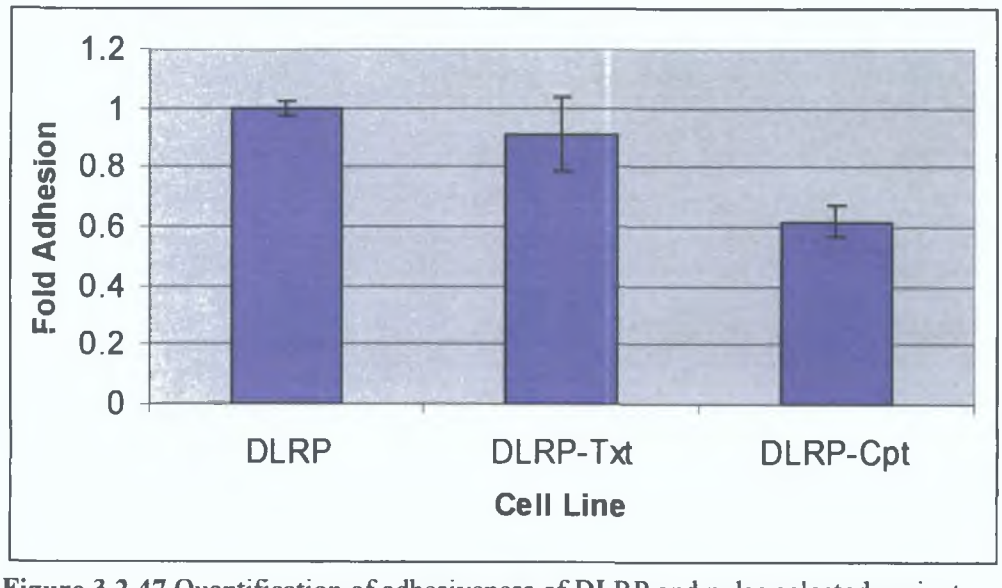

Figure 3.2.47 Quantification of adhesiveness of DLRP and pulse selected variants

3.2.20 Adhesion of DMS-53 and MDR variants

Table 3.2.9 and Figure 3.2.48 show no change in the adhesiveness of the non-invasive cell line DMS-53 and pulse selected variants to matrigel after 1 hour.

Cell Line	Fold Adhesion	P value
DMS-53	1± 0.092	-
DMS-Cpt	0.95 ± 0.15	0.7
DMS-Txl	1.03 ± 0.12	0.8
DMS-Txt	0.99 ± 0.09	0.3

Table 3.2.9 Quantification of adhesion of DMS-53 and selected variants to matrigel

The values are given as the fold adhesion to matrigel relative to the parental cell line ± the standard deviation on a minimum of three repeats.

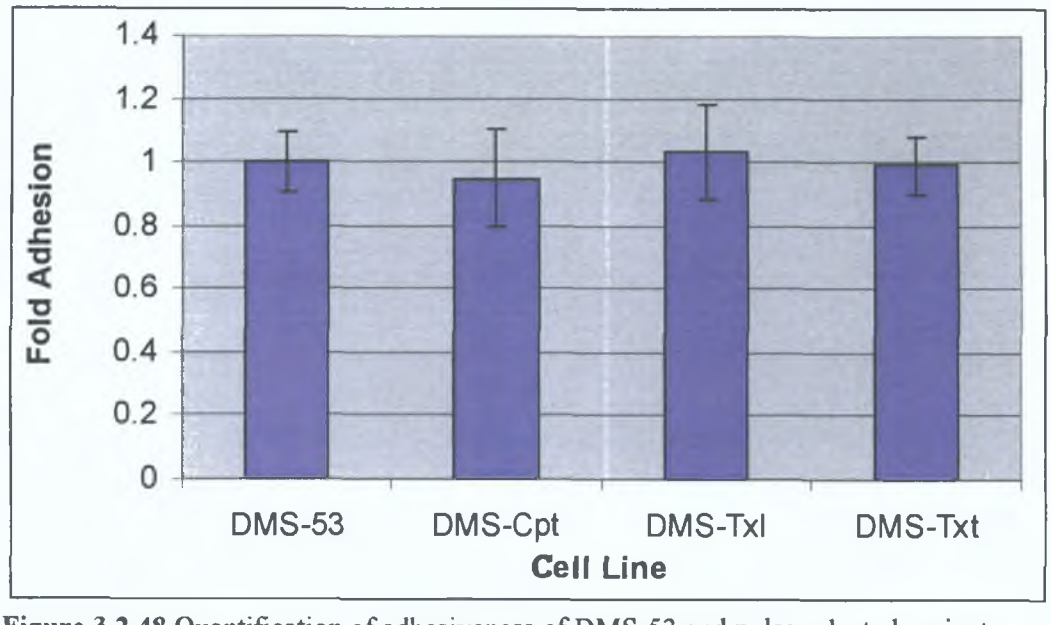

Figure 3.2.48 Quantification of adhesiveness of DMS-53 and pulse selected variants

3.2.21 Expression of gelatin degrading proteases from SKMES-1, DLRP and their MDR variants

Matrix metalloproteinases (MMPs), cysteine proteinases and serine proteineases are secreted by cells. They play an important role in degrading the extracellular matrix. To investigate the mechanism underlying the invasive phenotype of the two squamous cell lines and their drug-selected variants, studies of the proteineases were carried out as described in section 2.11.4.

The RPMI-Melphalan, DLKP and RPMI-2650 cell lines, which secrete MMP-2 (66kDa), MMP-9 (86kDa), and serine proteinases respectively, were used as positive controls in these studies. A band corresponding to MMP-9 is visible in all cell lines tested. A band corresponding to MMP-2 is apparent in all cell lines except DLRP-Cpt. SKMES-1 and both carboplatin-selected variants secrete proteinases, which are not MMPs (Figure 3.2.49).

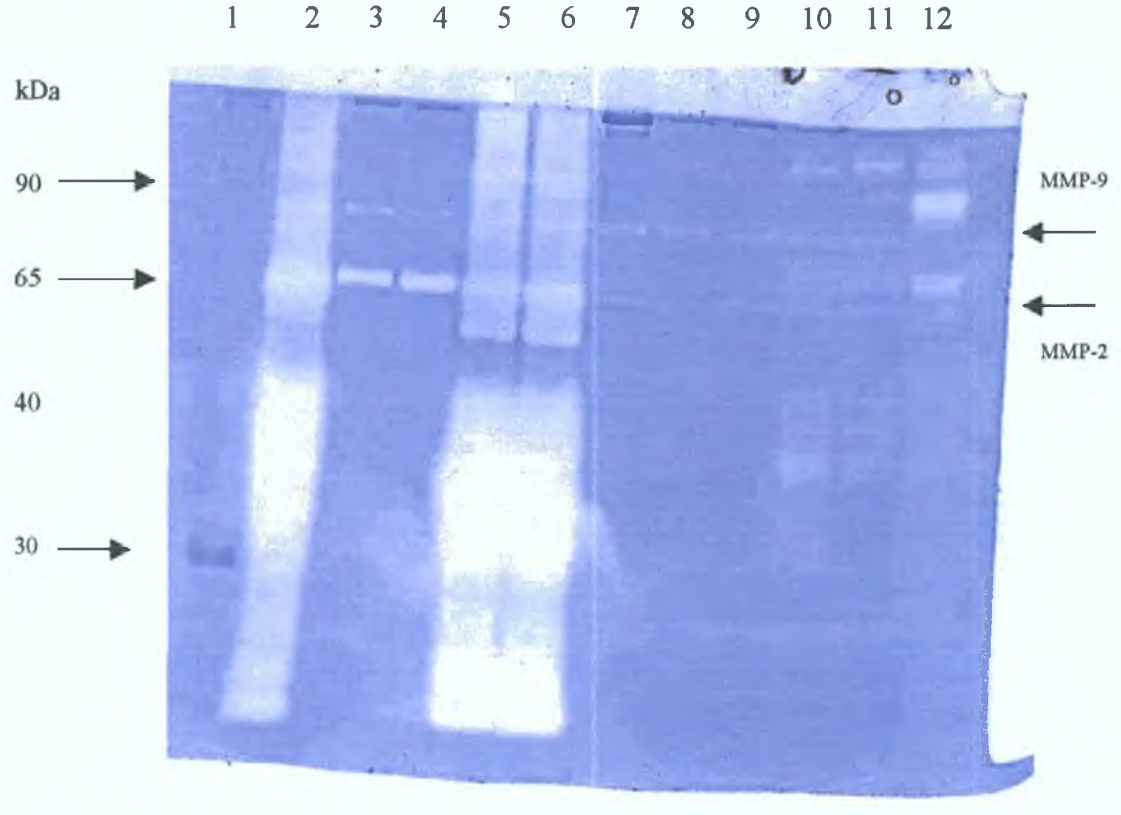

Figure 3.2.49 Zymograph of the proteinases in SKMES-1, DLRP and corresponding drug resistant variants. Lanes 1-12 = markers, SKMES-1, SKMES-Txt, SKMES-Txl, SKMES-Cpt30, SKMES-Cpt100, DLRP, DLRP-Cpt, DLRP-Txt, RPMI-2650, RPMI-melphalan and DLKP. Zympgraphy was carried out in triplicate and results were consistent.

3.2.22 Investigation with type of gelatin degrading protease from SKMES-1, DLRP and MDR variants

To confirm that the bands detected in Figure 3.2.50 were MMP-2 and MMP-9 and also to determine if the bands secreted by SKMES-1, SKMES-Cpt30 and SKMES-100 were MMPs, the inhibitor EDTA was added.

3.2.22.1 The effect of EDTA

EDTA is a chelating agent, which can bind zinc and calcium needed for the activation of MMPs. To confirm that the bands are MMPs, proteinase inhibitors were added to inactivate their corresponding substrates. After the gel was incubated with EDTA, the bands corresponding to MMP-2 and MMP-9 disappeared in all the cell lines. This indicates that the three bands are MMPs. Bands at ~90kDa in SKMES-Cpt30 and SKMEs-Cpt100 also disappeared indicating that they are MMPs. However, EDTA had no effect on the expression of the other bands in SKMES-1 and carboplatin selected variants (Figure 3.2.50).

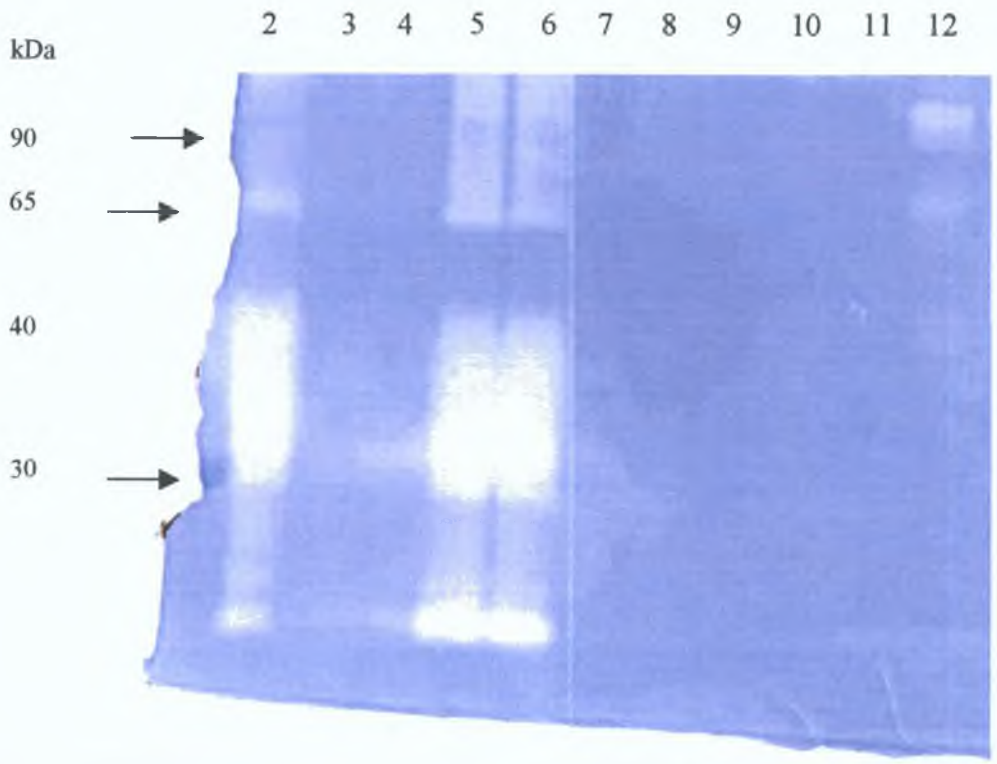

Figure 3.2.50 Zymograph of the proteinases in SKMES-1, DLRP and corresponding drug resistant variants with EDTA. Lanes 2-12 = markers, SKMES-1, SKMES-Txt, SKMES-Txl, SKMES-Cpt30, SKMES-Cpt100, DLRP, DLRP-Cpt, DLRP-Txt, RPMI-2650, RPMI-melphalan and DLKP. Zymography was carried out in triplicate and results were consistent.

3.2.22.2 The effect of PMSF

PMSF is a serine protease inhibitor, which does not inhibit MMP secretion. PMSF was used to establish that the bands observed were due to MMP secretion, not serine protease secretion. After the gel was incubated with PMSF, it was shown that all previously observed bands were MMP bands (Figure 3.2.51). The addition of PMSF to the substrate buffer did not suppress or reduce the expression of the protease bands of SKMES-1, SKMES-Cpt30 and SKMES-Cpt100, suggesting the proteases are not serine proteases.

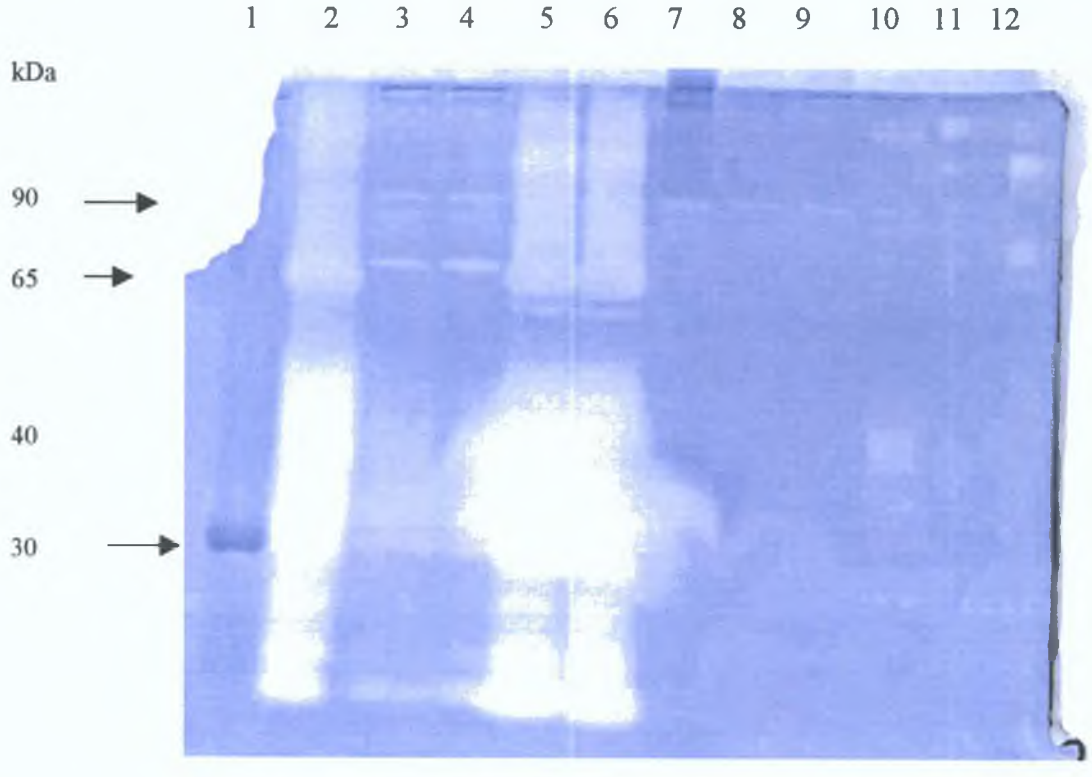

Figure 3.2.51 Zymograph of the proteinases in SKMES-1, DLRP and corresponding drug resistant variants with PMSF. Lanes 2-12 = markers, SKMES-1, SKMES-Txt, SKMES-Txl, SKMES-Cpt30, SKMES-Cpt100, DLRP, DLRP-Cpt, DLRP-Txt, RPMI-2650, RPMI-melphalan and DLKP. Zympgraphy was carried out in triplicate and results were consistent.

3.2.23 Expression of gelatine-degrading proteases from DMS-53, DMS-Txt, DMS-Cpt and DMS-Txl

Zymography gels were carried out on concentrated supernatants collected from the non-invasive cell lines DMS-53, DMS-Txt, DMS-Cpt and DMS-Txl. Figure 3.2.52 shows that DMS-53 has a band at ~66kDa corresponding to MMP-2. This band is not present in the two variants. Another band corresponding to pro-MMP-9 (92kDa) is also visible in this cell line and absent in the others. There are also bands expressed at approximately 50-60kDa in the three cell lines.

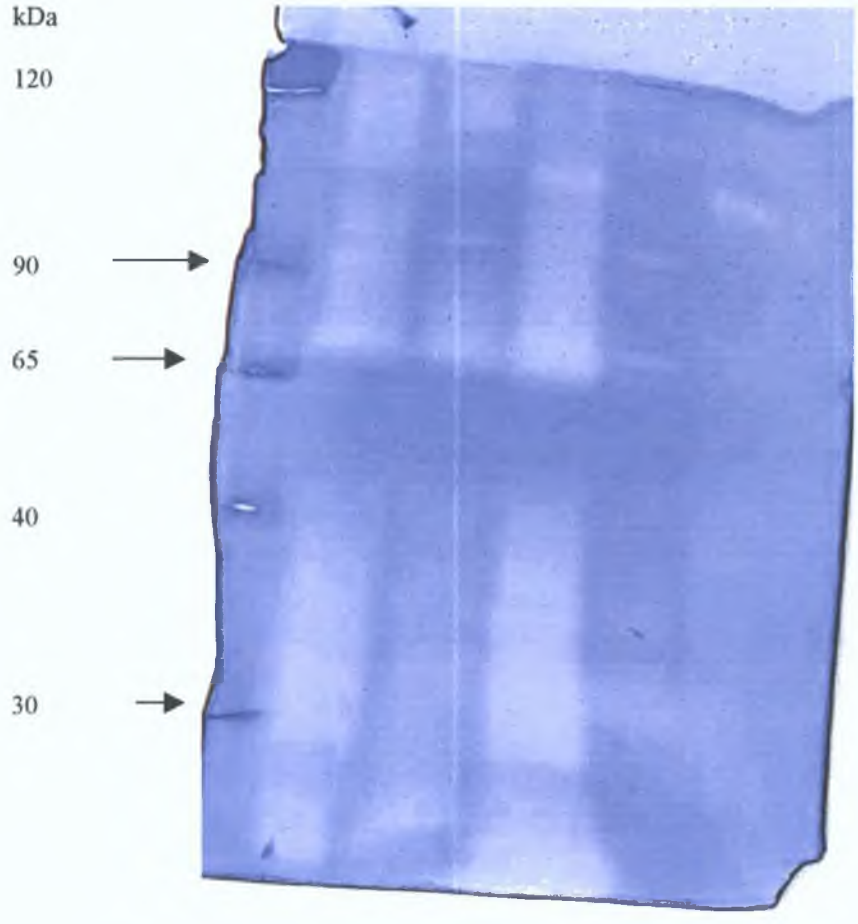

Figure 3.2.52 Zymograph of the proteinases in DMS-53, DMS-Txt, DMS-Cpt and DMS-Txl and. Lanes 1-6 – Markers, DMS-53, DMS-Txt, DMS-Cpt and DMS-Txl, DLKP. Zymography was carried out in triplicate and results were consistent.

3.2.23.1 The effect of cysteine

Cysteine keeps cysteine proteases in their reduced form thus making them more active. If the bands visible in Figure 3.2.52 were cysteine proteases, they would become stronger after incubating the gel with cysteine. Figure 3.2.53 suggests that the bands originally thought to be MMP-9 could be cysteine proteases in DMS-53 and DMS-Cpt.

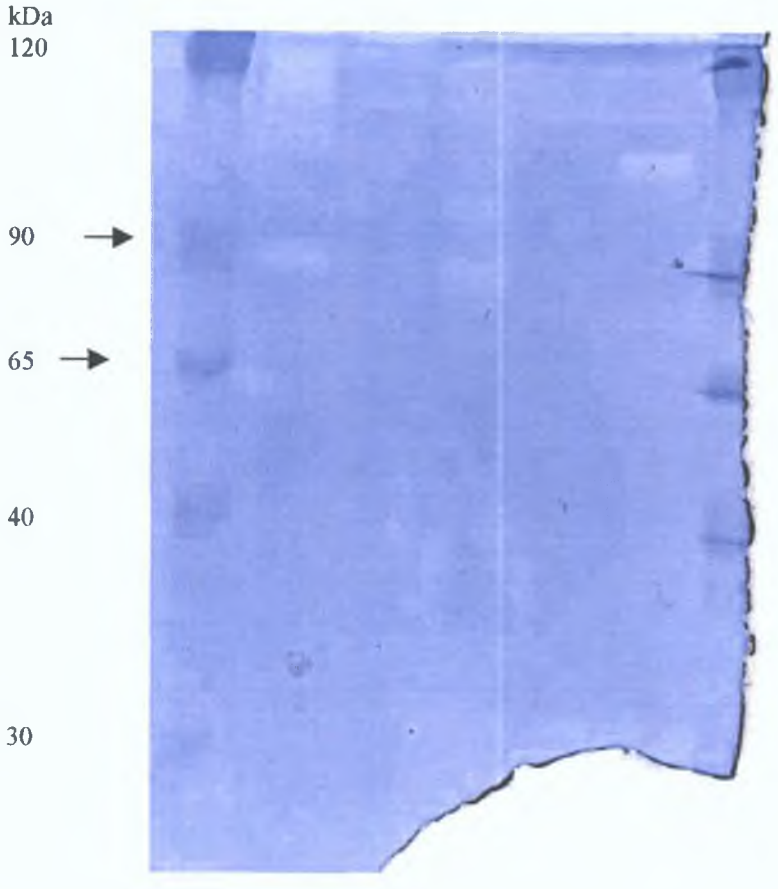

Figure 3.2.53 Zymograph of the cysteine proteinases in DMS-53, DMS-Txt, DMS-Cpt and DMS-Txl. Lanes 1-6 – Markers, DMS-53, DMS-Txt, DMS-Cpt and DMS-Txl, DLKP. Zympgraphy was carried out in triplicate and results were consistent.

3.2.23.2 The effect of EDTA

To determine if the bands at ~65 kDa are MMPs, or cysteine proteases, EDTA was included in the substrate buffer. After the gel was incubated with EDTA, the three bands did not disappear, indicating that they are probably not MMPs (Figure 3.2.54)

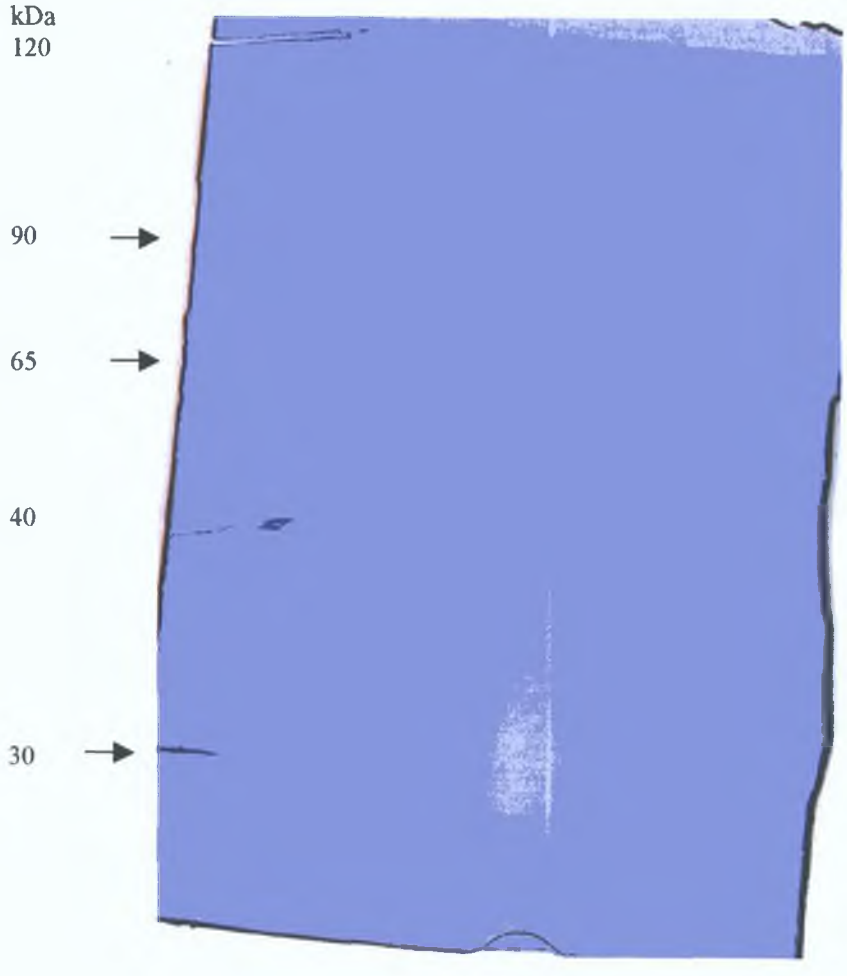

Figure 3.2.54 Zymograph of the proteinases in DMS-53, DMS-Txt, DMS-Cpt and DMS-Txl with the MMP inhibitor EDTA Lanes 1-6 – Markers, DMS-53, DMS-Txt, DMS-Cpt and DMS-Txl, DLKP. Zymography was carried out in triplicate and results were consistent.

3.2.23.3 The effect of PMSF

PMSF was used to establish that the bands observed were due to MMP secretion, not serine protease secretion. After the gel was incubated with PMSF, all previously observed bands were MMP bands. The addition of PMSF did not suppress or reduce the expression of the protease bands in the four cell lines suggesting the proteases are not serine proteases (Figure 3.2.55).

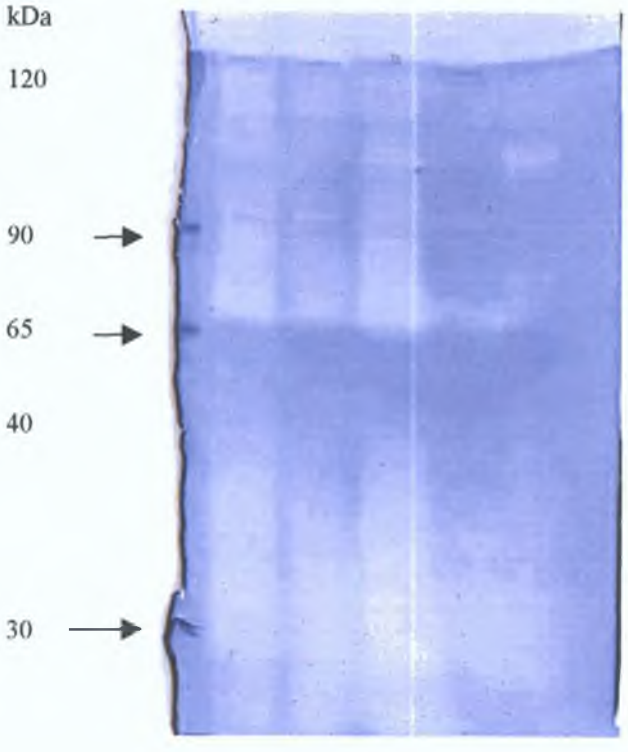

Figure 3.2.55 Zymograph of the proteinases in DMS-53, DMS-Txt, DMS-Cpt and DMS-Txl with the inhibitor PMSF. Lanes 1-6 – Markers, DMS-53, DMS-Txt, DMS-Cpt and DMS-Txl, DLKP. Zymography was carried out in triplicate and results were consistent.

3.2 24 Summary of zymography

Gelatine zymography of the taxane selected variants and corresponding parental cell lines in these studies revealed the presence of MMP-9 in all invasive cell lines tested A band corresponding to MMP-2 was also detected in all invasive taxane-selected variants A loss of secreted proteinases, which are not MMPs or serine proteinases was observed in the SKMES-Txt and SKMES-Txl compared to the parental cell line Gelatine zymography of the carboplatin-selected variants in these studies, revealed the presence of MMP-9 in all invasive cell lines tested A band corresponding to MMP-2 was also detected in the selected variants, except DLRP-Cpt SKMES-1 and both carboplatin-selected variants secrete proteinases which are not MMPs or serine proteinases

3.3 Combination assay summary

3.3.1 Circumvention of adriamycin and taxotere resistance

Toxicity assays were carried out on cell lines with (1) a combination of adriamycin, an MRP1 substrate, and the non steroidal anti-inflammatory drug sulindac, an MRP1 inhibitor or (2) a combination of taxotere, a P-gp substrate, with GF120918, a P-gp inhibitor (section 2.8.3). A summary of the results observed in all combination assays can be seen in Table 3.3.1. Western blotting revealed that P-gp levels, though expressed in DMS-53 and absent in SKMES-1 were overexpressed in all taxane-resistant variants of these cell lines as well as the carboplatin resistant variant of DMS-53. Combinations assays with GF12098 revealed a greater than 20% and 40% enhanced effect of taxotere toxicity in DMS-53 and SKMES-1 respectively. However, GF12098/taxotere resulted in a greater than 60% enhanced effect in DMS-Txl, DMS-Txt and SKMES-Txt. These results suggest that P-gp plays a major role in taxane resistance in these cell line. No P-gp was detected in DLRP or DLRP-Txt. Combinations assays with sulindac and adriamycin had a greater than 20% enhanced effect of adriamycin toxicity in both carboplatin selected variants of SKMES-1. The MRP1 status of these cell lines has not been fully completed due to problems with the primary antibody.

Cell line	Sulindac and adriamycin	MRP1 Expression	GF120918 and taxotere	P-gp Expression
SKMES-1	-	UK	++	Y
SKMES-Txt	-	UK	+++	Y
SKMES-Cpt100	+	UK	-	N
SKMES-Cpt30	+	UK	-	N
DLRP	-	UK	-	N
DLRP-Txt	+	UK	+	N
DLRP-Cpt	-	UK	-	N
DMS-53	+	UK	+	Y
DMS-Txt	-	UK	+++	Y
DMS-Txl	-	UK	+++	Y
DMS-Cpt	-	UK	++	Y

Table 3.3.1 Summary of effects observed in combination assays. + Indicates >20% enhanced effect, ++ indicates >40% enhanced effect, +++ indicates >60% enhanced effect, - indicates no effect. Y indicates expression, N indicates no expression, UK indicates unknown.

3.3.2 Adriamycin in combination with sulindac for SKMES-1

The combinations of three concentrations of sulindac were tested with 1.56ng/ml adriamycin for SKMES-1. The combination of sulindac with adriamycin did not enhance adriamycin cell kill indicating the possible absence of MRP1 in this cell line (Figure 3.3.1).

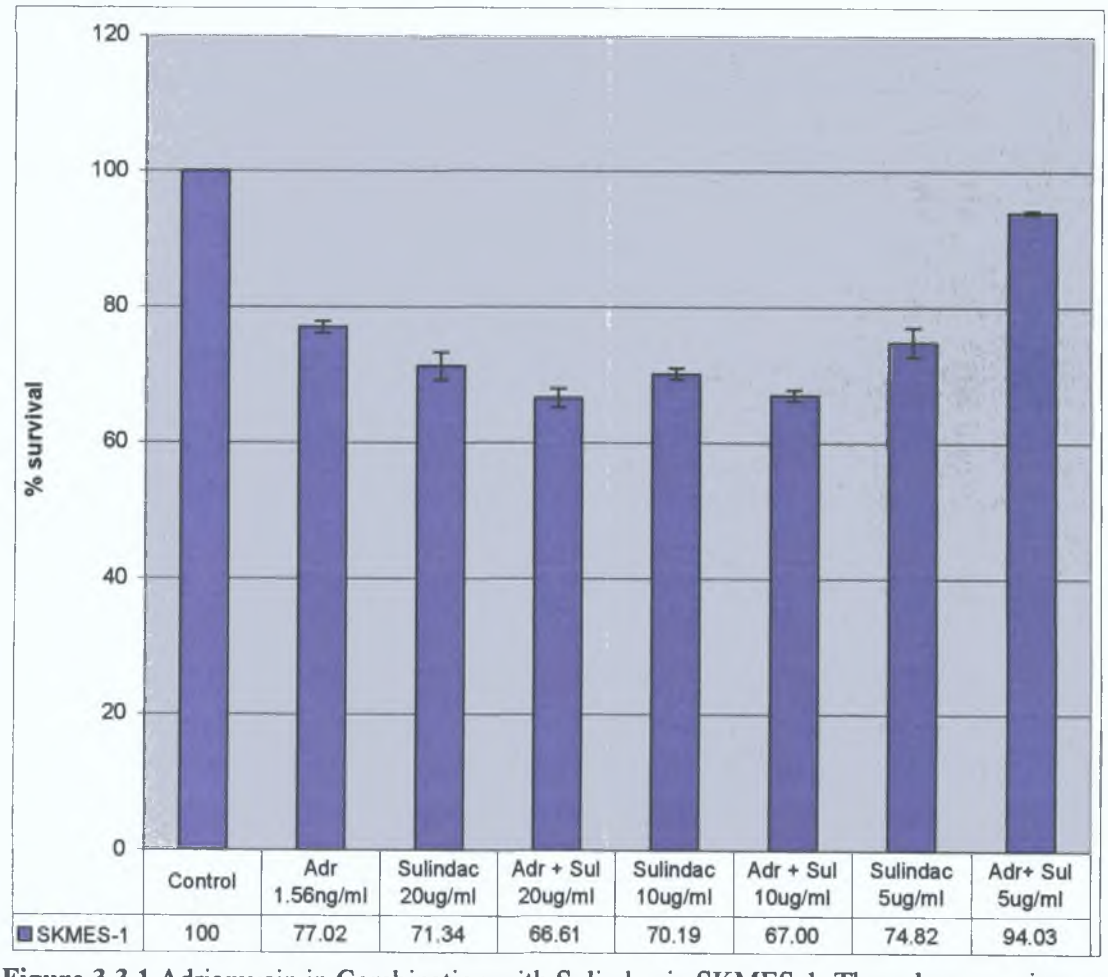

Figure 3.3.1 Adriamycin in Combination with Sulindac in SKMES-1. The values are given as the average % survival values ± the standard deviation on a minimum of three repeats. Adr = adriamycin, Sul = sulindac.

3.3.3 Adriamycin in combination with sulindac for SKMES-Cpt100

The combinations of three concentrations of sulindac were tested with 3ng/ml adriamycin for SKMES-Cpt100. The combination of adriamycin with the NSAID sulindac enhanced adriamycin toxicity in this cell line indicating the possible up-regulation of MRP1 (Figure 3.3.2).

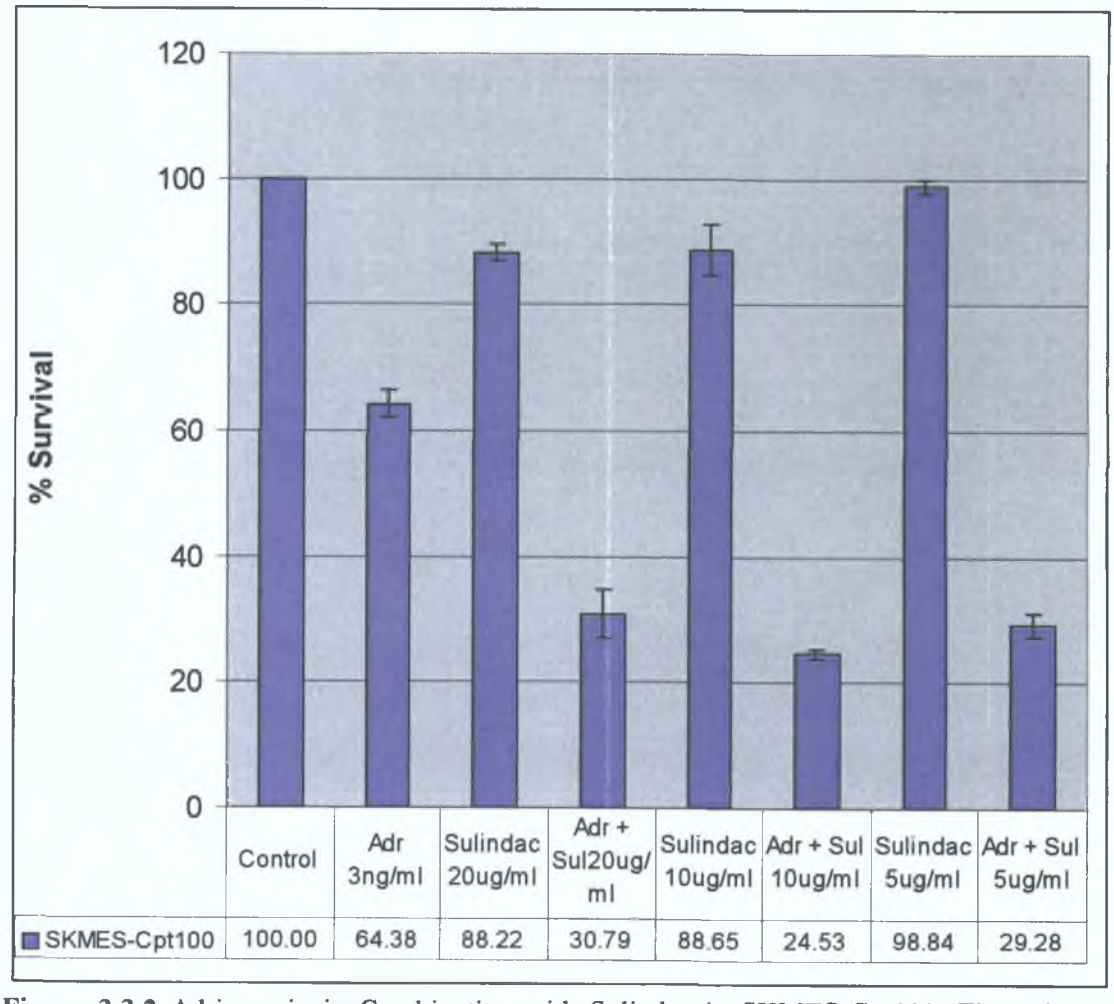

Figure 3.3.2 Adriamycin in Combination with Sulindac in SKMES-Cpt100. The values are given as the average & survival values ± the standard deviation on a minimum of three repeats. Adr = adriamycin, Sul = sulindac.

3.3.4 Adriamycin in combination with sulindac for SKMES-Txt

The combinations of three concentrations of sulindac were tested with 7.8ng/ml adriamycin for SKMES-Txt. The combination of sulindac with adriamycin did not enhance adriamycin toxicity indicating that MRP1 is probably absent in this cell line (Figure 3.3.3).

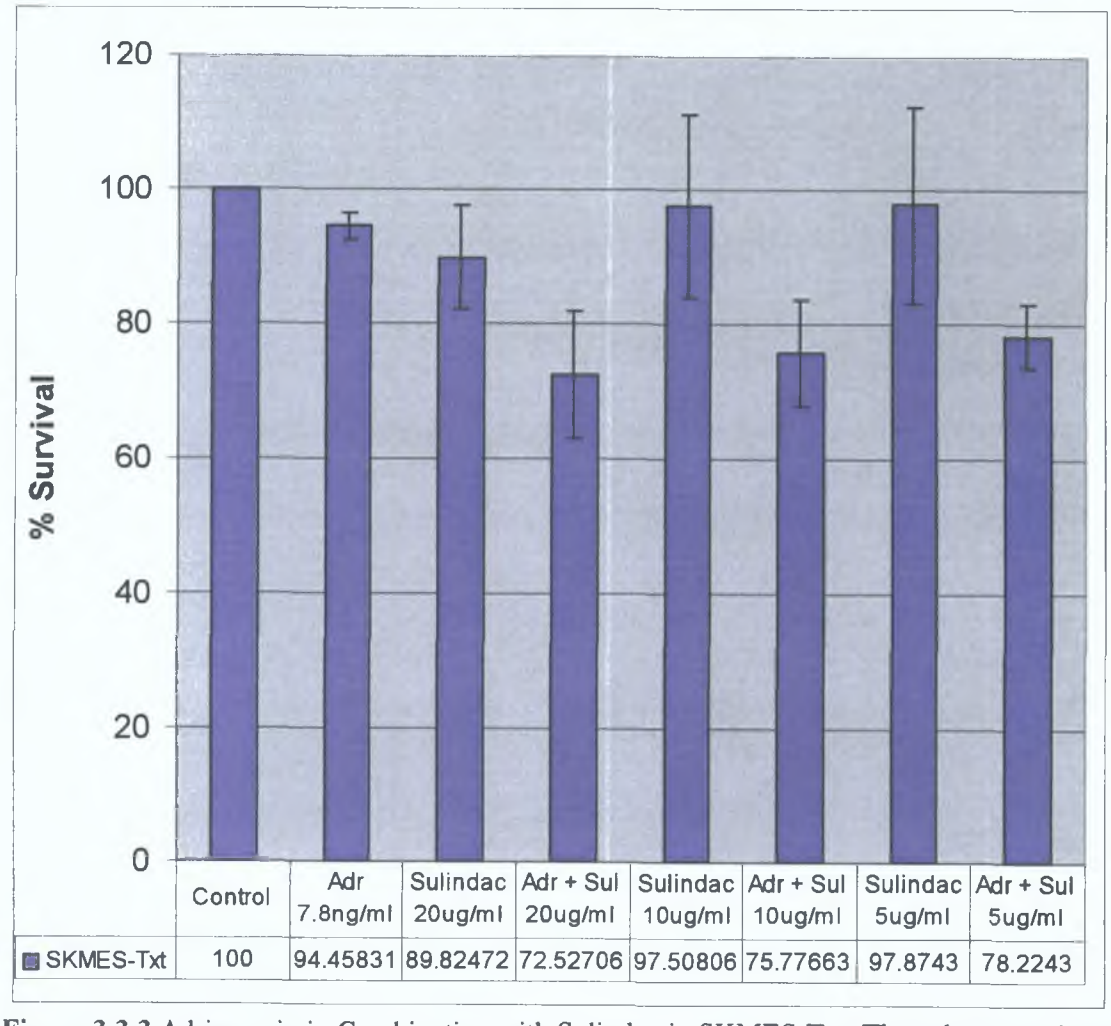

Figure 3.3.3 Adriamycin in Combination with Sulindac in SKMES-Txt. The values are given as the average % survival values ± the standard deviation on a minimum of three repeats. Adr = adriamycin, Sul = sulindac.

3.3.5 Adriamycin in combination with sulindac for SKMES-Cpt30

The combinations of three concentrations of sulindac were tested with 1.9ng/ml adriamycin for SKMES-Cpt30. The combination of sulindac with adriamycin enhanced adriamycin toxicity indicating the possible presence of MRP1 in this cell line (Figure 3.3.4).

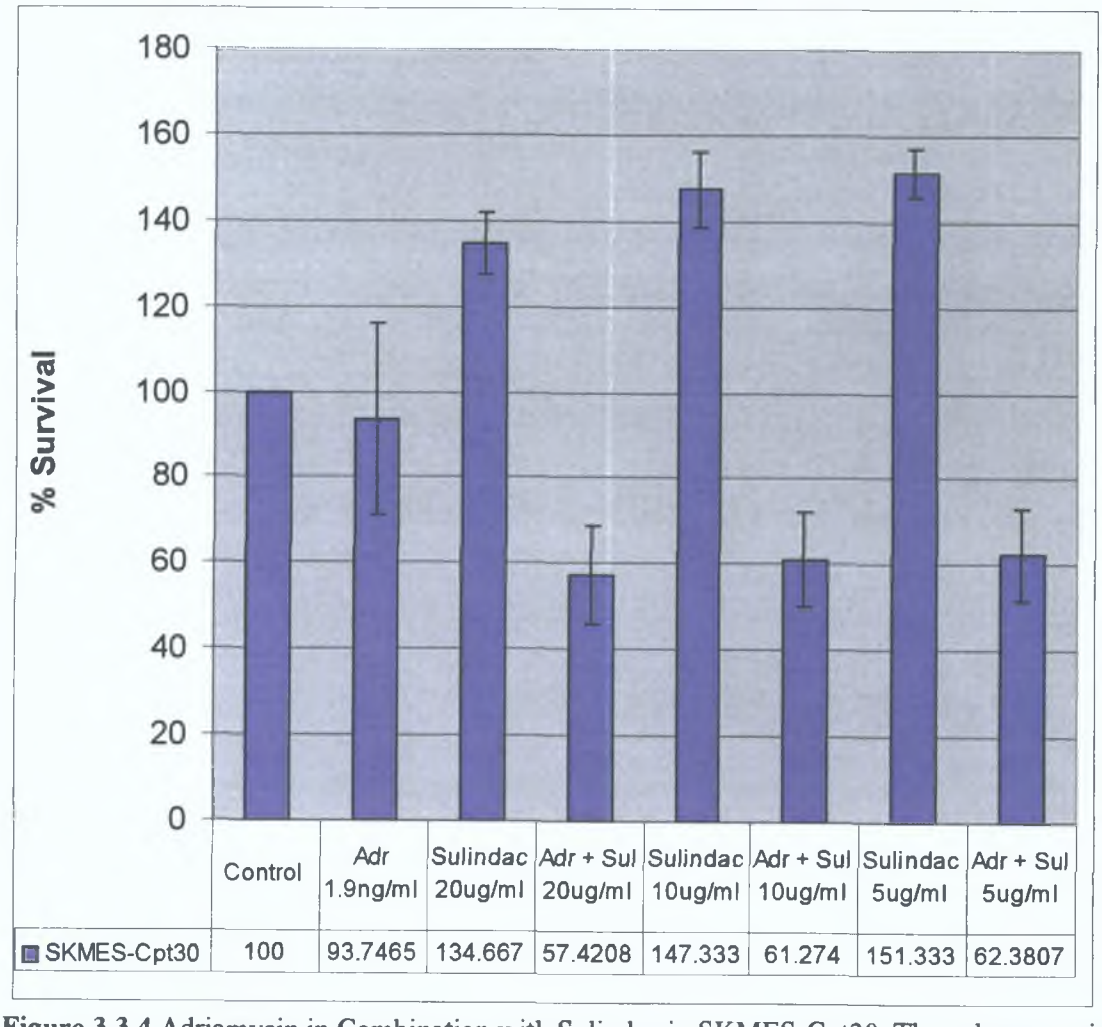

Figure 3.3.4 Adriamycin in Combination with Sulindac in SKMES-Cpt30. The values are given as the average IC value ± the standard deviation in duplicate. Adr = adriamycin, Sul = sulindac.

3.3.6 Adriamycin in combination with sulindac for DLRP and DLRP-Txt

The combinations of three concentrations of sulindac were tested with 0.3ng/ml adriamycin for DLRP and DLRP-Txt. The combination of sulindac with adriamycin had no effect on adriamycin toxicity in the parent cell line, DLRP indicating the absence of MRP1. However, the same combination in DLRP-Txt resulted in >20% enhanced toxicity indicating that MRP1 is most likely up-regulated (Figure 3.3.5).

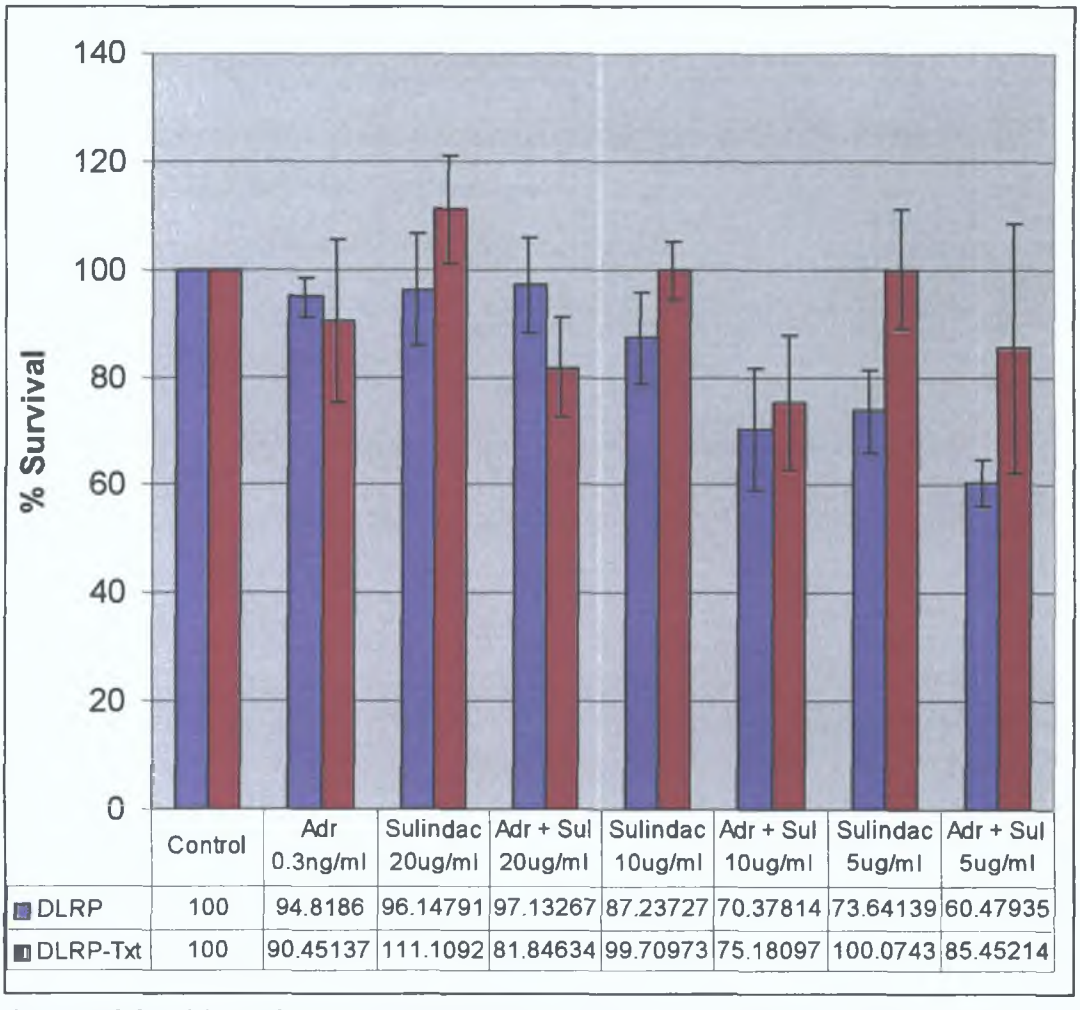

	Control	Adr 0.3ng/ml	Sulindac 20ug/ml	Adr + Sul 20ug/ml	Sulindac 10ug/ml	Adr + Sul 10ug/ml	Sulindac 5ug/ml	Adr + Sul 5ug/ml
DLRP	100	94.8186	96.14791	97.13267	87.23727	70.37814	73.64139	60.47935
DLRP-Txt	100	90.45137	111.1092	81.84634	99.70973	75.18097	100.0743	85.45214

Figure 3.3.5 Adriamycin in Combination with Sulindac in DLRP and DLRP-Txt. The values are given as the average % survival values ± the standard deviation on a minimum of three repeats. Adr = adriamycin, Sul = sulindac.

3.3.7 Adriamycin in combination with sulindac for DLRP-Cpt

The combinations of three concentrations of sulindac were tested with 0.3ng/ml adriamycin for DLRP. The combination of sulindac with adriamycin had no effect on adriamycin toxicity indicating the possible absence of MRP1 in this cell line (Figure 3.3.6).

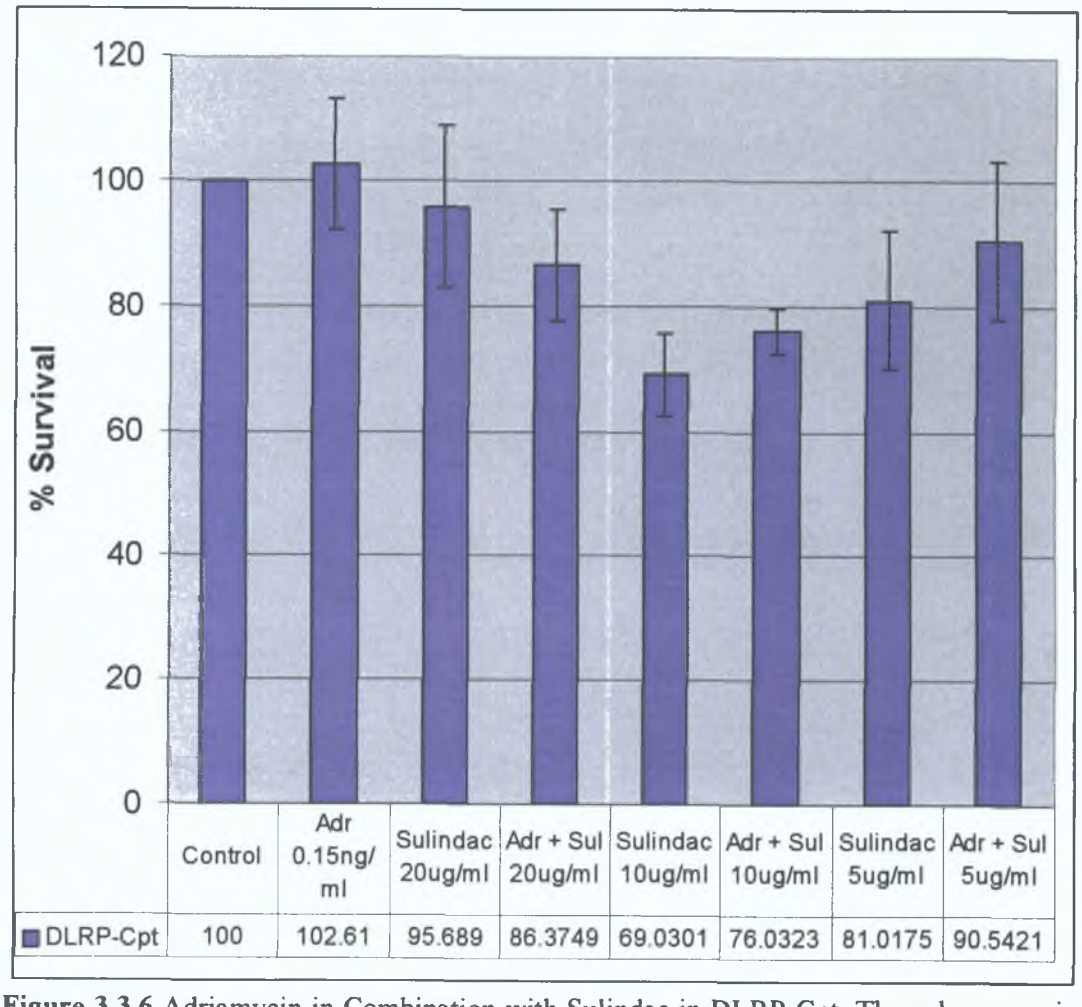

Figure 3.3.6 Adriamycin in Combination with Sulindac in DLRP-Cpt. The values are given as the average % survival values ± the standard deviation on a minimum of three repeats. Adr = adriamycin, Sul = sulindac.

3.3.8 Adriamycin in combination with sulindac for DMS-53 and variants

The combinations of three concentrations of sulindac were tested with 3.1ng/ml adriamycin for DMS-53 and drug resistant variants. The combination of sulindac with adriamycin in the parental cell line DMS-53 resulted in > 20% enhanced toxicity. However, in each of the variants no effect on adriamycin toxicity was observed indicating the probable absence of MRP1 (Figure 3.3.7).

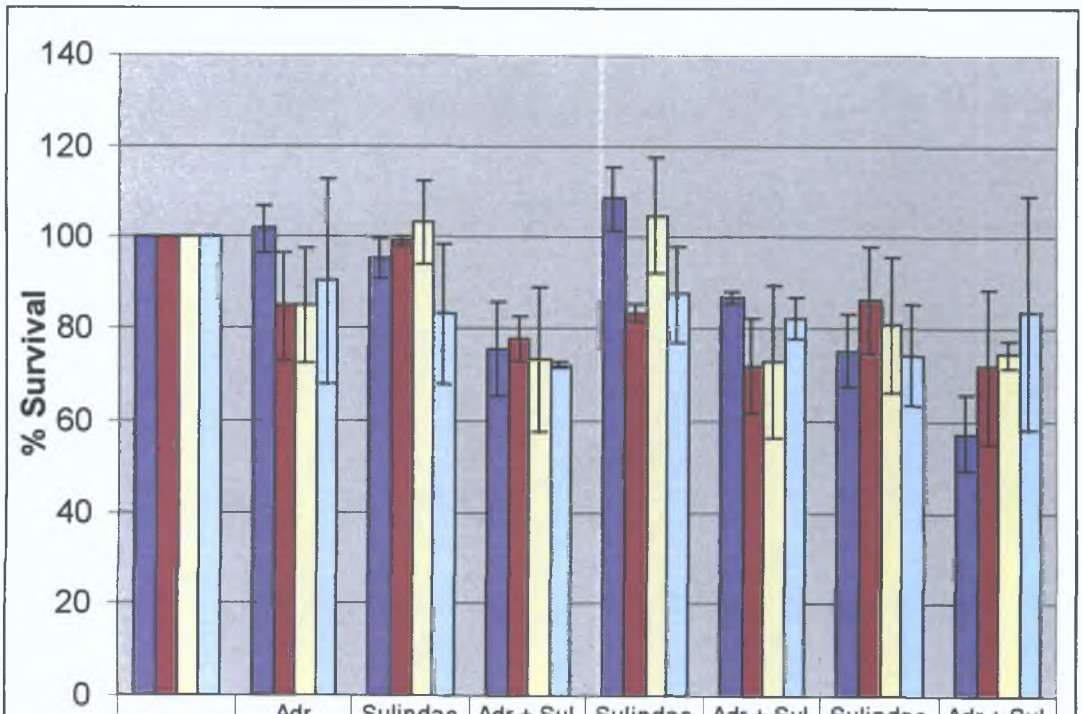

	Control	Adr 3.1ng/ml	Sulindac 20ug/ml	Adr + Sul 20ug/ml	Sulindac 10ug/ml	Adr + Sul 10ug/ml	Sulindac 5ug/ml	Adr + Sul 5ug/ml
DMS-53	100.00	101.80	95.23	75.63	108.62	86.74	75.28	57.35
DMS-Txl	100.00	84.81	99.17	77.82	83.40	72.04	86.32	71.90
DMS-Txt	100.00	84.96	103.19	73.52	104.87	72.78	80.91	74.50
DMS-Cpt	100.00	90.23	83.25	72.20	87.62	82.32	74.38	83.60

Figure 3.3.7 Adriamycin in Combination with Sulindac in DLRP-Cpt. The values are given as the average IC value ± the standard deviation on a *minimum* of three repeats. Adr = adriamycin, Sul = sulindac.

3.3.9 Taxotere in combination with GF120918 for SKMES-1

The combinations of three concentrations of GF120918 were tested with 0.45ng/ml taxotere for SKMES-1. The combination of GF120918 with taxotere in the parental cell line resulted in > 40% enhanced toxicity confirming the expression of P-gp (Figure 3.3.8).

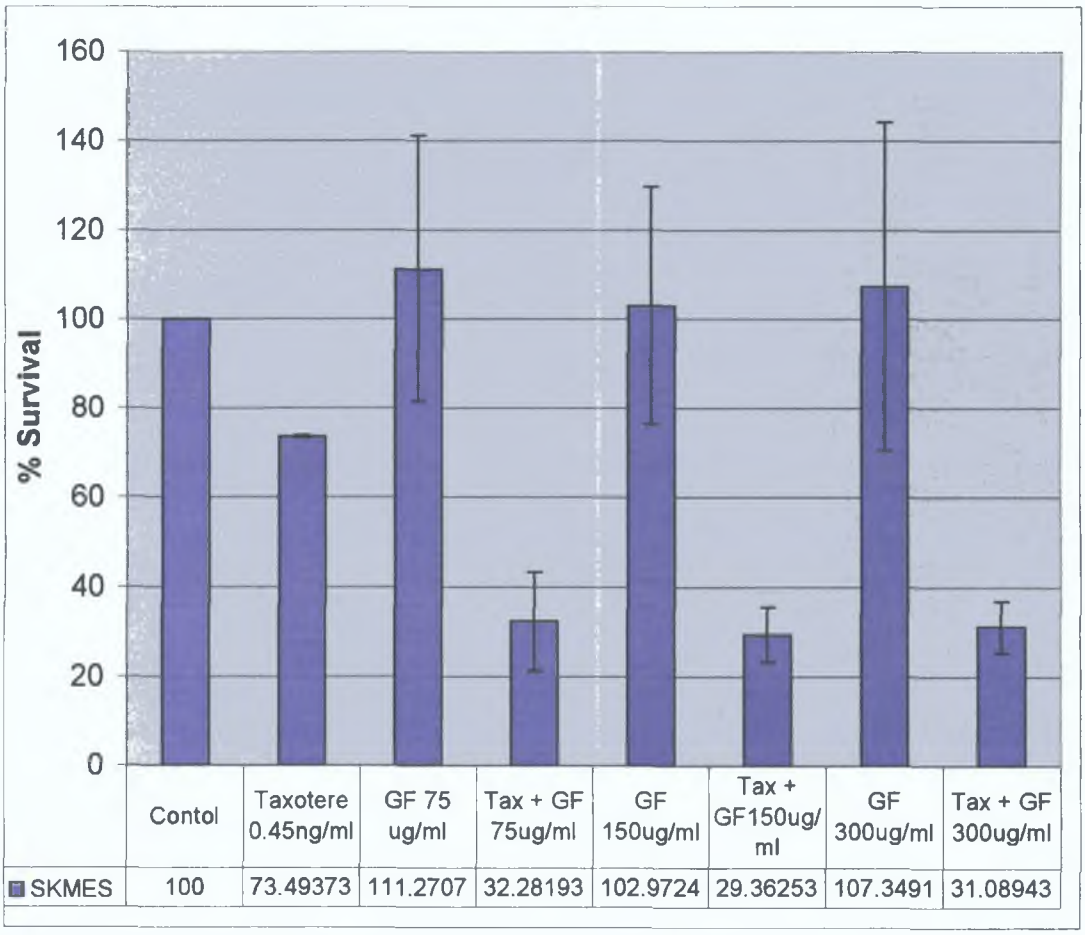

	Contol	Taxotere 0.45ng/ml	GF 75 ug/ml	Tax + GF 75ug/ml	GF 150ug/ml	Tax + GF150ug/ml	GF 300ug/ml	Tax + GF 300ug/ml
SKMES	100	73.49373	111.2707	32.28193	102.9724	29.36253	107.3491	31.08943

Figure 3.3.8 Taxotere in Combination with GF120918 in SKMES-1. The values are given as the average % survival value ± the standard deviation on a minimum of three repeats. Tax = taxotere, GF = GF120918.

3.3.10 Taxotere in combination with GF120918 for SKMES-Txt

The combinations of three concentrations of GF120918 were tested with 1.87ng/ml taxotere for SKMES-Txt. The combination of GF120918 with taxotere in the parental cell line resulted in > 60% enhanced toxicity indicating the expression of P-gp (Figure 3.3.9).

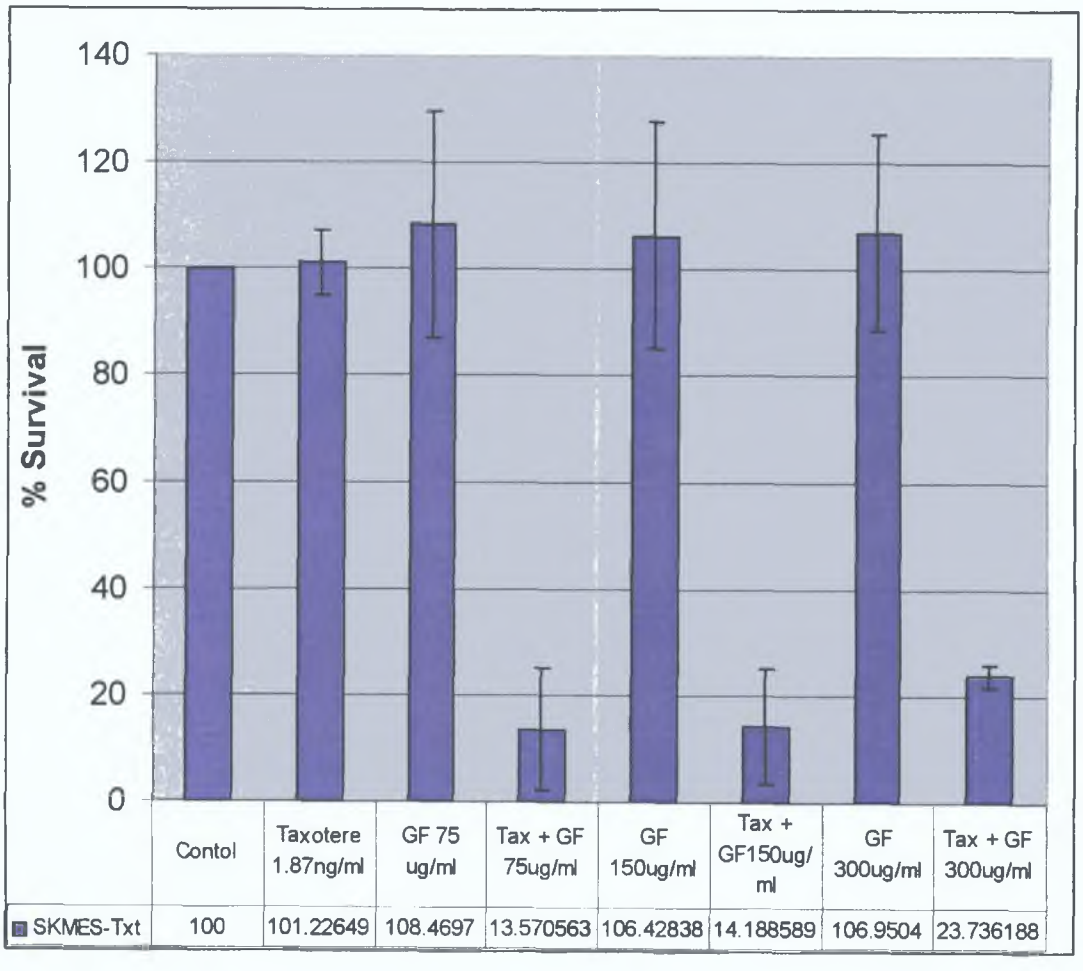

Figure 3.3.9 GF120918 in Combination with taxotere in the SKMES-Txt MDR resistant variant. The values are given as the average % survival values ± the standard deviation on a minimum of three repeats. Tax = taxotere, GF = GF120918.

3.3.11 Taxotere in combination with GF120918 for SKMES-1 and SKMES-Txt

A concentration of 1.8ng/ml taxotere on the parent cell line SKMES-1 results in ~ 30% survival. However, the same concentration of taxotere on SKMES-Txt with the lowest concentration of GF120918 (75µg/ml) results in 23.7 % survival (Figure 3.3.10).

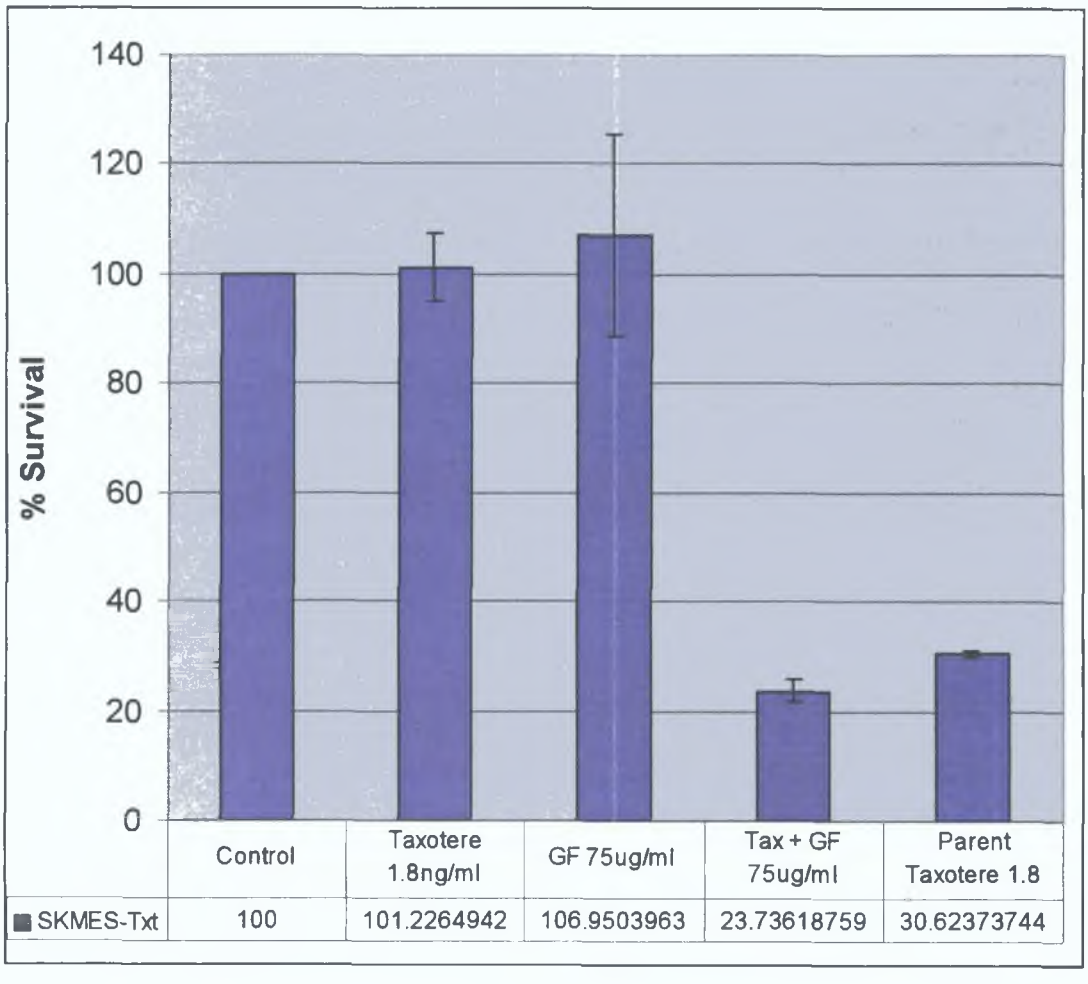

Figure 3.3.10 GF120918 in Combination with taxotere in the SKMES-Txt MDR resistant variant. The values are given as the average % survival values ± the standard deviation on a minimum of three repeats. Tax = taxotere, GF = GF120918.

3.3.12 Taxotere in combination with GF120918 for DLRP

The combinations of three concentrations of GF120918 were tested with 0.25ng/ml taxotere for DLRP. The combination of GF120918 with taxotere in the parental cell line did not enhance taxotere resistance at each concentration tested indicating the possible absence of P-gp in this cell line (Figure 3.3.11).

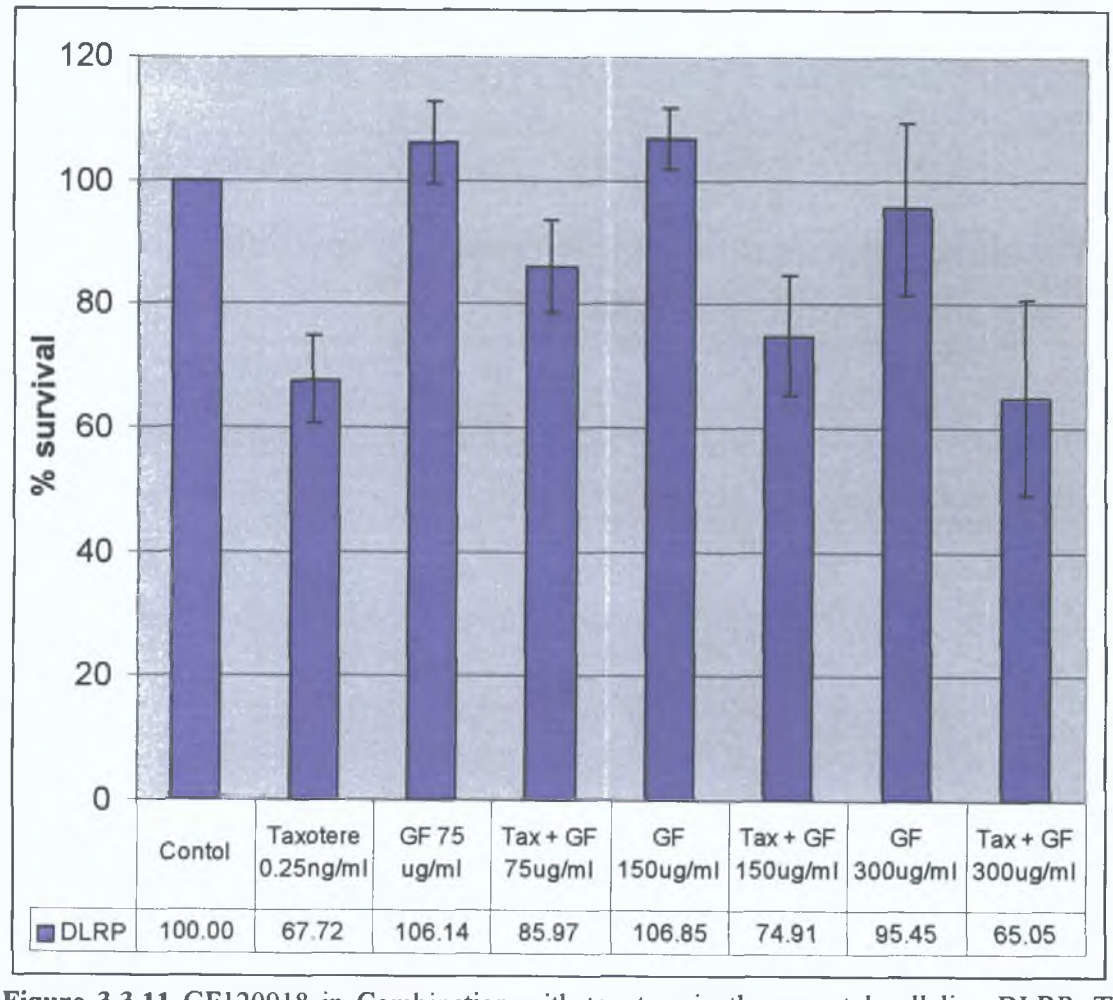

Figure 3.3.11 GF120918 in Combination with taxotere in the parental cell line DLRP. The values are given as the average % survival values ± the standard deviation on a minimum of three repeats. Tax = taxotere, GF = GF120918.

3.3.13 Taxotere in combination with GF120918 for DLRP-Cpt

The combinations of three concentrations of GF120918 were tested with 0.11ng/ml taxotere for DLRP-Cpt. The combination of GF120918 with taxotere in the parental cell line had no effect on taxotere resistance indicating that P-gp is most likely absent in this cell line (Figure 3.3.12).

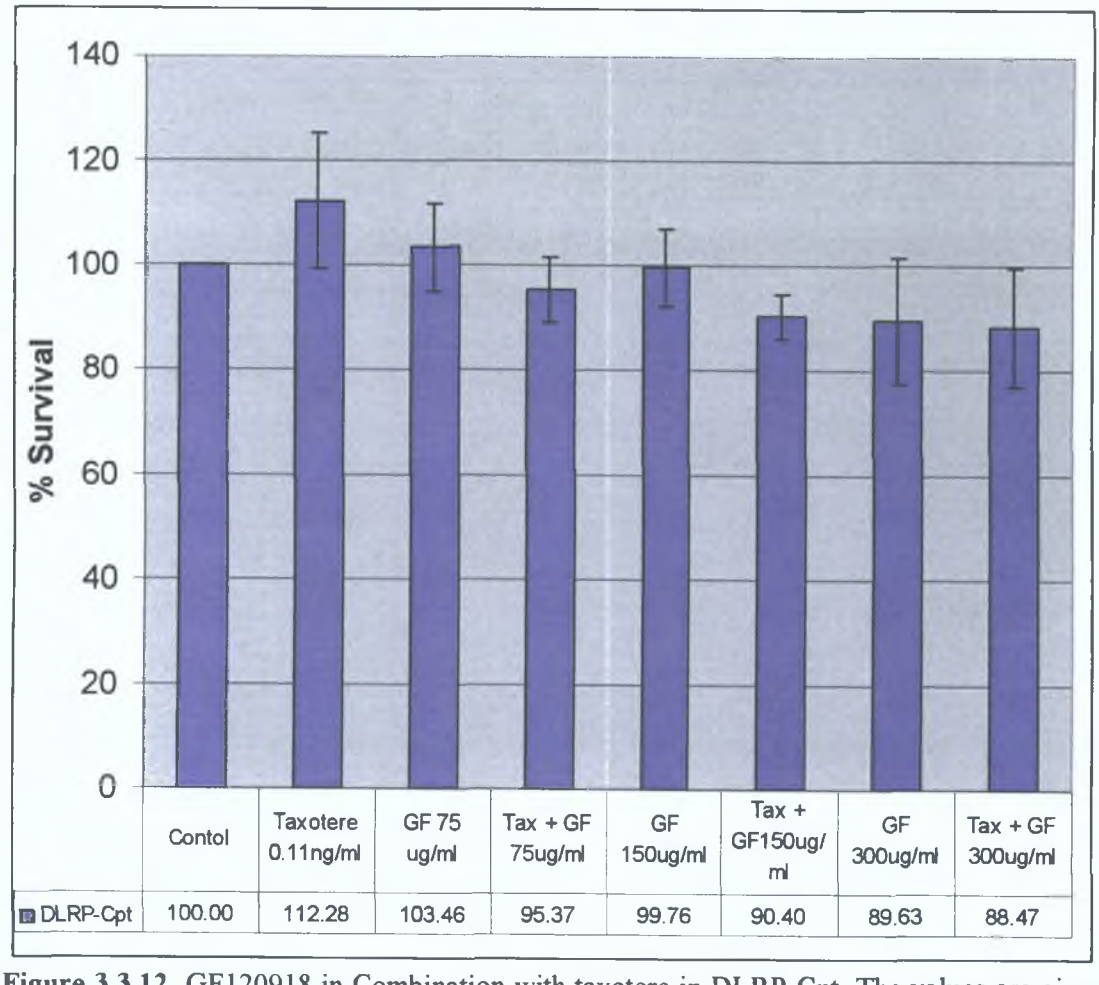

Figure 3.3.12 GF120918 in Combination with taxotere in DLRP-Cpt. The values are given as the average % survival values ± the standard deviation on a minimum of three repeats. Tax = taxotere, GF = GF120918.

3.3.14 Taxotere in combination with GF120918 for DLRP-Txt

The combinations of three concentrations of GF120918 were tested with 0.38ng/ml taxotere for DLRP-Txt. The combination of GF120918 with taxotere in the parental cell line had greater than 20% enhanced toxicity indicating the possible presence of P-gp (Figure 3.3.13).

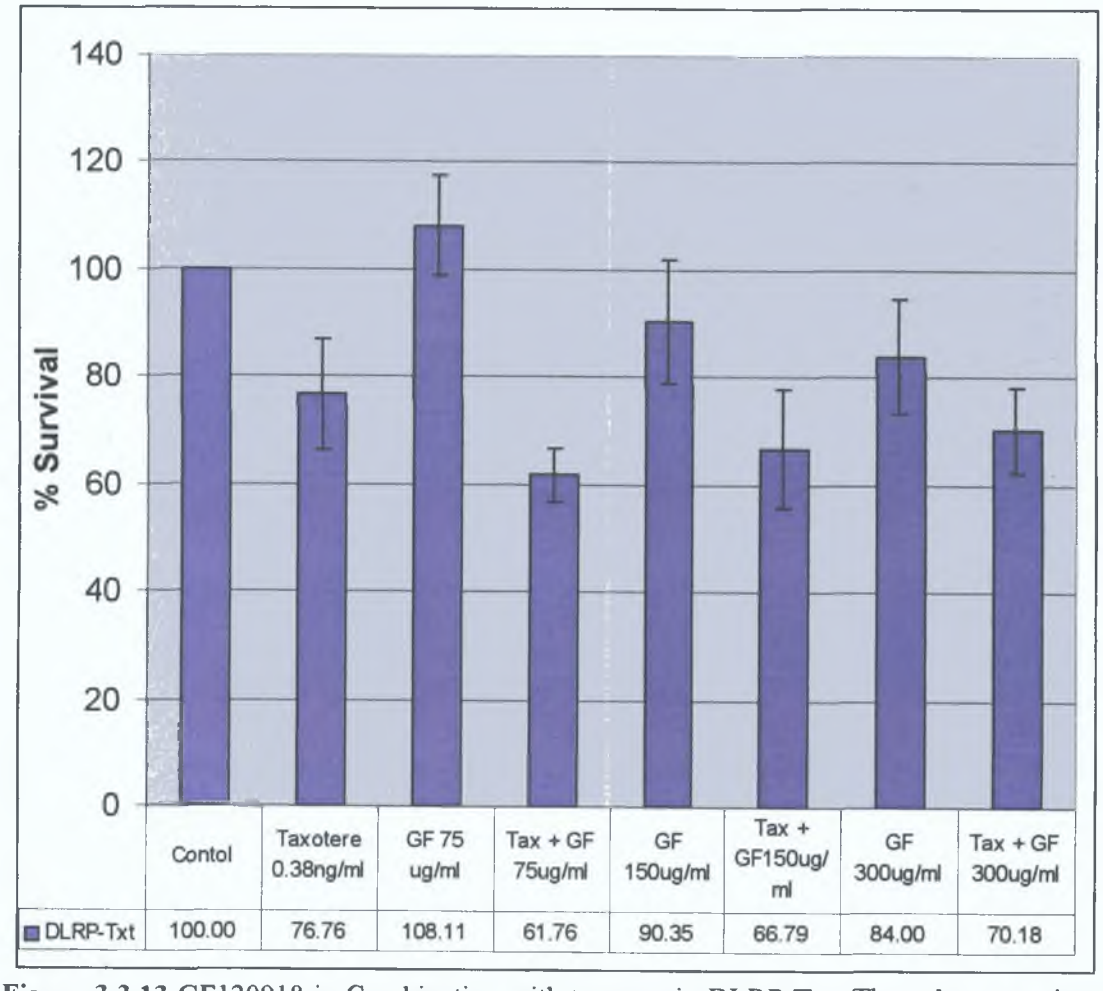

Figure 3.3.13 GF120918 in Combination with taxotere in DLRP-Txt. The values are given as the average % survival values ± the standard deviation on a minimum of three repeats. Tax = taxotere, GF = GF120918.

3.3.15 Taxotere in combination with GF120918 for DMS-53 and variants

The combinations of three concentrations of GF120918 were tested with 0.75ng/ml taxotere for DMS-53 and drug resistant variants. The combination of GF120918 with taxotere in the parental cell line DMS-53 and DMS-Cpt resulted in > 20% and 40% enhanced toxicity. However, in the taxane variants, greater than 60% enhanced toxicity was observed indicating the presence of P-gp in the parental cell line and its up-regulation in the variants (Figure 3.3.14)

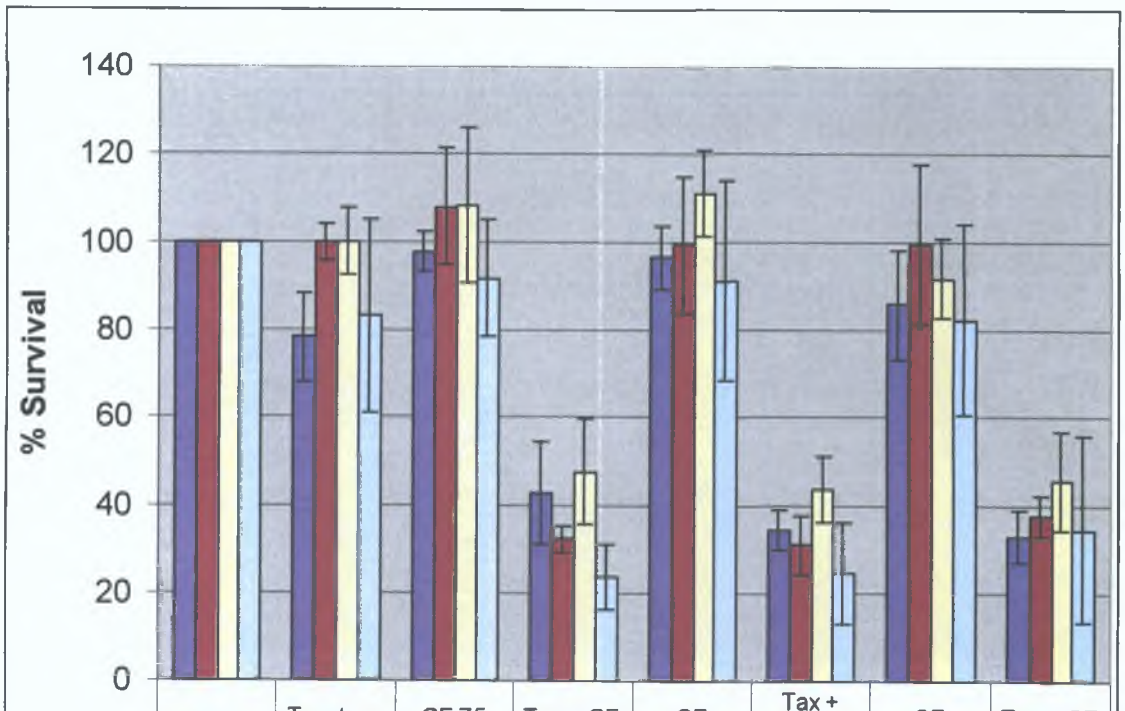

	Contol	Taxotere 0.75ng/ml	GF 75 ug/ml	Tax + GF 75ug/ml	GF 150ug/ml	Tax + GF150ug/ml	GF 300ug/ml	Tax + GF 300ug/ml
DMS-53	100.00	78.23	97.72	42.76	96.41	34.44	85.70	33.07
DMS-Txt	100.00	99.88	108.01	32.58	99.19	31.06	99.45	37.84
DMS-Txl	100.00	99.99	108.34	47.81	111.08	43.74	91.60	45.79
DMS-Cpt	100.00	83.18	91.60	23.71	91.07	24.73	82.33	34.58

Figure 3.3.14 GF120918 in Combination with taxotere in DMS-53 and MDR resistant variants. The values are given as the average IC value ± the standard deviation on a minimum of three repeats. Tax = Taxotere, GF = GF120918.

3 3 16 P-gp Expression in SKMES-1 and taxane-selected variants

Western blots were carried out to determine P-gp expression in the SKMES-1 taxane-selected cell lines There was up-regulation of P-gp in both taxane-selected variants of SKMES-1 Taxotere exposure resulted in a higher expression of P-gp compared to taxol exposure Protein samples were prepared at weeks 34, 36 and 38 from SKMES-Txl (see Figure 4 1) and at weeks 61, 63 and 65 from SKMES-Txt (see Figure 4 2) to determine if a correlation existed between fall of drug resistance with P-gp expression Results revealed no correlation β-actin is differentially expressed in SKMES-Txl (Wk3) according to proteomic results (see Table 3 6 7)

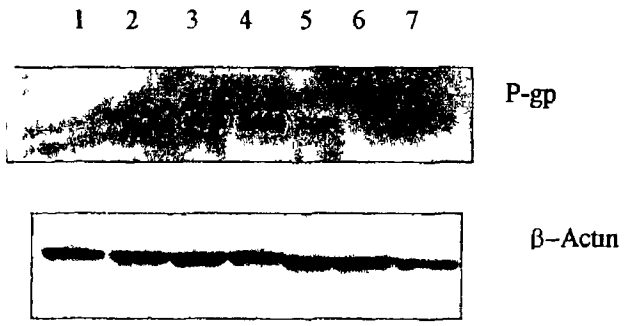

Figure 3 3 15 P-gp expression in SKMES-1 and taxane-selected variants Lane 1 SKMES-1, 2 SKMES-Txt (Wk2), 3 SKMES-Txt (W5), 4 SKMES-Txt (Wk6), 5 SKMES-Txl (Wk2), 6 SKMES-Txl (W5), 7 SKMES-Txl (Wk6) Western blots comparing parent with SKMES-Txt and SKMES-Txl (week 2) have been carried out in triplicate However, the comparison of taxane-selected variants at weeks 3 and 5 have only been carried out once

3 3 17 P-gp Expression in DMS-53 and drug selected variants

Western blots were carried out to determine P-gp expression in the carboplatin and taxane-selected variants of DMS-53 There was slight up-regulation of P-gp in the variants

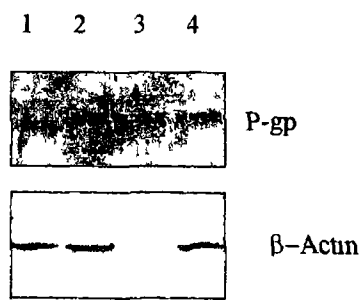

Figure 3 3 16 P-gp expression in DMS-53 and drug-selected variants Lane 1 DMS-53, 2 DMS-Txt, 3 DMS-Txl, 4 DMS-Cpt Western blots were only carried out once and need to be repeated

3.4 Two-dimensional-difference gel electrophoresis

Two-dimensional-difference gel electrophoresis (2D-DIGE), a new development in proteomics has made it possible to detect and quantify the differences between experimental pairs of samples on one gel. Protein samples are prelabelled with different fluorescent dyes (Cy2, Cy3 and Cy5) so they can be mixed together, co-separated and visualised distinctly on a single 2D gel. Pooling an aliquot of all biological samples in the experiment and labelling it with the Cy2 fluor creates the internal standard. The internal standard is then run on every gel along with each individual sample. Each protein from all samples is therefore represented in the internal standard, which is present on all gels resulting in co-migration of proteins originating from separate samples (Figure 3.4.1). For example, a control cell line and a corresponding drug-resistant variant can be labelled with the different dyes, combined and run on the same gel. The advantage of this method over conventional 2-DE is that the samples are exposed to the same chemical environments and electrophoretic conditions. Gel-to-gel variation is reduced as co-migration is guaranteed for identical proteins from separate samples.

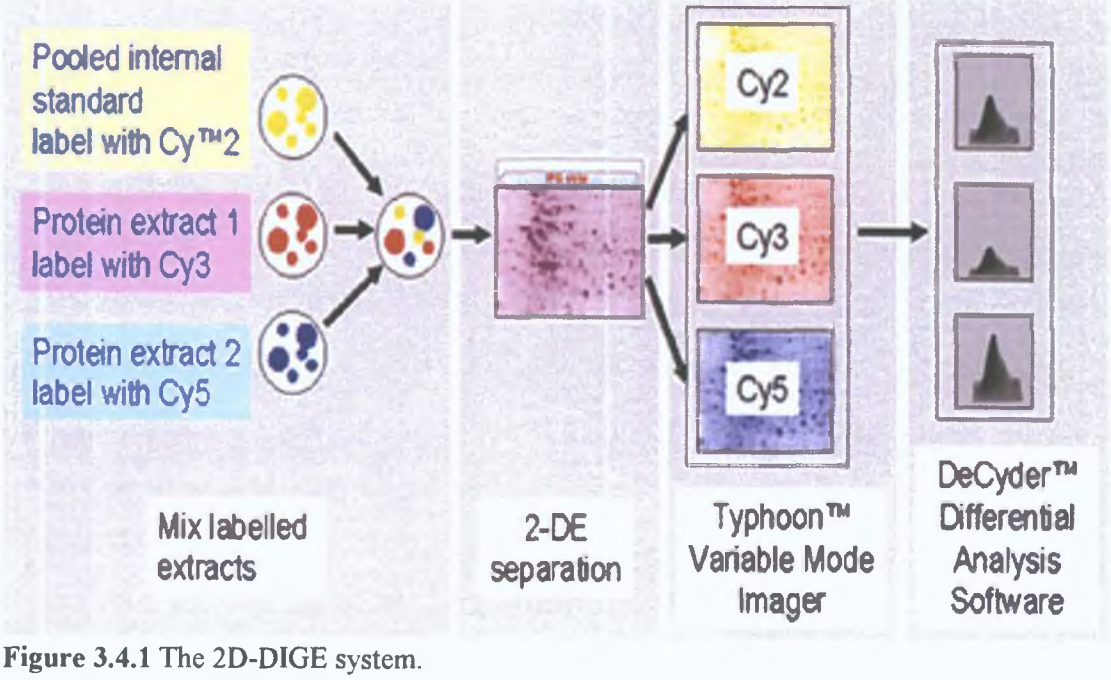

Figure 3.4.1 The 2D-DIGE system.

The two-dimensional DIGE system has greatly reduced inherent system variation to a level that allows detection of minor protein expression changes of as little as 20%. The result is new levels of statistical reliability in electrophoresis results. Each protein has

its own internal standard, which ensures high accuracy enabling even the smallest possible real differences in protein abundance to be detected The technique was used to look at differential protein expression in cancer and drug-resistant variants by labelling control and resistant variants with spectrally-resolvable fluorophores and as DIGE is multiplexed, an internal control was run to allow improved matching between gels

3 4 1 Outline of proteomic analysis of adriamycin resistant variants of DLKP

Investigations were carried out to establish differential protein expression caused by adriamycin resistance in DLKP, a squamous lung cell line displaying varying levels of resistance to adriamycin (Table 3 4 1) The adriamycin-resistant cell lines (produced by a number of researchers at the NCTCC (section 2 2)) were developed from the DLKP cell line DLKP was established from a lymph node biopsy of a 52-year-old male identified as a poorly differentiated squamous cell lung carcinoma (Law *et al*, 1992)

	Fold Resistance				
Cell Line	**Adriamycin**	**Cisplatin**	**Vincristine**	**VP-16**	**5-FU**
DLKP	1	1	1	1	1
DLKP-A10	765 3	0 8*	3000	63 3	0 9
DLKP-A5F	235 4	1 4	1275	50 6	0 98
DLKP-A	122 6	1 5	1504	60 7	1 8
DLKP-A2B	7	0 6	228 3	18 2	1 3

Table 3 4 1 Drug resistance profiles of adriamycin resistant variants of DLKP *Carboplatin Table was compiled from Cleary *et al*, 1997 and Heenan *et al*, 1997 Resistance to adriamycin was reconfirmed by toxicity assay Fold resistance was calculated with respect to DLKP

The DLKP-A variant was developed from DLKP by continuous exposure to increasing concentrations of adriamycin to a final concentration of 2 μg/ml (Clynes *et al*, 1992) The DLKP-A10 cell line was selected by continuous exposure of the DLKP-A cell line to further increasing concentrations of adriamycin to a final concentration of 10μg/ml (Cleary *et al*, *1997*) Two clonal sub-populations were also established from DLKP-A by clonal dilution, and named DLKP-A5F and DLKP-A2B (Heenan *et al*, 1997) All of the above four resultant variants have varying levels of resistance to adriamycin and also exhibit cross-resistance profiles to a number of other chemotherapeutic drugs (Table 3 4 1)

The DLKP-A10 cell line is 765 3-fold resistant to adriamycin when compared to DLKP The cell line is also 3 2-fold, 6 2-fold and 109 3-fold times more resistant to adriamycin when compared to DLKP-A5F, DLKP-A and DLKP-A2B respectively All cell lines exhibited very high levels of cross resistance to vincristine with DLKP-A10 being 3000-fold resistant when compared to the parent and 2 3-fold, 1 99-fold and 13-fold resistant when compared to DLKP-A5F, DLKP-A and DLKP-A2B respectively Cross-resistance to cisplatin did not correspond to adriamycin resistance, DLKP-A10 and DLKP-A2B are lower than the parent while DLKP-A and DLKP-A5F are marginally higher Some small cross-resistance is seen for DLKP-A and DLKP-A2B but the more resistant variants (DLKP-A5F and DLKP-A10) show sensitivity in comparison to DLKP-A, almost back to the same levels as DLKP

DLKP, DLKP-A, DLKLP-A2B and DLKP-A5F have stable expression and toxicity assays confirmed the fold resistance to adriamycin (Table 3 4 1) The DLKP-A10 variant requires exposure to drug every four passages in order to maintain resistance levels This was also confirmed by toxicity assays (data not shown)

3 4 1 1 Invasive status of the adriamycin resistant variants of DLKP

Invasion assays were performed, as described in Section 2 11, to assess the ability of each of the five DKLP cell lines to invade through matrigel Cell culture inserts were coated with matrigel and placed in medium containing 24-well plates prior to cell addition Cells were considered invasive if they migrated through the matrigel and the 8 μM porous membrane and attached to the underside of the membrane within 24 hours The images presented are representative of at least three separate experiments, are at a magnification of 10X and are stained with crystal violet

The DLKP parental cell line is invasive (Figure 3 4 2) Increased invasion was observed in DLKP-A (Figure 3 4 3) when compared to the parent Further exposure of DLKP-A to adriamycin resulted in a less invasive variant, DLKP-A10 (Figure 3 4 4) Similarly, the least resistant subclone of DLKP-A, namely DLKP-A2B is less invasive than DLKP-A In contrast, DLKP-A5F which is more resistant than DLKP-A is also more invasive (Figure 3 4 5)

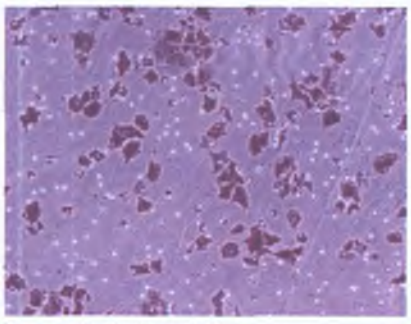

Figure 3.4.2 DLKP

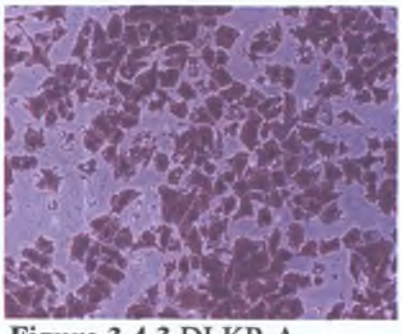

Figure 3.4.3 DLKP-A

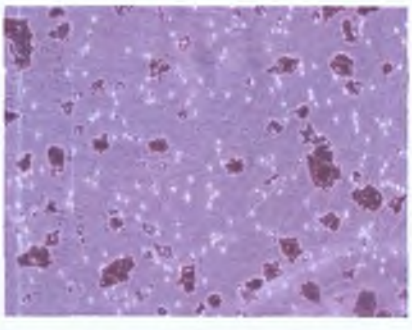

Figure 3.4.4 DLKP-A10

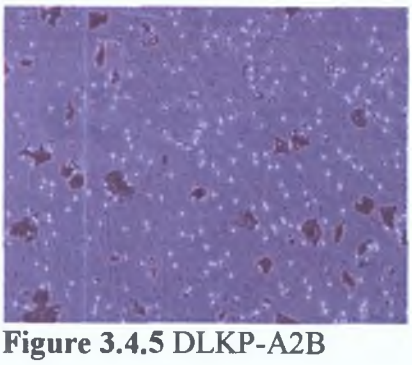

Figure 3.4.5 DLKP-A2B

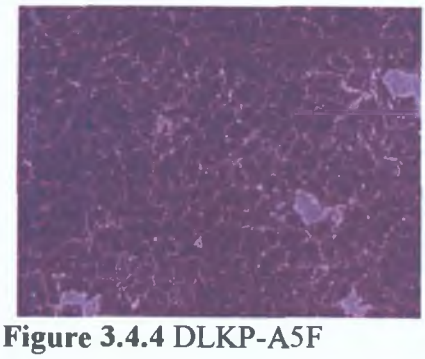

Figure 3.4.4 DLKP-A5F

3.4.1.2 Quantification of invasion

The invasion assays were quantified by counting cells with a graticule at 40X magnification (Table 4.2.2, Figure 3.4.5). Proteomic analysis was carried out on these cell lines. The data shows that DLKP, an invasive cell line was compared to the slightly more invasive DLKP-A. DLKP-A was compared to a more invasive cell line, DLKP-A5F and two less invasive cell lines, DLKP-A2B and DLKP-A10 respectively.

Cell Line	Average cell count/area/view	P value
DLKP	11.35 ± 1.09	-
DLKP-A2B	1.36 ± 0.35	0.002
DLKP-A	14.85 ± 1.41	0.029
DLKP-A5F	33.13 ± 2.15	0.0006
DLKP-A10	5.56 ± 0.68	0.001

Table 3.4.2 Quantification of DLKP and adriamycin-resistant variants. The values are given as the average cell counts/area/view ± the standard deviation. (n=3).

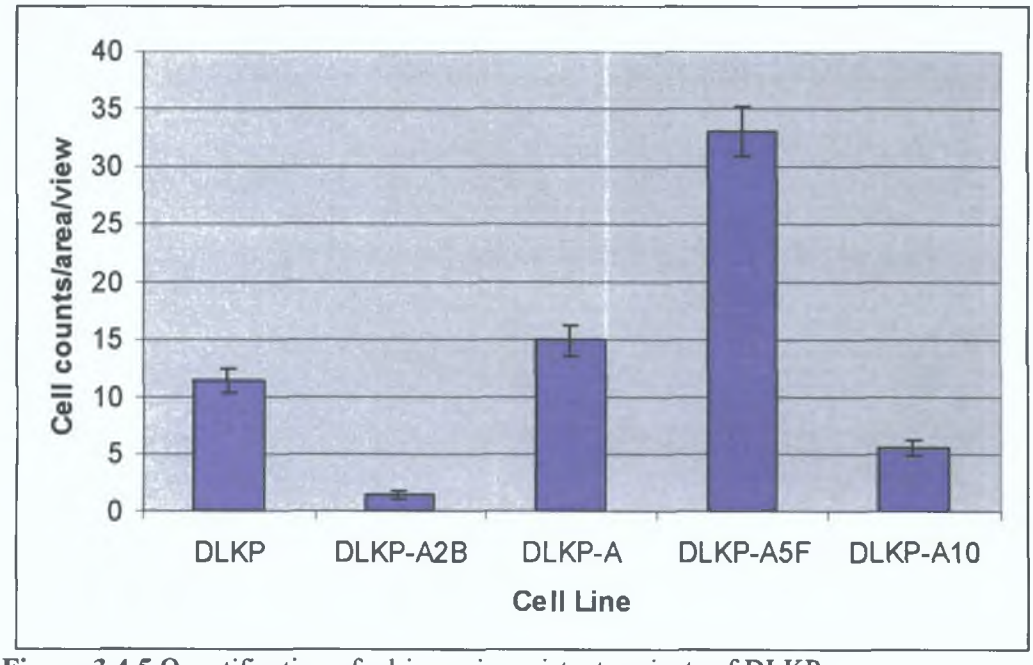

Figure 3.4.5 Quantification of adriamycin resistant variants of DLKP.

3.4.2 The overview of proteomic analyses

Initially DLKP was used as the control and compared only to DLKP-A (Table 3.4.3). So as not to confuse the lengthy proteomic procedure, when confidence had been built the remaining variants, A2B, A5F and A10 were compared to DLKP-A.

Experiment No.	Control	Treated
1	DLKP	DLKP-A
2	DLKP-A	DLKP-A2B
3	DLKP-A	DLKP-A5F
4	DLKP-A	DLKP-A10

Table 3.4.3 Overview of 2D-DIGE experiments carried out in this thesis

3.4 2 1 Screening of DLKP and variants protein samples

The DIGE system required six high quality protein samples per cell line per experiment (section 2 15) Many sample preparations were carried out to refine the procedure to generate good gels with many distinct protein spots and to ensure low levels of contaminating factors such as DNA, RNA, lipids and salts The gels were silver-stained and scanned at 300 resolution to ensure the quality of protein samples The best six samples showing most solubilised, well-defined protein spots free of streaking and salt fronts were selected

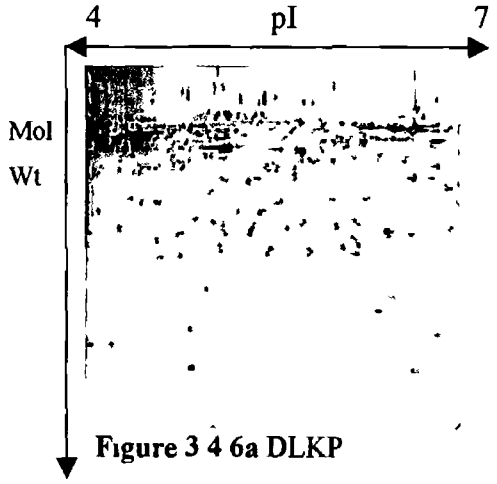

Figure 3 4 6a DLKP

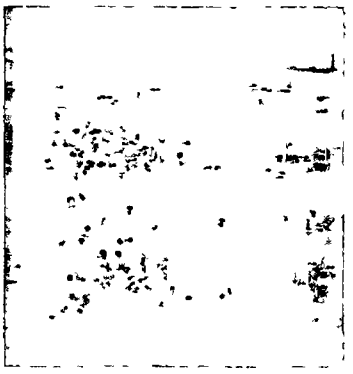

Figure 3 4 6b DLKP-A

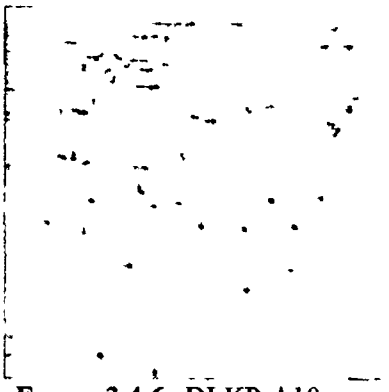

Figure 3 4 6c DLKP-A10

Figure 3 4 6d DLKP-A5F

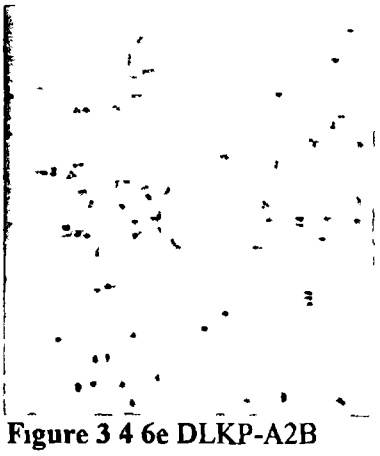

Figure 3 4 6e DLKP-A2B

Figures 3 4 6a-e A volume of 75 µg protein of all cell lysates for 2D-DIGE analysis were run on pH 4-7 IPG strips

3.4.3 Experimental outline of labelling of DLKP and DLKP-A protein samples

The experimental design for DIGE analysis of DLKP versus DLKP-A is outlined as follows: Six biological replicates of each cell line were reverse labelled with 200pmol of the Cy dyes (section 2.16.1.3) to allow for statistical analysis of protein expression using DeCyder™ software. Three replicates of DLKP and DLKP-A were labelled with Cy3 for gels 1-3 and 4-6 respectively. Three replicates of DLKP-A and DLKP were labelled with Cy5 for gels 1-3 and 4-6 respectively. Each replicate was also labelled with Cy2. A volume of 50μg protein was labelled with each Cy dye resulting in a total of 150μg/gel (50μg Cy2 internal standard, 50μg Cy3 and 50μg Cy5).

Once labelling was completed, six 2D gels were generated (sections 2.17 and 2.18) and scanned using the Typhoon scanner. All images generated were initially analysed in the DIA mode of the DeCyder™ software (section 2.20.1). In-depth analysis to identify spots with differential protein expression was carried out with the BVA module of the software (section 2.20.2). To identify these proteins, preparative 2D gels were generated and stained with colloidal blue coomassie, excised with the ETTAN spot picker and digested to be identified with a MALDI-TOF mass spectrometer (sections 2.22, 2.23 and 2.24 respectively).

3.4.3.1 DeCyder analysis of DLKP versus DLKP-A

Differential protein expression between the lung cell line DLKP and its adriamycin resistant variant DLKP-A was observed using 2D-DIGE. Difference In-gel Analysis using Decyder™ revealed a total of 3454 ± 303 protein spots between DLKP and DKLP-A. Biological variation analysis of these spots revealed a total of 282 spots showing a greater then 1.2-fold change in expression with a t-test score of 0.05 or less (Figure 3.4.7). Of these 282 spots, 38 have been identified using MALDI-TOF mass spectrometry.

A total of 244 of the differentially regulated spots were not identified (102 down-regulated and 142 up-regulated) as: (1) many failed to appear on a colloidal coomassie gel due to their relatively low abundance; (2) highly abundant proteins on the gel sometimes masked those proteins in low abundance and (3) some proteins, especially high molecular weight hydrophobic proteins do not fly well in the mass spectrometer.

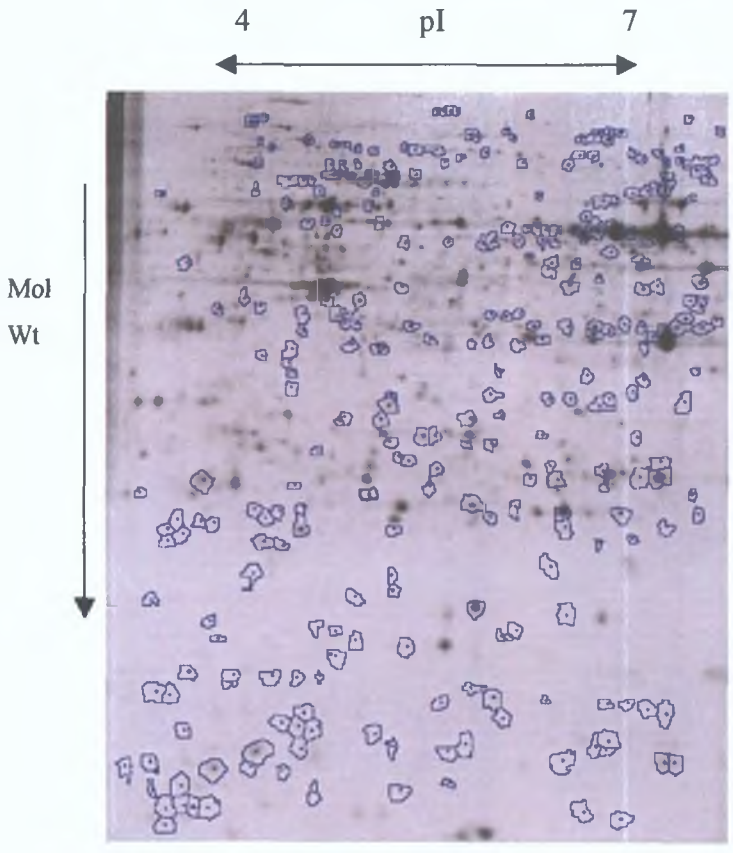

Figure 3.4.7 Representative Cy5 labelled DLKP-A gel showing completed BVA analysis of DLKP versus DLKP-A between pH4-7. Spots circled in blue are the 282 statistically significant differentially regulated proteins ($p \leq 0.05$, protein fold ≥ 1.2).

3.4.3.2 Identification of differentially regulated proteins

Matrix assisted laser desorption ionisation (MALDI) time of flight (TOF) mass spectrometry successfully identified 38 differentially regulated proteins between DLKP and DLKP-A (Figure 3.4.8). Of these 38 spots, 23 were found to be up-regulated and 15 down-regulated (Table 3.4.4). For visual clarity, the proteins were numbered as outlined in Table 3.4.4. Spots are numbered according to their relative molecular weight, from highest to lowest.

Over 65% of the proteins listed in Table 3.4.4a and 3.4.4b have been shown to be either increased or decreased in response to chemotherapy drug exposure. Proteins such as the heat shock proteins and the apoptotic response proteins are typically differentially regulated.

Above approximately 70kDa, out of 84 differentially expressed proteins only 4 were identified due to reasons (1) to (3) mentioned in section 3.4.3.1. Moreover, below approximately 17kDa, out of 53 differentially expressed proteins only 4 were identified. Therefore in the central part of the gel, out of 108 spots, 30 were identified.

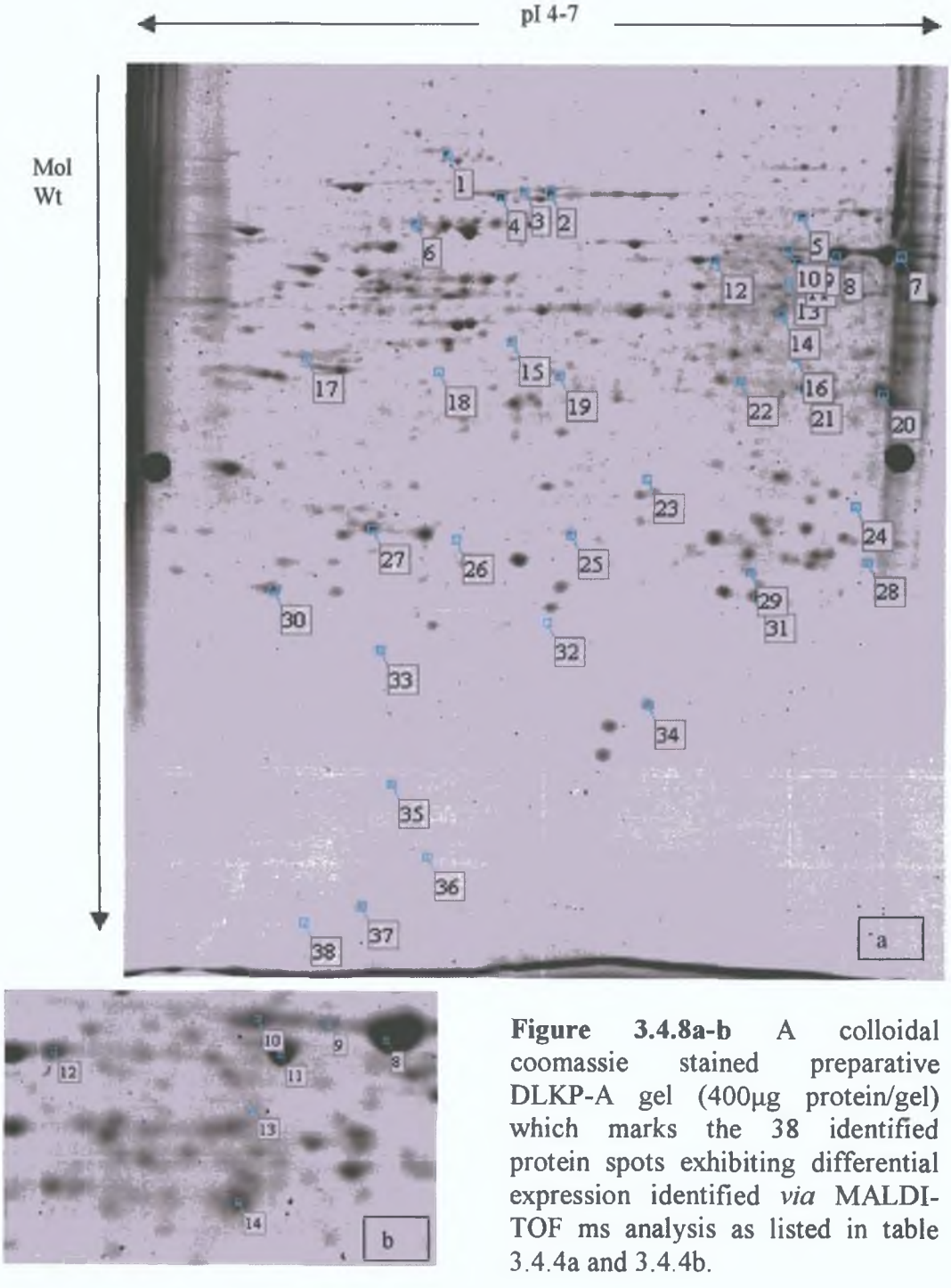

Figure 3.4.8a-b A colloidal coomassie stained preparative DLKP-A gel (400µg protein/gel) which marks the 38 identified protein spots exhibiting differential expression identified *via* MALDI-TOF ms analysis as listed in table 3.4.4a and 3.4.4b.

Spot No	Protein Name	gi Number	Gene Symbol	Fold	pI	M w
1	Valosin containing Protein	gi|48257098|	VCP	2 32	4 9	71 56
2	HSP70 kDa 9B (MTHsp75)	gi|292059|	HSPA9B	1 97	6	74 12
3	Lamin B1	gi|576840|	LMNB1	3 07	5 3	67 79
4	HSP 70 protein 8 isoform 2	gi|62896815|	HSPA8	3 21	5 6	53 6
5	Chaperonin containing TCP1 subunit 3	gi|58761484|	CCT3	2 58	6	57 78
6	hnRPK	gi|55958547|	HNRPK	1 93	5 4	42 02
7	Aldehyde dehydrogenase A1	gi|2183299|	ALDH1A1	1 65	6 3	55 44
8	Aldehyde dehydrogenase A1	gi|2183299|	ALDH1A1	1 52	6 3	55 44
9	Succinyl-CoA 3 ketoacid CoA transferase	gi|10280560|	OXCT1	2 3	7 2	56 6
10	Aldehyde dehydrogenase A1	gi|2183299|	ALDH1A1	1 47	6 3	55 44
11	CCT2	gi|48146259|	CCT2	2 58	6	57 78
12	hnRPH1	gi|48145673|	HNRPH1	1 52	5 9	49 5
13	Rab dissociation inhibitor beta	gi|4960030|	GDI2	1 69	5 9	41
14	Cham C, OAT Mutant Y85i	gi|78101704|	OATL1	-3 45	6 6	48 81
15	HSPC108 (stomatin)	gi|6841440|	STOML2	2 03	5 8	37 3
16	eIF 2b	gi|19353009|	EIF2	1 42	6 5	58 17
17	HSP 70 protein 8 isoform 2	gi|62896815|	HSPA8	-2 15	5 6	53 6
18	K alpha 1 protein	gi|62897609|	K-ALPHA-1	-1 55	5	50 49
19	Stress induced phosphoprotein	gi|54696884|	STIP1	-1 43	6 4	63 25

Table 3 4 4a Identified proteins from DLKP versus DLKP-A Gene symbol determined from "gi number" conversion software package "DAVID" and Entrez gene (OAT Ornithine Aminotransferase)

Spot No	Protein Name	gi Number	Gene Symbol	Fold	pI	M w
20	Annexin A1	gi|442631|	ANXA1	2 29	7 9	35 25
21	Annexin A1	gi|442631|	ANXA1	2 51	7 9	35 25
22	Annexin A1	gi|442631|	ANXA1	1 63	7 9	35 25
23	Replication A2 32, kDa	gi|56204165|	RPA2	1 5	6 4	30 25
24	Protein disulphide isomerase protein 5	gi|1710248|	p5	-2 18	5	46 52
25	HSP 27 kDa	gi|54696638|	HSPB1	1 47	6	22 82
26	Actin G protein	gi|178045|	ACTG1	-1 45	5 6	26 15
27	HSP 70 kDa protein 8 isoform 2	gi|62896815|	HSPA8	-1 25	5 6	53 6
28	Triosephosphate isomerase	gi|66360366|	TPI1	1 89	6 5	26 95
29	Triosephosphate isomerase	gi|66360366|	TPI1	-1 46	6 5	26 95
30	Thioredoxin peroxidase B chain J	gi|9955016|	PRDX5	-2 33	5 7	21 68
31	K130r mutant of human DJ-1	gi|33358056|	PARK7	1 54	6 5	21 14
32	Thioredoxin peroxidase B	gi|1617118|	PRDX2	-1 95	5 2	18 48
33	Sorcin isoform b	gi|38679884|	SRI	1 51	5 1	20 61
34	Nucleoside diphosphate kinase 1	gi|38045913|	NME1	1 54	5 4	19 86
35	eIF 5a	gi|33383425|	EIF5A	-2 63	5 1	16 98
36	Human tubulin chaperone cofactor A	gi|21730330|	TBCA	-1 26	5 3	12 29
37	Galectin-1	gi|42542977|	Galectin-1	-1 55	5 3	14 75
38	Thioredoxin delta 3	gi|1827674|	TXN	-1 17	4 8	11 86

Table 3 4 4b Identified proteins form DLKP versus DLKP-A continued

3.4.3.3 Ontology analysis of identified proteins

Ontology information was obtained through PubMed literature searches. Of the identified proteins, the majority have functions in the stress response (26%), glycolysis (16%), ion binding/transport (11%), apoptosis (11%) and cytoskeletal functions (8%). Cell signalling, translation, metabolism and transcription accounts for 5% each. Finally, 3% of the proteins are involved in protein turnover (Table 3.4.5, Figure 3.4.9).

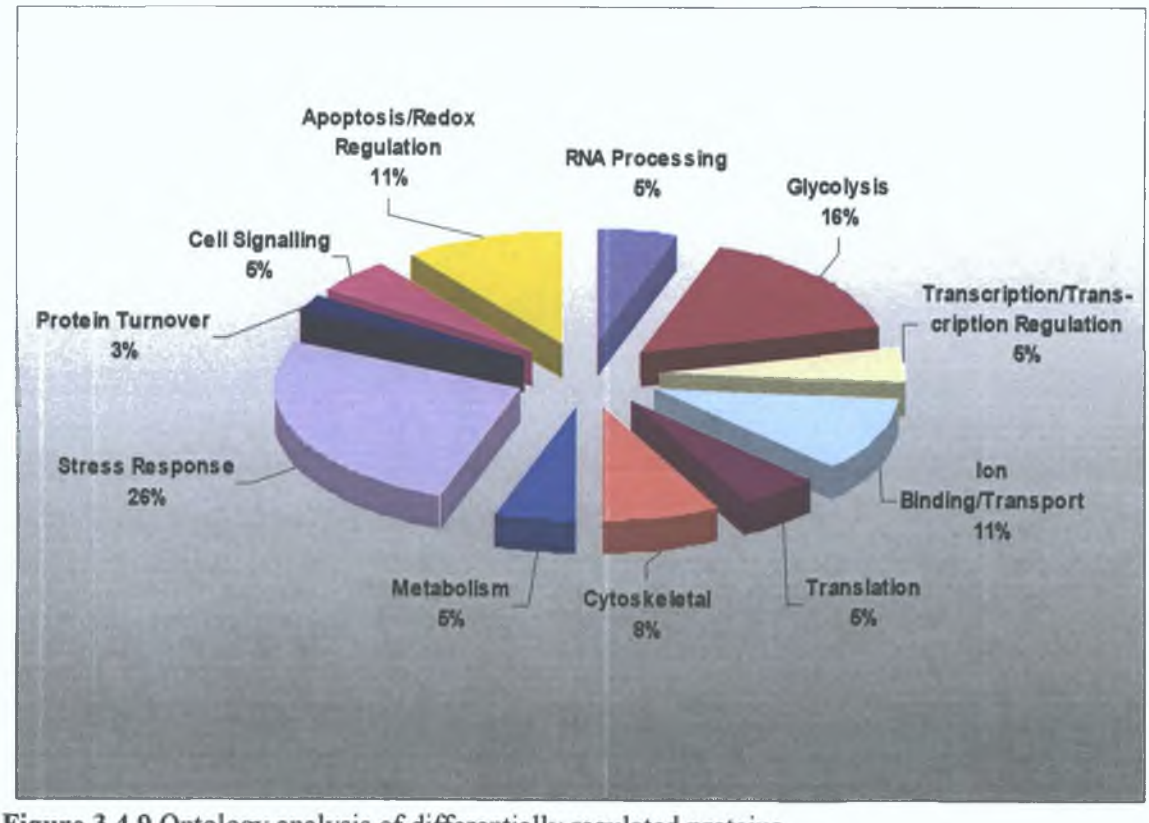

Figure 3.4.9 Ontology analysis of differentially regulated proteins.

The stress response proteins, which account for 26% of all differentially regulated proteins, were expected to be differentially regulated, as they are known to increase resistance to cell death induced by a variety of stimuli. The majority of these proteins are all up-regulated in DLKP-A. The apoptosis/redox regulation proteins have also been linked to overcoming drug-resistance through evading apoptosis. They are both up- and down-regulated in DLKP-A. Glycolysis was also regulated quite significantly in DLKP-A versus DLKP. This could be anticipated as drug-resistant variants may need energy for actively pumping out drugs.

Reported Function	Protein Name
Apoptosis/Redox regulation	Galectin 1, chain a Thioredoxin delta 3 Thioredoxin peroxidase B chain J K130r mutant of human DJ-1
Glycolysis	Aldehyde dehydrogenase A1 Peroxiredoxin 2 Triosephosphate isomerase
Transcription/Transcription Regulation	Nucleoside diphosphate kinase 1 Replication A2, 32kDa
Stress Response	HSP 27 kDa HSP 70 kDa protein 8 isoform 2 Human tubulin chaperone cofactor A HSPC108 (stomatin) Stress induced phosphoprotein HSP70 kDa 9B (MTHsp75) Chaperonin containing TCP1 subunit 3 CCT2
Ion Binding/Transport	Annexin A1 Sorcin isoform b
Translation	eIF 2b eIF 5a
Cytoskeletal	Lamin B1 K alpha 1 protein / TNF alpha Actin g1 protein
Protein Turnover	Protein disulphide isomerase protein 5
Cell Signalling	VCP protein Rab dissociation inhibitor beta
RNA Processing	hnRPK hnRPH1
Metabolism	Succinyl-CoA 3 ketoacid CoA transferase Ornithine mutant amine transferase Y85 chain c

Table 3 4 5 Ontology analysis of identified proteins from DLKP versus DLKP-A

3.4.3.4 PathwayAssist analysis of identified proteins

PathwayAssist literature mining software permits the identification of biological interactions among genes and proteins of interest from the published literature. This analysis was carried out on the 38 identified proteins in Table 3.4.4. The gene symbol list was imported into the software and from this both direct- and common-interacting pathways were built. Figure 3.4.10 shows only the direct links between differentially regulated proteins. Only the differentially regulated proteins were submitted for PathwayAssist analysis. These proteins are involved in stress response and redox reactions. Thioredoxin and thioredoxin peroxidase are linked components in a redox chain that couples peroxide reduction to NADPH oxidation. Thioredoxin peroxidase is also increased in Thioredoxin-1 transfected cells which results in enhanced protection against apoptosis caused by hydrogen peroxide but not by other agents including dexamethasone, etoposide and doxorubicin. Both of these proteins are decreased in DLKP-A. The stress induced phosphoprotein, VCP and HSPB1 have each been shown to interact with HSPA8.

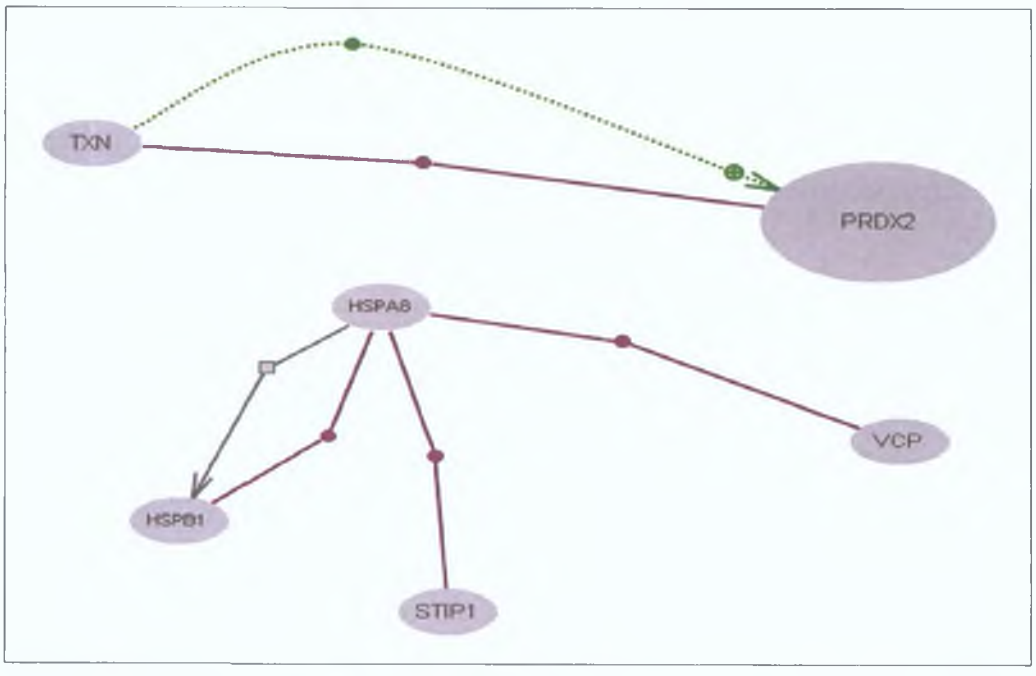

Figure 3.4.10 PathwayAssist analysis of direct interactions between proteins. This identifies only direct links between the proteins. This finds proteins that are regulated by all selected nodes. Green and purple lines mark regulatory and binding effects respectively. Grey lines indicate effect on expression.

Figure 3.4.11 shows the pathways built based on common targets for selected nodes (i.e. differentially regulated proteins). Pathway analysis found that processes of apoptosis, differentiation and proliferation are important in the development of adriamycin resistance in DLKP, reflecting ontology analysis to some extent.

Stimulators of apoptosis include STIP1, PARK7, LMNB1, ANAX1, NME, and LGALS1. The majority of these are up-regulated in response to adriamycin exposure. Inhibitors of apoptosis include HSPA9B, PRDX1, HSPB1, HSPA8 and ALDH1A1. Expression of all other proteins are increased in DLKP-A. Six proteins were observed to interact with the differentiation cell process. The single inhibitory protein of differentiation, NME1 was found to be increased in DLKP-A by 1.54-fold. The remaining stimulators of differentiation were both increased and decreased in DLKP-A. No proteins were found to have an inhibitory effect on proliferation in DLKP-A. The proteins that stimulated proliferation were predominantly down-regulated in DLKP-A

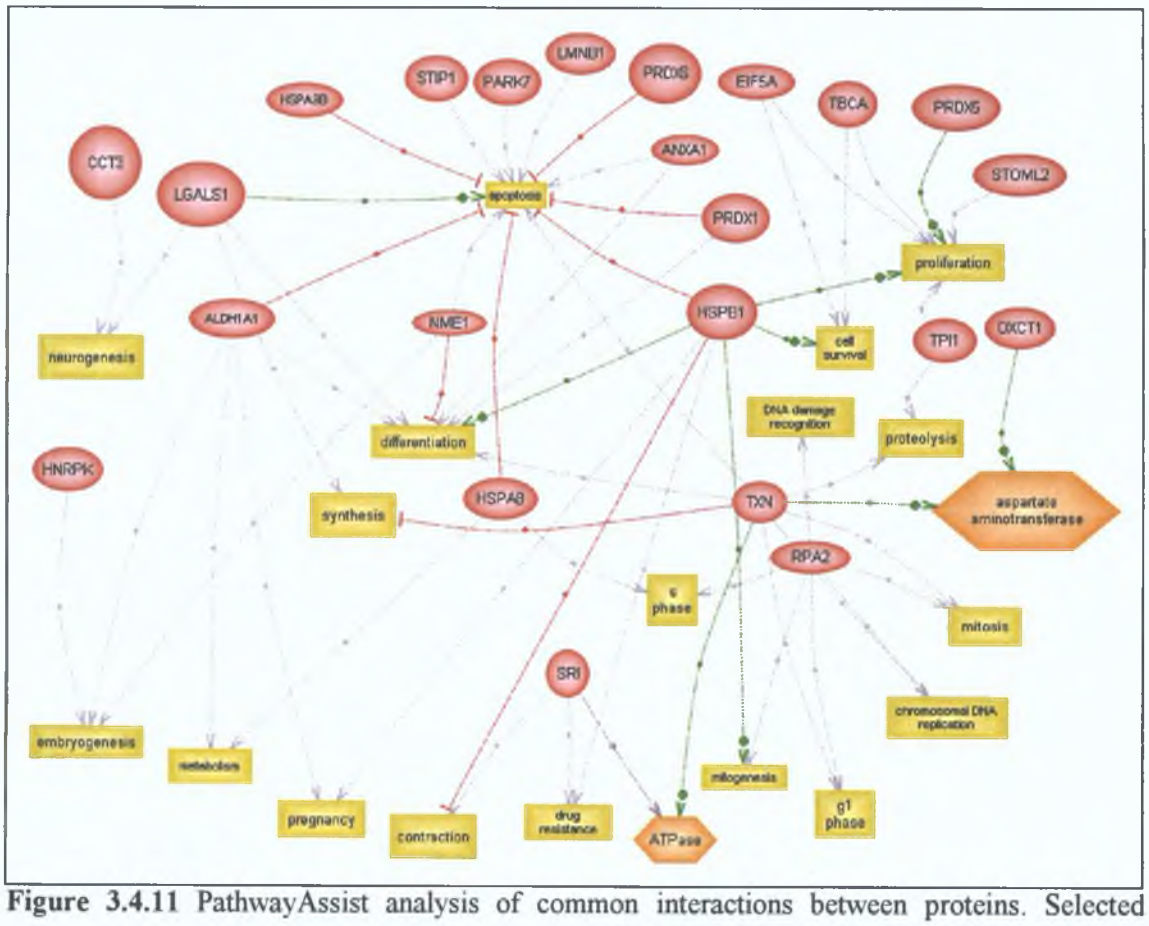

Figure 3.4.11 PathwayAssist analysis of common interactions between proteins. Selected protein nodes are shown in grey with the cellular processes in yellow and functional classes in orange. Green and red lines mark positive and negative regulatory effects respectively. Grey lines indicate an unknown regulatory effect.

3.4.4 DeCyder analysis of DLKP-A versus DLKP-A2B

This experiment was designed to compare DLKP-A to a less resistant subpopulation, DLKP-A2B in order to examine the protein expression changes resulting from a loss of resistance. DLKP was 254.14-fold resistant to adriamycin compared to DLKP while DLKP-A2B was only 36.8-fold resistant. The experimental design for DIGE analysis of DLKP-A compared to DLKP-A2B is identical to that of DLKP versus DLKP-A with DLKP-A as the control and 5 biological replicates.

Difference In-gel Analysis of DLKP-A (the control) compared to DLKP-A2B using Decyder™ revealed a total of 3483 ± 493 protein spots between DLKP-A and DKLP-A2B. Biological variation analysis revealed a total of 80 spots showing a greater than 1.2-fold change in expression with a t-test score of 0.05 or less (Figure 3.4.12). Of these 80 spots, 26 have been identified by MALDI-TOF mass spectrometry. A total of 54 differentially regulated spots were not identified (33 down-regulated and 21 up-regulated).

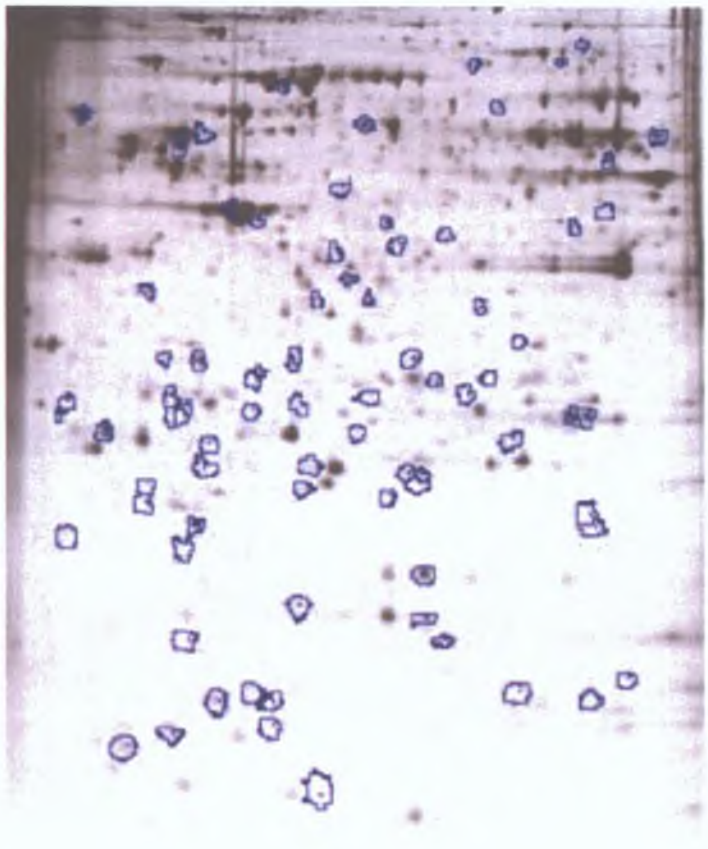

Figure 3.4.12 A representative Cy5 labelled DLKP-A2B gel showing completed BVA analysis of DLKP versus DLKP-A2B between pH 4-7. Spots circled in blue are the 80 statistically significant differentially regulated proteins ($p \leq 0.05$, protein fold ≥ 1.2).

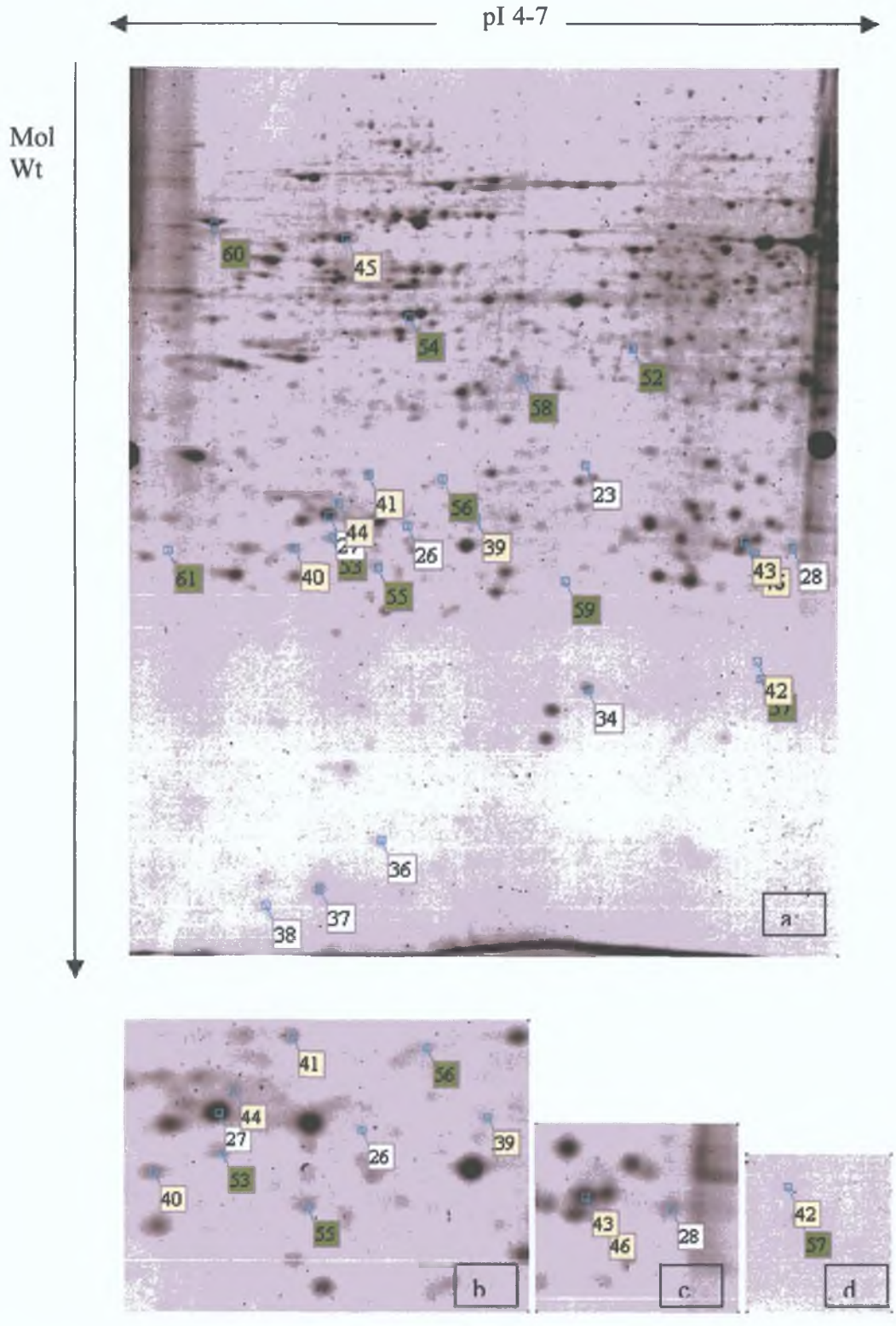

Figure 3.4.13a-d Colloidal coomassie stained preparative DLKP-A gel, which marks the proteins in common with DLKP versus DLKP-A – white spots (Figure 3.4.8). Yellow spots indicate the overlapping proteins from DLKP-A vs -A5F and -A10. Green proteins are unique to DLKP-A2B.

Comparisons between DLKP-A versus DLKP-A2B and DLKP versus DLKP-A revealed that 8 proteins were shared (white spots in Figure 3 4 13) Of the commonly shared proteins, many show a positive correlation with resistance when taking DLKP versus DLKP-A into account The transcription/transcription regulation proteins, replication A2 (RPA2) and nucleoside diphosphate kinase 1 (NDPK1) showed a decrease in protein expression as resistance fell This reflects a positive correlation with a fall of drug resistance In contrast, two proteins involved in apoptosis/redox regulation, namely galectin-1 and thioredoxin delta 3 are both decreased in DLKP versus DLKP-A, by 1 55 and 1 17-fold respectively However, in the less resistant cell line, DLKP-A2B, both proteins show an increase in expression, 1 71-fold and 1 6-fold respectively The same trend is seen for the cytoskeletal protein actin G1 and the stress response protein, HSP 70 kDa protein 8 isoform 2 The protein expression of human tubulin chaperone cofactor A protein was reduced from −1 26-fold to −1 88-fold whereas the expression of triosephosphate isomerase increased a further 1 87-fold from 1 89-fold in DLKP-A2B (Table 3 4 6)

PathwayAssist analysis of RPA2 and NDPK1 in DLKP versus DLKP-A revealed that RPA2 is involved in G1 and S phase, mitogenesis, mitosis chromosomal DNA replication and DNA damage recognition yet is only connected to s phase in DLKP-A2B (Figure 3 4 16) NDPK1 (labelled NME1 in PathwayAssist) functions in differentiation and apoptosis in DLKP versus DLKP-A (Figure 3 3 11) but is linked to recognition of signal transduction, shape, contraction and assemble in DLKP-A2B

Spot No	Protein Name	Fold	pI	M w.	DLKP vs DLKP-A
23	Replication A2, 32 kDa	-1 29	6 4	30 25	1 5
26	Actin G1 protein	2 95	5 5	26 68	-1 45
27	HSP 70 kDa protein 8 isoform 2	2 87	5 6	53 6	-1 25
28	Triosephosphate isomerase	1 87	6 5	26 95	1 89
34	Nucleoside diphosphate kinase 1	-1 28	5 4	19 86	1 54
36	Human tubulin chaperone cofactor A	-1 88	5 3	12 29	-1 26
37	Galectin-1	1 71	5 3	14 75	-1 55
38	Thioredoxin delta 3	1 6	4 8	11 86	-1 17

Table 3 4.6 Fold difference of overlapping protein spots between the comparisons DLKP versus DLKP-A and DLKP-A versus DLKP-A2B

Eight proteins that were found to be differentially regulated in DLKP-A versus DLKP-A2B were also seen in the comparison of DLKP-A versus DLKP-A5F or DLKP-A versus DLKP-A10 (Table 3 4 7)

Spot No	Protein Name	gi Number	Gene Symbol	Fold	pI	M W.
39	Actin G1 protein	gi|40226101|	ACTG1	6	5 5	26 68
40	Annexin 1	gi|442631|	ANXA1	-1 6	5 4	35 25
41	Chloride intracellular channel 1 variant	gi|62898319|	CSTD	-1 66	5 1	27 34
42	HSP 70 kDa protein 8 isoform 2	gi|62896815|	HSPA8	7 9	5 6	53 6
43	Chain B, Horf 6 a novel human peroxidase enzyme	gi|3318842|	-	-1 61	6	24 9
44	Eukaryotic translation elongation factor 1 delta isoform	gi|15215451|	EEF1D	-2 48	4 9	31 22
45	Vimentin	gi|37852|	VIM	-1 64	5 1	53 72
46	HPRT	gi|6730253	HPRT1	-1 71	5 5	39 3

Table 3 4 7 The 8 overlapping protein spots between the comparisons DLKP versus DLKP-A2B and/or DLKP-A versus DLKP-A5F, DLKP-A10 (Spots marked yellow in Figure 3 4 13)

Of the eight proteins shared with the two more resistant variants, DLKP-A5F and DLKP-A10 Three are shared with DLKP-A5F and five with DLKP-A10 Actin G1 shows an inverse relation between DLKP-A, DLKP-A5F and DLKP-A2B HPRT and the peroxidase enzyme do not correlate with resistance Between DLKP-A and DLKP-A2B, HSP 70 kDa protein 8 isoform 2 correlates inversely while vimentin correlates directly with resistance

Eleven proteins were determined to be unique to DLKP-A versus DLKP-A2B, the majority of which are involved in protein turnover and have both increased and decreased proteins expression HSP 70 kDa protein 8 isoform 2 and annexin 1 elicited the highest protein fold changes, 3 42 and 2 42 respectively Both of these proteins have previously been linked to the development of drug resistance (Table 3 4 8)

Spot No	Protein Name	gi Number	Gene Symbol	Fold	pI	M W
41	Chloride intracellular channel 1 variant	gi|62898319|	CSTD	-1 66	5 1	27 34
52	alpha tubulin 6 variant	gi|62897609|	TUBA6	1 81	5	50 49
53	Annexin 1	gi|442631|	ANXA1	2 42	7 9	35 25
54	Beta Actin	gi|15277503|	ACTB	-1 8	5 6	40 54
55	Chain D, Cathepsin B (E C 3 4 22 1)	gi|999911|	CSTB	-1 87	5 2	22 97
56	Chain H Cathepsin D at pH 7 5	gi|5822091|	CSTD	1 54	5 3	26 46
57	HSP 70 kDa protein 8 isoform 2	gi|62896815|	HSPA8	3 42	5 6	53 6
58	KIAA0002	gi|1136741|	KIAA0002	-2 02	5 8	59 06
59	Peroxiredoxin	gi|62896877|	PRDX3	1 72	7 1	27 95
60	Prolyl 4-hydrolase, beta subunit	gi|48735337|	P4HB	-1 89	4 8	57 5
61	Proteasome (prosome, macropain) subunit, alpha type 5	gi|54696300|	PSMA5	1 6	4 7	26 58

Table 3 4 8 Proteins unique to DLKP-A versus DLKP-A2B (Spots marked green in Figure 3 4 13)

3.4.4.1 Proteins identified between DLKP-A versus DLKP-A2B

Ontology analysis shows proteins with decreased protein expression are involved in translation, cytoskeleton, protein turnover, ion binding/transport, apoptosis/redox regulation and the stress response. Proteins showing increased expression have functions involving stress response, ion binding and transport, cytoskeleton, apoptosis/redox reactions glycolysis and protein turnover (Table 3.4.9, Figure 3.4.14). Interestingly, protein turnover and cytoskeletal proteins appear to be more important in the DLKP-A2B variant, 19% each in comparison to DLKP versus DLKP-A.

A decrease in glycolysis and stress response proteins is seen in DLKP-A2B, only 4% and 19% in comparison to 16% and 26% respectively in DLKP versus DLKP-A. In comparison to DLKP versus DLKP-A, no cell signalling, metabolic or RNA processing proteins were differentially regulated. Similar percentages of apoptosis/redox regulation, ion binding/transport, transcription/ transcription regulation and translation accounts were seen in DLKP versus DLKP-A and DLKP-A versus DLKP-A2B (Figure 3.4.14 and Figures 3.4.9).

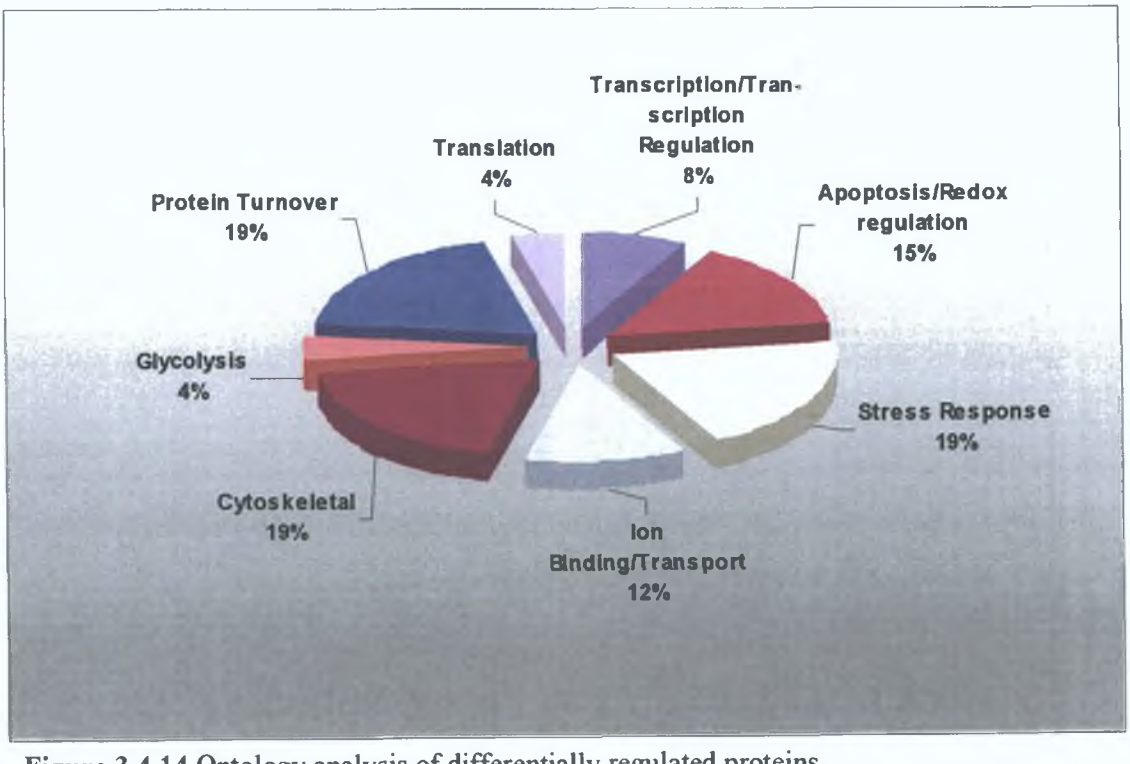

Figure 3.4.14 Ontology analysis of differentially regulated proteins

Reported Function	Protein Name
Apoptosis/Redox regulation	Galectin 1, chain a Thioredoxin delta 3 Peroxiredoxin Chain B, Horf 6 A Novel Human Peroxidase Enzyme
Glycolysis	Triosephosphate isomerase
Transcription/Transcription Regulation	Nucleoside diphosphate kinase 1 Replication A2, 32kDa
Stress Response	Human tubulin chaperone cofactor A KIAA0002 HSP 70 kDa protein 8 isoform 2
Ion Binding/Transport	Annexin A1 variant 3 Chloride intracellular channel 1
Cytoskeletal	ACTG1 Protein Alpha tubulin Beta Actin Vimentin
Protein Turnover	Chain D, Cathepsin B (E C 3 4 22 1) Chain H Cathepsin D at pH 7 5 HPRT Prolyl 4-hydrolase, beta subunit Proteasome (prosome, macropain) subunit, alpha type, 5
Translation	Eukaryotic translation elongation factor 1 delta isoform

Table 3 4 9 Ontology analysis of identified proteins from DLKP-A versus DLKP-A2B

3 4 4.2 PathwayAssist analysis of identified proteins between DLKP-A and DLKP-A2B

PathwayAssist analysis was carried out on the identified differentially regulated spots in DLKP-A versus DLKP-A2B to identify both direct and common pathways between the proteins Figure 3 4 15 shows only direct links between the list of differentially regulated proteins submitted to pathway analysis As with DLKP-A, proteins involved in stress response and apoptosis are shown Cathepsin D has been show to activate cathepsin B and that cathepsin B influences dephosphorlyation of cathepsin D

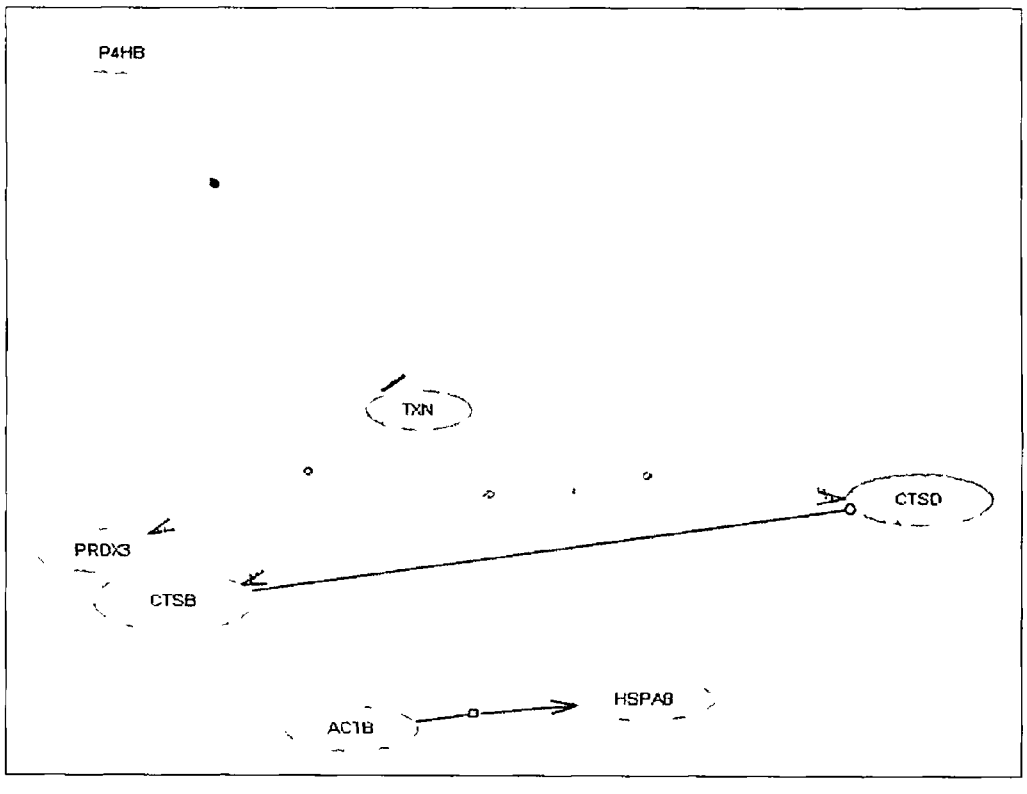

Figure 3 4 15 PathwayAssist analysis of direct interactions between proteins This identifies only direct links between the proteins This finds proteins that are regulated by all selected nodes The proteins with direct links are shown in grey Red line indicates an inhibitory effect Grey dashed lines indicate effect on expression

Figure 3.4.16 shows the pathways built based on common targets for selected nodes (i.e. differentially regulated proteins). Pathway analysis found that processes of regulation of signal transduction and assembly and that the proteins HPRT1 and galectin-1 are important in the loss of adriamycin resistance in DLKP-A2B compared to DLKP-A. Stimulators of signal transduction include NME1, HPRT1, PRDX3, HSPA8, ANAX1, TXN and LGALS1. The majority of these are up-regulated as resistance fell in DLKP-A2B. There are no inhibitors of signal transduction. The stimulators of assembly include NME1, TXN, HSPA8, ACTB and EEF1D.

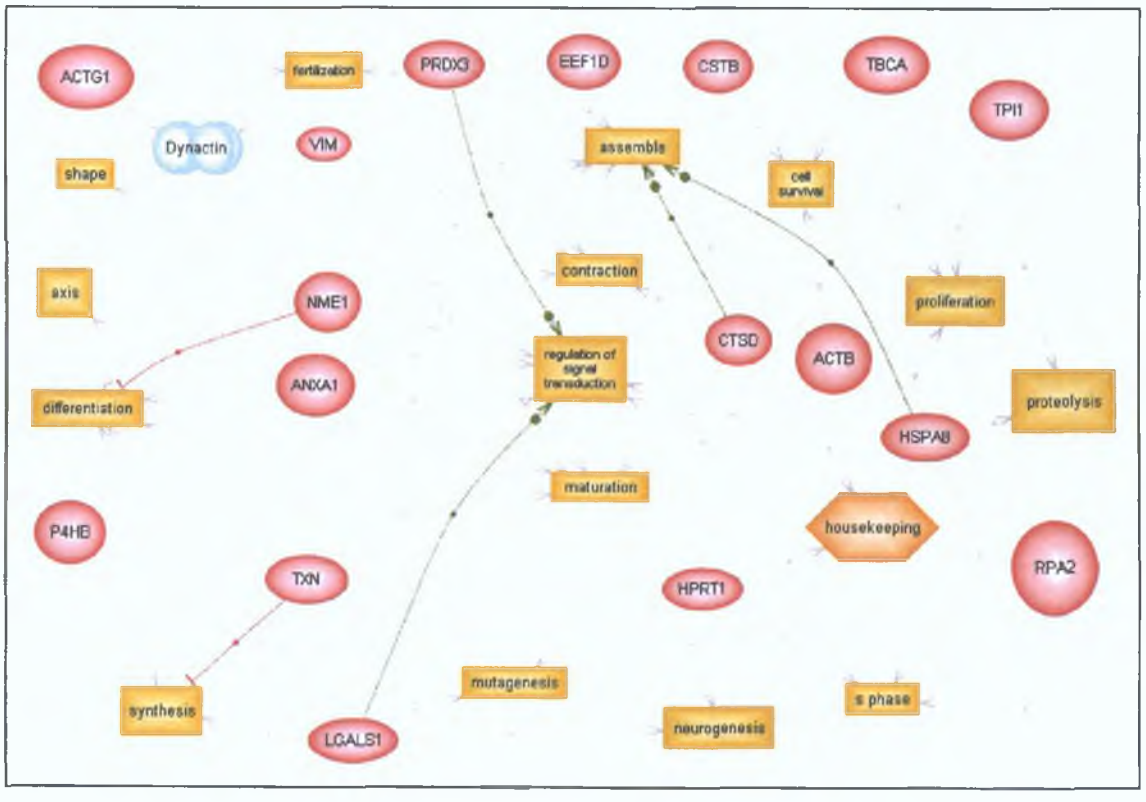

Figure 3.4.16 PathwayAssist analysis of common interactions between proteins. Selected protein nodes are shown in grey the picture with the cellular processes in yellow and functional classes in orange. Green and red lines mark positive and negative regulatory effects respectively. Grey lines indicate an unknown regulatory effect.

3.4.5 DeCyder analysis of DLKP-A versus DLKP-A5F

This experiment was designed to compare DLKP-A to a more resistant subpopulation, DLKP-A5F in order to examine the protein expression changes resulting from an increase in drug resistance. The experimental design for DIGE analysis of DLKP-A compared to DLKP-A5F is identical to that of DLKP versus DLKP-A.

Difference In-gel Analysis of DLKP-A (the control) compared to DLKP-A5F using Decyder™ revealed a total of 3323 ± 233 protein spots. Biological variation analysis revealed a total of 106 spots showing a greater than 1.2-fold change in expression with a t-test score of 0.05 or less. Of these 106 spots, 21 have been identified by MALDI-TOF mass spectrometry. A total of 85 differentially regulated spots were not identified (72 down-regulated and 13 up-regulated).

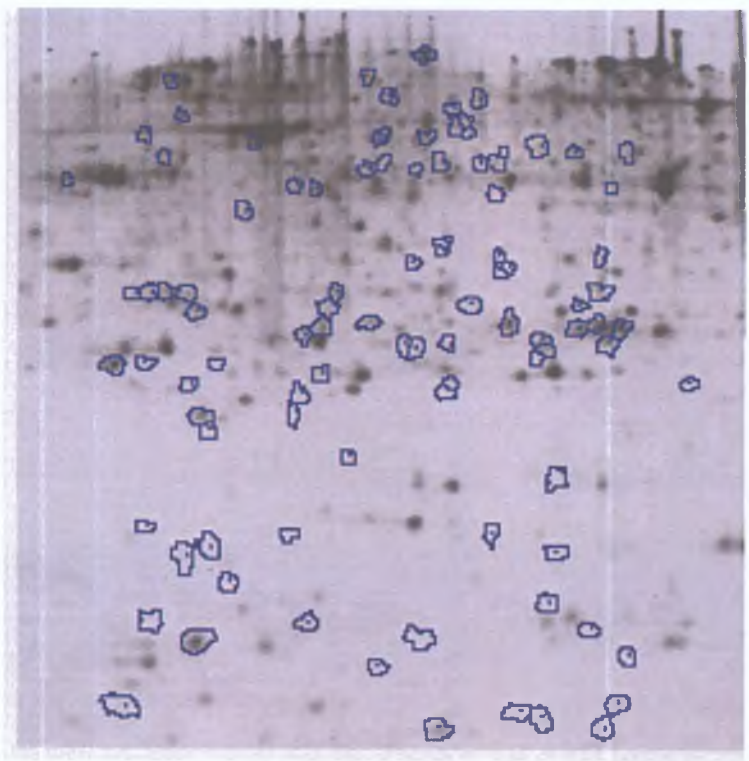

Figure 3.4.17 A representative Cy5 labelled DLKP-A5F gel showing completed BVA analysis of DLKP versus DLKP-A5F. Spots circled in blue are the 106 statistically significant differentially regulated proteins ($p \leq 0.05$, protein fold ≥ 1.2).

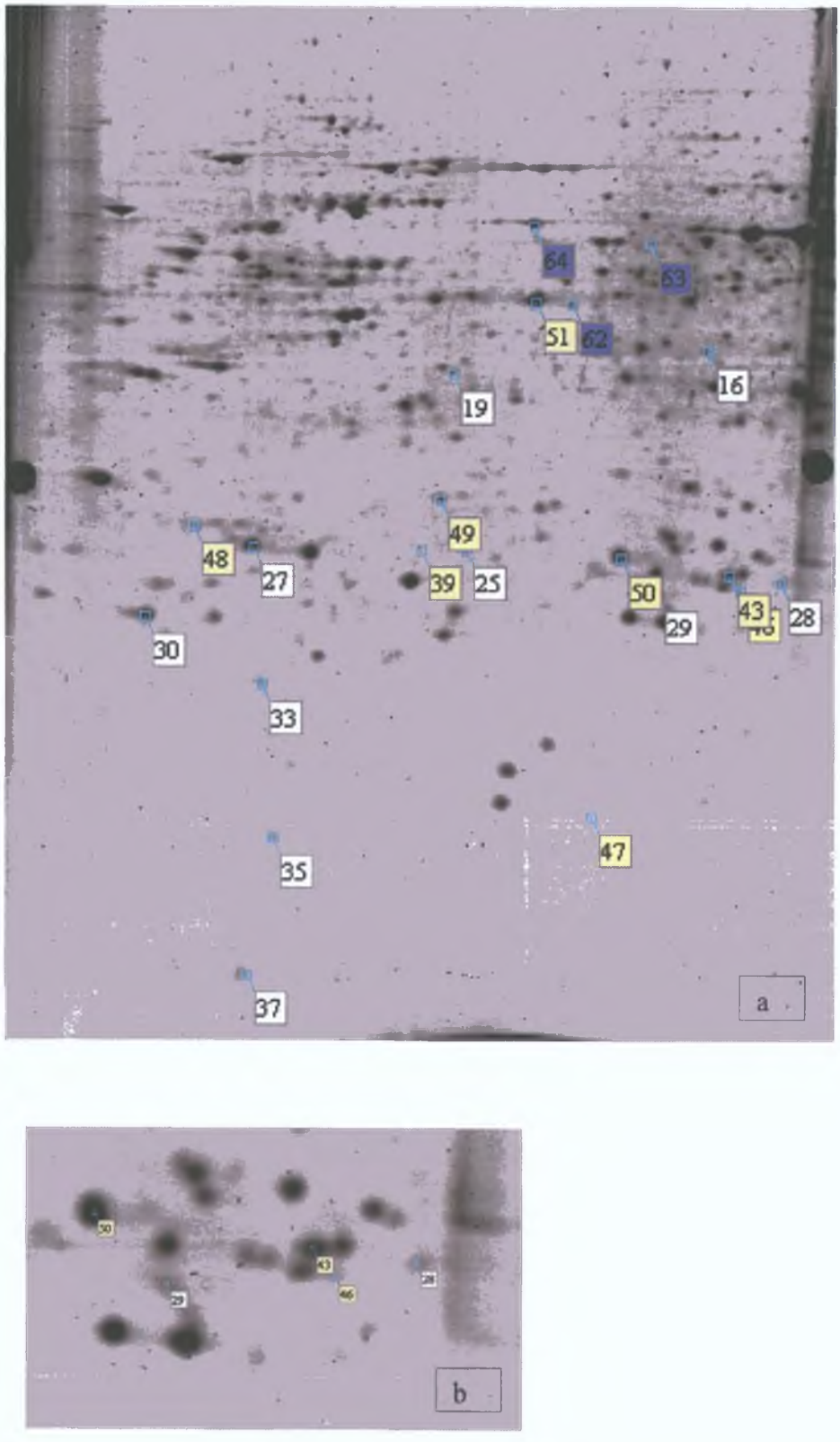

Figure 3.4.18a-b Colloidal coomassie stained preparative DLKP-A gel, which marks the proteins in common with DLKP versus DLKP-A – white spots (Figure 3.4.8). Yellow spots indicate the overlapping proteins from DLKP-A vs -A2B and/or -A10. Blue proteins are unique to DLKP-A5F.

Comparisons between DLKP-A versus DLKP-A5F and DLKP versus DLKP-A revealed that ten proteins were shared (white spots in Figure 3.4.8 Table 3.4.10). Of the commonly shared proteins, many show a positive correlation with an increase of resistance when taking DLKP versus DLKP-A into account. Heat shock protein 27 kDa developed a further increase in protein expression as resistance increased. PathwayAssist analysis of HSP 27 kDa reveals it to be involved in the regulation of signal transduction, contraction, assemble, differentiation and maturation. In DLKP vs DLKP-A it is also involved in the regulation of contraction, differentiation and is also involved in apoptosis, mitogenesis, cell survival, proliferation and drug resistance.

The protein expression of both apoptosis/redox regulation proteins increased with a rise in drug resistance, they include thioredoxin peroxidase B and galectin-1. Both of these proteins were previously down-regulated in DLKP versus DLKP-A but became increased in DLKP-A versus DLKP-A5F.

In contrast, the protein expression of eIF 2b and triosephosphate isomerase decreased in DLKP-A versus DLKP-A5F. A further decrease in expression is observed in two stress response proteins, (stress induced phosphoprotein and HSP 70 kDa protein 8 isoform 2) and the translation protein, eIF 5a.

Spot No.	Protein Name	A vs. A5F	pI	Mw	DLKP vs. DLKP-A
16	eIF 2b	-1.38	6.5	58.17	1.42
19	Stress induced phosphoprotein	-1.35	6.4	63.25	-1.43
25	HSP 27 kDa protein	1.55	6	22.82	1.47
27	HSP 70 kDa protein 8 isoform 2	-2.15	5.6	53.6	-1.25
28	Triosephosphate isomerase	-2.26	6.5	26.95	1.89
29	Triosephosphate isomerase		6.5	26.95	-1.46
30	Thioredoxin peroxidase B	1.44	5.7	21.68	-2.33
33	Sorcin	1.47	5.1	20.61	1.51
35	eIF 5a	-2.04	5.1	16.98	-2.63
37	Galectin-1	1.65	5.3	14.75	-1.55

Table 3.4.10 Overlapping protein spots between the comparisons DLKP versus DLKP-A and DLKP-A versus DLKP-A5F. Comparisons between both experiments revealed that 9 proteins were shared (white spots in Figure 3.4.18).

Comparisons between DLKP-A versus DLKP-A2B and DLKP-A versus DLKP-A5F revealed that three proteins overlapped namely, actin G, chain B, Horf 6 a novel human peroxidase enzyme and HRPT (Table 3 4 11) In the less resistant variant the protein expression of the apoptotic/redox regulation proteins, chain B, Horf 6 a novel human peroxidase enzyme, decreased from 1 34-fold in DLKP-A5F to –1 61-fold in DLKP-A2B In contrast, increased protein expression was observed in the cytoskeletal proteins actin G that was 4 07-fold decreased in DLKP-A5F but became 6-fold increased in DLKP-A2B Protein expression of the RNA processing protein HPRT was increased from –1 71 in DLKP-A2B to –1 33 in DLKP-A5F

Spot No	Protein Name	gi Number	Gene Symbol	Fold	pI	Mw
39	Actin G1 protein	gi|40226101|	ACTG1	-4 07	5 5	26 68
43	Chain B, Horf 6 a novel human peroxidase enzyme	gi|3318842|	-	1 34	6	24 9
46	HPRT	gi|6730253	HPRT1	-1 33	5 5	39 3
47	Synovial sarcoma breakpoint 3	gi|57162655|	SSX3	-1 73	6 1	11 37
48	BiP	gi|6470150|	GBP	-2 04	5	72 21
49	Prohibitin	gi|76879893|	PPA1	-2 13	5 6	29 87
50	Heat shock 27kDa protein	gi|54696638|	HSPB1	1 48	6	22 82
51	Beta tubulin	gi|18088719|	TUBB	-1 93	4 7	50 11

Table 3 4 11 Overlapping protein spots between the comparisons DLKP versus DLKP-A5F and DLKP-A versus DLKP-A2B, A10 (spots marked yellow in Figure 3 4 18)

Three proteins were determined to be unique to DLKP-A versus DLKP-A5F with functions including proteins turnover, cytoskeletal and RNA processing The PathwayAssist analysis software failed to find any common or direct interactions between the putative protein of Nbla 10058 and Alpha tubulin 6 variant proteins (Table 3 4 12) ER-60 is involved in the following cellular processes regulation of signal transduction, s phase, contraction and synthesis (Figure 3 4 21)

Spot No	Protein Name	gi Number	Gene Symbol	Fold	pI	Mw
62	Putative protein of Nbla 10058	gi|76879893|	PPA1	-1 76	5 9	49
63	Alpha tubulin 6 variant	gi|62897609|	TUBA6	-1 38	5	50 49
64	ER-60	gi|2245365|	PDIA3	1 45	6	57 18

Table 3 4 12 Protein spots unique to DLKP-A5F (spots marked blue in Figure 3 4 18)

3.4.5.1 Proteins identified between DLKP-A versus DLKP-A5F

Proteins with decreased protein expression are involved in all reported functions except ion binding/transport. Proteins showing increased expression have functions involving stress response, ion binding/transport, apoptosis/redox regulation and RNA processing (Table 3.4.16). Stress response, cytoskeletal and apoptosis/redox regulation proteins account for 25%, 15% and 15% respectively. Transcription/transcription regulation, glycolysis and RNA processing each accounts for 10%. The remainder of the proteins account for 5% each (Figure 3.4.19). A similar level of apoptosis/redox regulation, protein turnover and stress response proteins was observed in both DLKP versus DLKP-A and DLKP-A versus DLKP-A5F. There are approximately twice as many RNA processing, transcription, cytoskeletal and translation/translation regulation proteins regulated in DLKP-A versus DLKP-A5F compared to DLKP versus DLKP-A. In contrast, ion binding/transport accounts for 11% of the differentially regulated in DLKP versus DLKP-A, which is double that in DLKP-A5F. Glycolytic proteins are more differentially regulated in DLKP versus DLKP-A in comparison to DLKP versus DLKP-A5F (Table 3.4.13, Figure 3.4.19).

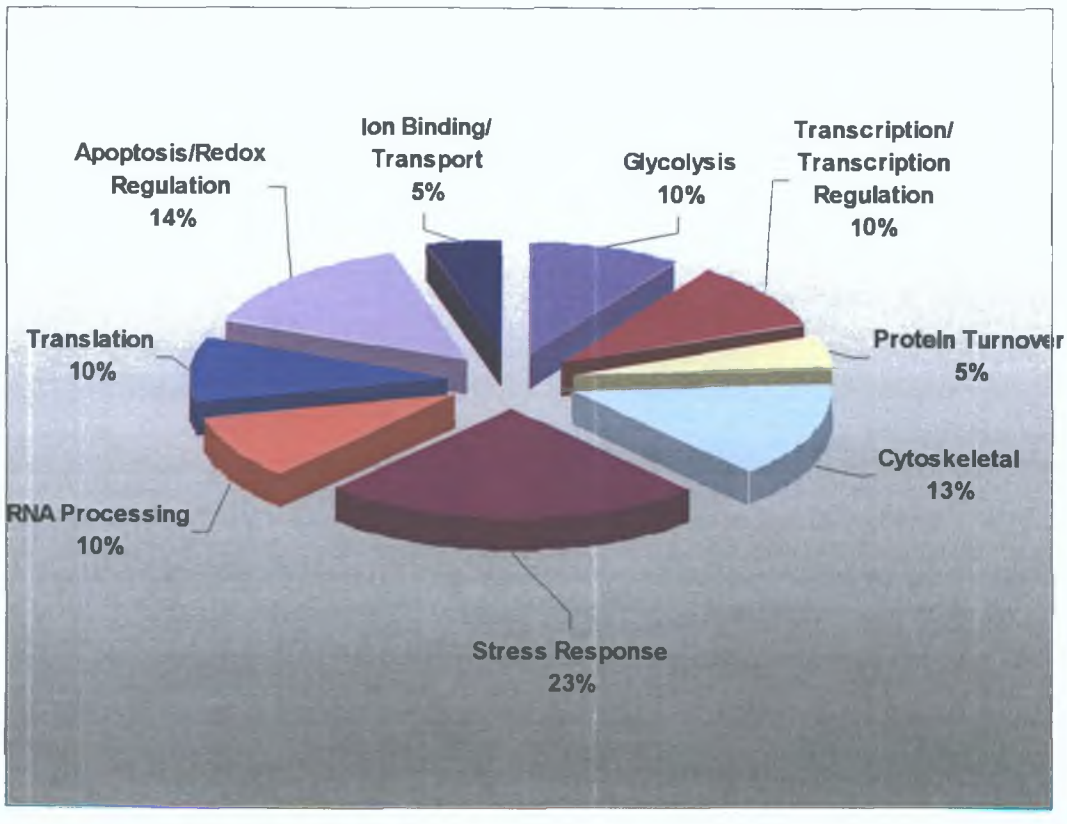

Figure 3.4.19 Ontology analysis of differentially regulated proteins.

Reported Function	Protein Name
Apoptosis/Redox regulation	Galectin 1, chain a Thioredoxin peroxidase B chain J Peroxidase
Glycolysis	Triosephosphate isomerase
Transcription/Transcription Regulation	Prohibitin Synovial sarcoma breakpoint 3
Stress Response	BiP HSP 27 kDa HSP 70 kDa protein 8 isoform 2 Stress induced phosphoprotein
Cytoskeletal	Actin G Alpha tubulin 6 Beta tubulin
Translation	EIF 2b EIF 5a
Ion Binding/Transport	Sorcin isoform b
RNA Processing	ER-60 HPRT
Protein Turnover	Putative protein of Nbla10058

Table 3 4 13 Ontology analysis of identified proteins from DLKP versus DLKP-A5F

3.4.5.2 PathwayAssist analysis of identified proteins between DLKP-A and DLKP-A5F

PathwayAssist analysis was carried out on identified differentially regulated spots in DLKP-A versus DLKP-A5F to identify both direct and common pathways between the proteins. Figure 3.4.20 shows only direct links between the list of differentially regulated proteins submitted to pathway analysis.

HSP 70 kDa protein 8 isoform 2, HSP 27 kDa and HSP 110kDa have been reported to spontaneously form a large complex and to directly interact with one another *in vitro* in mammalian culture systems. The stress-induced-phosphoprotein, STIP1 is also known as the Hsp70/Hsp90-organising protein as it binds to the HSPA8 proteins. The GRP58 proteins (also known as PDIA3 and ER-60) interact with high mobility group box proteins 1 and 2, HSPA8 and 3-phosphate dehydrogenase complex. It results after the incorporation of unnatural nucleosides into the DNA structure and is a determinant of cell sensitivity to DNA modifying chemotherapy. β-tubulin has also been shown to bind the HSP27 kDA protein.

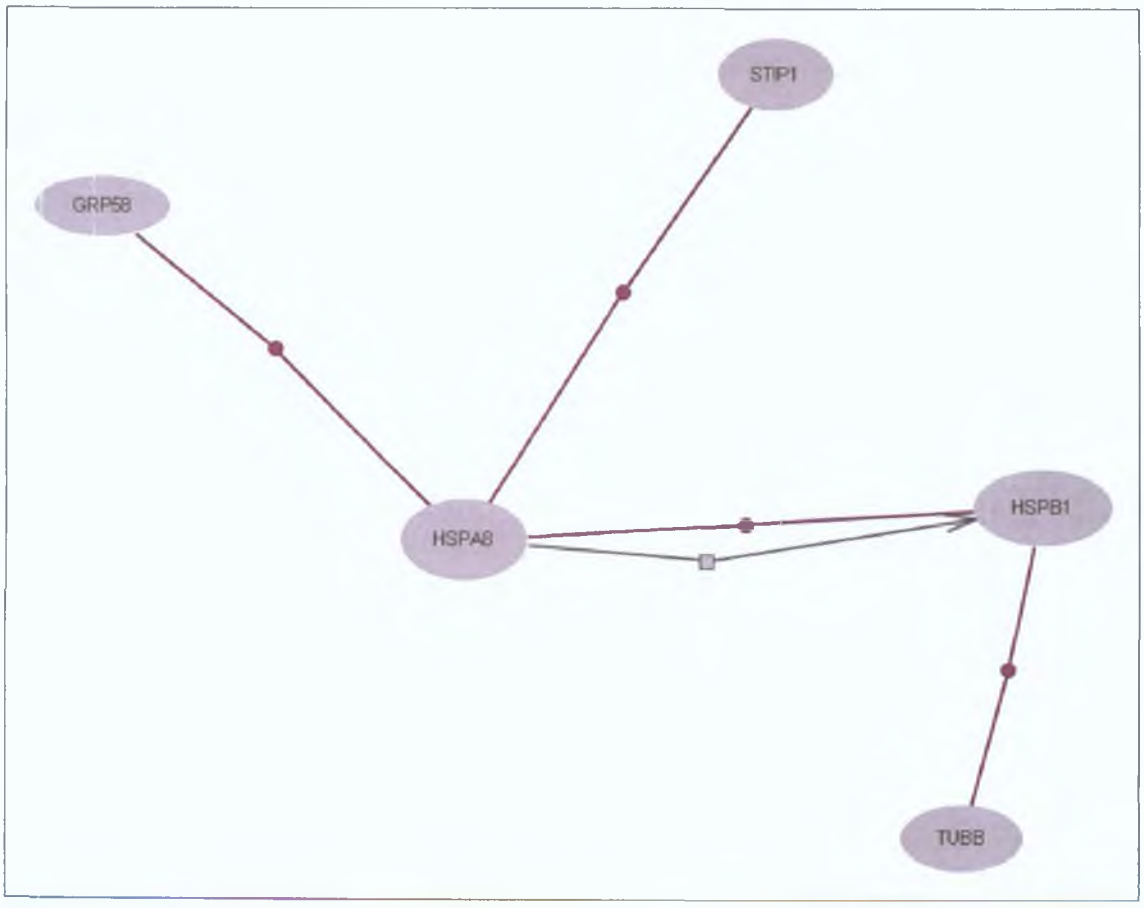

Figure 3.4.20 PathwayAssist analysis of direct interactions between proteins. The proteins involved in expression are shown in grey. Purple line indicates protein binding.

Figure 3.4.21 shows the pathways built based on common targets for selected nodes (i.e. differentially regulated proteins). Pathway analysis found that processes of differentiation, synthesis and regulation of signal transduction are important in the gain of adriamycin resistance in DLKP-A5F compared to DLKP-A. Important proteins include HSPB1, PHB and HPRT1.

The stimulators of differentiation include LGALS1, TUBB, HSPB1 and HPRT1, which are both increased and decreased in DLKP-A5F.

The two stimulators of synthesis include GRP58 and TUBB both of which are down-regulated in DLKP-A5F. PHB negatively affected synthesis and is down-regulated in DLKP-A5F.

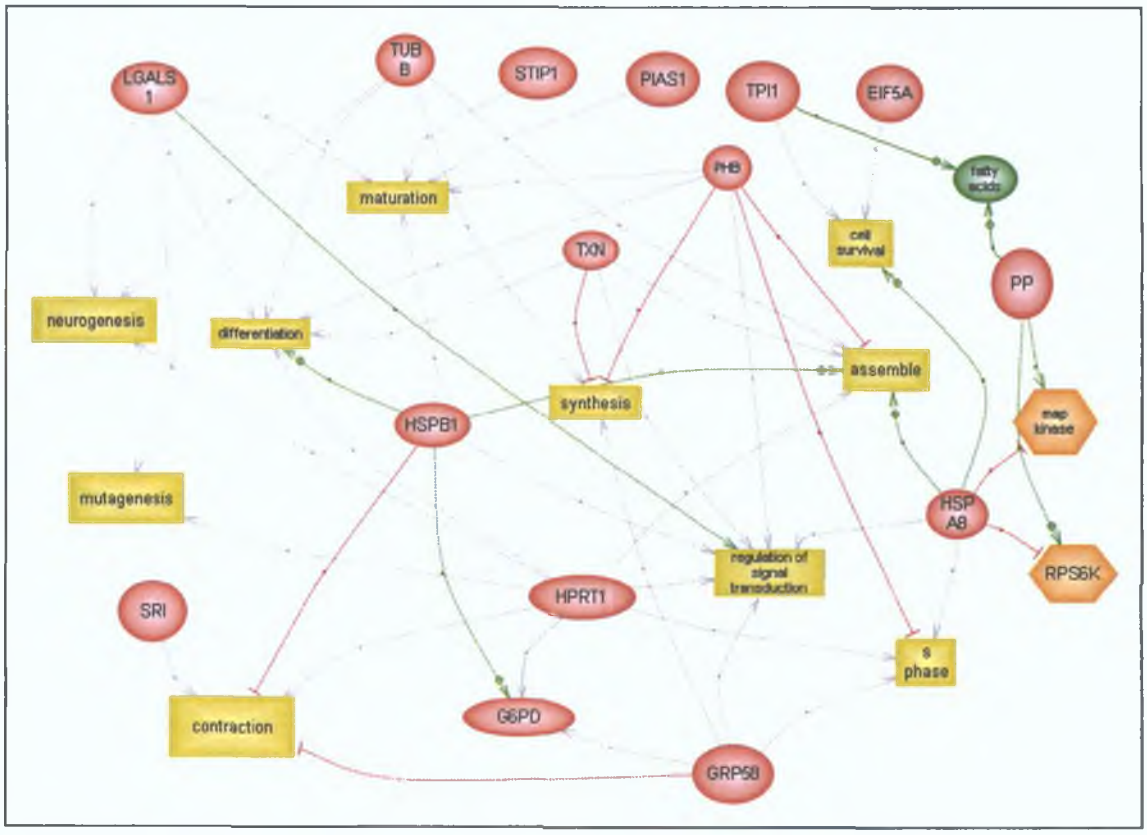

Figure 3.4.21 PathwayAssist analysis of common interactions between proteins. The selected proteins are shown in grey the picture with the cellular processes in yellow, small molecule in green and functional classes in orange. Green and red lines mark positive and negative regulatory effects respectively. Grey lines indicate an unknown regulatory effect.

3.4.6 DeCyder analysis of DLKP-A versus DLKP-A10

This experiment was designed to compare DLKP-A to a more drug-resistant variant, DLKP-A10 in order to examine the protein expression changes resulting from this increase in resistance. The experimental design for DIGE analysis is identical to that of DLKP versus DLKP-A as outlined in Table 3.4.3 with DLKP-A as the control and 6 biological replicates included.

Difference In-gel Analysis revealed a total of 3118 ± 524 protein spots between DLKP-A and DKLP-A10. Biological variation analysis revealed a total of 149 spots showing a greater than1.2-fold change in expression with a t-test p-value score of 0.05 or less (Figure 3.4.22). Of these 149 spots, 34 have been identified by MALDI-TOF mass spectrometry (Figure 3.4.23). A total of 34 differentially regulated spots 115 were not identified (76 down regulated and 39 up regulated).

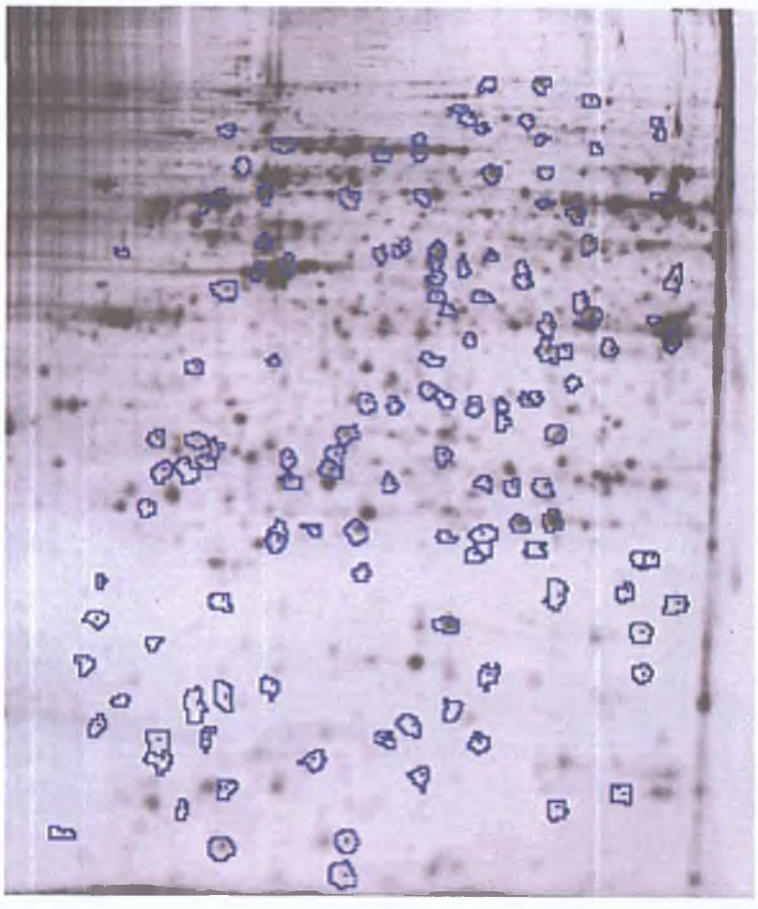

Figure 3.4.22 A representative Cy5 labelled DLKP-A10 gel showing completed BVA analysis of DLKP versus DLKP-A10. Spots circled in blue are the 149 statistically significant differentially regulated proteins ($p \leq 0.05$, protein fold ≥ 1.2).

Figure 3.4.23a-d Colloidal coomassie stained preparative DLKP-A gel which marks identified differentially regulated protein spots between DLKP-A and DLKP-A10. Spots in white are overlapping with DLKP-versus DLKP-A. Spots in yellow overlap with A5F and/or A2B. Spots in red are unique to A10. Due to problems with the ImageMaster software spots 35, 39 and 29 had to added separately and are not on the main picture.

Comparisons between DLKP-A versus DLKP-A10 and DLKP versus DLKP-A revealed that twelve proteins were shared (white spots in figure 3 4 13)

The K alpha 1 protein, 1 55-fold decreased in DLKP versus DLKP-A is now 1 81-fold increased in DLKP-A10, which correlates with an increase in drug resistance

The ion binding/transport proteins annexin and sorcin have lower levels of resistance in DLKP-A10 compared to DLKP versus DLKP-A A loss of protein expression was also observed with all other shared proteins

Spot No	Protein Name	Fold	pI	Mw	DLKP vs DLKP-A
4	HSP 70 protein 8 isoform 2	1 44	5 6	53 6	3 21
11	CCT2	1 8	6	57 78	2 58
16	eIF 2b	-1 63	6 5	58 17	1 42
18	K alpha 1 protein	1 81	5	50 49	-1 55
20	Annexin A1	2 06	7 9	35 25	2 29
21	Annexin A1	2 19	7 9	35 25	2 51
27	HSP 70 kDa protein 8 isoform 2	-6 5	5 6	53 6	-1 25
29	Triosephosphate isomerase	-3 21	6 5	26 95	-1 46
31	K130r mutant	1 54	6 5	21 14	1 54
33	Sorcin	-2 33	5 1	20 61	1 51
34	Nucleoside diphosphate kinase 1	1 27	5 4	19 86	1 54
35	eIF5a	-2 85	5 1	16 98	-2 63

Table 3 4 18 Overlapping protein spots between the comparisons DLKP-A versus DLKP-A10 and DLKP versus DLKP-A (spots marked white in Figure 3 4 23)

Comparisons between DLKP-A versus DLKP-A10 and DLKP-A versus DLKP-A2B revealed that four proteins overlapped namely, annexin 1, HSP 70 kDa protein 8 isoform 2, eukaryotic translation elongation factor 1 delta isoform and vimentin Annexin 1 was 1 6-fold decreased in the DLKP-A2B cell line, proteins expression decreased further in DLKP-A10 The heat shock protein while increased in DLKP-A2B (7 9-fold) is now 1 51-fold decreased in DLKP-A10 In contrast and in correlation wth drug resistance, vimentin is 1 64-fold decreased in DLKP-A2B but increased in DLKP-A10

A comparison between DLKP-A versus DLKP-A10 and DLKP-A versus DLKP-A5F again revealed that four proteins overlapped These included synovial sarcoma breakpoint 3, BiP, prohibitin and beta tubulin These proteins are further decreased in DLKP-A10 in comparison to DLKP-A2B (Table 3 4 19)

Spot No	Protein Name	gi Number	Gene Symbol	Fold	pI	M.W
39	Actin G	gi|40226101|	ACTG1	-4 69	5 5	26 68
40	Annexin 1	gi|442631|	ANXA1	-2 27	5 4	35 25
42	HSP 70 kDa protein 8 isoform 2	gi|62896815|	HSPA8	-1 51	5 6	53 6
44	Eukaryotic translation elongation factor 1 delta isoform	gi|15215451|	EEF1D	-1 67	4 9	31 22
45	Vimentin	gi|37852|	VIM	3 88	5 1	53 72
47	Synovial sarcoma breakpoint 3	gi|57162655|	SSX3	-1 9	6 1	11 37
48	BiP	gi|6470150|	GBP	-3	5	72 21
49	Prohibitin	gi|76879893|	PHB	-2 28	5 6	29 87
51	Beta tubulin	gi|18088719|	TUBB	-5 23	4 7	50 11

Table 3 4 19 Overlapping protein spots between the comparisons DLKP versus DLKP-A10 and/or DLKP-A versus DLKP-A5F, -A2B (spots marked yellow in Figure 3 4 23)

Sixteen proteins were determined to be unique to DLKP-A versus DLKP-A10, the majority of which are involved in the cytoskeleton and are predominantly down-regulated The remaining proteins also predominantly down-regulated have functions involving proteins turnover, cell signalling, glycolysis, stress, ion binding/transport, transcription regulation and RNA processing (Table 3 4 20)

Spot No	Protein Name	gi Number	Gene Symbol	Fold	pI	M W
65	26S proteasome-associated pad1 homolog variant	gi|62088020|	PSMD14	-1 54	6 5	18 99
66	Beta Actin	gi|15277503	ACTB	1 64	5 8	40 83
67	Beta Actin	gi|15277503	ACTB	1 63	5 6	40 54
68	Beta Actin	gi|15277503	ACTB	-2 03	5 6	40 54
69	Aldehyde Dehydrogenase A1	gi|2183299|	ALDH1A1	1 45	6 3	55 4
70	Actin G1	gi|178045|	ACTG	-2 85	5 5	29 68
71	Chloride intracellular channel 4	gi|55666469|	CLIC4	-4 69	5 5	28 98
72	hnRPF	gi|16876910|	HNRPF	1 92	5 4	46 02
73	HSP 60 kDa	gi|77702086|	HSPD1	1 33	5 7	61 37
74	HSPC124	gi|6841470|	PPA2	-2 48	5 6	36 96
75	LASP 1	gi|2135552|	Lasp-1	-1 48	6 1	30 19
76	Peroxiredixin 3 isoform a precursor variant	gi|62896877|	PRDX3	-1 45	8	27 95
77	Retinoblastoma binding protein 7	gi|57209889|	RBBP7	-2 43	4 9	47 6
78	Rho GDP dissociation inhibitor (GDI) alpha	gi|30582607|	ARHGDIA	-1 83	5	23 25
79	Peroxiredoxin 2	gi|1617118|	PRDX2	-1 86	5 2	18 48
80	Vimentin	gi|57471646|	VIM	-2 24	5	47 53

Table 3 4 20 Proteins unique to DLKP-A versus DLKP-A10 (spots marked in red in Figure 3 4 23)

3.4.6.1 Proteins identified between DLKP-A versus DLKP-A10

Proteins with decreased protein expression have all reported functions in Table 3.4.22 except RNA processing and glycolysis. In contrast, proteins with increased protein expression are involved in RNA processing, glycolysis, cytoskeleton, stress, apoptosis/redox regulation and ion binding/transport. The majority of protein changes are involved in cytoskeleton, stress response, ion binding/transport and transcription/ transcription regulation account for 25%, 21%, 15 and 12% respectively. Apoptosis/redox regulation proteins, proteins involved in glycolysis and translation each accounts for 6%. The remainder of the proteins account for 3% each (Figure 3.4.19). A similar level of protein turnover, translation/translation regulation, RNA processing, ion binding/transport, stress response and cell signalling proteins were observed in both DLKP versus DLKP-A and DLKP-A versus DLKP-A10. There are approximately twice as many transcription proteins in DLKP-A10 compared to DLKP versus DLKP-A and three times more cytoskeletal. In contrast, there are approximately twice as many glycolytic and apoptosis/redox regulation proteins in DLKP versus DLKP-A compared to DLKP-A versus DLKP-A10 (Table 3.4.21, Figure 3.4.24 and Figures 3.4.9).

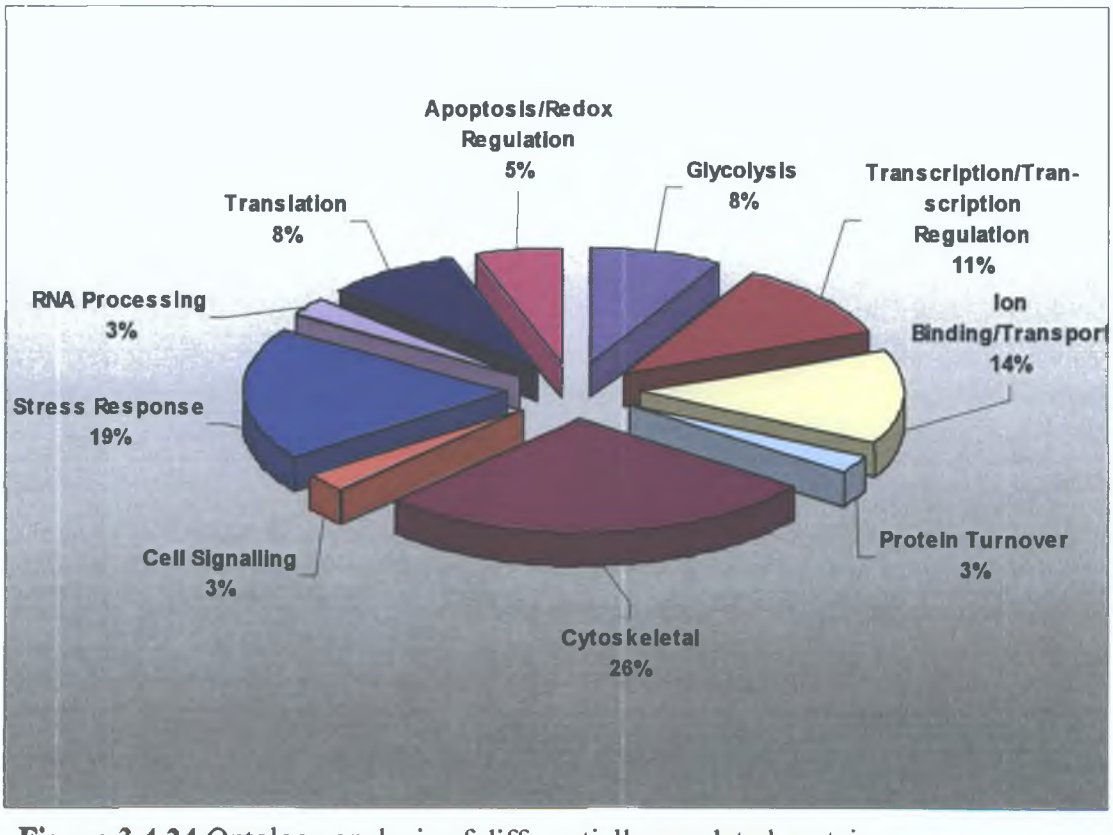

Figure 3.4.24 Ontology analysis of differentially regulated proteins.

Reported Function	Protein Name
Apoptosis/Redox regulation	K130r mutant of human DJ-1 Peroxiredoxin variant 2
Glycolysis	Peroxiredoxin 2 Aldehyde dehydrogenase 1
Stress Response	HSPC 124 HSP 70 kDa protein 8 isoform 2 HSP 60 BiP Protein CCT2
Ion Binding/Transport	Annexin A1 Chloride intreacellular channel 4 Sorcin isoform b
Translation	eIF 5a eIF 2b Eukaryotic translation elongation factor 1 delta, isoform 2
Cytoskeletal	ACTB Protein ACTG 1 Beta tubulin Tubulin alpha 6 Vimentin LASP 1
Protein Turnover	26S proteasome-associated pad1 homolog variant
Cell Signalling	Rho GDP dissociation inhibitor alpha
Transcription/Transcription Regulation	Prohibitin Retinoblastoma binding protein 7 Synovial sarcoma, X breakpoint 3 Nucleoside diphosphate kinase 1
RNA Processing	hnRPF

Table 3 4 21 Ontology analysis of DLKP-A10

3.4.6.2 PathwayAssist analysis of identified proteins between DLKP-A and DLKP-A10

PathwayAssist analysis was carried out on differentially regulated spots in DLKP-A versus DLKP-A10 to identify both direct and common pathways between the proteins. Figure 3.4.25 shows only direct links between the list of differentially regulated proteins submitted to pathway analysis.

The RhoGD protein inhibits the eukaryotic translation elongation factor 1 delta proteins which is a guanine nucleotide exchange protein. The CLIC4 protein has been shown to bind beta actin *in vivo*. NME1 forms molecular complexes with beta tubulin and that the number of complexes increases during the differentiation process of murine cells.

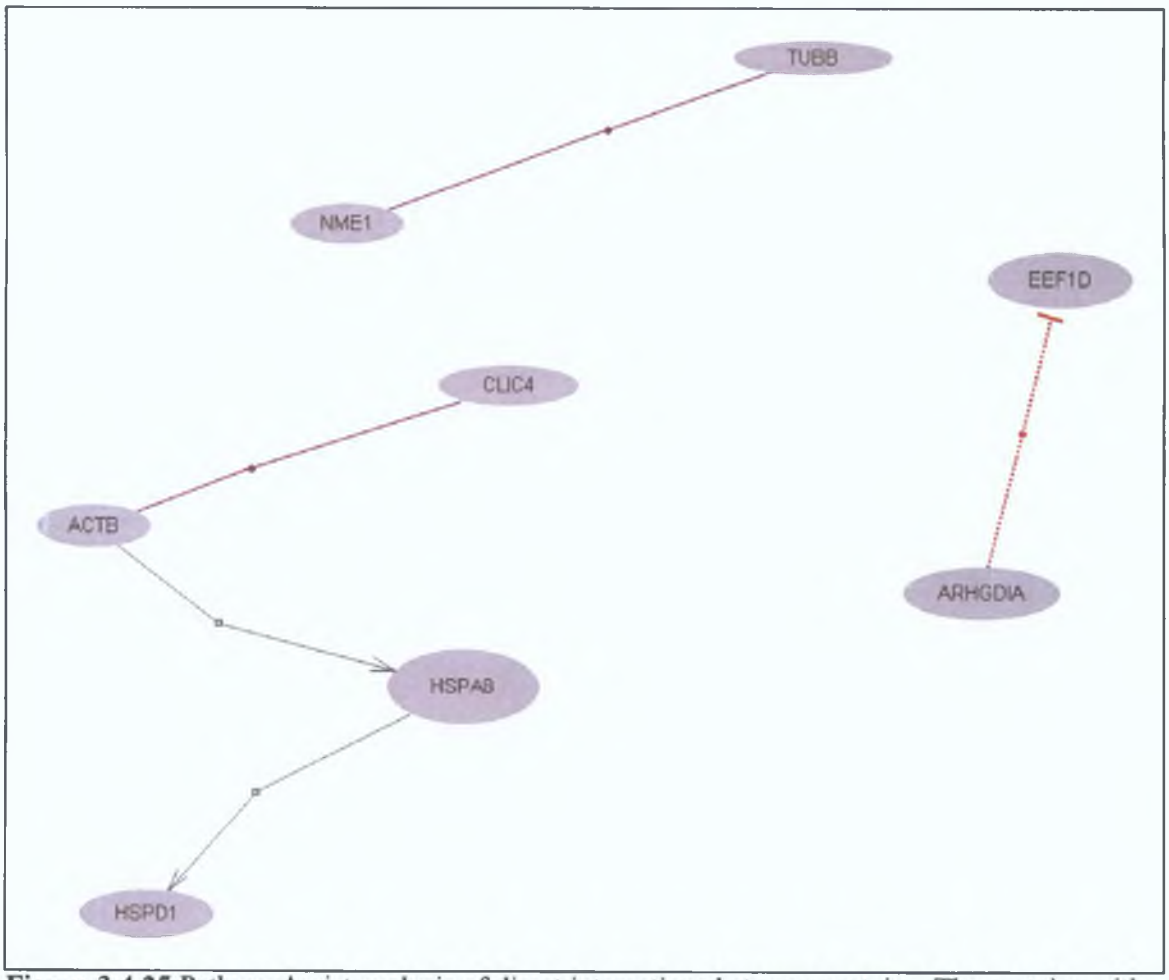

Figure 3.4.25 PathwayAssist analysis of direct interactions between proteins. The proteins with direct links are shown in grey. Purple lines indicate protein binding and the red line indicates an inhibitory effect.

Figure 3.4.26 shows the pathways built based on common targets for selected nodes (i.e. differentially regulated proteins). Pathway analysis found that processes of apoptosis and differentiation are important in the development of increased adriamycin resistance in DLKP-A. Stimulators of apoptosis include ARHGD1A, PHP, ANAX1, NME, EEF2, CLIC4, HSPD1, VIM, and RBBP7. The majority of these are down-regulated in DLKP-A10. Inhibitors of apoptosis include PRDX3 and PRDX2, HSPA8 and ALDH1A1. With the exception of ALDH1A1 the expression of all other proteins is decreased in DLKP-A10.

Eight proteins were observed to interact with the differentiation cell process. The single inhibitory protein of differentiation, NME1 was found to be increased in DLKP-A10 by 1.27-fold. The remaining stimulators of differentiation were all decreased except for ALDH1A1.

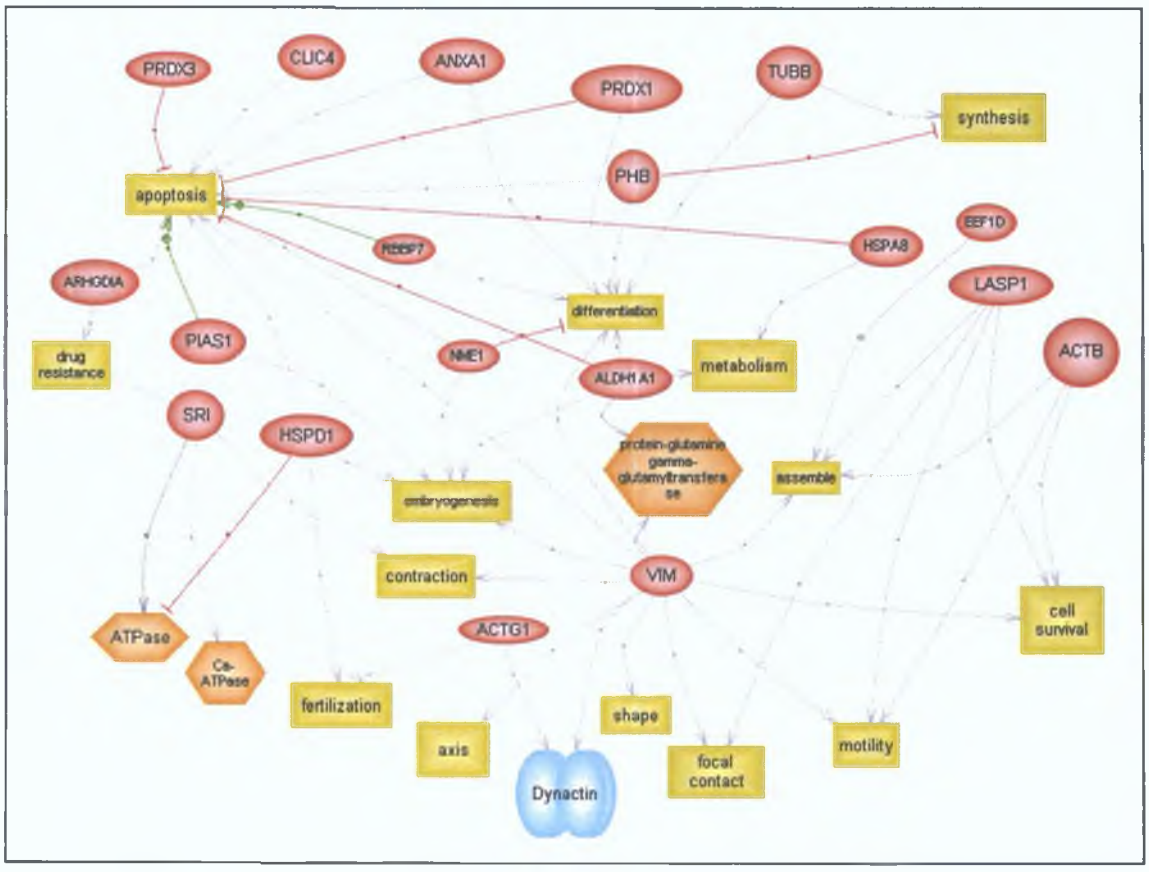

Figure 3.4.26 PathwayAssist analysis of common interactions between proteins. The selected protein nodes are shown in grey the picture with the cellular processes in yellow and functional classes in orange. Green and red lines mark positive and negative regulatory effects respectively. Grey lines indicate an unknown regulatory effect.

3 4 7 Correlation with drug resistance

Figure 3 4 27 and Table 3 4 22 shows differentially expressed proteins that correlate with drug resistance across the panel of adriamycin cell lines These proteins are all up-regulated in DLKP versus DLKP-A and are further increased in other cell lines in the panel Proteins involved in transcription/transcription namely nucleoside diphosphate kinase and replication A2 are similarly changed in DLKP-A2B with NME1 being further up-regulated in the most resistant cell line, DLKP-A10 The three stress response proteins especially CCT2 and HSPA8 are markedly increased in DLKP-A10 Similar results are seen for the apoptosis/redox regulation protein K130r mutant of human Dj-1 (PARK7) The two isoforms of the ion binding protein, annexin A1 are also strongly up-regulated in DLKP-A10

Spot No	Gene Name	DLKP	DLKP-A2B	DLKP-A	DLKP-A5F	DLKP-A10
34	NME1	-1 54	-1 28	1	1	1 27
22	RPA2	-1 5	-1 29	1	1	1
25	HSPB1	-1 47	1	1	1 48	1
11	CCT2	-2 58	1	1	1	1 8
31	PARK7	-1 54	1	1	1	1 26
4	HSPA8	-3 21	1	1	1	1 44
20	ANXA1	-2 29	1	1	1	2 06
21	ANXA1	-2 51	1	1	1	2 19

Table 3 4 22 Proteins correlating with drug resistance across the adriamycin-resistant panel

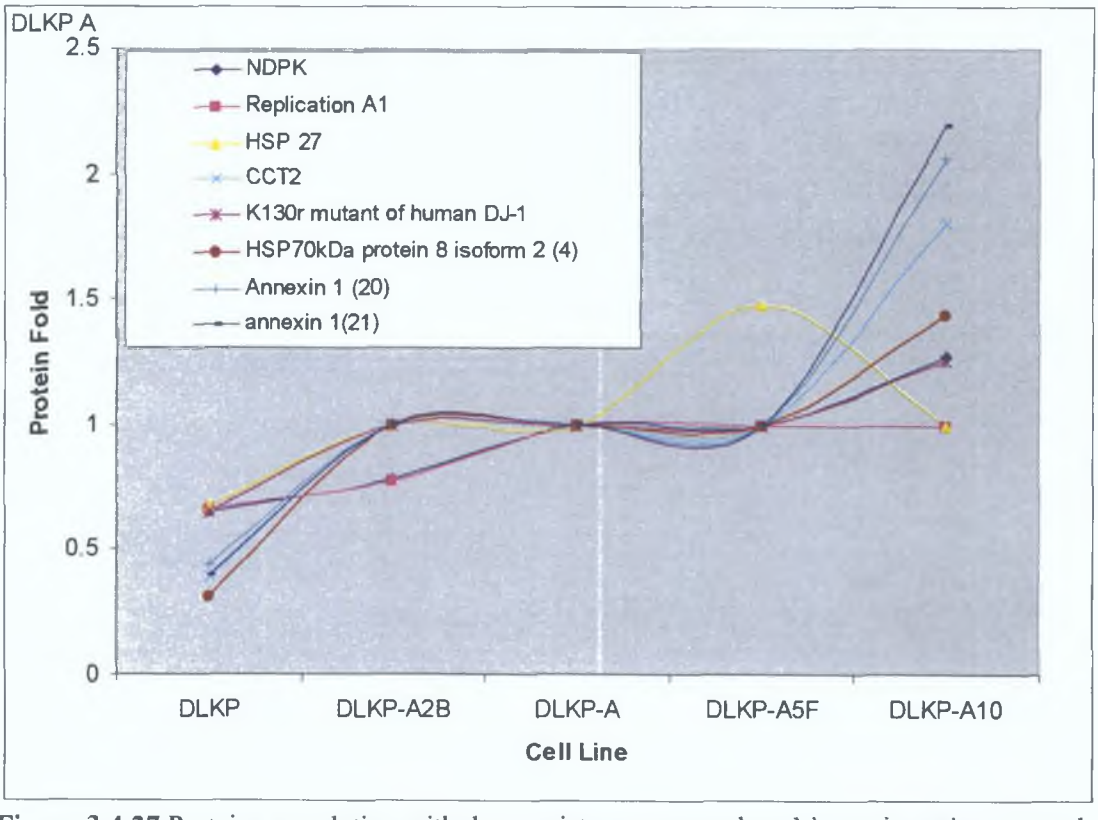

Figure 3.4.27 Proteins correlating with drug resistance across the adriamycin-resistant panel. Numbers in brackets indicate spot numbers.

Figure 3.4.28 and Table 3.4.23 shows differentially expressed proteins that inversely correlate with drug resistance across the panel. The stress response proteins stress induced phosphoprotein and HSP 70kDa protein 8 isoform 2 are further decreased in A5F and/or A10. BiP is unchanged in DLKP versus DLKP-A but decreased in A5F and A10. The transcription/transcription regulation proteins, prohibitin and synovial sarcoma breakpoint 3 though unchanged in DLKP versus DLKP-A but decreased in the more adriamycin-resistant variants. The glycolytic protein triosephosphate isomerase and the cytoskeletal protein, gamma actin are both decreased in DLKP versus DLKP-A, increased in A2B and decreased in both A5F and A10. The translation protein, eIF5a is decreased in DLKP-A and further decreased in DLKP-A5F and DLKP-A10.

Spot No.	Gene Name	DLKP	DLKP-A2B	DLKP-A	DLKP-A5F	DLKP-A10
19	STIP1	1.43	1	1	-1.35	1
27	HSPA8	1.25	2.87	1	-2.15	-6.5
49	PPAI	1	1	1	-2.13	-2.28
48	GPB	1	1	1	-2.04	-3.00
47	SSX3	1	1	1	-1.73	-1.9
35	EEF5A	2.63	1	1	-2.04	-2.85
39	ACTG	1	6	1	-4.07	-4.69
29	TPI	1.46	1.87	1	-2.06	-3.21

Table 3.4.23 Proteins inversely correlating with drug resistance across the adriamycin-resistant panel

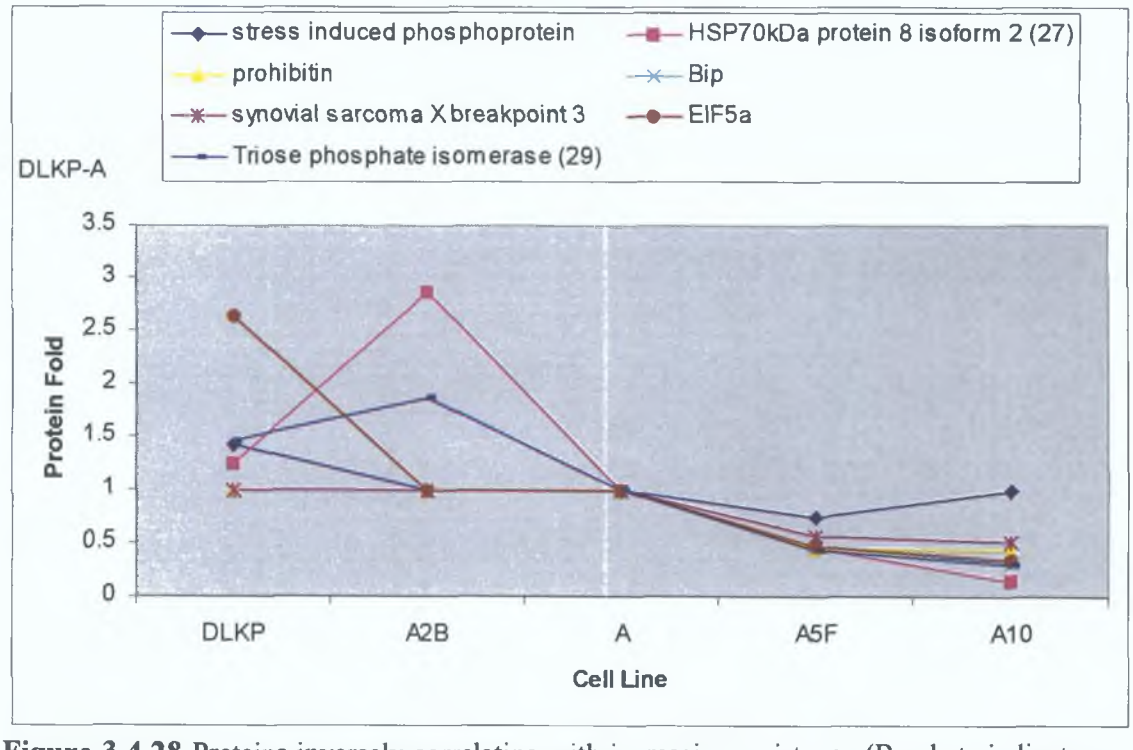

Figure 3.4.28 Proteins inversely correlating with increasing resistance (Brackets indicate spot number where isoforms are present).

Figure 3.4.29 and Table 2.4.24 shows the proteins increased in DLKP versus DLKP-A but show no change in the other adriamycin-resistant variants.

Spot No.	Gene Name	DLKP	DLKP-A2B	DLKP-A	DLKP-A5F	DLKP-A10
1	VCP	-2.32	1	1	1	1
2	HSPA9B	-1.97	1	1	1	1
3	LMNB1	-3.07	1	1	1	1
5	CCT3	-1.89	1	1	1	1
6	HNRPK	-1.93	1	1	1	1
7	ALDH1A1	-1.65	1	1	1	1
8	ALDH1A1	-1.52	1	1	1	1
9	OXCT1	-2.3	1	1	1	1
10	ALDH1A1	-1.47	1	1	1	1
12	HNRPH1	-1.52	1	1	1	1
13	GDI2	-1.69	1	1	1	1
15	STOML2	-2.03	1	1	1	1
22	ANXA1	-1.63	1	1	1	1
28	TPI	-1.89	1	1	1	1

Table 3.4.24 Proteins only increased in DLKP-A versus DLKP. There is no change across the rest of the panel.

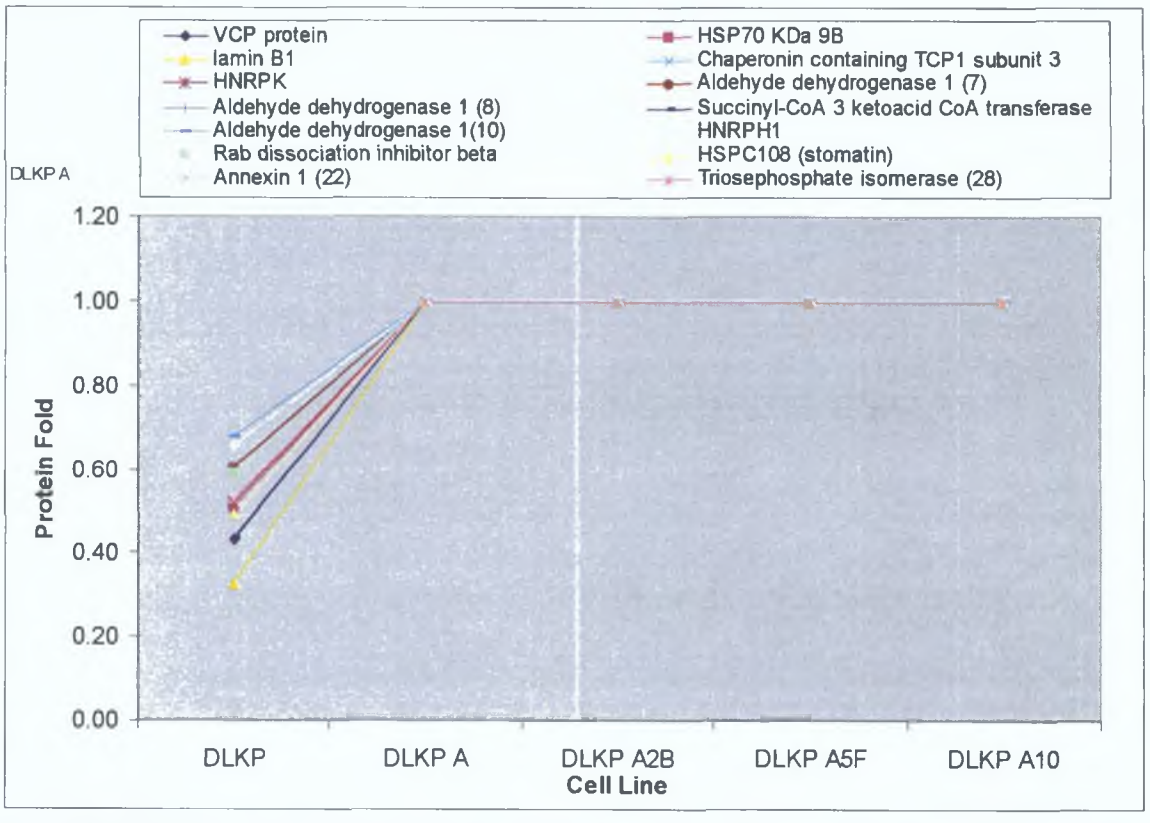

Figure 3.4.29 Proteins correlating with a baseline increase in resistance (Brackets indicate spot number where isoforms are present).

Figure 3.4.30 and Table 2.4.25 shows the proteins decreased in DLKP versus DLKP-A but show no change in the other adriamycin-resistant variants.

Spot No.	Protein Name	DLKP	DLKP-A2B	DLKP-A	DLKP-A5F	DLKP-A10
14	OATL1	3.45	1	1	1	1
17	HSPA8	2.15	1	1	1	1
24	p5	2.18	1	1	1	1
32	PRDX2	1.95	1	1	1	1

Table 3.4.24 Proteins decreased in DLKP versus DLKP-A only. There is no change across the rest of the panel

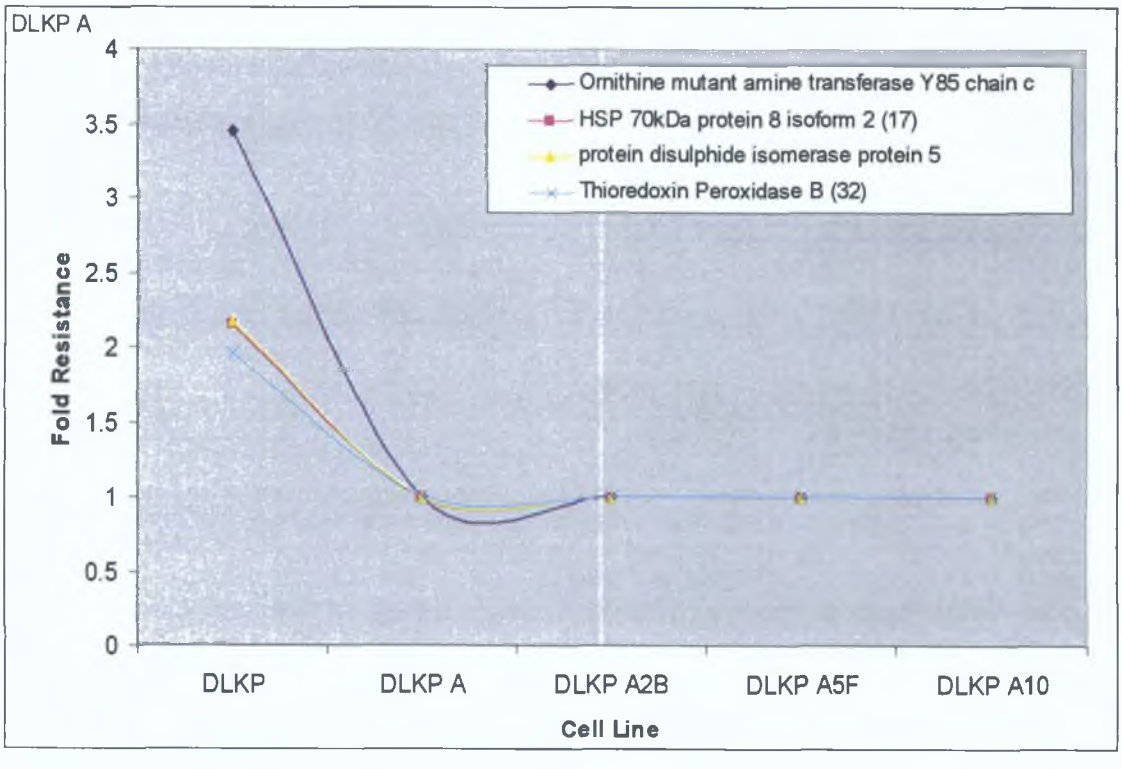

Figure 3.4.30 Proteins inversely correlating with a baseline resistance (Brackets indicate spot number where isoforms are present).

3 5 Proteomic analysis of DLKP-Mitox

Resistance to the chemotherapy drug mitoxantrone has been associated with several mechanisms such as drug accumulation defects, a decrease in its target proteins topoisomerase II α and β 4 and overexpression of the breast cancer resistance half transporter protein (BCRP1) While the main mechanism of resistance in DLKP-Mitox is associated with BCRP1, little information on cytoplasmic changes is available This work set out to investigate differential protein expression resulting from mitoxantrone resistance in DLKP Previously, the DLKP cell line was pulsed 5 times with 60ng/ml mitoxantrone to establish resistance (Liang *et al*, 2004) The resulting cell line, DLKP-Mitox was 5 8-fold stably resistant to mitoxantrone No cross-resistance developed to adriamycin or taxotere The cell line became sensitised to carboplatin (0 4-fold) Low cross-resistance developed to vincristine (1 6-fold) and methotrexate (1 4-fold) The mitoxantrone resistance was confirmed by toxicity assays (section 2 8 1) In this section of the thesis, DLKP was used as the control and compared to DLKP-Mitox It is also of interest to compare proteins altered in DLKP versus DLKP-A with DLKP versus DLKP-Mitox as both adriamycin and mitoxantrone are alkylating agents Mitoxantrone is an analogue of adriamycin and has less cardiotoxicity

3 5 1 Screening of DLKP and DLKP-Mitox protein samples

As previously mentioned, the DIGE system required six high quality protein samples of each cell line (section 2 15) The gels were silver-stained to ensure the quality of protein samples The best six samples showing most solubilised, well-defined protein spots, free of streaking and salt fronts were selected

Figure 3 5 1a DLKP

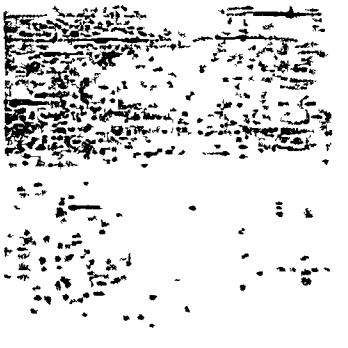

Figure 3 5 1b DLKP-Mitox

Figure 3 5 1a-b Silver stained images of DLKP and DLKP-Mitox A volume of 75 µg protein of all cell lysates for 2D-DIGE analysis were run on pH 4-7 IPG strips

3.5.2 The invasive status of the mitoxantrone-resistant variant of DLKP

Invasion assays were performed, as described in Section 2.11, to assess the ability DKLP and DLKP-Mitox to invade through matrigel. Cell culture inserts were coated with matrigel and placed in medium containing 24-well plates prior to cell addition. Cells were considered invasive if they migrated through the matrigel and the 8 μM porous membrane and attached to the underside of the membrane within 24 hours. The images presented are representative of at least three separate experiments, are at a magnification of 10X and are stained with crystal violet.

The DLKP parental cell line is invasive (Figure 3.5.2). Decreased invasion was observed in DLKP-Mitox (Figure 3.5.3) when compared to the parent.

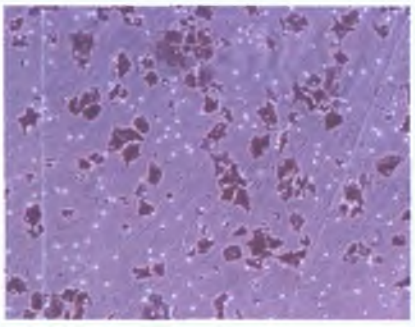

Figure 3.5.2 DLKP

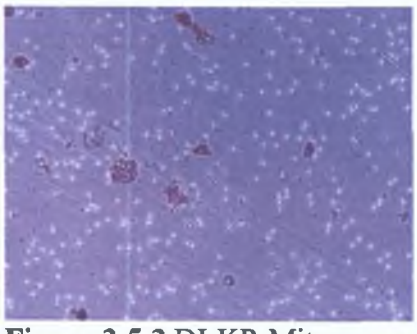

Figure 3.5.3 DLKP-Mitox

3.5.2.1 Quantification of invasion

The invasion assays were quantified by counting cells with a graticule at 40X magnification (Table 5.2.1, Figure 3.5.4). Proteomic analysis was carried out on these cell lines. The data shows that DLKP-Mitox is less invasive than DLKP.

Cell Line	Average cell count/area/view	P value
DLKP	11.35 ± 1.09	-
DLKP-Mitox	0.85 ± 0.05	0.003

Table 3.5.1 Quantification of DLKP and DLKP-Mitox. The values are given as the average cell counts/area/view ± the standard deviation. (n=3).

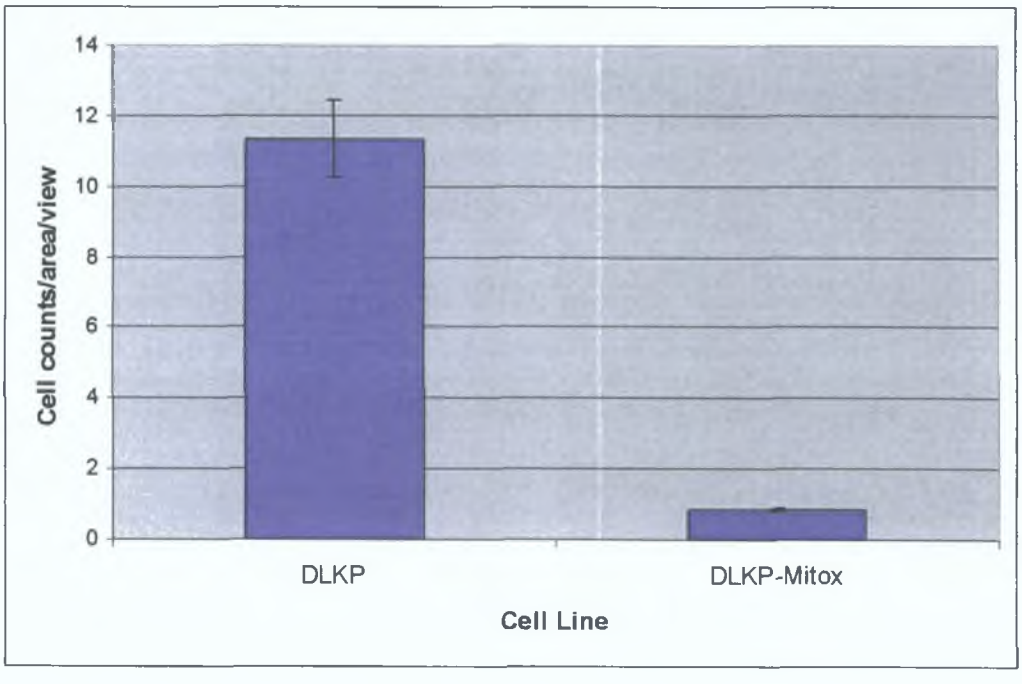

Figure 3.5.4 Quantification of mitoxantrone resistant variant of DLKP

3.5.3 Experimental outline of labelling of DLKP and DLKP-Mitox

The experimental design for DIGE analysis of DLKP versus DLKP-Mitox is outlined as follows: Six biological replicates of DLKP and DLKP-Mitox were labelled with 200pmol of Cy3 and Cy5 respectively (section 2.16.1.3). Each replicate was also labelled with Cy2 for the internal control. This generated a total of 150μg lysate/gel (50μg Cy2 internal standard, 50μg Cy3 and 50μg Cy5).

Difference In-gel Analysis of DLKP compared to DLKP-Mitox using Decyder™ revealed a total of 2221 ± 140 protein spots. BVA revealed a total of 343 spots showing a greater than 1.2-fold change in expression with a t-test score of 0.05 or less of which 147 had a p value less than 0.01 (Figure 3.5.5). Of these 343 spots, 60 have been identified by MALDI-TOF mass spectrometry. A total of 283 differentially regulated spots were not identified.

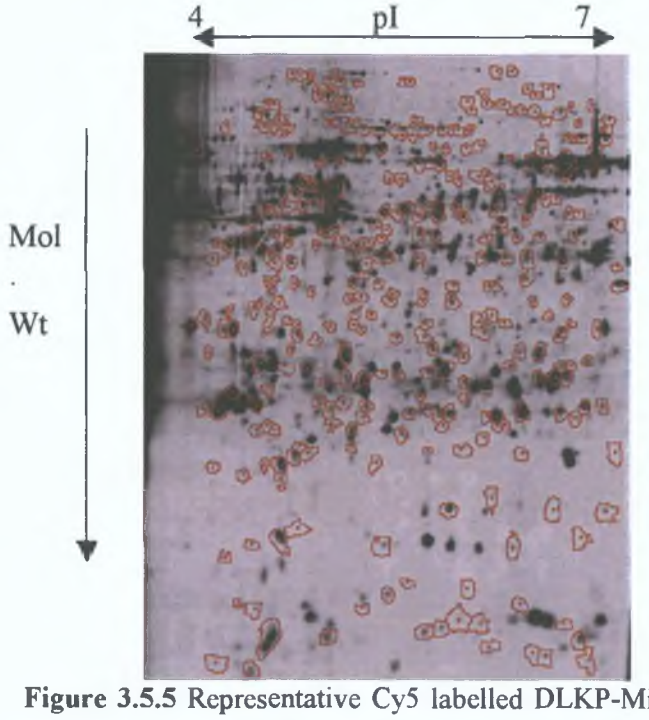

Figure 3.5.5 Representative Cy5 labelled DLKP-Mitox gel showing completed BVA analysis of DLKP versus DLKP-Mitox between pH4-7. Spots circled in red are the 343 statistically significant differentially regulated proteins ($p \leq 0.05$, protein fold ≥ 1.2).

3.5.4 Identification of differentially regulated proteins

MALDI-TOF mass spectrometry successfully identified 60 differentially regulated proteins between DLKP and DLKP-Mitox (Figure 3.5.6). Of these 60 spots, 31 were found to be up-regulated and 30 down-regulated (Table 3.5.2). For visual clarity, the proteins were numbered and the identification outlined in Table 3.5.2, 3.5.3 and 3.5.4. Table 3.5.2 shows the protein spots, which show shared expression between DLKP-A and DLKP-Mitox and are numbered to be consistent with those of DLKP versus DLKP-A. Table 3.5.3 shows the protein spots, which show shared expression between DLKP-Mitox and the DLKP-A variants A2B and A5F. Table 3.5.5 shows the differentially expressed protein spots, which are unique to DLKP-Mitox.

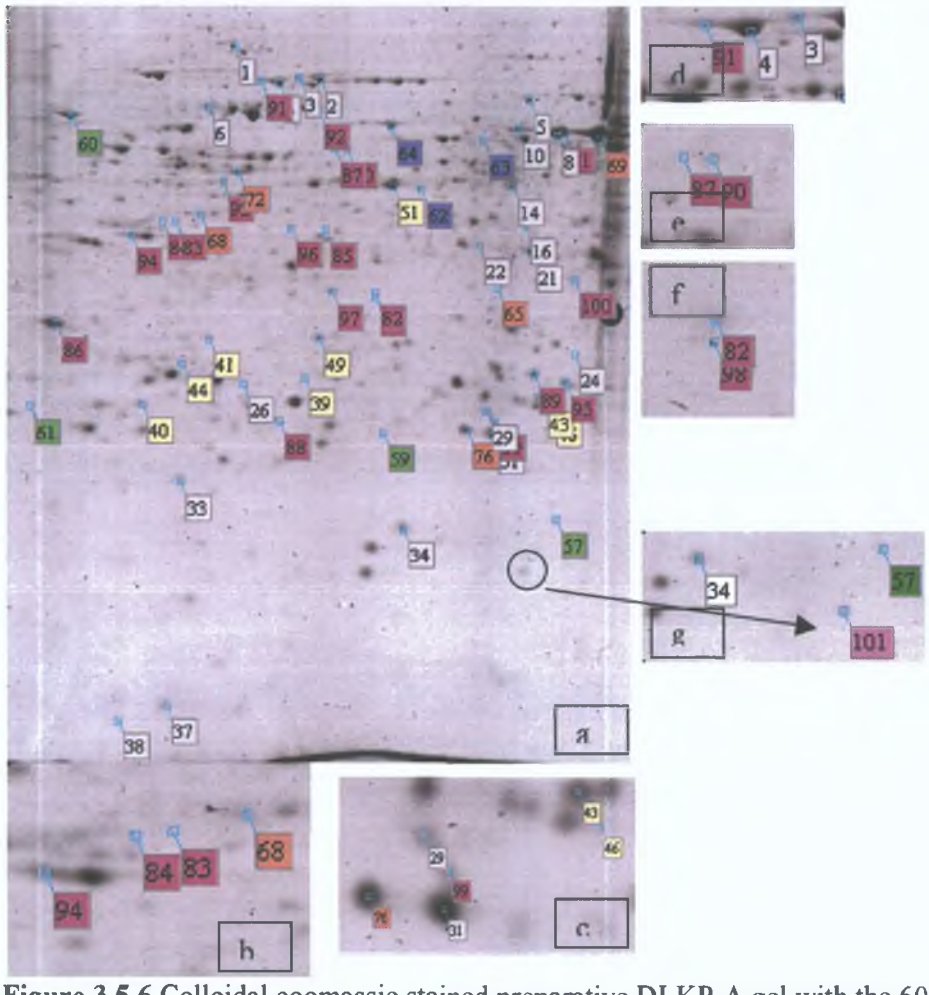

Figure 3.5.6 Colloidal coomassie stained preparative DLKP-A gel with the 60 identified protein spots exhibiting differential expression identified *via* MALDI-TOF MS analysis as listed in Tables 3.5.2, 3.5.3 and 3.5.5.

3 5 5 Shared differentially expressed proteins between DLKP-A and DLKP-Mitox

Spot No	Protein Name	gi Number	Gene Symbol	Fold	pI	Mw
1	Valosin containing Protein	gi|48257098|	VCP	-2 0	4 9	71 56
2	HSP70 kDa 9B (MTHsp75)	gi|292059|	HSPA9B	-2 53	6	74 12
3	Lamin B1	gi|576840|	LMNB1	-2 1	5 3	67 79
4	HSP 70 protein 8 isoform 2	gi|62896815|	HSPA8	-2 99	5 6	53 6
5	Chaperonin containing TCP1 subunit 3	gi|58761484|	CCT3	-2 02	6	57 78
6	hnRPK	gi|55958547|	HNRPK	-2 69	5 4	42 02
8	Aldehyde dehydrogenase A1	gi|2183299|	ALDH1A1	1 64	6 3	55 44
10	Aldehyde dehydrogenase A1	gi|2183299|	ALDH1A1	1 61	6 3	55 44
14	Chain C, OAT Mutant Y85i	gi|78101704|	OATL1	1 96	6 6	48 81
16	eIF 2b	gi|19353009|	EIF2B	-1 32	6 5	58 17
21	Annexin A1	gi|442631|	ANXA1	1 89	7 9	35 25
22	Annexin A1	gi|442631|	ANXA1	1 2	7 9	35 25
24	Protein disulphide isomerase protein 5	gi|1710248|	p5	2 82	5	46 52
26	Actin G protein	gi|178045|	ACTG1	-2 45	5 6	26 15
29	Triosephosphate isomerase	gi|66360366|	TPI1	-1 25	6 5	26 95
31	K130r mutant of human DJ-1	gi|33358056|	PARK7	1 25	6 5	21 14
33	Sorcin isoform b	gi|38679884|	SRI	3 85	5 1	20 61
34	Nucleoside diphosphate kinase 1	gi|38045913|	NME1	-1 45	5 4	19 86
37	Galectin-1	gi|42542977|	Galectin-1	-1 4	5 3	14 75
38	Thioredoxin delta 3	gi|1827674|	TXN	1 98	4 8	11 86

Table 3 5 2 Overlapping proteins form DLKP versus DLKP-Mitox and DLKP versus DLKP-A Gene symbol determined from DAVID software and PubMed Entrez gene (section 2 24) Where the same protein has two separate numbers this indicates the presence of isoforms e g annexin A1 Spots marked white in Figure 3 5 6

Spot No	Protein Name	gi Number	Gene Symbol	Fold	pI	Mw
39	Actin G protein	gi|178045|	ACTG1	3 19	5 6	26 15
40	Annexin A1	gi|442631|	ANXA1	2 21	7 9	35 25
49	Prohibitin	gi|46360168|	PHB	-1 36	5 6	29 86
43	Chain B, Horf 6 a novel human peroxidase enzyme	gi|3318842|	-	-1 62	6	24 9
44	Eukaryotic translation elongation factor delta isoform 2	gi|15215451|	EEF1D	2 04	4 9	31 22
57	HSP 70 kDa protein 8 isoform 2	gi|62896815|	HSPA8	1 79	5 6	53 6
46	Human Hprt	gi|47115227|	HPRT	2 25	5 5	39 3
59	Peroxiredoxin	gi|62896877|	PRDX3	2 2	7 1	27 95
60	prolyl 4-hydrolase beta subunit	gi|48735337|	P4HB	1 28	4 8	57 5
61	Proteasome subunit alpha type 5	gi|54696300|	PSMA5	-1 28	4 7	26 58
65	26S Proteasome-associated Pad1 homologue variant	gi|62088020|	PSMD14	1 44	6 5	18 99
68	Beta Actin	gi|15277503|	ACTB	2 01	40 54	5 6
69	Aldehyde dehydrogenase 1A1	gi|2183299|	ALDH1A1	1 57	6 3	55 44
41	Chloride intracellular channel 1	gi|62898319|	CLIC1	-1 34	5 1	27 34
72	HNRPF	gi|16876910|	HNRPF	-1 71	5 4	46 02
76	Peroxiredixin 3 isoform a precursor variant 2	gi|62896877|	PRDX3	1 61	8	27 95
62	putative protein of Nbla10058	gi|76879893|	PSMC2	-1 25	5 9	49
63	Alpha tubulin 6	gi|62897609|	TUBA6	1 39	5	50 49
64	ER-60 protease	gi|1208427|	PDIA3	-1 57	6	57 18
51	Beta Tubulin	gi|18088719|	TUBB	-1 48	4 7	50 11

Table 3 5 3 Overlapping proteins form DLKP versus DLKP-Mitox, and DLKP-A versus DLKP-A2B, -A5F and -A10 Gene symbol determined from "gi number" conversion software package "DAVID" and PubMed Entrez gene (section 2 24) (spots marked yellow, blue, green in Figure 3 5 6)

Table 3 5 4 and Figure 3 5 7 shows differentially expressed proteins that are shared between DLKP and the adriamycin and mitoxantrone resistant variants Taking the cellular functions of these cells into account a number of observations can be made Proteins involved in glycolytic activities such as aldehyde dehydrogenase and triosephosphate isomerase are similarly up- or down-regulated respectively Ion binding protein annexin A1 while up-regulated in both variants are more strongly so in DLKP-A Conversely, sorcin appears more important to the DLKP-Mitox cell line Of interest are the opposite changes in stress-related proteins, in DLKP-Mitox these are down-regulated while in DLKP-A, they are up-regulated Apoptosis/redox-related proteins galectin-1 and K130r mutant of human DJ-1 are similarly regulated in the two cell lines while thioredoxin delta 3 is more important in DLKP-Mitox than in DLKP-A

Spot No	Gene Symbol	DLKP vs DLKP-Mitox	DLKP vs DLKP-A	Function
26	ACTG 1	2 45	-1 45	Cytoskeleton
3	LMNB1	-2 1	3 07	
10	ALDH1A1	1 61	1 47	Glycolysis
8	ALDH1A1	1 64	1 52	
29	TPI	-1 25	-1 46	
22	ANXA1	1 2	1 63	Ion binding
21	ANXA1	1 89	2 51	
33	SRI	3 85	1 51	
5	CCT3	-2 02	1 89	Stress Response
2	HSPA9B	-2 53	1 97	
4	HSPA8	-2 99	3 21	
37	Galectin-1	-1 4	-1 55	Apoptosis/Redox
31	PARK7	1 25	1 54	
38	TRX	1 98	-1 17	
16	EIF2	-1 32	1 42	Translation
6	HNRPK	-2 69	1 93	RNA processing
14	OAT	1 96	-3 45	Metabolism
34	NDPK	-1 45	1 54	Transcription
24	PDI	2 82	-2 18	Protein turnover

Table 3 5 4 Interesting overlapping proteins form DLKP versus DLKP-Mitox, and DLKP versus DLKP-A

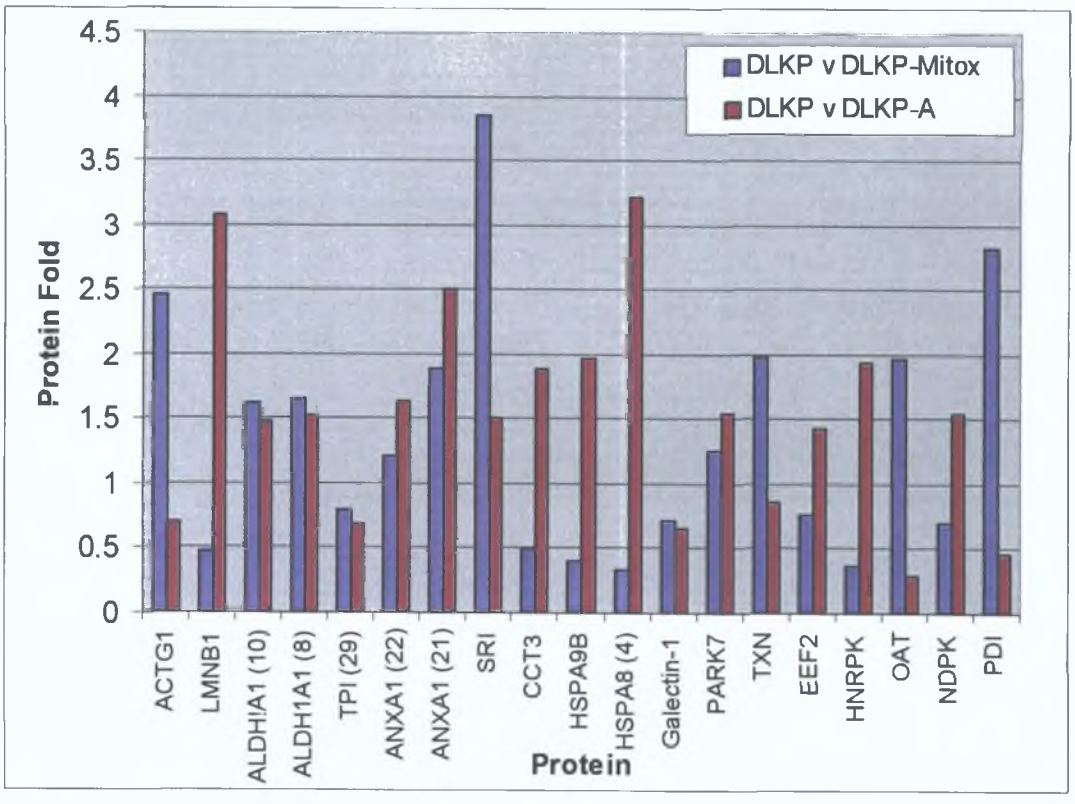

Figure 3.5.7 Shared differentially expressed proteins between DLKP versus DLKP-Mitox and DLKP versus DLKP-A.

3 5 6 Unique differentially expressed proteins between DLKP and DLKP-Mitox

Spot No	Protein Name	gi Number	Gene Symbol	Fold	pI	Mw
81	Aldehyde dehydrogenase 1A1	gi|2183299|	ALDH1A1	1 32	6 3	55 44
82	Annexin A4	gi|1703319|	ANXA4	1 51	5 8	36 09
83	Beta Actin	gi|15277503|	ACTB	2 97	5 6	40 54
84	Beta Actin	gi|15277503|	ACTB	2 53	5 6	40 54
85	Beta Actin	gi|15277503|	ACTB	-1 37	5 6	40 54
86	Tropomyosin	gi|825723|	TPM1	3 1	4 8	26 62
87	CGI-46 Protein	gi|4929561|	CGI-46	-1 35	6 3	48 5
88	GST-pi chain B	gi|23200511|	GSTP1	1 8	5 4	23 43
89	High mobility Group box 1	gi|55958717|	HMGB1	2 4	5 6	25 1
90	HLA-B associated transcript 1 variant	gi|62897383|	BAT1	-2 05	5 5	49 56
91	HSP 70kDa protein 8 isoform 2	gi|62896815|	HSPA8	-2 3	5 6	53 6
92	KIAA0098	gi|58257644|	CCT5	-1 73	5 5	61 49
93	Mannose-6-phosphate receptor binding protein	gi|16306789|	M6PRBP1	-1 26	5 3	47 19
94	nucleophosmin	gi|13536991|	NPM1	-1 37	4 5	29 62
95	Phosphoglycerate mutase 1 (brain) variant	gi|62897753|	PGAM1	-3 34	6 7	28 93
96	PKCq-interacting protein	gi|6840947|	TXNL2	-1 58	5 4	37 7
97	PP protein	gi|33875891	PP	-2 88	6	35 97
98	Proteasome activator subunit 3	gi|47523754|	PSME3	-1 71	5 7	29 6
99	Proteasome beta 3 subunit	gi|15278174|	PSMB3	1 45	6 1	23 22
100	Purine nucleoside phosphorlyase	gi|387033|	PNP	1 38	6 5	32 23
101	Cofilin (non muscle)	gi|30582531|	CFL1	-3 77	6 5	24 46

Table 3 5 5 Proteins unique to DLKP versus DLKP-Mitox (spots marked pink in Figure 3 5 6)

3.5.7 Ontology analysis of identified proteins

Ontology information was obtained through PubMed searches. Of the identified proteins, the majority have functions in cytoskeleton (19%), protein turnover (13%) with apoptosis/redox regulation, ion binding/transport and stress response accounting for 12% each. Glycolytic and RNA processing proteins account for 10% respectively. Transcription accounts for 5% with 3% of the proteins involved in cell signalling and metabolism. Finally, 2% are involved in tumour immunity and translation (Table 3.5.6, Figure 3.5.8).

Twice the amount of cytoskeletal and RNA processing proteins are found in DLKP-Mitox compared to DLKP-A. In contrast, twice the amount of stress response proteins is found in DLKP-A compared to DLKP-Mitox. Similar metabolic, translation, transcription, cell signalling and ion binding/transport responses are found in both cell lines (Figure 3.4.9, Figure 3.5.8).

Mitoxantrone was designed to produce less free radicals in comparison to adriamycin however, similar levels of apoptotic/redox response proteins were differentially regulated in both cell lines. However, in contrast to DLKP-A, the majority of these proteins are up-regulated in DLKP-Mitox.

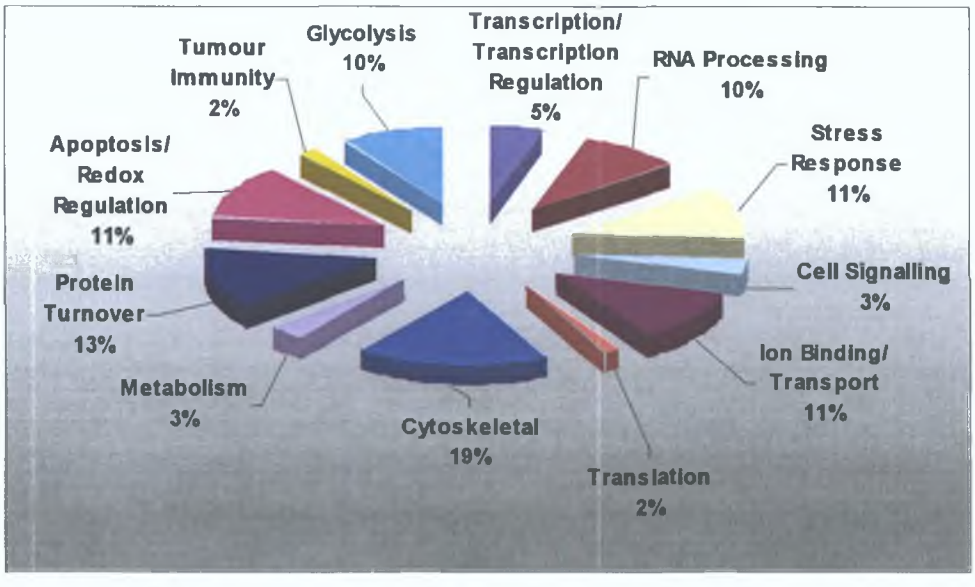

Figure 3.5.8 Ontology analysis of differentially regulated proteins.

Reported Function	Protein Name
Apoptosis/Redox regulation	Peroxiredoxin Peroxidase GST-pi chain B Galectin 1, Thioredoxin delta 3 K130r mutant of human DJ-1 Peroxiredixin 3 isoform a precursor variant 2
Glycolysis	Aldehyde dehydrogenase A1 Triosephosphate isomerase chain b Phosphoglycerate mutase 1 (brain) variant
Transcription/Transcription Regulation	Nucleoside diphosphate kinase 1 Prohibitin High mobility Group box 1
Stress Response	HSP 70 kDa protein 8 isoform 2 HSP70 kDa 9B (MTHsp75) Chaperonin containing TCP1 subunit 3 KIAA0098 CGI-46 Protein
Ion Binding/Transport	Annexin A1 Sorcin isoform b Chloride intracellular channel 1 Annexin A4 Nucleophosmin
Translation	eIF 2b
Cytoskeletal	Lamin B1 Alpha tubulin 6 Tropomyosin Actin g1 protein Beta Actin Beta Tubulin Cofilin
Cell Signalling	VCP protein Purine nucleoside phosphorlyase
RNA Processing	hnRPK hnRPF HPRT ER-60 Mannose-6-phosphate receptor binding protein EEF2
Metabolism	Chain C, OAT Mutant Y85i PP protein
Protein Turnover	Putative protein of Nbla10058 Proteasome subunit alpha type 5 26S Proteasome-associated Pad1 homologue variant Prolyl 4-hydrolase beta subunit Protein disulphide isomerase protein 5 Proteasome beta 3 subunit Proteasome activator subunit 3 PKCq-interacting protein
Tumour Immunity	HLA-B associated transcript 1

Table 3.5.6 Ontology analysis of identified proteins from DLKP versus DLKP-Mitox

3.5.8 PathwayAssist analysis of identified proteins

The gene symbol list was imported into the programme and from this both direct and common pathways were built. Only the differentially-regulated proteins were submitted for PathwayAssist analysis. Figure 3.5.9 shows only the direct links between differentially-regulated proteins between DLKP versus DLKP-Mitox. The NME1 protein forms complexes with beta-tubulin in *in vitro* tumour cell lines, but not in primary tumours. GRP58 and P4HB have been shown to bind in bovine and canine systems. These four proteins are decreased in DLKP-Mitox. The high mobility groups box proteins 1 and 2 (HMGB1) complexes with heat shock protein (HSPA8). In eukaryotic systems, HMGB1 interacts with hnRNP K and GSTP1 binds with prohibitin. The VCP protein has been shown to interact with HSPA8 in yeast.

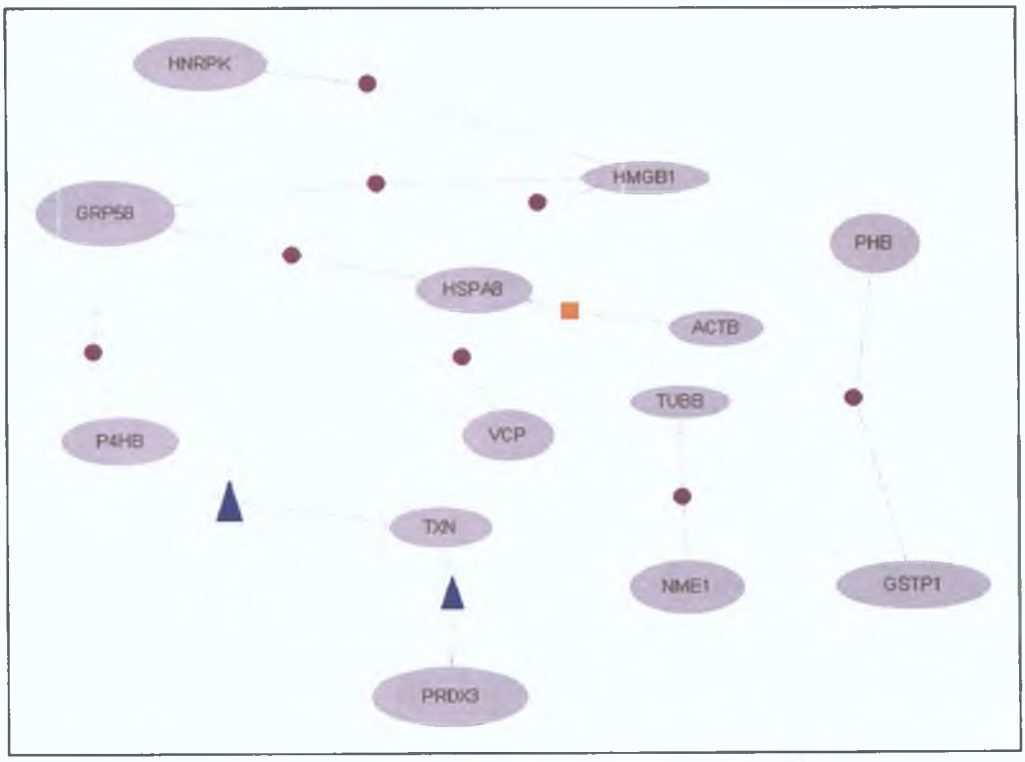

Figure 3.5.9 PathwayAssist analysis of direct interactions, identifying only direct links between the proteins. This finds proteins that are regulated by all selected nodes. Purple circles indicate binding, blue triangles indicate regulation and orange squares indicate effect on expression.

Figure 3.5.10 shows the pathways built based on common targets for selected nodes (i.e. differentially regulated proteins). Pathway analysis found that processes of apoptosis and differentiation are important in the development of increased mitoxantrone in DLKP-Mitox. Stimulators of apoptosis include NME1, PARK7, LMNB1, ANAX1, GSTP1, LGALS1 and NPM1. The majority of these are down-regulated in DLKP-Mitox. Inhibitors of apoptosis including HSPA9B, HSPA8, PRDX3, P4HB and ALDH1A1 are up-regulated in DLKP-Mitox. Stimulators of differentiation include BAT1, NP, TUBB, PSMC2, TXN, ALH1A1, HPRT1, PHB, GSTP1, HMGB1 and LGALS1. The majority of these are increased in DLKP-Mitox. NME1 inhibits differentiation and is down-regulated.

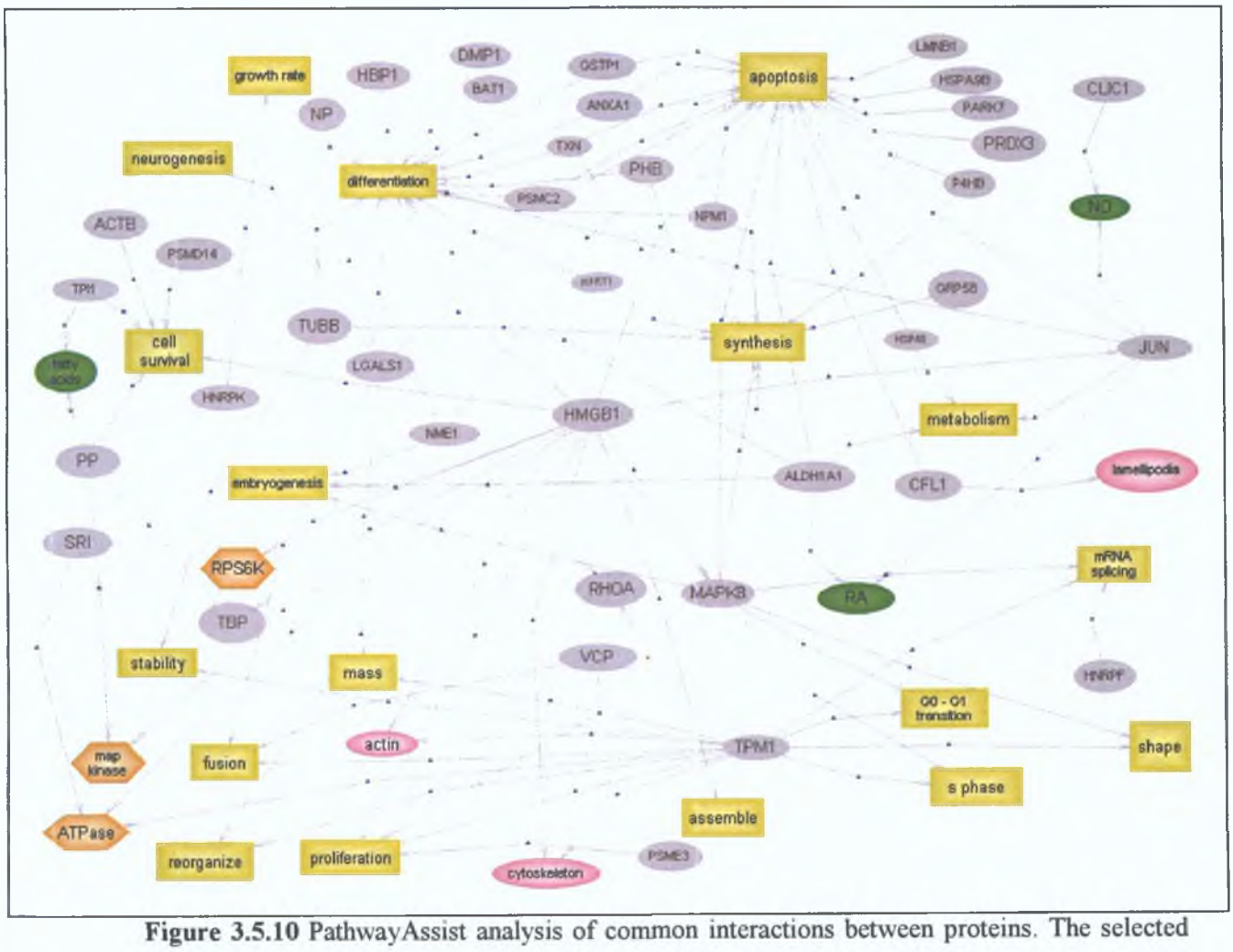

Figure 3.5.10 PathwayAssist analysis of common interactions between proteins. The selected protein nodes are shown in grey, the cellular processes in yellow, cell objects in pink, small molecules in green and functional classes in orange. Grey lines mark positive and negative regulatory effects.

3 6 Two-dimensional-difference gel electrophoresis of taxane-selected variants of SKMES-1

Investigations were carried out to establish differential protein expression caused by taxotere and taxol resistance in the squamous lung cell line SKMES-1, a cell line developed from a pleural effusion from a 65-year old male with squamous cell carcinoma of the lung The taxol and taxotere resistant cell lines were established from SKMES-1 during the course of this work Briefly, SKMES-1 was exposed to IC_{90} concentrations of taxotere (60ng/ml) and taxol (120ng/ml) for four hours, once a week for ten consecutive weeks The resulting cell lines were designated SKMES-Txt and SKMES-Txl respectively (Table 3 6 1) These resistance levels were the levels observed at week 61 for SKMES-Txt and week 34 for SKMES-Txl (Figures 4 1 and 4 2)

	Fold Resistance					
Cell Line	**Taxotere**	**Taxol**	**5-FU**	**Adriamycin**	**VCR**	**VP-16**
SKMES-1	1	1	1	1	1	1
SKMES-Txt (week 2)	5 9 ± 0 2	10 6 ± 0 6	9 6 ± 0 4	4 3 ± 0 4	4 5 ± 0 6	11 8 ± 0 97
SKMES-Txl (week 3)	6 7 ± 0 2	12 5 ± 0 1	7 5 ± 0 4	2 3 ± 0 1	5 6 ± 0 2	4 ± 0 1
SKMES-Txl (week 6)	2 95 ± 0 14	5 8 ± 0 3	7 8 ± 0 1	2 54 ± 0 04	5 1 ± 0 3	4 9 ± 0 5

Table 3 6 1 Drug resistance profiles of taxane resistant variants of SKMES-1

3 6 1 Overview of SKMES-Taxane resistance

The SKMES-Txt cell line is 5 9-fold and 10 6-fold resistant to taxotere and taxol respectively when compared to SKMES-1 The cell line is also approximately twice and three times more cross-resistant to adriamycin and VP-16 respectively when compared to SKMES-Txl (week 3 and week 6) The SKMES-Txl (week 3) cell line is 12 5-fold and 6 7-fold resistant to taxol and taxotere respectively when compared to SKMES-1 All cell lines exhibited cross-resistance to 5-FU and vincristine Resistance to taxol and taxotere fell in SKMES-Txl (week 6) to 5 8-fold and 2 95-fold respectively in comparison to SKMES-Txl (week 3)

3.6.2 Screening protein samples of SKMES-1 and variants

The DIGE system required six high quality protein samples per cell line per experiment. (section 2.15). Many sample preparations were carried out to refine the procedure to generate good gels with many distinct protein spots and to ensure low levels of contaminating factors such as DNA, RNA, lipids and salts. These lysates were generated from 7M urea/2M thiourea lysis buffer. The gels were silver-stained and scanned at 300 resolution to ensure the quality of proteins samples. The best six samples showing most solubilised, well-defined protein spots, free of streaking and salt fronts were selected.

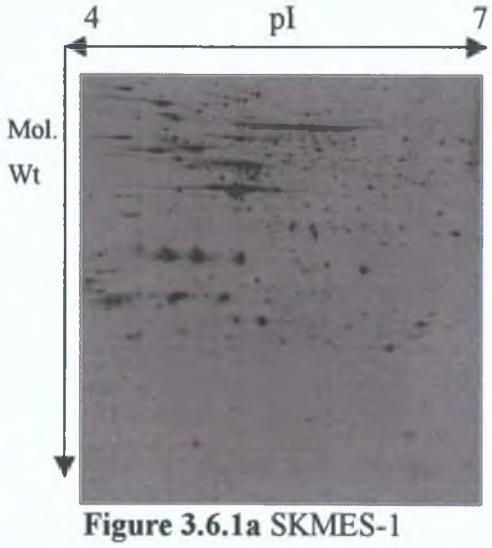

Figure 3.6.1a SKMES-1

Figure 3.6.1b SKMES-Txt (wk 2)

Figure 3.6.1c SKMES-Txl (wk 3)

Figure 3.6.1d SKMES-Txl (wk 6)

Figures 3.6.1a-d Silver stained images of SKMES-1 and taxanes-resistant variants. A volume of 75 μg protein of all lysates for 2D-DIGE analysis were run on pH 4-7 IPG strips.

3.6.3 Experimental outline of SKMES-1 versus and SKMES-Txt (Wk 2)

This experiment was designed to compare SKMES-1 to its taxotere-resistant variant (SKMES-Txt) at a time point when resistance was the highest (section 3.1.3.3). The aim was to determine the protein expression changes resulting from taxotere resistance.

The experimental design for DIGE analysis is outlined as follows: six biological replicates of each cell line were labelled with 150pmol of the Cy dyes. All SKMES and SKMES-Txt (Wk2) lysates were labelled with Cy3 and Cy5 respectively. A Cy2 labelled internal standard comprising of 6 SKMES, 6 SKMES-Txt (Wk2), 6 SKMES-Txl (Wk 2) and 5 SKMES-Txl (Wk6) was also included on each gel. A volume of 50μg protein was labelled with each Cy dye resulting in a total of 150μg/gel (50μg Cy2 internal standard, 50μg Cy3 and 50μg Cy5). Once labelling was completed, six 2D gels were generated, scanned, analysed and proteins of interest identified as previously described in section 3.4.

3.6.3.1 DeCyder analysis of SKMES-1 versus SKMES-Txt (Wk 2)

Differential protein expression between the lung cell line SKMES-1 and SKMES-Txt (Wk2) was observed using 2D-DIGE. Difference In-gel Analysis using Decyder™ (version 6) revealed a total of 1417 ± 131 protein spots. Biological variation analysis of these spots revealed a total of 157 spots showing a greater than 1.2-fold change in expression with a t-test score of 0.05 or less. Of these 157 spots, 40 have been identified using MALDI-TOF mass spectrometry. A total of 116 of the differentially regulated spots were not identified. As can be seen from Tables 3.6.3a and 3.6.3b, the fold changes are low, ranging from 1.98-fold increased to 1.68-fold decreased.

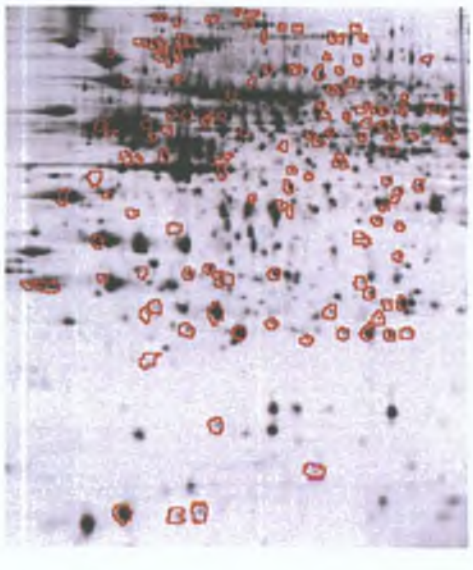

Figure 3.6.2 Representative Cy5 labelled SKMES-Txt (week 2) gel showing completed BVA analysis of SKMES-1 versus SKMES-Txt (week 2). Spots circled in red are the statistically significant differentially-regulated proteins.

Figure 3.6.3, Table 3.6.3a and 3.6.3b shows the identified differentially regulated proteins between SKMES-1 and SKMES-Txt.

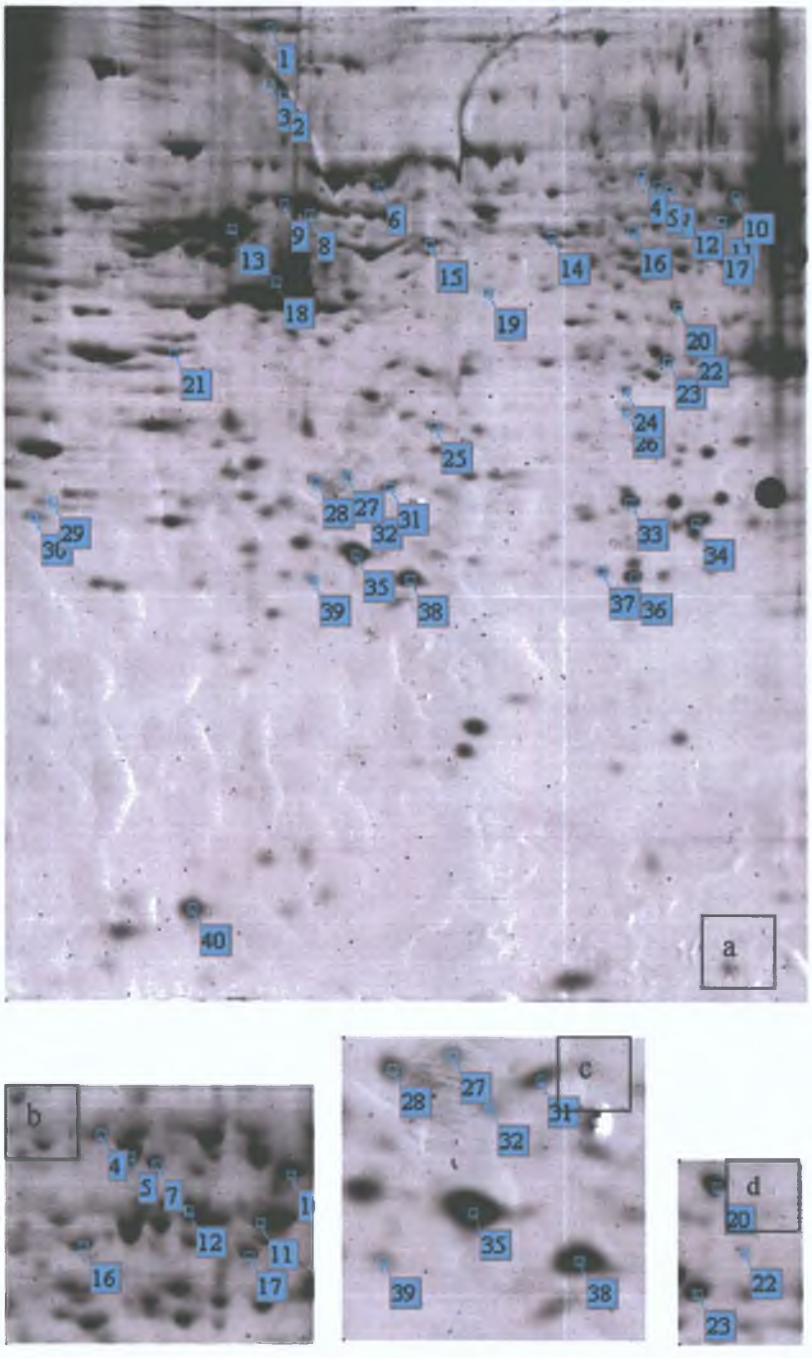

Figure 3.6.3a-d Colloidal coomassie stained preparative SKMES-Txt gel, which marks the proteins differentially-regulated between SKMES-1 versus SKMES-Txt - blue spots.

Spot No	Protein Name	gi Number	Gene Symbol	Fold	pI	M w
1	150kDa oxygen-regulated precursor	gi|10720185|	HYOU	1 33	5 2	111 6
2	Valosin containing Protein	gi|55662798|	VCP	-1 58	4 9	71 56
3	Valosin containing Protein	gi|55662798|	VCP	-1 87	4 9	71 56
4	Lamin A/C	gi|55957496|	LMNA	1 58	6 1	53 23
5	Chaperomn containing TCP1 subunit 3	gi|58761484|	CCT3	1 23	6	57 78
6	HSP 70 protein 8 isoform 2	gi|62896815|	HSPA8	1 24	5 6	53 6
7	Dihydropyrimidinase-like variant 2	gi|62087970|	CRMP-1	1 42	5 8	68 62
8	HSP 60 kDa	gi|77702086|	HSPD1	1 45	5 7	61 37
9	HSP 60 kDa	gi|77702086|	HSPD1	1 35	5 7	61 37
10	Glucose 6 phosphate dehydrogenase	gi|26224874	G6PD1	1 22	6 3	59 53
11	Glucose 6 phosphate dehydrogenase	gi|26224872|	G6PD1	1 55	6 3	59 53
12	Glucose 6 phosphate dehydrogenase	gi|26224874	G6PD1	1 2	6 7	55 21
13	Vimentin	gi|37852|	VIM	-1 63	5 1	53 72
14	hnRPH1	gi|48145673|	HNRPH1	1 57	5 9	49 5
15	Keratin 8	gi|62913980|	CARD2	-1 51	5 6	55 89
16	PMPCA protein	gi|48257293|	PMPCA	1 73	6 6	58 86
17	TATA binding protein interacting protein 49 kDa variant	gi|62896685|	GTF2D	1 32	6	50 54
18	Mannose-6-phosphate receptor binding protein	gi|16306789|	M6PRBP1	-1 22	5 3	47 19
19	Beta tubulin	gi|18088719|	TUBB	1 21	4 7	50 11
20	Septin 2	gi|15680208|	NEDD5	1 31	6 1	41 69
21	HNRPC protein	gi|58476967|	HNRPC	1 32	4 5	27 86
22	Mitochondrial ribosomal s22	gi|14424546|	MRPS22	1 19	7 8	41 43
23	Annexin A1	gi|442631|	ANXA1	1 43	7 9	35 25

Table 3 6 3a Identified proteins form SKMES-1 versus SKMES-Txt Gene symbol determined from "gi number" conversion software package "DAVID" and Entrez Gene

Spot No	Protein Name	gi Number	Gene Symbol	Fold	pI	M w
24	LASP 1	gi|2135552|	Lasp-1	1 61	6 1	30 19
25	Annexin A3	gi|47115233|	ANXA3	1 48	5 6	36 63
26	HSPC124	gi|6841470|	PPA2	1 77	5 6	36 96
27	Proteasome activator subunit 2	gi|48734793|	PSME2	1 62	5 4	27 51
28	Chain H Cathepsin D at pH 7 5	gi|5822091|	CTSD	1 98	5 3	26 46
29	Proteasome (prosome, macropain) subunit, alpha type 5	gi|54696300|	PSMA5	-1 26	4 7	26 58
30	Proteasome (prosome, macropain) subunit, alpha type 5	gi|54696300|	PSMA5	1 27	4 7	26 58
31	Prohibitin	gi|76879893|	PPA1	1 43	5 6	29 87
32	Chloride intracellular channel 4	gi|55666469|	CLIC4	1 74	5 5	28 98
33	High mobility Group box 1	gi|55958717|	HMGB1	1 46	5 6	25 1
34	Chain B, Horf 6 a novel human peroxidase enzyme	gi|3318842|	-	1 36	6	24 9
35	Ubiquitin Carboxy Hydrolase L1	gi|4185720|	PGP9 5	1 27	5 3	23 35
36	K130r mutant of human DJ-1	gi|33358056|	PARK7	1 23	6 5	21 14
37	Peroxiredoxin 2	gi|32483377|	PRDX2	1 72	7 1	27 95
38	GST-pi	gi|4139460|	GSTP1	-1 68	5 4	23 43
39	GST-pi chain B	gi|23200511|	GSTP1	-1 37	5 4	23 43
40	Galectin-1	gi|42542977|	Galectin-1	-1 55	5 3	14 75

Table 3 6 3b Identified proteins form SKMES-1 versus SKMES-Txt-continued

3.6.4 Ontology analysis of identified proteins

Ontology information was obtained through PubMed searches. Of the identified proteins, the majority have functions in protein turnover, stress response and cytoskeletal proteins with 21%, 15% and 12% of the differentially regulated proteins respectively. The stress response and protein turnover proteins were expected to be differentially regulated, as they are known to increase resistance to cell death induced by a variety of stimuli. The majority of these proteins are all up-regulated in SKMES-Txt. There are twice as many transcription/transcription regulation and metabolic proteins differentially regulated in contrast to cell signalling proteins in SKMES-Txt. The ion binding/transport, apoptosis/apoptosis regulation and RNA processing proteins account for 7% each. The apoptosis/redox regulation proteins have also been linked to overcoming drug-resistance through evading apoptosis, the majority of which are up-regulated in SKMES-Txt. Finally, 2% of the proteins are involved in glycolysis, cytokinesis and mitochondrial processing (Table 3.6.4, Figure 3.6.4).

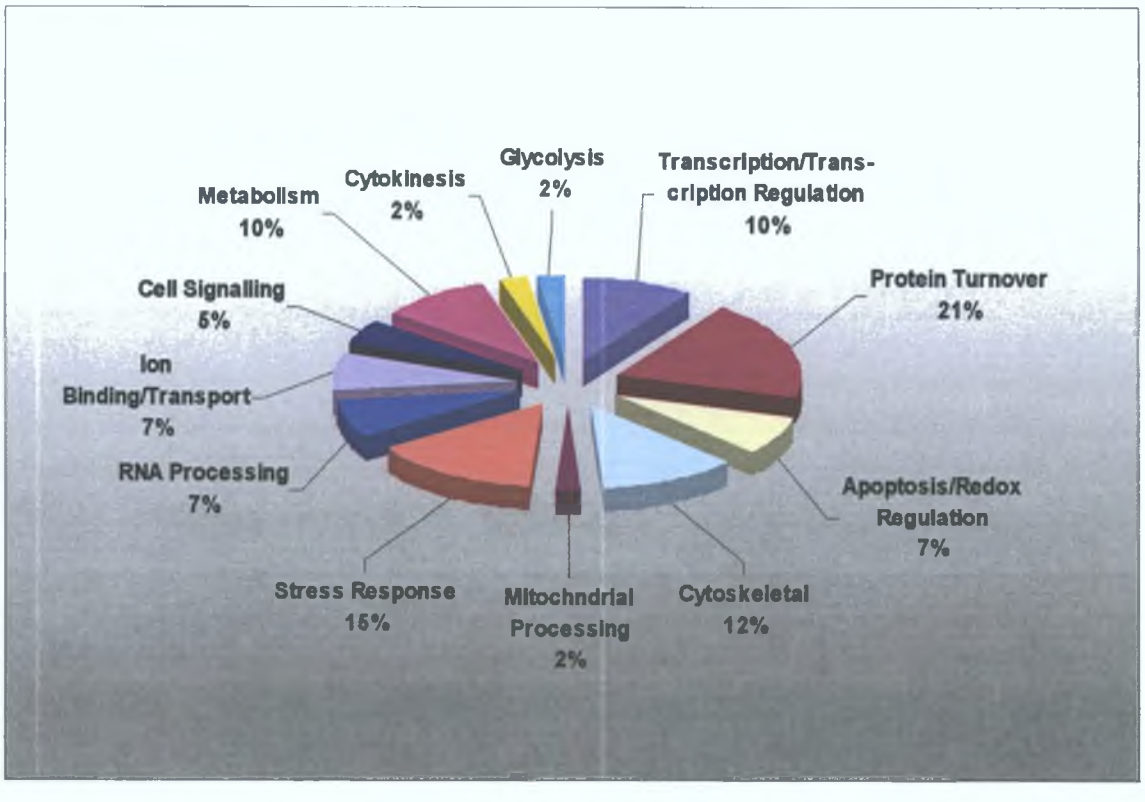

Figure 3.6.4 Ontology analysis of differentially regulated proteins.

Reported Function	Protein Name
Apoptosis/Redox regulation	Galectin-1 Cham B, Horf 6 a novel human peroxidase enzyme K130r mutant of human DJ-1
Glycolysis	Peroxiredoxin
Transcription/Transcription Regulation	Prohibitin TATA binding protein High mobility Group box Dihydropyrimidinase-like variant 2
Stress Response	HSP 60 kDa HSP 70 kDa protein 8 isoform 2 HSPC124 150kDa oxygen-regulated protein Chaperonin containing TCP1 subunit 3
Ion Binding/Transport	Annexin A1 Chloride intracellular channel 4 Annexin A3
Cytoskeletal	Vimentin Beta Tubulin Lamin A/C LASP 1 Keratin 8
Protein Turnover	Proteasome activator subunit 2 Chain H Cathepsin D at pH 7 5 Proteasome (prosome, macropain) subunit, alpha type 5 GST-pi chain B Proteasome beta 3 subunit GST-pi Ubiquitin Carboxy Hydrolase L1
Cell Signalling	VCP protein
RNA Processing	hnRPH1 Mannose-6-phosphate receptor binding protein hnRPC
Metabolism	Glucose 6 phosphate dehydrogenase Mitochondrial ribosomal s22
Cytokinesis	Septin 2
Mitochondrial Processing	PMPCA protein

Table 3 6 4 Ontology analysis of identified proteins from SKMES-1 versus SKMES-Txt

3 6 5 PathwayAssist analysis of identified proteins

PathwayAssist (version 3 0), which permits the identification of biological interactions among genes and proteins of interest from the published literature, was carried out on the 40 identified proteins The gene symbol list was imported into the programme and from this both direct and common pathways were built Figure 3 6 5 shows only the direct lines between differentially regulated proteins They are cytoskeletal, metabolic, cell signalling and stress response proteins The cytoskeletal and cell signalling proteins are all down-regulated whereas the stress response and metabolic proteins are up-regulated It has been shown that there is a specific interaction of the periplakin linker domain with keratin 8 and vimentin Glucose-6-phosphate dehydrogenase complexes with HSPD1 HSPA8 has a direct effect on the regulation of HSPD1 Finally, VCP has been shown to interact with HSPA8 in yeast

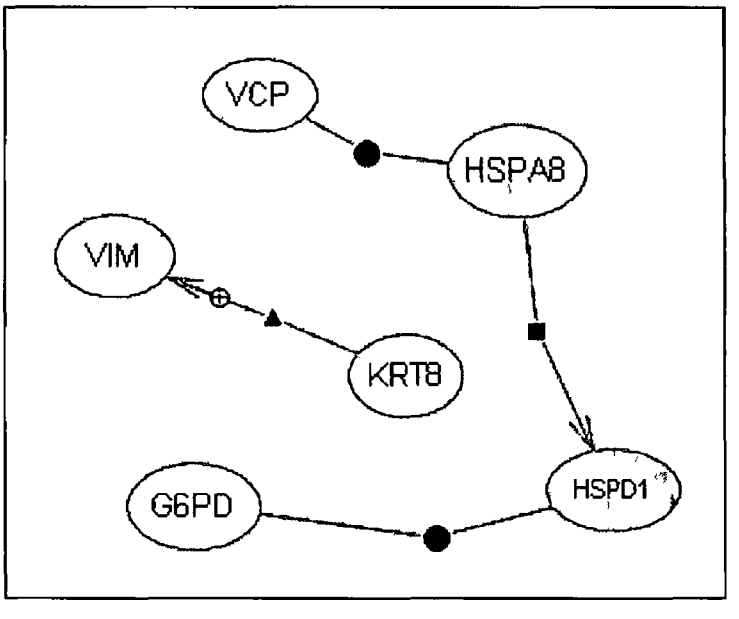

Figure 3 6 5 PathwayAssist analysis of direct interactions, identifying only direct links between the proteins This finds proteins that are regulated by all selected nodes Purple circles indicate binding, blue triangles indicate regulation and orange squares indicate an effect and direct effect on expression respectively

Figure 3.6.6 shows the pathways built based on common targets for selected nodes (i.e. differentially regulated proteins). Pathway analysis found that cellular processes of apoptosis, differentiation and proliferation and the proteins HSPD1 and G6PD are important in the taxotere resistant cell line, SKMES-Txt.

Stimulators of proliferation include HYOU, CRMP1, HSPA8, VCP, G6PD and HSPD1. All of these are up-regulated except VCP in SKMES-Txt versus SKMES-1. The two inhibitors of proliferation include TUBB and ANAX1 are both up-regulated. Stimulators of differentiation include TUBB, ANAX1, VIM and G6PD are up-regulated except VIM. There are no inhibitors of differentiation. The stimulators of apoptosis include VIM, G6PD, KRT8, CRMP1 and ANAX1. HSPA8 inhibits apoptosis. The majority of these proteins are up-regulated in SKMES-Txt.

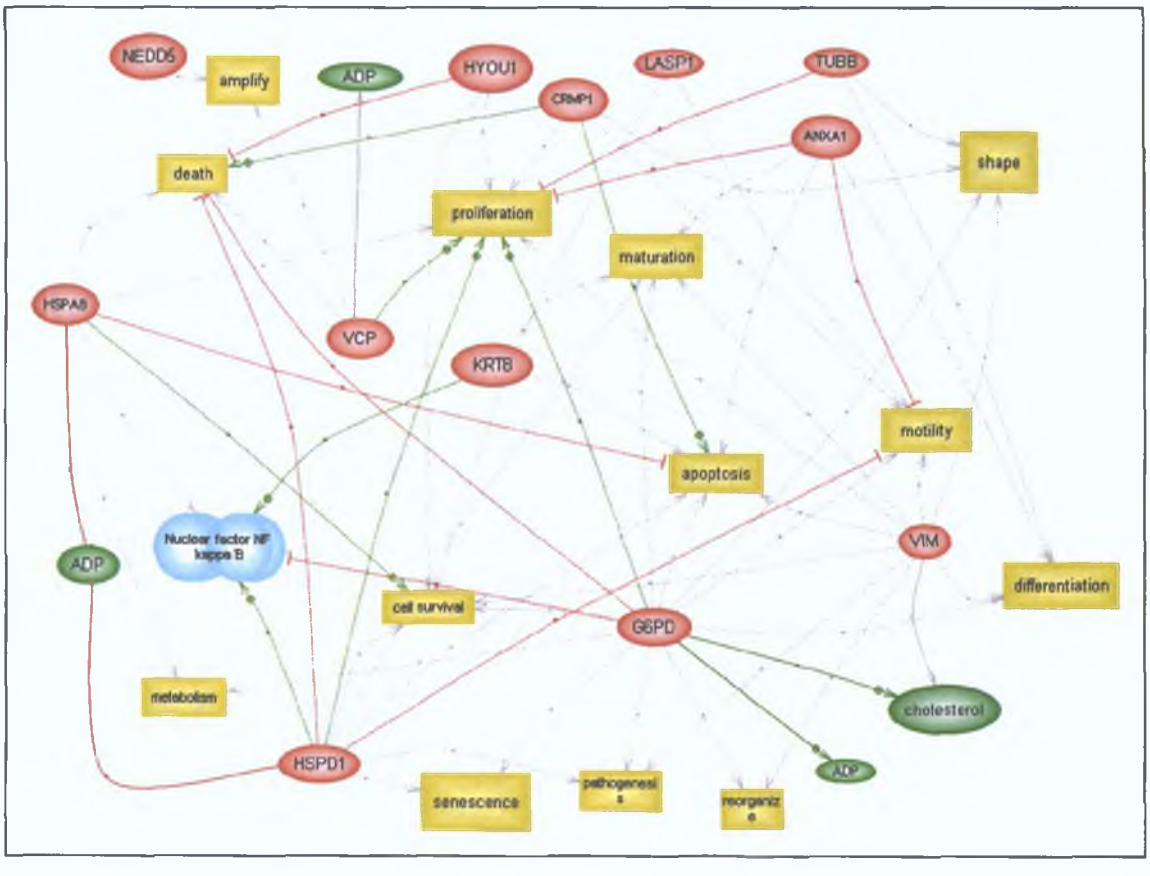

Figure 3.6.6 PathwayAssist analysis of common interactions between proteins. Selected protein nodes are shown in red with the cellular processes in yellow, small molecules in green and complexes in blue. Green, red and gray lines mark positive, negative and unknown regulatory effects respectively.

3.6.6 Experimental outline of SKMES-1 versus SKMES-Txl (Wk 3)

This experiment was designed to compare SKMES-1 to its taxol-resistant variant SKMES-Txl when resistance was the highest (12.5-fold). The aim was to determine the protein expression changes resulting from taxol resistance. The experimental design for DIGE analysis of SKMES compared to SKMES-Txl is identical to that of SKMES-1 versus SKMES-Txt as outlined in Table 3.6.3 with SKMES-1 as the control and 6 biological replicates.

3.6.6.1 DeCyder analysis of SKMES-1 versus SKMES-Txl (Wk 3)

Differential protein expression between the lung cell line SKMES-1 and SKMES-Txl(Wk3) was observed using 2D-DIGE. Difference In-gel Analysis using Decyder™ revealed a total of 1636 ± 102 protein spots. Biological variation analysis of these spots revealed a total of 193 spots showing a greater than 1.2-fold change in expression with a t-test score of 0.05 or less (Figure 3.6.7). Of these 193 spots, 55 have been identified using MALDI-TOF mass spectrometry. A total of 138 of the differentially-regulated spots were not identified (Figure 3.6.8).

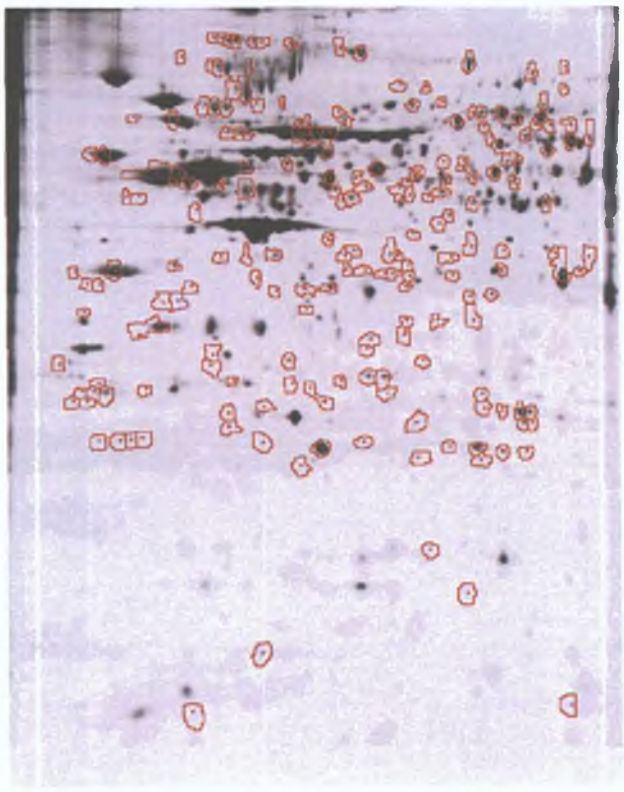

Figure 3.6.7 A representative Cy5 labelled SKMES-Txl (Wk 3) gel showing completed BVA analysis of SKMES-1 versus SKMES-Txl (Wk 3) between pH 4-7. Spots circled in red are the 193 statistically significant differentially regulated proteins ($p \leq 0.05$, protein fold ≥ 1.2).

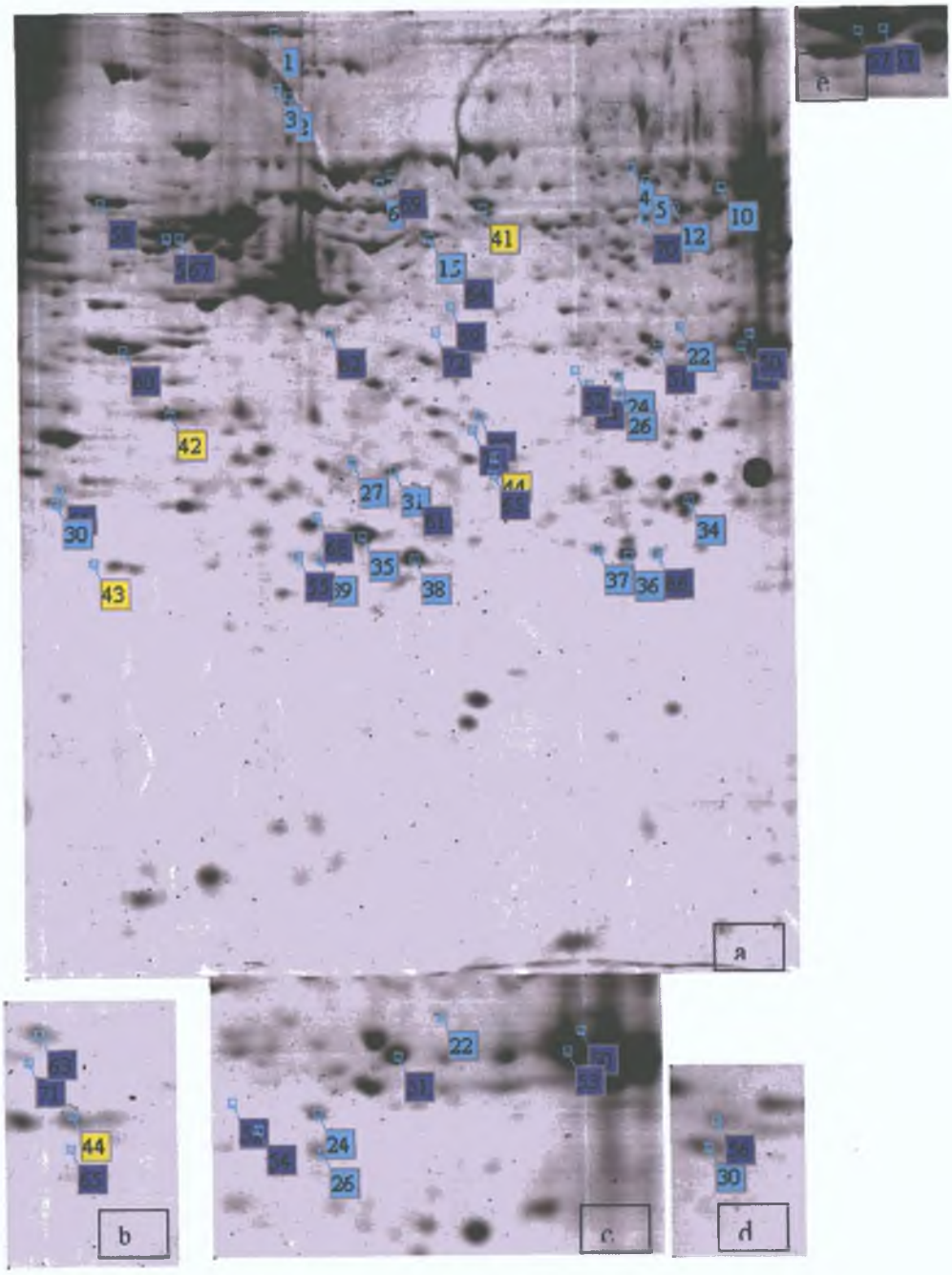

Figure 3.6.8a-e Colloidal coomassie stained preparative SKMES-Txt gel, which marks the proteins in common with SKMES-Txl – light blue spots. Yellow spots indicate the overlapping proteins from SKMES-Txl (Wk3) versus SKMES –Txl (Wk6). Dark blue spots are unique to SKMES-Txl (Wk3).

3 6 6 2 Table 3 6 5 highlights the overlapping proteins from SKMES-1 versus SKMES-Txl (wk3) and SKMES-1 versus SKMES-Txt Spots marked light blue in Figure 3 6 8

Spot No	Protein Name	gi Number	Gene Symbol	Fold	pI	M w
1	150kDa oxygen-regulated protein	gi|10720185|	ORP150	1 94	5 2	111 6
2	Valosin containing Protein	gi|55662798|	VCP	-1 31	4 9	71 56
3	Valosin containing Protein	gi|55662798|	VCP	-1 4	4 9	71 56
4	Lamin A/C	gi|55957496|	LMNA	1 71	6 1	53 23
5	Chaperomn containing TCP1 subunit 3	gi|58761484|	CCT3	1 41	6	57 78
6	HSP 70 protein 8 isoform 2	gi|62896815|	HSPA8	-1 55	5 6	53 6
10	Glucose 6 phosphate dehydrogenase	gi|26224874	G6PD1	1 23	6 3	59 53
12	Glucose 6 phosphate dehydrogenase	gi|26224872|	G6PD1	1 43	6 3	59 53
15	Keratin 8	gi|62913980|	CARD2	-1 57	5 6	55 89
22	HNRPC protein	gi|58476967|	HNRPC	1 4	4 5	27 86
24	LASP 1	gi|2135552|	Lasp-1	1 58	6 1	30 19
26	HSPC124	gi|6841470|	PPA2	1 58	5 6	36 96
27	Proteasome activator subunit 2	gi|48734793|	PSME2	-1 43	5 4	27 51
30	Proteasome (prosome, macropain) subunit, alpha type 5	gi|54696300|	PSMA5	1 21	4 7	26 58
31	Prohibitin	gi|76879893|	PPA1	1 44	5 6	29 87
34	Chain B, Horf 6 a novel human peroxidase enzyme	gi|3318842|	-	1 37	6	24 9
35	Ubiquitin Carboxy Hydrolase L1	gi|4185720|	PGP9 5	1 21	5 3	23 35
36	K130r mutant of human DJ-1	gi|33358056|	PARK7	1 29	6 5	21 14
37	Peroxiredoxin	gi|32483377|	PRDX2	1 19	7 1	27 95
38	GST-pi	gi|4139460|	GSTP1	-1 37	5 4	23 43
39	GST-pi chain B	gi|23200511|	GSTP1	-1 92	5 4	23 43

Table 3 6 5 Overlapping proteins form SKMES-1 versus SKMES-Txl (wk3) and SKMES-1 versus SKMES-Txt Spots marked light blue in Figure 3 6 8

Twenty-one proteins were found to be overlapping between SKMES-1 versus SKMES-Txt and SKMES-1 versus SKMES-Txl (Wk3). Similar levels of regulation resulted for the majority of the proteins with the exception of proteasome activator subunit 2 and peroxiredoxin 2, both of which are increased to a greater level in SKMES-Txt (Figure 3.6.9).

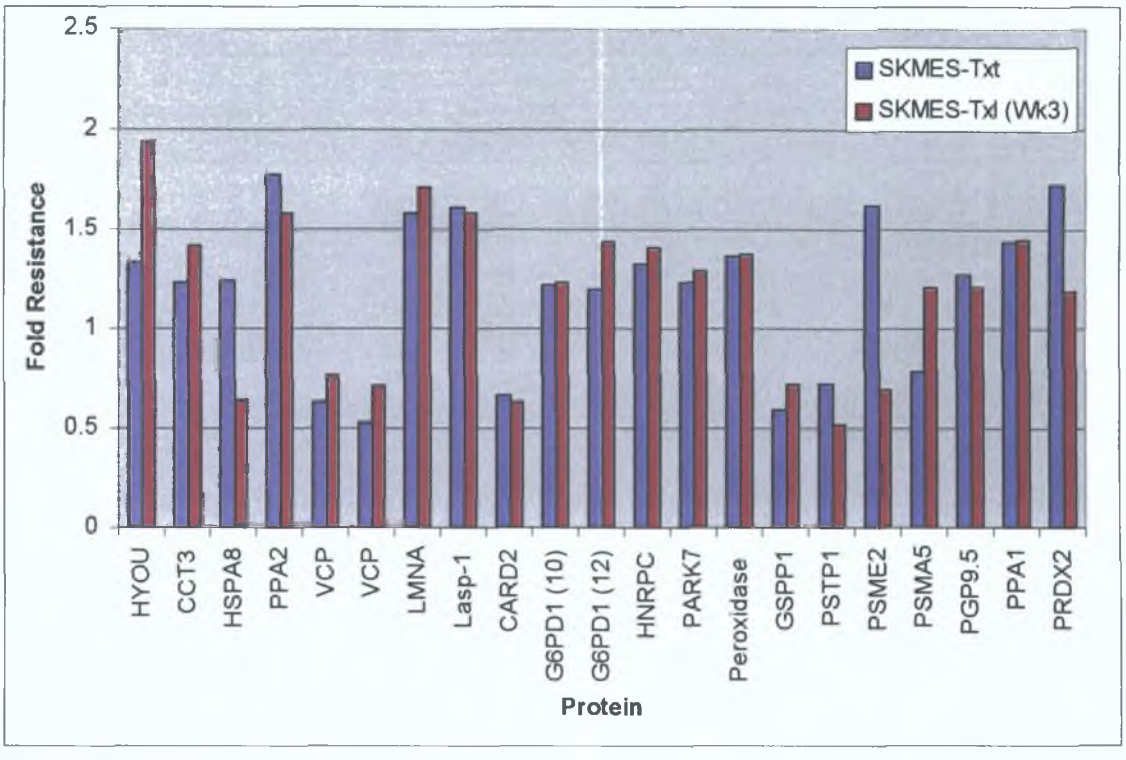

Figure 3.6.9 Review of shared proteins in SKMES-Txt and SKMES-Txl (Wk3)

Comparisons between SKMES-1 versus SKMES-Txl (Wk3) and SKMES-Txl (Wk3) versus SKMES-Txl (Wk6) revealed that 4 proteins were shared ER-60, thioredoxin peroxidase B and protein disulfide isomerase protein 5 are increased in SKMES-1 versus SKMES-Txl (wk3) (Table 3 6 6, Figure 3 6 8)

Spot No	Protein Name	gi Number	Gene Symbol	Fold	pI	M w
41	ER-60 protease	gi|1208427|	PDIA3	1 35	6	57 18
42	Annexin V	gi|809190|	ANXA5	1 56	4 9	35 84
43	Thioredoxin peroxidase B	gi|1617118|	PRDX2	2 02	4 8	20 16
44	Protein disulphide isomerase protein 5	gi|1710248|	p5	1 65	5	46 52

Table 3 6 6 The overlapping protein spots between the comparisons SKMES versus SKMES-Txl (wk3) with SKMES-Txl (wk3) versus SKMES-Txl (Wk6) Spots marked yellow in Figure 3 6 8

In contrast to the unique proteins differentially regulated in response to taxotere exposure, taxol exposure resulted in the differential expression of 23 unique proteins of which most were down-regulated The majority of these proteins have function in ion binding/transport, protein turnover and the stress response (Table 3 6 7)

Spot No.	Protein Name	gi Number	Gene Symbol	Fold	pI	M.w.
50	Annexin A1	gi|442631|	ANXA1	-1.26	7.9	35.25
51	Annexin A1	gi|442631|	ANXA1	-1.29	7.9	35.25
52	Annexin A1	gi|442631|	ANXA1	1.25	7.9	35.25
53	Annexin A1	gi|442631|	ANXA1	-1.31	7.9	35.25
54	26S Proteasome-associated Pad1 homologue variant	gi|62088020|	PSMD14	1.22	6.5	18.99
55	Chain D, Cathepsin B (E.C.3.4.22.1)	gi|999911|	CSTB	-1.77	5.2	22.97
56	Proteasome (prosome, macropain) subunit, alpha type 5	gi|54696300|	PSMA5	1.2	4.7	26.58
57	Beta tubulin	gi|18088719|	TUBB	-1.56	4.7	50.11
58	Prolyl 4-hydroxlyase, beta subunit	gi|48735337|	P4HB	1.26	4.8	57.5
59	Beta Actin	gi|15277503|	ACTB	-1.42	5.6	40.54
60	Nucleophosmin	gi|13536991|	NPM1	-1.15	4.5	29.62
61	HSP 27 kDa	gi|54696638|	HSPB1	-1.41	6	22.82
62	HSPC108	gi|7305503|	STOML2	1.31	5.8	37.3
63	Annexin A4	gi|1703319|	ANXA4	1.37	5.8	36.09
64	HLA-B associated transcript 1 variant	gi|62897383|	BAT1	1.26	5.5	49.56
65	6 phosphogluconolactonase	gi|6018458|	PGLS	1.22	2.7	27.81
66	ATP Synthase	gi|16741373|	ATP5B	1.61	6.6	20.15
67	ATPase beta subunit	gi|179279|	ATP5B	-1.33	5.0	50.52
68	Actin G1 protein	gi|40226101|	ACTG1	-1.26	5.5	26.68
69	HSP70 kDa 9B (MTHsp75)	gi|292059|	HSPA9B	-1.33	6	74.12
70	CCT2	gi|48146259|	CCT2	1.32	6	57.78
71	Replication A2 32, kDa	gi|56204165|	RPA2	1.22	6.4	30.25
72	eiF 3 subunit 2 beta 36 kDa	gi|47003155|	EIF3S2	-1.79	5.4	36.5

Table 3.6.7 Proteins unique to SKMES-1 versus SKMES-Txl(Wk2), Spots marked dark blue in Figure 3.6.8.

3.6.7 Ontology analysis of identified proteins

Ontology information was obtained through PubMed searches. Of the identified proteins, the majority have functions in protein turnover, cytoskeletal, the stress response and ion binding/transport and account for 21%, 17%, 15% and 13% respectively. The levels of stress response, metabolic and protein turnover proteins are similar to those obtained for SKMES-1 versus SKMES-Txt. The protein turnover proteins and ion binding/transport are both increased and decreased in SKMES-Txl (wk3). The majority of the stress response proteins are all up-regulated in SKMES-Txl (wk3) whereas the cytoskeletal proteins are predominantly decreased. Metabolic and apoptosis/redox regulation accounts for 10% and 6% respectively in SKMES-Txl (wk3). There are twice as many cell signalling, transcription/transcription regulation, and RNA processing proteins regulated in contrast to translation, tumour immunity and glycolysis proteins in SKMES-1 versus SKMES-Txl (wk3). There is a higher percentage of cytoskeletal and ion binding/transport proteins differentially regulated in SKMES-Txl (wk3) compared to SKMES-Txt. Taxotere exposure resulted in more than twice the amount of transcription/transcription regulation proteins being differentially regulated in comparison to taxol exposure. There are similar levels of cell signalling, glycolysis and apoptosis/redox regulation proteins in both cell lines whereas there are no cytokinesis or mitochondrial processing proteins differentially regulated in SKMES-1 versus SKMES-Txl (wk3) (Table 3.6.8, Figure 3.6.10).

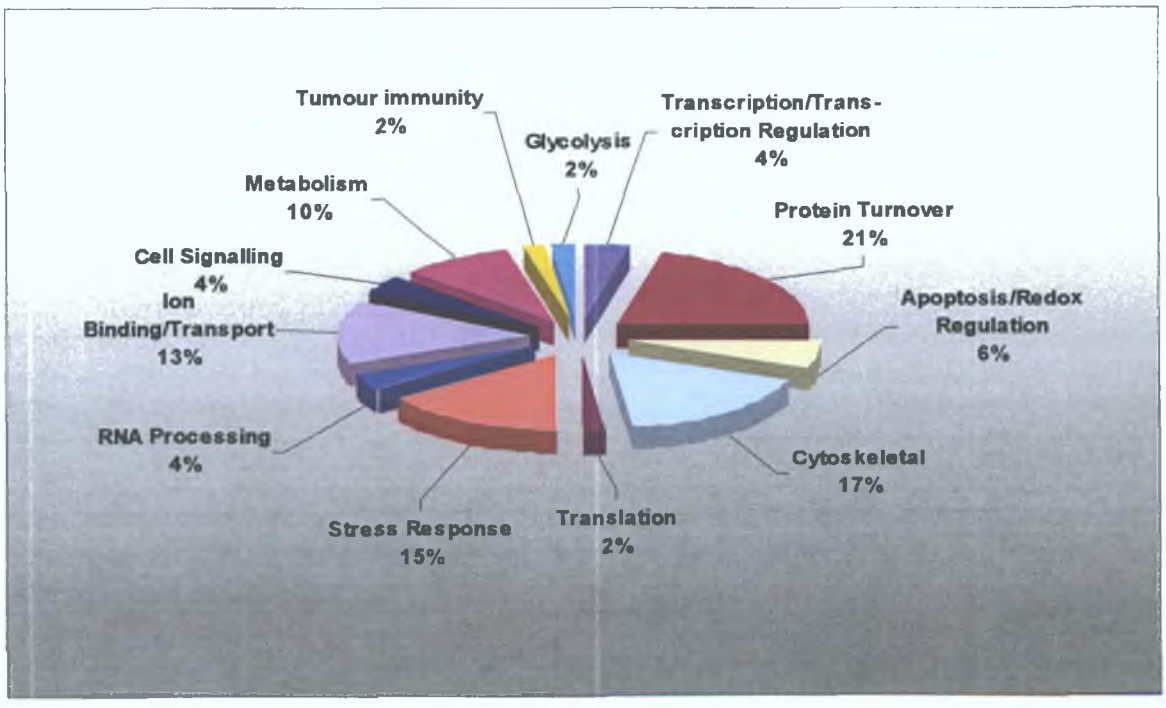

Figure 3.6.10 Ontology analysis of differentially regulated proteins

Reported Function	Protein Name
Apoptosis/Redox regulation	Thioredoxin peroxidase B K130r mutant of human DJ-1 Chain B, Horf 6 a novel human peroxidase enzyme
Glycolysis	Peroxiredoxin
Transcription/Transcription Regulation	Prohibitin Replication A2 32, kDa
Stress Response	HSP 27 kDa HSP 70 kDa protein 8 isoform 2 HSPC124 Chaperonin containing TCP1 subunit 3 HSP70 kDa 9B (MTHsp75) CCT2 HSPC108 150kDa oxygen-regulated protein
Ion Binding/Transport	Annexin A1 Annexin A4 Annexin V Nucleophosmin
Translation	eiF 3 subunit 2 beta 36 kDa
Cytoskeletal	Beta Actin Gamma Actin Beta Tubulin Lamin A/C LASP 1 Keratin 8
Protein Turnover	Proteasome activator subunit 2 Chain D, Cathepsin B (E C 3 4 22 1) Proteasome (prosome, macropain) subunit, alpha type 5 GST-pi chain B GST-pi Prolyl 4-hydrolase, beta subunit Protein disulphide isomerase protem 5 Ubiquitin Carboyxy Terminal hydrolase L1 26S Proteasome-associated Pad1 homologue variant
Cell Signalling	VCP protem
RNA Processing	HnRPC ER-60 protease
Metabolism	ATPase beta subunit ATP Synthase 6 phosphogluconolactonase Glucose 6 phosphate dehydrogenase
Tumour Immunity	HLA-B associated transcript 1

Table 3 6 8 Ontology analysis of identified proteins from SKMES versus SKMES-Txl (wk3)

3 6 8 PathwayAssist analysis of identified proteins

The gene symbol list was imported into the programme and from this both direct and common pathways were built Figure 3 6 11 shows only the direct lines between differentially regulated proteins between SKMES-1 versus SKMES-Txl (Wk3) The proteins with direct interactions include, cytoskeletal, ion binding, metabolic, protein turnover, transcription/transcription regulation and stress response proteins These proteins are both up- and down-regulated in SKMES-Txl Both α- and β-tubulin associate with HSPB1, which also associates with GSTP1 Annexin 5 promotes a dose-dependent inhibition of annexin 1 phosphorylation GRP58 binds to P4HB, the resultant complex inhibits further interactions VCP possesses chaperone-like activities and can functionally interact with HSPA8 Finally HSPA8 also binds with HSPB1

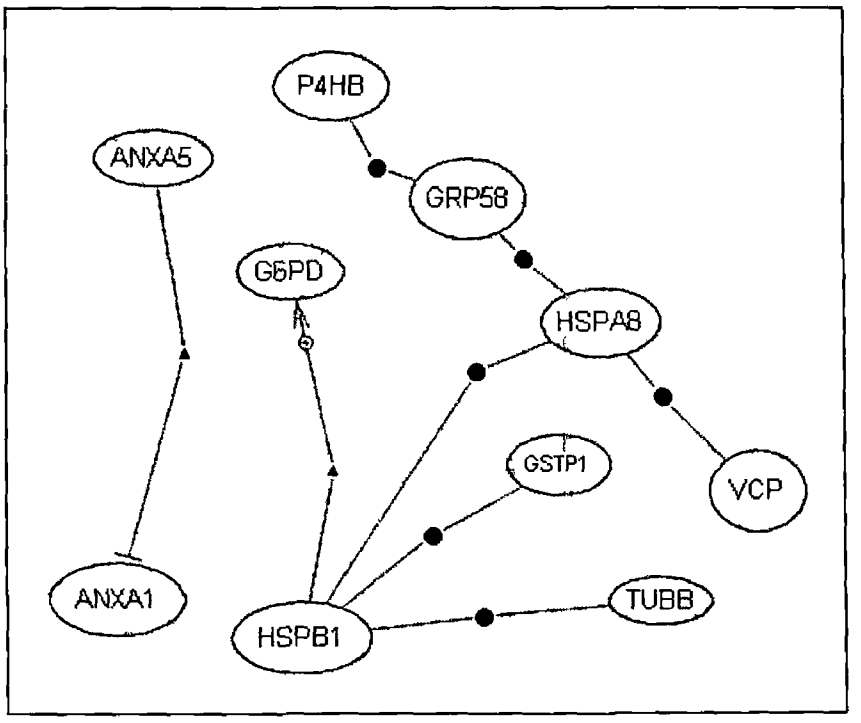

Figure 3 6 11 PathwayAssist analysis of direct interactions, identifying only direct links between the proteins This finds proteins that are regulated by all selected nodes Purple circles indicate binding, blue triangles indicate regulation of expression

Figure 3.6.12 shows the pathways built based on common targets for selected nodes (i.e. differentially regulated proteins). Pathway analysis found that cellular processes of apoptosis, differentiation and proliferation and the proteins HSPD1 and G6PD are also important in the taxol resistant cell line, SKMES-Txl (wk3). Stimulators of proliferation include GSTP1, ANAX5, BATL1, HSPB1, HSPA8, G6PD, HSPA9B, HYOU, UCHL1, PRDX2, GRP58, VCP, PRDX3 and PARK7. The three inhibitors of proliferation include NPM1, TUBB and ANAX1 the majority of these are down-regulated in SKMES-Txl whereas in SKMES-Txt both TUBB and ANAX1 are up-regulated. The stimulators of differentiation include NPM1, HSPB1, G6PD, ANAX1, ANAX5, PRDX2, GSTP1 and TUBB. Similarly to SKMES-Txt, there are no inhibitors of differentiation. The majority of these are decreased in SKMES-Txl (Wk3).

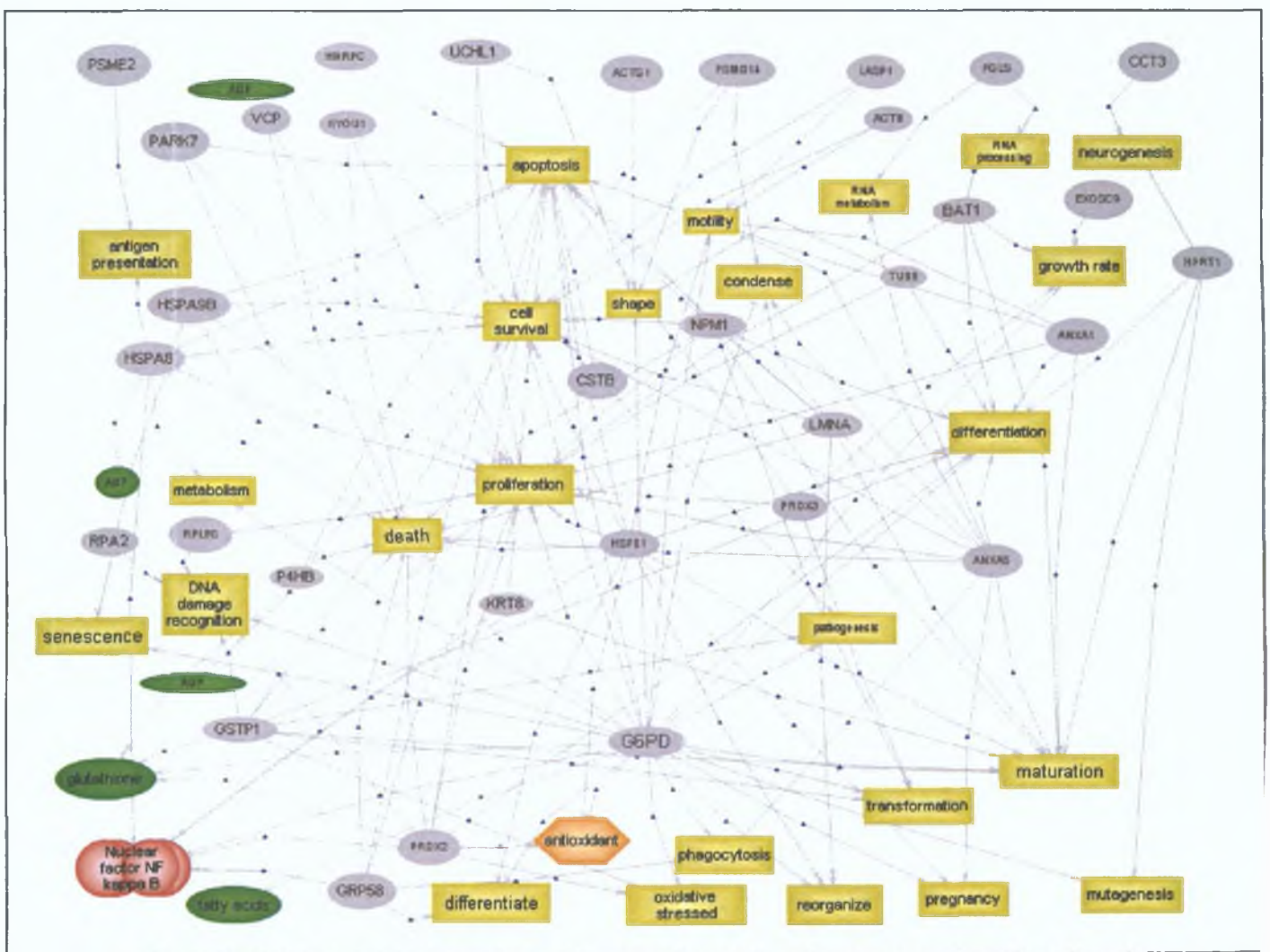

Figure 3.6.12 PathwayAssist analysis of common interactions between proteins. The selected protein nodes are shown in grey, the cellular processes in yellow, a complex in red, a small molecule in green and functional classes in orange. Grey lines indicate a negative and positive regulatory effect.

3.6.9 Experimental outline of SKMES-Txl (Wk3) versus SKMES-Txl (Wk 6)

This experiment was designed to compare SKMES-Txl (Wk3) to a less resistant variant, SKMES-Txl (Wk6) in order to examine the protein expression changes resulting from a loss of taxol resistance. SKMES-Txl (Wk3) was 12.5-fold resistant to taxol compared to SKMES-1 while SKMES-Txl (Wk6) was only 5.8-fold resistant. The experimental design for DIGE analysis of SKMES-Txl (Wk3) versus SKMES-Txl (Wk 6) is identical to that of SKMES-1 versus SKMES-Txt as outlined in Table 3.6.3 with SKMES-Txl (Wk3) as the control and 5 biological replicates.

3.6.9.1 DeCyder analysis of SKMES-Txl (Wk3) versus SKMES-Txl (Wk 6)

Differential protein expression between the lung cell line SKMES-Txl (Wk3) and SKMES-Txl (Wk6) was observed using 2D-DIGE. Difference In-gel Analysis using Decyder™ revealed a total of 1553 ± 213 protein spots. Biological variation analysis of these spots revealed a total of 159 spots showing a greater than 1.2-fold change in expression with a t-test score of 0.05 or less (Figure 3.6.13). Of these 159 spots, 28 have been identified using MALDI-TOF mass spectrometry (Figure 3.6.14).

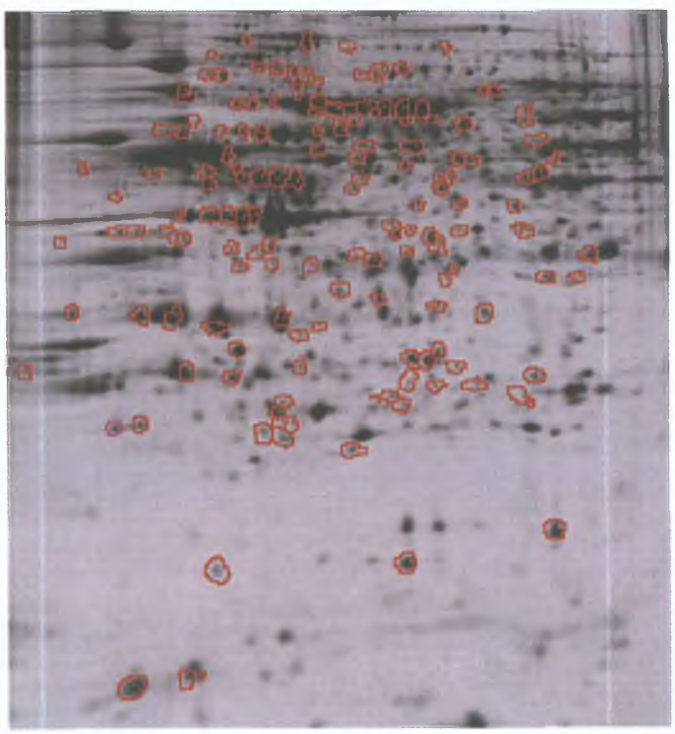

Figure 3.6.13 A representative Cy5 labelled SKMES-Txl (Wk6) gel showing completed BVA analysis of SKMES-Txl (Wk3) versus SKMES-Txl (Wk 6) between pH 4-7. Spots circled in red are the 159 statistically significant differentially regulated proteins ($p \leq 0.05$, protein fold ≥ 1.2).

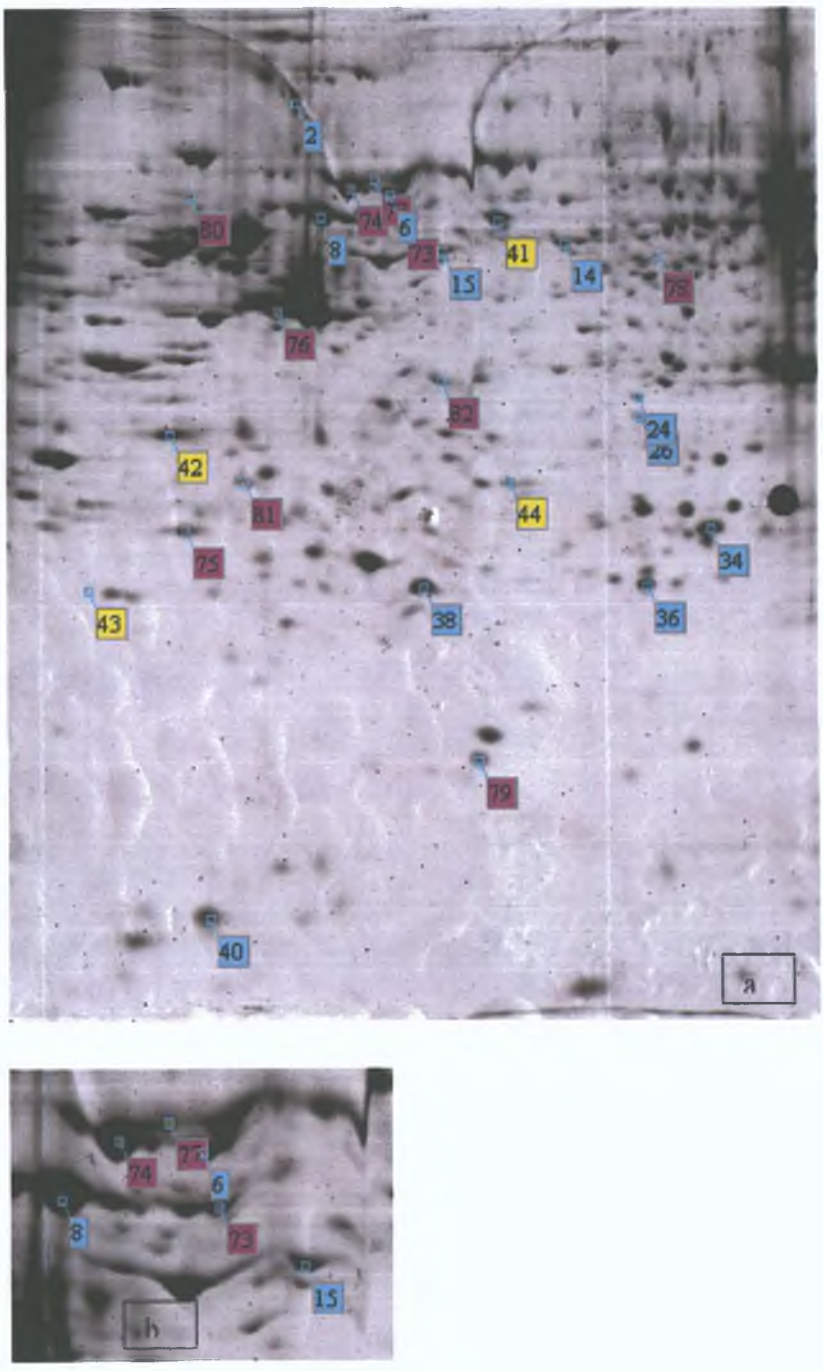

Figure 3.6.14a-b Colloidal coomassie stained preparative SKMES-Txt gel, which marks the proteins in common with SKMES-Txt – blue spots. Yellow spots indicate the overlapping proteins from SKMES-1 versus SKMES-Txl (Wk3). Purple proteins are unique to SKMES-Txl (Wk6).

Table 3 6 9 shows the 11 differentially expressed proteins that are shared between the comparisons SKMES-1 versus SKMES-Txt and SKMES-1 versus SKMES-Txl (Wk3) The majority of these proteins are up-regulated in SKMES-1 versus SKMES-Txt but decreased in this comparison The exceptions include, GST-pi which is decreased in SKMES-1 versus SKMES-Txt and peroxiredoxin 2 which is increased in SKMES-1 versus SKMES-Txt but decreased in this comparison

Spot No	Protein Name	gi Number	Gene Symbol	Fold	pI	M W
2	Valosin containing Protein	gi|55662798|	VCP	-1 31	4 9	71 56
8	HSP 60 kDa	gi|77702086|	HSPD1	1 6	5 7	61 37
6	HSP 70 protein 8 isoform 2	gi|62896815|	HSPA8	1 30	5 6	53 6
14	hnRPH1	gi|48145673|	HNRPH1	-1 24	5 9	49 5
19	Beta tubulin	gi|18088719|	TUBB	-1 94	4 7	50 11
24	LASP 1	gi|2135552|	Lasp-1	-1 49	6 1	30 19
25	Annexin A3	gi|47115233|	ANXA3	-1 39	5 6	36 63
33	High mobility Group box 1	gi|55958717|	HMGB1	1 2	5 6	25 1
37	Peroxiredoxin 2	gi|32483377|	PRDX2	-1 25	7 1	27 95
38	GST-pi	gi|23200511|	GSTP1	2 29	5 4	23 43
40	Galectin-1	gi|42542977|	Galectin-1	-1 32	5 3	14 75

Table 3 6 9 Overlapping proteins between SKMES-Txl (Wk3) versus SKMES-Txl (Wk6) and SKMES-1 versus SKMES-Txt

Comparisons between SKMES-1 versus SKMES-Txl (Wk3) and SKMES-Txl (Wk3) versus SKMES-Txl (Wk6) revealed that 4 proteins were shared. ER-60, thioredoxin peroxidase B and protein disulfide isomerase protein 5 show a decrease in protein expression as resistance falls. This reflects a positive correlation with a fall of drug resistance (Figure 3.6.15, Table 3.6.10).

Spot No.	Protein Name	gi Number	Gene Symbol	Fold	pI	M.W.
41	ER-60 protease	gi|1208427|	PDIA3	-1.55	6	57.18
42	Annexin V	gi|809190|	ANXA5	2.10	4.9	35.84
43	Thioredoxin peroxidase B	gi|1617118|	PRDX2	-1.33	4.8	20.16
44	Protein disulphide isomerase protein 5	gi|1710248|	p5	-1.48	5	46.52

Table 3.6.10 The 4 overlapping protein spots between the comparisons SKMES-1 vs. SKMES-Txl (wk3) and SKMES-Txl (wk3) vs SKMES-Txl (Wk6) (Spots marked yellow in Figure 3.6.8).

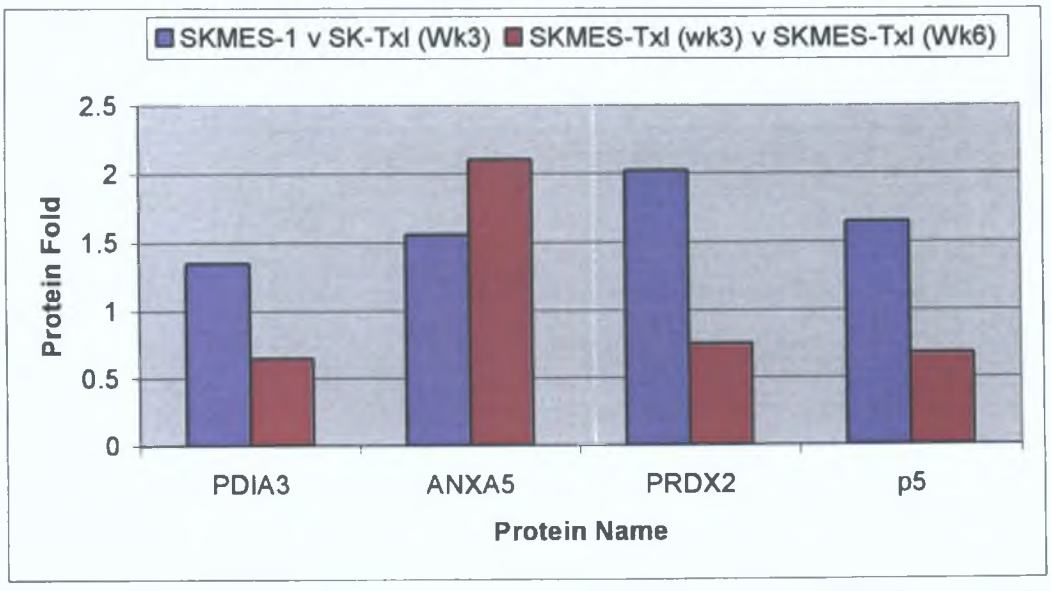

Figure 3.6.15 Review of shared proteins in SKMES-1 versus SKMES-Txl (Wk2) and SKMES-Txl (Wk3) versus SKMES-Txl (Wk6)

Ten proteins were found to be unique to SKMES-Txl (Wk6) The majority of these proteins are cytoskeletal and stress response proteins (Table 3 6 11)

Spot No	Protein Name	gi Number	Gene Symbol	Fold	pI	M w
73	KIAA0098	gi|58257644|	CCT5	-1 31	5 5	61 49
74	HSP 70 protein 8 isoform 2	gi|62896815|	HSPA8	-1 29	5 6	53 6
75	HSP 70 protein 8 isoform 2	gi|62896815|	HSPA8	-1 3	5 6	53 6
76	Beta Actin	gi|15277503|	ACTB	2 38	5 6	40 54
77	Lamin B1	gi|576840|	LMNB1	1 7	5 3	67 79
78	Rab dissociation inhibitor beta	gi|4960030|	GDI2	1 69	5 9	41
79	Stathmin	gi|57870|	STMN1	-1 24	6	17 15
80	hnRPK	gi|55958547|	HNRPK	-1 33	5 4	42 02
81	Chloride intracellular channel 1	gi|62898319|	CLIC1	-1 21	5 1	27 34
82	RPLPO	gi|47123412|	RPLPO	1 39	8 6	27 45

Table 3 6 11 Proteins unique to SKMES-Txl (Wk3) versus SKMES-Txl (Wk6), Spots marked purple in Figure 3 6 14

3.6.10 Ontology analysis of identified proteins

Ontology information was obtained through PubMed searches. Of the identified proteins, the majority have functions in the stress response, cytoskeletal, RNA processing and ion binding/transport and account for 18%, 18%, 12% and 12% respectively. There are twice as many cell signalling, apoptosis/redox regulation and proteins turnover differentially regulated proteins compared to transcription/transcription regulation, glycolysis and translation proteins. The levels of stress response, apoptosis/redox regulation, cytoskeletal, ion binding/transport and transcription proteins are similar to those obtained for SKMES-1 versus SKMES-Txl (wk3). There are twice as many cell signalling, glycolysis, translation and three times as many RNA processing proteins differentially regulated in SKMES-Txl (wk3) versus SKMES-Txl (wk6) compared to SKMES-1 versus SKMES-Txl (wk3). In contrast there are more proteins turnover proteins differentially regulated in SKMES-1 versus SKMES-Txl (wk3). There are no metabolic or tumour immunity proteins regulated in SKMES-Txl (wk3) versus SKMES-Txl (wk6) (Table 3.6.12, Figure 3.6.16).

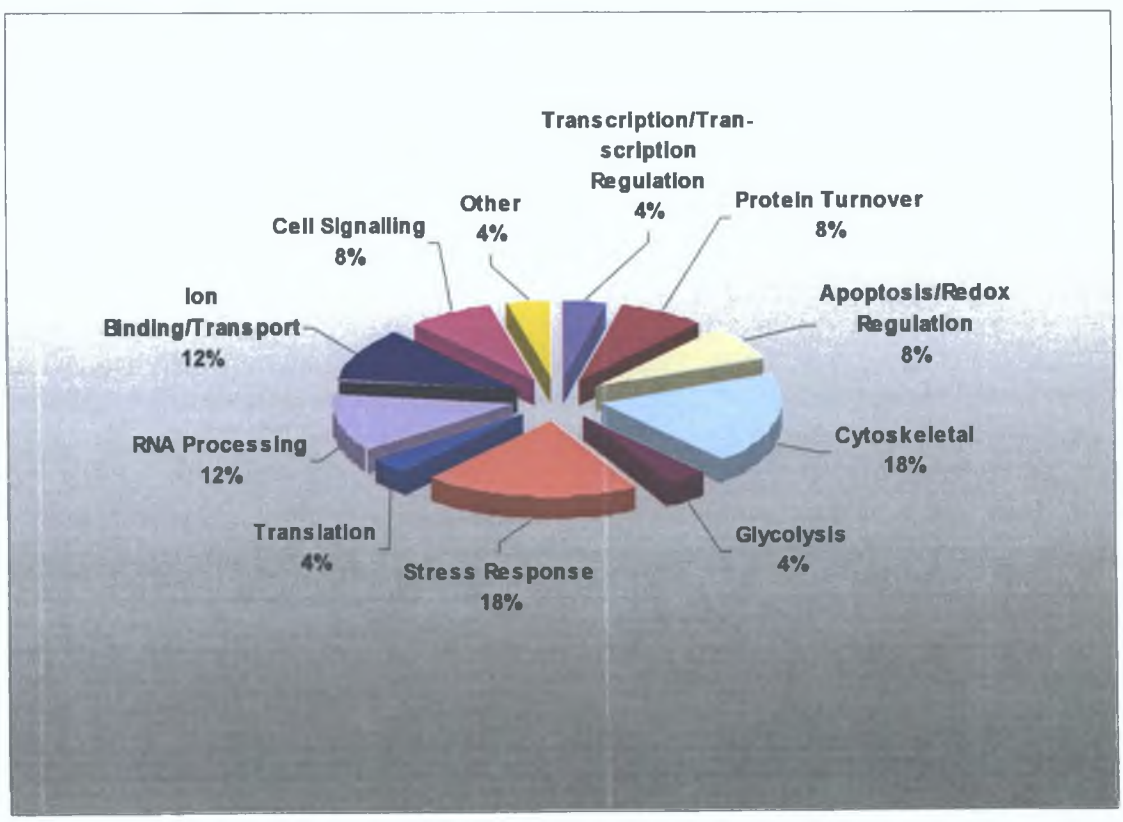

Figure 3.6.16 Ontology analysis of differentially regulated proteins

Reported Function	Protein Name
Apoptosis/Redox regulation	Thioredoxin peroxidase B Galectin-1
Glycolysis	Peroxiredoxin
Transcription/Transcription Regulation	High mobility Group box 1
Stress Response	HSP 70 kDa protein 8 isoform 2 HSP60 kDa KIAA0098
Ion Binding/Transport	Chloride intracellular channel 1 Annexin V Annexin A3
Translation	RPLPO
Cytoskeletal/cytoskeletal regulation	Beta Actin Alpha tubulin 6 variant Beta Tubulin Lamin B1 LASP 1 Stathmin
Protein Turnover	GST-pi chain B Protein disulphide isomerase protein 5
Cell Signalling	VCP protein Rab dissociation inhibitor beta
RNA Processing	hnRPK ER-60 protease HnRPH1

Table 3 6 12 Ontology analysis of identified proteins from SKMES-Txl (Wk3) versus SKMES-Txl (Wk6)

3 6 11 PathwayAssist analysis of identified proteins

The gene symbol list was imported into the programme and from this both direct and common pathways were built Figure 3 6 17 shows only the direct links between differentially regulated proteins High mobility group box protein interacts with HSPA8 and GRP58 and forms a complex HMGB1 also binds to hnRNP K VCP which possesses chaperone-like activities functionally interacts with HSPA8 Stathmin binds with HSPA8 This is most likely biologically relevant in their control of numerous intracellular signalling and regulatory pathways, and normal cell growth and differentiation Stathmin is also an important regulatory protein thought to control the dynamics of microtubules through the cell cycle in a phosphorylation-dependent manner Stathmin interacts with two molecules of dimeric alpha- beta-tubulin to form a tight ternary T2S complex

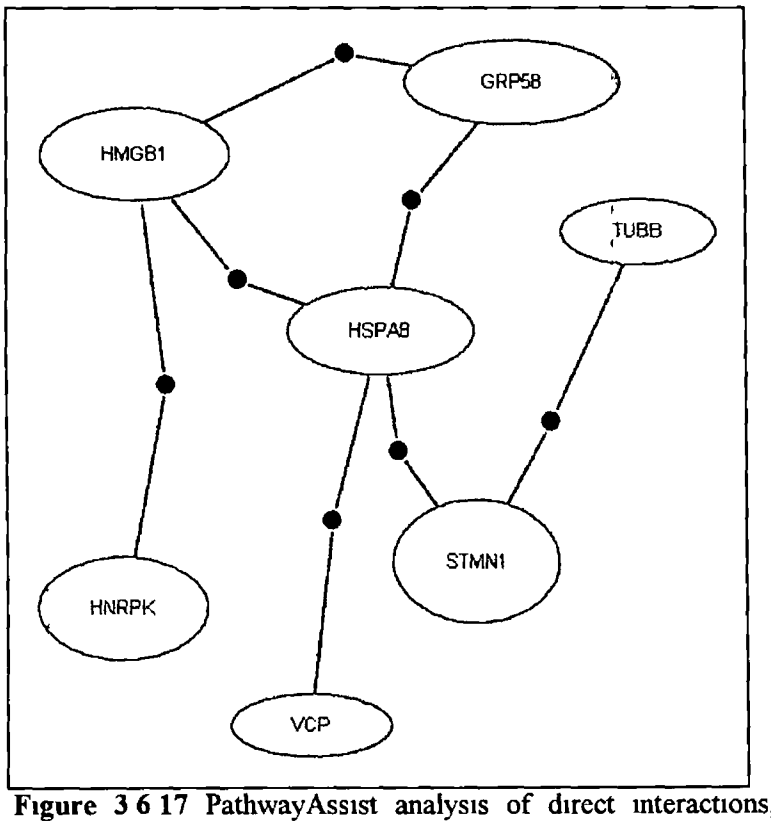

Figure 3 6 17 PathwayAssist analysis of direct interactions, identifying only direct links between the proteins This finds proteins that are regulated by all selected nodes Purple circles indicate binding

Figure 3.6.18 shows the pathways built based on common targets for selected nodes (i.e. differentially regulated proteins). Pathway analysis found that cellular processes of apoptosis, differentiation and proliferation and the proteins GSTP1, HMGB1, STMN1, HSPD1 and GRP58 are important in the loss of taxol resistance. Important cellular processes include apoptosis, proliferation and proliferation.

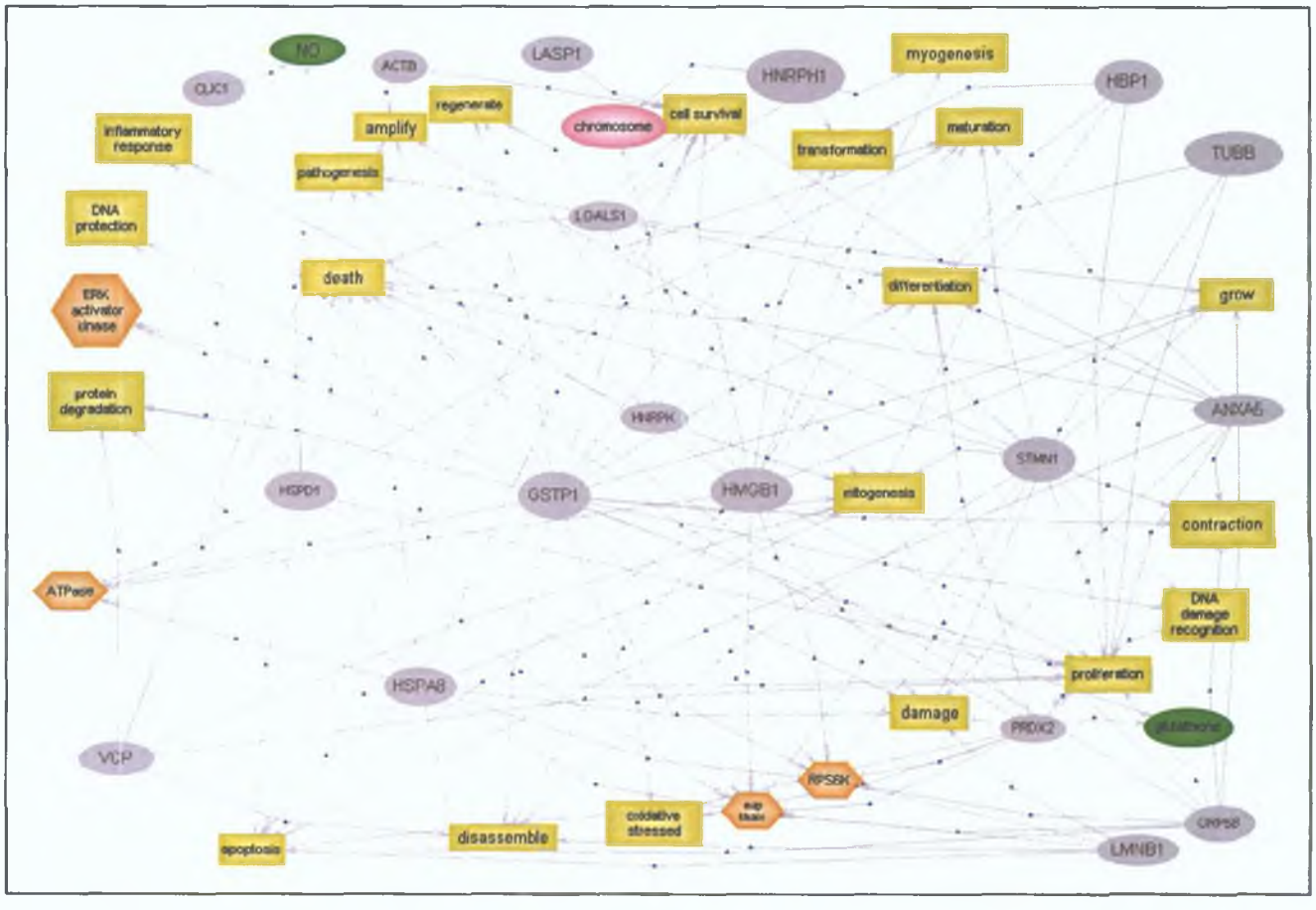

Figure 3.6.18 PathwayAssist analysis of common interactions between proteins. The selected protein nodes are shown in grey, the cellular processes in yellow, a small molecule in green, cell objects in pink and functional classes in orange. Grey lines indicate a negative and positive regulatory effect.

Section 4.0: Discussion

4 1 Development of MDR variants of squamous and small cell lung cancer cell lines

Lung cancer is the most prevalent and lethal of malignancies in the world (Akehurst *et al*, 2002) with deaths exceeding those from breast, colon and prostate combined (Danesi *et al*, 2003) Lung cancer can be categorised as non-small cell and small cell lung cancers which account for approximately 80% and 20% of lung cancer deaths respectively Chemotherapy and radiotherapy are important elements in the treatment of NSCLC with surgery to a lesser extent However, greater than 70% of patients present with advanced or metastatic disease so surgery is rarely an option (Akehurst *et al*, 2002) The use of chemotherapy in the treatment of NSCLC patients has greatly increased over the last twenty years, with agents being used in combination more effectively than alone The most commonly used drugs for the treatment of NSCLC are the taxanes and platinum drugs with platinum-based doublets remaining the preferred option (Socinski, 2004) However, the development of resistance to these drugs is frequent and a major obstacle in lung cancer treatment

Many *in vitro* studies have attempted to simulate resistance by continuously exposing cells to chemotherapeutics The result is highly resistant cell lines (100-1000-fold) which do not reflect the 5-10-fold resistance normally found *in situ* (Simon and Schindler, 1994) In order to satisfy the clinical situation, the following criteria were used

(1) use of chemotherapy naive cell lines Each of these cell lines had no previous exposure to chemotherapeutic drugs,

(2) pulsing rather than continuous selection This method of pulse-selection, instead of continuous exposure (often employed in *in vitro* studies) was used to try to mimic the clinical scenario, where drug is administered to patients every 1-3 weeks for a period of 2-3 months, depending on the type of cancer in question (Calderoni and Cerny 2001) The cell lines were exposed to low levels of the drugs in question for four hours once a week for ten weeks

(3) use of low levels i e pharmacologically achievable concentrations

To study the molecular events causing resistance, a panel of NSCLC (two adenocarcinomas, two large cell carcinomas and two squamous cell carcinomas) and SCLC were selected for developing resistant variants For this body of work, two squamous and two SCLC were studied, all of which were chemotherapeutically naive

Each parental cell line was pulsed separately with two or three clinically relevant drugs namely a taxane (taxotere and/or taxol) and the platinum drug, carboplatin The two squamous cell carcinomas (SKMES-1 and DLRP) and one small cell carcinoma, DMS-53 were pulse-selected with a taxane and carboplatin The NCI-H69 cell line was pulsed with carboplatin and VP-16 The pulse selections yielded a total of twelve drug-resistant variants and allowed for a comparison in the development of drug resistance as well as a comparison of two common subclasses of lung cancer

The following sections will outline the selections resulting initially to taxol (SKMES-1, DMS-53), taxotere (SKMES-1, DMS-53 and DLRP), VP-16 (NCI-H69) or to carboplatin (SKMES, DLRP, DMS-53 and NCI-H69) The process resulted in variants exhibiting modest changes in resistance with some cross-resistance As these drug-resistant variants were selected at or near sustainable pharmacological levels (Scripture *et al*, 2005, Oguri *et al*, 1988), they provide a suitable model for *in vitro* investigations

4 1 1 Analysis of SKMES-1 drug selected variants

The squamous cell carcinoma line, SKMES-1, was originally established from a pleural effusion from a 65-year-old male with squamous cell carcinoma of the lung (Fogh *et al*, 1977) Initial toxicity assays (section 3 1 1) indicated that the cell line along with DLRP was extremely sensitive to the taxanes, 5-FU and adriamycin in comparison to the other NSCLC cell lines in the panel In contrast, the cell line was most resistant to the platinum drugs In order to study the phenotypic features related to acquired-drug resistance, a taxol-selected variant was established by pulse selection A recent study by Scripture *et al* (2005) showed that the achievable levels of taxol in the plasma of a patient ranges from 1 2 - 5 3μg/ml, depending on the dose The drug concentration available in a tumour is only 25ng/ml (Gyorffy *et al*, 2006) SKMES-1 was exposed to 120ng/ml and 60ng/ml of taxol and taxotere rspectively for 4 hours, once a week for 10 weeks and the resulting cell lines were designated SKMES-Txl and SKMES-Txt

4 1 2 Stability of SKMES-Txl

Taxol, originally extracted from the bark of the Pacific yew, is a potent anticancer agent It has demonstrated remarkable antineoplastic effects against a wide range of human tumours, including ovarian, breast, head and neck, small-cell and non-small-cell lung cancers, as well as metastatic melanomas (Parekh *et al*, 1997) Studies of taxol-resistant tumour cell lines have shown that the cellular transport of taxol and drug efflux is typically associated with increased P-gp expression and its subsequent microtubule-binding activity play a major role in the development of resistance to taxol (Pratt *et al*, 1994) Other mechanisms of resistance include increased and changes in expression of apoptosis-related proteins such as caspases and the bcl-2 family (Wang *et al*, 2000)

Unstable resistance to taxol resulting from the selection process was revealed over time (Figure 4 1 1) Resistance is lost in culture and with storage in liquid nitrogen when tested one month from initial freezing and after eight months storage The cell line was frozen one week after the final pulse Following one-month storage and at the second week from thawing, SKMES-Txl was 72 9-fold resistant to taxol (section 3 1 3 2, Figure 4 1 1) After thirty-four weeks storage, taxol resistance had fallen from 72 9-fold to 12 9-fold Similar to the SKMES-Txt results, the cells appear more sensitive the first week after thawing Taxol resistance levelled out to between 8-fold at week 33 to 5 1-fold at week 37

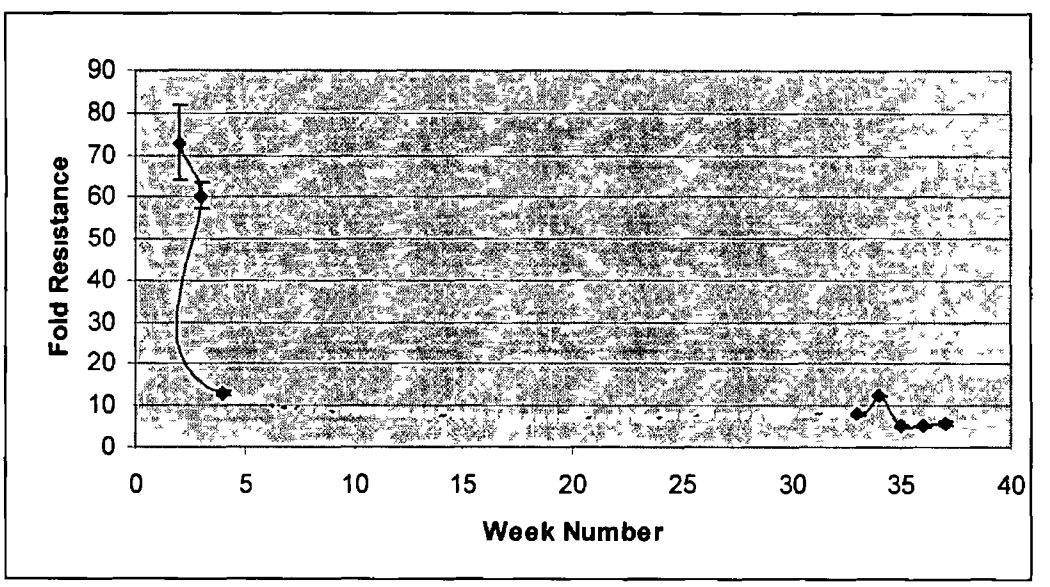

Figure 4 1 1 Summary of unstable resistance of SKMES-Txl The broken line indicates storage in liquid nitrogen Continuous lines indicate cells in culture

4.1.3 Stability of SKMES-Txl to other drugs

Cross-resistance to taxotere resistance also fell during storage and with culture. SKMES-Txl was 31.1-fold resistant after one month storage. This fell to 9.8-fold after one month in culture (Table 3.1.11). Taxotere resistance also fell with time in storage, SKMES-Txl was 31.1-fold resistant after one month but only 4.4-fold resistant after eight months (Table 3.1.13). Given the similarities of taxol and taxotere, it is not surprising that the taxol-resistant variant is also resistant to taxotere or that taxotere is twice as effective as taxol, in agreement with the literature. SKMES-Txl was found to be 14.7-fold resistant to vincristine (Table 3.1.11), which, like the taxanes, functions by disrupting the tubulin/microtubule equilibrium, resulting in cell cycle arrest at metaphase (Bruchovsky *et al.*, 1965; Gidding *et al.*, 1999).

Unstable resistance to most of the other drugs in the panel resulting from the selection process was revealed over time (Figure 4.1.2). When tested at week 2, SKMES-Txl is 4-fold resistant to adriamycin, an anthracycline with different structural and functional properties to the taxanes and the vinca alkaloids and 11.9-fold resistant to VP-16, an epipdophyllotoxin. Both these drugs are associated with classical MDR. Interestingly, cross-resistance developed to 5-FU (15.1-fold) but very low levels of resistance to the platinum drugs was seen.

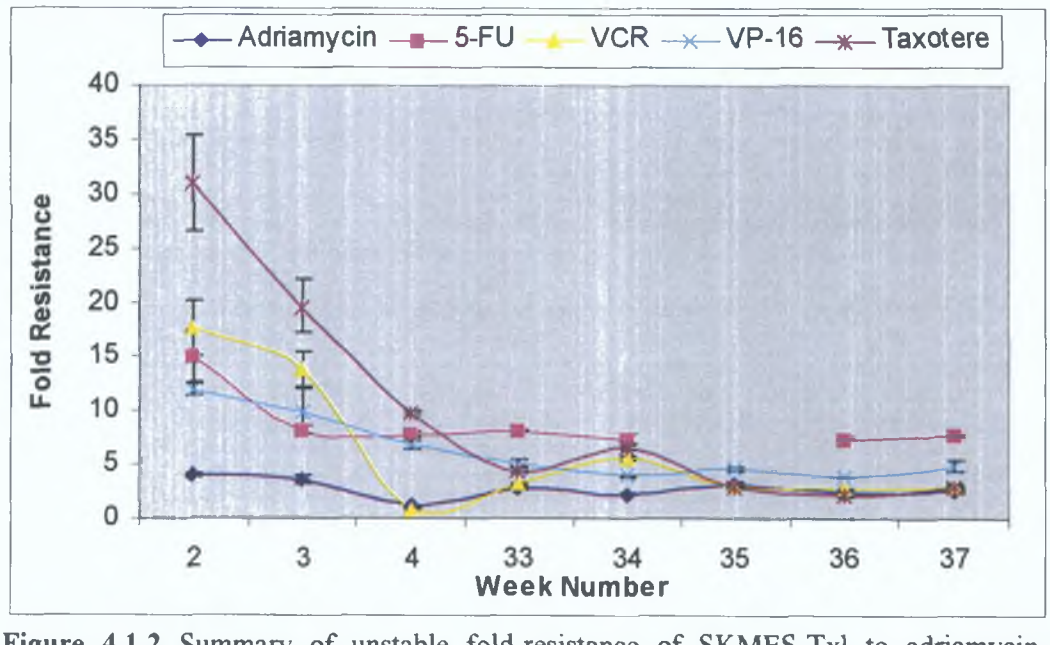

Figure 4.1.2 Summary of unstable fold-resistance of SKMES-Txl to adriamycin, 5-FU, vincristine, VP-16 and taxotere.

After eight-months storage, resistance to each of the drugs had levelled out in culture Unlike testing one month after pulsing, lower but stable cross-resistance developed to 5-FU, adriamycin (consistent with P-gp expression) and VP-16

Another pulse-selected cell line also showed unstable resistance, RPMI 2650 cell line pulse-selected with a range of chemotherapeutic agents, the initial resistance quickly reversed with increasing passage number (Rasha Linehan, PhD, 2003) A study carried out by Liang *et al* (2001) on the nasal carcinoma cell line, RPMI-2650, found that the RPMI-2650 taxol-resistant variant was 226-fold resistant to taxol and cross-resistant to adriamycin, vincristine, vinblastine and VP-16 There was no significant resistance to melphalan, cisplatin or 5-FU However, these were obtained through continuous selection starting with 4ng/ml and culminating with 200ng/ml Bhalla *et al* (1993) exposed the human myeloid leukemia cell line, HL-60, cell line to progressively higher concentrations of taxol This resulted in the development of two taxol-resistant cell lines The cells developed a variable degree of cross-resistance to taxotere, vincristine and adriamycin, however, they were sensitive to the antimetabolite, cytosine arabinoside (Ara-C) The LCLC cell lines NCI-H1299 and NCI-H460, pulsed at clinically relevant concentrations of taxol yielded approximately 2-4-fold increase in resistance to taxol and showed a low level of cross-resistance to vincristine and cisplatm but not to VP-16 or adriamycin (Laura Breen PhD thesis, 2005)

This loss/instability of resistance may be resulting from prolonged growth of cells in the absence of selection pressure The cell line was therefore cultured for seven weeks then exposed to 120ng/ml taxotere for four hours The resulting cell line, SKMES-Txl(11), was 14 4-fold resistant to taxol and 4-fold cross-resistant to taxotere Future experiments will involve testing the stability of this cell line to the panel of drugs It may therefore be beneficial to expose cells to their selecting agent occasionally to avoid loss of resistance in this cell line

The need to re-expose drug-resistant cell lines to their selection agent occasionally to maintain their resistance levels is not unique to pulse selections The DLKP-A10 cell line developed through continuous exposure of escalating concentrations of adriamycin-established in the NICB (Cleary, PhD, 1995) required periodic exposure to adriamycin to maintain resistance The lung large cell carcinoma cell line, CorL23R cell line must be exposed to 0 2ug/ml adriamycin after the first passage in culture (Twentyman *et al*, 1986) Chromosome instability with the loss of double minute chromosomes is one

mechanism of unstable resistance (Curt *et al*, 1984) or the presence of clonal variations Two subclonal population of DLKP-A are more (DLKP-A5F) and less resistant (DLKP-A2B) than DLKP-A

4 1.4 SKMES-Txt

Taxotere resistance has been attributed to a number of changes including increased expression of P-gp, alterations in the expression of tubulins and mutations at the taxane site of action in microtubules Other studies have demonstrated that resistance to taxol can be a independent of P-gp activity The main target of taxol and taxotere are the microtubules which are involved in a wide range of cellular functions, including mitosis and maintenance of cell shape The major component of the microtubules is tubulin, a protein containing two non-identical (alpha and beta) 50kDa subunits arranged head-to-tail in linear protofilaments A single microtubule is composed of 13 protofilaments, forming a hollow structure with a "minus" and "plus" end (Jordan, 2002) Microtubules exhibit dynamic instability This non-equilibrium behaviour occurs due to the association and dissociation of tubulin dimers from the microtubule ends leading to rapid growth and shrinkage of the microtubules Microtubule-associated proteins (MAPs) and proteins such as stathmin can stabilise microtubules through interaction with tubulin dimers and play a role in regulation of microtubule stability Taxol and taxotere disrupt the equilibrium and shifts them in the direction of assembly rather than disassembly The result is a stabilisation of ordinary cytoplasmic microtubules and the formation of abnormal bundles of microtubules (Schiff *et al*, 1980) Cells with alterations or mutations in microtubules have greater tolerance for taxane-induced stabilisation than those of the parental cells (Schibler and Cabral, 1986)

4 1 5 Stability of SKMES-Txt to taxotere

Unstable resistance to taxotere resulting from the selection process was revealed over time (Figure 4 1 3) Prior to storage in liquid nitrogen, SKMES-Txt was determined to be 16-fold at week 1 This resistance increased and stabilised at about 26-fold over the next three weeks The cells appear more sensitive the first week after freezing Following one-month storage in liquid nitrogen, the initial resistance to taxotere at week 1 had fallen to 5 6-fold but subsequently recovered While Figure 4.1 3 would suggest that freezing the cells in liquid nitrogen had a serious effect on loss of resistance, it may have been to soon after the thawing to have tested the cells and would suggest that the

cells are in a more "sensitive" form immediately after thawing so have lower fold resistance. However, looking at the drop from weeks 15-16 to week 60 it is clear that there is a drop in resistance as a result of the storage as well as a drop during culturing.

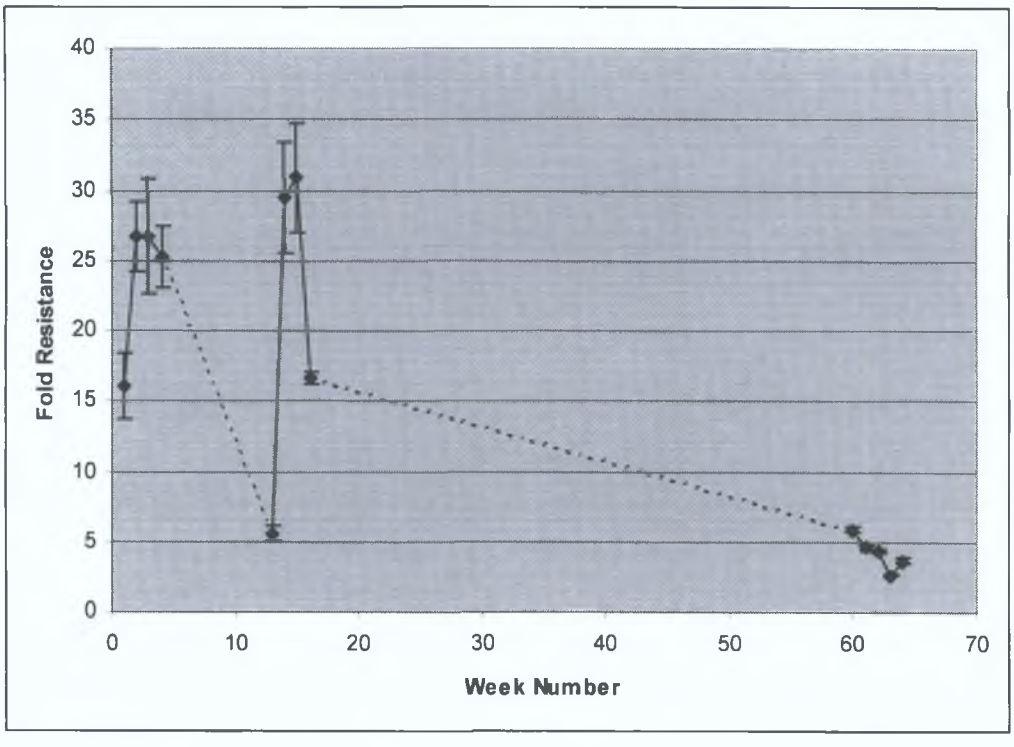

Figure 4.1.3 Summary of unstable resistance of SKMES-Txt to taxotere. Broken lines indicate storage in liquid nitrogen. Continuous lines indicate cells in culture.

4.1.6 Stability of SKMES-Txt to other drugs

Taxol resistance, 52.5-fold at week 2 was reduced by half at week 4 (Figure 3.1.5). Given the similarities of these two taxane drugs, it is not surprising that the taxotere-resistant variant is also resistant to taxol and has been well reported in the literature. After fifteen months storage, taxol resistance had again fallen significantly, being 10.6-fold resistant at week 60 (Table 3.1.8).

After fifteen months storage SKMES-Txt lost further resistance to all drugs tested when compared to one-month and fifteen-months storage in liquid nitrogen (Figure 4.1.4). Stable cross-resistance developed to 5-FU, VP-16, adriamycin and vincristine when tested for four weeks in culture, before freezing, after one month and fifteen months storage. No cross-resistance to the platinum drugs was observed at each time point. However, resistance to vincristine and 5-FU falls with long-term storage in liquid nitrogen (Figure 4.1.4). Interestingly, VP-16-resitance is stable over the fifteen-month storage period. The squamous cell lines selected by pulsing at clinically relevant

concentrations (SKMES-Txl, DLRP) show cross-resistance to 5-FU. This is not observed in the DLKP or hepatocellular carcinoma (Zhou *et al.*, 2001) cell lines as they were pulsed by continuous selection.

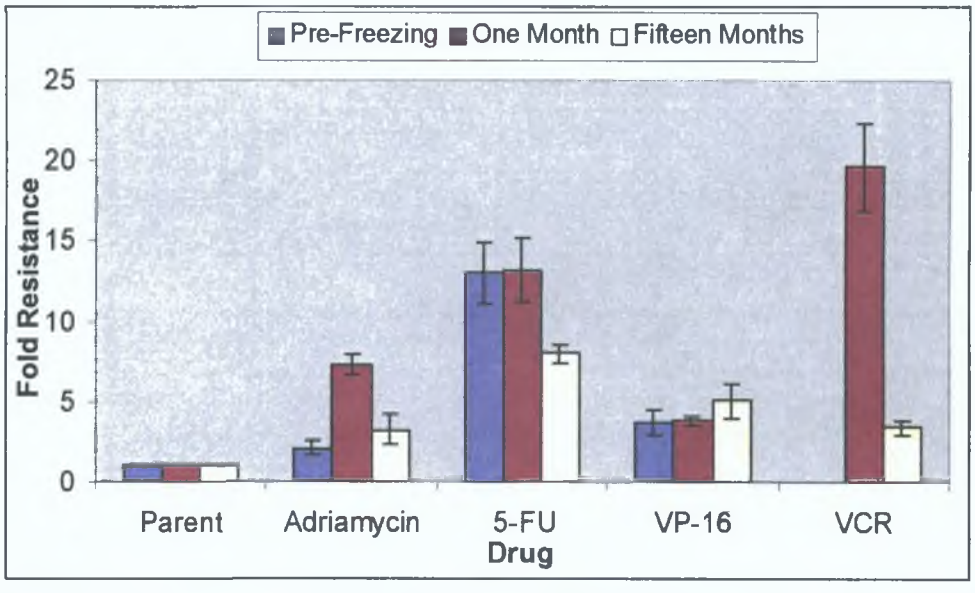

Figure 4.1.4 Summary of fold-resistance of SKMES-Txt to adriamycin, 5-FU, VP-16 and vincristine before freezing, after one and fifteen months storage. Values are given as fold increase in resistance with respect to SKMES-1 as determined by comparing IC_{50} values on a minimum of three repeats.

Similar to results obtained from SKMES-Txl, this loss (and instability) of resistance may be resulting from prolonged growth of cells in the absence of selection pressure. The cell line was therefore cultured for seven weeks then exposed to 60ng/ml taxotere for four hours. The resulting cell line, SKMES-Txt(11), was 169-fold resistant to taxotere and 41-fold cross-resistant to taxol. Future experiments will involve testing the stability of this cell line to the panel of drugs. It may therefore be beneficial to expose cells to their selecting agent occasionally to avoid loss of resistance in this cell line.

Western blotting detected low levels of P-gp protein in H1299 and H1299-tax with combinations of GF120918 and taxol having a potent toxic effect. A small combination effect was observed in A549-txl and SKLU-1-txl suggesting a low level of P-gp protein in these cell lines, which may be enough to contribute to taxol resistance. Studies have shown that even a small increase in P-gp expression can result in an MDR phenotype and also explain the cross-resistance pattern of the SKLU-1-tax cell line (Laura Breen, PhD thesis 2005). Since only small effects can be seen in the taxol-selected variants

when P-gp is inhibited with GF120918, it is reasonable to assume these cell lines possess alternative mechanisms of taxol resistance

4 1 7 Analysis of carboplatin-selected SKMES-1 variants

Toxicity assays indicated that the parental cell line exhibited high resistance to both carboplatin and cisplatin in comparison to the other drugs in the panel (Table 3 1 2) However, on a molar basis and consistent with the literature, cisplatin was the most potent of the two

In order to study the phenotypic features related to carboplatin-resistance, two carboplatin-selected variants of SKMES-1 were established by pulse selection with 100μg/ml and 30μg/ml of the drug respectively The resulting cell lines were designated SKMES-Cpt100 and SKMES-Cpt30 Achievable plasma concentrations in patients for carboplatin range from 9-55μg/ml, depending on the dose (Oguri *et al*, 1988) while 0 5μg/ml was clinically achievable in the tumour (Gyorffy *et al*, 2006) The 100μg/ml concentration is very high and is not clinically achievable compared to the taxol pulse selections The remaining carboplatin-resistant cell lines are valuable models for the study of carboplatin resistance

Stable, but notably less, resistance to carboplatin developed in both cell lines, SKMES-Cpt100 and SKMES-Cpt30 The SKMES-Carboplatin cell lines developed cross-resistance to cisplatin, which was expected since these drugs share a common mechanism of action Both SKMES-1 variants developed about 3-fold cross-resistance to taxol, however, SKMES-Cpt30 developed cross-resistance to taxotere and VP-16 SKMES-Cpt100 became sensitised to taxotere The SKMES-Cpt100 cell line, like the SKMES-Txl developed unusual cross-resistance to 5-FU (5 2-fold) This contrasts to the SKMES-Cpt30 cell line All variants became sensitised to adriamycin

Two adenocarcinomas of the lung and two large cell lung carcinomas pulse-selected with carboplatin resulted in variants displaying fold resistance in the range of 1 3- to 2 7-fold (Laura Breen, PhD thesis 2005) There was no common cross-resistance pattern observed in the resistant cell lines SKLU1-cpt displayed the most cross-resistance to adriamycin and VP-16 (MRP1 was upregulated) The resistance observed in the carboplatin-selected cells was unstable

The combination of adriamycin and sulindac in SKMES-1 had no effect on toxicity indicating that MRP-1 is not present in the parent cell line However, this combination

in SKMES-Cpt100 and SKMES-Cpt30 resulted in greater than 20% enhanced toxicity in both cases indicating the up-regulation of MRP1 and suggest that carboplatin may lead to an increase in MRP-mediated drug resistance for this variant GF120918 failed to circumvent the approximately 3-fold taxol resistance in both cell lines, suggesting MDR-1 is not expressed Duffy *et al* (1998) showed, in agreement with our findings, that sulindac circumvented MRP-1 mediated drug resistance *in vitro* In another study in our laboratories, A549 and H460 carboplatin-selected cell lines showed increased MRP1 expression (Laura Breen, PhD thesis 2005) Combination assays with adriamycin and sulindac led to enhanced adriamycin toxicity

A study by Ikuta *et al* (2005) examined the expression of MDR1, MRP1 and LRP in NSCLC cells and compared this with sensitivity to cisplatin No correlation between expression of these markers and sensitivity to cisplatin in the NSCLC cells was found Combination assays were performed to further elucidate mechanisms of resistance to taxotere in these cell lines The combination of GF120918 and taxotere in the three parental and three taxotere-selected cell lines resulted in all cell lines (except DLRP and DLRP-Txt) becoming sensitised to taxotere The effect was greatest in SKMES-Txt and DMS-Txt suggesting that P-gp plays a role in taxotere resistance in these cell lines No effect was seen with the combination of sulindac and adriamycin in all cell lines indicating the absence of MRP-1 In a study by Liu *et al* (2001), intrinsic and acquired taxotere-resistant cell lines have shown expression of the mdr-1 gene The group also confirmed that taxotere resistance was not mediated by MRP, using RT-PCR and the MRP-specific inhibitor indomethacin

4 1.8 Analysis of DLRP selections

Toxicity assays indicated that DLRP is highly sensitive to taxotere but intrinsically resistant to carboplatin, 5-FU and VP-16 (Table 3 1 2) DLRP was pulsed with 5 ng/ml of taxotere and 15μg/ml of carboplatin respectively The cell lines resulting from this exposure were designated DLRP-Txt and DLRP-Cpt No resistance to carboplatin developed in DLRP-Cpt This cell line, in comparison to the others in the panel selected with carboplatin, retained sensitivity to carboplatin throughout the selection process and took longer to recover from each pulse implying that resistance had not developed Interestingly, DLRP-Cpt developed cross-resistance to taxotere and VP-16 and became sensitised to adriamycin The combination of sulmdac with adriamycin in both DLRP

and DLRP-Cpt had no effect on adriamycin toxicity indicating the possible absence of MRP1 in these cell lines

DLRP-Txt developed low and stable resistance to taxotere (4 4-fold) and was cross-resistant to adriamycin (2 7-fold) and to a lesser degree carboplatin, 5-FU, vincristine and VP-16 (1 3-fold, 1 5-fold, 1 4-fold and 1 2-fold respectively)

Western blotting revealed that P-gp levels were increased in SKMES-Txt in comparison to the parental cell line, which had very low expression levels of P-gp No P-gp was detected in DLRP or DLRP-Txt

4 1 9 Analysis of DMS-53 selections

The small cell lung carcinoma cell line DMS-53, obtained from the ECACC had been established from a mediastinal biopsy of a 54-year-old male prior to treatment Toxicity assays indicated that DMS-53 exhibits high intrinsic resistance to taxotere in contrast to DLRP and SKMES-1, which are highly sensitive to the drug This cell line is also the most sensitive to carboplatin DMS-53 was pulsed with 40ng/ml and 60ng/ml taxotere and taxol and designated DMS-Txt and DMS-Txl DMS-53 was selected with 5μg/ml of carboplatin and designated DMS-Cpt

DMS-Txl was 6 3-fold resistant to taxol and stable after six weeks in culture Stable cross-resistance also developed to adriamycin (1 6-fold), vincristine (3 3-fold) and carboplatin (1 2-fold) No cross-resistance to taxotere, cisplatin, VP-16 or 5-FU developed DMS-Txt developed low but stable resistance to taxotere, taxol, adriamycin, vincristine and cisplatin (1 8-fold, 5 9-fold, 1 3-fold, 1 6-fold and 1 4-fold respectively) No change in resistance to carboplatin, 5-FU or VP-16 was observed DMS-Cpt became resistant to taxol and sensitised to taxotere The cell line became sensitised or developed no resistance to vincristine and adriamycin respectively

Liang *et al* (2003), found that the DLKP-taxotere resistant variant was approximately 36-fold resistant to taxotere, 262-fold and 33-fold cross-resistant to vincristine and adriamycin respectively No cross-resistance developed to cisplatin (resistance to 5-FU was not determined) These results are in agreement with our findings

Western blotting revealed that P-gp levels were increased in DMS-Txt and DMS-Txl in comparison to the parental cell line, which had high levels of P-gp intrinsically and was the most resistant of the parental cell lines to the taxane drugs Combinations assays with GF120918 revealed a greater than 20% enhanced effect of taxotere toxicity in the

parent cell line However, the GF12098/taxotere combination resulted in a greater than 60% enhanced effect in both DMS-Txl and DMS-Txl and greater than 40% enhanced effect in DMS-Cpt (Figure 3 3 14) These results suggest that P-gp plays a major role in taxol resistance in this cell line DLKP-Txt, a taxotere resistant variant of the poorly differentiated squamous lung cell line, DLKP developed by pulsing also showed an increase in P-gp as determined by RT-PCR and Western blotting (Rasha Linehan PhD Thesis 2003)

The combination of sulindac with adriamycin in DMS-53 resulted in greater than 20% enhanced toxicity indicating the presence of MRP1 However, in each of the variants, no effect on adriamycin toxicity was observed indicating the probable absence of MRP1 (Figure 3 3 7)

4.1.10 Analysis of NCI-H69 selections

In contrast to both squamous and the DMS-53 cell lines, the NCI-H69 are more sensitive to both platinum drugs, VP-16 and taxotere (Table 3 1 2) The NCI-H69 variant was pulsed with 10μg/ml and 5μg/ml of carboplatin The resulting variants were designated H69-Cpt10 and H69-Cpt5 respectively The cell line was also pulsed with 480ng/ml VP-16, resulting in H69-VP480

Similar to results from squamous carboplatin selections, all small cell variants developed low carboplatin and cisplatin cross-resistance Both H69-Carboplatin variants and H69-VP480 developed cross-resistance to taxotere and became sensitised to taxol, adriamycin and vincristine The three variants developed cross-resistance to 5-FU Only H69-Cpt5 and H69-VP480 developed resistance to VP-16 No combination assays were carried out on NCI-H69 or variants as the cell line is non-adherent and grows as spheroids in culture

4.1.11 Taxane resistance – mechanism of action

Resistance to the taxanes has been reported to involve the amplification of the *MDR1* gene for the 170-kDa membrane glycoprotein, P-gp. This protein functions in pumping various hydrophobic agents (e.g. the taxanes, adriamycin, vincristine and etoposide) out of the cell in an ATP-dependent manner. Cells positive for P-gp expression exhibit resistance to taxol but are also cross-resistant to an array of structurally unrelated compounds such as adriamycin, vincristine, vinblastine, VP-16 and show little or no cross resistance to alkylating agents, platinum drugs and antimetabolites. SKMES-Txl displays a MDR profile consistent with classic mdr-1-conferred drug resistance. Immunohistochemical analysis of P-gp expression in cell lines and tumour samples have revealed a correlation with resistance and P-gp expression (Mechetner *et al,*. 1998) and with taxol-based chemotherapy in NSCLC (Chou *et al.,* 2003).

A number of studies using high taxane concentrations have generated cell lines with several mechanisms in addition to P-gp.

A taxol-resistant subline, SKOV-3TR, isolated from the human ovarian cancer cell line SKOV-3, was established by increasing the taxol concentration from 0.03 nM to 0.3 μM. The resulting subline was 100-fold more resistant to taxol compared to SKOV-3. Differential display analysis of the cell lines identified a new gene, TRAG-3 (Taxol Resistance Associated Gene-3) whose expression is associated with the chemotherapy-resistant and neoplastic phenotype. TRAG-3 mRNA was overexpressed in SKOV-3TR as well as MDA 435TR (a taxol-resistant breast cancer cell line). Further analysis revealed its overexpression in the adriamycin-resistant myeloma cell lines 8226/DOX40 and 8226/MDR10V (Duan *et al.*, 1999).

Parekh *et al.* (1997) established a series of taxol-resistant human ovarian carcinoma clones by step-wise sequential exposure starting from 0.05μM to 0.5 μM displayed resistance to taxol in the range of 250 to greater than 1500–fold. Resistance to taxol developed via P-gp-mediated and non-P-gp-mediated mechanisms. Non-P-gp-mediated resistance to taxol may be due to alterations in the taxol-binding affinity of the microtubules and alterations in tubulins. Giannakakou *et al.* (1997) discovered alterations in the β270 and β364 regions of the tubulin that abrogated the effect of taxol *in vitro* and conferred resistance in taxol-resistant sublines from a human ovarian carcinoma cell line, A2780, in the presence of verapamil, a P-gp antagonist.

Han *et al* (2000) developed a taxol-resistant large cell lung cancer variant of the NCI-H460 cell line (H460/T800), which is 1000-fold resistant to taxol and showed cross-resistance to colchicine, vinblastine and doxorubicin Increased expression of P-gp and overexpression of α- and β-tubulin are observed in the resistant cell line Down-regulation of the α-tubulin expression by antisense resulted in an increased drug sensitivity of the cell line

Burns *et al* (2001) exposed the osteosarcoma cell line, TE-85, to increasing doses of taxol or taxotere over a nine-month period Two highly resistant variants were developed, TE-85TXL and TE-85TXR The taxol-resistant variant was greater than 1000-fold resistant to taxol and taxotere and 60-fold resistant to adriamycin The taxotere-resistant variant developed greater than 1000-fold resistance to taxol and 800-fold and 80-fold resistance to taxotere and adriamycin respectively and not surprisingly both taxol- and taxotere-resistant variants overexpress P-gp Little cross-resistance to topotecan developed and both cell lines became sensitised to cisplatin Verapamil, a P-gp circumventing agent partially reversed taxane and adriamycin resistance and flow cytometry analysis revealed reduced accumulation of adriamycin in both variants

4 1 12 Clinically-relevant taxane selections

Other investigations, using clinically relevant drug concentrations also revealed P-gp and non-P-gp mechanisms Zhou *et al* (2001) developed a taxol-resistant variant of the hepatocellular carcinoma cell line, QGY-7703 through continuous selection by increasing the concentrations of taxol from 2nM to 50nM The resulting cell line, QGY-TR50, was more than 250-fold resistant to taxol and exhibited cross-resistance to adriamycin (6-fold), vincristine (12 4-fold), vinblastine (5 7-fold) and actinomycin D (4 5-fold) No cross-resistance to 5-FU developed Western blot analysis revealed P-gp over-expression in the taxol-resistant variant RT-PCR analysis of the expression of the 6 isotypes of β-tubulin revealed no overall change in the levels of expression of β-tubulin However, lowly expressed β_{II}-tubulm was increased and β_{III}-tubulin was decreased Increased expression of β_{III}-tubulin has been shown in taxol-resistant cells and is thought to contribute to taxol-resistance by offering the cells a survival advantage Overexpression of β_{II}-tubulin and β_{IVa}-tubulin has also been linked to cell survival

Martello *et al* (2003) studied two taxol-resistant variants of the adenocarcinoma cell line A549 called A549-T12 and A549-T24 A549-T12 is 9-fold resistant to taxol and does not express P-gp A549-T24 is 17-fold resistant to taxol and expresses low levels of P-gp Both cell lines are dependent of taxol for normal growth as tubulin polymerisation is taxol-dependent There is a mutation in the major α-tubulin iso-type Kα1 This report highlights the complexity of taxol resistance in mammalian cells

4 2 13 Apoptosis and taxane resistance

Padar *et al* (2004) suggested that altered intracellular calcium homeostasis could contribute to the taxol-resistant phenotype They determined whether intracellular calcium levels have a regulatory role in the development of taxol resistance in A549 and the resistant subclone A549-T24 Similar basal levels of calcium were found in both cell lines However, a decreased response to thapsigargin (a sarcoplasmic/endoplasmic reticulum Ca^{2+}-ATPase inhibitor) in A549-T24 cells compared to the parent cell line suggested a lower ER Ca^{2+} content in these cells An altered calcium influx pathway in the taxol-resistant cell line was found Western blot and RT-PCR analysis revealed an increase of the anti-apoptotic protein Bcl-2 and sorcin m the resistant variant compared to the parent, both of which have previously been implicated in resistance as they can modulate calcium levels

Zaffaroni *et al* (2002) implicated apoptotic factors in taxol resistance in an ovarian cancer cell line Stable transfection with survivin cDNA resulted in a 4-fold to 6-fold increase in resistance to taxotere and taxol with a concomitant reduction in the apoptotic response to taxol There was no effect on sensitivity to cisplatin or oxaliplatin High expression of the survivin protein, detected by immunohistochemistry in advanced ovarian carcinomas, was significantly associated with clinical resistance to a taxol/platinum-based regimen but unrelated to tumour shrinkage following cisplatin-including combinations (non-taxol based)

Ooe *et al* (2006) investigated the relationship between p53 mutation status and response to taxotere in breast cancers Mutational analysis of p53 was carried out in 50 primary breast cancer samples and 17 locally recurrent breast cancer patients before taxotere therapy The response of the p53-mutated tumours was lower (44%) than that of the p53-wild tumours (62%) Gene expression profiling of 186 tumour samples identified 2412 genes, 13 of which were significantly altered in mRNA expression

between p53-wild and p53-mutated tumours and three were significantly increased in the p53-mutated tumours The expression of CCT5, RGS3, and YKT6 mRNA was up-regulated in p53-mutated tumours and was associated with a low response rate to taxotere Silencing RNA specific for the chaperone protein, CCT5 the regulatory protein RGS3 or the trafficking protein YKT6 in MCF-7 cells resulted in a significant enhancement of taxotere-induced apoptosis

4 1.14 Carboplatin resistance

In 1965, Rosenberg and co-workers first reported the inhibition of cell division in *Escherichia coli* by the electrolysis products from a platinum electrode Besides their effect on lung cancer, the platinum drugs are extremely effective when used on most testicular cancers, head and neck and on a subset of ovarian and bladder tumours The mechanisms of resistance to carboplatin are not as well characterised as those to taxol

The ability of cisplatin or carboplatin to form covalent intra-strand and inter-strand cross-links with the genomic DNA is thought to cause its cytotoxic effects Mechanisms of cellular platinum resistance include decreased drug accumulation *via* increased drug inactivation by protein and glutathione/thiol conjugates enhanced DNA adduct repair, alteration in the sorts of platinum-DNA adducts formed and increased tolerance to platinum-DNA damage However, the underlying molecular bases for these chemoresistance mechanisms are still poorly understood (Johnson *et al*, 1996) Chemoresistance to the platinum drugs remains one of the major obstacles to the successful treatment of NSCLC In this work, a range of carboplatin concentrations was used for pulse-selection of the cell lines

4.1 15 Cross-resistance to carboplatin

Compared to the literature, SCLC cell lines treated with cisplatin showed no cross-resistance to the anti-microtubule agents, namely, taxotere and taxol' (Ikubo *et al*, 1999)

Osmak *et al* (1995) exposed human larynx carcinoma cells to incremental concentrations of carboplatin over 5 days to a final clinical level of 9 23 μg/ml The result was the development of three clones, CBP-3, CBP-6 and CBP-7 which were 2 0-fold, 2 1-fold and 2 9-fold resistant to carboplatin respectively The CBP-7 and CBP-6 clones exhibited cross-resistance to cisplatin CBP-7 clone became markedly more

sensitive and CBP-3 slightly more sensitive to 5-FU CBP-6 became sensitive to VP-16 and vinblastine CBP-7 developed resistance to vinblastine None of the three clones developed resistance to mitomycin C, adriamycin or vincristine A significant increase in glutathione levels and glutathione transferase were observed in CBP-7 only There was an increase in the expression of the *c-los* and *c-Ha-ras* oncogenes in CBP-6 and CPB-7 The cross-resistance profiles, GSH and GST biochemistry and oncogene expression indicate that the acquired resistance to carboplatin is a complex, multifactorial process in these carboplatin-selected cell lines In our studies, all cell lines resistant to carboplatin, developed cross-resistance to cisplatin Moreover, no cross-resistance to adriamycin or vincristine developed SKMES-Cpt30 became sensitized to 5-FU None of the cell lines became sensitized to VP-16

Fram *et al* (1990) have shown that human colon carcinoma cells, resistant to cisplatin and cross-resistant to carboplatin, became resistant to adriamycin and VP-16 but sensitized to 5-FU Carboplatin-resistant ovarian tumour cells became cross-resistant to mitomycin C and depending on the treatment schedule, either retained their sensitivity to adriamycin or became resistant to the drug (Kuppen *et al*, 1988) In contrast, all cell lines in these studies developed no significant resistance or became sensitised to adriamycin

From the literature, carboplatin resistant cells are cross-resistant to cisplatin and resistance ratios are similar for both drugs However, our resistance ratios were different (H69-Cpt10) than those published in the literature, probably due to the drug concentrations used in resistance development Our results, as well as the above-mentioned experimental data clearly show that induction of carboplatin resistance is a very complex, multifactorial process The changes induced in cells during resistance development depend on the cell line used and on the schedule of resistance development Furthermore, with the same cell line and different pulse concentrations, the variants produced can have opposite sensitivities to a range of drugs, as is the case of SKMES-Carboplatin selections and cross resistance to taxotere and 5-FU

4 1.16 Other mechanisms of carboplatin resistance

Cytogenic alterations have also been implicated in platinum resistance (Osterberg *et al*, 2005) Comparative genomic hybridization revealed more frequent cytogenetic alterations in carboplatin resistant ovarian tumours compared to carboplatin sensitive tumours Differences in tumour histology were also found There were gams of 1q, 5q14~q23, 13q21~q32, and losses of 8p and 9q associated with clinical carboplatin resistance Moreover, differences were found between primary resistant and secondary resistant tumours

Daubeuf *et al* (2003) investigated the effect of G-glutamyltransferase (GGT) overexpression on cell viability after carboplatin treatment compared to cisplatin Carboplatin exposure of HeLa cells induced GGT and glutamate-cysteine ligase (GCL) activities by 2-fold and 1 4-fold respectively and increased glutathione levels (1 5-fold) HeLa-GGT cells Stable transfection of GGT in the parent to yield HeLa-GGT, facilitated a study of the role of GGT Culturing the cell lines with low levels of cysteine resulted in a dramatic decrease (90%) of the intracellular GSH level and a 2 5-fold increase of carboplatin cytotoxicity A decrease in carboplatin resistance was observed with the inclusion of GSH in the media in the HeLa-GGT cells only Using partially purified GGT from HeLa-GGT cells, cisplatin forms adducts with cysteinylglycine, depending only on GGT activity whereas carboplatin did not efficiently react with cysteinylglycine GGT activity can affect platinum cytotoxocity by two different ways cisplatin can be detoxified extracellularly after reaction with the –SH group of cysteinylglycine, in the case of carboplatin, the supply of GSH precursors, initiated by GGT, increases the intracellular level of the tripeptide and provides enhanced defensive mechanisms to the cell

Changes in control of apoptosis have been implicated in carboplatin resistance Itoh *et al* (2002) demonstrated that the Bcl-2 family member Bcl-xL provide resistance to chemotherapeutic agents including carboplatin Using Morpholino Bcl-xL antisense oligonucleotides (oligos) to down-regulate Bcl-xL in carboplatin-resistant (MIT8, MIT16) and carboplatin-sensitive (MIT7) squamous cell carcinoma cell lines resulted in a reduction in Bcl-xL levels and substantially prevented cell growth of both carboplatin-sensitive and resistant cells This reduction in cell growth was further augmented the addition of Bcl-xL oligos

Ribosomal proteins and elongation factors were found to be a common characteristic of cisplatin resistant cell lines (Wu *et al.,* 2005). To survive cisplatin exposure, it was hypothesised that cells have to synthesize DNA repair proteins, antiapoptotic proteins and growth-stimulating proteins. Therefore, blocking the translation of these proteins could restore cisplatin sensitivity. CCI-779, an ester analogue of rapamycin, could restore cisplatin sensitivity in SCLC cell lines selected for cisplatin resistance and cell lines derived from patients who failed cisplatin treatment. By disabling mTOR, translation is inhibited and cisplatin sensitivity was restored. The addition of CCI-779 decreased the amount of 4E-BP phosphorylation and p-70S6 kinase phosphorylation and lowered the amount of elongation factor. The compound is effective at 10 ng/ml. At this concentration, it can increase the growth inhibition of cisplatin by 2.5-fold to 6 fold. It can also enhance the apoptotic effect of cisplatin in cisplatin-resistant cell lines. However, at achievable clinical concentrations CCI-779 had no effect on the growth of P-gp or MRP1 overexpressing cells.

4.1.17 Analysis of VP-16 resistance in the NCI-H69 cell line

Etoposide/VP-16 is a semi-synthetic derivative of podophyllotoxin used in the treatment of testicular cancers, acute myeloid leukaemia, Hodgkin's disease, non-Hodgkin's lymphoma, lung, gastric, breast and ovarian cancers as well as Kaposi's sarcoma (Hande, 1998). The major toxicities attributable to VP-16 are bone marrow depression, nausea, diarrhoea, mucositis and hypotension.

4.1.18 Mechanism of VP-16 resistance

VP-16 works as a topoisomerase II (topo II) poison whose function is to temporarily break DNA strands and reseal the breaks. This results in the DNA being sufficiently untangled to allow transcription and replication to occur.

VP-16 increases the steady state concentration of the covalent DNA cleavage complexes, converts the topoisomerases into toxins that introduce high levels of transient protein-associated breaks in the genome of the treated cells. Development of resistance to VP-16 can be due to reduced levels of topoisomerase II within the target cells. Moreover, mutations or alterations in drug binding sites on topoisomerase II are associated with resistance to VP-16. Increased expression of MDR-1 also confers resistance to VP-16.

Overexpression of P-gp or MRP1 is a mechanism of resistance to VP-16 It results in decreased intracellular drug accumulation (Sinha *et al*, 1998) Minato *et al* (1990) developed a 9 4-fold etoposide-resistant variant of the NCI-H69 cell line The cell line was cross-resistant to adriamycin, teniposide, vindesine and vincristine as opposed to our NCI-H69 VP-16 resistant variant Topoisomerase II levels between the parent and variants were almost unchanged The catalytic level of the enzyme was lower in the resistant variant Northern blot analysis revealed that P-gp levels were significantly increased in H69/VP suggesting that it has a typical MDR phenotype

VP-16 treatment also prevents the activation of $p34^{cdc2}$ protein kinase, which usually becomes activated at the end of the G_2 phase of the cell cycle It is believed to have a critical role in allowing cells to start mitosis It is possible that the arrest of cells in the G_2 phase of the cell cycle which is seen with VP-16 is due to interference with $p34^{cdc2}$ Ikubo *et al* (1999) studied the cytotoxicity of anti-microtubule agents in SCLC cell lines, including a primary cell line from an untreated patient and cell lines from treated patients The panel consisted of representatives of intrinsic drug-resistance and cell lines selected by continuous exposure to increasing concentrations of adriamycin, etoposide or cisplatin, as representative of acquired drug resistance Results showed that the cell lines treated with adriamycin or etoposide were highly resistant to taxol, taxotere, vincristine, vindesine and vinblastine as well being resistant to their selection agents (unlike our variants)

Hill *et al* (1994) established four epipodophyllotoxin-selected cell lines, which had alterations in topoisomerase II No cross-resistance to taxotere developed suggesting that taxotere cross-resistance is not automatically expressed by classic MDR tumour cells

A phenotype has been identified in which cells that are resistant to VP-16 retain normal sensitivity to the vinca alkaloids and normal drug transport characteristics It arises from the expression of different forms of topoisomerase II with altered catalytic activities (Glisson *et al*, 1986) Another form of resistance has been traced to a mutation that resulted in decreased expression of the topoisomerase II protein with otherwise normal catalytic activity (Deffie *et al*, 1989)

4.1 19 Summary

The criteria required to mimic the clinical situation, namely the use of chemotherapy-naive cell lines, pulsing rather than continuous selection and the use of pharmacologically achievable concentrations were adhered to in the generation of clinically relevant drug-resistant variants Resistant tumour cells *in situ* are usually no more than 5 to10-fold resistant (Simon and Schindler, 1994) Excluding the unstable SKMES-Taxane selections, selection with taxol resulted in a variant with a fold resistance of 6 3-fold compared to the parent Selection with taxotere resulted in variants with fold resistance differences between 1 8-fold and 4 4-fold compared to the parent cell lines Unstable resistance developed to both taxane-selected variants of SKMES contrasting to the taxane selected variants arising from DLRP and DMS-53 Carboplatin selection resulted in variants with stable fold resistance differences between 1-fold and 2 2-fold compared to the parent

The resistance in taxane-selected variants may be due to a number of mechanisms including alterations in tubulin dynamics, mutations in tubulin and increased expression of P-gp The carboplatin-resistance observed might be due in part to increased MRP-1 expression

The resulting selected variants displayed relatively low-level resistance to the pulsing drug (1-76 7-fold) and therefore provide excellent models for the study of taxotere, taxol, VP-16 and carboplatin resistance

4 1 20 Cell invasion, motility and adhesion

Invasion is one of the most critical steps of metastasis in cancer and is a major cause of cancer deaths as approximately 50% of all cancer patients develop metastasis (Fidler *et al*, 1994) Tumour progression requires the dispersion of epithelial cells from the neoplastic cluster and cell invasion into adjacent tissue The development of metastasis is a multistep process involving attachment to the basement membrane, local proteolysis and migration into surrounding tissues, lymph or bloodstream and re-attach at a different site Tumour cells must initiate and successfully complete all of these steps in order to enter the circulatory and lymphatic systems to form distant metastases It is thought that some tumour cells acquire favoured phenotypes that give them an advantage in disseminating from the primary tumour and invading other areas Understanding the relationship between cell dispersion and cell invasion represents a challenge in elucidating the mechanisms contributing to the acquisition of an invasive phenotype A good tumour metastasis model is not yet available to analyse the metastatic potential of lung cancer cells It is difficult to correlate *in vitro* the cellular and molecular modifications, which lead to invasion with a precise cell behaviour At present, models cannot analyse cell adhesion and the individual ability of each cell to disperse and be invasive

Widespread metastasis is common in non-small-cell lung cancer The adenocarcinomas typically metastasise at an early stage whereas squamous cell lines occur relatively late Small cell lung carcinomas are very malignant tumours, grow aggressively and metastasize early Damstrup *et al* (1998) correlated *in vitro* invasiveness with expression of epidermal growth factor receptor (EGFR) in a panel of 21 SCLC cell lines They determined that only EGFR-positive SCLC cell lines had the *in vitro* invasive phenotype suggesting that the EGFR might play an important role for the invasion potential of SCLC cell lines The inclusion of the EGFR-neutralizing monoclonal antibody mAb528 in six EGFR-positive SCLC cell lines resulted in a significant reduction in *in vitro* invasion in three of the cell lines

4.1.21 MDR and invasion

Studies have begun to focus on a correlation between cancer invasion, metastasis and drug resistance There is increasing evidence that drug resistance may induce an invasive phenotype in cancer cells and *vice versa* (Kondo *et al*, 1961, Takenaga *et al*, 1986, McMillan *et al*, 1987) Previous studies in our laboratories have shown that selection with some chemotherapeutic agents can lead to increased *in vitro* invasiveness (Liang *et al*, 2001) The aim of this part of the thesis was to determine whether invasion could be induced in non-invasive cells (DMS-53 and NCI-H69) and whether an already invasive phenotype be altered as a result of drug selection (SKMES-1 and DLRP)

4.1.22 SKMES-1

Pulse selection of SKMES-1 with taxotere and taxol resulted in more invasive variants, with the taxotere variant being the most invasive in comparison to the parent cell line (2 17-fold and 1 34-fold respectively) Due to the unstable nature of both SKMES-Txt and SKMES-Txl variants, their invasiveness was also assessed after long-term storage at week 7 where drug resistance had fallen by approximately 2 2-fold in both cell lines The taxol variant SKMES-Txl, was 5-fold more invasive compared to the control at week 7, and 1 3-fold invasive at week 2 The taxotere-selected variant SKMES-Txt was 3 3-fold more invasive at week 7 compared to the control (2 1-fold invasive at week 2) The invasiveness of the parental cell line remained unchanged over the same period

Selection of SKMES-1 with the high concentration of carboplatin resulted in a more invasive (1 4-fold) cell line whereas pulse selection with a lower concentration resulted in a less invasive (3-fold) and less motile (1 5-fold) cell line No change in motility was observed in SKMES-Cpt100 These cell lines provide a model for the future study of invasion SKMES-Cpt100 is 2 5 times more adhesive than the parent cell line with the SKMES-Cpt30 cell line being only 1 2 times more adhesive

The most widely accepted method to measure and quantify *in vitro* invasiveness is the use of the monolayer Boyden Chamber assay, where cells are placed into a microporous membrane insert pre-coated in e g matrigel (section 2 11 1) However, this assay is limited and does not fully reflect the *in vivo* tumour situation Therefore, invasion assays were also carried out on SKMES-1, SKMES-Txt and SKMES-Txl, whereby cells

were induced to grow as spheroids (to try and mimic the *in vivo* situation), then transferred to a well of a 24-well plate coated in collagen type I. Components of the extracellular matrix play a fundamental role in the process of tumour invasion and metastasis. During metastasis, invasive cells must traverse tissue barriers which are mainly comprised of type I collagen. This process is dependent on the ability of tumour cells to degrade the surrounding collagen matrix and migrate through. The results revealed that both SKMES-1 and the taxane variants are invasive after 24 hours. However, the taxol and taxotere variants are approximately half as invasive as the parent when tested over the seven days.

Taxotere was found to greatly increase the invasiveness and motility of the DLKP-Taxotere cells (Rasha Linehan, PhD thesis 2003). The invasiveness of DLKP-taxotere was reversed using MMP inhibitor III which inhibits MMP-1, -2, -3, -7, -13.

Adhesion assays to matrigel compared to a control with no matrigel determined that SKMES-Txt (3.85-fold) is more adhesive to matrigel than either the parent or taxol-selected variant (0.83-fold) with the taxol-selected variant being less adhesive than the parent. Loss of adhesion was seen in both taxane cell lines with respect to time, SKMES-Txt and SKMES-Txl being 1.4-fold and 0.44-fold less adhesive at week 7 compared to week 2 respectively with respect to SKMES-1 (Table 3.2.7). Loss of adhesion to matrigel is greater in the taxol-selected variant than in taxotere-selected variant, 2.5 times versus 1.5-times respectively. Taxol-mediated stabilisation of microtubules and subsequent cell death may be more effective if the tumour is adhered to the extracellular matrix. It may be advantageous to a tumour or cell line to become less adhesive to extracellular matrix components, in order to lessen the effects of taxol or taxotere on microtubules. A study on the invasive breast cancer cell line MDA-MB-435S-F found that selection with the agents taxol and adriamycin led to a more aggressive invasive phenotype termed "superinvasive" (Glynn *et al.*, 2004). These variants were also considerably less adhesive to laminin, fibronectin, collagen type IV and matrigel.

Gelatine zymography of the taxane selected variants and corresponding parental cell lines in these studies revealed the presence of MMP-9 in all invasive cell lines tested. A band corresponding to MMP-2 was also detected in all invasive taxane-selected variants. A loss of secreted proteinases, which are not MMPs or serine proteinases was observed in the SKMES-Txt and SKMES-Txl compared to the parental cell line.

4 2 23 DLRP

Exposure to taxotere resulted in the DLRP-taxotere becoming only slightly more invasive No change in motility was observed However, DLRP-Txt (0 91-fold) was less adhesive than the parent cell line Carboplatin selection had no effect on drug resistance, motility or invasiveness of DLRP-Cpt However, this cell line was considerably less adhesive than the parent

4.1 24 DMS-53 and NCI-H69

Exposure of the non-invasive cell line, DMS-53, to taxol and taxotere did not induce an invasive or motile phenotype or a change in adhesiveness Previous findings showed taxol did not induce a strong invasive phenotype in the non-invasive cell line RPMI-2650 (Liang *et al* , 2001) The SCLC cell lines (DMS-Cpt, H69-Cpt10 and H69-Cpt5) remained non-invasive after pulse selection with carboplatin

However, when cultured *in vitro*, such as the classic SCLC cell line NCI-H69, grow in floating aggregates and express negligible proteolytic activity Sage *et al* (2004) selected for adherent NCI-H69 cells, which expressed tissue factor as well as gelatinolytic activity, namely MMP-2 and MMP-9 If this occurs in SCLC patients it might increase the understanding of the steps involved in the spreading of this highly metastatic type of lung cancer

4 1 25 Taxol and invasion

Taxol treatment has been linked to decreased invasion and motility Belotti *et al* (1996) determined the effect of taxol on the adhesive and motility properties of human ovarian carcinoma cell lines, OVCAR 5, SK-OV-3, and HOC-1OTC Taxol significantly inhibited the motility of these cell lines but it did not affect their adhesion to the subendothelial matrix Taxol is therefore a potent inhibitor of ovarian carcinoma cell motility and this activity is independent of its cytotoxic activity In a different study by the same group, results indicated that taxol has a strong antiangiogemc activity, a property that might contribute to its antineoplastic activity *in vivo* (Belotti *et al* , 1996)

In another ovarian cancer cell line, Ovcar-3, taxol was also found to suppress invasion, motility and cell attachment of ovarian cell line and was accompanied by an increase of TIMP-2 protein release (Westerlund *et al*, 1997) Motile and invasive cells were trypsinised from the invasion chamber and counted These invasion results do not correlate with the results obtained from SKMES-Txl which became more invasive after

pulse selection Similar increases in invasion were also seen in taxol-selected H460 and SKLU1 cell lines (Laura Breen, PhD thesis 2005)

In the study, RPMI-2650Ml (melphalan-resistant) and RPMI-2650Tx (taxol-resistant) cell lines were established through continuous selection with melphalan and taxol, respectively The variants exhibited a multiple drug resistant phenotype However, RPMI-2650Ml but not RPMI-2650Tx, exhibited a highly invasive phenotype, with increased expression of MMP-2 and MMP-9 as well as increased adhesion to collagen type IV, laminin, fibronectin and matrigel (Liang *et al* , 2001)

Terzis *et al* (1997) tested taxol for its anti-migrational, anti-invasive and anti-proliferative effect on two human glioma cell lines, GaMg and D-54Mg, which were grown as spheroids Both cell lines showed a dose-dependent growth and migratory response to the drug taxol The GaMg cells were 5-10 times more sensitive than the D-54Mg cell line It was also highly effective in preventing invasion in a co-culture system in which tumour spheroids were confronted with foetal rat brain cell aggregates Confocal microscopy of both cell lines showed an extensive random organisation of the microtubules in the cytoplasm After exposure, the GaMg and the D-54Mg cells displayed a fragmentation of the nuclear material, indicating a possible induction of apoptosis Flow cytometric DNA histograms showed an accumulation of cells in the G2/M phase of the cell cycle after 24 hours of exposure Forty-eight hours resulted in a deterioration of the DNA histograms indicating nuclear fragmentation

4 1 26 Carboplatin and invasion

Carboplatin selection of other lung cell lines namely, H460, H1299, A549 and SKLU1 in our laboratories resulted in a less invasive phenotype (Laura Breen, PhD thesis 2005) In contrast, pulse-selection with cisplatin led to increased *in vitro* invasiveness in lung cancer cell line DLKP (Liang *et al* , 2004) This increased invasiveness was associated with increased expression of the matrix metalloproteinases MMP-2 and MMP-13

Gelatine zymography of the carboplatin-selected variants in these studies, revealed the presence of MMP-9 in all invasive cell lines tested A band corresponding to MMP-2 was also detected in the selected variants except DLRP-Cpt SKMES-1 and both carboplatin-selected variants secrete proteinases which are not MMPs or serine proteinases

It is suggested that tumour growth, angiogenesis and metastasis are dependent on MMP activity. They break down matrix barriers, thereby allowing tumour cells to penetrate tissues, gain access to blood vessels, exit blood vessels and metastasise to distant sites. Koivunen *et al.* (1999) developed a specific MMP-2 and MMP-9 synthetic peptide inhibitor, CTTHWGFTLC (CTT1) and CCT2 to prevent the migration of human endothelial and tumour cells. It also inhibited tumour growth and invasion in animal models and improved the survival of mice with human tumours. CTT1-displaying phage could specifically target angiogenic blood vessels *in vivo*. However, CTT2 did not inhibit the type I collagen degradation by human collagenases (MMP-1, MMP-8 and MMP-13) in tongue SCC. It reduced the blood vessel density and improved the survival of the mice bearing human tongue carcinoma xenografts (Heikkila *et al.*, 2006). The development of matrix metalloproteinase inhibitors as an anti-cancer agents, is therefore very important and may prove useful in tumour targeting and anticancer therapies.

The tumour microenvironment, which consists of soluble factors, components of the extracellular matrix as well as cell–cell interactions is often overlooked when considering tumour response to chemotherapeutic agents. Anti-apoptotic pathways initiated by cell adhesion are operative in tumour cells and cause resistance to mechanistically-distinct cytotoxic drugs. Cell adhesion of hematopoietic cancers (e.g. the human myeloma 8226 cell line) to fibronectin is sufficient to inhibit apoptosis induced by mechanistically distinct chemotherapy drugs. The results in blocking cell cycle progression result in increased p27kip1 levels. This correlates with cell cycle arrest and drug resistance. A reduction in initial DNA damage induced by topo II inhibitors has also been seen in adherent hematopoietic cancer cell lines (Hazelhurst and Dalton, 2004).

It has been proposed that extracellular effectors namely, cytokines, matrix components and adjacent cells may provide sanctuary to cancer cells and inhibit stress-induced cell death. Cell adhesion has been shown to confer a protective advantage to adherent cancer cells against classical chemotherapeutic agents and irradiation and prevent cell death through a number of mechanisms. Shain and Dalton (2001) observed that fibronectin adhesion of K562, the chronic myelogenous leukemia cell line reduced the effectiveness of the BCR-Abl kinase inhibitors STI-571 and AG957. The results show that the microenvironment of the cancer cell can provide a sanctuary conferring resistance to cancer therapy.

Hikawa *et al* (2000) used a glioma cell line, IN157 to study changes in cell adhesion and invasion on acquiring drug-resistance to VP-16, vincristine and adriamycin The drug-resistant cells had increased expression of integrins alpha 2, 3 and 5 and beta 1 The adhesiveness of the variants increased to laminin, fibronectin and type IV collagen Reduced invasion was observed The development of drug-resistance and an increase in the expression of integrins may have enhanced the adhesion to ECM proteins

Pulse selection of NCI-H69 cells with VP-16 had no effect on the invasive phenotype of the cells In solid tumours, cancer cells are exposed to various micro-environmental stresses such as hypoxia, nutritional depletion and low pH Cancerous cells adapt to these conditions and circumvent cell death by acquiring physiologic functions, such as invasiveness Mutsuko *et al* (2005) treated rat ascites hepatoma MM1 cells with VP-16 and hypoxia and acidic conditions Under stress conditions, the cells became invasive and changed morphologically This was induced by caspase-3 activation In contrast, acid-induced invasiveness was not activated by caspase-3 inhibition

4 1 27 Summary

Studies have begun to focus on a correlation between cancer invasion, metastasis and drug resistance There is increasing evidence that drug resistance may induce an invasive phenotype in cancer cells The aim of this part of the thesis was to determine whether invasion could be induced in non-invasive cells (DMS-53 and NCI-H69) and whether an already invasive phenotype be altered as a result of drug selection (SKMES-1 and DLRP)

Invasion was not induced in a non-invasive cell line (NCI-H69 and DMS-53) when pulsed with carboplatin and/or taxotere, taxol and VP-16 Pulse selection of an already invasive cell line was found to alter the invasiveness Taxane selection resulted in increased invasion whereas carboplatin induced different levels of invasiveness depending on the concentration used

Pulse selection of SKMES-1 with both taxanes resulted in more invasive variants, with the taxotere variant being the more invasive of the two when checked over two and seven weeks A correlation between a fall in drug resistance and adhesiveness with increase in the invasive phenotype was observed in both cell lines over this period Exposure of DLRP to taxotere resulted in the DLRP-Txt cell line becoming only slightly more invasive and as seen in SKMES-Taxane selection a loss of adhesion was observed Pulse selection of the non-invasive small cell lung carcinoma cell line, DMS-53, to taxol and taxotere did not induce an invasive or motile phenotype or a change in adhesiveness Gelatine zymography of the taxane selected variants in these studies revealed the presence of MMP-9 and MMP-2 in all invasive cell lines tested A loss of secreted proteinases, which are not MMPs or serine proteinases was observed in the SKMES-Txt and SKMES-Txl compared to the parental cell line

Collagen type I is a major component of the extracellular matrix which plays a fundamental role in the process of tumour invasion and metastasis To try and mimic the *in vivo* situation, SKMES-1 and both taxane-selected variants were induced to grow as spheroids and transferred to collagen type I The results revealed that both SKMES-1 and the taxane variants are invasive after 24 hours However, the taxol and taxotere variants are approximately half as invasive as the parent when tested over the seven days

Selection of SKMES-1 with the high concentration of carboplatin resulted in a more invasive cell line whereas pulse selection with a lower concentration resulted in a less invasive and less motile cell line No change in motility was observed in SKMES-Cpt100 Both carboplatin selections are more adhesive than the parent cell line Carboplatin selection had no effect on drug resistance, motility or invasiveness of DLRP-Cpt However, this cell line was considerably less adhesive than the parent Similar results to the taxane selections on the DMS-53 cell line were observed with carboplatin selection on NCI-H69 and DMS-53 No change in the invasive and motile phenotype was observed Gelatine zymography of the carboplatin-selected variants and parental cell lines in these studies, revealed the presence of MMP-9 in all invasive cell lines tested A band corresponding to MMP-2 was also detected in the selected variants, except DLRP-Cpt SKMES-1 and both carboplatin-selected variants secrete proteinases which are not MMPs or serine proteinases This increased invasiveness was associated with increased expression of the matrix metalloproteinases MMP-2 These cell lines therefore provide a model for the future study of invasion

Pulse selection of NCI-H69 cells with VP-16 had no effect on the invasive phenotype of the cells

4.2 Proteomic analysis of drug-resistant variants of squamous lung carcinomas

Cancer is a multi-faceted disease, presenting many challenges to clinicians and cancer-researchers alike who search for more effective ways to combat this devastating disease. Tumour development is a complex process, requiring the co-ordinated interactions of many proteins, signal pathways and cell types (Negm *et al.,* 2002) and as such, is an ideal candidate for proteomic analysis. Cancer proteomics seeks to understand how networks become dysfunctional, predict how their function can be altered through interventions by drugs or genetic manipulations (Anderson *et al.,* 2000) and enables the identification of disease-specific proteins, drug targets and markers of drug efficacy and toxicity. Improving diagnosis, classification of tumours and defining targets for more effective therapeutic measures are among the central challenges of this disease (Simpson and Dorrow, 2001). Proteomic approaches hold the promise of identifying specific protein modifications in tumour tissues to aid in individualising treatments for certain cancers.

Lung cancer is the most lethal of cancers with 1.2 million cases diagnosed each year and 1.1 million deaths (Seve and Dumontet, 2005). Poor survival rates are due to: the propensity for early spread; the lack of effective screening for early diagnosis (75% present with advanced stage disease); the inability of systemic therapy to cure metastatic disease and the poor understanding of the biology of the tumours and the development of resistance to chemotherapeutics (Bunn, 2002; Niklinski and Hirsch, 2002).

4.2.1 Drug resistance and cancer

The development of resistance to drug therapy is one of the major problems in cancer treatment and a main cause of limited long-term survival. Intrinsic and acquired drug resistance are believed to cause treatment failure in over 90% of patients with metastatic cancer (Longley and Johnston, 2005). Tumours can be initially sensitive to a chemotherapy drug but through drug selection acquire resistance. In contrast, other tumours are intrinsically resistant before treatment. Non-small cell lung carcinomas often show intrinsic multidrug resistance (Wilhelm and Kolesar, 2005), whereas small cell lung carcinomas usually respond well to various anticancer agents initially and then acquire resistance. Treatment with one chemotherapeutic agent can often lead to associated resistance to a number of unrelated agents, a phenomenon called multiple drug resistance (MDR). MDR is caused by a variety of changes in the cancer cells and

is almost always multifactorial A better understanding of the mechanisms of drug resistance would help to overcome this obstacle Huge advances have been made in understanding the biology of lung cancer and the mechanisms of drug resistance Mechanisms include drug inactivation (GSTs), alterations in the target, decreased drug accumulation, increased drug efflux, enhanced processing of drug-induced damage and evasion of apoptosis (Longley and Johnston, 2005) MDR categories based on the specific cellular targets include – classical multidrug resistance (MDR/P-gp), non P-gp MDR (MRP) and atypical MDR (mediated through altered expression of topoisomerases II) (Scagliotti, *et al*, 1999)

Cellular pathways that are mutated in cancer and associated with resistance may provide cancer therapy approaches Increased overall survival and resistance to unfavourable growth conditions develop as the consequence of several mechanisms such as mutations in p53, up-regulation of PI3K-AKT signalling and growth factor receptor associated pathways, resistance to hypoxia-induced apoptosis Anticancer therapy should therefore be directed against targets that represent weaknesses in the armour of tumour cells and not their strong points Some apoptosis mechanisms are unlikely to be mutated during tumour progression and are interesting potential therapeutic targets One such potential mechanism is the lysosomal apoptotic pathway The high protein turnover in tumour cells is another example of a possible weak point to be exploited The protein-folding compartment of the endoplasmic reticulum (ER) is particularly sensitive to disturbances, which, if severe, could trigger apoptosis (Chen *et al*, 2005)

In addition to developing MDR, some cells also become metastatic and migrate to distant sites in the body (Lucke-Huhle, 1994) Conversely, metastatic cells may also develop drug resistance more readily than their non-invasive counterparts (Cillo *et al*, 1987) A better understanding of the relationship between chemotherapeutic drug resistance and invasion in cancer could lead to a more effective treatment for the disease (Liang *et al*, 2002)

In this work, proteomic tools were used to study the chemoresistance mechanisms in cell culture systems derived from squamous lung carcinomas The parental cell lines along with the chemoresistant variants were cultured and analysed for differential proteins expression using 2D-DIGE Differentially expressed proteins were identified by MALDI-TOF mass spectrometry

4 2 2 Proteomic analysis of adriamycin-resistant variants of DLKP

Proteomics has emerged as a valuable tool for identifying proteins, which play a role in chemotherapeutic efficacy In these studies, we used the ETTAN DIGE two-dimensional electrophoresis system, where protein samples were labelled with three different charge- and size-matched fluorescent cyanine dyes possessing distinct excitation and emission spectra Proteomic analysis was carried out to study differential protein expression caused by adriamycin resistance in a range of established cell lines displaying varying levels of resistance to adriamycin DLKP, a poorly differentiated squamous lung cell line, was previously exposed continuously to increasing concentrations of adriamycin resulting in the cell line, DLKP-A (Clynes *et al*, 1992) This cell line was further selected continuously with adriamycin creating DLKP-A10 (Cleary *et al*, 1997) Several clonal sub-populations were also established from DLKP-A by clonal dilution including, DLKP-A5F and DLKP-A2B (Heenan *et al*, 1997) Each of the above four cell lines has differing levels of resistance to adriamycin and also exhibits cross-resistance profiles to a number of chemotherapeutic drugs (Table 4 2 1) While the main mechanism of resistance in these cell lines is associated with P-gp (no detectable levels of MRP), little information on cytoplasmic changes was available This work set out to investigate such changes to increase our understanding of the mechanisms involved in adriamycin resistance and to identify putative markers with possible prognostic/diagnostic value

	Fold Resistance				
Cell Line	**Adriamycin**	**Cisplatin**	**Vincristine**	**VP-16**	**5-FU**
DLKP-A10	765 3	0 825*	3000	63 3	0 92
DLKP-A5F	235 4	1 39	1275 04	50 6	0 98
DLKP-A	122 6	1 46	1504	60 67	1 75
DLKP-A2B	7	0 57	228 32	18 17	1 28

Table 4 2 1 Drug resistance profiles of adriamycin resistant variants of DLKP

*Carboplatin Table was compiled from Cleary *et al*, 1997 and Heenan *et al*, 1997 Resistance to adriamycin was reconfirmed by toxicity assay Fold resistance was calculated with respect to DLKP

4.2.3 Summary of identified proteins

Proteomic analysis was carried out whereby DLKP was compared to DLKP-A. DLKP-A was then compared to DLKP-A2B, DLKP-A5F and DLKP-A10.

DLKP-A versus the parent yielded a total of 300 proteins of which 38 were identified. Of the total number of proteins identified (68) from all the comparisons, the most interesting, with respect to drug resistance, were those that increased with resistance (8 proteins) (Figure 3.4.27; those that decreased with resistance (7 proteins) (Figure 3.4.28) and those that showed a baseline change across the cell lines (11 increased and 8 decreased proteins) (Figures 3.4.29 and Figure 3.4.30). In the following sections some of the differentially expressed proteins will be discussed.

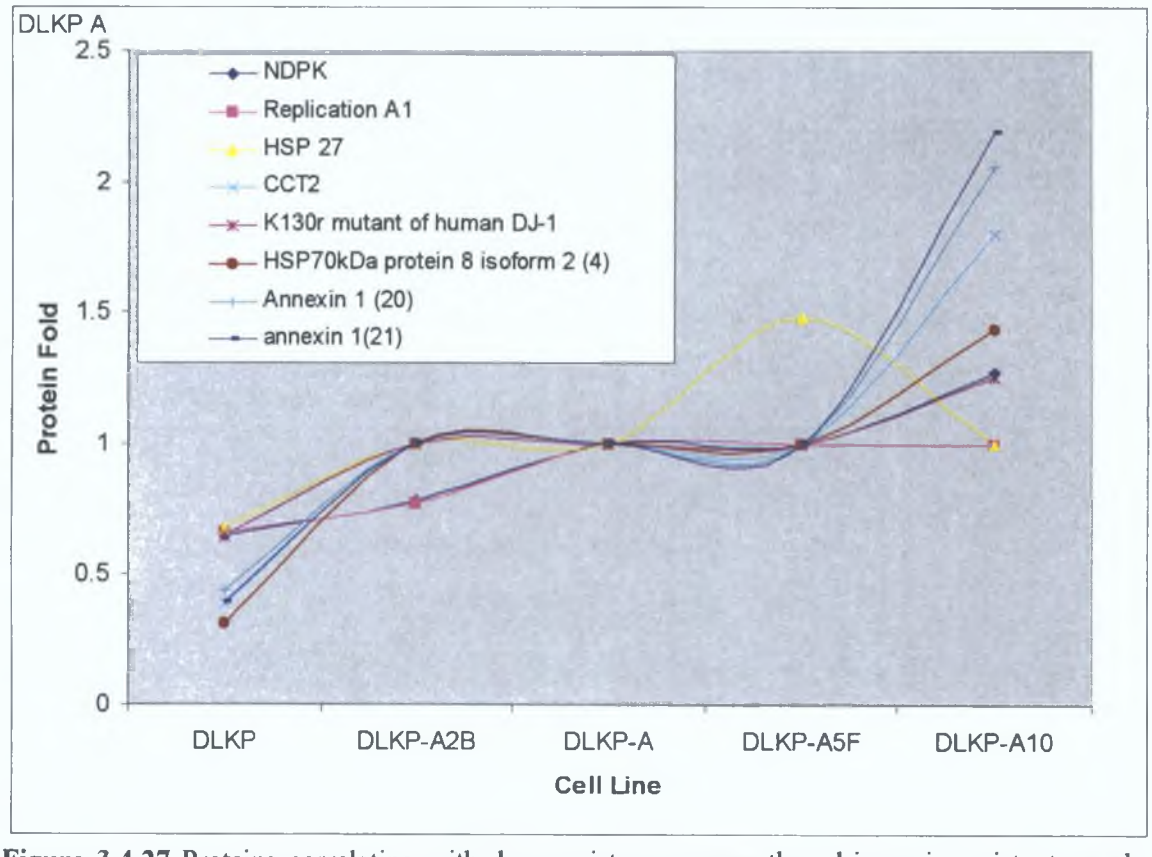

Figure 3.4.27 Proteins correlating with drug resistance across the adriamycin-resistant panel. Numbers in brackets indicate spot numbers.

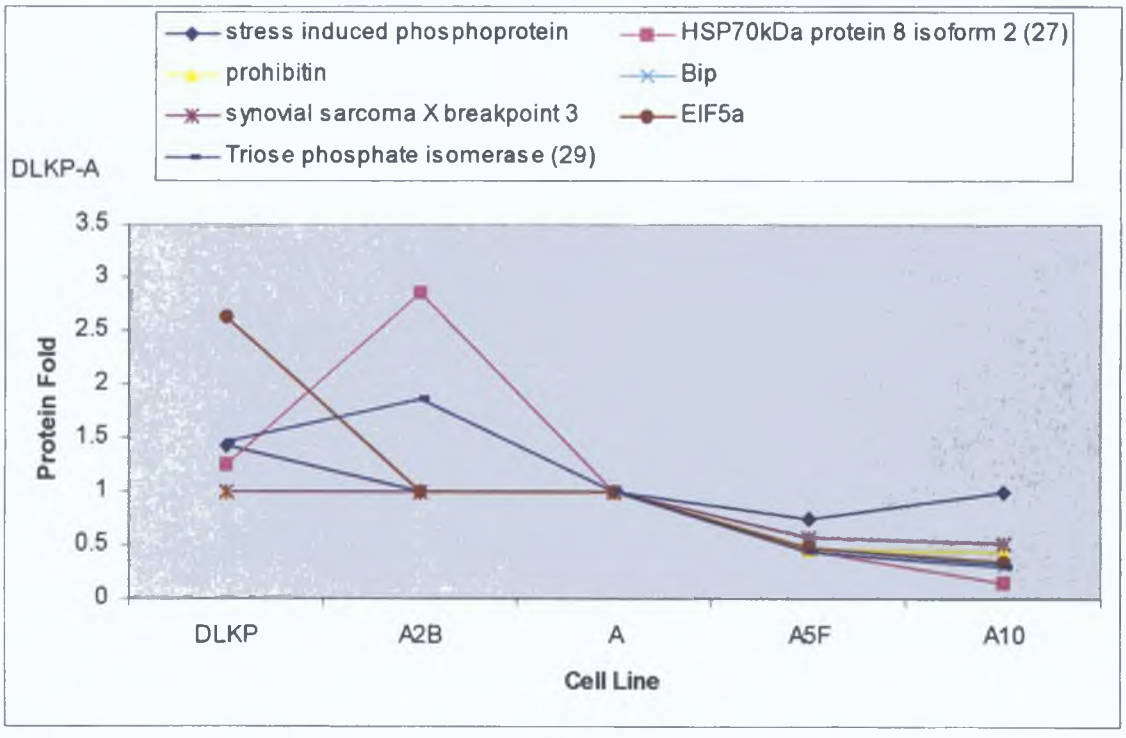

Figure 3.4.28 Proteins inversely correlating with increasing resistance (Brackets indicate spot number where isoforms are present).

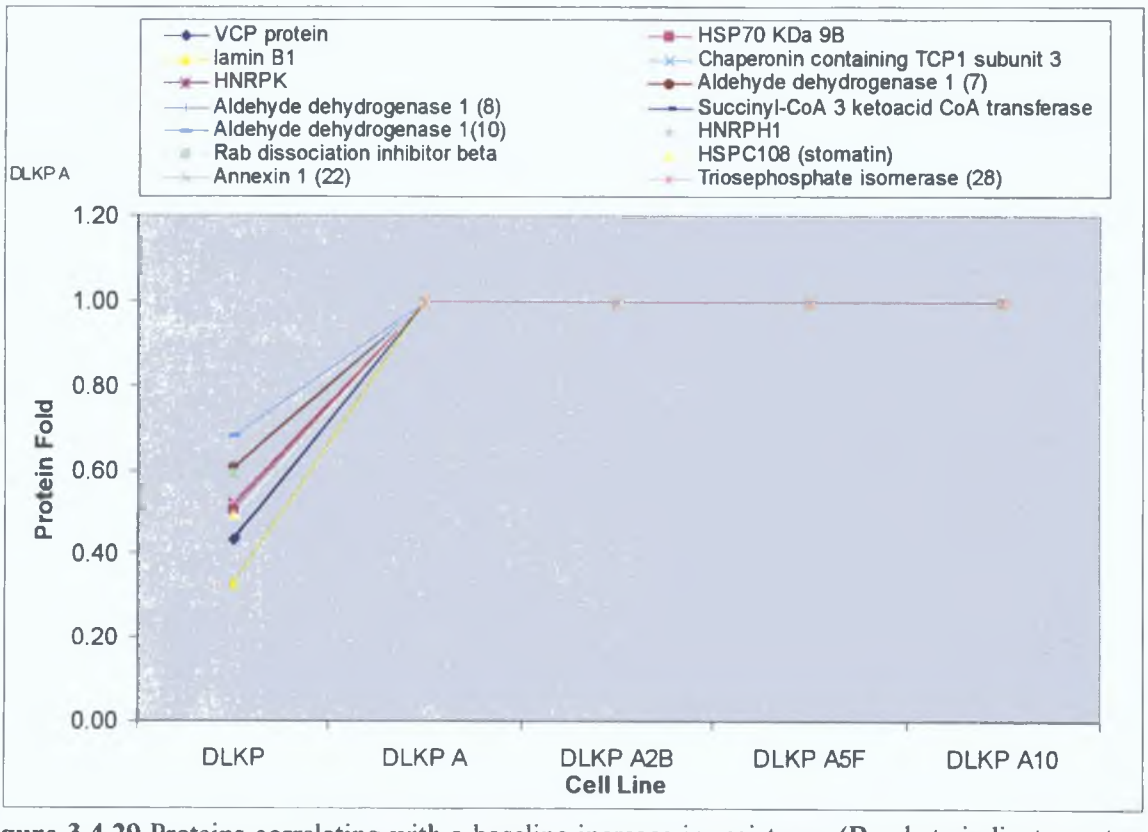

Figure 3.4.29 Proteins correlating with a baseline increase in resistance (Brackets indicate spot number where isoforms are present).

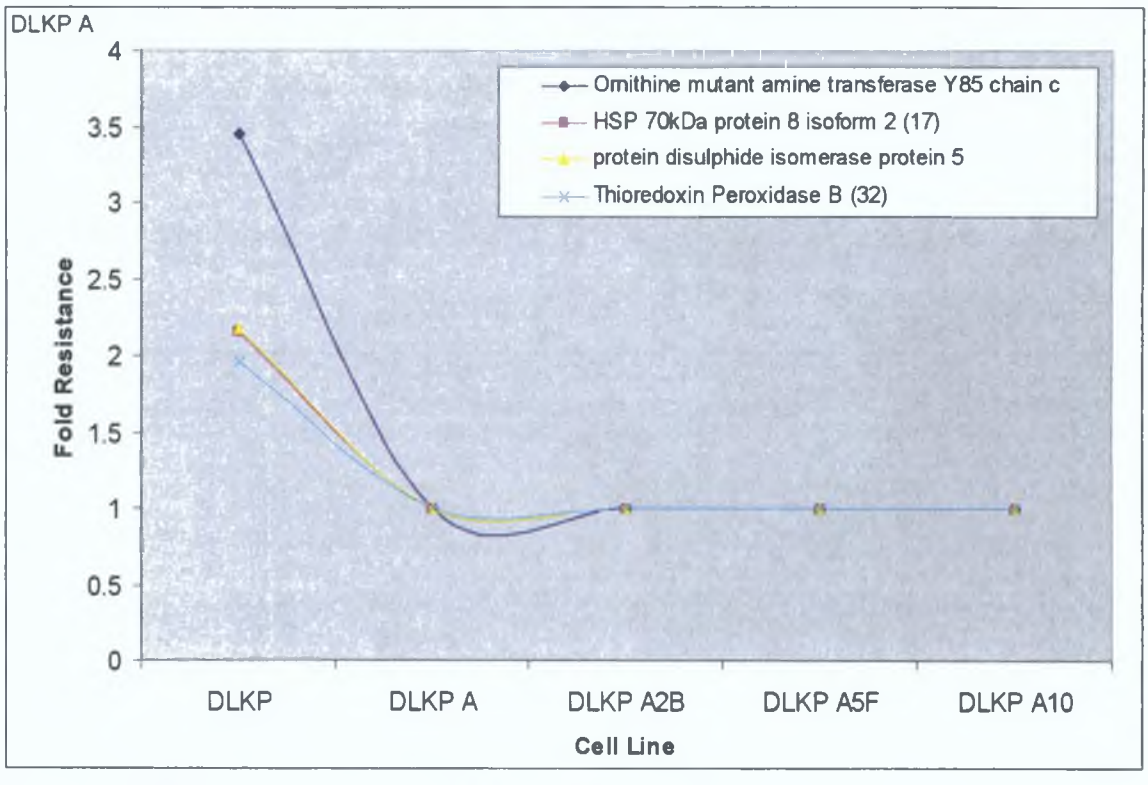

Figure 3.4.30 Proteins inversely correlating with a baseline resistance (Brackets indicate spot number where isoforms are present).

4.2.4 Overview of proteins that increased with drug resistance

4.2.4.1 Annexin A1

The annexins are a family of structurally related water-soluble calcium- and phospholipid-binding proteins, which total 20 (Vishwanatha *et al.*, 2004). Annexin A1 is a 35-kDa member of this annexin superfamily. Each annexin has a very conserved C-terminal domain, composed of four (or 8 for ANXA6) repeated sequences of seventy amino acids. In contrast, the N-terminal sequence of all annexins is unique and confers the biological specificity of the individual proteins. The N-terminal domain of ANXA1 is composed of 44 amino acids and includes sites for protein kinase C, tyrosine kinase phosphorylation, glycosylation, acetylation and proteolysis (Mulla *et al.*, 2004). The protein was first identified to be an important mediator of the anti-inflammatory actions of glucocorticoids in the immune system. Further work revealed that it plays important roles in many other physiological and pathological processes including, cell growth, differentiation, apoptosis, membrane fusion, endocytosis and exocytosis (John *et al.*, 2004; Bai *et al.*, 2004). It has been identified in every major peripheral endocrine organ in the body (pancreas, testis, ovary, thyroid, adrenal gland, thymus and placenta). Cell

fractionation studies determined that ANXA1 is found in three distinct pools namely, the cytoplasm, embedded in the membrane structures and finally attached to the outer surface of the plasma membrane (John *et al.*, 2004). It is a critical mediator of apoptosis. Overexpression has been observed in pancreatic, breast, hepatocellular, pituitary adenoma and gastric cancers. Reduced or no expression of annexin I has been reported in prostate, endometrial and esophageal cancers. Differential regulation of annexin I in a tissue specific manner could be associated with the development of cancers in these sites (Vishwanatha *et al.*, 2004; Bai *et al.*, 2004). Five isoforms of annexin A1 were found to be differentially expressed across the adriamycin resistant panel (Figure 4.2.1). Multiple isoforms of annexin A1 exist, which may be the result of post translational modifications.

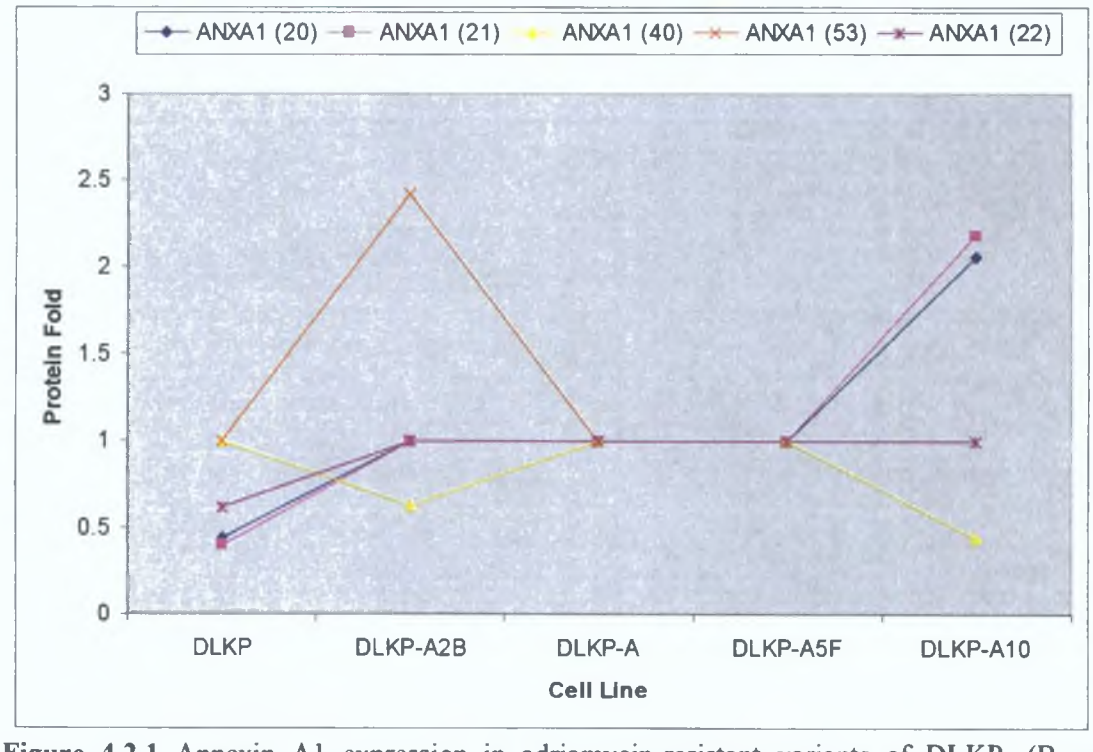

Figure 4.2.1 Annexin A1 expression in adriamycin-resistant variants of DLKP. (Brackets indicate protein number where isoforms are present).

The role of annexins in tumour biology is attracting more interest as members of the annexin family are being increasingly implicated in the signalling processes that regulate the cell cycle and also because dysregulation of annexin expression has been described in a variety of cancerous and precancerous cells and tissues. Decreased expression of annexins 1, 2, 4 and 7 have been found in prostrate cancers but not in benign prostatic hyperplasia (Smitherman *et al.*, 2004). Similarly, reduced expression of

annexins 1 and 5 have been discovered in malignant endometrial tissue (Mulla *et al*, 2004) In contrast, annexin 1 expression is significantly increased in malignant breast, liver, gliomas and stomach tumours (Liu *et al*, 2002) Further analysis of both expression and function of the annexin family members may lead to the identification of new markers of tumour progression and of potential targets for therapeutic intervention

Annexin I is thought to be involved in cell proliferation and differentiation and has been shown to be expressed on the surfaces of lymphoma cells where it functions as an endothelial cell adhesion molecule Ahn *et al* (1997) used biopsy tissues to determine the expression of annexin I in relation to breast cancer development and progression Immunohistochemical analysis of paraffin-embedded ductal epithelial cells revealed that annexin I was generally expressed in the various types of breast cancers, including noninvasive ductal carcinoma *in situ*, invasive and metastatic breast tumours (n = 33) This suggests that annexin I expression may correlate with malignant breast cancer progression and is most likely to be involved at an early stage of human breast cancer development

Muller *et al* (2004) suggests that ANXA1 is expressed in abundance by normal cells that proliferate rapidly (buccal and alveolar epithelial cells) Moreover, experiments on lung-derived cell lines (epithelial carcinoma and ANXA1-null fibroblast) provided evidence that ANXA1 mediates the inhibitory effects of glucocorticoids on EGF-stimulated cell growth, by disrupting EGF-signalling via a process involving tyrosine phosphorylation of ANXA1 However, other data suggests that tyrosine phosphorylation increases the growth of primary hepatoma cells

The up-regulation of annexin I has been found to correlate with increased synthesis of epidermal growth factor (EGF) and therefore with increased phosphorylation of the tyrosine kinase, EGF receptor (EGFR) Annexm 1 is a substrate for tyrosine kinases and serine/threonine kinases such as protein kinase C It is able to modulate the extracellular signal-regulated kinase (ERK) signal cascade at an upstream site Overexpression of annexin 1 may result in constitutive activation of ERK1-2 kinase in macrophages Abnormally high expression levels of a number of important tyrosine kinase growth factors and receptors, especially from the EGF family were found in pancreatic cancer (Bai *et al* 2004) This may contribute to the neoplastic growth by autocrine and paracrine effects Annexin 1 expression was up regulated in 84 6% of pancreatic cancers and multi-tissue microarrays showed that annexin 1 was 71 4% positive compared to

normal pancreatic tissue (18 4%) (P<0 01) High expression of annexin 1 has since been correlated with the differentiation of pancreatic adenocarcinoma during tumourigenesis Detection of annexin 1 expression could be an aid to a clinical diagnosis and may assess the prognosis of pancreatic cancer They found that annexin 1 expression was correlated with the poorly differentiated type of pancreatic cancer suggesting that annexin 1 may be involved in histological differentiation (Bai *et al* , 2004)

Both annexin 1 and annexin 5 translocate to the cell surface Annexin 5 is a marker of apoptosis Mulla *et al* (2004) examined the expression, phosphorlyation status and distribution of annexin 1 and 5 in 42 pituitary adenomas, normal pituitary tissue and in two carcinomas (an astrocytoma and a GH-secreting carcinoma) by Western blot and RT-PCR Their results provide evidence for the modest expression of ANXA1 by pituitary adenomas localised mainly but not exclusively to nonendocrine cells ANXA5 expression was more variable and was found in both endocrine and nonendocrine cells However, there was marked expression of both annexins in the tumour and non-tumour cells of the two carcinomas The results also provide some insight into the phosphorylation status of ANXA1 as a serine-phosphorylated species of ANXA1 was detected in all pituitary tumours In contrast, only four adenomas and the GH carcinoma expressed a tyrosine-phosphorylated ANXA1 Expression of ANXA1 and ANXA5 in human pituitary tumours raise the possibility that these proteins influence the growth and/or functional activity of the tumours Cell surface overexpression of annexin 2 may contribute to the development of metastases and invasion by increasing the detachment of tumour cells

Annexm A1 binds to F-actin and also interacts with profilin, a G-actin binding protein and regulator of actin polymerization Partial overlapping intracellular localization of the two proteins suggests that the annexin A1-profilin interaction may participate in regulating the membrane-associated cytoskeleton (Gerke and Moss, 2002, Hayes *et al* , 2004) The role of annexm A1 in membrane interaction with actin structures and regulation of the membrane-associated cytoskeleton could contribute to differences in invasiveness

4 2 4 2 Nucleoside diphosphate kinase 1

Nucleoside diphosphate kinase (NDPK) is a tumour metastasis suppressor An inverse correlation exists between the metastatic invasion and the level of NDPK observed in melanomas, hepatocellular carcinomas and, in some studies, breast carcinomas Overexpression of NDPK positively correlates with aggressiveness in the case of neuroblastomas (Lacombe, 1993) Nucleoside diphosphate kinase is decreased in DLKP and DLKP-A2B by 1 54-fold and 1 28-fold respectively with respect to DLKP-A However, the protein is increased in DLKP-A10 by 1 27-fold Low expression of NDPK has been correlated with poor patient prognosis and survival, lymph node infiltration and histopathological indicators of high metastatic potential in a number of cancer types, including mammary and ovarian carcinomas and melanoma In other tumour types, no correlation has been established Transfection of NDPK cDNA into highly metastatic breast, melanoma, prostrate and squamous cell carcinomas and colon adenocarcinoma cells significantly reduced the metastatic competency of the cells in vivo In culture, cell motility, invasion and colonisation were inhibited, whereas tumourigenicity and cellular proliferation were not affected, indicating that NDPK acts as a metastasis suppressor (Hartsough and Steeg, 2000)

4 2.4.3 K130r mutant of human DJ-1

K130r Mutant of human DJ-1 (PARK7), originally cloned as a putative oncogene, is capable of transforming NIH-3T3 cells in cooperation with H-ras It has also been implicated in fertilisation, regulation of androgen receptor signalling and oxidative stress Mutations of the DJ-1 gene are associated with autosomal early-onset Parkinson's disease It has been suggested that DJ-1 may play a role in tumourigenesis, in breast, NSCLC and prostate cancers It was identified as a negative regulator of the tumour suppressor PTEN, promoting cell survival in primary breast and lung cancer patients It has also been described as a circulating tumour antigen in serum from 37% of newly diagnosed patients with breast cancer (Pardo *et al*, 2006) This protein is up-regulated in DLKP versus DLKP-A and DLKP-A versus DLKP-A10 Mitoxantrone and taxane exposure also resulted in increased expression of this protein

4 2 4 4 Replication A2, 32kDA

The replication A2 32 kDa protein correlated directly with resistance in the DLKP variants being 1 5-fold lower in DLKP and DLKP-A2B compared to DLKP-A Replication protein A (RPA) is a single-stranded DNA (ssDNA) binding protein involved in various processes including nucleotide excision repair and DNA replication It is a heterotrimer composed of three subunits - 70, 32 and 14 kDa The 32 kDa subunit of RPA (RPA32) differentially expressed in these studies is phosphorylated in response to various DNA-damaging agents Two protein kinases, ataxia-telangiectasia mutated (ATM) and the DNA-dependent protein kinase (DNA-PK) have been implicated in DNA damage-induced phosphorylation of RPA32 Phosphorylation occurs in a cell cycle-dependent manner and begins at the G1/S transition and extends until late mitosis The DNA-damaging agents include ionising and ultraviolet radiation, camptothecin and adriamycin (Wang *et al*, 2001) Block *et al* (2004) produced an RPA32 Thr21 phosphospecifc antibody and identified Thr21 as an *in vitro* phosphorylation site of both DNA-PK and ATM Both DNA-PK and ATM phosphorylate RPA32 on Thr21 *in vitro* This phosphorylation was ATM dependent in response to IR, UV and adriamycin However, the relative roles of ATM and DNA-PK in the site-specific DNA damage-induced phosphorylation of RPA32 have not been reported Thus, the regulation of RPA32 Thr21 phosphorylation by multiple DNA damage response protein kinases suggests that Thr21 phosphorylation of RPA32 is a crucial step within the DNA damage response Adriamycin and VP-16, both topo II poisons, induced Thr21 phosphorylation However, only the adriamycin-induced Thr21 phosphorylation was ATM dependent Topo II poisons stabilize the topo II-DNA cleavage complexes (Powis *et al*, 1994) These can lead to the induction of DNA double-strand breaks chromosomal translocations and other mutagenic events (Powis *et al*, 1994) The varied ATM dependency with which adriamycin and VP-16 induced RPA32 Thr21 phosphorylation may reflect the ability of adriamycin to generate ROS or to intercalate DNA

4.2.5 Overview of proteins correlating with baseline drug-resistance

4.2.5.1 Aldehyde dehydrogenase 1A1

One of the toxic effects of the reactive oxygen species is the production of toxic aldehydes by lipid peroxidation. Aldehydes are highly reactive molecules that can be generated from a limitless number of endogenous sources such as amino acids, biogenic amines, or lipid metabolism and exogenous sources including aldehydes derived from xenobiotic metabolism. While some aldehyde-mediated effects such as vision are beneficial, many are deleterious including cytotoxicity, mutagenicity and carcinogenicity. The aldehyde dehydrogenase enzymes have evolved to metabolize aldehydes to less reactive forms (Lindahl, 1992). Three isoforms of aldehyde dehydrogenase are consistently up-regulated in DLKP versus DLKP-A. There are twelve known human *ALDH* genes which encode for 12 corresponding enzymes (Yoshida *et al.*, 1997). The aldehyde dehydrogenases are a family of NADP-dependant isoenzymes, which are expressed in many tissue types and in all subcellular fractions. They catalyze the oxidation of a broad spectrum of aliphatic and aromatic aldehydes (Lindahl, 1992) e.g. benzaldehyde and aldehydes derived from the lipid peroxidation process and those derived from drugs which are metabolised by cells into active compounds (Canuto *et al.,* 2001). Three major classes of mammalian ALDHs have been identified. Classes 1 and 3 both contain constitutively expressed and inducible cytosolic forms. Class 2 consists of constitutive mitochondrial enzymes. The classes appear to oxidize a variety of aldehydes (Lindahl, 1992). Aldehyde dehydrogenase is implicated in the sensitisation of certain cells to aldehydes. Canuto *et al.* (2001) developed a synthetic suicide inhibitor of ALDH1 which is also an irreversible inhibitor of ALDH3. This inhibitor induced bcl2-overexpressing cells to undergo apoptosis. Four hours after treatment with 25 μM ATEM, ALDH activity using benzaldehyde or propionaldehyde in hepatoma cells was decreased by 40% and cell number by 15% compared with controls. As cell growth did not resume when the inhibitor was removed from the culture medium, it strongly suggested that ALDHs play a pivotal role in mediating cell death. ALDHs have also been attributed to a protective role against ROS-induced apoptosis, in particular ALDH2 (Ohsawa *et al.*, 2003). Tsukamoto *et al.* (1998) attributed increased aldehyde dehydrogenase with resistance to cyclophosphamide in mouse leukaemia cells. A link has been found between DNA-damage and apoptosis induced by ROS-dependent Fas aggregation (Huang *et al.*, 2003).

Sladek *et al.* (2002) semi-quantified the cellular levels of ALDH1A1 and ALDH3A1 to predict the clinical responses to cyclophosphamide-based chemotherapeutic regimens. However, while the levels of both varied widely, retrospective analysis revealed that cellular levels of only ALDH1A1 were significantly higher in the metastatic breast cells that had survived the exposure to cyclophosphamide than in those that had not been exposed. Interestingly, the therapeutic outcome of cyclophosphamide-based chemotherapy corresponded to cellular ALDH1A1 levels in 77% of cases with partial or complete responses occurring 2.3 times more often when the ALDH1A1 level was low than when it was high. This could provide a rational basis of individualised therapeutic regimens.

Succinyl-CoA:3-ketoacid CoA transferase is a mitochondrial enzyme in mammals that is essential for the metabolism of ketone bodies. It is responsible for the transfer of coenzyme A (CoA) from succinyl-CoA to acetoacetate. Once activated, acetoacetyl-CoA is further metabolized into acetyl-CoA, which can either enter the citric acid cycle or be stored ultimately as a fatty acid. This protein is increased (2.3-fold) in DLKP versus DLKP-A.

4.2.5.2 Messenger RNA Processing Proteins - HnRNP F, K and H1

Heterogeneous nuclear ribonucleoproteins (hnRNPs/HNRPs) are a large family of nucleic acid-binding proteins that bind heterogeneous nuclear RNA (hnRNA), the transcripts produced by RNA polymerase II and precursors to mRNAs. This family of proteins includes, hnRPA, H, C, K and F. They are involved in the processing of RNA molecules from transcription to translation, including splicing, transportation from nucleus to cytoplasm, degradation and translation of RNAs. HnRNPs have been overexpressed in several cancers. In lung cancer, hnRNP A2/B1 have been suggested as useful early detection markers for lung carcinoma (Pino *et al.,* 2003) with higher levels of hnRNP mRNA in SCLC than NSCLC. Some of these proteins (hnRNP C1 and C2) are substrates for activated caspases during apoptosis. All these proteins are involved in maintaining a balance between cell death and cell survival. Their overexpression might be responsible for a greater ability of cells to counteract adriamycin effects, for example adriamycin-induced oxidative stress is strongly limited by the overexpression of peroxiredoxin 1 and RNA synthesis is conserved by the overexpression of hnRNPK.

Differential protein expression of both hnRPK and H1 were seen in the adriamycin resistant variant of DLKP. HnRNP appeared to be involved in baseline resistance as it

was increased by 1 52-fold from the parent and remained unchanged in the variants HnRPK on the other hand appeared in the more resistant variant DLKP-A10

HnRNP F is a regulator of pre-mRNA splicing It binds preferentially to Cap Binding Complex-RNA complexes but not to naked RNA HnRNP F is involved in regulating the splicing of Bcl-x, a member of the Bcl-2 family of proteins which, are key regulators of apoptosis The Bcl-x pre-mRNA is alternatively spliced to yield Bcl-x_S and Bcl-x_L, two isoforms that have been associated, respectively, with the promotion and prevention of apoptosis A 30-nucleotide G-rich element (B2G) which is responsible for regulating mRNA splicing of Bcl-x was found to bind to hnRNP F Depletion of hnRNP F from HeLa cell nuclear extract was found to decrease the efficiency of pre mRNA splicing (Gamberi *et al*, 1997) The addition of hnRNP F to a HeLa extract improved the production of the Bcl-x_S variant Consistent with the *in vitro* results, small interfering RNA targeting hnRNP F and H decreased the Bcl-x_S/Bcl-x_L ratio of plasmid-derived and endogenously produced Bcl-x transcripts These results show a positive role for the hnRNP F proteins in the production of the proapoptotic regulator Bcl-x_S (Garneau *et al*, 2005)

Heterogeneous nuclear ribonucleoprotein K protein has been found in the nucleus, cytoplasm and mitochondria and is implicated in chromatin remodelling, transcription, splicing and translation processes It contains multiple modules that on the one hand, bind kinases while on the other hand recruit chromatin, transcription, splicing and translation factors These protein-mediated interactions are regulated by signalling cascades These observations are consistent with hnRNP K protein acting as a docking platform to integrate signalling cascades by facilitating cross talk between kinases and factors that mediate nucleic acid directed processes (Bomsztyk *et al*, 2004) HnRNP K binds to CU rich repetitive stretches known as DICE (differential control elements) elements in mRNA 3'UTRs and can block translation initiation by blocking the recruitment of the 60S ribosomal subunit and the formation of the translation competent 80S ribosome (Bomsztyk *et al*, 2004)

4 2 6 Overview of proteins inversely correlating with increasing and baseline resistance

4 2 6 1 Prohibitin

Prohibitin (PHB) was decreased in DLKP-A versus DLKP-A5F and DLKP-A versus DLKP-A10 by 2 13-fold and 2,28-fold respectively PHB is a highly conserved 32 kDa protein with homologues in all animal species, yeast and plants (Gamble *et al*, 2006) Upon discovery, it was suspected to be a tumour suppressor protein (Nuell *et al*, 1991) It was found in the inner membrane of the mitochondria, where it acts as a chaperone in a complex with the structurally similar protein BaP37/REA (repressor of oestrogen receptor activity) (Coates *et al*, 1997) Prohibitin has multiple functions in aging, epithelial cell migration, cell cycle control, apoptosis and as associated molecules in cell surface receptors in mammalian cells Evidence shows it has a nuclear function in transcription regulation (Peng *et al*, 2006) PHB has been found in the nucleus of ovarian granulosa, breast epithelial and prostate epithelial cells (Thompson *et al*, 2001, Wang *et al*, 2002, Gamble *et al*, 2004) whereby it interacts with proteins such as nuclear corepressor (NCoR), histone deacetylase 1 (HDAC1) and retinoblastoma (Rb) to repress activation of genes regulated by the E2F family of transcription factors (Wang *et al*, 1999) This repression of E2F1 activity has been shown to be important in the protection of Ramos B cells from camptothecin-induced apoptosis (Fusaro *et al*, 2002) Recruitment of PHB and BRG1/BRM has been shown to inhibit E2F activation and cause growth arrest in breast cancer cells treated with tamoxifen It is also involved in the mitogen-activated protein kinase pathway (Rajalingam *et al*, 2005)

4 2.6.2 Eukaryotic translation initiation factor 5A (eIF 5a)

Eukaryotic translation initiation factor 5A is the only cellular protein that contains the unusual amino acid hypusine Vertebrates carry two genes that encode two eIF 5A isoforms, eIF5A-1 and eIF5A-2, which, are 84% identical m humans Stimulation of eIF 5A leads to methionyl-puromycin synthesis, although the true physiological activity of this factor has yet to be elucidated (Clement *et al*, 2006) It has been proposed to be a mRNA-specific initiation factor (Kang and Hershey, 1994) The protein is decreased in DLKP versus DLKP-A by 2 63-fold The protein is further decreased in DLKP-A versus DLKP-A5F and DLKP-A versus DLKP-A10 by 2 04-fold and 2 85-fold respectively Essential for sustained proliferation of mammalian cells, eIF 5A and may therefore contribute to malignant cell transformation and eIF 5A probably acts in the

final stage of the initiation phase of protein synthesis by promoting the formation of the first peptide bond (Hershey, 1991)

Chen *et al* (2003) examined eIF-5A expression in lung adenocarcinomas Increased expression was present in tumours showing poor differentiation, 12/13th codon K-*ras* mutations, p53 nuclear accumulation and tumours with positive lymphocytic response Patients having a higher eIF-5A protein expression showed a relatively poorer survival suggesting the use of eIF-5A as prognostic marker in lung adenocarcinoma

Proteins inversely correlating with base line drug resistance include protein disulfide isomerase protein 5, ornithine mutant amino transferase chain c, heat shock protein 70 kDa protein 8 isoform 2 (17) and thioredoxin peroxidase B The latter two are discussed in sections 4 2 6 and 4 2 7

4 2.7 Overview of proteins correlating with invasion

DLKP and the drug resistant variants also display differential invasion potential in the order DLKP-A2B < DLKP-A10 < DLKP < DLKP-A < DLKP-A5F with DLKP-A2B being the least invasive and DLKP-A5F the most invasive (section 3 4 1 2) A number of proteins were found to correlate with this increase in invasion namely, eukaryotic translation elongation factor 1D, annexin 1, horf 6a human peroxidase enzyme and HPRT (Figure 4 2 2) Gamma actin is inversely correlated with invasion

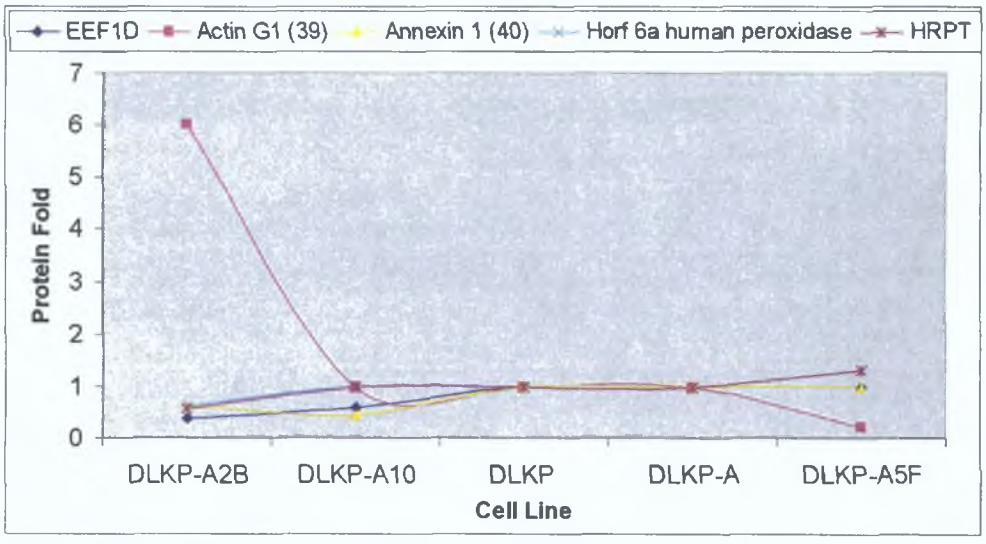

Figure 4.2.2 Proteins correlating and inversely correlating with invasion

Actin is largely responsible for cell motility and altered expression in some malignancies may facilitate aggressive invasion. In vertebrates, 3 main groups of actin isoforms, alpha, beta and gamma have been identified. The alpha actins are found in muscle tissues and are a major constituent of the contractile apparatus. The beta and gamma actins coexist in most cell types as components of the cytoskeleton and as mediators of internal cell motility (Christian *et al.*, 2001).

EEF1D was overexpressed in chemoresistant melanoma cells (Sinha *et al.*, 2000) and its expression along with RPL30 and RPS20 correlated adversely with survival in medullobalstoma (Bortoli *et al.*, 2006).

4.2.8 Proteomic analysis of the mitoxantrone resistant variant of DLKP

A proteomic investigation was carried out to study the differential protein expression caused by mitoxantrone resistance in the already established DLKP-Mitox cell line. While the main mechanism of resistance in this cell line is associated with BCRP (no detectable levels of P-gp and MRP1), little information on cytoplasmic changes is available. Resistance to mitoxantrone has shown changes in ABC membrane pumps Pgp, MRP-1 (McMorrow *et al.*, 2006) and BCRP (Doyle *et al.*, 1998), alterations in topoisomerase activity or translational modification (Chen *et al.*, 2002) and apoptosis induction (Nakanishi *et al.*, 2005). This work has yielded a total of 50 differentially expressed proteins (61 including all isoforms) that may present targets for drug resistance/invasion intervention. None of the ABC transporters were identified as differentially expressed. This is not surprising given the limitations of detecting high molecular weight and hydrophobic proteins on two-dimensional gel electrophoresis.

Previous work revealed thioredoxin, stratafin, annexin 1, cofilin, Rho-GDP inhibitor, FaBP and APRT to be differentially regulated in mitoxantrone-resistant variants of colon, fibrosarcoma and pancreatic adenocarcinomas (Sinha *et al.*, 1999a; Sinha *et al* 1999b; Sinha *et al.*, 1998). Further studies in mitoxantrone-resistant MCF-7 breast cells showed tropomyosin, HMG-1, prohibitin, HSP 70, heterogeneous nuclear ribonucleoproteins (H and K) and nucleophosmin to be differentially regulated (Fu and Fenselau, 2005; An *et al.*, 2005). Many of these proteins have been differentially regulated in DLKP-Mitox, consistent with previous reports (PDI, annexin I, P4HB, thioredoxin, HMG1, NDPK and nucleophosmin). Tropomyosin, prohibitin, ER-60, HNRPF, TPI and cofilin are not consistent with previous results.

According to PathwayAssist, two of the most highly interacting proteins are tropomyosin and HMG1. Tropomyosin acts as an anti-oncogene and tumour suppressor and decreased expression has been observed in many transformed cells (Shah *et al.*, 1998). Invasion assays on DLKP and DLKP-Mitox revealed that the mitoxantrone variant was less invasive than the parent cell line used in these studies. A number of proteins directly involved in metastasis and invasion are differentially regulated, the majority of which are all down-regulated in DLKP-Mitox. They include nucleoside diphosphate kinase, nucleophosmin, phosphoglycerate mutase 1, prohibitin, tropomyosin and galectin-1. However, other proteins also linked to invasion, namely high mobility group box protein and annexin 1, are up-regulated. Tropomyosin, down-

regulated in MCF-7/MX and in SNU-drug resistant gastric cancers (Yoo *et al*, 2000), was up regulated in DLKP-Mitox This is unexpected as DLKP-Mitox is less invasive than the parent and suppression of tropomyosin has been related to a metastatic phenotype (Barkin *et al*, 2005)

4 2.8 1 Nucleophosmin

Nucleophosmin (NPM) is a nucleolar phosphoprotein that binds the tumour suppressors p53 and $p19^{Arf}$ It is thought to be indispensable for ribogenesis, cell proliferation and survival after DNA damage The NPM gene is the most frequent target of genetic alterations in leukaemia's and lymphomas However, its role in tumourigenesis is unknown Mouse cells null for both p53 and NPM grow faster than control cells and are more susceptible to transformation by activated oncogenes, such as mutated Ras or overexpressed Myc NPM regulates DNA integrity and through Arf, inhibits cell proliferation (Colombo *et al*, 2005) Overexpression of nucleophosmin mRNA was independently associated with bladder cancer recurrence and progression In patients with muscular invasion disease, Overexpression of mRNA was associated with the greatest risk of recurrence and progression (Tsui *et al*, 2004)

4 2 8.2 Sorcin

Sorcin, also known as VP19 and CP22, is a 22 kDa calcium-binding protein first identified in a VCR-resistant Chinese hamster lung cell line, DC-3F/VCRd-5L (Van der Bliek *et al*, 1986) A direct binding assays showed that it is a calcium-binding protein with four 'E-F hand' structures typical of calcium-binding sites, two of which contain putative recognition sites for cAMP-dependent protein kinase It has been implicated in the development of resistance to a variety of chemotherapy drugs including colchicines, actinomycin D, taxol, vinblastine, temposide, VP-16 and doxorubicin in a variety of cancers (Roberts *et al* 1989, Wang *et al*, 1995) Overexpression of sorcin in three MDR solid tumour cell lines including an adriamycin-resistant MCF-7/ADR (breast carcinoma), a cisplatin $A549^{DDP}$ (lung carcinoma) and a VCR-resistant KBv200 (epidermoid carcinoma line) line was not observed This indicates that sorcin may represent a significant and independent indicator of leukaemia resistance to chemotherapies (Zhou *et al*, 2006)

Sorcin was 1 51-fold increased in DLKP-A and a further 1 47-fold increased in DLKP-A5F In contrast, sorcin was down-regulated by 2 33-fold in the most adriamycin-resistant cell line, DLKP-A10 (Figure 4 2 7) Interestingly, the protein is overexpressed to a greater extent (3 85-fold) in the mitoxantrone-resistant variant, DLKP-Mitox compared to the adriamycin-resistant variants

Its function in drug-resistance has been controversial Hamada *et al* (1988) reported that overexpression of sorcin was not sufficient or even necessary for the development of MDR in human myelogenous leukaemia cell line K562/ADR Further studies with this cell line revealed that overexpression of sorcin in K562/ADR cells may play an important role in the development of the multidrug resistance through its interactions with free ribosomes (Sugawara *et al*, 1989)

Up-regulation of sorcin in patients with acute myeloid leukaemia was similar to that of *mdr1* and associated with low complete response to chemotherapies as well as poor overall clinical prognosis In K562 cells, sorcin-transfection resulted in increased resistance to adriamycin (2 7- to 7 9-fold) and like the *mdr1*-amplified K562 cells, were cross-resistant to several other chemotherapeutic agents (Zhou *et al*, 2006) Sorcin-targeted small interfering RNA (siRNA) resulted m approximately 80% reversal of adriamycin resistance in human leukemia cells (Zhou *et al*, 2006) However, in MDR lymphoma cell lines with increasing resistance, sorcin was found to be co-amplified with MDR-1 due to its close proximity to the mdr-1 gene (Lee, 1996, Tan *et al*, 2003)

Sorcin has been implicated in apoptosis Qi *et al* (2006) examined the effects of sorcin overexpression on both chemotherapeutic agent-induced apoptosis and the expression of apoptosis-related proteins Bcl-2 expression was upregulated and Bax was moderately reduced with increased resistance to etoposide-induced apoptosis Sorcin may also regulate cell apoptosis by modulating intracellular calcium level and/or distribution as it may sequester significant amounts of cytosolic calcium It may be translocated to the endoplasmic reticulum membrane and block calcium release mediated by the cardiac ryanodine receptor The overexpression of sorcin in leukemia cells leads to significantly reduced intracellular calcium concentration which contributes to the decreased sensitivity of cancer cells to cytotoxic agent-mediated apoptosis, leading to the development of drug resistance

Parekh *et al* (2002) induced low levels of resistance to taxol by transfecting a human breast cancer cell line with sorcin cDNA However, high expression of sorcin did not induce high level resistance to taxol

The results in this study together with those of previous observations, further confirm that sorcin plays an important role in the drug-resistant phenotype Sorcin may therefore represent a good target for modulation and in the development more efficacious MDR reversal agents

4 2 8 3 High mobility group box protein

HMG-1, the high mobility group 1 box protein, was up-regulated in MCF-7/MX and DLKP-Mitox HMG-1 is involved in nuclear complex formation and DNA repair, inflammation, apoptosis and differentiation and may contribute to drug resistance by enhancing these activities Significantly, HMG1 was found to elicit activation of metalloproteases MMP-2 and MMP-9 (Taguchi *et al*, 2000), both of which were previously found to be increased in DLKP-Mitox (Liang *et al*, 2001) Prohibitin (PHB) is a mitochondrial chaperone involved in cell cycle control, cellular immortalisation (Tsai *et al*, 2006) and is up-regulated in MCF-7/MX and cisplatin-resistant head and neck tumors (Johnsson *et al*, 2000) PHB was down-regulated in DLKP-Mitox Proteins such as protein disulphide isomerase and TPI are commonly found to be expressed in a variety of cancers and may contribute to drug resistance (Liu *et al*, 2006) Gst M4, prolyl 4-hydroxylase B and TPI were significantly overexpressed in lung adenocarcinomas (Chen *et al*, 2002)

Sinha and colleagues (1998) suggested a mechanism of mitoxantrone resistance involving apoptosis (via Rho-GDP dissocation inhibitors and thioredoxin) and concerted actions on PKC activity (downstream effector of GST, Topo II and Pgp) Consistent with this, apoptosis in DLKP-Mitox may become more resistant to apoptotic signals through reduced expression of proteins stimulating apoptosis and elevated inhibitory proteins Fifteen of the differentially-expressed proteins have a role in apoptosis as shown in PathwayAssist Two of the three inhibitors (ALDH and PRDX3) are up-regulated while 7 of 12 stimulators are down-regulated

4 2 8.4 Cathepsin B and Cathepsin D

Cathepsins are proteases and the best characterised of the lysosomal hydrolases They are among many proteolytic enzymes involved in metastasis (Krueger *et al*, 1999) Proteases of the cathepsin family are the best-characterized lysosomal hydrolases Most cathepsins are cysteine-proteases (cathepsin B, C, H, F, K, L, O, S, V, W and X/Z) Two are aspartyl proteases (cathepsin D and E) and one is a serine protease (cathepsin G) (Linder and Soshan, 2005) The cytosol contains endogenous cysteine cathepsin inhibitors, cystatins (Turk and Bode, 1991) In contrast, no endogenous cathepsin D/E inhibitors have been found The degree of lysosomal permeabilization determines the amounts of cathepsins released into the cytosol A complete breakdown of all lysosomes results in necrosis, whereas partial breakdown (sufficient to overcome protection by the cystatins) may trigger apoptosis (Bursch, 2001)

Cathepsin B has been linked to tumour invasion and metastasis Malignant tumour cells (lung, colon, breast, stomach and prostate) express higher levels of cathepsin B mRNA and protein and activity levels (Hughes *et al*, 1998) *In vitro* invasion assays with Cathepsin B protease inhibitors such as the MMP inhibitor Batimastat, reduced invasion (Kobayashi *et al*, 1993, Kolkhorst *et al,* 1998) Cathepsin B is often overexpressed in premalignant lesions, primary cancers and especially in preneoplastic lesions, suggesting it might have pro-apoptotic features Expression of cathepsin B is regulated at many different levels, from gene amplification, use of alternative promoters, increased transcription and alternative splicing, to increased stability of transcripts Cathepsin B is synthesized as a preproenzyme and the primary pathways for its normal trafficking to the lysosome utilize mannose 6-phosphate receptors (Roshy *et al*, 2003) A change in the localisation of cathepsin B occurs during the transition to malignancy, as seen by the presence of cathepsin-containing vesicles at the cell periphery and the basal pole of polarized cells Active cathepsin B is also secreted from tumours, a mechanism likely to be facilitated by lysosomal exocytosis or extracellular processing by surface activators Cathepsin B is localised to caveolae on the tumour surface and bind to the annexin II heterotetramer Activation of cathepsin B on the cell surface leads to the regulation of downstream proteolytic cascades (Podgorski and Sloane, 2003)

Cathepsin B was decreased in the less invasive subclone of DLKP-A, namely DLKP-A2B by 1 87-fold However, Cathepsin D was increased in this cell line also

Cathepsin D is the major intracellular aspartyl protease and a mediator of IFN-gamma and TNF-alpha induced apoptosis Cathepsin D has been implicated in apoptosis

induced by a number of conventional anti-cancer agents including adriamycin, etoposide, cisplatin and 5-fluorouracil (Emert-Sedlak *et al*, 2005) The mechanisms leading to release of cathepsin from the lysosomes after treatment with these agents are unclear as is the relative importance of the lysosomal pathway for the cytotoxicity of these compounds

Injection of cathepsin D to the cytosol of fibroblasts induces caspase-dependent apoptosis Some cathepsins can induce pro-apoptotic cleavage of the BH3-only (Bcl-2 homology-3) protein Bid, leading to activation of the ability of Bid to act on other pro-apoptotic members of the Bcl-2 family (Linder and Soshan, 2005)

Cathepsin D has been associated with p53 status mRNA levels of cathepsin were increased in the wild-type p53-expressing PA1, ML1 leukemia and U1752 lung cancer cells but not in mutant p53-expressing cells following adriamycin exposure Pepstatin A, a cathepsin D inhibitor, suppressed p53-dependent apoptosis in lymphoid cells linking cathepsin D to p53-dependent tumour suppression and chemosensitivity (Wu *et al*, 1998)

Cathepsin D expression correlates with invasion and metastasis and poor prognosis Overexpression of Cathepsin D inhibited growth of colon, liver and ovarian cancer cells (Wu *et al*, 1998) Exposure to adriamycm, VP-16 or gamma-radiation increased cathepsin D exposure in leukaemia and ovarian cancer cells, breast cancer but not significantly in lung (Inoue *et al*, 1998)

Cathepsins have been shown to be important in cancer development and diagnosis However the mechanisms by which they exert their role is still not fully understood Therefore the presence of cathepsin D in lung tumours should be studied further as this protein could be of clinical relevance for the diagnosis and/or prognosis of lung cancer and other types of cancer (Alfonso *et al*, 2004)

4.2.8.5 Comparison between adriamycin and mitoxantrone resistance in DLKP

It was also of interest to compare proteins altered in DLKP versus DLKP-A with DLKP versus DLKP-Mitox as both adriamycin and mitoxantrone are alkylating agents and mitoxantrone is an analogue of adriamycin with less cardiotoxicity (i.e. it is supposed to produce less reactive oxygen species). Interestingly, mitoxantrone exposure resulted in lower fold changes in the chaperon and stress response proteins namely, chaperonin containing TCP subunit 3, mortalin (HSPA9B) and HSP 70 proteins 8 as would be expected. Both drugs induced relatively similar levels of two apoptotic/redox regulation proteins, galectin-1 and PARK7 and the overlapping glycolytic proteins namely the aldehyde dehydrogenases and triosephosphate isomerase. Mitoxantrone induced a significantly higher fold change in the protein turnover and metabolic proteins, protein disulfide isomerase (PDI) and ornithine aminotransferase respectively. Adriamycin exposure resulted in higher levels of annexin induction. However, mitoxantrone induced over twice the amount of sorcin and hnRPK (Figure 3.5.7).

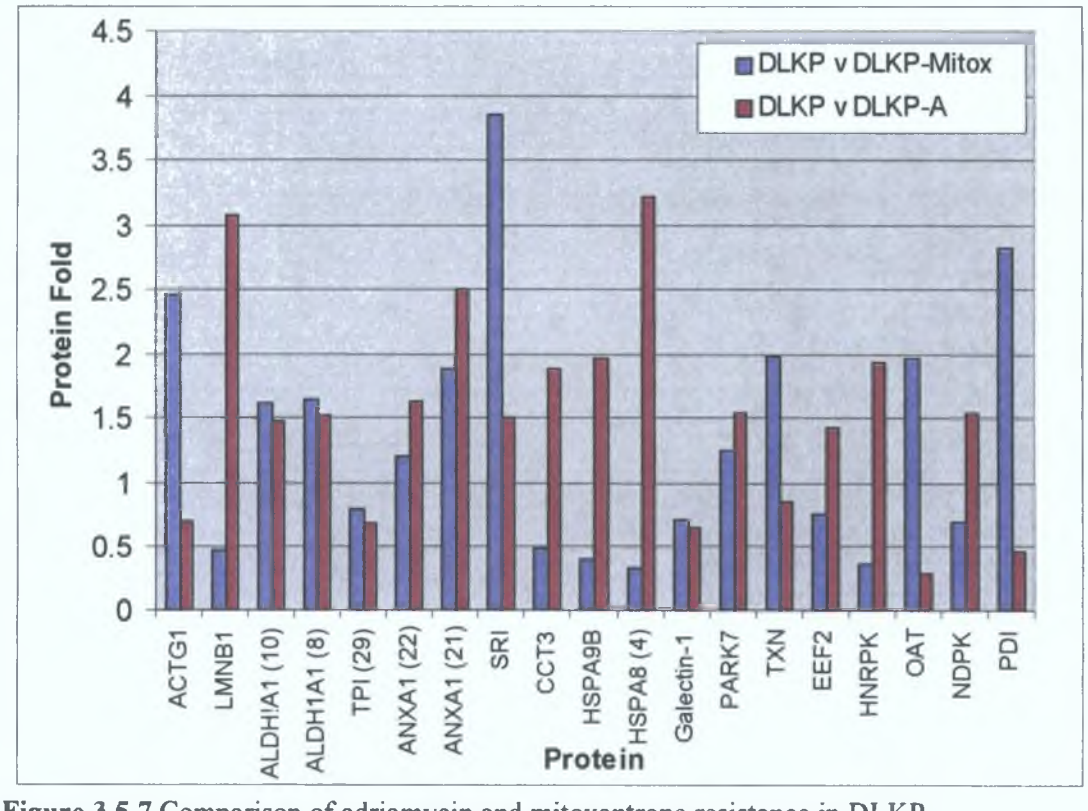

Figure 3.5.7 Comparison of adriamycin and mitoxantrone resistance in DLKP.

4.2.9 Proteomic analysis of taxane-resistant variants of SKMES-1

Proteomic analysis was carried out to study differential protein expression associated with taxane resistance in two cell lines developed in these studies, namely SKMES-Txt and SKMES-Txl (Wk3) The parental cell line, SKMES-1, not previously documented to be exposed to drug was selected with clinically relevant concentrations of the taxanes, taxol or taxotere, drugs traditionally used in the treatment of lung cancer The main mechanism of resistance in these cell lines is the membrane protein P-gp and therefore would not be expected to be identified by proteomics Pulse selection with taxotere yielded a total of 40 differentially expressed proteins Of these 40 proteins, 19 were unique to taxotere-selection Taxol exposure resulted in a total of 48 differentially expressed proteins Of these 48 proteins, 21 overlapped with SKMES-Txt, 23 were unique to SKMES-Txl (Wk3) and 4 overlapped with SKMES-Txl (Wk3) versus SKMES-Txl (Wk6) comparison

An unforeseen but fortunate result of taxane selection of SKMES-1 was the observed loss of resistance in both taxane-resistant variants Proteomic analysis was also carried out to study differential protein expression caused by loss of taxol resistance Twenty-five proteins were identified in the comparison of SKMES-Txl (Wk3) versus SKMES-Txl (Wk6), 11 of which overlapped with SKMES-1 versus SKMES-Txt, 4 with SKMES-1 versus SKMES-Txl (Wk3) and 10 were unique to SKMES-Txl (Wk3) versus SKMES-Txl (Wk6)

The stress response and chaperonin proteins, namely HSP 70 protein 8 isoform 2, HSP 60, 150kDa oxygen-regulated protein, CCT3 and HSPC124 are all increased in SKMES-Txt In contrast, three heat shock proteins, two of which are unique to SKMES-Txl (Wk3), HSP 70 protein 8 isoform 2, HSP27 and HSP 70kDa 9B are all decreased in SKMES-Txl (Wk3) Taxol-selection resulted in a greater fold decrease in the chaperonin proteins when compared to taxotere exposure

Loss of taxol resistance resulted in the HSPs being both up and down-regulated HSP60 and an isoform of HSP70A8 were 1 6-fold and 1 3-fold increased respectively However, the chaperonin protein KIAA0098 was decreased as well as two isoforms of HSPA8

4.2.10 Comparison between taxotere and taxol resistance in SKMES-1

Currently, much is known about the mechanism of action of the taxanes, little is known about the differences induced by taxol and taxotere. Taxol and taxotere have similar mechanisms of action even though taxotere is approximately twice as potent an inhibitor of microtubule depolymerisation relative to taxol (Gelman, 1994). Pulse selection with taxotere yielded a total of 40 differentially expressed proteins. Of these 40 proteins, 19 were unique to taxotere-selection. Taxol exposure resulted in a total of 48 differentially expressed proteins of which 23 were unique to SKMES-Txl (Wk3) and 21 overlapped with SKMES-Txt.

4.2.10.1 Overlapping proteins between taxotere and taxol resistance in SKMES-1

A number of proteins were differentially regulated in response to both taxotere and taxol exposure. Similar levels of regulation resulted for the majority of proteins with the exception of proteasome activator subunit 2 and peroxiredoxin 2, both of which are up-regulated at a greater level in SKMES-Txt (Figure 4.2.3).

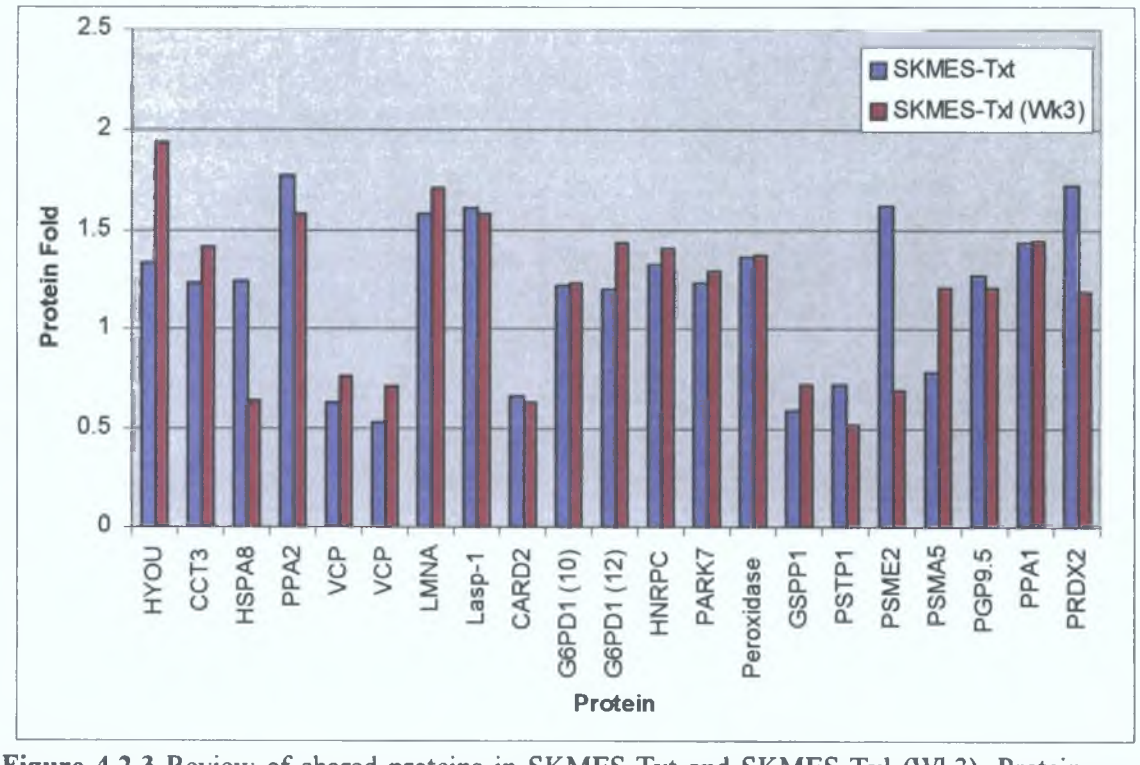

Figure 4.2.3 Review of shared proteins in SKMES-Txt and SKMES-Txl (Wk3). Proteins are grouped according to ontology. Brackets indicate spot number where isoforms are present.

4 2 10 2 Glucose-6-phosphate dehydrogenase

Glucose-6-phosphate dehydrogenase is the first and a rate limiting enzyme of the hexose monophosphate shunt It replenishes NADPH needed to maintain glutathione in concentrations to support the redox environment in the taxane-resistance cell lines This protein, present as three isoforms, is increased in both SKMES-Txt and SKMES-Txl (Wk3) to the same extent but not in SKMES-Txl (Wk6) Only taxol exposure resulted in the increase of the protein 6-phosphogluconolactonase, another enzyme involved in normal intermediary metabolism (Galperin *et al*, 2006)

Cytoskeletal disruption can lead to activation of NADPH oxidase and the production of intracellular ROS (Kustermans *et al*, 2004) Studies have described NF-κB activation in response to microtubule depolymerization such as taxol (Rosette *et al*, 1995) NF-κB activation is characterized by a reorganization of actin filaments, such as cellular adhesion on fibronectin, chemotaxis or phagocytosis (Kustermans *et al*, 2004) Taxol and taxotere exposure resulted in both increases and decreases in expression of cytoskeletal proteins

4 2 10 3 Keratin 8

The expression of keratin 8 was decreased in both taxotere and taxol resistant variants of SKMES There was no change in expression when SKMES-Txl (Wk3) was compared to SKMES-Txl (Wk6)

The intermediate filaments (IFs) constitute a large proportion of the cytoskeleton and nuclear envelope in most types of eukaryotic cells Although structural components of other major cytoskeletal proteins, like actin and tubulin are highly conserved in different cell types, constituent proteins of the IFs exhibit molecular diversity The keratins are a subfamily consisting of over 20 members (keratin 1-20) and are preferentially expressed in epithelial cells (Inada *et al*, 2001) Keratin 8 (K8) and 18 (K18) are the major components of the IFs of simple or single-layered epithelia and are found in the gastrointestinal tract, liver, exocrine pancreas and mammary gland, from which many carcinomas arise (Oshima *et al*, 1996) Functional studies with different cell models have suggested that K8 and K18 are involved in simple epithelial cell resistance to several forms of stress that may lead to cell death Caulin *et al* (2000) found knockout mice are deficient in K8 and K18 are approximately 100 times more sensitive to tumour necrosis factor (TNF)–induced cell death K8 and K18 both bind to the cytoplasmic domain of TNF receptor type 2 (TNFR2) and moderate the effects of TNF While

K8/K18 deprived hepatocytes are more sensitive to Fas mediated apoptosis (Gilbert *et al*, 2004) This may be a fundamental function of K8/18 seen in liver regeneration, inflammatory bowel disease, hepatotoxin sensitivity and the persistent expression of these keratins in many carcinomas As these proteins have a frequent and persistent expression in carcinomas, they are considered as tumour markers (Oshima, 2002) They could also play an important role in tumoural migration and invasion (Hembrough, *et al*, 1995) Bichat *et al* (1997) exposed human breast cancer cell line MCF7S to adriamycin The result was an increase in keratin 8 expression but no change in vimentin expression A much weaker ERK1/2 activation occurs in K8-null hepatocytes This then resulted in impaired ERK1/2 activation in K8-null hepatocytes and is associated with a drastic reduction in c-Flip protein This points to a new regulatory role of simple epithelium keratins in the c-Flip/ERK1/2 antiapoptotic-signalling pathway

Taxol is known to inhibit cell growth and trigger significant apoptosis Park *et al* (2004) transfected lymphoblastic leukemia cells with a dominant-negative FADD plasmid and demonstrated for the first time that taxol induces FADD-dependent apoptosis primarily through activation of caspase-10 but independently of death receptors Taxol induced activation of caspases-10, -8, -6, and -3, cleaved Bcl-2, Bid, poly(ADP-ribose) polymerase, lamin B and down-regulated cellular levels of FLICE-like inhibitory protein (FLIP) and X-chromosome-linked inhibitor of apoptosis protein (XIAP) The drug caused a decrease of mitochondrial membrane potential and a significant increase in ROS generation However, increased ROS production was not directly involved in taxol-triggered apoptosis Inhibitors of caspases-8, -6 or -3 partially inhibited taxol-induced apoptosis, whereas the caspase-10 inhibitor totally abrogated this process Keratin 8 and 18 are able to modulate trafficking and interactions of many molecules involved in cisplatin-induced apoptosis They could play a role in acquired chemoresistance of IGROV1-R10 ovarian cancer cell line (Le Moguen *et al*, 2005)

4 2 10 4 LASP-1

Lasp-1 is an actin binding protein, which, along with Krp1 protein co-localises with actin at the tips of pseudopodia This localisation is maintained by continued AP-1 (a transcription factor) mediated down-regulation of fibronectin that in turn suppresses integrin and Rho-ROCK signalling and allows pseudopodial protrusion and mesenchyme-like invasion (Spence *et al*, 2006) The function of Lasp-1 is not known

It is necessary for cell migration on ECM but not adhesion (Lin *et al*, 2004) Lasp-1 expression is increased in metastatic breast cancers, suggesting that protein amplification may contribute to the migratory properties of these cells (Tomasetto *et al*, 1995) Lasp-1 is increased in both SKMES-Txt (1 61-fold) and SKMES-Txl (1 58-fold) both of which are more invasive than the parent In contrast, it is decreased in the more invasive SKMES-Txl (Wk6) cell line with respect to SKMES-Txl (Wk3) by 1 49-fold

4 2 10 5 Ubiquitin carboxy-terminal hydrolase L1 (PGP9 5)

Taxane exposure resulted in an increase in the expression of ubiquitin carboxy-terminal hydrolase L1 A large proportion of regulatory proteins are modified by conjugation with ubiquitin or ubiquitin-like proteins This modification acts as a targeting signal, delivering the modified protein to different locations in the cell and modifying its activity, half-life or interaction with other molecules (Hochstrasser, 2000) Ubiquitin modification of proteins is important in the regulation of the cell cycle, modulation of the cellular response to stress and extracellular effectors, DNA repair, regulation of the immune and inflammatory responses, down-regulation of cell surface receptors and ion channels and biogenesis of organelles (Ciechanover *et al*, 2000) PGP9 5 represents one of the members of the ubiquitin carboxy terminal hydrolase family It plays a role in lung cancer tumourigenesis Expression of PGP9 5 is strongly associated with advanced stage lung cancers It is highly expressed in 54 % of 98 primary NSCLC lung cancers and 22 of 24 lung cancer cell lines (Hibi *et al*, 1999) Little is known regarding PGP9 5 specific substrates or its biological activity *in vivo* There is an interaction between PGP9 5 and JAB1, a co-activator of c-*jun* which promotes the phosphorylation and cytoplasmic translocation of $p27^{Kip1}$ for its subsequent degradation in the cytoplasm (Claret *et al*, 1996, Tomoda *et al*, 1999) They form a heteromeric complex that includes $p27^{Kip1}$ and can co-localise to the nucleus of lung cancer cells Cells, contact inhibited redistributed both PGP9 5 and JAB1 in the cytoplasm PGP9 5 may therefore play a role in lung cancer growth by regulating the level of nuclear JAB1, which can then lead to an increased degradation of $p27^{Kip1}$ (Caballero *et al*, 2002)

Liu *et al* (2003) showed that enzymatic activity of PGP9 5 is antiproliferative Cells do not grow and invade at the same time It interacts with p27, a cyclin-dependant kinase inhibitor This results in cell cycle arrest at G1 phase Up-regulation of PGP9 5 is associated with cell cycle retardation and p27 over-expression in myeloma cells (Otsuki *et al*, 2004) *In vitro* studies show that p27 up-regulation is essential for growth

inhibition by EGFR-TKIs (Busse *et al.*, 2000). Ubiquitin carboxy-terminal hydrolase L1 is a marker for aggressive and invasive colorectal carcinoma, pancreatic and lung cancer (Hathout *et al.*, 2004). The protein was also found to be over-expressed in the MCF-7/Adr (Hathout *et al.*, 2004).

4.2.11 Proteins unique to taxol-resistance in SKMES-1

In contrast to the unique proteins differentially regulated in response to taxotere, taxol exposure resulted in the differential expression of more unique proteins (23) of which most were down-regulated. The majority of these proteins have functions in ion binding/transport, protein turnover and the stress response (Figure 4.2.4).

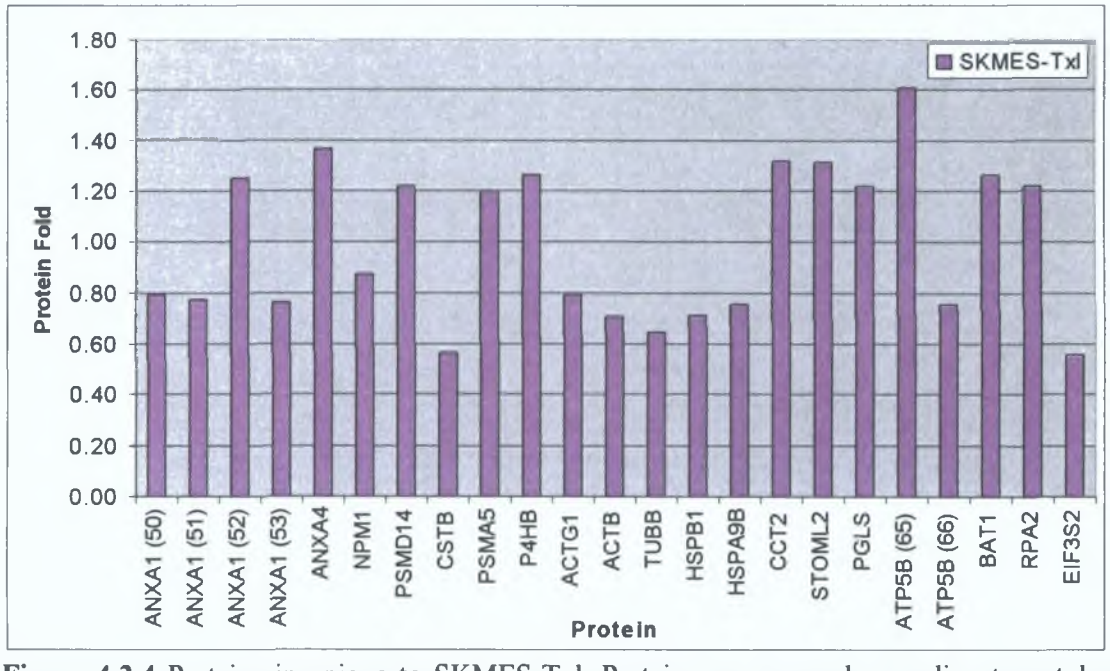

Figure 4.2.4 Proteins in unique to SKMES-Txl. Proteins are grouped according to ontology. Brackets indicate protein number where isoforms exist.

4.2.11.1 Annexin IV

The expression of annexin IV was determined to be overexpressed in the taxol resistant variant of SKMES-1 and the mitoxantrone resistant variant of DLKP by 1.37-fold and 1.51-fold respectively. Little data exists linking the expression of annexin IV to cancer. However, taking the functions of the annexins into consideration, alterations in the expression of these proteins could have important consequences on cancer cell behaviour. Discrepancies in the role of annexins in cancer have been observed. High annexin 1 expression in MCF-7 cells resulted in increased resistance to various cell lines while in ovarian SKOV-3 sensitivity increased (Wang *et al.*, 2000). Annexin IV

expression is up-regulated in the taxol resistant lung cancer cell line (Han *et al* 2003) In contrast two cisplatin-resistant ovarian carcinoma and hormone refractory prostate cancer cell lines was determined to express less annexin IV (Le Moguen *et al* 2006, Stewart *et al*, 2006, Xin *et al*, 2003)

4 2 12 Proteins unique to taxotere-resistance in SKMES-1

Taxotere exposure resulted in the differential expression of 19 proteins of which most were up-regulated The majority of proteins have functions in transcription/transcription regulation and ion binding/transport and are all up-regulated to approximately the same degree Cathepsin D is the most up-regulated protein (1 98-fold) and may contribute to increased invasiveness of SKMES-Txt (Figure 4 2 5)

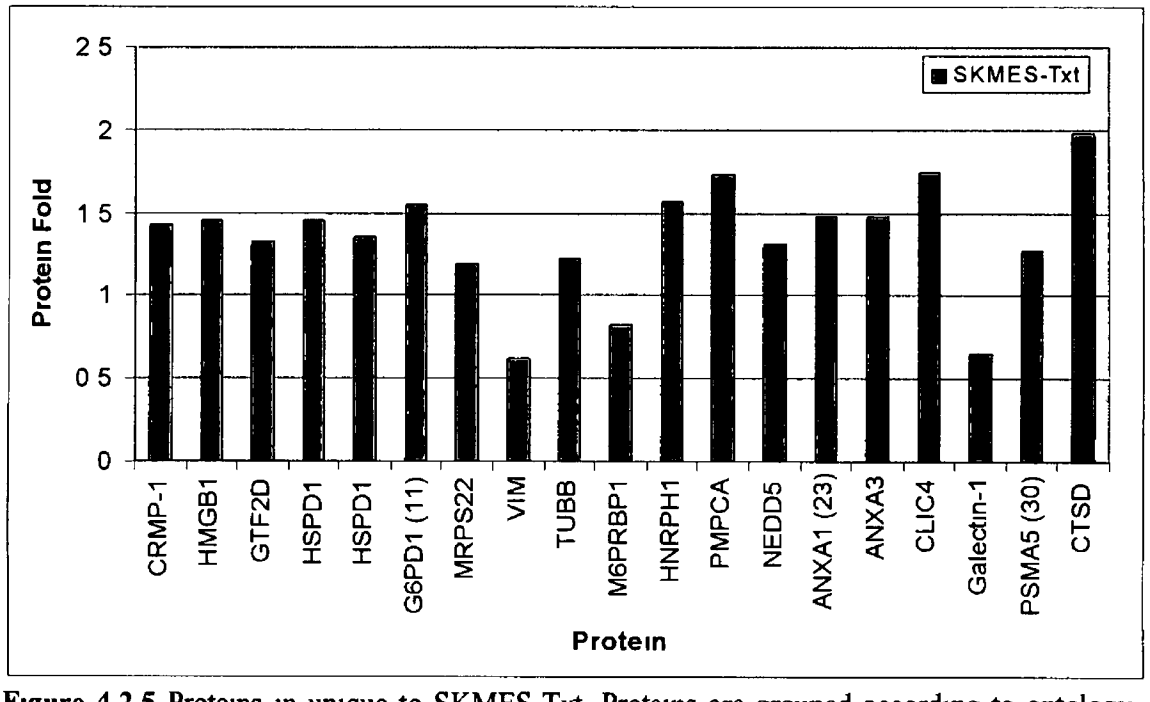

Figure 4 2 5 Proteins in unique to SKMES-Txt Proteins are grouped according to ontology Brackets indicate protein number where isoforms exist

4 2.12 1 Vimentin

Interestingly in the DLKP-adriamycin resistant cell lines, changes in vimentin expression may be more related to resistance than invasion While both DLKP-A2B and DLKP-A10 show low invasive potential, DLKP-A10 (more resistant) has a 3 88-fold increased expression compared to DLKP-A and DLKP-A2B, which is less resistant variant with 1 64-fold decreased expression of vimentin

This protein is also down-regulated in SKMES-Txt compared to SKMES-1 and as such does not correlate with resistance It does however, correlate with 3D-invasion assays which show SKMES-Txt to be less invasive Thus in DLKP-A10 vimentin may play an important role in the development of increased resistance and may represent a molecular mechanism to replace the caspase-cleaved vimentin to maintain cell integrity and to counteract programmed cell death

Vimentin belongs to the type III family of intermediate filaments and plays an important role in the dynamic remodelling of the cell during development of the neoplastic phenotype Vimentin is also a caspase substrate and is therefore part of the execution phase of apoptosis (Byun *et al*, 2001) However, evidence has accumulated which shows that atypical expression of vimentin in epithelial cancer cells is associated with invasiveness and metastasis potential for a variety of cancers including hepatocellular carcinoma (Hu *et al*, 2004), prostate carcinoma (Lang *et al*, 2002), breast carcinoma (Hendrix *et al*, 1997) and cervical carcinoma (Gilles *et al*, 1999) Analysis of vimentin expression in migrating MCF10A breast carcinoma cells using an *in vitro* wound assay model revealed induction of vimentin mRNA and protein in migrating cells Decreased vimentin expression using antisense cDNA caused a reduction in the migration of these cells also (Gilles *et al*, 1999) These studies show that vimentin is strongly associated with cellular motility and invasiveness The reduced expression of vimentin in DLKP-A2B cells may therefore contribute to the decreased mvasiveness of these cells However, other factors may be a work in the DLKP-A5F, which showed no change in vimentin expression, but were the most invasive of the DLKP cell lines tested in this study

4.2.12.2 Galectin-1

The galectins are a conserved family of carbohydrate binding proteins, which have an affinity for β-galactosidases. Galectin-1 has both intracellular and extracellular functions. It exhibits the characteristics of typical cytoplasmic proteins as well as an acetylated N-terminus and a lack of glycosylations. It has also been found in cell nuclei as well as cytosols and translocates to the intracellular side of cell membranes. When secreted, it can be found on the extracellular surface of all cell membranes as well as in the extracellular matrices of various normal and neoplastic tissues. The β-galactoside binding site may be the primary targeting site for galectin export machinery using β-galactoside-containing surface molecules as export receptors for intracellular galectins.

Galectin-1 (Gal-1) is involved in numerous biological functions including cell-cell and cell-substrate interactions and the three cell migration processes, adhesion, motility and invasion. The protein increases adhesion of many normal and cancer cells to the ECM by cross-linking the integrins exposed to the cell surfaces with carbohydrate moieties of the ECM components e.g. laminin and fibronectin (Clausse *et al.*, 1999). It binds to a number of extracellular matrix (ECM) components (laminin > cellular fibronectin > thrombospondin > plasma fibronectin > vitronectin > osteopontin) and is involved in ECM assembly and remodelling. It inhibits the incorporation of vitronectin and chondroitin sulphate B into the ECM of vascular smooth muscle cells. Galectin-1 binds integrin adhesion receptors and membrane glycoproteins which are essential for normal cellular function and survival. Gal-1 is secreted during skeletal muscle differentiation and accumulates with laminin in the basement membrane (Clausse *et al.*, 1999). Galectin-1 has been implicated in Ras signalling cascade leading to increased transformation (Paz *et al.*, 2001).

The expression or increased expression of galectin-1 in either a tumour or the tissue surrounding a tumour is considered a sign of its malignant progression and therefore a poor prognosis for patients. This prognosis is often related to tumour immune-escape, metastasis or its presence in the surrounding normal tissue. Galectin-1 could also play a role in tumour angiogenesis as it is expressed in both vascular smooth muscle and endothelial cells. Galectin-1 has been reported to increase motility in gliomal cells and colon cancer cells (Hittelet *et al.*, 2003). Harvey *et al.* (2001) used a proteomic approach to identify membrane expression of galectin-1 as a signature of cell invasiveness in mammary carcinoma. Galectin-1 accumulation around prostate cancer cells could act as

an immunological shield as it induces activated T-cell apoptosis (Van den Brule *et al*, 2001)

Galectin-1 expression was differentially expressed across the adriamycin resistant DLKP cell lines and did not always correlate with invasion Increased invasion correlated with increased expression of galectin-1 when DLKP-A was compared to the extremely invasive DLKP-A5F In contrast, decreased invasion correlated with decreased expression of galectin-1 when DLKP was compared to the less invasive DLKP-Mitox

Pulse selection with taxol and taxotere resulted in more invasive cell lines when examined in a monolayer on the Boyden Chamber Assay precoated in matrigel However, when induced to grow as spheroids and placed in collagen type I (to try and mimic the *in vivo* situation), both taxane-selected variants were less invasive than the parent Proteomic analysis revealed that galctin-1 was decreased in SKMES-Txt and unchanged in SKMES-Txl suggesting that gal-1 may not be the mam component relating to invasive potential

Le *et al* (2005) used SELDI-TOF mass spectrometry and tandem MS to identify galectin-1 and CD3 (a T-cell marker) in the FaDu HNSCC cells were significant predictors of overall survival The results suggest hypoxia can affect the malignant progression and therapeutic response of solid tumours by regulating the secretion of proteins that modulate immune privilege

The targeted inhibition of galectin-1 expression may be novel treatment in the fight against cancer progression The knock-down of galectin-1 in migrating tumour cells (e g gliomas and melanomas) may impair malignancy development in different ways It could delay cancer cell migration within the host tissue or at a distance (metastases), and the sensitisation of migrating cancer cells to apoptosis Migrating cancer cells are protected against apoptosis therefore down-expressing galectin-1 could restrict migration as the cells would be sensitised to cell death and importantly chemotherapeutic drugs

4.2.13 Proteins involved in unstable resistance to taxol in SKMES-Txl (Wk3) versus SKMES-Txl (Wk6)

Comparisons between SKMES-1 versus SKMES-Txl (Wk3) and SKMES-Txl (Wk3) versus SKMES-Txl (Wk6) revealed that 4 proteins were shared. The cellular redox proteins, ER-60, peroxiredoxin 2 and protein disulfide isomerase protein 5 show a decrease in protein expression as resistance falls (Figure 4.2.6). For example, PDIA3 was 1.35-fold increased in SKMES-Txt (Wk3) when resistance was highest but was 1.55-fold decreased when resistance was at its lowest. Peroxiredoxin 2 (PRDX2) was 2.02-fold up-regulated in SKMES-Txl (Wk3) but –1.33-fold in SKMES-Txl (Wk6). Peroxiredoxin 2 and 3 expression was increased in SKMES-1 versus SKMES-Txt and SKMES-Txl (Wk3) respectively. Peroxiredoxin 2 plays an important role in regulating cell differentiation and proliferation by modulating the hydrogen peroxide-mediated responses and has anti-apoptotic properties (Noh *et al.*, 2001). The up-regulation of these cellular redox proteins in the more resistant SKMES-Txl (Wk3) reflects an attempt of the cells to survive and proliferate in response to taxol exposure. The glutathione-related detoxification pathway is commonly discussed as one of the major mechanisms of MDR. Both isoforms of GST π were decreased in SKMES-Txt and SKMES-Txl (Wk3). However, one isoform of GST π was increased (2.29-fold) in SKMES-Txl (Wk6). Annexin 5 on the other hand, increases with decreasing resistance.

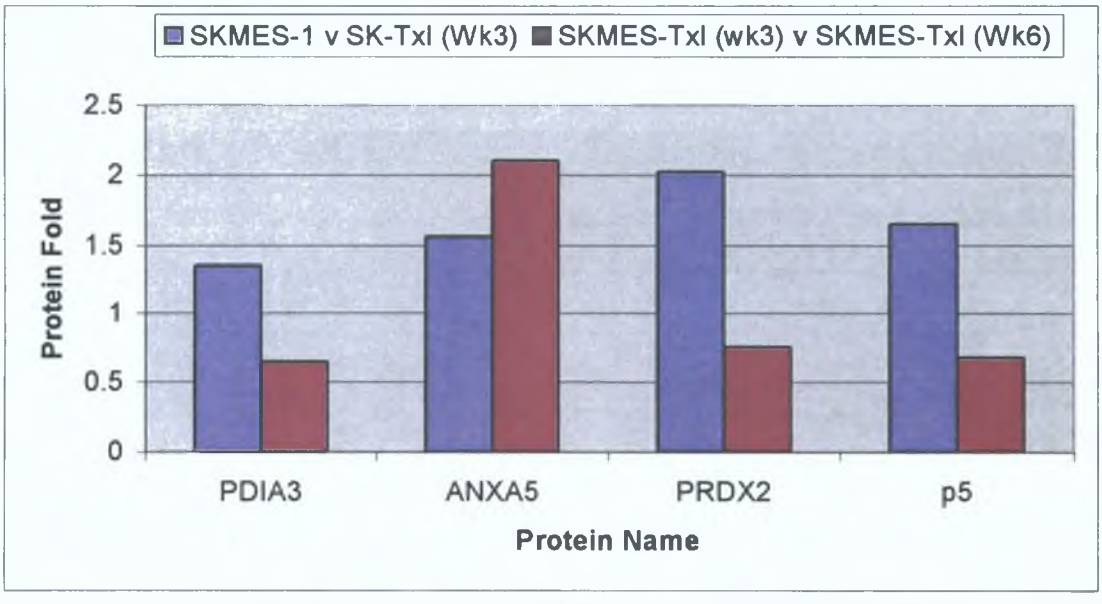

Figure 4.2.6 Review of shared proteins in SKMES-1 versus SKMES-Txl (Wk3) and SKMES-Txl (Wk3) versus SKMES-Txl (Wk6).

Loss of taxol-resistance also resulted in the differential expression of 10 proteins, of which most were down-regulated. The majority of proteins have cytoskeletal and stress response functions. Interestingly, the three stress response proteins, KIAA0098 and HSP 70kDa protein 8, are all down-regulated which may contribute to a fall in drug-resistance. β-actin is a member of the actin family of genes, which play important role in maintaining cytoskeletal structure, cell motility, cell division, intracellular movements and contractile processes. Beta actin and lamin B1 are the most up-regulated of the proteins and may contribute to increased invasiveness of SKMES-Txl (Wk6) (Figure 4.2.7).

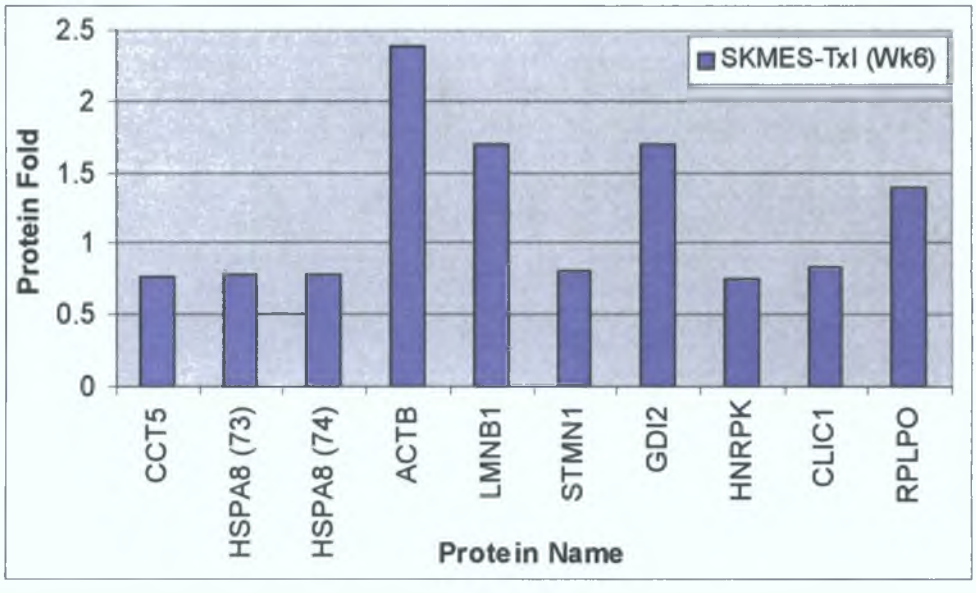

Figure 4.2.7 Unique proteins to SKMES-Txl (Wk6) when compared to week 3.

4.2.14 Mechanism of taxane resistance

Taxol and taxotere have similar mechanisms of action even though taxotere is approximately twice as potent an inhibitor of microtubule depolymerisation relative to taxol (Gelman, 1994). The taxanes promote the stable assembly of microtubules from α- and ß-tubulin heterodimers and inhibit their de-polymerization. Interestingly, both taxanes bind to the β-subunit of tubulin but the microtubules produced by taxotere are larger than those produced by taxol. This may explain why taxotere appears to be approximately twice as potent as taxol (Vaishampayan *et al.*, 1999). In these studies taxotere exposure resulted in an increase (1.21-fold) whereas taxol exposure resulted in a decrease of 1.56-fold of β–tubulin. Loss of taxol resistance also resulted in a decrease in β-tubulin expression by 1.94-fold. The mechanism of taxol and taxotere toxicity

remains controversial. The antitumour effects of these drugs may result from interference with the normal function of microtubules and from blocking of cell cycle progression in late G_2-M phases (Donaldson *et al.*, 1994). Taxol-induced apoptosis in hepatoma cells is mediated through G_2-M arrest and DNA fragmentation (Lin *et al.*, 2000). Cells with a defective G_1 checkpoint and with an increased percentage of G_2-M fractions were found to have increased sensitivity to taxol (DiPaola, 2002). However, pulse exposure to taxol can cause apoptosis but not G_2-M arrest suggesting that taxol-induced apoptosis may occur without a prior G_2-M arrest (Dziadyk *et al.*, 2004). Taxol has been reported to induce the formation of reactive oxygen species (ROS) and alter mitochondrial membrane permeability (Varbiro *et al.*, 2001). Moreover, treatment of the human T-cell lymphoblastic leukemia cell line CCRF-HSB-2 with an antioxidant showed inhibition of taxol-induced ROS production but did not prevent taxol-induced apoptosis indicating that it is independent (Park *et al.*, 2004).

4.2.14.1 Reactive oxygen species

Many chemotherapeutic agents exert their toxic effects on cancer cells by producing free radicals, leading to irreversible cell injury and overproduction of ROS in cancer cells may exhaust the capacity of superoxide dismutase and other adaptive antioxidant defences. Depletion of cellular antioxidant capacity enhanced taxol toxicity (Kong *et al.*, 2000). Taxol chemoresistance correlates with intracellular antioxidant capacity, ROS and reactive nitrogen species, inducing the production of O_2^-, H_2O_2 and NO and causing oxidative DNA damage. Agents that decrease H_2O_2 and NO production suppress taxol-induced DNA damage. The inhibition of superoxide dismutase or glutamylcysteine synthase increases taxol-induced apoptosis. Finally, cell lines with higher total antioxidant capacity are more resistant to taxol cytotoxicity (Ramanathan *et al.*, 2005).

Increases in protein disulfide isomerases may act as a protective response against DNA damage and have been reported for other models of oxidative stress (Tanaka *et al.*, 2000). Interestingly, protein disulfide isomerase 5 is increased in SKMES-Txl (Wk3) only and decreased in SKMES-Txl (Wk6). ER-60 is increased by 1.35-fold in SKMES-Txl (Wk3) and decreased in SKMES-Txl (Wk6). Increases in these proteins can lead to a greater inhibition of p53-dependent apoptosis, a decrease in the inhibition of c-myc survival pathways and an increase in the signalling of Ras oncogene. Decreases in these

proteins in SKMES-Txl (Wk3) compared to SKMES-Txl (Wk6) correlates with a decrease in drug resistance

The thioredoxins are ubiquitous redox proteins that are reduced by NADPH and thioredoxin reductase, which in turn reduces oxidized cysteine groups on proteins Elevated levels result in increased cell growth and resistance to the normal mechanism of programmed cell death Mechanisms by which thioredoxin increases cell growth include an increased supply of reducing equivalents for DNA synthesis, activation of transcription factors that regulate cell growth and an increase in the sensitivity of cells to other cytokines and growth factors The mechanisms for the inhibition of apoptosis by thioredoxin have been elucidated (Powis *et al* , 2000) Thioredoxin as a stimulator of cancer cell growth and an inhibitor of apoptosis, offers a target for new chemotherapeutics Thioredoxin plays an important role in cell viability, activation, and proliferation and is widely distributed in normal tissues and is highly expressed in a variety of cancers such as lung, cervical, pancreatic, hepatoma, gastric, and breast cancers (Kim *et al* , 2005) This high expression of thioredoxin in cancers is associated with a biologically aggressive phenotype, increased proliferation and decreased apoptosis (Kakolyris *et al* , 2001) High expression has been associated with resistance to cisplatin, mitomycin C, adriamycin, taxotere and etoposide (Yokomizo *et al* , 1995, Kim *et al* , 2005) Taxotere or taxol exposure in these studies did not result in the differential regulation of thioredoxin However, thioredoxin peroxidase is increased in SKMES-Txl (Wk3) by 2 02-fold but decreased in SKMES-Txl (Wk6) when compared to SKMES-Txl (Wk3)

The glutathione and thioredoxin systems represent two major mechanisms for maintaining the intracellular redox environment through the reduction and oxidation of thiol groups The glutathione and thioredoxin systems have been studied individually, but both systems seem to work cooperatively in taxotere-resistance

4.2.15 Overall mechanisms of resistance - The stress response proteins

One of the major groups found to be predominantly increased in all the drug resistant cell lines are the group of stress response proteins namely the heat shock proteins. Figure 4.2.13 shows differentially expressed heat shock proteins that both correlate and inversely correlate with drug resistance across the panel of adriamycin cell lines. HSP 27 kDa (25), HSP 70 kDa protein 8 isoform 2 protein (4) and HSPA9B appear to be involved in baseline resistance as they are increased in DLKP-A versus DLKP and have similar expression in all the resistant variants. In contrast, HSP70A8 (17) is consistently decreased in the resistant variants. HSP70 kDa protein 8 isoform 2 (4) correlated with increasing drug resistance and HSPA8 (27), except for DLKP-A2B, inversely correlated with drug-resistance.

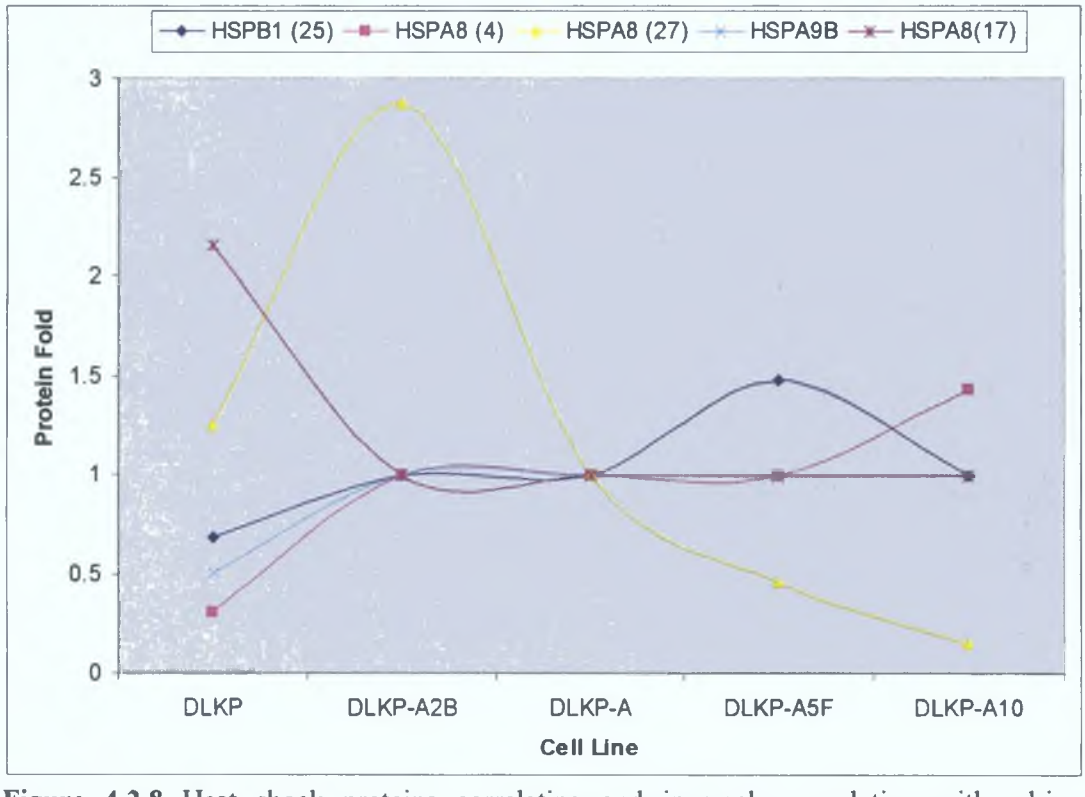

Figure 4.2.8 Heat shock proteins correlating and inversely correlating with adriamycin resistance. Numbers in brackets indicate protein identification number where isoforms existed.

4 2 15 1 Heat Shock Proteins –function and background

Heat shock proteins are the products of several distinct gene families that are required for cell survival during stress and are named according to the approximate relative molecular mass of their encoded proteins They include the following - HSP10, HSP27, HSP40, HSP60, HSP70, HSP90 and HSP110 They interact with diverse protein substrates to assist in the recovery from stress by repairing damaged proteins (protein refolding), thus restoring protein homeostasis and promoting cell survival (Calderwood *et al* , 2006) The cytoprotective properties of the HSPs are closely associated with their main functions as chaperones The intracellular reactions catalyzed by HSPs are divided into two categories namely, 'protein holding' and 'protein folding' The major holding proteins belong to the HSP70 and HSP90 families They bind to unfolded sequences in polypeptide substrates and prefer hydrophobic regions Holding interactions occur (a) during mRNA translation, when HSP70 binds to the elongating polypeptide chain to prevent premature self-association in the nascent protein, (b) during heat shock, when proteins partially unfold and expose hydrophobic sequences that are subsequently bound by HSP and (c) constitutively, when HSP90 binds to proteins with unstable tertiary structures (Calderwood *et al* , 2006)

HSP70 and HSP90 function in large complexes or 'chaperone machines' containing several accessory proteins or co-chaperones that bind the primary chaperone to mediate substrate selection and cycles of association with, and disassociation from, the substrate After completion of their molecular chaperone function, HSP70 and HSP90 are actively released from protein substrates by means of their intrinsic ATPase domains They have therefore become targets for rational anti-cancer drug design (Calderwood *et al* , 2006) Overexpression of HSPs in tumour cells is due to the loss of p53 function and to increased expression of the proto-oncogenes HER2 and c-Myc and is crucial to tumourigenesis

4 2 15 2 HSPs Molecular mechanisms in cancer

The molecular mechanisms involving HSP27 and other HSPs in cancer and chemotherapy resistance can be explained in several ways (1) they can confer cytoprotection by repairing more efficiently the damaged proteins resulting from cytotoxic drug administration as they are molecular chaperones, (2) they protect tumour cells from apoptosis (Arrigo *et al* , 2003), (3) they protect the microvasculature inside tumours (HSP27 is found in endothelial cells) (Ciocca *et al* , 2003) and finally (4) they enhance DNA repair (Nadin *et al* , 2003)

The rate of tumour growth depends on the relative rate of turnover of tumour cells Figure 4 2 14 illustrates cell death inhibition through the ability of HSP70 and HSP27 to block programmed cell death (PCD) The intrinsic pathway of caspase-mediated apoptosis is stimulated by c-Jun kinase, leading to a release of signals including cytochrome *c* from the mitochondria and activation of a caspase cascade, involving caspase 8 and 3 Increases in HSP70 (red triangles) inhibit this pathway at several stages, including at the level of c-Jun kinase, cytochrome *c* release and after the caspase 3 step The extrinsic pathway is stimulated through death receptors such as Fas and *via* downstream activation of the caspase cascade by caspase 9, a step that is inhibited by increased levels of HSP27 (red squares) Members of the HSP70 family are also inhibitors of replicative senescence Several HSP70 family members inhibit senescence by acting upstream to block the pro-senescence effects of the wild-type p53 protein

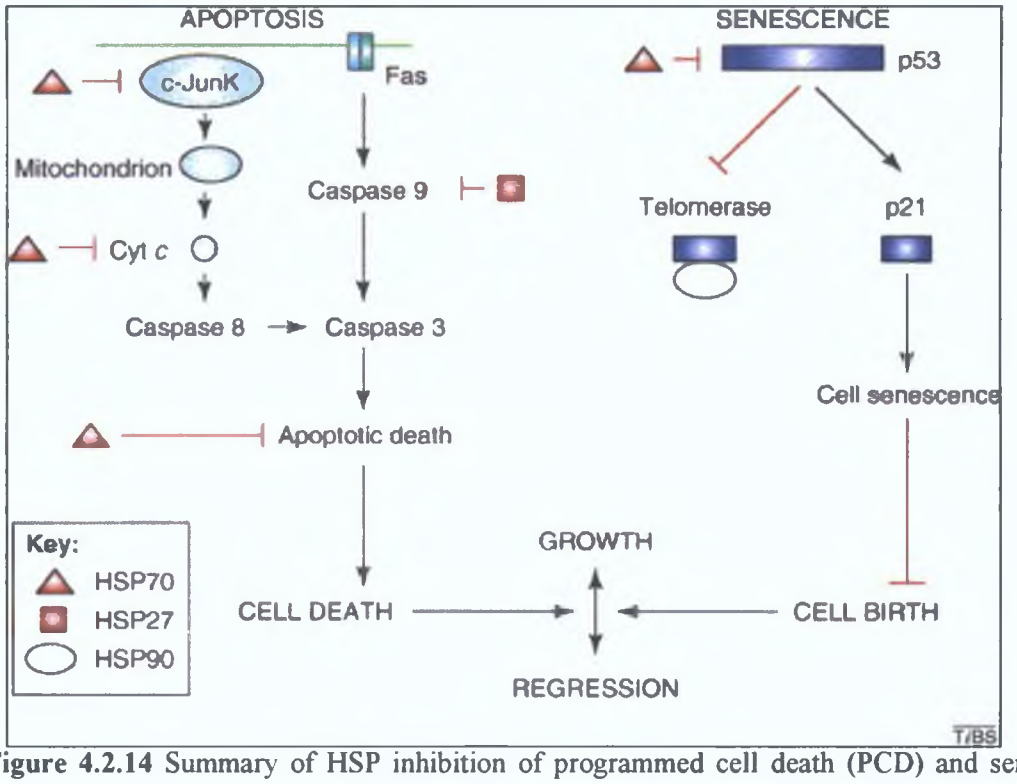

Figure 4.2.14 Summary of HSP inhibition of programmed cell death (PCD) and senescence (Calderwood *et al.*, 2006).

In addition, the enzyme telomerase binds HSP90 (white oval), delaying the onset of replicative senescence. Increased expression of HSPs in cancer thus further shifts the balance between cell death and birth, and promotes tumour growth.

Mortalin (HSPA9B), a member of the HSP70 family of proteins has differential subcellular distribution in normal and immortal cells (Wadhwa *et al.*, 2003). It has previously been identified as an intracellular FGF-1-binding protein and appears to be involved in diverse regulatory processes including cellular senescence, glucose regulation, mitochondrial transport, nephrotoxicity and antigen processing. While heat shock proteins are generally considered to function in folding, assembly and degradation of newly synthesised proteins, increasing evidence indicates that they also associate with regulatory proteins such as receptor kinases and transcription factors (Mizukoshi *et al.*, 2001).

In contrast to HSP27 and 90 which are phosphorylated on Ser/Thr residues, HSP75 and HSPA8 undergo acute tyrosine phosphorylation in response to vanadate and hydrogen peroxide suggesting that HSP proteins could be involved in the regulation of signalling pathways (Wadhwa *et al.*, 2003). HSP70 is found in many subcellular sites and is known to bind p53 causing its inactivation. The leukaemia cell line, HL-60, developed a growth advantage with the overexpression of mortalin. Overexpression also resulted in

malignant transformation of mouse NIH 3T3 cells and life span extension of normal human fibroblasts (Wadhwa *et al* , 2003)

HSP is a potential target for apoptosis-based cancer chemotherapy HSP70 and HSPA8 can interact, *via* the Bag1 protein, with several proteins, which participate in signal transduction and apoptosis, including the Bcl-2 protein The transient complex chaperone-Bag1-Bcl-2 could facilitate the insertion of the anti-apoptotic protein into the mitochondrial membrane thus preventing apoptosis (Takayama *et al* , 1998) HSP70 does not inhibit fas-induced apoptosis suggesting that its inhibitory function is only effective against those agents that produce ROS Protection against TNF-induced apoptosis, has been shown to involve HSP70 (Creagh and Cotter, 1999)

Direct or indirect association with antiapoptotic bcl-2 family members may confer HSP70 protection Inducible and constitutive forms of HSP70 associate with the bcl-2 binding protein, BAG-1 inhibiting apoptosis As a result an increased bcl-2 expression often occurs with HSP70 overexpression (Townsend *et al* , 2003) Zhao *et al* (2005) inhibited HSP70 using antisense RNA resulting in accelerated apoptosis

4 2.15 4 HSP and chemotherapy treatment

HSPs are overexpressed in a wide range of human cancers and have been implicated in tumour cell proliferation, differentiation, invasion, metastasis, death and recognition by the immune system (Ciocca and Calderwood, 2005) They are useful biomarkers for carcinogenesis in some tissues and signal the degree of differentiation and the aggressiveness of some cancers, hyperplastic endometrium, uterine cervix, colon and hepatocellular carcinoma (Ciocca and Calderwood, 2005)

Circulating levels of HSP and anti-HSP antibodies in cancer patients could be useful in tumour diagnosis HSP27 expression is associated with poor prognosis in gastric, liver, and prostate carcinoma (Takeno *et al* , 2001, King *et al* , 2000 and Bostwick, 2000) HSP70 is correlated with poor prognosis in breast, endometrial, uterine cervical, and bladder carcinomas (Ciocca and Calderwood, 2005) Increased HSP expression may also predict the response to some anticancer treatments Both HSP27 and HSP70 expression are implicated in chemotherapy resistance in breast cancer (Vargas-Roig *et al* , 1998) HSP27 expression is correlated with a poor response to chemotherapy in leukemia patients

The implication of heat shock proteins in tumour progression and response to therapy has led to its successful targeting in therapy by 2 main strategies Firstly,

pharmacological modification of HSP expression or molecular chaperone activity and secondly, their use in anticancer vaccines, exploiting their ability to act as immunological adjuvants (Calderwood *et al* , 2006)

HSP70 is a weak predictive marker in lung caner (Volm and Rittgen, 2000) but a predictor of better response to chemotherapy in osteosarcoma (Trieb *et al* , 1998) Chauhan *et al* (2003) identified several HSPs including HSP70 to confer resistance to dexamethasone in multiple myeloma and oestrogen receptor-α in breast cancer HSP27 overexpression has been correlated with a shorter disease-free survival in advanced breast cancer and in ovarian cancers (Langdon *et al* , 1995) Low constitutive levels of HSP27 in testicular germ cell tumours has facilitated the successful use of cisplatin (80% cure rate) Co-transfection of HSP27 plasmid resulted in resistance to cisplatin (Richards *et al* , 1996) Similarly suppression of HSP27 with anti-sense improved the sensitivity of the gastric carcinoma SG7901 cell line to vincristine (Yang *et al* , 2006) Morino *et al* (1997) revealed that HSP27 expression correlated with metastasis and tumouregenisis in mammary and prostate cancers The results also correlated overexpression of HSP27 with a shorter disease-free survival period, suggesting that it could be a prognostic marker for malignancy of these tumours

In predictory responses to chemotherapy (table 4 2 2), overexpression of HSP27 has been linked to adriamycin resistance in breast cancer cells (Oesterreich *et al* , 1993) by increasing the efficiency of repair of adriamycin-induced DNA damage (Nadin *et al* , 2003) Both HSP27 and HSP70 were shown to inhibit apoptosis caused by chemotherapeutic drugs especially those that target topoisomerase II enzymes i e the anthracyclines, VP-16, H_2O_2 and staurosporine (Garrido *et al* , 1999) HSP27 can decrease the level of reactive oxygen species (ROS) and increase levels of glutathione High levels of GSH are effective against intracellular stress caused by ROS HSP27 can stabilise microfilaments and protect against toxicants (Lavoie *et al* , 1995)

Phosphorlyation of HSP27, a result of PKC up-regulation, was found in gefitinib-resistant colorectal cell lines HSP27 antisense techniques reversed resistance mechanisms in lymphoma cells to the proteasome inhibitor bortezomib (Chauhan *et al* , 2003) HSP27 directly interacts with cytochrome C and two effectors of the EGFR pathway, namely AKT and p38 MAPK, to confer protection against cell death (Loeffler-Ragg *et al* , 2005)

Sinha *et al* (2003) used 2-DE to analyse chemoresistance in melanoma, stomach, pancreatic, fibrosarcoma and colorectal carcinoma cell lines All cell lines were grown in the presence of cisplatin and daunorubicin, leading to the development of classical MDR and mitoxantrone, VP-16, vindesine and fotemustine leading to atypical MDR The heat shock proteins 27, 70, 60 and 60 variant were all found to be overexpressed in the resistant melanoma variants Creagh *et al* (2000) showed that these drugs produce ROS, which play a major role in apoptosis induction Treatment with antioxidants increases cellular resistance to these agents HSP27 can reduce intracellular levels of ROS in a glutathione-dependant manner It can inhibit apoptosis-mediated cell death via receptor induced pathways e g death receptors Fas/CD95 and tumour necrosis factor alpha It increases glutathione (GSH) as high GSH is effective against cellular stress caused by ROS Koomagi *et al* (1996) used immunohistochemistry techniques to analyze 20 tumoural and peritumoural tissues from patients with lung cancer (14 smokers and 6 non-smokers) for drug resistance proteins P-gp, topoisomesare II (topo-II), glutathione S-transferase-π (GST-π), metallothionein (MT), HSP-70 and the putative regulators of resistance (ErbBl, Fos and Jun) The study set out to look for a link between expression of resistance-related proteins with their regulators and smoking Results revealed that protein expression of topo-II, GST-π, MT, HSP-70, ErbB 1, Fos and Jun were overexpressed in tumour tissue compared to normal tissue The expression of the proteins (especially HSP70 and MT) was frequently increased in smokers and correlated with differences between the tumoural and non-tumoural tissue

Zhang *et al* (2006) exposed the HL-60 leukaemia cell line to the natural tyrosine kinase inhibitor geneticin and applied 2-DE to analyse the response Forty protein spots out of 600 in total showed a greater than 2-fold changes in spot intensity, 15 of which were identified by MALDI-TOF HSP70 kDa protein 8 isoform 2 was up-regulated (5 9-fold) Proteins involved in glycolysis and ATP production such pyruvate kinase and isocitrate dehydrogenase were also highly over expressed Proteins implicated in RNA processing (hnRPA1 and hnRPC) were decreased due to genetisin However, hnRPH1 was 5 1-fold up-regulated The RNA processing proteins hnRPH1 and hnRPK was also up-regulated in DLKP versus DLKP-A HnRPF were increased in DLKP-A versus

Hsp	Author(s)	Findings
Breast cancer		
Hsp27	Seymour et al (1990)	+ better response to combination therapy (chemotherapy and tamoxifen for ER+)
	Damstrup et al (1992)	Does not predict response to endocrine therapy
	Ciocca et al (1998)	Does not predict response to tamoxifen
	Vargas Roig et al (1998)	Shorter DFS (neoadjuvant chemotherapy)
Hsp70	Ciocca et al (1993)	Predictor of recurrence (adjuvant therapy)
	Liu et al (1996)	Higher <resp. radiation and hyperthermia
	Ciocca et al (1998)	Does not predict response to tamoxifen
	Vargas Roig et al (1998)	Shorter DFS (neoadjuvant chemotherapy)
Ovarian cancer		
Hsp27	Langdon et al (1995)	>Hsp27 resistant to chemotherapy
	Germain et al (1996)	No correlation with chemoresistance
	Arts et al (1999)	Univariate analysis absence of Hsp27 correlated with longer median progression free survival
	Piura et al (2002)	Overexpression poor response to chemoth
Cervical (uterine) cancer		
Hsp27	Vargas-Roig et al (1993)	Hsp27 no correlation with response to tamoxifen
Head and neck cancer		
Hsp27	Fortin et al (2000)	Expression did not correlate with local response to radiotherapy (transfected cells with >Hsp27 thermoresistance and chemoresistance)
Oesophageal cancer		
Hsp27	Takeno et al (2001b)	Hsp27 involved in resistance to neoadjuvant C+R (scc)
Rectal cancer		
Hsp27/70	Rau et al (1999)	No correlation with treatment (H+R+C)
Lung cancer		
Hsp70	Volm and Rittgen (2000)	Weak correlation with resistance to doxorubicin (nsclc)
Bladder cancer		
Hsp27	Kassem et al (2002)	Downregulation in radiosensitive bcc
Hsp60	Zlotta et al (1997)	Increased anti-Hsp 60 IgG after BCG therapy ↗tumor recurrence
Prostate cancer		
Hsp27	Bubendorf et al (1999)	Overexpression 31% of hormone refractory tumors 5% of primary tumors
Leukemia		
Hsp27	Kasimir Bauer et al (1998)	Coexpression of Hsp27 and other molecules predicts response to induction chemother
CNS tumors		
Hsp27 70 90	Hermisson et al (2000)	Does not predict response to induction radiochemothera py However glioblastoma cells express high levels of Hsps
Osteosarcomas		
Hsp60 70	Trieb et al (1998)	Hsp72+ better response to neoadjuvant chemotherapy
Hsp90	Trieb et al (2000a)	Antibodies >response to neoadjuvant chemotherapy
Malignant fibrous histiocytoma		
Hsp27	Têtu et al (1992)	Expression no correlation with response to chemotherapy

Abbreviations bcd bladder carcinoma cell line C chemotherapy scc, squamous cell carcinoma H hyperthermia, nsclc non-small cell lung carcinoma R radiotherapy

DLKP-A10

Table 4 2 2 Review of studies exploring the use of the HSPs to predict the response (or lack of response) of a set of cancer patients to a specific treatment(s) (Ciocca and Calderwood, 2005)

A comparison of lung tumoural and peritumoural tissue revealed that several tumour proteins were differentially expressed including, annexin 2, prohibitin, stathmin, Cathepsin D The normal tissue 2-DE patterns were reasonably reproducible among patients, the tumour samples showed notable variation depending on tumour type (i e adenocarcinoma, squamous cell carcinoma and neuroendocrine carcinoma) and on stage Some proteins were found in most patients e g HSP27, but some were only found in one patient Cathepsin D and HSP27 are markers in current use for breast and lung cancer respectively The induction of HSP27, prohibitin and chaperones under stress conditions has been linked to apoptosis (Alfonso *et al* , 2004)

The HSP family could provide a true Achilles heel for cancer therapy because they seem to be required for cell survival during tumour progression and metastasis New classes of drugs targeting HSPs are beginning to be generated, for example HSP90 inhibitors are currently showing much promise in clinical trials, whereas the increased expression of HSPs in tumours are forming the basis of chaperone-based immunotherapy (Calderwood *et al* , 2006)

The ATPase domain of HSP90 has been effectively targeted A very active and unique family of anti-cancer drugs has been produced and are showing considerable promise in phase I and II clinical trials whereby tumour cells are selectively sensitised with anti-HSP90 drug 17AAG (Workman, 2004, Neckers, 2002) In tumour cells, the principal effect of HSP90 inhibition is the degradation of proteins required for autonomous growth and cytoprotection The selectivity of HSP90-targeted drugs also affects the increased concentration of HSP90 substrates found in tumor cells, including overexpressed oncogenes and mutant proteins generated through the 'mutator phenotype' of advanced cancers (Calderwood *et al* , 2006)

The other HSPs have not been effectively targeted yet, although efforts to do this are proceeding There is great promise for such drugs owing to the widespread role of HSP27 and HSP70 in blocking PCD and senescence during tumour progression However, the high concentrations of these proteins might place constraints on the feasibility of this approach Drugs that target HSP70 family proteins in general are likely to be toxic through inhibition of the basic molecular chaperone function needed to fold most intracellular proteins However, individual members of the HSP70 family, many of which are overexpressed in cancer, have distinct mechanisms for increasing cell survival and could be targeted individually (Tang *et al* , 2005)

Immunotherapy treatment may be a tempting target as they are able to chaperone tumour antigens and act as biological adjuvants to break tolerance to tumour antigens and cause immune killing by cytotoxic T lymphocytes and tumour regression The identification of proteins already in use as cancer markers (HSP27, stathmin and cathepsin) support the validity of the technique and stresses the potential of proteomics

4 2 16 Cellular redox system

Generation of oxidative stress in response to various external stimuli has been implicated in the activation of transcription factors and in the triggering of apoptosis Several anticarcinogenic agents have been shown to inhibit ROS production and oxidative DNA damage, inhibiting tumour promotion Other mechanisms, apart from P-gp are also responsible for the development of MDR Antioxidants govern intracellular redox status Inside cells, GSH, glutaredoxin and thioredoxin represent the major reducing agents (Figure 4 2 15) The glutathione-related detoxification pathway is commonly discussed as one of the major mechanisms of MDR however, GST pi expression was unchanged across the adriamycin resistant cell lines in the panel but increased in DLKP-Mitox (1 8-fold)

Other members of the thioredoxin system include peroxiredoxin 1, 2 and 3 Peroxiredoxin 1 was overexpressed in the least-resistant variant DLKP-A2B Thioredoxin reductase, thioredoxin, and thioredoxin peroxidase/peroxiredoxin are three linked components in a redox chain that couple peroxide reduction to NADPH oxidation Thioredoxin (TRX), thioredoxin peroxidase, peroxiredoxin 2 and 2 were all down-regulated in each of the other proteomic comparisons with the exception of thioredoxin peroxidase which is increased in DLKP-A versus DLKP-A5F

The lower level of these proteins may therefore render these cells more susceptible to oxidant injury Interestingly, reduced expression of TRX led to the sensitisation of bladder cancer cell lines towards adriamycin, etoposide and mitomycin C (Yokomizo *et al*, 1995) Thioredoxin regulates the activity of DNA-binding proteins including, Jun/Fos and nuclear factor B It also interacts with an intranuclear reducing molecule redox factor 1, which enhances the activity of Jun/Fos

Tumourigenesis results in the disruption of the fine balance between cell death and survival Increased levels of antioxidant enzymes such as MnSOD, peroxiredoxin 2, peroxiredoxin 6, aldehyde dehydrogenase A2, and thioredoxin 1 are associated with accumulation of ROS Accumulation of ROS may lead to activation of the

protooncogene NF-kb, induces DNA damage but inhibits the function of the AP-1 transcription factor

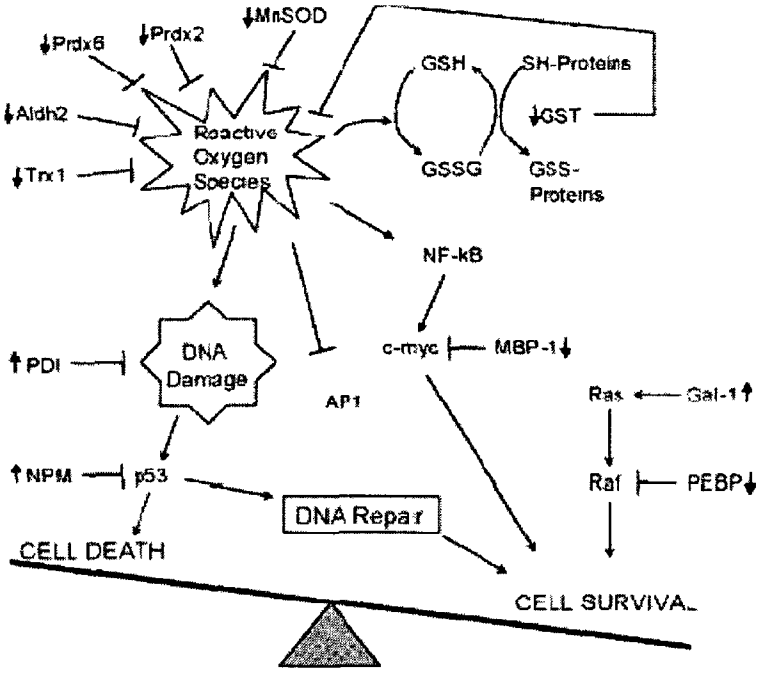

Figure 4 2 15 The Cellular Redox System Small arrows in bold next to the protein indicate changes in level during tumour progression

The RAS-RAF-MAP kinase oncogenic pathway can be activated by an increase in the levels of galectin-1, which acts as an amplifier of Ras signaling (Elad-Sfadia *et al*, 2002) and by a decrease in the Raf kinase inhibitor protein (Yeung *et al*, 1999) Increases in protein disulfide isomerases may act as a protective response against DNA damage and have been reported for other models of oxidative-reductive stress (Tanaka *et al*, 2000) Interestingly, protein disulfide isomerase 5 is down-regulated in DLKP versus DLKP-A by –2 18-fold whereas ER-60 is increased by 1 45-fold in DLKP-A5F These changes in the levels of these proteins can lead to a greater inhibition of p53-dependent apoptosis, a decrease in the inhibition of c-myc survival pathways and an increase in the signaling of Ras oncogene

Nucleophosmin (NPM) is up-regulated in cancer cells and has been described as a repressor of p53 activity (Maiguel *et al*, 2004) Since p53 transcriptional activity can be activated by DNA damage caused by the increase of ROS levels in tumour cells, the

increased expression of nucleophosmin can be important to maintain cell viability and to aid escaping apoptotic signalling Nucleophosmin (NPM) is unchanged in the adriamycin resistant variants but decreased in DLKP-Mitox

Liu *et al* (2006) compared the protein profiles of parental MCF-7 and an adriamycin resistant variant Proteomic analysis identified 17 proteins including nucleophosmin (-1 7-fold), peroxiredoxin 1 (2 3-fold) and peroxiredoxin 2 (-4 5-fold), protein disulfide isomerase (2 3-fold) cathepsin D chain B (3 5-fold), HSP27 (1 6-fold), triosephosphate isomerase (2 2-fold) and inorganic pyrophosphatase (-1 9-fold) Nucleophosmin, protein disulfide isomerase, HSP27 and cathepsin D have all been associated with the development of drug resistance and poor prognosis In these studies an isoform of triosephosphate isomerase is increased in DLKP versus DLKP-A (1 89-fold) and further increased in DLKP-A versus DLKP-A2B (1 87-fold) but decreased in DLKP-A versus DLKP-A5F (-2 26-fold) In contrast, a second isoform of triosephosphate isomerase is decreased in DLKP versus DLKP-A (-1 46-fold) and further decreased in DLKP-A versus DLKP-A10 (-3 21-fold) Peroxiredoxin 2, a protein uniquely differentially regulated in DLKP-A versus DLKP-A10, the cell line most resistant to adriamycin is also decreased (-1 86-fold)

Section 5.0: Conclusions and Future Work

5.1 Conclusions

The objectives of this thesis were to investigate the factors involved in the development of resistance to a number of chemotherapeutic drugs. This work has generated valuable models for the study of drug resistance and invasion, which reflect the clinical scenario.

- Pulse selections with clinically relevant drug concentrations were carried out on four lung cancer cell lines, two squamous (SKMES-1 and DLRP) and two small cell (NCI-H69 and DMS-53) lung carcinoma cell lines with either taxol, taxotere, carboplatin or VP-16. The result was twelve novel cell lines with relatively low clinically-relevant resistance.

- All selected cell lines developed resistance to the selecting drug (except DLRP-Cpt) and cross-resistance to structurally unrelated drugs. Taxotere selection of SKMES-1 resulted in increased expression of P-gp compared to the taxol-selected variant of SKMES-1. Pulse selection of DMS-53, a cell line intrinsically resistant to the taxanes, induced low levels of resistance to the drugs and also resulted in increased P-gp expression.

- Unstable resistance to both taxol and taxotere resulted in SKMES-Txt and SKMES-Txl. Resistance in both cell lines was unstable over time in culture and following storage in liquid nitrogen.

- Stable cross-resistance to 5-FU was observed in both taxane-selected variants of SKMES-1, each of the NCI-H69 drug selected variants and SKMES-Cpt100 suggesting a different mechanism of resistance in each of these cell lines.

- The resistance in DMS-Cpt and SKMES-1 and DMS taxane-selected variants may be due to a combination of mechanisms including alterations in tubulin dynamics, mutations in tubulin (β–tubulin expression is increased in SKMES-Txt) and increased expression of P-gp.
- Pulse selection of NCI-H69 with VP-16 and carboplatin resulted in cross-resistance to taxotere and sensitisation to adriamycin, vincristine and taxol in each case. In

contrast, SKMES-Cpt100 became cross-resistant to taxol and sensitised to vincristine and adriamycin, whereas SKMES-Cpt30 developed cross-resistance to both taxanes and was sensitised to vincristine, adriamycin and 5-FU

- Drug resistance has been previously associated with an invasive phenotype in cancer cells In the work described here however, no consistent correlation was observed Invasion was not induced in either of the non-invasive cell lines when pulsed with carboplatin and/or taxotere, taxol and VP-16 However, pulse selection of an already invasive cell line was found to alter the invasiveness Pulse selection of SKMES-1 with both taxanes resulted in more invasive variants, with the taxotere variant being the more invasive of the two when checked over two and seven weeks A correlation between a fall in drug resistance and adhesiveness with increase in the invasive phenotype was observed in both SKMES-Txt and SKMES-Txl over this period Exposure of DLRP to taxotere resulted in the DLRP-Txt cell line becoming only slightly more invasive and as seen in SKMES-Taxane selected variants a loss of adhesion was observed Pulse selection of the non-invasive small cell lung carcinoma cell line, DMS-53 to taxol and taxotere did not induce an invasive or motile phenotype or a change in adhesiveness

- Selection of SKMES-1 with a high concentration of carboplatin resulted in a more invasive cell line whereas pulse selection with a lower, more clinically relevant concentration resulted in a less invasive and less motile cell line These cell lines therefore provide a model for the future study of invasion No change in motility was observed in SKMES-Cpt100 Both carboplatin selections are more adhesive than the parent cell line Carboplatin selection had no effect on drug resistance, motility or invasiveness of DLRP-Cpt However, this cell line was considerably less adhesive than the parent Similar results to the taxane selections on the DMS-53 cell line were observed with carboplatin selection on NCI-H69 and DMS-53 No change in the invasive and motile phenotype was observed

- A fall in taxol and taxotere resistance in SKMES-Taxane-selected cells resulted in more invasive and less adhesive cell lines

The second major section of the thesis investigated the altered protein expression resulting from adriamycin exposure in a model system displaying varying levels of resistance to adriamycin.

It is also of interest to compare proteins altered in the adriamycin-resistant model with a mitoxantrone-resistant cell line as both drugs are alkalyating agents and mitoxantrone has less cardiotoxicity. Finally, resistance to the taxane drugs and the loss of resistance to taxol in SKMES-Txl (Wk3) was also examined by proteomic technologies.

As resistance to chemotherapy drugs is considered to be multifactorial, proteomic strategies have provided insights into the global changes in protein expression. The combination of proteomic techniques and suitable *in vitro* models presents an excellent setting for dissecting the processes and players involved in drug resistance.

- Proteomic analysis was carried out to study differential protein expression associated with adriamycin resistance in a series of clonal subpopulations of the adriamycin-resistant cell line DLKP-A, displaying varying levels of resistance to adriamycin and a number of other chemotherapeutic drugs (DLKP-A2B, -A5F and -A10). While the main mechanism of resistance in these cell lines is associated with P-gp, little information on cytoplasmic changes was available. This work identified eight proteins whose expression positively correlated with increasing resistance (e.g. the heat shock proteins 70kDa and 27 kDa, chaperonin containing TCP subunit 2, annexin A1, replication A2, K130r mutant of human Dj-1 and nucleoside diphosphate kinase 1). The expression of fourteen proteins correlated with baseline adriamycin resistance (ALDH1A1, VCP, HSPB1, CCT3, hnRPK, OXCT1, hnRNPH1, GDI2, STOML2 and ANXA1). These proteins represent ideal targets for future inhibitory work. The expression of twelve proteins inversely correlated with increasing adriamycin resistance (e.g. prohibitin and eIF 5A).

- DLKP and the adriamycin resistant variants also display differential invasion potential in the order DLKP-A2B < DLKP-A10 < DLKP < DLKP-A < DLKP-A5F with DLKP-A2B being the least invasive and DLKP-A5F the most invasive. The expression of four proteins was found to positively correlate with this increase in invasion namely, eukaryotic translation elongation factor 1D, annexin 1, horf 6 a

human peroxidase enzyme and HPRT The expression of gamma actin inversely correlated with invasion

- Proteomic analysis was carried out to study differential protein expression associated with mitoxantrone resistance in the DLKP-Mitox cell line While the main mechanism of resistance in this cell line is associated with BCRP overexpression (no detectable levels of P-gp and MRP1), little information on cytoplasmic changes is available This work identified 60 proteins with differential expression relating to mitoxantrone exposure The majority are involved in protein turnover and have cytoskeletal functions (e g nucleophosmin and high mobility group box protein)

- Of the sixty proteins identified as differentially expressed with regards to mitoxantrone resistance, nineteen were also differentially expressed in the DLKP versus DLKP-A comparison and twelve with the other adriamycin-resistant variants of DLKP Mitoxantrone exposure resulted in lower fold changes in the chaperone and stress response proteins namely, chaperonin containing TCP subunit 3, mortalm (HSPA9B) and HSP 70 proteins 8 as would be expected Both drugs induced relatively similar levels of two apoptotic/redox regulation proteins, galectin-1 and PARK7 and the overlapping glycolytic proteins, namely the aldehyde dehydrogenases and triosephosphate isomerase However, mitoxantrone induced a significantly higher fold change in the protein turnover and metabolic proteins, protein disulfide isomerase and ornithine aminotransferase respectively Adriamycin exposure resulted in higher levels of annexin induction However, mitoxantrone induced over twice the amount of sorcin and hnRPK Mitoxantrone was designed to produce less free radicals in comparison to adriamycin, similar levels of apoptotic/redox response proteins were differentially regulated in both cell lines However, in contrast to DLKP-A, the majority of these proteins are up-regulated in DLKP-Mitox

- Proteomic analysis was carried out to study differential protein expression caused by taxane resistance in two cell lines developed in these studies, namely SKMES-Txt and SKMES-Txl (Wk3) The parental cell line, SKMES-1, not previously documented to be exposed to drug was selected with clinically-relevant concentrations of the taxanes, taxol and taxotere The main mechanism of resistance in these cell lines is the overexpression of the membrane protein P-gp Pulse selection with taxotere yielded a total of 40 differentially expressed proteins Of these 40 proteins, 19 were unique to taxotere-selection (e g vimentin and galectin-1) when compared to SKMES-Txl (Wk3) and SKMES-Txl (Wk6) The majority of the differentially-regulated proteins have functions, as expected, in protein turnover and the stress response These proteins are known to increase resistance to cell death induced by a variety of stimuli

- Taxol exposure in SKMES-1 resulted in a total of 48 differentially-expressed proteins Of these 48 proteins, 21 overlapped with SKMES-Txt (e g keratin 8 and glucose-6-phosphate dehydrogenase) Taxol and taxotere exposure resulted in similar expression levels of the majority of these proteins with the exception of proteasome activator subunit 2 and peroxiredoxin 2, both of which are increased to a greater extent in SKMES-Txt In contrast to the unique proteins differentially-regulated in response to taxotere exposure, taxol exposure resulted in the differential expression of 23 unique proteins, of which most were down-regulated The majority of these proteins have function in ion binding/transport, protein turnover and the stress response

- An unforeseen but fortunate result of taxane-selection of SKMES-1 was the observed loss of resistance in both taxane-resistant variants which resulted from culturing and storage in liquid nitrogen Proteomic analysis was also carried out to study differential protein expression caused by loss of taxol resistance Twenty-five proteins were identified in the comparison of SKMES-Txl (Wk3) versus SKMES-Txl (Wk6) Four of these proteins showed contrasting protein-fold level in comparison to SKMES-1 versus SKMES-Txl (Wk3) Ten proteins were found to be unique to SKMES-Txl (Wk3) versus SKMES-Txl (Wk6) These shared proteins involved in loss of resistance function in the cellular redox cycle They are involved

in the regulation of cellular differentiation and proliferation *via* the modulation of hydrogen peroxide mediated responses The up-regulation of these cellular redox proteins in the more resistant SKMES-Txl (Wk3) may reflect an attempt by the cells to survive and proliferate in response to taxol exposure This response is no longer required once taxol is removed

- Exposure to adriamycin, mitoxantrone, taxol and taxotere predominantly resulted in differential expression of the stress and cellular redox proteins which may contribute to drug resistance in these cell lines

5 2 Future Work

Proteomic strategies have allowed the simultaneous analysis of differential protein expression that may contribute to the understanding of drug resistance and/or invasion These results confirm the multifactorial nature of both processes (i e drug resistance and invasion) and proteins involved in drug resistance and may provide biomarkers for future intervention of drug-induced resistance

- The taxol, taxotere and carboplatin-selected cell lines in this thesis represent valuable models for the study of mechanisms of resistance to these drugs Most of the analysis in this thesis focussed on the taxane-resistant cell lines of SKMES-1 Similar proteomic analysis on the other taxane-selected cell lines would be necessary to check for similar patterns in these other models

- The carboplatin-resistant cell lines could also be examined by proteomic analysis and candidate proteins for development of carboplatin resistance could be identified

- During pulse-selection of the cell lines SKMES-Txt cell stocks were frozen in liquid nitrogen after 2, 4, 6 and 8 pulses before the cells received the full ten pulses These intermediate cell lines have not been characterised for drug resistance, invasion or expression of any markers Using these cell lines, it may be possible to track the development of resistance to taxotere through proteomic technologies

- The proteins identified *via* proteomic analysis in this thesis as potentially involved in drug-resistance should be further validated by Western blotting and analysed by inhibitory work (siRNA) Drug-resistance remains a serious problem in the treatment of cancer and the proteins identified here could help increase our knowledge of the complex mechanisms involved

Section 6.0: Bibliography

Ahn, S H , Sawada, H , Ro, J Y and Nicolson, G L (1997) Differential expression of annexin I in human mammary ductal epithelial cells in normal and benign and malignant breast tissues *Clin Exp Metastasis* **15,** 151-160

Akehurst, R L Beinert, T , Crawford, J , Crino, L , Debus, J , Eckersberger, F , Fischer, J , Georgoulias, V , Gridelli, C , Hirsch, F R , Jassem, J , Kosmidis, P , Krainer M , Krzakowski, M , Mansgold, Ch , Niklinski, J , Pirker, R , Pujol, J L , Scagliotti, G , Thatcher, N , Tomek, S , Tonato, M , van Zandwijk, N , Zielinski, C C , Zochbauer, S , Zitter, M , (2002) Consensus on medical treatment of non-small cell lung cancer *Lung Cancer* **38,** S3-S7

Adriaenssens, E , Lemoine, J , El Yazidi-Belkoura, I and Hondermarck, H (2002) Growth signaling in breast cancer cells outcomes and promises of proteomics *Biochemical Pharm* **64,** 797-803

Ahmed, N , Oliva, K T , Barker, G , Hoffmann, P , Reeve, S , Smith, I A , Quinn, M A and Rice, G E (2005) Proteomic tracking of serum protein isoforms as screening biomarkers of ovarian cancer *Proteomics* **5,** 4625-4636

Alaiya, A A , Franzen, B , Moberger, B , Silfversward, C , Linder, S and Auer, G (1999) Two-dimensional gel analysis of protein expression of ovarian tumours shows a low degree of intratumoral heterogeneity *Electrophoresis* **20,** 1039-1046

Alaiya, A A , Franzen, B , Auer, G and Linder, S (2000a) Cancer proteomics From identification of novel markers to creation of artificial learning models for tumour classification *Electrophoresis* **21,** 1210-1217

Alaiya, A A , Franzen, B , Hagman, A , Silfversward, C , Moberger, B , Linder, S , Auer, G (2000b) Classification of human ovarian tumours using multivariate data analysis of polypeptide expression patterns *Int J Cancer* **86,** 731-736

Alaiya, A A , Roblick, U J , Franzen, B Brunch, H-P and Auer, G (2002) Protein expression profiling in human lung, breast, bladder, renal, colorectal and ovarian cancers *J Chromatography B* In Press

Albini, A (1998) Tumor and endothelial cell invasion of basement membranes The matrigel chemoinvasion assay as a tool for dissecting molecular mechanisms *Pathol Oncol Res* , **4,** 230-241

Alderden, R A , Mellor, H R , Modok, S , Hambley, T W , Callaghan, R (2006) Cytotoxic efficacy of an anthraquinone linked platinum anticancer drug *Biochem Pharmacol* **71,** 1136-45

Alfonso, P Catala, M , Rico-Morales, M L , Durante-Rodriguez, D , Moro-Rodriguez, E , Fernandez-Garcia, H , Escribano, J M , Alvarez-Fernandez, E and Garcia-Poblete, E (2004) Proteomic analysis of lung biopsies Differential protein expression profile between peritumoral and tumoral tissue *Proteomics* **4,** 442-447

An, Y , Fu, Z , Gutierrez, P and Fenselau, C (2005) Solution isoelectric focusing for peptide analysis comparative investigations of an insoluble nuclear protein fraction *J Proteome Res* **4,** 2126-2132

Anderson, N L and Seilhamer, J (1997) A comparison of selected mRNA and protein abundance in human liver *Electrophoresis* **18,** 533-537
Anderson, N L , Matheson, A D , Steiner, S (2000) Proteomics applications in basic and applied biology *Curr Opin Biotechnol* **11,** 408-412

Arrigo, A.P., Paul, C. and Duchase, C. (2002). Small stress proteins: novel negative modulators of apoptosis induced independently of reactive oxygen species. *Prog. Mol. Subcell. Biol.* **28**, 185-204.

Arrigo, A.P. (2005). Heat shock proteins as molecular chaperones, *Med.. Sci. (Paris)* **21**, 619–625.

Aschele, C., Debernardis, D., Bandelloni, R., Cascinu, S., Catalano, V., Giordani, P., Barni, S. Turci, D., Drudi, G.S., Lonardi, L., Gallo, L., Maley, F. and Monfardini, S, (2002). Thymidylate synthase protein expression in colorectal cancer metastases predicts for clinical outcome to leucovorinmodulated bolus or infusional 5-fluorouracil but not methotrexate-modulated bolus 5-fluorouracil. *Annals of Oncol,* **13,** 1882-1892.

Bai, X.F., Ni, X.G., Zhao, P., Liu, S.M., Wang, H.X., Guo, B., Zhou, L.P., Zhang, J.S., Wang, K., Xie, Y.Q., Shao, Y.F. and Zhao, X.H. (2004). Overexpression of annexin 1 in pancreatic cancer and its clinical significance. *World J. Gastroenterol.* **10,** 1466-1470.

Banks, R.E., Dunn, M.J., Forbes, M.A., Stanley, A., Papin, D., Naven T., Gough, M., Harnden, P. and Selby, P.J. (1999). The potential use of laser capture microdissection to selectively obtain distinct populations of cells for proteomic analysis - preliminary findings. *Electrophoresis* **20**, 689-700.

Barkin, A., Varga, A., Zheng, Q. and Safine, A. (2005). Epigenetic silencing of tropomyosin alters transforming growth factor beta control of cell invasion and metastasis. *Breast Cancer Res.* 7, 40.

Belotti, D., Vergani, V., Drudis, T., Borsotti, P., Pitelli, M. R., Viale, G., Giavazzi, R. and Taraboletti, G. (1996). The microtubulea affecting drug paclitaxel has antiangiogenic activity. *Clin. Cancer Res.* **2**, 1843-1849.

Bergman, A.C., Benjamin, T., Alaiya, A.A., Waltham, M. Sakaguchi, K, Franzen, B., Linden, S. Bergman, T., Auer, G., Appello, E., Wirth, P.J. and Jarnval, H. (2000). Identification of gel-separated tumor marker proteins by mass spectrometry. *Electrophoresis* **21**, 679-686.

Besada, V., Diaz, M., Becker, M., Ramos, Y., Castellanos-Serra, L. and Fichtner, I. (2006). Proteomics of xenografted human breast cancer indicates novel targets related to tamoxifen resistance. *Proteomics,* **6,** 1038-1048.

Bhalla, K., Huang, Y., Tang, C., Self, S., Ray, S., Mahoney, M.E., Ponnathpur, V., Tourkina, E., Ibrado, A.M., Bullock, G. (1994). Characterisation of a human myeloid leukemia cell line highly resistant to taxol. *Leukemia*, **8**, 465-475.

Bi, X., Lin, Q., Foo, T.W., Joshi, S., You, T., Shen, H.M., Ong, C.N., Cheah, P.Y., Eu, K.W. and Hew, C.L. (2006). Proteomics analysis of colorectal cancer reveals alterations in metabolic pathways - mechanism of tumorigenesis. *Mol. and Cell. Proteomics* **5**, 1119-1130

Bichat, F., Mouawad, R., Solis-Recendez, G., Khayat, D. and Bastian, G. (1997). Cytoskeleton alteration in MCF7R cells, a multidrug resistant human breast cancer cell line. *Anticancer Res.* **17**, 3393-3401.

Bjellquist, B., Ek, K., Richetti, P., Gianazza, E., Gorg, A., Westermeir, R. and Postel, W. (1982). Isoelectric focusing in immobilised pH gradients principle, methodology and some applications. *J. Biochem. Biophys. Methods* **6**, 317-339.

Blackstock, W.P. and Weir, M.P. (1999). Proteomics: quantitative and physical mapping of cellular proteins. *Trends Biotechnol.* **17**, 121-127.

Block, W.D., Yu, Y. and Lees-Miller, S.P. (2004). Phosphatidyl inositol 3-kinase-like serine/threonine protein kinases (PIKKs) are required for DNA damage-induced phosphorylation of the 32 kDa subunit of replication protein A at threonine 21. *Nucleic Acids Res.* **32**,997-1005.

Bomsztyk, K., Denisenko, O. and Ostrowski, J. (2004). hnRNP K: one protein multiple processes. *Bioessays*, **26,** 629-638.

Boonstra, R., Timmer-Bosscha, H., van Echten-Arends, J. (2004). Mitoxantrone resistance in a small cell lung cancer cell line is associated with ABCA2 upregulation. *Br. J. Cancer.* **90**, 2411-7

Borst, P. Evers, R., Kool, M. and Wijnholds, J. (1999). The multidrug resistance protein family. *Biochim. Biophys. Acta*, **1461**, 347-357.

Bortoli, M.D., Casteool, R.C., Lu, X.Y., Deyo, J., Sturla, L.M., Adesina, A.M., Perlaky, L., Pomeroy, S.L. (2006). Medulloblastoma outcome is adversely associated with overexpression of EEF1D, PRL30 and RPS20 on the long arm of chromosome 8. *BMC.* **6,** 223.

Bostwick, D.G. (2000). Immunohistochemical changes in prostate cancer after androgen deprivation therapy. *Mol. Urol.* **4,** 101–106.

Breen, L., PhD, Dublin City University, **2005.**

Brichory, F.M., Misek, D.E., Yim, A.M., Krause, M.C., Giordano, T.J., Beer, D.G. and Hanash, S.M. (2001a). An immune response manifested by the common occurrence of annexins I and II autoantibodies and high circulating levels of IL-6 in lung cancer. *PNAS,* **98,** 9824-9829.

Brichory, F., Beers, D., LeNaour, F., Giordano, T. and Hanash, S. (2001b). Proteomics-based identification of protein gene product 9.5 as a tumour antigen that induces a humoral immune response in lung cancer. *Cancer Res.,* **61,** 7908-7912.

Bruchovsky, N., Owen, A. A., Becker, A. J. and Till, J. E. (1965). Effects of vinblastine on the proliferative capacity of and their progress through the division cycle. *Cancer Res. 25*, 1232-1237.

Bukau, B. and Horwich, A.L. (1998). The Hsp70 and Hsp60 chaperone machines, *Cell* **92**, 351–366.

Bunn, P.A., (2002). Molecular biology and early diagnosis in lung cancer. *Lung Cancer,* **38,** S5-S8.

Burns, B.S., Edin, M.L., Lester, G.E., Tuttle, H.G., Wall, M.E., Wani, M.C. and Bos, G.D. (2001). Selective drug resistant human osteosarcoma cell lines. *Clin. Orthop. Relat Res.* **383,** 259-267.

Bursch, W. (2001). The autophagosomal-lysosomal compartment in programmed cell death. *Cell Death Differ.* **8**, 569-581.

Byun, Y., Chen, F., Chang, R., Trivedi, M. (2001). Caspase cleavage of vimentin disrupts intermediate filaments and promotes apoptosis. *Cell Death Differ.* 2001, *8*, 443-450.

Caballero, O L , Resto, V , Parrurajan, M , Meerzaman, D , Gou, M Z , Engles, J Yochem, R , ratovitski, E , Sidransky, D and Jen, J (2002) Interaction and colocalisation of PGP9 5 with JAB1 and $p27^{kp1}$ *Oncogene*, **21**, 3003-3010

Cahill, D J (2001) Protein and antibody arrays and their medical applications *J Immunological Methods* **250**, 81-91

Calderoni, A and Cerny, T (2001) Taxanes in lung cancer a review with focus on the European experience *Clin Rev in Oncology/Hematology*, **38**, 105-127

Calderwood, S K , Khalegue, M A , Sawyer, D B and Ciocca, D R (2006) Heat shock proteins in cancer chaperones of tumorigenesis *Trends Biochem Sci* **31**, 164-72

Campostrini, N , Pascali, J , Hamdan, M , Astner, H , Marimpietri, D , pastorino, F , Ponzoni, M and Righetti, P G (2004) Proteomic analysis of an orthotopic neuroblastoma xenograft animal model *J Chromatogr B Analyt Technol Biomed Life Sci* **808**, 279-286

Canuto, R A , Muzio, G , Salvo, R A and Maggiora, M , Trombetta, A , Chantepie, J , Fournet, G , Reichert, U and Quash, G (2001) The effect of a novel irreversable inhibitor of aldehyde dehydrogenase 1 and 3 on tumour cell growth and death *Chem Biol Interact* 2001, **130**, 209-218

Cascinu, S , Aschele, C , Barni, S , Debernardis, D , Baldo, C , Tunesi, G , Catalano, V , Staccioli, M P , Brenna, A , Muretto, P , Catalano, G (1999) Thymidylate Synthase Protein Expression in Advanced Colon Cancer Correlation with the Site of Metastasis and the Clinical Response to Leucovorin-modulated Bolus 5-Fluorouracil *Clin Can Res* **5**, 1996-1999

Castagna, A , Antonioli, P , Astner, H , Hamdan, M , Rigetti, S C , Perego, P , Zunino, F and Rigetti, P G (2004) A proteomic approach to cisplatin resistance in the cervix squamous cell carcinoma cell line A431 *Proteomics*, **4**, 3246-67

Caulin, C , Ware, C F , Magin, T M and Oshima R G (2000) Keratin-dependent, epithelial resistance to tumor necrosis factor-induced apoptosis *J Cell Biol* **149**, 17–22

Celis, J E and Gromov, P (1999) 2D protein electrophoresis can it be perfected? *Curr Opin Biotechnol* **10**, 16-21

Celis, J E , Celis, P , Ostergaard, M , Basse, B , Lauridsen, J B , Ratz, G , Rasmussen, H H , Orntoft, T F , Hein, B , Wolf, H and Celis, A (1999) Proteomics and immunohistochemistry define some of the steps involved in the squamous differentiation of the bladder transitional epithelium a novel strategy for identifying metaplastic lesions *Cancer Res* **59**,3003-3009

Celis, J E , Kruhoffer, M , Gromova, I , Frederiksen, C , Ostergaard, M , Thykjear, T , Gromov, P , Jinsheng, Y , Palsdottir, H , Magnusson, N and Orntoft, T F (2000) Gene expression profiling monitoring transcription and translation products using DNA microarrays and proteomics *FEBS Lett* **480**, 2-16

Chauncey, T R (2000) Chemotherapy resistance in acute leukaemia *Turk J Haematol* **17**, 155-162

Chauhan, D , Li, G , Shringarpure, R , Podar, K , Ohtake, Y , Hideshima, T and Anderson, K C (2003) Blockade of Hsp27 overcomes Bortezomib/proteasome inhibitor PS-341 resistance in lymphoma cells *Cancer Res* **63**, 6174-6177

Chauhan, D , Li, G , Auclair, D and Hideshima, T (2003) Identification of genes regulated by 2-methoxyestradiol (2ME2) in multiple myeloma cells using oligonucleotide arrays *Blood* **101**, 3606-3614

Chen, S , Gomez, S P , McCarley, D , Mainwaring, M G (2002) Topotecan-induced topoisomerase II α expression increases the sensitivity of the CML cell line K562 to subsequent etoposide plus mitoxantrone treatment *Cancer Chemother Pharmacol* **49**, 347-355

Chen, G , Gharib, T G , Huang, C C , Thomas, D G , Shedden, K A , Taylor, J M G , Kardia, S L R , Misek, D E , Giordano, T J , Iannettoni, M D , Orringer, M B , Hanash, S H and Beer, D G (2003) Proteomic analysis of lung adenocarcinoma identification of a highly expressed set of proteins in tumors *Clin Cancer Res* **8**, 2298-2305

Chen, C , Gomez, S P , McCarley, D and Mainwaring, M G (2002) Topotecan-induced topoisomerase IIalpha expression increases the sensitivity of the CML cell line K562 to subsequent etoposide plus mitoxantrone treatment *Cancer Chemother Pharmacol* **49**, 347-55

Chen, G , Gharib, T G , Thomas, D G , Huang, C C , Misek, D E , Kuick K , Giordano, T J , Lannettoni, M D , Orringer, M B , Hanash, S M and Beer, D G (2003) Proteomic analysis of eIF-5A in lung adenocarcinomas *Proteimics*, **3**, 496-504

Chen, W , Li, N , Chen, T , Han, Y , Li, C , Wang, Y , He, W , Zhang, L , Wan, T and Cao, X (2005) The lysosome-associated apoptosis-inducing protein containing the pleckstrin homology (PH) and FYVE domains (LAPF), representative of a novel family of PH and FYVE domain-containing proteins, induces caspase-independent apoptosis via the lysosomal-mitochondrial pathway*J Biol Chem* **280**, 40985-95

Chiou, J -F , Liang, J -A , Hsu, -H , Wang, J -J , Ho, S -T and Kao, A (2003) Comparing the relationship of taxol-based chemotherapy response with P-glycoprotein and lung resistance-related protein expression in non-small cell lung cancer *Lung*, **181**, 267-273

Chu, Y-W , Yang, P W , Yang, S C , Shyu, Y C , Hendrix, M J C , Wu, R and Wu, C W (1997) Selection of invasive and metastatic subpopulations from a human lung adenocarcinoma cell line *Am J Respir Cell Mol Biol*, **17**, 353-360

Chuman, Y , Bergman, A-C , Ueno, T , Saito, S , Sakaguchi, K , Alaiya, A A , Franzen, B , Bergman, T , Arnott, D , Auer, G , Appella, E , Jornvall, H and Linder, S (1999) Napsin A, a member of the aspartic protease family, is abundantly expressed in normal lung and kidney tissue and is expressed in lung adenocarcinomas *FEBS Lett* **462**, 129-134

Christian, M M , Moy, R , Wagner, R F , Moore, A (2001) A correlation of alpha smooth muscle actin and invasion in micronodular basal cell carcinoma *Dermatologic Surgery*, **27**, 1524-1547

Ciechanover, A , Orian, A and Schwartz, A L (2000) Interaction and colocalization of PGP9 5 with JAB1 and $p27^{Kip1}$ *J Cell Biochem* **34**, (Suppl) 40-51

Cillo, C , Dick, J E , Ling, V and Hill, R P (1987) Generation of drug-resistant variants in metastatic B16 mouse melanoma cell lines *Cancer Res* **47**, 2604-2608

Ciocca, D R , Oesterreeich, S , Chamness, G C , McGuire, W L and Fuqua, S A (1993) Biological and clinical implications of heat shock protein 27,000 (Hsp27) a review *J Natl Cancer Inst* **85**, 1558-1570

Ciocca, D R and Calderwood, S K (2005) Heat shock proteins in cancer diagnostic, prognostic, predictive, and treatment implications *Cell Stress Chaperones* **10,** 86-103

Ciocca, D R , Rozados, V R , Cuello-Carrión, F D , Gervasoni, S I , Matar, P and Scharovsky, O G (2003) Heat shock proteins 25 and 70 in rodent tumors treated with doxorubicin and lovastatin *Cell Stress Chaperones* **8,** 26-36

Claret, F X Hibi, M , Dhut, S , Toda, T and Karin, M (1996) A new group of conserved coactivators that increase the specificity of AP-1 transcription factors *Nature,* **383,** 453-457

Clausse, N , Van den Brule, F , Waltregny, D , Garnier, F and Castronovo, V (1999) Galectin-1 expression in prostate tumor-associated capillary endothelial cells is increased by prostate carcinoma cells and modulates heterotypic cell-cell adhesion *Angiogenesis* **3,** 317-325

Cleary, I , Doherty, G , Moran, E and Clynes, M (997) The multidrug-resistant human lung tumour cell line, DLKP-A10, expresses novel drug accumulation and sequestration systems *Biochem Pharmacol* **53**, 1493-502

Clement, P M , Johansson, H E , Wolffi , E C and Park, M H (2006) Differential expression of eIF5A-1 and eIF5A-2 in human cancer cells *FEBS J* **273**, 1102–1114

Clynes, M , Redmond, A , Moran, E, and Gilvarry, U (1992) Multiple drug-resistance in variant of a human non-small cell lung carcinoma cell line, DLKP-A *Cytotechnology* **10**, 75-89

Clynes M, Daly C, NicAmhlaoibh R, Cronin D, Elliott C, O'Connor R, O'Doherty T, Connolly L, Howlett A, Scanlon K (1998) Recent developments in drug resistance and apoptosis research *Crit Rev Oncol Hemato* **28**, 181-205

Coates, P J , Jamieson, D J , Smart, K , Prescott, A R and Hall, P A (1997) The prohibitin family of mitochondrial proteins regulate replicative lifespan *Curr Biol* 7, 607–610

Cohen, L S , Escobar, P F , Scharm, C , Glimco, B , Fishman, D A (2001) Three-dimensional power Doppler ultrasound improves the diagnostic accuracy for ovarian cancer prediction *Gynecol Oncol* **82**, 40-48

Cole, S and Bhardwaj, G Overexpression of a transporter gene in a Multidrug resistant human lung cancer cell line *Science* **1992**, *258*, 1650-1654

Colombo, E , Bonetti, P , Lazzerini, D E , Martinelli, P , Zamponi, R , Marine, J C , Helin, K , Falini, B and Pelicci, P G (2005) Nucleophosmin is required for DNA integrity and p19Arf protein stability *Mol Cell Biol* **25**, 8874-86

Cordwell, S J , Nouwens, A S , Verrills, N M , Basseal, D J and Walsh, B J (2000) Subproteomics based upon protein cellular location and relative solubilities in conjunction with composite two-dimensional electrophoresis gels *Electrophoresis* **21**, 1094-1103

Costello, C (1999) Bioanalytic applications of mass spectrometry *Curr Opin Biotechnol* **10**, 22-28

Cragg, G M and Newman, D J (2005) Plants as a source of anti-cancer agents *J of Ethnopharmacology,* **100,** 72-79

Creagh, E M and Cotter, T G (1999) Selective protection by hsp 70 against cytotoxic drug-, but not Fas-induced T-cell apoptosis *Immunology* **97,** 36-44

Creagh, E.M., Sheehan, D. and Cotter, T.G. (2000). Heat shock proteins--modulators of apoptosis in tumour cells. *Leukemia.* **14,** 1161-73.

Curt, G.A., Carney, D.N., Cowan, K.H., Bailey, B.D., Drake, J.C., Kao-Shan, C.S., Minna, J.D. and Chabner, B.A. (1984). Unstable methotrexate resistance in numan small cell carcinoma associated with double minute chromosomes. *New England J. of Medicine* **308,** 199-202.

Damstrup, L., Voldberg, R.B., Spang-Thomsen, M., Brunner, N and Poulsen, S.H. (1998). In vitro invasion of small-cell lung cancer cell lines correlates with expression of epidermal growth factor receptor. *Br. J. Cancer.* **78,** 631-640.

Danesi, R., De Braud, F., Fogli, S., De Pas, T.M. Di Paolo, A., Curigliano, G. and Del Tacca, M. (2003). Pharmacogenetics of anticancer drug sensitivity in non-small cell lung cancer. *Pharmacological Rev.,* **55,** 57-103.

Daubeuf, S., Balin, D., Leroy, P. and Visvikis, A. (2003). Different mechanisms for γ-glutamyltransferase-dependent resistance to carboplatin and cisplatin. *Biochem. Pharmacol.* **66,** 595-604.

De Bruin, M., Miyake, K., Litman, T., Robey, R., Bates, S.E. (1999). Reversal of resistance by GF120918 in cell lines expressing the ABC half-transporter, MXR. *Cancer Letts.* **146,** 117-126

Debatin, K-M. (2000). Activation of apoptosis pathways by anticancer treatments. *Toxicol. Lett.* **112,** 41-48.

Deffie AM, Batra JK, Goldenberg GJ. (1989). Direct correlation between DNA topoisomerase II activity and cytotoxicity in adriamycin-sensitive and -resistant P388 leukemia cell lines. *Cancer Res.* **49,** 58-62.

DiPaola, R.S. (2002). To arrest or not to G(2)-M Cell-cycle arrest. *Clin Cancer Res.* **8,** 3311–4.
Donaldson, K., Goolsby, G., Kiener, P.A. and Wahl, A.F. (1994). Activation of $p34^{cdc2}$ coincident with taxol-induced apoptosis. *Cell Growth and Differentiation.* **5,** 1041-1051.

Doyle, L.A., Yang, W., Abruzzo, L.V., Krogmann, T., Gao, Y., Rishi, A.K. and Ross D.D. (1998). A multidrug resistance transporter from human MCF-7 breast cancer cells. *PNAS,* **95,** 15665-15670.

Duan, Z., Feller, A.J., Chong Toh, H., Makastorsis, T. and Seiden, M.V. (1999). TRAG-3, a novel gene, isolated from a taxol-resistnt ovarian carcinoma cell line. *Gene,* **229,** 75-81.

Dutt, M.J. and Lee, K.H. (2000). Proteomic analysis. *Curr. Opin. Biotechnol.* **11**, 176-179.

Duffy, C.P., Elliott, C.J., O'Connor, R.A., Heenan, M.M., Coyle, S., Cleary, I.M., Kavanagh, K., Verhaegen, S., O'Loughlin, C.M., NicAmhlaoibh, R. and Clynes, M. (1998). Enhancement of chemotherapeutic drug toxicity to human tumour cells *in vitro* by a subset of non-steroidal anti-inflammatory drugs (NSAIDs). *Eur. J. Cancer*, **34**, 1250-1259.

Dvorzhinski, D., Thalasila, A., Thomas, P.E., Nelson, D., Li, H., White, E. and DiPaola, R.S. (2004) A novel proteomic coculture model of prostate cancer cell growth. *Proteomics,* **4,** 3268-3275.

Dziadyk, J.M., Sui, M., Zhu, X., Fan, W. (2004). Paclitaxel-induced apoptosis may occur without a prior G2/M-phase arrest. *Anticancer Res.* **24,** 27–36.

Easton, D P , Kaneko, Y Subjeck, J R (2000) The hsp110 and Grp1 70 stress proteins newly recognized relatives of the Hsp70s, *Cell Stress Chaperones* **5**, 276–290

Ekstrom, S , Onnerfjord, P , Nilsson, J , Bengtsson, M , Laurell, T and Marko-Varga, G (2000) Integrated microanalytical technology enabling rapid and automated protein identification *Anal Chem* **72**, 286-293

Elad-Sfadia, G , Haklai, R , Ballan, E , Gabius, H J and Kloog, Y (2002) Galectin-1 augments Ras activation and diverts Ras signals to Raf-1 at the expense of phosphoinositide 3-kinase *J Biol Chem* **277**, 37169-75

Emert-Sedlak, L , Shangary, S , Rabinovitz, A , Miranda, M B , Delach, S M and Johnson, D E (2005) Involvement of cathepsin D in chemotherapy-induced cytochrome *c* release, caspase activation, and cell death *Mol Cancer Ther* **4**, 733-742

Ferlini, C , Ojima, I , Distefano, M , Gallo, D , Riva, A , Morazzoni, P , Bombardelli, E , Mancuso, S and Scambia, G (2003) Second Generation Taxanes from the Natural Framework to the Challenge of Drug Resistance *Current Medicinal Chemistry - Anti-Cancer Agents,* **3**, 133-138

Fields, S (2001) Proteomics in genomeland *Science,* **291**, 1221-1224

Filipits, M (2004) Mechanisms of cancer multidrug resistance *Drug Discovery Today Disease Mechanisms,* **1**, 229-234

Fokkema, E , De Vries, E G , Groen, H J Meijer, C and Timens, W (2003) Expression of apoptosis-related proteins and morphological changes in a rat tumor model of human small cell lung cancer prior to and after treatment with radiotherapy, carboplatin, or combined treatment *Virchows Arch* **442**, 349-355

Fram, R J , Woda, B A , Wilson, J M and Robichaud, N (1990) Characterization of acquired resistance to cis-diammminedichloroplatinum(II) in BE human colon carcinoma cells *Cancer Res* **50**, 72-77

Friedman, D B , Hill, S , Keller, J W , Merchant, N B , Levy, S E , Coffey, R J and Caprioli, R M (2004) Proteome analysis of human colon cancer by two-dimensional difference gel electrophoresis and mass spectrometry *Proteomics* **4**, 793-811

Fogh, J , Wright, W C and Loveless, J D (1977) Absence of HeLa cell contamination in 169 cell lines derived from human tumours *J Nat Cancer Inst* **58**, 209-14

Fox, E J (2004) Mechanism of action of mitoxantrone *American Academy of Neurology* **63**, S1-S18

Fu Z, Fenselau C (2005) Proteomic evidence for roles for nuleolin and Poly[ADP-ribosyl] transferase in Drug resistance *J Proteome Res* 4, 1583-1591

Fujii, K , Kondo, T , Yokoo, H , Yamada, T , Iwatsuki, K and Hirohashi, S (2005) Proteomic study of human hepatocellular carcinoma using two-dimensional difference gel electrophoresis with saturation cysteine dye *Proteomics* **5**,1411-1422

Fung, E (2001) Ciphergen ProteinChip technology A platform for protein profiling and biomarker identification *Nat Genetics,* **27**, 54-62

Fusaro, G., Wang, S. and Chellappan, S. (2002). Differential regulation of Rb family proteins and prohibitin during camptothecin-induced apoptosis. *Oncogene* **21**, 4539–4548.

Futscher, B.W., Abbaszadegan, M.R., Domann, F. and Dalton, W.S. (1994) Analysis of MRP mRNA in mitoxantrone-selected, multidrug-resistant human tumour cells. *Biochem. Pharmacol,* **47,** 1601-6.

Gamberi, C., Izaurralde, E., Beisel, C. and Mattaj, I.W. (1997). Interaction between the Human Nuclear Cap-Binding Protein Complex and hnRNP F. *Mol. Cell. Biol.*, **17**, 2587-2597.

Gamble, S.C., Odontiadis, M., Waxman, J., Westbrook, J.A., Dunn, M.J. and Wait, R. (2004). Androgens target prohibitin to regulate proliferation of prostate cancer cells. *Oncogene* **23**, 2996–3004.

Galperin, M.Y., Moroz, O.V., Wilson, K.S. and Murzin, K.S. (2006). House cleaning, a part of good housekeeping. *Molecular Microbiology.* **59,** 5-19.

Gamble, S.C., Chotai, D., Odontiadis, D.A., Brooke, G.N., Powell, S.M. Reebye, V., Valera-Carver, A., Kawano, Y., Waxamn, J. and Bevan, C.L. (2006). Prohibitin, a protein downregulated by androgens, represses androgen receptor activity. *Oncogene.* 1-12.

Garneau, D., Revil, T., Fisette, J.F. and Chabot, B. (2005). Heterogeneous Nuclear Ribonucleoprotein F/H Proteins Modulate the Alternative Splicing of the Apoptotic Mediator Bcl-x. *J. Biol. Chem.*, **280,** 22641-22650.

Garrido, C., Bruey, J.M., Fromentin, A., Hammann, A., Arrigo, A.P. and Solary, E. (1999). HSP27 inhibits cytochrome c-dependent activation of procaspase-9. *FASEB J.* **13,** 2061-70.

Gazdar, A.F., Carney. D.N., Nau, M.M., Minna, J.D. (1985). Characterization of variant subclasses of cell lines derived from small cell lung cancer having distinctive biochemical, morphological, and growth properties. *Cancer Res.*;**45,** 2924–2930

Gehrmann, M.L., Hathout, Y. and Fenselau, C. (2004). Evaluation of metabolic labeling for comparative proteomics in breast cancer cells. *J. Proteome Res.* **3**, 1063-1068.

Gelman, K. (1994). The taxoids: paclitaxel and docetaxel. *Lancet,* **344,** 1267-1272.

Geney, R., Chen, J. and Ojima, I. (2005) Recent advances in the new generation taxane anticancer agents. *Med. Chem.* **1**, 125-139.

Gharbi, S., Gaffney, P., Yang, A., Marketa, J., Zvelebil, M.J., Cramer, R., Waterfield, M.D. and Timms, J.F. (2002). Evaluation of two-dimensional differential gel electrophoresis for Proteomic expression analysis of a model breast cancer cell system. *Mol. and Cell.Proteomics* **1**, 91-98.

Giannakakou, P., Sackett, D.L., Kang, Y.K., Zhan, Z., Buters, J.T.M., Fojo, T., Poruchynsky, M.S. (1997). Paclitaxel-resistant human ovarian cancer cells have mutant β-tubulins that exhibit impaired paclitaxel-driven polymerization. *J. Biol. Chem.*, **272**, 17118-17125.

Gidding, C.E., Kellie, S.J., Kamps, W.A., de Graaf, S.S. (1999). Vincristine revisited. *Crit. Rev. Oncol. Hematol.*, **29**,267-287.

Gilbert, S., Loranger, A. Marceau, N. (2004) Keratins modulate c-Flip/extracellular signal-regulated kinase 1 and 2 antiapoptotic signaling in simple epithelial cells. *Mol. Cell Biol.* **24**, 7072-7081.

Gilles, C , Polette, M , Zahm, J M , Tournier, J M , Volders, L , Foidart, J M , Birembaut, P (1999) Vimentin contributes to human mammary epithelial cell migration *J Cell Sci* , **112,** 4615-4625

Glisson, B , Gupta, R , Smallwood-Kentro, S and Ross, W (1986) Characterization of acquired epipodophyllotoxin resistance in a Chinese hamster ovary cell line loss of drug-stimulated DNA cleavage activity *Cancer Res* **46**, 1934-1938

Glynn, S A , Gammell, P , Heenan, M , O'Connor, R , Liang, Y , Keenan, J , Clynes, M (2004) A new superinvasive in vitro phenotype induced by selection of human breast carcinoma cells with the chemotherapeutic drugs paclitaxel and doxorubicin *Br J Cancer*, **91**, 1800-1807

Gorg, A , Boguth, G , Obermaier, C and Weiss, S (1988) Two-dimensional electrophoresis of proteins in an immobilized pH 4-12 gradient *Electrophoresis* **19**, 1516-1519

Gorg, A , Obermaier, C , Boguth, G and Weiss, S (1999) Recent developments in two-dimensional gel electrophoresis with immobilized pH gradients wide pH gradients up to pH 12, longer separation distances and simplified procedures *Electrophoresis* **20**, 712-717

Gorg, A , Obermaier, C , Boguth, G , Harder, A , Scheibe, B , Wildgruber, R and Weiss, W (2000) The current state of two-dimensional electrophoresis with immobilised pH gradients *Electrophoresis* **21**, 1037-1053

Gregory, B W , Baggerly, K A , Peng, B , Koomen, J , Kuerer, H M , Esteva, F J , Symmans, F , Wagner, P , Hortobagyi, G N , Laronga, C , Semmes, J , Wright, G L Jr , Drake, R R and Vlahou, A (2004) Pharmacoproteomic analysis of prechemotherapy and postchemotherapy plasma samples from patients receiving neoadjuvant or adjuvant chemotherapy for breast carcinoma *Cancer **100,*** 1814 -1822

Grem, J L (2000) 5-Fluorouracil forty decades and still ticking A review of its preclinical development *Investigational new drugs,* **18,** 299-313

Guicciardi, M E , Leist, M and Gores, G J (2004) Lysosomes in cell death *Oncogene* **23**, 2881-2890

Guo, H , Zhang, Q L Zhang, J , Wang, C W , Kong, J X , Liu, F S , Ma, D X and Bian, J F (2005) Inhibition of multidrug resistance related P-gp expression in human neuroblastoma by antisense peptide nucleic acid *Zhongguo Yi Xue Ke Xue Yuan Xue Bao,* **27,** 300-304

Gutiererez, P L (2000) The role of AND(P)H oxidoreductase (dt-diaphorase) in the bioactivation of quinone-containmg antitumour agents a review *Free Radical Biology & Medicine*, **29**, 263-275

Gygi, S , Rist, B , Gerber, S , Turecek, F , Gelb, M and Aebersold, R (1999) Quantitative analysis of complex protein mixtures using isotope-coded affinity tags *Nat Biotechnol* **10**, 994-999

Gygi, S , Rist, B and Aebersold, R (2000) Measuring gene expression by quantitative proteome analysis *Curr Opin Biotechnol* **11**, 396-401

Gygi, S P and Aebersold R (2000) Mass spectrometry and proteomics *Curr Opin Chem Biol* **4**, 489-494

Gyorffy, B., Surowiak, P., Kiesslich, O., Denkert, C., Schafer, R., Dietel, M. and Lage, H. (2006). Gene expression profiling of 30 cancer cell lines predicts resistance towards 11 anticancer drugs at clinically achieved concentrations. *Int J Cancer.* **118**, 1699-712.

Hamada, H., Okochi, E., Oh-hara, T. and Tsurou, T. (1988). Purification of the Mr 22,000 calcium-binding protein (sorcin) associated with multidrug resistance and its detection with monoclonal antibodies. *Cancer Res.* **48**, 3173-3178.

Han, E.K.H., Gehrke, L., Tahir, S.K., Credo, R.B., Cherian, S.P., Sham, H., Rosenberg, S.H. and Ng, S. (2000). Modulation of drug resistance by alpha-tubulin in paclitaxel-resistant human lung cancer cell lines. *Eur. J. Cancer*, **36**, 1565-1571

Han, E. K., Tahir, S. K., Cherian, S. P., Collins, N. (2000). Modulation of paclitaxel by annexin IV in human cancer cell lines. *Br. J. Cancer* **83**, 83-88.

Hanash S.M., Strahler J.R., Neel J.V., Hailat N., Melhem R., Keim D., Zhu X.X., Wagner D., Gage G.A. and Watson J.T. (1991). Highly resolving two-dimensional gels for protein sequencing. *Proc. Natl. Acad. Sci. USA* **88**, 5709-5713.

Hande, K.R. (1998). Etoposide: four decades of development of a topoisomerase II inhibitor. *Eur. J. Cancer*, **34**, 1514-1521.

Hartsough, M.L. and Steeg, P.S. (2000). Nm23/nucleoside diphosphate kinase in human cancers. *J. Bioenerg. Biomembr.* **32,** 301-308.

Harvey, S., Zhang, Y., Landry, F., Miller, C. and Smith, J.W. (2001). Insights into a plasma membrane signature. *Physiol Genomics*. **5**, 129-36.

Hathout, Y., Riordan, K., Gehrmann, M. and Fenselau, C. (2002). Differential protein expression in the cytosol fraction of an MCF-7 breast cancer cell line selected for resistance toward melphalan. *J Proteome Res*. **1,** 435-42.

Hayes, M.J., Rescher, U., Gerke, V., Moss, S.E. (2004). Annexin-actin interactions. *Traffic*, **5,** 571-576.

Hazlehurst, L.A., Foley, N. E., Gleason-Guzman, M.P., Hacker, M.P., Cress, A.E., Greenberger, L.E., De Jong, M.C. and Dalton, W.S. (1999). Multiple Mechanisms Confer Drug Resistance to Mitoxantrone in the Human 8226 Myeloma Cell Line. *Cancer Res.* **59**, 1021-1028.

He, L., Orr, G.A. and Horwitz, S,B. (2001). Novel molecules that interact with microtubules and have functional activity similar to taxol. *DDT,* **6,** 1153-1164.

He, Q.Y., Chen, J., Kung, H.F., Yuen, A. P. and Chiu, J.F. (2004). Identification of tumor-associated proteins in oral tongue squamous cell carcinoma by proteomics. *Proteomics,* **4,** 271-278.

Heenan, M., O'Driscoll, L., Cleary, I., Connolly, L. and Clynes. (1997). Isolation from a human MDR lung cell line of multiple clonal subpopulations which exhibit significantly different drug resistance. *Int. J. Cancer.* **71**, 907-15.

Heikkila, P., Suojanen, J., Pirila, E., Vaananen, A., Koivunen, E., Sorsa, T. and Salo, T. (2006). Tongue carcinoma growth is inhibited by selective antigelatinolytic peptides. *Int. J. Cancer.* **118,** 2202-2209.

Hendrix, M.J., Seftor, E.A., Seftor, R.E., Trevor, K.T. (1997). Experimental co-expression of vimentin and keratin intermediate filaments in human breast cancer cells results in phenotypic interconversion and increased invasive behavior. *Am. J. Pathol.*, **150,** 483-495.

Herbert, B.R., Harry, J.L., Packer, N.H., Gooley, A.A., Pedersen, S.K. and Williams, K.L. (2001). What place for acrylamide in proteomics? *Trends Biotechnol.* **19**, (Suppl.), S3-S9.

Hershey, J.W.B. (1991) Translational control in mammalian cells. *Annu. Rev. Biochem.* **61**, 717–755.

Hibi, K., Westra, W.H., Borges, M., Goodman, S., Sidranski, D. Jen, J. (1999). PGP9.5 as a candidate tumor marker for non-small-cell lung cancer. *Am. J. Pathol.*, **155:** 711-715.

Hikawa, T., Mori, T., Abe, T and Hori, S. (2000). The ability in adhesion and invasion of drug-resistant human glioma cells. *J Exp Clin Cancer Res.* **19,** 357-362.

Hill, B.T., Whelan, R.D., Shellard, S.A., McClean, S. and Hosking, L.K. (1994). Mammalian tumor cell lines and certain drug resistant sublines in vitro. *Invest New Drugs.* **12**, 169-82.

Hirano, T., Fujioka, K., Franzen, B., Okinawa, K., Urdu, K., Shibanuma, H., Numata, K., Konata, C., Ebihara, Y., Takahashi, M., Kato, H. and Auer, G. (1997). Relationship between TA01 and TA02 polypeptides associated with lung adenocarcinomas and histolocytological features. *Br. J. Cancer* **75**, 978-985.

Hittelet, A., Legendre, H., Nagy, N., Bronckart, Y., Perctor, J.C., Salmon, I., Yeaton, P., Gabius, H.J., Kiss, R. Camby, I. (2003). Up-regulation of galectins-1 and –3 in human colon cancer and their role in regulating cell migration. *Int. J. Cancer.* **103,** 370-379.

Ho, E., Hayden, A. and Wilkins, M.R. (2006). Characterisation of organellar proteomes: a guide to subcellular fractionation and analysis. *Proteomics.* **6,** 5746-5757.

Hochstrasser M. (2000). Biochemistry. All the ubiquitin family. *Science,* **289,** 563-564.

Hortobagiyi, G.N. (1997). Anthracyclines in the treatment of cancer. An overview. *Drugs* **54,** (Suppl. 4), 1-7.

Hu, L., Lau, S.H., Tzang, C.H., Wen, J.M., Wang, W., Xie, D., Huang, M., Wang, Y., Wu, M.C., Huang, J.F., Zeng, W.F., Sham, J.S., Yang, M. and Guan, X.Y. (2004). Association of Vimentin overexpression and hepatocellular carcinoma metastasis. *Oncogene*, **23,** 298-302.

Huang, H.L., Fang, L. W., Lu, S.P., Chou, C. K., Luh, T.Y. and Lai, M.Z. (2003). DNA damaging reagents induce apoptosis through highly reactive ozygen species-dependant Fas aggregation. *Oncogene.* **22,** 8168-8177.

Hughes, S.J., Glover, T.W., Zhu, X., Kuik, R., Thoraval, D., Orringer, M.B.,Beer, D.G. and Hanash, S. (1998). A novel amplicon at 8p22-23 results in overexpression of cathepsin B in esophageal adenocarcinomas. *PNAS.* ***95,*** 12410-12415.

Hutchens, T.W. and Yip, T.-T. (1993). New desorption strategies for the mass spectrometric analysis of macromolecules. *Rapid Commun. Mass Spectrum* **7**, 576-580.

Ikubo, S., Takigawa, N., Ueoka, H., Kiura, K., Tabata, M., Shibayama, T., Chikamori, M., Aoe, K., Matsushita, A., Harada, M. (1999). *In vitro* evaluation of antimicrotubule agents in human small-cell lung cancer cell lines. *Anticancer Res.* **19,** 3985-3988.

Ikuta, K., Takemura, K., Sasaki, K., Kihara, M., Nishimura, M., Ueda, N., Naito, S., Lee, E., Shimizu, E., Yamauchi, A. (2005). Expression of multidrug resistance proteins and accumulation of cisplatin in human non-small cell lung cancer cells. *Biol. Pharm. Bull.*, **28**, 707-712.

Inada, H., Izawa, I., Nishizawa, M., Kiyono, T., Takashashi, T., Momoi, T. and Inagaki, M. (2001). Keratin attenuates tumour necrosis factor-induced cytotoxicity through association with TRADD. *The Journal of Cell Biology*, **155**, 415-426.

Inoue, H., Kawada, A., Takasu, H., Maruyama, R., Hata, Y., Hiruma, M., Tajima, S and Ishibashi, A. (1998). Cathepsin D expression in skin metastasis of breast cancer. J. Cutan Pathol. **25**, 365-369.

Itoh, M., Noutomi,T. Chiba, H. and Mizuguchi, H. (2002). Bcl-xL antisense treatment sensitizes Bcl-xL -overexpressing squamous cell carcinoma cells to carboplatin. *Oral Oncology,* **38,** 752-756.

John, C.D., Christian, H.C., Morris, J.F., Flower, R.J., Solito, E. and Buckingham, J.C. (2004). Annexin 1 and the regulation of endocrine function. *Trends Endocrinol Metab.***15**, 103-9.

Johnson, S.W., Shen, D.W., Pastan, I., Gottesman, M.M. and Hamilton, T.C. (1996). Cross-resistance, cisplatin accumulation, and platinum-DNA adduct formulation and removal in cisplatin-sensitive and -resistant human hepatoma cell lines. *Experimental Cell Research,* **226,** 133-139.

Johnsson, A., Seelenberg, I., Min, Y., Hilinski, J., Berry, C., Howell, S. and Brit, G. (2000). Identification of genes differentially expressed in association with acquired cisplatin resistance. *Brit J Cancer* **83**, 1047-1054.

Jordan, M.A. (2002). Mechanism of action of antitumor drugs that interact with microtubules and tubulin. *Curr. Med. Chem.*, **2**, 1-17.

Jensen, O.N., Podtelejnikov, A.V. and Mann, M. (1997). Identification of the components of simple protein mixtures by high-accuracy peptide mass mapping and database searching. *Anal. Chem.* **69**, 4741-4750.

Kakolyris, S., Giatromanolaki, A. and Koukourakis, M. (2001). Thioredoxin expression is associated with lymph node status and prognosis in early operable non-small cell lung cancer. *Clin Cancer Res.* **7,** 3087–91.

Kang, H.A. and Hershey, J.W. (1994) Effect of initiation factor 5A depletion on protein synthesis and proliferation of Saccharomyces cerevisiae. *J Biol Chem.* **269**, 3934–3940.

Kennedy, S. (2001). Proteomics profiling from human samples: the body fluid alternative. *Toxicology Letters* **120**, 379-384.

Kerbel, R.S. (1997). A cancer therapy resistant to resistance. *Nature* **390**, 335-336.

Khuri, F.R. and Cohen, V. (2004). Molecular targeted approaches to the chemoprevention of lung cancer. *Clin. Cancer Res.*, **10 (Suppl)**, 4249s-4253s.

Kim, S.J., Miyoshi, Y., Taguchi, T., Tamaki, Y., Nakamura, H., Yodoi, J., Kato, K. and Noguchi, S. (2005). High thioredoxin expression is associated with resistance to docetaxel in primary breast cancer. *Clin Cancer Res.* **11,** 8425-30.

King, K.L., Li, A.F., Chau, G.Y., Chi, C.W., Wu, C.W., Huang, C.L. and Lui, W.Y. (2000). Prognostic significance of heat shock protein-27 expression in hepatocellular carcinoma and its relation to histologic grading and survival. *Cancer.* **88**, 2464–2470.

Klose J. (1975). Protein mapping by combined isoelectric focusing and electrophoresis of mouse liver: a novel approach to testing for induced point mutations in mammals. *Humangenetik* **26**, 231-243.

Krueger, S., Haeckel, C., Buehling, F. and Roessner, A. (1999). Inhibitory effects of antisense cathepsin B cDNA transfection on invasion and motility in a human osteosarcoma cell line. *Cancer Res.* **59**, 6010-4.

Koivunen, E., Arap, W., Valtanen, H., Rainisalo, A., Medina, O.P., Heikkila, P., Kantor, C., Gahmberg, C.G., Salo, T., Konttinen, Y.T., Sorsa, T., Rouslahti, E. and Pasqualine, R. (1999). Tumour targeting with a selective gelatinase inhibitor. *Nat. Biotechnol.* **17,** 768-774.

Kobayashi, H., Moniwa, N., Sugimura, M., Shinohara, H., Ohi, H., Terao, T. (1993). Effects of membrane-associated cathepsin B on the activation of receptor-bound prourokinase and subsequent invasion of reconstituted basement membranes. *Biochim Biophys Acta.* **1178,** 55-62.

Kolkhorst, V., Sturzebecher, J., Wiederanders, B. (1998). Inhibition of tumour cell invasion by protease inhibitors: correlation with the protease profile. *Cancer Res. Clin. Oncol.* **124**, 598-606.

Kondo, T. and Moor, G. E. (1961). Production of metastases by treatment with carcinostatic agents. Effects of carcinostatic agents on the host. *Cancer Res.* **21**, 1396-1399.

Kong, Q., Beel, J.A. and Lillehei, K.O. (2000). A threshold concept for cancer therapy. *Med Hypotheses* **55**, 29–35.

Koomagi, R., Stammler, G., Manegold, C., Mattern, J. and Volm. M. (1996). Expression of resistance-related proteins in tumoral and peritumoral tissues of patients with lung cancer. *Cancer Lett.* **110,** 129-36.

Kustermans, G., El Benna, J., Piette, J. and Legrand-Poels, S. (2004). Perturbation of actin dynamics induces NF-B activation in myelomonocytic cells via a NADPH oxidase-dependent pathway. *Biochem J.* **387**, 531–40.

Lafky, J.M. and Maihle, N.J. (2002). The parable of the proteome: cancer biomarkers. *Trends Cell Biol.* **12**, 358.

Lacombe, M.L. (1993). Nucleoside diphosphate kinase/Nm23 and metastatic potency. *Bull Cancer,* **80,** 712-722.

Lang, S.H., Hyde, C., Reid, I.N., Hitchcock, I.S., Hart, C.A., Bryden, A.A., Villette, J.M., Stower, M.J. and Maitland, N.J. (2002) Enhanced expression of vimentin in motile prostate cell lines and in poorly differentiated and metastatic prostate carcinoma. *Prostate*, **52,** 253-263.

Langdon, S.P., Rabiasz, G.J., Hirst, G.L., King, R.J., Hawkins, R.A., Smyth, J.F., Miller, W.R. (1995). Expression of the heat shock protein HSP27 in human ovarian cancer. *Clin Cancer Res.* **1**, 1603-9.

Langen, H. and Roder, D. (2000). Separations of proteins from human embryonic kidney cells on narrow-range IPG strips. *Life Science News* **4**, 1-3.

Larroque, A.L., Dubois, J., Thoret, J., Aubert, G., Guénard, D. and Guéritte, F. (2005). Novel C2-C3' N-peptide linked macrocyclic taxoids. Part 1: Synthesis and biological activities of docetaxel analogues with a peptide side chain at C3'. *Bioorganic & Medicinal Chemistry Letters,* **15,** 4722-76

Lavie, Y and Liscovitch, M (2000) Changes in lipid and protein constituents of refts and caveolae in multidrug resistant cancer cells and their functional consequences *Glycoconjugate Journal,* **17,** 253-259

Lavoie, J N , Lambert, H , Hickey, E , Weber, L A and Landry, J (1995) Modulation of cellular thermoresistance and actin filament stability accompanies phosphorylation-induced changes in the oligomeric structure of heat shock protein 27 *Mol Cell Biol* **15,** 505-16

Le, Q T , Shi, G , Cao, H , Nelson, D W , Wang, Y , Chen, E Y , Zhao, S , Kong, C , Richardson, D , O'Byrne, K J , Giaccia, A J and Koong, A C (2005) Galectin-1 a link between tumor hypoxia and tumor immune privilege *J Clin Oncol* **23,**8932-41

Le Moguen, K , Lincet, H , Deslandes, E , Hubert-Roux, M , Lange, C , Poulain, L , Gauduchon, P and Baudin, B (2006) Comparative proteomic analysis of cisplatin sensitive IGROV1 ovarian carcinoma cell line and its resistant counterpart IGROV1-R10 *Proteomics,* **6,** 0000-0000

Lee, K H (2001) Proteomics a technology-driven and technology-limited discovery science *Trends Biotechnol* **19,** 217-222

Lee, W P (1996) Purification, cDNA cloning, and expression of human sorcin in vincristine-resistant HOB1 lymphoma cell lines *Arch Biochem Biophys* **325,** 217-226

Lee, K H , Yim, E K , Kim, C J , Namkoong, S E , Um, S J and Park, J S (2005) Proteomic analysis of anti-cancer effects by paclitaxel treatment in cervical cancer cells *Gynecol Oncol* **98,** 45-53

Leslie, E M , Deeley, R and Cole, P C (2001) Toxicological relevance of the multidrug resistance protein 1, MRP1 (ABCC1) and related transporters *Toxicology,* **167,** 3-23

Levner, I, (2005) Feature selection and nearest centroid classification for protein mass spectrometry *BMC Bioinformatics,* **6,** 68-72

Li, J , Orlandi, R , White, C N , Rosenzweig, J , Zhao, J , Seregni, E , Morelli, D , Yu, Y , Meng, X Y , Zhang, Z , Davidson, N E , Fung, E T and Chan, D W (2005) Independent validation of candidate breast cancer serum biomarkers identified by mass spectrometry *Clin Chem,* **51,** 2229-35

Li, J , Zhang, Z , Rosenberg, J , Wang, Y Y and Chen, D W (2002) Proteomics and bioinformatics approaches for identification of serum biomarkers to detect breast cancer *Clin Chem* **48,** 1296-1304

Liang, Y , PhD, Dublin City University, **1999**

Liang, Y , Meleady, P , Cleary, I , McDonnell, S , Connolly, L and Clynes, M (2001) Selection with melphalan or paclitaxel (Taxol) yields variants with different patterns of multidrug resistance, integrin expression and *in vitro* invasiveness *Eur J Cancer* **37** 1041-1052

Liang, Y , O'Driscoll, L , McDonnell, S , Doolan, P , Oglesby, I , Duffy, K , O'Connor, R , Clynes, M (2004) Enhanced *in vitro* invasiveness and drug resistance with altered gene exppression patterns in a human lung carcinoma cell line after pulse selection with anticancer drugs *Int J Cancer,* **111,** 484-493

Lindahl, R (1992) Aldehyde dehydrogenases- the 1992 perspective *Crit Rev Biochem Mol Biol* **27**, 283-335

Liu, B , Staren, E D , Iwamura, T , Appert, H E , Howard, J M (2001) Mechanisms of taxotere-related drug resistance in pancreatic carcinoma *J Surg Res* **99**, 179-186

Liu, S H , Lin, C Y , Peng, S Y , Jeng, Y M , Pan, H W , Lai, P L , Liu, C L and Hsu, H C (2002) Down-Regulation of annexin A10 in hepatocellular carcinoma is associated with vascular invasion, early recurrence, and poor prognosis in synergy with p53 mutation *Am J of Pathology*, **160**, 1831-1837

Liu, Y , Chen, Q and Zhang, T J (2004) Tumor suppressor gene 14-3-3σ is down-regulated whereas the proto-oncogene translation elongation factor 1δ is up-regulated in non-small cell lung lancers as identified by proteomic profiling *J Proteomic Res* **3**, 728-735

Liang, Y , McDonnell, S and Clynes, M (2002) Examining the relationship between cancer invasion/metastasis and drug resistance *Curr Cancer Drug Targets*, **2**, 257-277

Lin, H L , Liu, T Y , Chau, G Y , Lui, W Y and Chi, C W (2000) Comparison of 2-methoxyestradiol-induced, docetaxel-induced, and paclitaxel-induced apoptosis in hepatoma cells and its correlation with reactive oxygen species *Cancer* **89**, 983–994
Lin, Y H , Park, Z Y , Lin, D , Brahmbhatt, A A , Rio, M C , Yates III, J R and Klemke, R L (2004) Regulation of cell migration and survival by focal adhesion targeting of Lasp-1 *The Journal of Cell Biology*, **165**, 421–432

Linder, S and Shoshan, M C (2005) Lysosomes and endoplasmic reticulum targets for improved, selective anticancer therapy *Drug Resist Updat* **8**, 199-204

Linehan, R , PhD, Dublin City University, **2003**

Lockhart A C , Tirona, R G and Kim, R B (2003) Pharmacogenetics of ATP-binding Cassette Transporters in Cancer and Chemotherapy *Mol Cancer Therpaeutics*, **2**, 685-698

Loeffler-Ragg, J , Skvortsov, S , Sarg, B , Skvortsova, I , Witsch-Baumgartner, M , Mueller, D , Lindner, H and Zwierzina, H (2005) Gefitinib-responsive EGFR-positive colorectal cancers have different proteome profiles from non-responsive cell lines *Eur J Cancer* **1**, 2338-46

Lofgren, C , Hjortsberg, L , Blennow, M , Lofti, K , Paul, C , Eriksson, S and Albertioni, F (2004) Mechanisms of cross-resistance between nucleoside analogues and vincristine or daunorubicin in leukemic cells *Biochem and Biophysical Res Communications*, **320**, 825-832

Longley, D B , Harkin, D P and Johnston, P G (2003) 5-Fluorouracil mechanisms of action and clinical strategies *Nature Revs Cancer*, **3**, 330-338

Longley, D B , Johnston, P G (2005) Molecular mechanisms of drug resistance *J Pathology*, **205**, 275-292

Lopez, M F (1999) Proteome analysis I Gene products are where the biological action is *J Chromatogr B* 722, 191-202

Lucke-Huhle, C (1994) Permissivity for methotrexate-induced DHFR gene amplification correlates with the metastatic potential of rat adenocarcinoma cells *Carcinogenesis*, **15(4)**, 695-700

Maiguel, D A , Jones, L , Chakravarty, D , Yang, C Carrier, F (2004) Nucleophosmin sets a threshold for p53 response to UV radiation *Mol Cell Biol* 24, 3703-3711

Maring, J G , Groen, H M J , Wachters, F M , Uges, D R A and Vries, E G E (2005) Genetic factors influencing Pyrimidine-antagonist chemotherapy *The Pharmacogenomics J* **5,** 226-243

Martello, L A , Verdier-Pinard, P , Shen, H J , He, L , Torres, K , Orr, G A , Horwitz, S B (2003) Elevated levels of microtubule destabilizing factors in a taxol-resistant/dependent A549 cell line with an α-tubulin mutation *Cancer Res* **63**, 1207-1213

Mayer, M P and Bukau, B (2005) Hsp70 chaperones cellular functions and molecular mechanism, *Cell Mol Life Sci* **62**, 670–684

McDonald, W H and Yates, J R (2000) Proteomic tools for cell biology *Traffic* **1**, 747-754

McMillan, T J and Hart, I R (1987) Can cancer chemotherapy enhance the malignant behaviour of tumours? Cancer *Met Rev* **6**, 503-520

McMorrow, C S , Peklak-Scott, C , Bishwokarma, B , Kute, T E , Smitherman, P K and Townsend, A J (2006) Multidrug resistance protein 1 (MRP1, ABCC1) mediates resistance to mitoxantrone via glutathione-dependent drug efflux *Mol Pharmacol* **69**, 1499-1505

Merchant, M and Weinberger, R S (2000) Recent advancements in surface-enhanced laser desorption ionisation-time of flight mass spectrometry *Electrophoresis* **21**, 1164-77

Mechetner, E , Kyshtoobayeva, A , Zonis, S , Kim, H , Stroup, R , Garcia, R , Parker, R J , Fruehauf, J P (1998) Levels of multidrug resistance (MDR1) P-glycoprotein expression by human breast cancer correlate with *in vitro* resistance to taxol and doxorubicin *Clin Cancer Res* , **4**, 389-398

Minato, K , Kianzawa, F , Nishio, K , Nauagawa, K , Fujiwara, Y and Saijo, N (1990) Characterisation of an etoposide-resistant human small cell lung cancer cell line *Cancer Chemother Pharmacol* **26,** 313-317

Minderman, H , Brooks, T A , O'Loughlin, K L , Ojima, I , Bernacki, R J and Baer, M R (2004) Broad-spectrum modulation of ATP-binding cassette transport proteins by the taxane derivatives ortataxel (IDN-5109, BAY 59-8862) and tRA96023 *Cancer Chemother Pharmacol* , **53,** 363-369

Molloy, M P (2000) Two-dimensional electrophoresis of membrane proteins using immobilised pH gradients *Anal Biochem* **280**, 1-10

Monneret, C (2001) Recent developments in the field of antitumour anthracyclines *Eur J Med Chem,* **36,** 483-493

Morino, M , Tsuzuki, T , Ishikawa, Y , Shirakami, T , Yoshimura, M , Kiyosuke, Y , Matsunaga, K , Yoshikumi, C and Saijo, N (1997) Specific expression of HSP27 in human tumor cell lines in vitro *In Vivo* **11**, 179-84

Mulla, A , Christian, H C , Solito, E , Mendoza, N and Morris J F (2004) Expression, subcellular localization and phosphorylation status of annexins 1 and 5 in human pituitary adenomas and a growth hormone-secreting carcinoma *Clin Endocrinology* **60,** 107-111

Mukai, M , Kusama, T , Hamanaka, Y , Koga, T , Endo, H , Tatsuta, M Inoue, M (2005) Cross talk between apoptosis and invasion signaling in cancer cells through caspase-3 activation *Cancer Res* , **65,** 9121-9125

Myers, C E , McGuire, W P and Liss R H (1977) Adriamycin the role of lipid peroxidation in cardiac toxicity and tumour response *Science,* **197,** 165-169

Nadin, S , Vargas-Roig, L M , Cuello-Carrion, F D and Ciocca, D R (2003) Deoxyribonucleic acid damage induced by doxorubicin in peripheral blood mononuclear cells possible roles for the stress response and the deoxyribonucleic acid repair process *Cell Stress Chaperones* **8,** 361-371

Nakanishi, T , Karo, J E , Tan, M , Doyle, L A , Peters, T , Yang, W , Wei, D and Ross, D D (2005) Quantitative analysis of breast cancer resistance protein and cellular resistance to flavopiridol in acute leukaemia patients *Clin Cancer Res* **9,** 3320-3328

Neckers, L (2002) Hsp90 inhibitors as novel cancer chemotherapeutic agents *Trends Mol Med* **8,** S55–S61

Negm, R , Verma, M , Srivastava, S (2002) The promise of biomarkers in cancer screening and detection *Trends Mol Sci* **8,** 288-293

Neubauer, G and Mann, M (1999) Mapping of phosphorlyation sites of gel-isolated proteins by nanoelectrospray tandem mass spectrometry potentials and limitations *Anal Chem* **71,** 235-241

Nielsen, D , Maare, C and Skovsgaard, T (1996) Cellular resistance to anthracyclines *Gen Pharmac,* **27,** 251-255

Niklinski, J and Hirsch, F R (2002) Molecular approaches to lung cancer evaluation *Lung Cancer,* **38,** S9-S17

Nobili, S , Landini, I , Giglioni, B and Mini, E (2006) Pharmacological strategies for overcoming multidrug resistance *Curr Drug Targets,* **7,** 861-879

Nuell, M J , Stewart, D A , Walker, L , Friedman, V , Wood, C M and Owens, G A (1991) Prohibitin, an evolutionarily conserved intracellular protein that blocks DNA synthesis in normal broblasts and HeLa cells *Mol Cell Biol* **11,** 1372–1381

O'Farrell, P H (1975) High resolution two-dimensional electrophoresis of proteins *J Biol Chem* **250,** 4007-4021

Oguri, S , Sakakibara, T , Mase, H , Shimizu, T , Ishikawa, K , Kimura, K and Smyth, R D (1988) Clinical pharmacokinetics of carboplatin *J Clin Pharmacol* **28,** 208-215

Ohsawa, M , Ikura, Y , Fukushima, H , Shirai, N , Sugama, Y , Suekane, T , Hirayama, M , Hino, M and Ueda, M (2005) Immunohistochemical expression of multidrug resistance proteins as a predictor of poor response to chemotherapy and prognosis in patients with nodal diffuse large B-cell lymphoma *Oncology,* **68,** 422-431

Okada, A , Bellocq, J P , Rouyer, N , Chenard, M P , Rio, M C , Chambon, P , Basset, P (1995) "Membrane-type matrix metalloproteinase (MT-MMP) gene is expressed in stromal cells of human colon, breast, and head and neck carcinoma" *PNAS* **92,** 2730-2734

Ooe, A , Kato, K and Noguchi, S (2006) Possible involvement of CCT5, RGS3, and YKT6 genes up-regulated in p53-mutated tumors in resistance to docetaxel in human breast cancers *Breast Cancer Res Treat* In press

Ohsawa, I , Nishimaki, K , C , Kamino, K (2003) Deficiency in a mitochondrial aldehyde dehydrogenase increases vulnerability to oxidative stress in PC12 cells *J Neurochem* **84,** 1110-1117

Oshima, R G , Baribault, H and Caulin (1996) Oncogenic regulation and function of keratins 8 and 18 *Cancer Metastasis Rev* **15,** 445–471

Osmak, M , Bizjak, L , Jernej, B and Kapitanovid, S (1995) Characterization of carboplatin-resistant sublines derived from human larynx carcinoma cells *Mutation Research,* **347,** 141-150

Osterberg, L , Levan, K , Partheen, K , Helou, K and Horvath, G (2005) Cytogenetic analysis of carboplatin resistance in early-stage epithelial ovarian carcinoma *Cancer Genetics and Cytogenetics,* **163,** 144-150
Padar, S Breemen, C , Thomas, D W , Uchizono, J A , Livesey, J C and Rahimian, R (2004) Differential regulation of calcium homeostasis in adenocarcinoma cell line A549 and its Taxol-resistant subclone *British Journal of Pharmacology,* **142,** 305-316

Page, M J , Amess, B , Townsend, R R , Parekh, R , Hearth, A , Brute, L , Zvelebil, M J , Stein, R C , Waterfield, M D , Davies, S C and O'Hare, M J (1999) Proteomic definition of normal human luminal and myoepithelial breast cells purified from reduction mammoplasties *PNAS* **96,** 12589-12594

Park, S J , Wu, C H , Gordon, J D , Zhong, X , Emami, A and Safa, A (2004) Taxol induces caspase-10-dependent apoptosis *J Biol Chem* , **279,** 51057-51067

Patterson, S D , (2000) Proteomics the industrialization of protein chemistry *Curr Opin Biotechnol* **11,** 413-418

Paz, A , Haklai, R , Elad-Sfadia, G , Ballan, E and Kloog, Y (2001) Galectin-1 binds oncogenic H-Ras to mediate Ras membrane anchorage and cell transformation *Oncogene* **20,** 7486-7493

Patton, W F , Schulenberg, B and Steinberg, T H (2002) Two-dimensional gel electrophoresis, better than a poke in the ICAT? *Curr Opin Biotechnol* **13,** 321-328

Pardo, M , Garcia, A , Thomas, B , Pineiro, A , Akoulitchev, R and Zitman N (2006) The characterization of the invasion phenotype of uveal melanoma tumour cells shows the presence of MUC18 and HMG-1 metastasis markers and leads to the identi cation of DJ-1 as a potential serum biomarker *Int J Cancer,* **119,** 1014-1022

Parekh, H , Wiesen, K , Simpkins, H (1997) Acquisition of taxol resistance via p-glycoprotein and non-p-glycoprotein-mediated mechanisms in human ovarian carcinoma cells *Biochem Pharmacol* , **53,** 461-470

Parekh, H K , Deng, H B , Choudhary, K , Houser, S R and Simpkins, H (2002) Overexpression of sorcin, a calcium-binding protein, induces a low level of paclitaxel resistance in human ovarian and breast cancer cells *Biochem Pharmacol* **63,** 1149-1158

Park, S J , Wu, C H , Gordon, J D , Zhong, X , Emami, A and Safa, A R (2004) Taxol induces caspase-10-dependent apoptosis *J Biol Chem* **279,** 51057–67

Parker, B.S., Rephaeli, A., Audeelman, A., Phillips, D.R. and Cutts, S.M. (2004). Formation of mitoxantrone adducts in human tumor cells: potentiation by AN-9 and DNA methylation. *Oncol. Res.* **14,** 279-290.

Peng, X., Mehta, R., Wang, S., Chellappan, S. and Mehta, R.G. (2006). Prohibitin Is a Novel Target Gene of Vitamin D Involved in Its Antiproliferative Action in Breast Cancer Cells. *Cancer Research* **66**, 7361-7369.

Peterson, D.S. (2006). Matrix-free methods for laser desorption/ionization mass spectrometry. *Mass Spectrometry Reviews,* (Articles online in advance of print).

Petricoin, E.F. III, Ardekani, A.M., Hitt, B.A. (2002) Use of proteomic patterns in serum to identify ovarian cancer. *Lancet* **359,** 572-575.

Pino, I., Pio, R., Toledo, G., Zabalegui, N., Vicent, S., Rey, N., Lozano, M.D., Torre, W., Garcia-Foncillas, J. and Montuenga, L.M. (2003). Altered patterns of expression of members of the heterogeneous nuclear ribonucleoprotein (hnRNP) family in lung cancer. *Lung Camcer.* **41,** 131-143.

Pinedo, H.M., Peters, G.J. (1988). Fluorouracil: biochemistry and pharmacology. *J Clin Oncol* **6,** 1653-1664.

Podgorski, I. and Sloane, B.F. (2003). Cathepsin B and its role(s) in cancer progression. *Biochem. Soc. Symp.* **70,** 273-276.

Powis, G., Bonjouklian, R., Berggren, M. M., Gallegos, A., Abraham, R., Ashendel, C., Zalkow, L., Matter, W. F., Dodge, J., Grindley, G., and Vlahos, C. J. (1994). Wortmannin, a potent and selective inhibitor of phosphatidylinositol-3-kinase. *Cancer Res.*, **54,** 2419–2423.

Powis, G., Mustacich, D. and Coon A. (2000). The role of the redox protein thioredoxin in cell growth and cancer. *Free Radic Biol Med.* **29**, 312–22.

Pratt, W. B., Ruddon, R. W., Ensminger, W. D. and Maybaum, J. *The Anticancer drugs*. (1994). (second Edition).

Pratt, W.B. and Toft, D.O. (2003). Regulation of signalling protein function and trafficking by the hsp90/hsp70-based chaperone machinery, *Exp. Biol. Med. (Maywood)* **228**, 111–133.

Qi, J., Liu, N., Zhou, Y., Tan. Y., Cheng, Y., Yang, Y., Zhu, Z. and Xiong, D. (2006). Overexpression of sorcin in multidrug resistant human leukemia cells and its role in regulating cell apoptosis. *Biochemical and Biophysical Res. Communications.* **349,** 303-309

Qu, Y., Adam, B.L., Yasui, Y., Ward, M.D., Cazares, L.H., Schellhammer, P.F. (2002). Boosted decision tree analysis of surface-enhanced laser desorption/ionization mass spectral serum profiles discriminates prostate cancer from noncancer patients. *Clin Chem.* **48**, 1835-1843.

Qian, L., Zhang, Z., Shi, M., Yu, M., Hu, M., Xia, Q., Shen, B. and Guo, N. (2006). Expression and distribution of HSP27 in response to G418 in different human breast cancer cell lines. *Histochem. Cell Biol.* **126,** 593-601.

Rabilloud, T., Valette, C. and Lawrence, J.J. (1994). Sample application by in-gel rehydration improves the resolution of twp-dimensional electrophoresis with immobilized pH gradients in the first dimension. *Electrophoresis* **15**, 1552-1558.

Rabilloud, T (1996) Solubilization of proteins for electrophoretic analysis *Electrophoresis* **17**, 813-829

Rabilloud, T , Adessi, C , Giraudel, A and Lunardi, J (1997) Improvement of the solubilisation of proteins in two-dimensional electrophoresis with immobilized pH gradients *Electrophoresis* **18**, 307-316

Rabilloud, T (2002) Two-dimensional gel electrophoresis in proteomics Old, old fashioned, but it still climbs up the mountains *Proteomics* **2**, 3-10

Rajalingam, K , Wunder, C , Brinkmann, V , Churin, Y , Hekman, M and Sievers, C (2005) Prohibitin is required for Ras-induced Raf-MEK-ERK activation and epithelial cell migration *Nat Cell Biol* 7, 837–843

Ramanathan, B , Jan, K Y , Chen, C H , Hour, T C , Yu, H J and Pu, Y S (2005) Resistance to paclitaxel is proportional to cellular total antioxidant capacity *Cancer Res* **65**, 8455-8460

Reymond, M A , Sanchez, J -C , Hughes, G J , Gunther, K , Riese, J , Tortola, S , Peinado, M A , Kirchner, T , Hohenberger, D F and Kockerling, F (1997) Standardized characterization of gene expression in human colorectal epithe lium by two-dimensional electrophoresis *Electrophoresis* **18**, 2842-2848

Richards, E H , Hickey, E , Weber, L and Master, J R (1996) Effect of overexpression of the small heat shock protein HSP27 on the heat and drug sensitivities of human testis tumor cells *Cancer Res* **56**, 2446-51

Roberts, D , Meyers, M B , Biedler, J L and Wiggins, L G (1989) Association of sorcin with drug resistance in L1210 cells *Cancer chemotherapy pharmacology* **1**, 19-25

Rosel, R , Felip, E , Taron, M , Majo, J , Mendez, P , Sanchez-Ronco, M , Queralt, C , Sanchez, J J and Maestre, J (2004) Gene expression as a predictive marker of outcome in stage IIB-IIIA-IIIB non-small cell lung cancer after induction gemcitabine-based chemotherapy followed by resectional surgery *Clin Cancer Res* , **10 (suppl)**, 4215s-4219s

Rosette C and Karin, M (1995) Cytoskeletal control of gene expression depolymerization of microtubules activates NF-kappa B *J Cell Biol* **128**, 1111–1119

Roshy, S , Sloane, B F and Mom, K (2003) Pericellular cathepsin B and malignant progression *Cancer Metastasis Rev* **22**, 271-286

Rutters, H , Zurbig, P , Halter, R and Borlak, J (2006) Towards a lung adenocarcinoma proteome map Studies with SP-C/c-raf transgenic mice *Proteomics*, **6**, 3127-3137

Salge, U , Seitx, R , Wimmel, A , Schuermann, M , Daubner, E , Heiden, M (2004) Transition from suspension to adherent growth is accompanied by tissue factor expression and matrix metalloproteinase secretion in a small cell lung cancer cell line *J of Cancer Research and Clinical Oncol* **127**, 139-141

Sanchez, J C , Rouge, V , Pisteur, M , Ravier, F , Tonella, L , Moosmayer Wilkins, M R and Horchstrasser, D F (1997) Improved and simplified in-gel sample application using reswelling of dry immobilized pH gradients *Electrophoresis* **18**, 324-327

Sandler, A B , Johnson,D H and Herbst, R S (2004) Anti-vascular endothelial groth factors monoclonals in non-small cell lung cancer *Clin Cancer Res* , **10 (suppl)**, 4258s-4262s

Sano, D , Matsuda, H , Ishiguro, Y , Nishimura, G , Kawakami, M and Tsukuda, M (2006) Antitumour effects of IDN5109 on head and neck squamous cell carcinoma *Oncol Rep* **15,** 329-334

Santoni, V , Molloy, M and Rabilloud, T (2000) Membrane proteins and proteomics un amour impossible *Electrophoresis* **21**, 1054-1070

Scagliatti , G V , Novello, S and Selvaggi, G (1999) Multidrug resistance in non-small cell lung cancer *Annals of Oncol* , **10 (Suppl 5),** S83-S86

Schibler, M and Cabral, F (1986) Taxol-dependent mutants of Chinese hamster ovary cells with alterations in α- and ß-tubulin *J Cell Biol* **102**,1522 -1531

Schiff, P B , Fant, J , Horwitz, S B (1979) Promotion of microtubule assembly in vitro by taxol *Nature* **277**, 665-667

Schrenk, D , Baus, P R , Ermel, N E Klein, C , Vorderstemann, B and Kauffmann, H-M (2001) Up-regulation of transporters of the MRP family by drugs and toxins *Toxicology Lett* **120,** 51-57

Scripture, C D , Szebeni, J , Loos, W J , Figg, W D , Sparreboom, A (2005) Comparative in vitro properties and clinical pharmacokinetics of placlitaxel following the administration of taxol and paxene *Cancer Biol Ther* **4**, 555-560

Seike, M , Kondo, T , Fujii, K , Okano, T , Yamada, T , Matsuno, Y , Gemma, A , Kudoh, S and Hirohashi, S Proteomic signatures for histological types of lung cancer *Proteomics,* **5,** 2939-2948

Seow, T K , Ong, S-E , Liang, R C M Y , Ren, E-C , Ou, K and Chung, M C M (2000) Two-dimensional electrophoresis map of the human hepatocellular carcinoma cell line, HCC-M and identification of separated proteins by mass spectrometry *Electrophoresis* **21**, 1787-1813

Seve, P and Dumontet, C (2005) Chemoresistance in non-small cell lung cancer *Curr Med Chem - Anti Cancer Agents* **5,** 73-88

Shah, T , Braverman, R and Prasad, G L (1998) Suppression of neoplastic transformation and regulation of cytoskeleton by tropomyosins Somat *Cell Mol Genet* **24**, 273-80

Sham, K H and Dalton W S (2001) Cell Adhesion Is a Key Determinant in *de Novo* Multidrug Resistance (MDR) New Targets for the Prevention of Acquired MDR *Mol Cancer Therapeutics*, **1,** 69-78

Shaw, M M and Riederer, B M (2002) Sample preparation for two-dimensional gel electrophoresis *SPS Proceedings 2nd Annual Congress Lausanne*, **3,** 1408-1417

Shin, Y K , Yoo, B C , Chang, H J , Jeon, E , Hong, S H , Jung, M S , Lim, S J and Park, J G (2005) Down-regulation of mitochondrial F1F0-ATP synthase in human colon cancer cells with induced 5-fluorouracil resistance *Cancer Res* **65**, 3162-70

Shionoya, M , Jimbo, T , Kitagawa, M , Soga, T and Tohgo, A (2003) DJ-927, a novel oral taxane, overcomes P-glycoprotein-mediated multidrug resistance *in vitro* and *in vivo Cancer Sci* **94,** 459-466

Simon, S M , Schindler, M (1994) Cell biological mechanisms of multidrug resistance in tumours *PNAS*, **91**, 3497-3504

Simpson, R J and Dorrow, D S (2001) Cancer proteomics from signalling to tumour markers *Trends Biotechnol* **19**, (Suppl) S40-S48

Sinha, P , Hutter, G , Kottgen, E , Dietel, M , Schadendorf, D and Lage, H (1998) Increased expression of annexin I and thioredoxin detected by two-dimensional gel electrophoresis of drug resistant human stomach cancer cells *J Biochem Biophys Meth* **37**, 105-116

Sinha, P , Hutter, G , Kottgen, E , Dietel, M , Schadendorf, D and Lage, H (1999) Search for novel proteins involved in the development of chemoresistance in colorectal cancer and fibrosarcoma cells in vitro using two-dimensional electrophoresis, mass spectrometry and microsequencing *Electrophoresis* **20,** 2961-2969

Sinha, P , Hutter, G , Kottgen, E , Dietel, M , Schadendorf, D and Lage, H (1999b) Increased expression of epidermal fatty acid binding protein, cofilin and 14-3-3-σ (stratifin) detected by two-dimensional electrophoresis, mass spectrometry and microsequencing in drug-resistant human adenocarcinoma of the pancreas *Electrophoresis* **20,** 2652-2660

Sinha, P , Kohl, S , Fischer, J , Hutter, G , Kern, M , Kottgen, E , Dietel, M , Lage, H , Schnolzer, M , Schadendorf, D (2000) Identification of novel proteins associated with the development of chemoresistance in malignant melanoma using two-dimensional electrophoresis *Electrophoresis* **21,** 3048-3057

Sinha, P , Poland, J , Kohl, S , Schnolzer M , Helmbach, H , Hutter, G , Lage, H and Schadendorf, D (2003) Study of the development of chemoresistance in melanoma cell lines using proteome analysis *Electrophoresis* **24,** 2386-404

Skovsgaard T, Nielsen D, Maare C, Wassermann K (1994) Cellular resistance to cancer chemotherapy *Int Rev Cytol*, 156, 77-157

Sladek, N E , Kollander, R , Sreerama, L and Kiang, D T (2002) Cellular levels of aldehyde dehydrogenases (ALDH1A1 and ALDH3A1) as predictors of therapeutic responses to cyclophosphamide-based chemotherapy of breast cancer a retrospective study Rational individualization of oxazaphosphorine-based cancer chemotherapeutic regimens *Cancer Chemother Pharmacol* **49,** 309-21

Smitherman, A B , Mohler, J L , Maygarden, S J and Ornstein, D K (2004) Expression of annexin I, II and VII proteins in androgen stimulated and recurrent prostate cancer *J Urol* **171,** 916-920

Socinski, M A (2004) Cytotoxic chemotherapy in advanced non-small lung cancer a review of standard treatment paradigms *Clinical Cancer Res* **10, (Suppl),** 4210s-4214s

Sorrentino, B (2002) Gene therapy to protect haematopoietic cells from cytotoxic cancer drugs *Nat Rev Cancer*, **2**, 431-441

Spence H J , McGarry, L , Chew, C S , Carragher, N O , Carragher, S A , Zhengquiang, Y , Croft, D R , Olson, M F , Frame, M and Ozanne, B W (2006) AP-1 differentially expressed proteins Krp1 and fibronectin co-operatively enhance Rho-ROCK-independent mesenchymal invasion by altering the function, localisation, and activity of nondifferentially expressed proteins *Mol and cell boil* , **26** 1480-1495

Spiess, C , Meyer, A S , Reissmann, S and Frydman, J (2004) Mechanism of the eukaryotic chaperonin protein folding in the chamber of secrets, *Trends Cell Biol* **14** 598–604

Stewart, J. J., White, J. T., Yan, X., Collins, S. (2006). Proteins assiciated with cisplatin resistance in ovarian cancer cells identified by quantitative proteomic technology and integrated with mRNA expression levels. *Mol. Cell. Proteomics.* **5,** 433-443.

Strassheim, D., Shafer, S.H., Phelps, S.H. and williams, C.L. (2000). Small cell lung carcinoma exhibits greater phospholipase C-B1 expression and edelfosine resistance compared with non-small cell lung carcinoma. *Cancer Res.* **60,** 2730-2736.

Sugawara, I., Mizumoto, K., Ohkochi, E., Hamada, H., Tsuro, T. Mori, S. (1989). Immunocytochemical identification and localization of the Mr 22,000 calcium-binding protein (sorcin) in an adriamycin-resistant myelogenous leukemia cell line. *Jpn. J. Cancer Res.* **80,** 469-74.

Swerts, K., De Moerloose, B., Dhooge, C., Laureys, G., Benoit, Y. and Philippe, J. (2006). Prognostic significance of multidrug resistance-related proteins in childhood acute lymphoblastic leukaemia. *Eur. J. Cancer,* **42**, 295-309.

Taguchi, A., Blood, D.C., del Toro, G., Canet, A., Lee, D.C., Qu, W., Tanji, N., Lu, Y., Lalla, E., Fu, C., Hofmann, M.A., Kislinger, T., Ingram, M., Lu, A., Tanaka, H., Hori, O., Ogawa, S., Stern, D.M. and Schmidt, A.M. (2000). Blockade of RAGE-amphoterin signalling suppresses tumour growth and metastasis. *Nature* **405**, 354–360.

Tang, D. Knaleque, M.A., Jones, E.L., Theriault, J.R., Li, C., Wong, W.H., Stevenson, M.A. and Calderwood, S.K. (2005). Expression of heat shock proteins and HSP messenger ribonucleic acid in human prostate carcinoma in vitro and in tumors in vivo. *Cell Stress Chaperones* **10,** 46–59.

Takayama, S., Krajewski, S., Krajewski, M., Kitada, S., Zapada, S., Kochel, J.M., Knee, D., Scudiero, D., Tudor, G., Miller, G.J., Miyashita, T., Yamada, M. and Reed, K.C. (1998). Expression and location of Hsp70/Hsc-binding anti-apoptotic protein BAG-1 and its variants in normal tissues and tumor cell lines. *Cancer Res.*, **58**, 3116-3131.

Takenaga, K. (1986). Modification of the metastatic potential of tumour cells by drugs. Cancer *Met. Rev.* **5**, 67-75.

Takeno, S., Noguchi, T., Kikuchi, R., Sato, T., Uchida, Y. and Yokoyama, S. (2001). Analysis of the survival period in respectable stage IV gastric cancer. *Ann Surg Oncol.* **8**, 215–221.

Tan, Y., Li, G., Zhao, H., Xue, Y., Han, M. Yang, C. (2003). Expression of sorcin predicts poor outcome in acute myeloid leukaemia. *Leuk. Res.* **27,** 125-131.

Tanaka, S., Uehara, T. and Nomura, Y. (2000). Up-regulation of protein-disulfide isomerase in response to hypoxia/brain ischemia and its protective effect against apoptotic cell death. *J. Biol. Chem.* **275,** 10388-93.

Tannu, N. and Hemby, S.E. (2006). Quantitation in two-dimensional fluorescence difference gel electrophoresis. Effect of protein fixation. *Electrophoresis.* **27,** 2011-2015.

Tellingen, O. (2001). The importance of drug-transporting P-glycoproteins in toxicology. *Toxicology Letters,* **120,** 31-41.

Terzis, A.J., Thornsen, F., Heese, O., Visted, T., Bjerkvig, R., Dahl, O. and Arnold, H. (1997). Proliferation, migration and invasion of human glioma cells exposed to paclitaxel (Taxol) in vitro. *Br. J. Cancer,* **75,** 1744-1752.

Tewey, K.M., Rowe, T.C., Yang, L.C., Halligan, B.D. and Liu L.F. (1984). Adriamycin-induced DNA damage mediated by mammalian DNA topoisomerase II. *Science,* 226, 466-468.

Tham, Y.L., Gutierrez, C., Weiss, H., Mohsin, S., Hilsenbeck, S., Elledge, R., Chamness, G., Osborne, C.K., Allred, D.C. and Chang, J.C. (2005). Clinical response to neoadjuvant docetaxel predicts improved outcome in patients with large locally advanced breast cancer. *J. Clinical Onco.* **23,** 279-284.

Thompson, W.E., Branch, A.,Whittaker, J.A., Lyn, D., Zilberstein, M. and Mayo, K.E. (2001). Characterization of prohibitin in a newly established rat ovarian granulosa cell line. *Endocrinology* **142**, 4076–4085.

Tomasetto, C., Regnier, C., Moog, L., Mattei, M.G., Chenard, M.P., Lidereau, R., Basset, P. and Rio. M.C. (1995). Identification of four novel human genes amplified and overexpressed in breast carcinoma and localized to the q11-q21.3 region of chromosome 17. *Genomics.* **28,** 367–376.

Tomoda, K., Kubota, K. and Kato, J. (1999). Degradation od cyclin-dependant kinase inhibitor p27KIP1 is instigated by Jab1. *Nature,* **398,** 160-165.

Tonge, R., Shaw, J., Middleton, B., Rowlinson, R., Rayner, S., Young, J., Pognan, F., Hawkins, E., Currie, I. And Davidson, M. (2001). Validation and development of fluorescence two-dimensional differential gel electrophoresis proteomics technology. *Proteomics* **1**, 377-396.

Towatari, M., Adachi, K., Marunouchi, T. and Saito, H. (1998). Evidence for a critical role of DNA topoisomerase IIα in drug sensitivity revealed by inducible antisense RNA in a human leukaemia cell line. *Br. J. of Haematology* **101,** 548-551.

Towbin, H., Staehelin, T. and Gordon, J. (1979) Electrophoretic transfer of proteins from polyacrylamide gels to nitrocellulose sheets: procedures and some applications. *PNAS* **76**, 4350-4354.

Townsend, P.A., Cutress, R.I., Sharp, A., Brimmell, M. and Packham, G. (2003). BAG-1 prevents stress-induced long-term growth inhibition in breast cancer cells via a chaperone-dependent pathway. *Cancer Res.* **63**, 4150-4157.

Trieb K, Lechleitner T, Lang S, Windhager R, Kotz R, Dirnhofer S. (1998). Heat shock protein 72 expression in osteosarcomas correlated with good response to neoadjuvant chemotherapy. *Human Pathol.* **29**, 1050-1055.

Tsai, H.W., Chow, N.H., Lin, C.P., Chan, S.H., Chou, C.Y., Ho, C.L. (2006). The significance of prohibitin and c-Met/hepatocyte growth factor receptor in the progression of cervical adenocarcinoma. *Human Pathology* **37**, 198-204

Tsui, K., Cheng, A., Chang, P, Pan, T. and Yung, B. (2004). Association of nucleophosmin/B23 mRNA expression with clinical outcome in patients with bladder carcinoma. *Urology,* **64,** 839-844.

Tsukamoto, N., Chen, J. and Yoshida, A. (1998). Enhanced expression of glucose-6-phosphate dehydrogenase and cytosolic aldehyde dehydrogenase and elevation of reduced glutathione level in cyclophosphamide-resistant human leukaemia cells. *Blood Cells Mol. Dis.* **24**, 231-238.
Turk, V. and Bode, W. (1991). The cystatins: protein inhibitors of cysteine proteinases, *FEBS Lett.* **285**, 213-219.

Twentyman, P.R., Fox, N.E., Wright, K.A. and Bleehen, N.M. (1986). Derivation and preliminary characterisation of adriamycin resistant lines of human lung cancer cells. *Br. J. Cancer.* **53,** 529-537.

Tyan, Y.C., Wu, H.Y., Su, W.C., Wei, P. and Liao, P.C. (2005). Proteomic analysis of human pleural effusion. *Proteomics,* **5,** 1062-1074.

Unlu, M., Morgan, M.E. and Minden, J.S. (1997). Difference gel electrophoresis: a single gel method for detecting changes in protein extracts. *Electrophoresis* **18,** 2071-2077.

Urbani, A., Poland, J., Bernardini, S., Bellincampi, L., Biroccio, A., Schnölzer, M. Sinha, P. (2005). A proteomic investigation into etoposide chemo-resistance of neuroblastoma cell lines. *Proteomics,* **5,** 796-804.

Vaishampayan, U., Parchment, R.E., Jasti, B.R. and Hussain, M. (1999) Taxanes: an overview of the pharmacokinetics and pharmacodynamics. *Urology*, **54 (Suppl 6A),** 22-29.

Van der Bliek, A.M., Meyers', M.B., Biedlerl, J.L., Hes, E. and Borst, P. (1986). A 22-kd protein (sorcin/V19) encoded by an amplified gene in multidrug-resistant cells, is homologous to the calcium-binding light chain of calpain. *The EMBO Journal.* **5,** 3201 -3208.

Van den Brule, F., Califice, S. and Castronovo, V. (2004). Expression of galectins in cancer: a critical review. *Glycoconj J.***19**, :537-42.

Varbiro, G., Veres, B., Gallyas, F. Jr. and Sumegi, B. (2001). Direct effect of Taxol on free radical formation and mitochondrial permeability transition. *Free Radic Biol Med* **31**, 548–58.

Vargas-Roig, L.M., Gago, F.E., Tello, O., Aznar, J.C. and Ciocca, D.R. (1998). Heat shock expression and drug resistance in breast cancer patients treated with induction chemotherapy. *Int J Cancer (Pred Oncol).* **79**, 468–475.

Verrills, N.M., Liem, N.L., Liaw, T.Y., Hood, B.D., Lock, R.B. and Kavallaris, M. (2006). Proteomic analysis reveals a novel role for the actin cytoskeleton in vincristine resistant childhood leukemia-an in vivo study *Proteomics* **6,** 1681-1694.

Vishwanatha, J.K., Salazar, E. and Gopalakrishnan, V.K. (2004). Absence of annexin I expression in B-cell non-Hodgkin's lymphomas and cell lines. *BMC Cancer.***4**, 8-12.

Volm, M. and Rittgen, W. (2000). Cellular predictive factors for the drug response of lung cancer. *Anticancer Res.* **20,** 3449-3458.

Wadhwa, R., Ando, H., Kawasaki, H., Taira, K. and Kaul, S.C. (2003). Targeting mortalin using conventional and RNA-helicase-coupled hammerhead ribozymes. *EMBO Rep.* **4,** 595-601.
Wang, S.L., Tam, M.F., Ho, Y.S., Pai, S.H. Kao, M.C. (1995). Isolation and molecular cloning of human sorcin a calcium binding protein in vincristine-resistant HOB1 lymphoma cells. *Biochim. Biophys Acta..* **1260,** 285-293.

Wang, S., Nath, N., Adlam, M. and Chellappan, S. (1999). Prohibitin, a potential tumor suppressor, interacts with RB and regulates E2F function. *Oncogene* **18**, 3501–3510.

Wang, H., Guan, J., Wang, H., Perrault, A. R., Wang, Y. and Iliakis, G. (2001). Replication Protein A2 Phosphorylation after DNA Damage by the Coordinated Action of Ataxia Telangiectasia-Mutated and DNA-dependent Protein Kinase 1. *Cancer Research.* **61,** 8554-8563.

Wang, S , Fusaro, G , Padmanabhan, J and Chellappan, S P (2002) Prohibitin co-localizes with Rb in the nucleus and recruits N-CoR and HDAC1 for transcriptional repression *Oncogene* **21**, 8388–8396

Wang, Y , Serfass, L , Roy, M O , Wong, J (2004) Annexin I expression modulates drug resistance in tumour cells *Biochem Biophys Res Commun* **314**, 565-570

Wang, D and Lippard, S J (2005) Cellular processing of platinum anticancer drugs *Nature Rev Drug Discov* **4**, 307-320

Wasinger, V , Cordwell, S , Cerpa-Poljak, A , Gooley, A , Wilkins, M , Duncan, M , Harris, R , Williams, K and Humprey-Smith, I (1995) Progress with gene-product mapping of the mollicutes *Mycoplasma genitalium Electrophoresis* **16**, 1090-1094

Wasinger, V and Corthals, G L (2002) Proteomic tools for biomedicine *J Chromatogr B* **771**, 33-48

Weinberger, S R , Dalmasso, E A and Fung, E T (2000) Current achievements using ProteinChip Array technology *Curr Opin Chem Biol* **6**, 86-91

Wernyj, R P and Morin, P J (2004) Molecular mechanisms of platinum resistance still searching for the Achilles' heel *Drug Resistance Updates*, **7**, 227-232

Westerlund, A , Hujanen, E , Hoyhtya, M , Puistola, U , Turpeenniemi-Hujanen, T (1997) Ovarian cancer cell invasion is inhibited by paclitaxel *Clin Exp Metastasis*, **15**, 318-328

Wilhelm, L and Kolesar, J M (2005) Role of adjuvant chemotherapy in the treatment of non small cell lung cacner *American Journal of Health-System Pharmacy* **62**, 1365-1369

Workman, P (2004) Altered states selectively drugging the Hsp90 cancer chaperone *Trends Mol Med* **10**, 47–51

Wu, C , Wangpaichitr, M , Feun, L , Kuo M T , Robles, C , Lampidis, T and savaraj, N (2005) Overcoming cisplatin resistance by mTOR inhibitor in lung cancer *Mol Cancer*, **4**, 25

Wu, G S , Saftig, P , Peters, C and El-Deiry, W S (1998) Potential role for cathepsin D in p53-dependent tumor suppression and chemosensitivity *Oncogene* **16**, 2177-2183

Xang, Y , and Xiao, Z Q Chen, Z C , Zhang, G Y , Yi, H , Zhang, P F , Li, J L and Zhu, G (2006) Proteome analysis of multidrug resistance in vincristine-resistant human gastric cancer cell line SGC7901/VCR *Proteomics* **6**, 2009-2021

Xin, W , Rhodes, D R , Ingold, C , Chinnaiyan, A M (2003) Dysregulation of the annexin family protein family is assiciated with prostate cancer progression *Am J Pathol* 2003, **162**, 255-261

Yakirevich, E , Sabo, E , Naroditsky, I , Sova, Y , Lavie, O and Resnick, M B (2006) Multidrug resistance-related phenotype and apoptosis-related protein expression in ovarian serous carcinomas *Gynecol Oncology*, **100**, 152-159

Yang, S Y , Xiao, X Y , Zhang, W G , Zhang, L J , Zhang, W , Zhou, B , Chen, G and He, D C (2005) Application of serum SELDI proteomic patterns in diagnosis of lung cancer *BMC Cancer*, **5**, 83

Yang, Y X , Xiao, Z Q , Chen, Z C , Zhang, G Y , Yi, H , Zhang, P F , Li, J L and Zhu, G (2006) Proteome analysis of multidrug resistance in vincristine-resistant human gastric cancer cell line SGC7901/VCR *Proteomics,* **6,** 2009-21

Yates, J R (2000) Mass spectrometry from genomics to proteomics *Trends Biotechnol* **16,** 5-8

Yeung, K , Seitz, T , Li, S , Janosch, P , McFerran, B , Kaiser, C , Fee, F , Katsanakis, K D , Rose, D W , Mischak, H , Sedivy, J M and Kolch, W (1999) Suppression of Raf-1 kinase activity and MAP kinase signalling by RKIP *Nature* **401,** 173-177

Yokomizo, A , Ono, M and Nanri, H (1995) Cellular levels of thioredoxin associated with drug sensitivity to cisplatin, mitomycin C, doxorubicin, and etoposide *Cancer Res* **55,** 4293–6
Yoshida, A , Rzhetsky, A , Hsu, L C and Chang, C (1998) Human Aldehyde Dehydrogenase Gene Family *Eur J Biochem* , **251,** 549-557

Yoo, B C , Ku, J L , Hong, S H , Shin, Y K , Park, S Y , Kim, K and Park, J G (2004) Decreased pyruvate kinase M2 activity linked to cisplatin resistance in human gastric carcinoma cell lines *Int J Cancer* **108,** 532-539

Young, L C , Campling, B G , Voskoglou-Nomikos, T , Cole, S P C , Deeley, R G and Gerlach, J H (1999) Expression of multidrug resistance protein-related genes in lung cancer correlation with drug response *Clin Cancer Res* , **5,** 673-680

Young, J C , Agashe, V R , Siegers, K , Hartl, F U (2004) Pathways of chaperone-mediated protein folding in the cytosol *Nat Rev Mol Cell Biol* **5,** 781–791

Young, L C , Campling, B G , Cole, S P C , Deeley, R G and Gerlach, J H (2001) Multidrug resistance proteins MRP3, MRP1, and MRP2 in lung cancer correlation of protein levels with drug response and messenger RNA levels *Clin Cancer Res* , **7,** 1798-1804

Yvon, A-M C , Wadsworth, P and Jordan, M A (1999) Taxol suppresses dynamics of individual microtubules in living human tumour cells *Mol Biol Cell,* **10,** 947-959

Zaffaroni, N , Pennati, M , Colella, G , Perego, P , Supino, R , Gatti, L , Pilotti, S , Zunino, F and Daidone, M G (2002) Expression of the anti-apoptotic gene survivan correlates with taxol resistance in human ovarian cancer *Cell Mol Life Sci* **59,** 1406-1412

Zhang, Z , Bast, R C , Yu, Y H , Li, J N and Sokoll, L J (2004) Three biomarkers identified from serum proteomic analysis for the detection of early stage ovarian cancer *Cancer Res* **64,** 5882-5890

Zhang, D , Tai, Y C , Wong, C H , Tai, L K , Koay, E S and Chen, C S (2006) Molecular response of leukemia HL-60 cells to genistein treatment, a proteomics study *Leuk Res* **31,** 75-82
Zhao, Z G and Shen, W L (2005) Heat shock protein 70 antisense oligonucleotide inhibits cell growth and induces apoptosis in human gastric cancer cell line SGC-7901 *World J Gastroenterol* **7,** 73-8

Zhong, L , Hidalgo, G E , Stromberg, A J , Khattar, N H , Jett, J R and Hirschowitz, E A (2005) Using Protein Microarray as a Diagnostic Assay for Non-Small Cell Lung Cancer *Am J. Respir Crit Care Med* **172,** 1308-1314

Zhou, J , Chak-Sum Cheng, S , Luo, D and Xie, Y (2001) Study of Multi-drug resistant mechanisms in a taxol-resistant hepatocellular carcinoma QGY-TR 50 cell line *Biochemical and Biophysical Res Communications,* **280,** 1237-1242

Zhou, G , Li, H , Gong, Y , Zhao, Y , Cheng, J , Lee, P and Zhao, Y (2005) Proteomic analysis of global alteration of protein expression in squamous cell carcinoma of the esophagus *Proteomics* **5,** 3814-3821

Zhou, Y , Xu, Y , Tan, Y , Qi, J , Xiao, Y , Yang, C , Zhu, Z and Xiong, D (2006) Sorcin, an important gene associated with multidrug-resistance in human leukemia cells *Leukaemia research* **30,** 469-476

Zhukov, T A , Johanson, R A , Cantor, A B , Clark, R A and tockman, M S (2003) Discovery of distinct protein profiles specific for lung tumours and pre-malignant lung lesions by SELDI mass spectrometry *Lung Cancer,* **40,** 267-279

Appendix 1 - Identified proteins from DLKP versus DLKP-A

Spot No	Protein Name	Fold	P value	Sequence Coverage	No of Peptides
1	Valosin containing Protein	2 32	0 03	26 4	15 of 32
2	HSP70 kDa 9B (MTHsp75)	1 97	0 026	28	8 of 17
3	Lamin B1	3 07	0 001	24	15 of 27
4	HSP 70 protein 8 isoform 2	3 21	0 0052	23 3	8 of 22
5	Chaperonin containing TCP1 subunit 3	2 58	0 04	26 3	13 of 19
6	hnRPK	1 93	0 0087	20	6 of 14
7	Aldehyde dehydrogenase A1	1 65	0 023	23 8	8 of 18
8	Aldehyde dehydrogenase A1	1 52	0 0067	12 6	5 of 10
9	Succinyl-CoA 3 ketoacid CoA transferase	2 3	0 0012	24	7 of 17
10	Aldehyde dehydrogenase A1	1 47	0 046	6 3	10 of 15
11	CCT2	2 58	0 013	43	10 of 17
12	hnRPH1	1 52	0 025	23 6	7 of 19
13	Rab dissociation inhibitor beta	1 69	0 012	22 6	5 of 12
14	Chain C, OAT Mutant Y85i	-3 45	0 052	16 4	6 of 11
15	HSPC108 (stomatin)	2 03	0 0084	17 5	4 of 8
16	eIF 2b	1 42	0 029	18 4	7 of 14
17	HSP 70 protein 8 isoform 2	-2 15	0 0013	17 7	7 of 16
18	K alpha 1 protein	-1 55	0 034	29 4	9 of 16
19	Stress induced phosphoprotein	-1 43	0 047	12 3	5 of 14
20	Annexin A1	2 29	0 017	32 8	9 of 14
21	Annexin A1	2 51	0 0033	38 7	7 of 15
22	Annexin A1	1 63	0 027	26 4	7 of 15
23	Replication A2 32, kDa	1 5	0 033	26 3	6 of 13
24	Protein disulphide isomerase protein 5	-2 18	0 0032	20 9	6 of 11
25	HSP 27 kDa	1 47	0 031	30 9	5 of 11
26	Actin G protein	-1 45	0 012	40 7	6 of 14
27	HSP 70 kDa protein 8 isoform 2	-1 25	0 021	23 3	8 of 22
28	Triosephosphate isomerase	1 89	0 00077	21 6	4 of 9
29	Triosephosphate isomerase	-1 46	0 015	52 8	8 of 19
30	Thioredoxin peroxidase B chain J	-2 33	0 037	40 1	
31	K130r mutant of human DJ-1	1 54	0 0022	50 3	10 of 19
32	Thioredoxin peroxidase B	-1 95	0 0027	17 7	3 of 7
33	Sorcin isoform b	1 51	0 018	48 6	10 of 25
34	Nucleoside diphosphate kinase	1 54	0 011	51 4	7 of 12
35	eIF 5a	-2 63	0 027	19 5	4 of 11
36	Human tubulin chaperone cofactor A	-1 26	0 012	24 1	4 of 8
37	Galectin-1	-1 55	0 013	41	5 of 9
38	Thioredoxin delta 3	-1 17	0 018	43 8	4 of 13

Table 3 4 4a-ctd Identified proteins from DLKP versus DLKP-A (OAT Ornithine Aminotransferase)

Appendix 2 - Identified proteins from DLKP-A versus DLKP-A2B

Spot No	Protein Name	Fold	P value	Sequence Coverage	No of Peptides
23	Replication A2, 32 kDa	-1 29	0 0044	26 3	6 of 13
26	Actin G1 protein	2 95	0 032	40 7	6 of 14
27	HSP 70 kDa protein 8 isoform 2	2 87	0 0017	23 3	8 of 22
28	Triosephosphate isomerase	1 87	0 0047	46	7 of 15
34	Nucleoside diphosphate kinase 1	-1 28	0 013	51 4	7 of 12
36	Human tubulin chaperone cofactor A	-1 88	0 012	24 1	4 of 8
37	Galectin-1	1 71	0 014	50 7	5 of 12
38	Thioredoxin delta 3	1 6	0 0035	43 8	4 of 13

Table 3 4 6-ctd Fold difference of overlapping protein spots between the comparisons DLKP versus DLKP-A and DLKP-A versus DLKP-A2B

Spot No	Protein Name	Fold	P value	Sequence Coverage	No of Peptides
39	Actin G1 protein	6	0 018	40 7	6 of 16
40	Annexin 1	-1 6	0 013	60 8	9 of 22
41	Chloride intracellular channel 1 variant	-1 66	0 0011	54 8	9 of 14
42	HSP 70 kDa protein 8 isoform 2	7 9	0 0034	32 9	12 of 15
43	Chain B, Horf 6 a novel human peroxidase enzyme	-1 61	0 05	41 1	14 of 26
44	Eukaryotic translation elongation factor 1 delta isoform	-2 48	0 02	26 7	5 of 15
45	Vimentin	-1 64	0 046	30 7	13 of 22
46	HPRT	-1 71	0 013	24 2	8 of 15

Table 3 4 7-ctd The 8 overlapping protein spots between the comparisons DLKP versus DLKP-A2B and/or DLKP-A versus DLKP-A5F, DLKP-A10

Spot No	Protein Name	Fold	P value	Sequence Coverage	No of Peptides
41	Chloride intracellular channel 1 variant	-1 66	0 0011	54 8	9 of 14
52	alpha tubulin 6 variant	1 81	0 015	29 4	9 of 16
53	Annexin 1	2 42	0 0064	49	6 of 13
54	Beta Actin	-1 8	0 0018	27 5	7 of 13
55	Chain D, Cathepsin B (E C 3 4 22 1)	-1 87	0 016	29 3	4 of 14
56	Chain H Cathepsin D at pH 7 5	1 54	0 012	44	7 of 16
57	HSP 70 kDa protein 8 isoform 2	3 42	0 0098	21 9	7 of 12
58	KIAA0002	-2 02	0 041	21	8 of 14
59	Peroxiredoxin	1 72	0 041	28 5	7 of 12
60	Prolyl 4-hydrolase, beta subunit	-1 89	0 046	15	6 of 12
61	Proteasome (prosome, macropain) subunit, alpha type 5	1 6	0 034	42 3	7 of 16

Table 3 4 8-ctd Proteins unique to DLKP-A versus DLKP-A2B

Appendix 3 - Identified proteins from DLKP-A versus DLKP-A5F

Spot No	Protein Name	Fold	P value	Sequence Coverage	No of Peptides
16	eIF 2b	-1 38	0 0059	18 4	7 of 14
19	Stress induced phosphoprotein	-1 35	0 017	12 3	5 of 14
25	HSP 27 kDa protein	1 55	0 023	30 9	5 of 11
27	HSP 70 kDa protein 8 isoform 2	-2 15	0 004	23 3	8 of 22
28	Triosephosphate isomerase	-2 26	0 002	52 8	8 of 19
29	Triosephosphate isomerase		0 015	52 8	8 of 19
30	Thioredoxin peroxidase B	1 44	0 014	40 1	16 of 21
33	Sorcin	1 47	0 013	48 6	10 of 25
35	eIF 5a	-2 04	0 0022	19 5	4 of 11
37	Galectin-1	1 65	0 04	41	5 of 9

Table 3 4 10-ctd Overlapping protein spots between the comparisons DLKP versus DLKP-A and DLKP-A versus DLKP-A5F Comparisons between both experiments revealed that ten proteins were shared

Spot No	Protein Name	Fold	P value	Sequence Coverage	No of Peptides
39	Actin G1 protein	-4 07	0 015	40 7	6 of 16
43	Chain B, Horf 6 a novel human peroxidase enzyme	1 34	0 018	41 1	14 of 26
46	HPRT	-1 33	0 041	24 2	8 of 15
47	Synovial sarcoma breakpoint 3	-1 73	0 0025	34	4 of 11
48	BiP	-2 04	0 0022	19 5	4 of 11
49	Prohibitin	-2 13	0 044	39 3	9 of 13
50	Heat shock 27kDa protein	1 48	0 0074	22 8	4 of 7
51	Beta tubulin	-1 93	0 038	30	8 of 19

Table 3 4 11-ctd Overlapping protein spots between the comparisons DLKP versus DLKP-A5F and DLKP-A versus DLKP-A2B, A10

Spot No	Protein Name	Fold	P value	Sequence Coverage	No of Peptides
62	Putative protein of Nbla 10058	-1 76	0 0013	27 9	9 of 15
63	Alpha tubulin 6 variant	-1 38	0 023	31 4	10 of 15
64	ER-60	1 45	0 033	37	17 of 30

Table 3 4 12-ctd Protein spots unique to DLKP-A5F

Appendix 4- Identified proteins from DLKP-A versus DLKP-A10

Spot No	Protein Name	Fold	P value	Sequence Coverage	No of Peptides
4	HSP 70 protein 8 isoform 2	1 44	0 045	40 4	14 of 27
11	CCT2	1 8	0 013	26 4	10 of 17
16	eIF 2b	-1 63	0 026	18 4	7 of 14
18	K alpha 1 protein	1 81	0 001	29 4	9 of 16
20	Annexin A1	2 06	0 0062	32 8	9 of 14
21	Annexin A1	2 19	0 00064	38 7	7 of 15
27	HSP 70 kDa protein 8 isoform 2	-6 5	0 003	23 3	8 of 22
29	Triosephosphate isomerase	-3 21	0 026	52 8	8 of 19
31	K130r mutant	1 54	0 0022	49	6 of 11
33	Sorcin	-2 33	0 031	48 6	10 of 25
34	Nucleoside diphosphate kinase 1	1 27	0 046	35	5 of 7
35	eIF5a	-2 85	0 046	19 5	4 of 11

Table 3 4 18-ctd Overlapping protein spots between the comparisons DLKP-A versus DLKP-A10 and DLKP versus DLKP-A

Spot No	Protein Name	Fold	P value	Sequence Coverage	No of Peptides
39	Actin G	-4 69	0 041	40 7	6 of 16
40	Annexin 1	-2 27	0 023	60 8	9 of 22
42	HSP 70 kDa protein 8 isoform 2	-1 51	0 014	32 9	12 of 15
44	Eukaryotic translation elongation factor 1 delta isoform	-1 67	0 028	26 7	5 of 15
45	Vimentin	3 88	0 0048	30 7	13 of 22
47	Synovial sarcoma breakpoint 3	-1 9	0 0057	34	4 of 11
48	BiP	-3	0 022	15 8	9 of 17
49	Prohibitin	-2 28	0 025	39 3	9 of 13
51	Beta tubulin	-5 23	0 0043	30	8 of 19

Table 3 4 19-ctd Overlapping protein spots between the comparisons DLKP versus DLKP-A10 and/or DLKP-A versus DLKP-A5F, -A2B

Spot No	Protein Name	Fold	P value	Sequence Coverage	No of Peptides
65	26S proteasome-associated pad1 homolog variant	-1 54	0 038	30 1	4 of 8
66	Beta Actin	1 64	0 04	24 2	6 of 16
67	Beta Actin	1 63	0 01	18 9	5 of 8
68	Beta Actin	-2 03	0 02	21 1	6 of 11
69	Aldehyde Dehydrogenase A1	1 45	0 0096	21 8	9 of 16
70	Actin G1	-2 85	0 041	40 7	6 of 16
71	Chloride intracellular channel 4	-4 69	0 017	37 9	5 of 12
72	hnRPF	1 92	0 018	26	7 of 14
73	HSP 60 kDa	1 33	0 037	26 4	9 of 11
74	HSPC124	-2 48	0 023	24 8	5 of 8
75	LASP 1	-1 48	0 018	35 6	9 of 15
76	Peroxiredixin 3 isoform a precursor variant	-1 45	0 0039	23 8	5 of 10
77	Retinoblastoma binding protein 7	-2 43	0 045	11 9	5 of 12
78	Rho GDP dissociation inhibitor (GDI) alpha	-1 83	0 0078	25 5	6 of 17
79	Peroxiredoxin 2	-1 86	0 021	28 7	5 of 15
80	Vimentin	-2 24	0 0038	15 1	7 of 13

Table 3 4 20-ctd Proteins unique to DLKP-A versus DLKP-A10

Appendix 5 - Identified proteins from DLKP versus DLKP-Mitox

Spot No	Protein Name	Fold	P value	Sequence Coverage	No of Peptides
1	Valosin containing Protein	-2 0	0 0059	26 4	15 of 32
2	HSP70 kDa 9B (MTHsp75)	-2 53	0 0066	28	8 of 17
3	Lamin B1	-2 1	0 015	24	15 of 27
4	HSP 70 protein 8 isoform 2	-2 99	0 011	25 6	9 of 19
5	Chaperonin containing TCP1 subunit 3	-2 02	0 019	21 7	6 of 15
6	hnRPK	-2 69	9 80E-05	19 5	6 of 13
8	Aldehyde dehydrogenase A1	1 64	0 0011	26 7	12 of 19
10	Aldehyde dehydrogenase A1	1 61	0 0015	20 4	8 of 13
14	Chain C, OAT Mutant Y85i	1 96	0 043	16 4	6 of 11
16	eIF 2b	-1 32	0 035	18 4	7 of 14
21	Annexin A1	1 89	0 00049	35	8 of 15
22	Annexin A1	1 2	0 039	36 6	9 of 22
24	Protein disulphide isomerase protein 5	2 82	0 004	20 9	6 of 10
26	Actin G protein	-2 45	0 0067	40 7	6 of 14
29	Triosephosphate isomerase	-1 25	0 035	52 8	8 of 19
31	K130r mutant of human DJ-1	1 25	0 0059	50 3	6 of 16
33	Sorcin isoform b	3 85	0 0049	48 6	10 of 25
34	Nucleoside diphosphate kinase	-1 45	0 016	51 4	7 of 12
37	Galectm-1	-1 4	0 0024	41	5 of 9
38	Thioredoxin delta 3	1 98	0 007	43 8	4 of 13

Table 3 5 2-ctd Overlapping proteins form DLKP versus DLKP-Mitox and DLKP versus DLKP-A

Spot No	Protein Name	Fold	P value	Sequence Coverage	No of Peptides
39	Actin G protein	3 19	0 035	40 7	6 of 16
40	Annexin A1	2 21	0 019	44 6	7 of 12
49	Prohibitin	-1 36	0 025	39 3	9 of 13
43	Chain B, Horf 6 a novel human peroxidase enzyme	-1 62	1 10E-05	41 1	14 of 26
44	Eukaryotic translation elongation factor delta isoform 2	2 04	0 0013	26 7	5 of 15
57	HSP 70 kDa protein 8 isoform 2	1 79	0 0035	32 9	12 of 15
46	Human Hprt	2 25	0 0011	24 2	8 of 15
59	Peroxiredoxin	2 2	0 048	28 5	7 of 12
60	Prolyl 4-hydrolase beta subunit	1 28	0 035	15	6 of 12
61	Proteasome subunit alpha type 5	-1 28	0 025	42 3	7 of 16
65	26S Proteasome-associated Pad1 homologue variant	1 44	0 028	30 1	4 of 8
68	Beta Actin	2 01	0 0042	21 1	6 of 11
69	Aldehyde dehydrogenase 1A1	1 57	0 01	27 9	12 of 25
41	Chloride intracellular channel 1	-1 34	0 043	54 8	9 of 14
72	HNRPF	-1 71	0 015	26	7 of 14
76	Peroxiredixin 3 isoform a precursor variant 2	1 61	1 00E-05	28 5	7 of 12
62	putative protein of Nbla10058	-1 25	0 034	27 9	9 of 18
63	Alpha tubulin 6	1 39	0 022	31 4	10 of 15
64	ER-60 protease	-1 57	0 014	28 5	11 of 18
51	Beta Tubulin	-1 48	0 035	30	8 of 19

Table 3 5 3-ctd Overlapping proteins form DLKP versus DLKP-Mitox, and DLKP-A versus DLKP-A2B, -A5F and -A10

Spot No	Protein Name	Fold	P value	Sequence Coverage	No of Peptides
81	Aldehyde dehydrogenase 1A1	1 32	0 0011	26 7	12 of 19
82	Annexin A4	1 51	0 019	33 5	10 of 13
83	Beta Actin	2 97	0 032	21 1	6 of 11
84	Beta Actin	2 53	0 0049	27 5	7 of 13
85	Beta Actin	-1 37	0 0048	26 2	6 of 12
86	Tropomyosin	3 1	0 012	28 6	7 of 14
87	CGI-46 Protein	-1 35	0 043	31 7	11 of 23
88	GST-pi chain B	1 8	0 035	54 1	9 of 21
89	High mobility Group box 1	2 4	1 80E-07	35 8	9 of 22
90	HLA-B associated transcript 1	-2 05	0 0001	22 2	8 of 12
91	HSP 70kDa protein 8 isoform 2	-2 3	0 017	23 3	8 of 22
92	KIAA0098	-1 73	0 025	23 1	14 of 19
93	Mannose-6-phosphate receptor binding protein	-1 26	0 034	30 4	9 of 18
94	nucleophosmin	-1 37	0 05	23 6	4 of 12
95	Phosphoglycerate mutase 1 (brain) variant	-3 34	0 00029	37 4	7 of 11
96	PKCq-interacting protein	-1 58	0 0038	28 1	8 of 18
97	PP protein	-2 88	0 00021	48 7	12 of 24
98	Proteasome activator subunit 3	-1 71	0 016	33 4	6 of 11
99	Proteasome beta 3 subunit	1 45	0 0076	30 7	4 of 7
100	Purine nucleoside phosphorlyase	1 38	0 034	27 3	6 of 13
101	Cofilin (non muscle)	-3 77	0 00015	28 2	6 of 12

Table 3 5 5-ctd Proteins unique to DLKP versus DLKP-Mitox

Appendix 6 - Identified proteins from SKMES-1 versus SKMES-Txt

Spot No	Protein Name	Fold	P value	Sequence Coverage	No of Peptides
1	150kDa oxygen-regulated precursor	1 33	0 019	17 6	13 of 22
2	Valosin containing Protein	-1 58	0 036	18 5	9 of 16
3	Valosin containing Protein	-1 87	0 0004	15 4	8 of 16
4	Lamin A/C	1 58	0 0082	24 1	10 of 17
5	Chaperonin containing TCP1 subunit 3	1 23	0 0077	21 7	6 of 15
6	HSP 70 protein 8 isoform 2	1 24	0 041	17 6	6 of 11
7	Dihydropyrimidinase-like variant 2	1 42	0 023	14 3	5 of 10
8	HSP 60 kDa	1 45	0 00027	32 7	11 of 17
9	HSP 60 kDa	1 35	0 0019	31 8	11 of 18
10	Glucose 6 phosphate dehydrogenase	1 22	0 032	15	6 of 11
11	Glucose 6 phosphate dehydrogenase	1 55	0 0068	33 7	13 of 16
12	Glucose 6 phosphate dehydrogenase	1 2	0 036	27 2	10 pf 19
13	Vimentin	-1 63	0 0074	25 8	11 of 36
14	hnRPH1	1 57	5 80E-06	31	9 of 27
15	Keratin 8	-1 51	9 10E-05	31 7	18 of 24
16	PMPCA protein	1 73	0 0029	17 3	7 of 16
17	TATA binding protein interacting protein 49 kDa variant	1 32	0 0009	37 3	12 of 24
18	Mannose-6-phosphate receptor binding protein	-1 22	0 042	20 7	7 of 19
19	Beta tubulin	1 21	0 041	16 4	6 of 9
20	Septin 2	1 31	0 0081	26 6	6 o 16
21	HNRPC protein	1 32	0 0005	29 2	6 of 15
22	Mitochondrial ribosomal s22	1 19	0 0018	17 5	6 of 10
23	Annexin A1	1 43	0 02	32 8	9 of 17

Table 3 6 3a-ctd Identified proteins form SKMES-1 versus SKMES-Txt

Spot No	Protein Name	Fold	P value	Sequence Coverage	No of Peptides
24	LASP 1	1 61	0 0051	35 6	9 of 15
25	Annexin A3	1 48	0 05	49 8	13 of 20
26	HSPC124	1 77	4 40E-06	24 8	5 of 8
27	Proteasome activator subunit 2	1 62	0 0043	26 8	6 of 10
28	Chain H Cathepsin D at pH 7 5	1 98	0 0069	29 3	4 of 14
29	Proteasome (prosome, macropain) subunit, alpha type 5	-1 26	0 032	34	5 of 10
30	Proteasome (prosome, macropain) subunit, α type 5	1 27	0 0021	42 6	7 of 16
31	Prohibitin	1 43	0 0021	21 3	4 of 9
32	Chloride intracellular channel 4	1 74	0 028	37 9	5 of 12
33	High mobility Group box 1	1 46	0 0047	28 7	6 of 14
34	Chain B, Horf 6 a novel human peroxidase enzyme	1 36	0 0028	31 7	7 of 16
35	Ubiquitin Carboxy Hydrolase L1	1 27	0 0055	46 2	7 of 16
36	K130r mutant of human DJ-1	1 23	0 0013	40 6	6 of 13
37	Peroxiredoxin 2	1 72	0 001	18 5	4 of 7
38	GST-pi	-1 68	1 20E-05	31 6	4 of 7
39	GST-pi chain B	-1 37	0 0032	31 6	4 of 7
40	Galectin-1	-1 55	0 019	50 7	5 of 12

Table 3 6 3b-ctd Identified proteins form SKMES-1 versus SKMES-Txt

Appendix 7 - Identified proteins from SKMES-1 versus SKMES-Txl (Wk3)

Spot No	Protein Name	Fold	P value	Sequence Coverage	No of Peptides
1	150kDa oxygen-regulated precursor	1 94	3 50E-05	17 6	13 of 22
2	Valosin containing Protein	-1 31	0 011	18 5	9 of 16
3	Valosin containing Protein	-1 4	0 0088	15 4	8 of 16
4	Lamin A/C	1 71	7 60E-05	24 1	10 of 17
5	Chaperonin containing TCP1 subunit 3	1 41	0 00013	21 7	6 of 15
6	HSP 70 protein 8 isoform 2	-1 55	0 0001	17 6	6 of 11
10	Glucose 6 phosphate dehydrogenase	1 23	0 0036	15	6 of 11
12	Glucose 6 phosphate dehydrogenase	1 43	0 0036	27 2	10 pf 19
15	Keratin 8	-1 57	0 00023	31 7	18 of 24
22	HNRPC	1 4	7 50E-05	17 5	6 of 10
24	LASP 1	1 58	0 0067	35 6	9 of 15
26	HSPC124	1 58	4 10E-08	24 8	5 of 8
27	Proteasome activator subunit 2	-1 43	0 00075	26 8	6 of 10
30	Proteasome (prosome, macropain) subunit, alpha type 5	1 21	0 043	42 6	7 of 16
31	Prohibitin	1 44	0 025	21 3	4 of 9
34	Chain B, Horf 6 a novel human peroxidase enzyme	1 37	0 0013	31 7	7 of 16
35	Ubiquitin Carboxy Hydrolase L1	1 21	0 0098	46 2	7 of 16
36	K130r mutant of human DJ-1	1 29	0 00061	40 6	6 of 13
37	Peroxiredoxin 2	1 19	0 0047	18 5	4 of 7
38	GST-pi	-1 37	0 00011	31 6	4 of 7
39	GST-pi chain B	-1 92	4 50E-05	31 6	4 of 7

Table 3 6 5 Overlapping proteins form SKMES-1 versus SKMES-Txl (wk3) and SKMES-1 versus SKMES-Txt

Spot No	Protein Name	Fold	P value	Sequence Coverage	No of Peptides
41	ER-60 protease	1 35	0 03	37	17 of 30
42	Annexin V	1 56	0 0045	49 8	11 of 19
43	Thioredoxin peroxidase B	2 02	0 00016	40 1	16 of 21
44	Protein disulphide isomerase protein 5	1 65	8 50E-07	20 9	6 of 10

Table 3 6 6-ctd The overlapping protein spots between the comparisons SKMES versus SKMES-Txl (wk3) with SKMES-Txl (wk3) versus SKMES-Txl (Wk6)

Spot No	Protein Name	Fold	P value	Sequence Coverage	No of Peptides
50	Annexin A1	-1 26	0 02	35	8 of 15
51	Annexin A1	-1 29	0 038	36 6	9 of 22
52	Annexin A1	1 25	0 03	32 2	9 of 19
53	Annexin A1	-1 31	0 014	53 4	8 of 18
54	26S Proteasome-associated Pad1 homologue variant	1 22	0 028	30 1	4 of 8
55	Chain D, Cathepsin B (E C 3 4 22 1)	-1 77	0 007	29 3	4 of 14
56	Proteasome (prosome, macropain) subunit, alpha type 5	1 2	0 043	42 3	7 of 16
57	Beta tubulin	-1 56	1 60E-05	16 4	6 of 9
58	Prolyl 4-hydroxlyase, beta subunit	1 26	0 025	15	6 of 12
59	Beta Actin	-1 42	0 042	21 1	6 of 11
60	Nucleophosmin	-1 15	0 0028	23 6	4 of 12
60	HSP 27 kDa	-1 41	0 011	30 9	5 of 11
62	HSPC108	1 31	0 0075	17 5	4 of 8
63	Annexin A4	1 37	0 0011	33 5	10 of 13
64	HLA-B associated transcript 1 variant	1 26	0 022	22 2	8 of 12
65	6 phosphogluconolactonase	1 22	0 032	26	4 of 9
66	ATP Synthase	1 61	2 00E-05	21 7	8 of 16
67	ATPase beta subunit	-1 33	0 0038	35 7	15 of 20
68	Actin G1 protein	-1 26	0 013	40 7	6 of 16
69	HSP70 kDa 9B (MTHsp75)	-1 33	0 00042	28	9 of 20
70	CCT2	1 32	0 0013	43	8 of 24
71	Replication A2 32, kDa	1 22	0 0039	26 3	6 of 13
72	eiF 3 subunit 2 beta 36 kDa	-1 79	0 025	21 8	6 of 13

Table 3 6 7-ctd Proteins unique to SKMES versus SKMES-Txl(Wk2), Spots marked dark blue in Figure 3 6 8

Spot No	Protein Name	Fold	P value	Sequence Coverage	No of Peptides
2	Valosin containing Protein	-1 31	1 50E-05	18 5	9 of 16
8	HSP 60 kDa	1 6	3 40E-06	32 7	11 of 17
6	HSP 70 protein 8 isoform 2	1 30	0 011	17 6	6 of 11
14	hnRPH1	-1 24	0 037	31	9 of 27
19	Beta tubulin	-1 94	0 014	16 4	6 of 9
24	LASP 1	-1 49	0 00065	35 6	9 of 15
25	Annexin A3	-1 39	0 0019	49 8	13 of 20
33	High mobility Group box 1	1 2	0 0057	28 7	6 of 14
37	Peroxiredoxin 2	-1 25	0 033	18 5	4 of 7
38	GST-pi	2 29	0 00021	31 6	4 of 7
40	Galectin-1	-1 32	0 012	50 7	5 of 12

Table 3 6 9-ctd Overlapping proteins between SKMES-Txl (Wk3) versus SKMES-Txl (Wk6) and SKMES-1 versus SKMES-Txt

Spot No	Protein Name	Fold	P value	Sequence Coverage	No of Peptides
50	Annexin A1	-1 26	0 02	35	8 of 15
51	Annexin A1	-1 29	0 038	36 6	9 of 22
52	Annexin A1	1 25	0 03	32 2	9 of 19
53	Annexin A1	-1 31	0 014	53 4	8 of 18
54	26S Proteasome-associated Pad1 homologue variant	1 22	0 028	30 1	4 of 8
55	Chain D, Cathepsin B (E C 3 4 22 1)	-1 77	0 007	29 3	4 of 14
56	Proteasome (prosome, macropain) subunit, alpha type 5	1 2	0 043	42 3	7 of 16
57	Beta tubulin	-1 56	1 60E-05	16 4	6 of 9
58	Prolyl 4-hydroxlyase, beta subunit	1 26	0 025	15	6 of 12
59	Beta Actin	-1 42	0 042	21 1	6 of 11
60	Nucleophosmin	-1 15	0 0028	23 6	4 of 12
60	HSP 27 kDa	-1 41	0 011	30 9	5 of 11
62	HSPC108	1 31	0 0075	17 5	4 of 8
63	Annexin A4	1 37	0 0011	33 5	10 of 13
64	HLA-B associated transcript 1 variant	1 26	0 022	22 2	8 of 12
65	6 phosphogluconolactonase	1 22	0 032	26	4 of 9
66	ATP Synthase	1 61	2 00E-05	21 7	8 of 16
67	ATPase beta subunit	-1 33	0 0038	35 7	15 of 20
68	Actin G1 protein	-1 26	0 013	40 7	6 of 16
69	HSP70 kDa 9B (MTHsp75)	-1 33	0 00042	28	9 of 20
70	CCT2	1 32	0 0013	43	8 of 24
71	Replication A2 32, kDa	1 22	0 0039	26 3	6 of 13
72	eIF 3 subunit 2 beta 36 kDa	-1 79	0 025	21 8	6 of 13

Table 3 6 7-ctd Proteins unique to SKMES versus SKMES-Txl(Wk2), Spots marked dark blue in Figure 3 6 8

Spot No	Protein Name	Fold	P value	Sequence Coverage	No of Peptides
2	Valosin containing Protein	-1 31	1 50E-05	18 5	9 of 16
8	HSP 60 kDa	1 6	3 40E-06	32 7	11 of 17
6	HSP 70 protein 8 isoform 2	1 30	0 011	17 6	6 of 11
14	hnRPH1	-1 24	0 037	31	9 of 27
19	Beta tubulin	-1 94	0 014	16 4	6 of 9
24	LASP 1	-1 49	0 00065	35 6	9 of 15
25	Annexin A3	-1 39	0 0019	49 8	13 of 20
33	High mobility Group box 1	1 2	0 0057	28 7	6 of 14
37	Peroxiredoxin 2	-1 25	0 033	18 5	4 of 7
38	GST-pi	2 29	0 00021	31 6	4 of 7
40	Galectin-1	-1 32	0 012	50 7	5 of 12

Table 3 6 9-ctd Overlapping proteins between SKMES-Txl (Wk3) versus SKMES-Txl (Wk6) and SKMES-1 versus SKMES-Txt

Spot No	Protein Name	Fold	P value	Sequence Coverage	No of Peptides
41	ER-60 protease	-1 55	2 60E-06	37	17 of 30
42	Annexin V	2 10	0 017	49 8	11 of 19
43	Thioredoxin peroxidase B	-1 33	0 017	40 1	16 of 21
44	Protein disulphide isomerase protein 5	-1 48	9 80E-06	20 9	6 of 10

Table 3 6 10-ctd The 4 overlapping protein spots between the comparisons SKMES-1 vs SKMES-Txl (wk3) and SKMES-Txl (wk3) vs SKMES-Txl (Wk6)

Spot No	Protein Name	Fold	P value	Sequence Coverage	No of Peptides
73	KIAA0098	-1 31	0 0051	23 1	14 of 19
74	HSP 70 protein 8 isoform 2	-1 29	0 006	25 6	9 of 19
75	HSP 70 protein 8 isoform 2	-1 3	0 011	23 3	8 of 22
76	Beta Actin	2 38	0 0061	27 5	7 of 13
77	Lamin B1	1 7	0 00051	24	15 of 27
78	Rab dissociation inhibitor beta	1 69	0 022	22 6	5 of 12
79	Stathmin	-1 24	0 019	35 6	5 of 12
80	hnRPK	-1 33	0 00094	20	6 of 14
81	Chloride intracellular channel 1	-1 21	0 05	54 8	9 of 14
82	RPLPO	1 39	0 026	32 3	4 of 7

Table 3 6 11-ctd Proteins unique to SKMES-Txl (Wk3) versus SKMES-Txl (Wk6)

Abstract

This thesis sets out to increase our knowledge of mechanisms by which lung cancer cells develop resistance to chemotherapeutic agents To further investigate drug resistance in lung cancer, a panel of four cell lines were chosen for pulse-selection with chemotherapeutic agents The cell lines include two squamous (SKMES and DLRP) and two small cell lung carcinoma (DMS-53 and NCI-H69) cell lmes The chemotherapy naive cell lines were purposely pulse-selected rather than continuously selected with clinically relevant concentrations of taxotere, taxol, carboplatin and/or VP-16 The resulting twelve novel cell lmes were tested for resistance to a cross-section of chemotherapeutic agents, for changes in invasiveness, motility, adhesiveness and for expression of the multidrug resistance (MDR) efflux pump proteins, P-gp and MRP-1 The SKMES-taxane selected variants were chosen for further analysis because the resistance profile was unstable and the concentration of drug used for selection was at a clinically achievable level Proteomic analysis was used to identify proteins associated with the development of taxol and taxotere resistance in these cell lines Proteomic analysis also revealed the differences between resistance to taxol and taxotere Loss of resistance was observed in both taxane resistant variants of SKMES By monitoring the differential protein expression over time, proteins involved in the loss of resistance were identified

Adriamycin and mitoxantrone resistance was also studied in the squamous lung cell line DLKP While the main mechanism of resistance in these cell lines is associated with a drug pump, little information on cytoplasmic changes is available Proteomic analysis investigated these changes and elucidated the mechanisms involved in adriamycin and mitoxantrone resistance to identify putative markers with possible prognostic/diagnostic value A comparison of the proteins altered in adriamycin and mitoxantrone-resistant variants was carried out as these drugs are alkylating agents with mitoxantrone being an analogue of adriamycin and inducing less cardiotoxicity Multidrug resistance is a major problem in lung cancer, there is a need to understand the common mechanisms involved The proteins involved in the development of taxane resistance in SKMES showed some cross over with other chemotherapeutic drugs namely adriamycin or mitoxantrone in DLKP